

# **Advancing Stoichiometric and Catalytic Applications of Cooperative Bimetallics in Organic Synthesis**



**Marco De Tullio Meana**

Department of Pure and Applied Chemistry

University of Strathclyde

A thesis submitted to the Department of Pure and Applied Chemistry, University of Strathclyde, in part fulfilment of the requirements for the degree of Doctor of Philosophy.

**March 2017**

## **Declaration**

This thesis is the result of the author's original research. It has been composed by the author and has not been previously submitted for examination which has led to the award of a degree.

The copyright of this thesis belongs to the author under the terms of the United Kingdom Copyright Acts as qualified by the University of Strathclyde Regulation 3.50. Due acknowledgement must always be made of the use of any material contained in, or derived from, this thesis

Marco De Tullio

March 2017

*Dedicated to Maria, my love  
For the bright future that awaits us*

## Acknowledgments

I would like to take the opportunity to acknowledge different people which in one way or another have helped me during this important period of my life.

First and foremost I would like to thank my supervisor and friend Professor Eva Hevia, all her support, guidance and motivation throughout the 4 and a half years of the PhD is hugely appreciated. Also her patience in correcting this thesis an uncountable number of times along with all the suggestions which transformed many of my meaningless phrases into this work, it is sincerely appreciated. Eva, I feel very lucky to have had the opportunity to work in your group. Thank you particularly for making me the researcher I am today, there is no space enough in this thesis to express my respectful gratitude.

In addition I would like to thank Professor Robert Mulvey, his help, support and friendship is greatly appreciated. I won't forget some of the football games we've attended at Celtic Park, I remember Celtic-Inter Milan 3:3 as one of the best games I have ever attended, great feelings and atmospheres. I would also like to thank Dr. Charlie O'Hara and Dr. Stuart Robertson for all their suggestions, help and friendship. Great are the memories from the pool tournaments played in Rothesay and Largs. I have lost against Charlie and Stuart several times, but I was lucky to beat Rab more than once (hope you remember that Rab ☺). I was even lucky to win the tournament in one occasion, so I am glad I'll be on the winner's list for ever.

Furthermore I would also like to thank the post-doctoral researchers within Mulvey-Hevia and O'Hara group, Alberto for all the help in the lab and all the great moments and for mentoring me during this period. Tobi for the generous help and advice over the first year of my PhD. Sharon for helping me although only for a very short period of time, Ross for all the good times spent both in the lab, lunching or playing football, and Javi for all the good time spent together in Glasgow, Antonio, Maria and Markus and Marius for all your help.

A special thank goes to Lewis and Marina, we have started the PhD together and we became friends in no time. Great are the memories of this journey we began together back in October 2012. Lewis thanks for teaching me a lot about food (especially coffee), you are the PhD friend every group should have. A sport lover and a great party organiser, I will never forget all the great time spent in 95 Morrison's street. Marina thanks for all the motivation and for helping me during the bad moments of the PhD. I will never forget all the good time we've had in St. Vincent Street, during our flat sharing. I am laughing at thinking of all the Marinol moments

and stories, and remembering our trip to Japan and all the great time spent there. I would also like to thank Silvia, she also started a PhD with me and I have only great memories of all the time spent together both in the lab and outside (Sure she remembers Elain's party). Thanks to Ana, which has also started her PhD at the same time as I did.

A special thank goes to Laia, she started her PhD a year after I did, and she is since become one of my best friends in the lab. She is an awesome climber and we shared our pains for not being able to dedicate much time to the sport we love. Thank you Laia.

I also want to thank Sam, a PhD student from Mulvey's group, for all the great time spent next to me in the lab (God that was indeed the toughest part of the PhD, no doubt about it Sam...haha), thanks Sam.

A special thanks to Etienne and Andy for all the great time we've shared. I would like to thank all the people I have worked with in the beta-lab, Marco, Thomas, Tracy, Donna and all the past members of the Mulvey, Hevia and O'Hara group, Jan, Elaine, Jenny, Sarah, Ben, Emma and the new Vicky and Michael.

I would like to thank some of the people that have helped me with the technical aspects of my PhD, Craig Irving, for the constant help with NMR aspects in particular with the endless kinetic studies. I am thankful to Alexander Clunie for running my elemental analysis samples and Patricia Keating for all the help with the GC-MS.

A special thank goes to Janie-Anne Pickrell who has always helped me in the lab with anything needed, and has always provided me with all the best glassware. I am very grateful also to Isabel Scott for the help with administration issues.

This thesis would not have been possible without the encouragement and unconditional love of my family; my awesome parents Mercedes and Andrea, my sister Claudia and brother Nico, all of them are an inspiration for me and have guided me constantly.

## Abstract

Advancing the exploitation of alkali metal-magnesiates and alkali metal-manganates in a variety of fundamental organic transformations, this thesis presents an extensive study, which assesses synergistic behaviours in these systems and their ability to promote catalytic transformations.

Using novel potassium magnesiates such as  $(\text{PMDETA})_2\text{K}_2\text{Mg}(\text{CH}_2\text{SiMe}_3)_4$  (**1b**), selective magnesiation of aromatic and heterocyclic substrates has been accomplished under mild reaction conditions, using a hydrocarbon solvent. These studies have revealed an important alkali metal effect; thus when the K atom in **1b** is replaced by Li or Na, the direct magnesiation processes are inhibited.

The ability of sodium magnesiates to perform catalytic transformations has been disclosed, finding that higher order sodium magnesiate  $(\text{TMEDA})_2\text{Na}_2\text{Mg}(\text{CH}_2\text{SiMe}_3)_4$  (**1d**) catalyses the cycloaddition of alkynes to azides with the corresponding formation of a wide range of 1,5-disubstituted-1,2,3-triazoles. Structural elucidation of key organometallic intermediates along with  $^1\text{H}$  DOSY NMR studies has revealed sodium magnesiate  $[(\text{THF})_4\text{Na}_2\text{Mg}\{\text{C}\equiv\text{C}(\text{p-tolyl})\}_4]$  (**1j**) is a reaction intermediate in these processes. Mechanistic insights have been gained by kinetic studies which revealed that the reaction rate is zero-order in alkyne and order one in azide and catalyst, thus indicating the insertion/intramolecular nucleophilic attack is the rate determining step of the reaction.

$\text{NaMg}(\text{CH}_2\text{SiMe}_3)_3$  (**1f**) was found to perform the guanylation and hydrophosphination of multiple amines/phosphines upon reactions with carbodiimides at ambient temperature and in very short periods of time. Comprehensive stoichiometric and kinetic studies revealed this reaction takes place via tris amido sodium magnesiate (**1m**) and mixed amido/guanidinate (**1o**) intermediates. Interestingly, a concerted transition state is proposed which agrees with the first order observed in amine and carbodiimide.

Lithium manganate  $(\text{THF})_x\text{Li}_2\text{Mn}(\text{CH}_2\text{SiMe}_3)_4$  (**1u**) was found to be an excellent reagent for the Mn/I exchange reaction of iodoaryls followed by homocoupling for the synthesis of a variety of symmetric biaryl reagents. Interestingly the activity of **1u** could be upgraded to catalytic conditions, with the use of Mg(s) as reducing agent. Preliminary mechanistic studies have revealed that Li plays a major role in these transformations.

## Publication and Conference Presentations

### Publications in Peer Reviewed Journals

1. Potassium-Alkyl Magnesiates: Synthesis, Structures and Mg–H exchange Applications of Aromatic and Heterocyclic Substrates, *Chem. Commun.*, **2014**, 50, 12859-62 (DOI:10.1039/C4CC05305B) Authors: Dr. Sharon E. Baillie, Dr. Tobias D. Bluemke, Prof. William Clegg, Dr. Alan R. Kennedy, Dr. Jan Klett, Dr. Luca Russo, Marco De Tullio and Prof. Eva Hevia.

Chapter 2 is adapted from the publication above.

2. Structural and Mechanistic Insights into s-Block Bimetallic Catalysis: Sodium Magnesiates-Catalyzed Guanylation of Amines *Chem. Eur. J.*, **2016**, 22, 17646-56 (DOI: 10.1002/chem.201602906) Marco De Tullio, Dr. Alberto Hernán-Gómez, Dr. Zoe Livingstone, Prof. William Clegg, Dr. Alan R. Kennedy, Dr. Ross W. Harrington, Prof. Antonio Antiñolo, Antonio Martínez, Dr. Fernando Carrillo-Hermosilla, Prof. Eva Hevia.

Chapter 4 is adapted from the publication above.

### Conference Presentations (Oral)

1. *Tailoring Alkali-Metal Magnesiates for New Stoichiometric and Catalytic Applications*, University of Strathclyde Inorganic Section West Brewery Talks, 11<sup>th</sup> June **2014**, West Brewery, Glasgow (UK)
2. *Tailoring Alkali-Metal Magnesiates for New Stoichiometric and Catalytic Applications*, Universities of Scotland Inorganic Chemistry Conference, Heriot-Watt University 3<sup>th</sup> July **2015**, Edinburgh (UK)

### Conference Presentations (Poster)

1. *Synthesis and Reactivity of Novel Homoleptic Alkylpotassium Magnesiates*, 20<sup>th</sup> EuCheMS Conference on Organometallic Chemistry, 30<sup>th</sup> June-4 July **2013**, St Andrews (UK).

2. *Synthesis and Reactivity of Novel Homoleptic Alkylpotassium Magnesiates*, Universities of Scotland Inorganic Chemistry Conferences (USIC) 25<sup>th</sup>–26<sup>th</sup> July-**2013** University of Edinburgh (UK)
3. *New Potassium-Magnesiate Approaches for the Chemoselective Magnesiation of Aromatic and Heteroaromatic Substrates*, XXVI International Conference on Organometallic Chemistry (ICOMC), 13<sup>th</sup>-18<sup>th</sup> July **2014**, Sapporo, (Japan)
4. *New Potassium-Magnesiate Approaches for the Chemoselective Magnesiation of Aromatic and Heteroaromatic Substrates*, Universities of Scotland Inorganic Chemistry Conferences, 4<sup>th</sup>-5<sup>th</sup> September **2014** University of Glasgow (UK)
5. *Sodium-magnesiate catalysed synthesis of 1,5-disubstituted-1,2,3-triazoles*, The Main Group Interest Group Annual Meeting, 11<sup>th</sup> September **2015**, Royal Society of Chemistry, Burlington House, London (UK)
6. *Sodium-magnesiate catalysed synthesis of 1,5-disubstituted-1,2,3-triazoles*, 11<sup>th</sup> International Symposium on Carbanion Chemistry, 17<sup>th</sup>-21<sup>th</sup> July **2016**, Rouen, (France)
7. *Structural and mechanistic insights into s-block bimetallic catalysis: Sodium magnesiate catalysed guanylation of amines*, Universities of Scotland Inorganic Chemistry Conferences (USIC), 11<sup>th</sup>-12<sup>th</sup> August **2016** University of Strathclyde (UK)

## List of abbreviations

Å	Angstroms
∞	Infinity
σ	Sigma
°	Degrees
<i>o</i>	<i>Ortho</i>
<i>m</i>	<i>Meta</i>
<i>p</i>	<i>Para</i>
<b>AMMMg</b>	Alkali-metal-mediated-magnesium
<b>Ar</b>	Aryl
<b>Bu</b>	Butyl
<b>Cyc-C<sub>6</sub>D<sub>12</sub></b>	Deuterated cyclohexane
<b>CIP</b>	Contacted Ion-Pair
<b>DCM</b>	Dichloromethane
<b>DFT</b>	Density functional theory
<b>DoM</b>	Direct- <i>ortho</i> -metallation
<b>DOSY</b>	Diffusion ordered spectroscopy
<b>E</b>	Electrophile
<b>eq</b>	Equivalent/equivalents
<b>FG</b>	Functional group
<b>GC</b>	Gas chromatography
<b>KOR</b>	Potassium <i>tert</i> -butoxide
<b>LDA</b>	Lithium diisopropylamide
<b>LIC</b>	Butyllithium
<b>mg</b>	Milligrams
<b>mL</b>	Millilitres
<b>mmol</b>	Millimoles
<b>Np</b>	Neopentyl
<b>NMR</b>	Nuclear magnetic resonance
<b>s</b>	Singlet

<b>d</b>	Doublet
<b>t</b>	Triplet
<b>q</b>	Quartet
<b>m</b>	Multiplet
<b>Nu</b>	Nucleophile
<b>PMDETA</b>	<i>N,N,N', N'',N''</i> -pentamethyldiethylenediamine
<b>Ph</b>	Phenyl
<b>Pr</b>	Propyl
<b>RT</b>	Room Temperature
<b>T</b>	Temperature
<b>THF</b>	Tetrahydrofuran
<b>THP</b>	Tetrahydropyran
<b>TMP</b>	2,2,6,6-tetramethylpiperidide
<b>TMEDA</b>	<i>N,N,N',N'</i> -tetramethylethylenediamine
<b><sup>t</sup>Bu</b>	<i>Tert</i> -Butyl
<b><sup>n</sup>Bu</b>	<i>Normal</i> -butyl
<b><sup>n</sup>BuLi</b>	<i>n</i> -butyllithium
<b><sup>s</sup>BuLi</b>	<i>Sec</i> -butyllithium

# Table of Contents

Declaration	II
Dedication	III
Acknowledgments	IV
Abstract	VI
Publication and Conference Presentations	VII
List of Abbreviations	IX
Table of Contents	XI

## Chapter 1 Introduction

<b>1.1</b>	<b>General Introduction</b>	1
1.1.1	Mixed-metal organometallic reagents	1
1.1.2	Historical background	2
<b>1.2</b>	<b>Deprotonative metallation in synthesis</b>	3
1.2.1	Importance of metallation chemistry	3
1.2.2	Organolithium reagents in metallation chemistry	3
1.2.3	Lochmann-Schlosser superbases reagents	7
1.2.4	Applications of magnesium reagents in deprotonative metallation chemistry	13
<b>1.3</b>	<b>Kinetic activation of magnesium reagents: magnesiate formation</b>	15
1.3.1	Turbo-Hauser bases	15
1.3.2	Alkali-metal magnesiates	17
1.3.3	Alkali-metal-mediated-dimetallations: a template base approach to deprotonation	20
<b>1.4</b>	<b>Applications of group 2 complexes in catalysis</b>	24
1.4.1	Introduction	24
1.4.2	Group 2 organometallic components in catalysts	24
1.4.3	Organomanganese complexes in C-C bond forming processes	30
<b>1.5</b>	<b>Aims</b>	35
<b>1.6</b>	<b>References</b>	36

## Chapter 2 Alkali-Metal Mediated Magnesiations of Aromatic and N-heterocyclic Substrates Using Homoleptic Higher-Order Potassium Magnesiates

<b>II</b>	<b>Table of compounds</b>	42
<b>2.1</b>	<b>Summary</b>	44
<b>2.2</b>	<b>Introduction</b>	45
<b>2.2.1</b>	Alkali- Metal-Mediated-Magnesiations (AMMMg)	45
<b>2.3</b>	<b>Results and discussion</b>	49
2.3.1	Synthesis of starting material	49
2.3.2	Assessing metallating ability of alkyl potassium magnesiates <b>1a</b> , <b>1b</b> and <b>1c</b> .	53
2.3.3	Magnesiation of substituted aromatic substrates	61
<b>2.4</b>	<b>Magnesiation studies on N-heterocyclic substrates.</b>	72
2.4.1	Studies using methoxy substituted pyridines.	72
2.4.2	Magnesiation of aromatic five-membered ring heterocycles.	76
<b>2.5</b>	<b>Conclusions</b>	87
<b>2.6</b>	<b>Experimental section</b>	88
2.6.1	Synthesis of inorganic compounds	88
2.6.2	Synthesis of iodoaryl derivatives	91
<b>2.7</b>	<b>References</b>	101

**Chapter 3 Sodium-magnesiate catalysed synthesis of 1,5-disubstituted-1,2,3-triazoles**

<b>III</b>	<b>Table of compounds</b>	106
<b>3.1</b>	<b>Summary</b>	109
<b>3.2</b>	<b>Introduction</b>	110
<b>3.3</b>	<b>Results and Discussion: Synthesis of starting material</b>	115
3.3.1	Synthesis of bimetallic pre-catalysts	115
3.3.2	Synthesis of organic azides	116
<b>3.4</b>	<b>Assessing catalytic ability of homoleptic alkyl sodium magnesiates <b>1f</b>, <b>1d</b>.</b>	118
<b>3.5</b>	<b>Stoichiometric studies</b>	134
<b>3.6</b>	<b>Kinetic Analysis</b>	148
3.6.1	Azide order	149
3.6.2	Alkyne order	150
3.6.3	Catalyst order	152
3.6.4	Proposed mechanism	153
<b>3.7</b>	<b>Conclusions</b>	159
<b>3.8</b>	<b>Experimental section</b>	159

3.8.1	Synthesis of inorganic compounds	160
3.8.2	Synthesis of organic compounds	168
3.8.3	Synthesis of azides	169
3.8.4	Synthesis of 1,5-disubstituted-1,2,3-triazoles	171
3.9	<b>References</b>	186

## Chapter 4 Structural and mechanistic insights into s-block bimetallic catalysis: sodium magnesiate catalysed guanylation of amines

IV	<b>Table of compounds</b>	189
4.1	<b>Summary</b>	191
4.2	<b>Introduction</b>	192
4.3	<b>Results and Discussion</b>	195
4.3.1	Catalytic synthesis of guanidines and phosphaguanidine	195
4.3.2	Stoichiometric investigations	199
4.3.3	Mechanistic Studies	211
4.4	<b>Conclusions</b>	217
4.5	<b>Experimental section</b>	218
4.5.1	Synthesis of $[\{(THF)_3NaMg(NHAr)_3\}_2]$ ( <b>1m</b> ) (Ar = 2,6-Me <sub>2</sub> C <sub>6</sub> H <sub>3</sub> )	220
4.5.2	Synthesis of $[Na(THF)_5]^+[Mg\{(CyN)_2C(NPh_2)\}_2(NPh_2)]^-$ ( <b>1o</b> )	221
4.5.3	Stoichiometric studies: reaction between $[\{(THF)_3NaMg(NHAr)_3\}_2]$ ( <b>1m</b> ) (Ar = 2,6-Me <sub>2</sub> C <sub>6</sub> H <sub>3</sub> ) and 3 equivalents of diisopropylcarbodiimide ( <b>8a</b> )	221
4.5.4	Synthesis of dimer $[\{Na(NHAr)\}_2]$ ( <b>1r</b> ) (Ar = 2,6-Me <sub>2</sub> C <sub>6</sub> H <sub>3</sub> )	222
4.5.5	Synthesis of $[Na\{(iPrN)C(NAr)(HN^iPr)\}(THF)]_2$ ( <b>1q</b> ) (Ar = 2,6-Me <sub>2</sub> C <sub>6</sub> H <sub>3</sub> ).	222
4.6	<b>References</b>	224

## Chapter 5 Using Lithium Manganates to access symmetric biaryl compounds: Tandem Mn-I exchange, C-C homocoupling processes

V	<b>Table of contents</b>	228
5.1	<b>Summary</b>	231
5.2	<b>Introduction</b>	232
5.3	<b>Results and Discussion</b>	237
5.3.1	Synthesis of starting material	237
5.3.2	Assessing the ability of lithium manganates to promote Mn/halogen exchange reactions followed by homocoupling.	238

<b>5.3.3</b>	Optimisation of reaction conditions	239
<b>5.3.4</b>	Substrate scope	249
<b>5.4</b>	<b>Conclusions</b>	260
<b>5.5</b>	<b>Experimental section</b>	261
<b>5.5.1</b>	Synthesis of biaryl compounds.	261
<b>5.5</b>	<b>References</b>	271

## **Chapter 6    Conclusions and Further Work**

<b>6.1</b>	<b>Conclusions</b>	273
<b>6.2</b>	<b>Further work</b>	275

## **Chapter 7    General Experimental Techniques and Procedures**

<b>7.1</b>	<b>Schlenk line techniques</b>	278
<b>7.2</b>	<b>Glove Box techniques</b>	279

# **CHAPTER 1**

## **Introduction**

## 1.1 General Introduction

### 1.1.1 Mixed-metal organometallic reagents

Over the past decade the synthesis and exploitation of bimetallic reagents, which combine two metals of markedly different polarities have truly revolutionised organometallic chemistry.<sup>1-4</sup> Pioneered by Wanklyn more than 150 years ago with the synthesis of  $\text{NaZnEt}_3$ ,<sup>5</sup> these bimetallic reagents exhibit unique synergic chemical profiles which cannot be replicated by their homometallic components. Thus mixed-metal reagents have come to the fore as a new family of versatile and effective organometallic reagents which can participate in several key organic transformations such as metallations, metal-halogen exchange reactions and nucleophilic additions, to name just a few. Important landmarks in this evolving area of chemistry involve Knochel's "turbo-Grignard" reagents, the Lochmann-Schlosser "superbase"<sup>3</sup> as well as Mulvey's contributions towards understanding the synergic effects taking place in alkali-metal-mediated metallation reactions (**Figure 1.1**).<sup>4</sup>

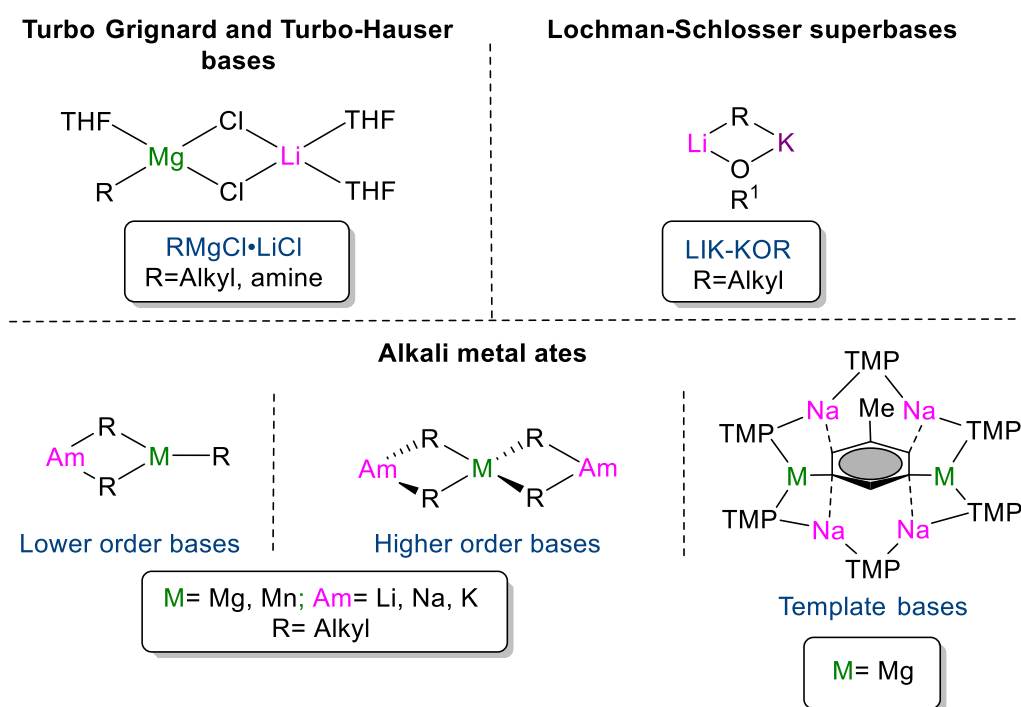
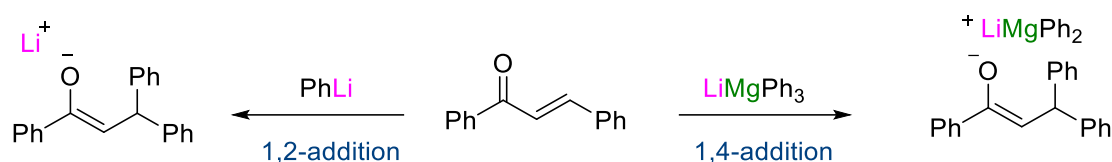


**Figure 1.1:** Chem Draw representation of a selection of mixed metal reagents

### 1.1.2 Historical background

Despite Wanklyn's early discovery, these systems received little attention until the twentieth century. Almost a hundred years after Wanklyn's discovery, Wittig described the bimetallic species  $\text{LiZnPh}_3$  and  $\text{LiMgPh}_3$ , which were prepared by mixing the homometallic components  $\text{PhLi}$  with  $\text{ZnPh}_2$  and  $\text{PhLi}$  with  $\text{MgPh}_2$  respectively.<sup>6</sup> Wittig introduced the term 'ate' to distinguish these complexes from classical organomagnesium and organolithium complexes and noted their special reactivities. Initial studies about the reactivity of these compounds with  $\alpha$ - $\beta$  unsaturated ketones showed that  $\text{LiMgPh}_3$  afforded the product of 1,4-addition, whereas  $\text{PhLi}$  on its own yields mainly the 1,2-addition product (**Scheme 1.1**).<sup>6,7</sup>



**Scheme 1.1:** 1,2- and 1,4-addition products obtained from the reaction of  $\alpha$ - $\beta$  unsaturated ketones with  $\text{PhLi}$  and  $\text{LiMgPh}_3$  respectively

NMR studies carried out by L. M. Seitz and T. L. Brown of the reaction of methyllithium and dimethylmagnesium in 1967 strongly supported the formation of lithium trimethylmagnesiates.<sup>8,9</sup> Finally, in 1978, X-ray crystallographic analysis by Thoennes and Weiss unambiguously proved the formation of mixed metal organomagnesiates.<sup>10</sup>  $\text{LiMgPh}_3$  was the first alkali-metal magnesiates compound to be described. An 'ate' compound can be defined as a combination of one metal of lower polarity, for example magnesium or zinc, with a more electropositive alkali metal (such as Li, Na or K), and containing an array of anionic ligands (alkyl, amine, halide, etc). Ate complexes can commonly be classed as either tri- or tetraorganometallates with the general formula  $\text{M}^{\text{I}}\text{M}^{\text{II}}\text{R}_3$  and  $\text{M}^{\text{I}}_2\text{M}^{\text{II}}\text{R}_4$  respectively where  $\text{M}^{\text{I}}$  represents the alkali metal,  $\text{M}^{\text{II}}$  is the divalent metal and R is the anionic ligand.

Weiss made a further step into the research of ate compounds by stabilising the X-ray molecular structures of many important organo-alkali-metal-compounds from the early 1960s and beyond.<sup>2</sup> One of the structures characterised by Weiss was  $[(\text{TMEDA})_2\text{Li}_2\text{MgMe}_4]$  (**Figure 1.2**). The monomeric structure of this magnesiates exhibits a tetrahedral coordination around magnesium with the methyl groups forming unsymmetrical  $\mu_2$  bridges between the magnesium and the TMEDA-solvated lithium atoms.<sup>1</sup>

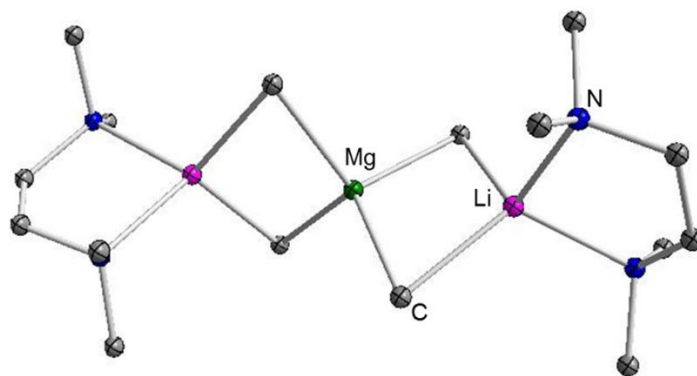


**Figure 1.2:** Molecular geometry of [(TMEDA)<sub>2</sub>Li<sub>2</sub>MgMe<sub>4</sub>]. Hydrogen atoms omitted for clarity

While these mixed metal systems have been utilised in a myriad of organic transformations, this introduction will focus on their applications in deprotonative metallation which are more relevant to the original research reported in this thesis.

## 1.2 Deprotonative metallation in synthesis

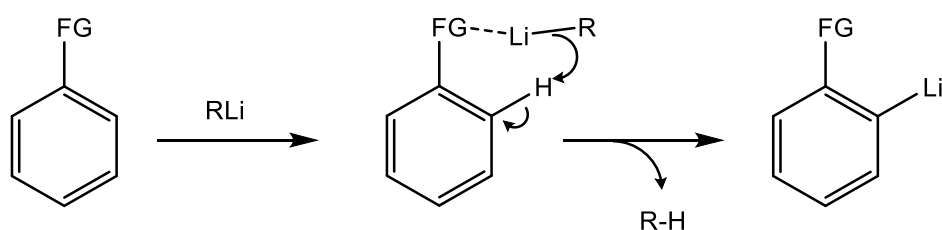
### 1.2.1 Importance of metallation chemistry

Deprotonative metallation is one of the most powerful and widely used synthetic methodologies. In general terms metallation involves the transformation of a relatively inert carbon-hydrogen bond to a more polar, therefore highly reactive carbon-metal bond. Typically highly reactive organometallic compounds such as organolithium compounds are employed. However these reagents suffer from major drawbacks, such as the low functional group tolerance, and limited selectivity which imposes the use of extremely low temperatures to preclude side reactions. In order to overcome these drawbacks several alternative metallating reagents have been developed, such as the Lochmann-Schlosser superbases (described in **chapter 1.2.3**) or the Turbo-Hauser bases (described in **chapter 1.3.1**) which have truly revolutionised the landscape of metallation chemistry.

### 1.2.2 Organolithium reagents in metallation chemistry

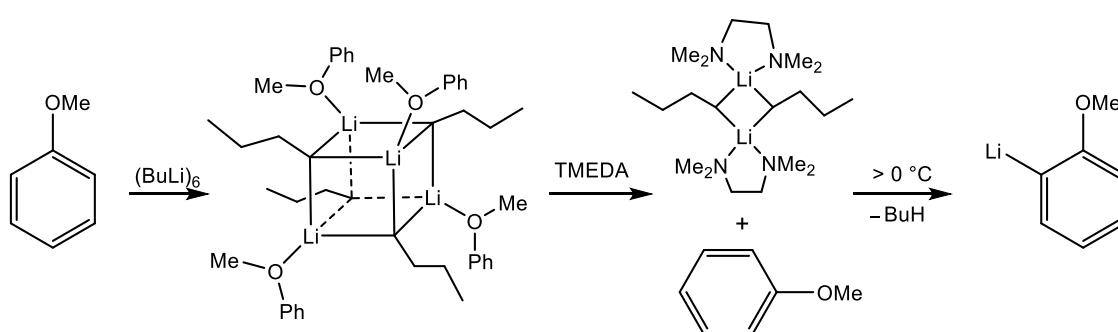
Organolithium reagents are indispensable reagents in organic synthesis. An estimated 95% of manufactured pharmaceuticals involve the use of this family of polar organometallic reagents at some stage of their preparation.<sup>11</sup> Several key features of this family of organometallic reagents have made them become commodity reagents in synthesis. Firstly, organolithium compounds exhibit excellent solubility in hydrocarbon solvents, therefore they are commercially available in hexane solution. In addition they are more stable in these solutions,

so they can be prepared, stored and transported. Secondly, the high polarity of the C-Li bond means they have high reactivity, thus these compounds can be employed in a variety of applications. For example they can be employed as strong bases, nucleophiles or as reagents for metal-halogen exchange reactions.<sup>12</sup> Directed *ortho*-lithiation (DoM), the directed metallation of an aromatic hydrogen located at the *ortho*-position of a functional group (FG) (**Scheme 1.2**), has overtaken classical electrophilic aromatic substitution as the principal tool for the regiospecific functionalisation of substituted aromatic molecules.



**Scheme 1.2:** Directed *ortho*-metallation process.

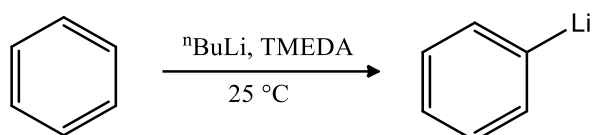
This approach was pioneered by Gilman<sup>13</sup> and Wittig<sup>14</sup> who reported the *ortho*-lithiation of anisole. It is known that BuLi is stabilised in hydrocarbon solutions by forming an hexameric complex.<sup>15</sup> As shown in **Scheme 1.3**, the *ortho*-lithiation of anisole proceeds through the deaggregation of the BuLi hexamer to form a tetrameric BuLi anisole complex. The addition of TMEDA displaces the anisole from the tetramer to give a BuLi-TMEDA dimer which is able to deprotonate anisole at temperatures above 0 °C yielding the final *ortho*-lithiated anisole product.



**Scheme 1.3:** BuLi mediated *ortho*-deprotonation of anisole

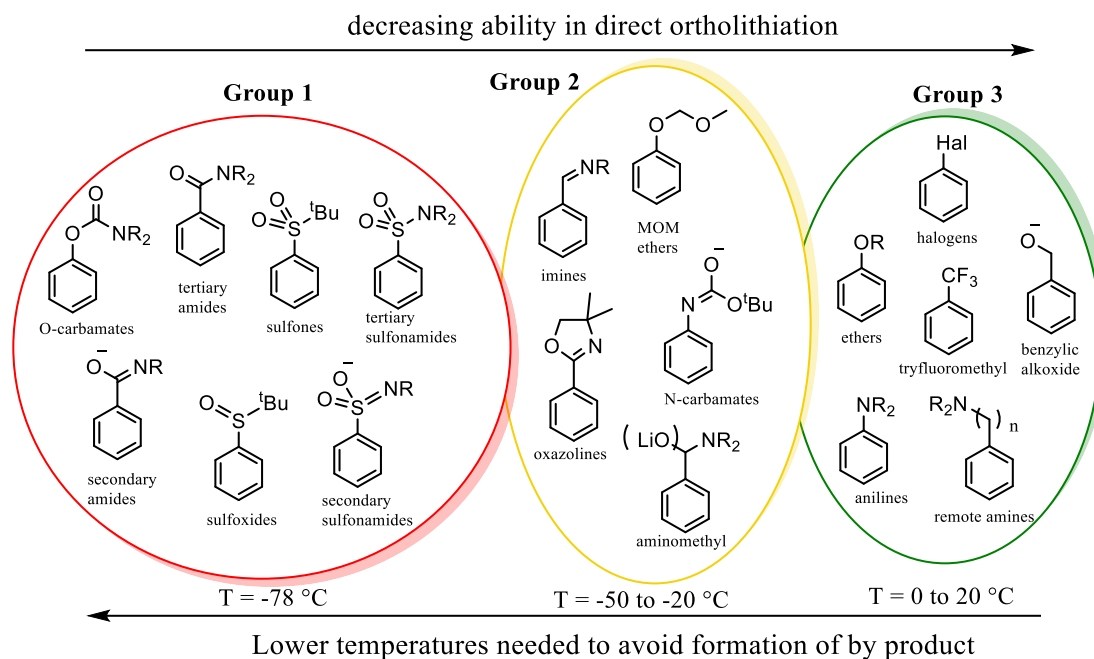
*Ortho*-lithiations involve the deprotonation of a substituted aromatic ring by an organolithium reagent such as BuLi or <sup>t</sup>BuLi, or a lithium amide reagent (such as lithium diisopropylamide, LDA, or lithium 2,2,6,6-tetramethylpiperidide, LiTMP). Considering that benzene is 10 orders of magnitude more acidic than butane, the removal of any aromatic proton by butyllithium is

thermodynamically favoured. Surprisingly, when benzene is added to a solution of  ${}^n\text{BuLi}$  in hexane only a negligible amount of deprotonation is observed after 3 hours at room temperature.<sup>16,17</sup> This can be rationalised in terms of the structure of  $\text{BuLi}$  in solution in this solvent, which is a hexamer that reacts slowly with benzene.<sup>18</sup> By adding TMEDA this hexameric aggregate can be broken up into a smaller oligomeric form  $[(\text{TMEDA})\text{BuLi}]_2$  which is now able to react efficiently at room temperature to form  $\text{PhLi-TMEDA}$  in almost quantitative yields (**Scheme 1.4**).<sup>17</sup>



**Scheme 1.4:** Room temperature lithiation of benzene in the presence of TMEDA.

Functional groups play an important role in *ortho*-lithiations. Snieckus divided the typical *ortho*-lithiation-directing groups into classes, according to the ease with which they allow the aromatic molecule to be lithiated.<sup>19</sup> The most powerful classes comprise carboxylic acids and carbonate-derived functions containing both nitrogen and oxygen such as secondary and tertiary amides,<sup>20</sup> oxazolines,<sup>21</sup> and carbamates.<sup>20</sup> These functional groups contain highly Lewis basic heteroatoms (for example a carbonyl group is amongst the strongest neutral Lewis bases which contains oxygen atoms). In addition they are strongly electron-withdrawing groups which reduce the aromaticity of the ring, thus increasing the acidity of the aromatic protons of the ring (group 1 of **Scheme 1.5**).

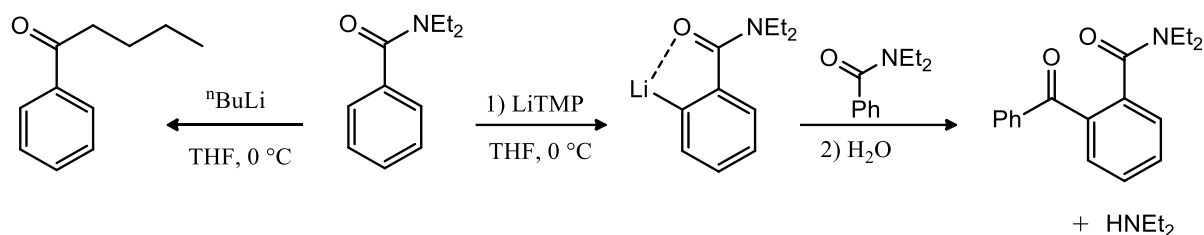


**Scheme 1.5:** Classes of directing groups for direct *ortho*-lithiation

It should also be noted that these groups are also electrophilic, which can suffer attack from the organolithium compound. A synthetic strategy is to use sterically hindered groups to prevent this, which can consequently hinder their proton removal. Sulfones and sulphonamides are powerful directors<sup>22</sup> and do not undergo nucleophilic attack at sulphur, although they can suffer from side reactions on the aromatic ring,<sup>23</sup> and they have more limited synthetic applications.<sup>24</sup> Functional groups containing only oxygen or nitrogen (group 3 in **Scheme 1.5**) are weak with regard to directing ability, due to their lower Lewis basicity and lower acidity of the protons adjacent to the functional group. The most powerful compounds of group 3 are those containing a nitrogen lone pair to coordinate to the organolithium, and also the oxygen containing compounds with the oxygen attached to the ring, inductively acidifying nearby protons. Group 2 in **Scheme 1.5** contains oxazolines which are resistant to nucleophilic attack and can be lithiated using  ${}^n\text{BuLi}$ .<sup>25</sup>

Despite their vast applications, organolithium reagents also have major drawbacks. As previously mentioned, they can suffer from a lack of selectivity and poor functional group tolerance towards direct *ortho*-metallation of organic substrates. By way of example, the reaction of *N,N*-diethylbenzamide with  ${}^n\text{BuLi}$  in THF at  $0\text{ }^{\circ}\text{C}$  gives 1-phenylpentan-1-one as major product which results from the butyl addition to the electrophilic  $\text{C}=\text{O}$  of the amide (**Scheme 1.6**).<sup>26,27</sup> By employing the hindered, non-nucleophilic LiTMP base with the same substrate it is possible to avoid attack at the  $\text{C}=\text{O}$  group obtaining *ortho*-lithiation. However the

*ortho*lithiated product reacts immediately with another molecule of starting material to form 2-benzoyl-*N,N*-diethylbenzamide as a by-product (**Scheme 1.6**).



**Scheme 1.6:** Side reactions of BuLi and LiTMP in the reaction with *N,N*-diethylbenzamide.

The poor functional group tolerance of organolithium reagents imposes the use of low temperatures to avoid side reactions. In addition organolithium compounds react with common organic solvents such as THF.<sup>28,29</sup> In order to overcome these limitations, a large amount of research effort has been dedicated to develop new metallating devices.

### 1.2.3 Lochmann-Schlosser superbases

In the 1960s the independent simultaneous work carried out by Lochmann and Schlosser introduced the “LIC-KOR” superbase (LIC denoting the alkyl lithium and KOR denoting the potassium alkoxide).<sup>30,31</sup> The base is formed by combining *n*-butyllithium and potassium *tert*-butoxide. These two species form a mixed aggregate of greater reactivity than either reagent alone. Studies on the addition reaction of BuLi in the presence of  $\text{NaO}^t\text{Bu}$  or  $\text{KO}^t\text{Bu}$  have shown that the reactivity of these compounds can be increased by a factor of more than  $10^6$  when compared to BuLi.<sup>32</sup> The exact nature of this base, in structural terms, remained uncertain for many years, and the characterisation of the metallated products upon deprotonation with this superbase has proved to be complicated.<sup>33–36</sup> In 2014 Strohmman and collaborators unveiled the structure of the intermediate derived from the metallation of benzene using  $n\text{BuLi}/t\text{BuOK}$  in THF at  $-78\text{ }^\circ\text{C}$ , being  $[(\text{PhK})_4(\text{PhLi})(^t\text{BuOLi})(\text{THF})_6(\text{Ph})_2]$  (**Figure 1.3**).<sup>37</sup>

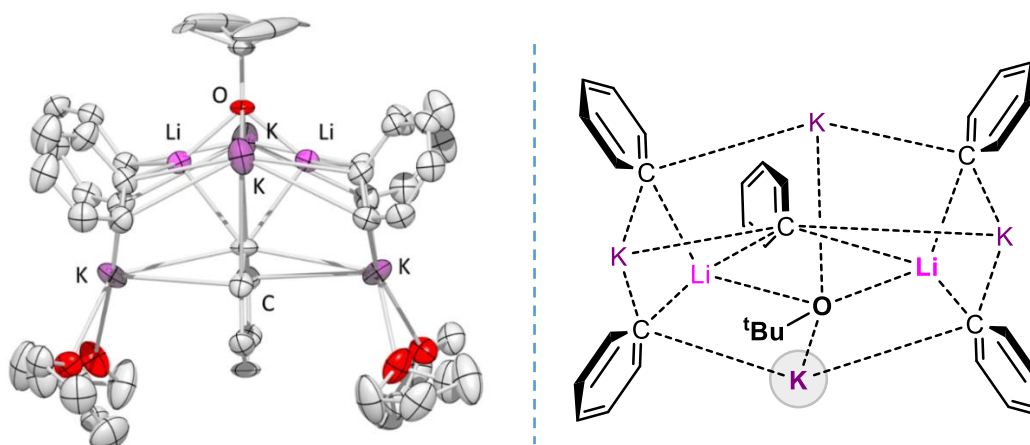
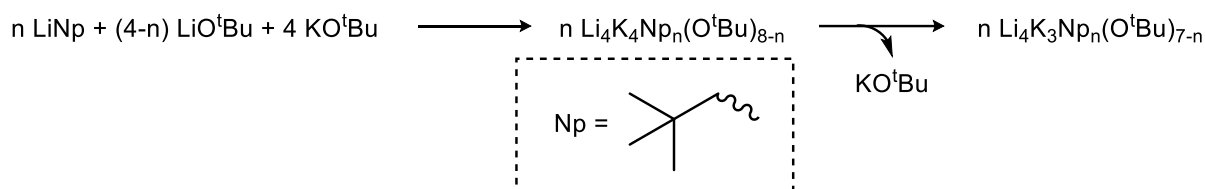


**Figure 1.3:** Strohmann's intermediate for the metallation of benzene using  $n\text{BuLi}/t\text{BuOK}$ . Free phenyl groups omitted for clarity.

The composition of the intermediate contains each of the superbases's components. Very recently Klett *et al* unveiled the formation of alkane-soluble and room-temperature-stable "LIC-KOR" superbases obtained upon reaction between neopentyl lithium and potassium *tert*-butoxide. Using  $^1\text{H}$  and  $^{13}\text{C}$  NMR spectroscopic studies authors were able to characterise different mixtures of lithium/potassium and neopentyl/*tert*-butoxy aggregates of varying compositions of the type  $[\text{Li}_x\text{K}_y\text{Np}_z(\text{O}^t\text{Bu})_{x+y-z}]$  depending on the ratio of neopentyl lithium:potassium *tert*-butoxide employed (**Scheme 1.7**).<sup>38</sup>



**Scheme 1.7:** Different mixtures of Li/K and Np/ $t\text{BuO}$  aggregates obtained.

In addition these compounds were also characterised by X-Ray studies which confirmed the close interaction of lithium, potassium, alkyl, and alkoxy groups.

The increased basicity found by the presence of an alkoxide had been reported twenty years previously by Morton *et al.* who applied the "alkoxide effect" to polymerisation reactions. Morton observed an increase in reaction rate and higher yields of metallated product with the addition of sodium *isopropoxide*, or potassium *isopropoxide*, to a suspension of the already highly basic *n*-pentylsodium.<sup>39,40</sup> Notably, Morton also reported that this combination of *n*-pentylsodium with sodium *isopropoxide* could metallate ethene directly to form vinyl

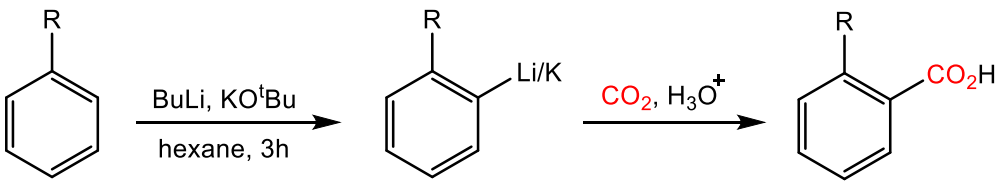
sodium.<sup>41</sup> The reactivity of LIC-KOR has been described as intermediate between *n*-butyllithium and *n*-butylpotassium, however, unlike *n*-butylpotassium, LIC-KOR is stable in THF at -75 °C.<sup>42</sup> These reagents can be used as a very successful deprotonating agent against relatively non-acidic C-H bonds such as allylic,<sup>43,44</sup> vinylic,<sup>44</sup> benzylic<sup>45</sup> and aromatic hydrogen atoms.<sup>46</sup> For example when stoichiometric amounts of <sup>n</sup>BuLi and <sup>t</sup>BuOK react with benzene in THF at -75 °C, the monometallation product is observed. The same reaction in hexane at ambient temperature forms *meta*- and *para*-disubstituted products (**Table 1.1**).<sup>46</sup>

**Table 1.1:** Different regioselectivity observed for LIC-KOR deprotonation of benzene when using THF or hexane solvents.

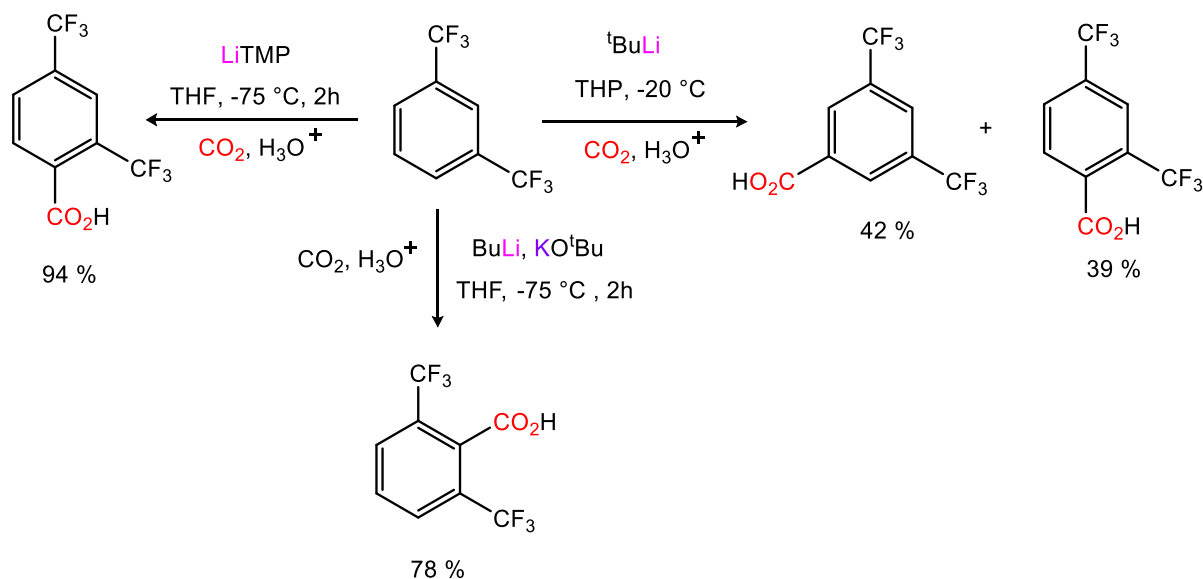
		Conversion (%)				
Time (h)	Mono substitution	<i>Meta</i> di-substitution	<i>Para</i> di-substitution	Time (h)	Conversion (%)	
0.25	65	3	7	0.1	2	
0.5	61	3	9	0.5	4	
1	65	6	9	5	13	
5	52	8	11	25	22	

The regioselectivity of these superbases tends to be directed by means of acidity (superbases deprotonate the most acidic proton of the substrate); in addition, coordination effects do not particularly influence these reagents. For example, with groups that direct mainly by acidification, selective *ortho*-metallation occurs. Thus the use of BuLi/<sup>t</sup>BuOK allows the selective metallation of the weak *ortho* directing group category of substrates, fluorobenzene and trifluorotoluene (**Scheme 1.5** for further details), in good yields and in a selective manner (**Table 1.2**):<sup>47,48</sup>

**Table 1.2:** *Ortho*-metallation of different fluoro-substituted aromatic substrates with the LiK-KOR superbase.

						
	Entry	R	T (°C)	Time (h)	Yield (%)	
	1	F	-75	3	98	
	2	CF <sub>3</sub>	-75	3	94	
	3	CF <sub>3</sub>	25	2	52	

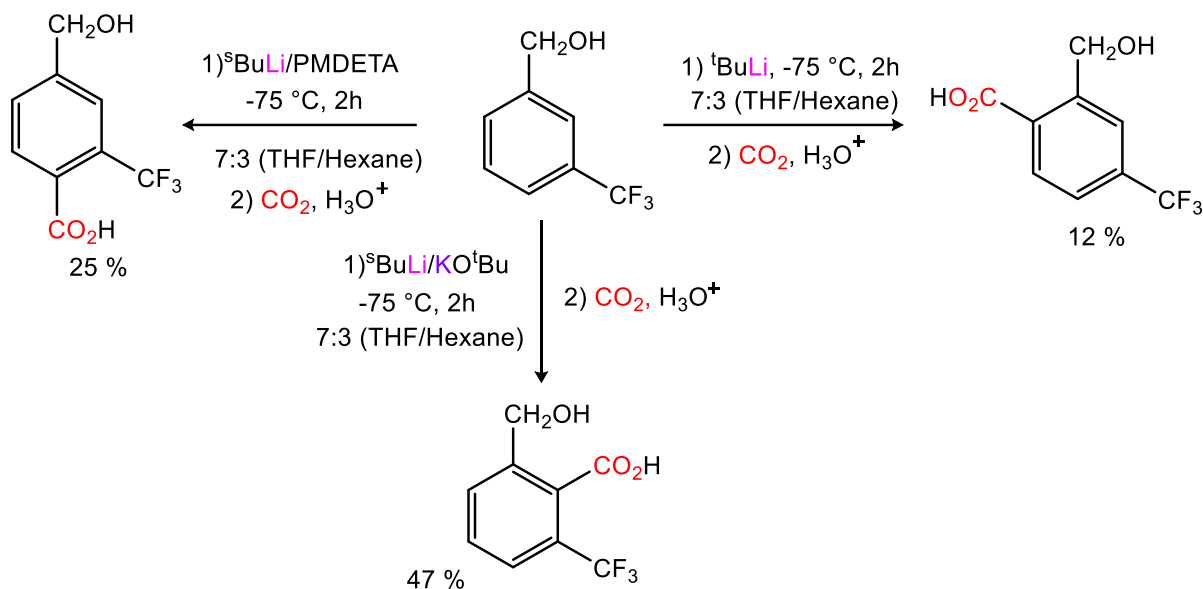
In the case of the reaction of LIC-KOR with 1,3-bis(trifluoromethyl)benzene at (-75 °C) metallation occurs exclusively at the C<sub>2</sub> position whereas employing <sup>t</sup>BuLi a mixture of the C<sub>4</sub> and C<sub>5</sub> metallated products is observed, and LiTMP yields exclusively the product of C<sub>4</sub> metallation (**Scheme 1.8**).<sup>46,49</sup>



**Scheme 1.8:** Different regioselectivities between LiTMP, <sup>t</sup>BuLi and LIC-KOR towards deprotonation of 1,3-bis(trifluoromethyl)benzene

3-(Trifluoromethyl)benzyl alcohol offers different choices of regioselectivity depending on the metallating reagent employed for the reaction. Treatment of this substrate in THF with <sup>t</sup>BuLi and subsequent quenching with carbon dioxide generated a product with a carboxyl group

(CO<sub>2</sub>H) in the C<sub>6</sub> position. Using LIC-KOR under the same reaction conditions the carboxyl group was inserted in the C<sub>2</sub> position. Contrastingly *sec*-BuLi/PMDETA affords the carboxyl group in the C<sub>4</sub> position (**Scheme 1.9**).<sup>47</sup>



**Scheme 1.9:** Different regioselectivity in the deprotonation of 3-(trifluoromethyl) benzyl alcohol.

In the metallation of low acidity C-H bonds, the superbases are an excellent reagent, however its regioselectivity can sometimes be a major drawback. For example in the metallation of one equivalent of naphthalene using one equivalent of BuLi/KO<sup>t</sup>Bu a mixture of monosubstituted and di-substituted carboxylic acids are obtained after quenching with carbon dioxide (**Table 1.3**).<sup>46</sup>

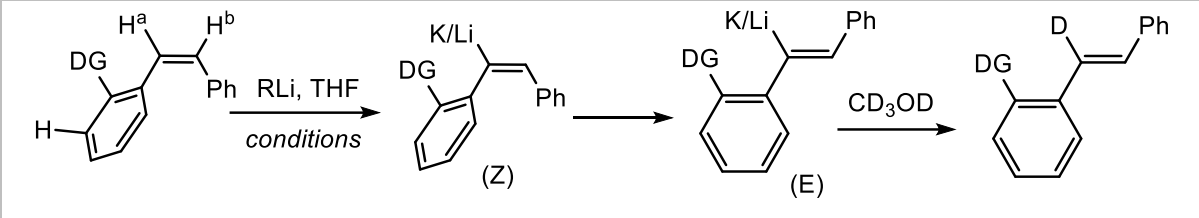
**Table 1.3:** Different regioselectivity in the deprotonation naphthalene.

	Reaction conditions	Mono substitution (%) (Alpha:beta)	di-substitution	
	THF, 1h, -50 °C	23 (52:48)	3	
	Hexane, 24h, 25 °C	28 (45:55)	25	

The LIC-KOR superbases are often too aggressive; therefore another limit of this reagent is the low functional group tolerance.

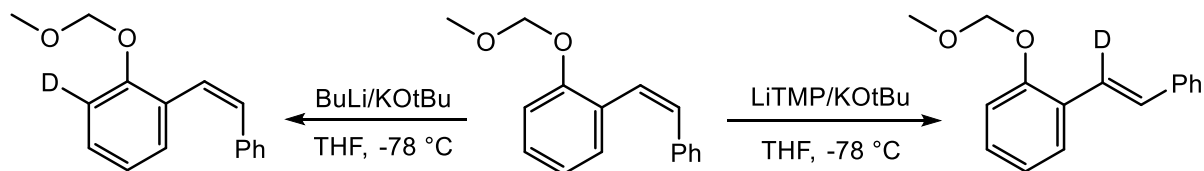
Other versions of mixed lithium potassium metallating reagents can be found in the literature. One of them is the amide version of the LIC-KOR mixed metal reagent, known as LINK bases which consists of a combination of BuLi/KO<sup>t</sup>Bu/TMP. LINK reagents can in some cases react differently compared to LIC-KOR. Schlosser and collaborators have described direct metallation reactions using this reagents.<sup>50</sup> Recently O'Shea *et al* have used LIC-KOR reagents for the carbolithiation reactions. Carbolithiations are addition reactions of alkyl, vinyl and aryllithiums to unactivated alkenes and alkynes.<sup>51</sup> The difficulty in this procedure is controlling regio- and stereoselectively of the process. O'Shea and collaborators have efficiently carried out the C-H lithiation of *cis*-stilbenes employing a variety of different Li reagents (**Table 1.4**).<sup>52</sup>

**Table 1.4:** direct lithiation of *cis*-stilbenes employing a variety of different Li reagents



Entry	DG	RLi/additive	T (°C)	Yield (%)
1	H	BuLi/KO <sup>t</sup> Bu	-78	80
2	SiMe <sub>3</sub>	BuLi/KO <sup>t</sup> Bu	-78	80
3	OMe	BuLi	-25	71
4	OMOM	LiTMP/ KO <sup>t</sup> Bu	-78	85

Particularly interesting is the reaction with the substrates having OMOM as directing group. In fact to achieve the regioselective vinyl C-H metalation of *o*-OMOM *cis*-stilbene mixed metal amide system LiTMP/ KO<sup>t</sup>Bu is needed. Differences in the reactivity of LIC-KOR and LINK bases are highlighted by O'Shea *et al* in the metallation of this substrate (**Scheme 1.10**).<sup>53,54</sup>

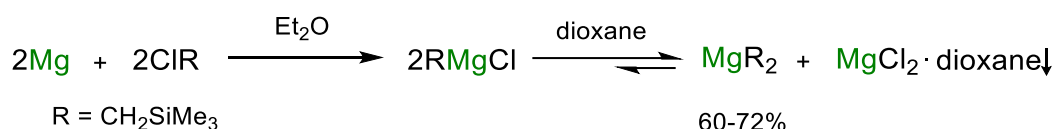


**Scheme 1.10:** Differences in the reactivity of LIC-KOR and LINK bases with *o*-OMOM *cis*-stilbene

Using BuLi/KO<sup>t</sup>Bu superbases the metallation occurs in the *ortho* position relative to the OMOM group in the aromatic ring.<sup>53</sup>

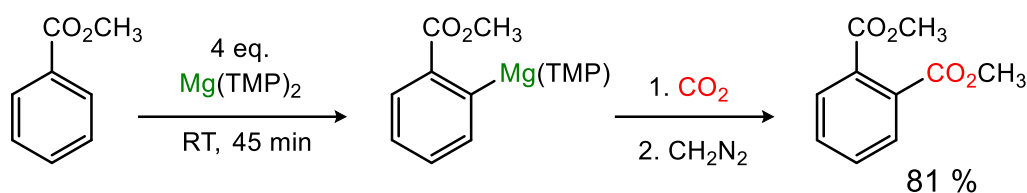
## 1.2.4 Applications of magnesium reagents in deprotonative metallations:

Diorganomagnesium compounds can be prepared by manipulation of Schlenk equilibrium present in Grignard reagents (RMgX, R=Alkyl, X=halogen) which in ethereal solvents coexists in equilibrium with the relevant diorganomagnesium species (MgR<sub>2</sub>) and magnesium dihalide (MgX<sub>2</sub>).<sup>55</sup> This equilibrium can be shifted towards the formation of the MgR<sub>2</sub> species by adding dioxane which forms an extremely insoluble complex with MgX<sub>2</sub> (**Scheme 1.11**).



**Scheme 1.11:** Chem Draw representation of Schlenk equilibrium in Grignard reagents

Furthermore, magnesium bisamides, (R<sub>2</sub>N)<sub>2</sub>Mg, have recently attracted attention and are fast becoming pop star reagents in organic synthesis.<sup>56</sup> In particular, their milder reactivity when compared with lithium amides, and great functional tolerance have increased the number of applications reported for these reagents.<sup>57,58</sup> Traditionally a typical process for the preparation of organomagnesium compounds would involve initial lithiation of a substrate followed by a transmetallation reaction with either a Grignard reagent or a metal halide.<sup>59</sup> However by using magnesium bases capable of promoting direct Mg-H exchange reactions, it is possible to grant access to functionalised organomagnesium intermediates in a much more efficient manner, minimising the risk of side reactions taking place. Eaton developed the use of Mg(TMP)<sub>2</sub> (TMP=2,2,6,6-tetramethylpiperidide) as a selective deprotonating agent.<sup>60</sup> The reaction of 4 equivalents of Mg(TMP)<sub>2</sub> with one equivalent of methyl benzoate for 45 minutes in THF solution at room temperature followed by quenching with carbon dioxide, acidification and esterification gave dimethyl *o*-phthalate in 81 % isolated yield (**Scheme 1.12**). It is interesting to note that BuLi cannot be employed to perform the same reaction as it would lead to side product formation from the nucleophilic addition of butane to the ester group (CO<sub>2</sub>Me). The lower reactivity of the magnesium base allows formation of *ortho* metallated product after carboxylation and esterification, however high excess of magnesium base is needed for this reaction to take place.



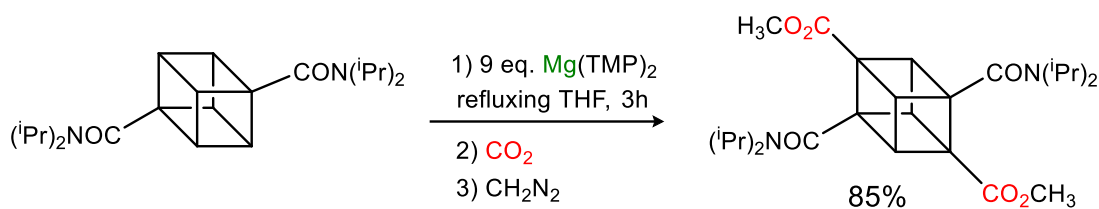
**Scheme 1.12:**  $\text{Mg(TMP)}_2$  mediated *ortho*-deprotonation of methyl benzoate followed by carboxylation and esterification.<sup>60</sup>

Effective *ortho*-magnesiation reactions can be carried out using the bisamido base  $\text{Mg(TMP)}_2$  in the presence of esters, which are normally more susceptible to nucleophilic attack using conventional Li-based reagents.<sup>61</sup> In addition, indoles may be deprotonated exclusively at the 2-position by  $\text{Mg(iPr}_2\text{N)}_2$  at ambient temperature. Subsequent quenching with a variety of electrophiles leads to 2-substituted indoles in good to excellent yields (**Table 1.5**).<sup>62</sup>

**Table 1.5:** Deprotonation of different *N*-substituted indoles using magnesium amide bases.

R	Mg amide	Electrophile	E	Yield (%)
SO <sub>2</sub> Ph	$\text{Mg(N}^i\text{Pr}_2)_2$	PhCHO	CH(OH)Ph	93
SO <sub>2</sub> Ph	$\text{Mg(N}^i\text{Pr}_2)_2$	I <sub>2</sub>	I	85
SO <sub>2</sub> Ph	$\text{MgBr(N}^i\text{Pr}_2)$	PhCHO	CH(OH)Ph	83
SO <sub>2</sub> Ph	$\text{MgBr(N}^i\text{Pr}_2)$	I <sub>2</sub>	I	60
CO <sub>2</sub> tBu	$\text{Mg(N}^i\text{Pr}_2)_2$	PhCHO	CH(OH)Ph	0
CO <sub>2</sub> tBu	$\text{Mg(N}^i\text{Pr}_2)_2$	I <sub>2</sub>	I	52
Me	$\text{Mg(N}^i\text{Pr}_2)_2$	I <sub>2</sub>	I	0
H	$\text{Mg(N}^i\text{Pr}_2)_2$	CO <sub>2</sub> -CH <sub>2</sub> N <sub>2</sub>	CO <sub>2</sub> Me	58

Interestingly  $\text{Mg(TMP)}_2$  is stable in THF solutions even when heating to reflux over several hours. As an example, 1,4-bis(*N,N*-diisopropylcarboxamido)-cubane can be metallated using excess of  $\text{Mg(TMP)}_2$  in refluxing THF, which after carboxylation and esterification yields the corresponding di-ester cubane (**Scheme 1.13**).<sup>60</sup>



**Scheme 1.13:**  $\text{Mg}(\text{TMP})_2$  mediated magnesiation of 1,4-bis(*N,N*-diisopropylcarboxamido)-cubane in refluxing THF.

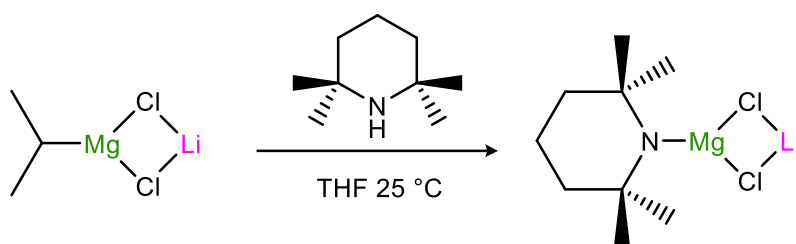
This feature allows its use at higher temperatures than organolithium reagents which decompose very rapidly under these conditions. Notwithstanding, the main limitation of these compounds is their reduced metallating power when compared to organolithium bases. For example  $\text{Mg}(\text{TMP})_2$  cannot deprotonate substrates such as benzene or anisole. In addition when this base successfully carries out the deprotonation reaction, a high excess of base is required which clearly reflects the lower efficiency as a metallating reagent of  $\text{Mg}(\text{TMP})_2$ .

### 1.3 Kinetic activation of magnesium reagents: magnesiate formation

#### 1.3.1 Turbo-Hauser bases:

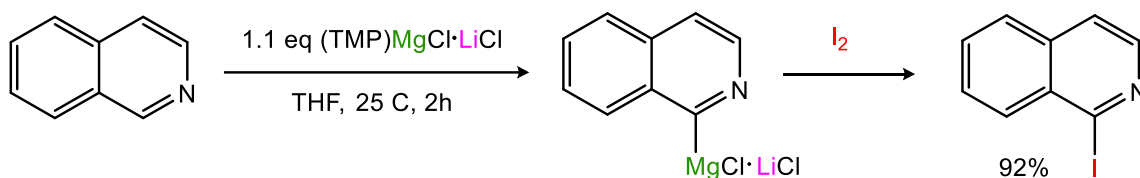
In 1994 Knochel and co-workers reported that the addition of stoichiometric amounts of  $\text{LiCl}$  to Grignard reagents could greatly enhance the reactivity of the latter. Thus, compounds like  $i\text{PrMgCl}\cdot\text{LiCl}$  can be effectively used to promote direct  $\text{Mg-X}$  exchange reactions ( $\text{X} = \text{Br}, \text{I}$ ) of a wide range of organic substrates.<sup>63</sup> These bimetallic combinations are known in the literature as turbo-Grignard reagents and recently they have become commercially available.<sup>64</sup>

The analogue version of this reagent, but employing Hauser base  $\text{TMPMgCl}$  combined with  $\text{LiCl}$  (turbo-Hauser base), has also been developed by the same research group.<sup>65,66</sup>  $(\text{TMP})\text{MgCl}\cdot\text{LiCl}$  shows high kinetic activity and extremely good solubility making it soluble in THF (**Scheme 1.14**).



**Scheme 1.14:** synthesis of the turbo-Hauser reagent (TMP)MgCl·LiCl

This Turbo-Hauser base can promote a variety of metal-hydrogen exchange reactions of challenging substrates showing a high degree of regioselectivity.<sup>67–69</sup> As an example, isoquinoline can be magnesiated in the C<sub>1</sub> position after 2 hours at ambient temperature giving an excellent yield (92%) after iodine quenching (**Scheme 1.15**).<sup>66</sup>



**Scheme 1.15:** Magnesiumation followed by iodine quench of Isoquinoline using the Turbo-Hauser (TMP)MgCl·LiCl.

Additionally, (TMP)MgCl·LiCl has been found to be an extremely effective regioselective base. For example, different organic 5 membered heterocyclic compounds can be magnesiated with excellent yields and high regioselectivity (**Table 1.6**).<sup>66,69</sup>

**Table 1.6:** Magnesiumation followed by iodine quench of different 5-membered ring heterocyclic substrates using the turbo-Hauser base (TMP)MgCl·LiCl.

Entry	X	Y	E	R	Temp (°C)	Time (h)	Yield (%)		
1	O	CH	DMF	CHO	25	24	81		
2	S	CH	DMF	CHO	25	24	90		
3	S	N	PhCHO	CH(OH)Ph	0	0.1	94		

The bimetallic constitution of (TMP)MgCl·LiCl has been demonstrated by Mulvey *et al* who have managed to structurally define this compound using X-ray crystallography (**Figure 1.4**).<sup>64</sup>

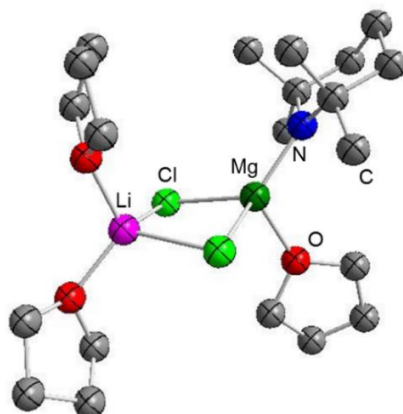


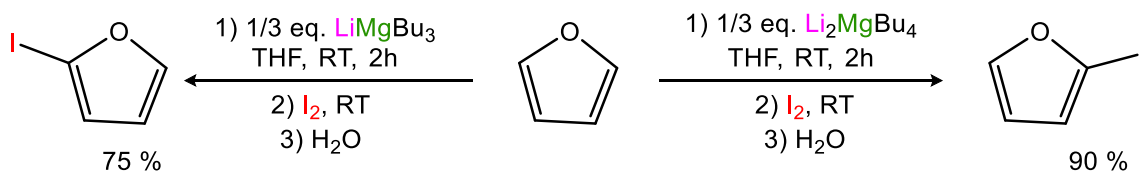
**Figure 1.4:** Molecular structure of the “turbo-Hauser Grignard” [(THF)<sub>2</sub>Li(μ-Cl)<sub>2</sub>Mg(THF)(TMP)]

As shown in **Figure 1.4**, the molecular structure of turbo-Hauser base (TMP)MgCl·LiCl is a molecular halide contacted ion-pair magnesiate, rather than a salt-like motif. The sterically hindered TMP, which is the active base, binds solely to magnesium and not to lithium. Magnesium is tetra-coordinated and a potentially labile THF molecule is bonded to it, geminal to the active TMP ligand. By losing this THF a new vacant coordination site will be potentially available for the substrate to coordinate with the base prior to the metallation.

### 1.3.2 Alkali-metal magnesiates

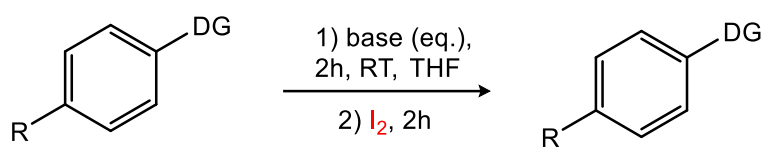
Alkali-metal magnesiates have emerged as a synthetic alternative to traditional single metal reagents to promote regioselective direct Mg-H exchange processes. For metallation chemistry two main types of magnesiates have been employed, homoleptic alkyl or amido magnesiates such as M<sub>2</sub>MgR<sub>4</sub><sup>70-72</sup> and MMgR<sub>3</sub><sup>72-74</sup> and heteroleptic species such as MMg(TMP)<sub>2</sub>R<sup>75,76</sup> and (TMP)MgCl·LiCl (where M is an alkali metal).<sup>64</sup>

Recently Mongin has successfully employed lithium magnesiate chemistry in the deprotonation of several heteroaryl molecules including pyridines,<sup>77</sup> fluoroaromatics,<sup>78</sup> thiophenes,<sup>79</sup> furan,<sup>80</sup> benzoxazoles and oxazoles,<sup>81</sup> with the resulting metallated intermediate being trapped with a variety of electrophiles. In the magnesiation of furan Mongin used both lithium tributylmagnesiate and dilithium tetrabutylmagnesiate under the same reaction conditions obtaining a higher percentage yield when Li<sub>2</sub>MgBu<sub>4</sub> was employed (**Scheme 1.16**).



**Scheme 1.16:** Comparison of the deprotonation of furan with a trialkyl and a tetraalkyl lithium magnesiate, followed by  $\text{I}_2$  quenching.<sup>80</sup>

Mixing together an alkali metal such as lithium with a less polar metal, such as magnesium, results in a mixed metal aggregate which exhibits higher reactivity when compared to  $\text{MgBu}_2$  which is unable to perform the deprotonation of furan on its own. Interestingly this approach exhibits polybasic behaviour, as when 1 equivalent of  $\text{LiMgBu}_3$  or  $\text{Li}_2\text{MgBu}_4$  are employed for the deprotonation of 3 equivalents of furan, high percentage yields of iodinated products can be obtained after iodine quench of the magnesium intermediate (75% and 90% respectively). This approach significantly reduces the amount of magnesiate base employed for the deprotonation of the aromatic substrate. Mongin however has not studied the alkali metal effect on the reactivity of these compounds, as the only compound used in these reactions was a lithium magnesiate. The trialkyl- and tetraalkylmagnesiates have also been employed for *ortho*-deprotonation of different arene substrates (**Table 1.7**).<sup>82</sup>

**Table 1.7:** Reactivity of different lithium magnesiates in DoM.

entry	substrate	R	base (eq.)	product	yield(%) <sup>a</sup>
1		H	LiMgBu <sub>3</sub>		75
2		Cl	(0.4)		68
3		OMe			71
4		H	Li <sub>2</sub> MgBu <sub>4</sub>		82
5		Cl	(0.55)		76
6		OMe			84
7		H	Li <sub>2</sub> MgBu <sub>4</sub>		88
8		Cl	(0.55)		82
9		OMe			87
10		H	Li <sub>2</sub> MgBu <sub>4</sub>		70 <sup>b</sup>
			(1)		
11		H	Li <sub>2</sub> MgBu <sub>4</sub>		75 <sup>b</sup>
12		OMe	(0.3)		91 <sup>b</sup>

<sup>a</sup> Yield of isolated products  
<sup>b</sup> Reflux, 2h

Marsais and collaborators also carried out the deprotonation of pyridine carboxamides using homoleptic alkyl, homoleptic amide and heteroleptic lithium magnesiates (Table 1.8).<sup>83</sup>

**Table 1.8:** Reactivity of lithium magnesiates in DoM of *N*-methylnicotinamide.

			Yield (%)		
	Entry	Base	Deprotonation	addition	
	1	LiMgBu <sub>3</sub>	-	100	
	2	LiMgBu <sub>2</sub> TMP	-	48	
	3	LiMgBu(TMP) <sub>2</sub>	82	-	
	4	LiMgBu(TMP) <sub>3</sub>	80	-	
	5	LiMg(TMP) <sub>3</sub>	61	-	

One equivalent of base was reacted with 1 equivalent of *N*-methylnicotinamide at ambient temperature for 2 hours in THF, and the intermediates were quenched with D<sub>2</sub>O. Depending on the base employed two possible reaction pathways were observed. C<sub>4</sub> deprotonation on one hand, and C<sub>4</sub> butyl addition on the other hand. The best results (when the desired reaction pathway was metallation) were obtained using LiMgBu(TMP)<sub>2</sub> where an 82% yield of *ortho*-*N*-methylnicotinamide was obtained and no butyl addition was observed.

### 1.3.3 Alkali-metal-mediated-dimetallations: A template base approach to deprotonation

One of the main challenges in metalation chemistry is the development of a new metalation strategies allowing the synthesis of new chemical structures. Chemists for decades have been particularly challenged by the difficulty that arises from promoting metal/hydrogen exchange reactions in one position, leaving other positions untouched (regioselective metalations). Regioselectivity is particularly important in substrates containing multiple C-H bonds. As previously mentioned in chapter 1.2.2 the presence of specific functional groups can facilitate metalation in the *ortho* position (direct-*ortho* metalation) but very limited applications have

been described for other regioselective deprotonations. In 2005 Mulvey and collaborators showed that mixing BuNa and Mg(TMP)<sub>2</sub> to form [Na(Bu)-(TMP)Mg(TMP)] and reacting it with toluene in hexane it is possible to isolate an intermediate where toluene has been dimetallated at its 2 and 5 positions (**Figure 1.5**).<sup>75</sup>

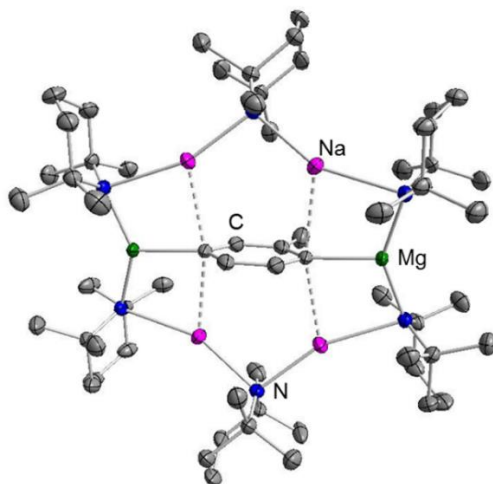
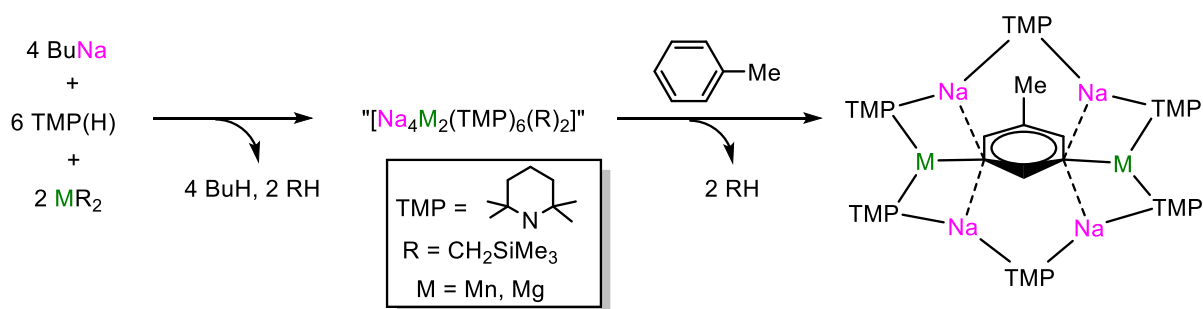


**Figure 1.5:** Monomeric structure of inverse-crown product [(TMP)<sub>6</sub>Na<sub>4</sub>(2,5-Mg<sub>2</sub>C<sub>6</sub>H<sub>3</sub>CH<sub>3</sub>)]

Macrocyclic compounds of this type are known as *inverse crowns*, due to their inverse topological relationship to conventional crown ethers.<sup>84–86</sup> Inverse crowns exhibit a positively charged *s*-block metal based ring capturing O, C or H based anions at its core.<sup>87</sup> These materials are of great interest to synthetic chemists as they selectively (and often multiply) deprotonate a range of organic substrates.<sup>88,89</sup>

In 2008 Mulvey carried out the dimetalation of toluene using a mixture of BuNa, TMP(H) and M(CH<sub>2</sub>SiMe<sub>3</sub>)<sub>2</sub> (M=Mn, Mg) in a 4:6:2 stoichiometry in hexane solution, to one molar equivalent of toluene (**Scheme 1.17**).<sup>90</sup> In this case the regioselectivity of the reaction changed from 2,5 dimetalated toluene (product [(TMP)<sub>6</sub>Na<sub>4</sub>(2,5-Mg<sub>2</sub>C<sub>6</sub>H<sub>3</sub>CH<sub>3</sub>)] (**Figure 1.5**) to 3,5 dimetalated toluene in product [(TMP)<sub>6</sub>Na<sub>4</sub>(3,5-M<sub>2</sub>C<sub>6</sub>H<sub>3</sub>CH<sub>3</sub>)] (**Figure 1.6**).<sup>90</sup>



**Scheme 1.17:** Dimetalation of toluene in position C<sub>3</sub> and C<sub>5</sub>, inverse-crown product [(TMP)<sub>6</sub>Na<sub>4</sub>(3,5-M<sub>2</sub>C<sub>6</sub>H<sub>3</sub>CH<sub>3</sub>)] (M=Mn, Mg)

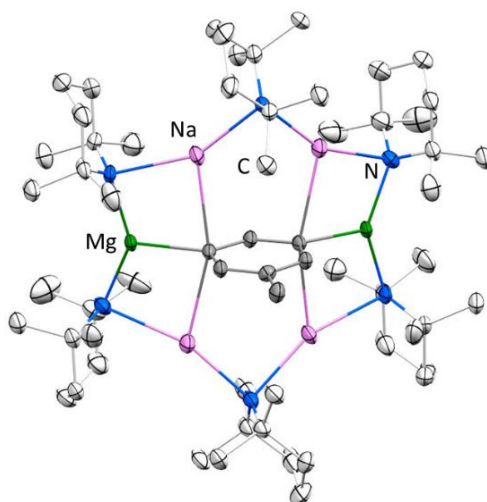
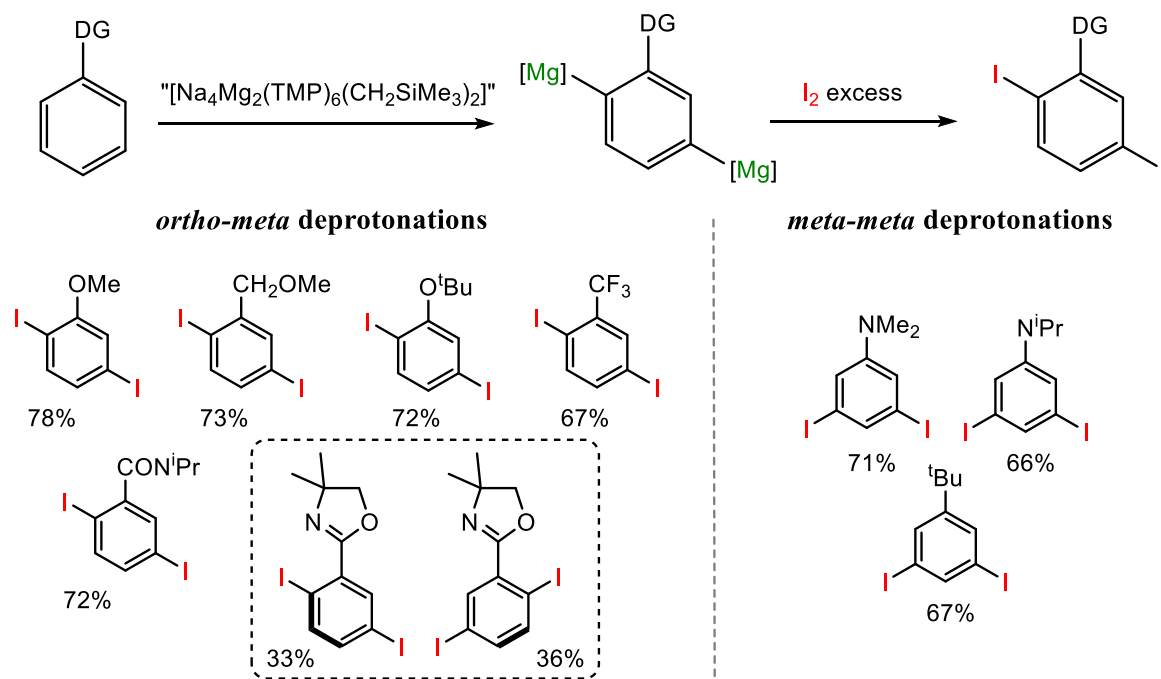


**Figure 1.6:** Monomeric structure of inverse-crown product  $[(\text{TMP})_6\text{Na}_4(3,5\text{-Mg}_2\text{C}_6\text{H}_3\text{CH}_3)]$

Interestingly once more the  $\text{CH}_3$  group which is the most acidic position of toluene is left untouched. The trimethylsilylmethyl ligand appears to be a key factor in switching the regioselectivity from the 2,5-regioisomer (where only Bu and TMP ligands were used) compared to the 3,5-regioisomer (which requires  $\text{CH}_2\text{SiMe}_3$  and TMP ligands) together with the synergic bimetallic sodium manganese or sodium magnesium bases employed. Highlighting the marked alkali-metal effects in these reactions, when benzene or toluene are treated with a 1:1:3 mixture of  $^n\text{BuK}$ ,  $\text{Bu}_2\text{Mg}$ , and TMPH a novel 24-atom polymetallic host ring  $[\text{K}_6\text{Mg}_6(\text{TMP})_{12}(\text{arene-ide})_6]$  is formed hosting 6 molecules of the mono metallated arene (this reaction procedure along with other potassium mediated magnesiation reactions will be discussed in detail in **chapter 2.2.1**).<sup>88</sup> In 2014 O'Hara has studied the co-complexation reaction between  $\text{KTMP}$  and  $^n\text{BuMgTMP}$  to form different potassium magnesiates such as  $[\text{KMg}(\text{TMP})_2^n\text{Bu}]_\infty$ ,  $[\text{KMg}(\text{TMP})_2^n\text{Bu}]_4$  and  $[\text{KMg}(\text{TMP})_2^n\text{Bu}]_6$  which could be employed as efficient metallating reagents; This upon reaction with equimolar amounts of toluene or benzene formed  $[\text{K}_6\text{Mg}_6(\text{TMP})_{12}(\text{C}_6\text{H}_4(\text{R}))_6]$  ( $\text{R}=\text{H}, \text{CH}_3$ ) respectively in a 44% and 93% yield (See **chapter 2.2.1**).<sup>89</sup> These metallating reagents are known as pre inverse crowns, as they constitute the chemical templates formed prior to the formation of inverse crowns. These findings provided strong evidence for a base template approach mechanism in this transformations. In 2014 O'Hara, Mulvey *et al* expanded the template base metalation approach to a variety of different substrates using a sodium magnesiate “ $[\text{Na}_4\text{Mg}_2(\text{TMP})_6(^n\text{Bu})_2]$ ”.<sup>91</sup> In this procedure double deprotonations occur at the *ortho-meta* positions for aromatic substrates such as anisole, (methoxymethyl)benzene, *tert*butoxybenzene, (trifluoromethyl)benzene, *N,N*-diisopropylbenzamide, 4,4-dimethyl-2-phenyl-4,5 dihydrooxazole and phenyl-*N,N*-diethyl-O-carbamate. This outstanding

methodology could also be expanded to a double deprotonation at the *meta-meta* positions (with *ortho* positions left untouched) for substrates such as *N,N*-diisopropylaniline, *N,N*-dimethylaniline and *tert*-butylbenzene in a counterintuitive way to that obtained in direct *ortho* metalations (**Scheme 1.18** and **Figure 1.7**).



**Scheme 1.18:** dimetalations of different substrates in the *ortho-meta* and *meta-meta* positions using the template approach.

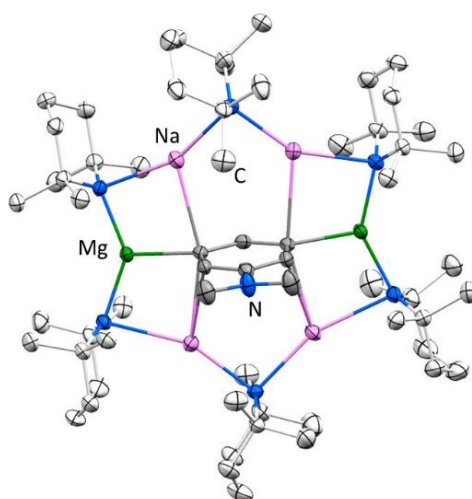


**Figure 1.7:** Monomeric structure of inverse-crown product  $[(\text{TMP})_6\text{Na}_4(3,5\text{-Mg}_2\text{C}_6\text{H}_3\text{NMe}_2)]$

## **1.4 Applications of group 2 complexes in catalysis:**

### **1.4.1 Introduction**

Chemical processes are crucial in our society for a variety of different reasons. In the sixteenth century Alchemists wanted to convert metals to gold, and they also wanted to find a chemical mixture that would enable people to live longer and cure all diseases. Those were the challenges faced by society at the time. Nowadays we face similar challenges. World population has increased drastically with time (during the 20th century alone, the population in the world has grown from 1.65 billion to 6 billion). Ideally we would like to sustain a society where everybody has access to health care. Therefore resources are key and chemists need to find green and efficient methods in order to meet the global demand. From a chemistry prospective, it would be ideal to move from stoichiometric reactions to catalytic ones for reasons that will be discussed later.<sup>92</sup>

Catalysis is a process which allows the transformation of one or more chemical feedstocks to desired products. These processes generally require small amounts of catalysts, the active species that carry out the transformation. Catalysts act by reducing the activation energy for a reaction to take place. Many of the most useful catalysts incorporate precious metals such as ruthenium, rhodium, palladium, and platinum. Furthermore some of these metals are highly toxic, which is particularly problematic when they are employed in the synthesis of biologically active compounds. Therefore there is a need for the development of cheap and low toxic catalysts which can carry out low energy chemical transformation with minimum cost in terms of energy and environmental impact.<sup>93</sup>

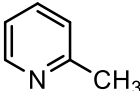
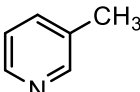
### **1.4.2 Group 2 organometallic components in catalysts:**

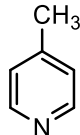
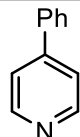
Group 2 containing organometallic reagents have been widely employed in stoichiometric applications such as dihydrocoupling reactions for Si-N, Si-S, Si-O, and B-N bond synthesis,<sup>94</sup> and metal\hydrogen exchange,<sup>60-62</sup> to name a few, however their usage as catalysts has only recently started to gain the deserved attention. Heavier group 2 metals as catalysts have as a main limitation the lack of stability in solution. This makes them inactive or non-selective in catalytic transformations. Recently some developments have been described regarding the preparation of stable heavier group 2 complexes which can act as catalysts.<sup>95-97</sup> Organomagnesium complexes are more stable than their heavier analogues.

Organomagnesium compounds have more covalent M-C bonds, due to the ionic radii and electronegativity of magnesium compared to other group 2 elements.<sup>98</sup> As previously mentioned in **chapter 1.2.4** stable organomagnesium compounds can be prepared using the Schlenk equilibrium that can be quite easily controlled by the choice of ligands and conditions.<sup>55</sup> For the heavier alkaline earth metals, the Schlenk equilibrium poses a significant synthetic challenge that can be somewhat overcome by kinetic stabilisation with suitable ligands (bulky ligands that hinder the redistribution process).<sup>99</sup>

Organomagnesium complexes were employed for the first time in catalysis more than 50 years ago to carry out polymerisations, Diels-Alder and Aldol reactions. Most of this initial applications were limited to the ability of  $Mg^{2+}$  to act as a Lewis acid.<sup>98,100,101</sup> In the last two decades there has been an increased interest for the development of catalytic applications where the Mg complexes are involved in deprotonation and addition processes. For example,  $\beta$ -diketiminato magnesium complexes have been employed to catalyse hydroboration and hydrosilylation of pyridines (**Table 1.9**).<sup>102,103</sup>

**Table 1.9:**  $\beta$ -diketiminato magnesium catalysed hydroboration of pyridines

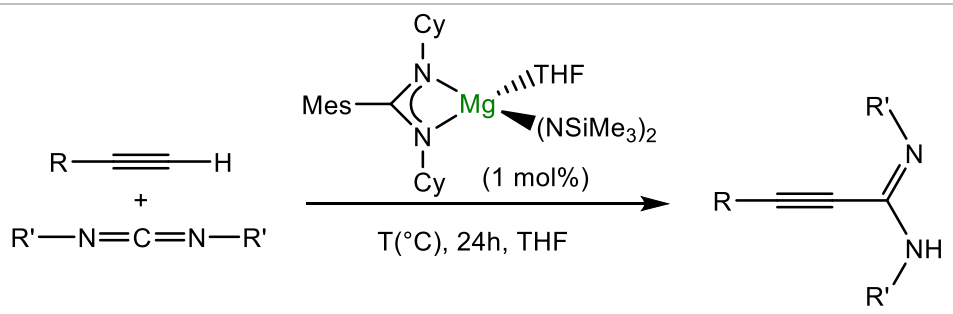
Entry	Substrate	1,2-:1,4-adduct	Conditions	Yield (%) <sup>a</sup>
1		37:63	17 h 70 °C	92 (59)
2		0:100	4 d 70 °C	51
3		48:52	3.5 h 70 °C	91 (62)

4		81:19	23 h 70 °C	91 (68)
5		100:0	8 h 70 °C	95
<sup>a</sup> NMR Yield and isolated yield shown in parenthesis				

However this protocol has as principal limitation the formation of mixtures between the 1,2- and 1,4-adducts (entries 1, 3 and 4), while formation of one stereoisomer exclusively is restricted to cases where C<sub>2</sub> position is blocked (for the corresponding formation of the 1,4-adduct, entry 2) and where the C<sub>4</sub> position is blocked (for the synthesis of 1,2-adduct, entry 5).

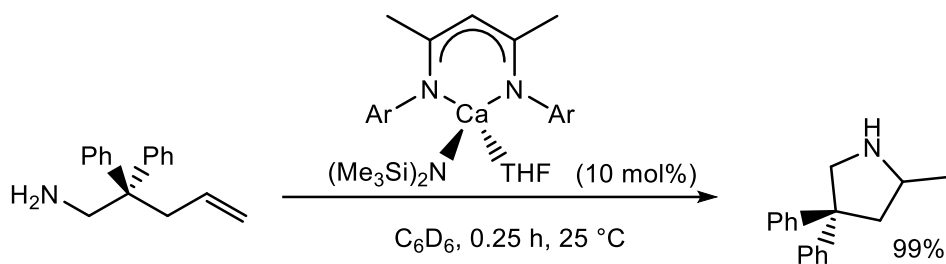
Furthermore organomagnesium complexes are key catalysts involved in C-H bond activation reactions such as alkyne-carbodiimide coupling reactions.<sup>104,105</sup> Long reaction times and the high temperatures required for the reaction to take place (80°C) are the main drawbacks of this methodology, in addition to the low yields obtained in some cases (**Table 1.10**).

**Table 1.10:** Mg-catalysed alkyne-carbodiimide coupling reactions

				
Entry	R	R'	Temp (°C)	Yield <sup>a</sup>
2	Ph	<sup>i</sup> Pr	80	72
3	Ph	<sup>t</sup> Bu	80	7
4	Ph	Ar	80	0
5	SiMe <sub>3</sub>	<sup>i</sup> Pr	80	63
6	<sup>t</sup> Bu	<sup>i</sup> Pr	80	12
<sup>a</sup> Yields from <sup>1</sup> H NMR integrals using THF as internal standard (average of two runs);				
<sup>b</sup> Ar = 2,6-diisopropylphenyl.				

The heavier group 2 organocatalysts have been employed in multiple bond heterofunctionalisations and cross coupling reactions.<sup>106</sup> Alkene and alkyne hydroamination

and hydrophosphination reactions have been developed to allow the synthesis of a wide variety of acyclic and heterocyclic molecules. In 2005 Hill and co-workers reported the first example of a well-defined molecular catalysis mediated by a group 2 centre. Here a  $\beta$ -diketiminato calcium complex was employed as a catalyst to carry out the intramolecular hydroamination of aminoalkenes (Scheme 1.17).<sup>96</sup>



**Scheme 1.19:** Ca-catalysed intramolecular hydroamination of aminoalkenes

Further research showed that other group 2 bisamide type of complexes could also be employed in the same reaction procedure (Figure 1.8)<sup>107,108</sup>

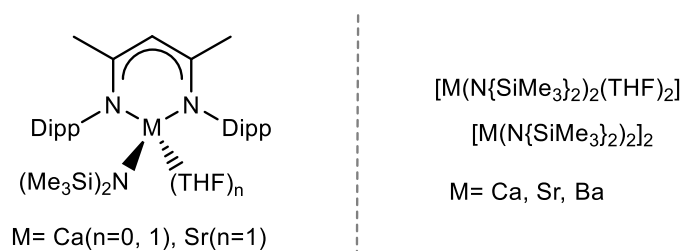
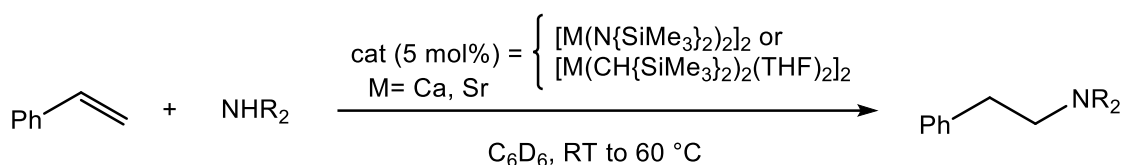


**Figure 1.8:** Efficient group 2 pre catalysts for the intramolecular hydroamination of aminoalkenes

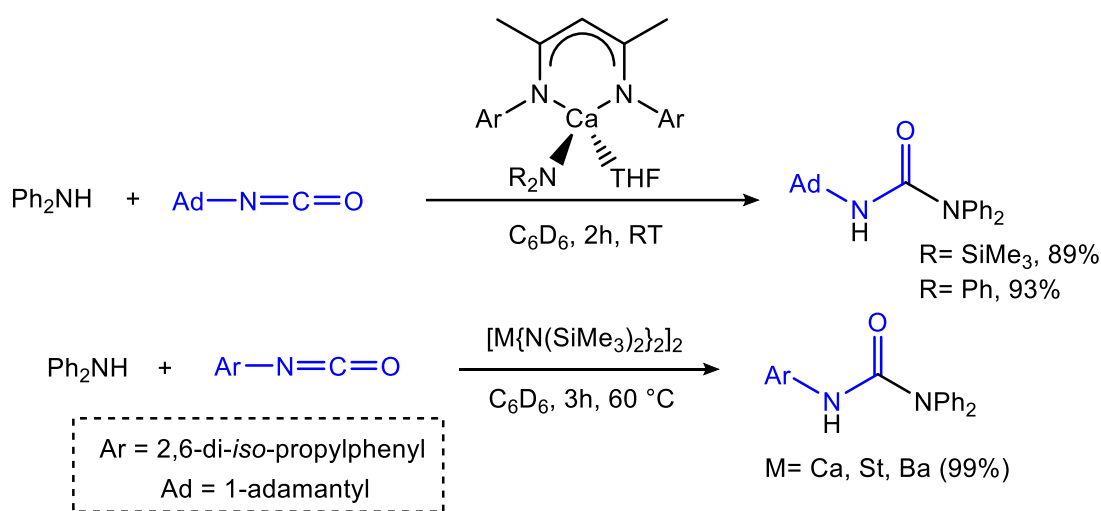
Although it has been shown that  $\beta$ -diketiminato magnesium complexes can also catalyse this reaction, they are significantly less efficient requiring longer reaction times (2 hours) whereas Ca-catalysed protocol requires only 15 minutes.<sup>108,109</sup> Hydroamination reactions could also be extended to the more energetically demanding intermolecular hydroaminations of styrene using primary or secondary amines with bisamide and bisalkyl group 2 pre catalysts (Scheme 1.20).<sup>108,110</sup>



**Scheme 1.20:** Group 2-catalysed Intermolecular hydroaminations of styrene using primary or secondary amines

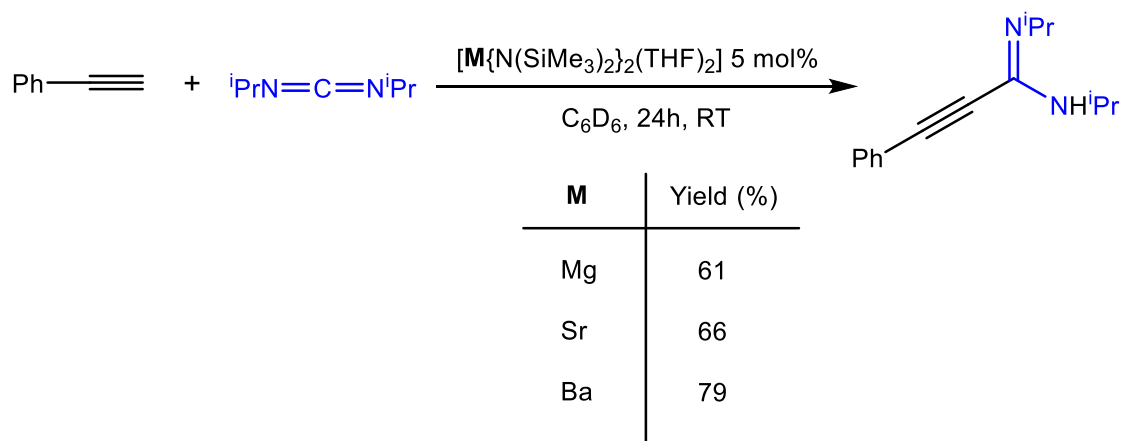
Interestingly when the same reaction was carried out using the barium and magnesium pre catalysts, several days were necessary despite the use of a potentially more reactive magnesium alkyl pre-catalyst. Magnesium pre catalysts are generally less efficient than the heavier analogues. The general trend as activity of the ML pre catalysts in Group 2 organometallic reagents is the following ( $\text{Mg} \ll \text{Ca} < \text{Sr} < \text{Ba}$ ), independent of the ligand employed. Thus, the catalytic activity of these compounds increases with the size of the metal.<sup>111</sup>

Related to this is Hill's hydroaminations of isocyanates using Ca, Sr and Ba complexes. Although the substrate scope is limited, these studies greatly contribute towards understanding how these reactions work (**Scheme 1.21**).<sup>112</sup>



**Scheme 1.21:** Group 2 catalysed hydroaminations of isocyanates

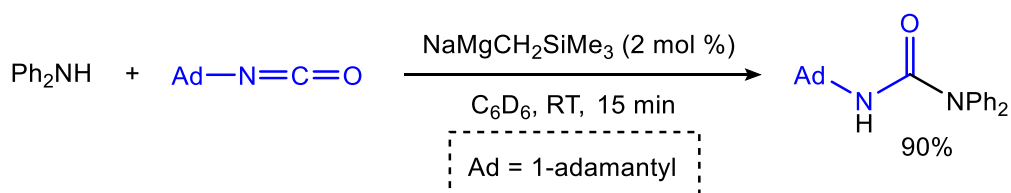
Strictly related is Hill's work on group 2 catalysed hydroacetylenation of carbodiimides using homoleptic alkaline earth hexamethyldisilazides  $[\text{M}\{\text{N}(\text{SiMe}_3)_2\}_2(\text{THF})_2]$  ( $\text{M} = \text{Mg}; \text{Ca}; \text{Sr}$ ) (**Scheme 1.22**).<sup>113</sup>



**Scheme 1.22:** Group 2 catalysed hydroacetylenation of carbodiimides

Once again, the Mg precatalyst is less active than the Sr and Ba analogues.

Furthermore the use of heavier alkaline earth hydride derivatives as pre-catalysts and intermediates in multiple bond hydrogenation, hydrosilylation and hydroboration was also described along with the emergence of these and related reagents in a variety of dehydrocoupling processes that allow the catalytic construction of Si–C, Si–N and B–N bonds.<sup>106</sup> Similarly to what is observed for stoichiometric applications, where activation of magnesium by forming alkali-metal magnesiate leads to enhanced metallating and nucleophilic power compared with single-metal systems (see **chapter 1.3**) it has been demonstrated in our own group that sodium magnesiate such as  $\text{NaMgCH}_2\text{SiMe}_3$  can be employed as pre catalysts for the hydroamination reactions of isocyanates under very mild reaction conditions. Thus activation of magnesium can also be achieved for catalytic purposes (**Scheme 1.23**).<sup>114</sup>



**Scheme 1.23:** Example of  $\text{NaMgCH}_2\text{SiMe}_3$  catalysed hydroamination of isocyanates.

In contrast with the Ca catalysed hydroamination of isocyanates previously described (See **Scheme 1.21**) where full conversion of the final urea is obtained in 2 hours, using  $\text{NaMgCH}_2\text{SiMe}_3$  under the same reaction conditions, the final urea is obtained quantitatively in only 15 minutes. This contribution represents the first ever catalytic applications of alkali

metal magnesiates in synthesis, thus it can be anticipated that it exists substantial scope for development of this protocol.

### 1.4.3 Organomanganese complexes in C-C bond forming processes:

Manganese is a widely distributed transitional element in nature.<sup>115,116</sup> Manganese is in fact the third most abundant transition metal in the Earth's upper continental crust after iron and titanium (**Figure 1.9**).<sup>117</sup>

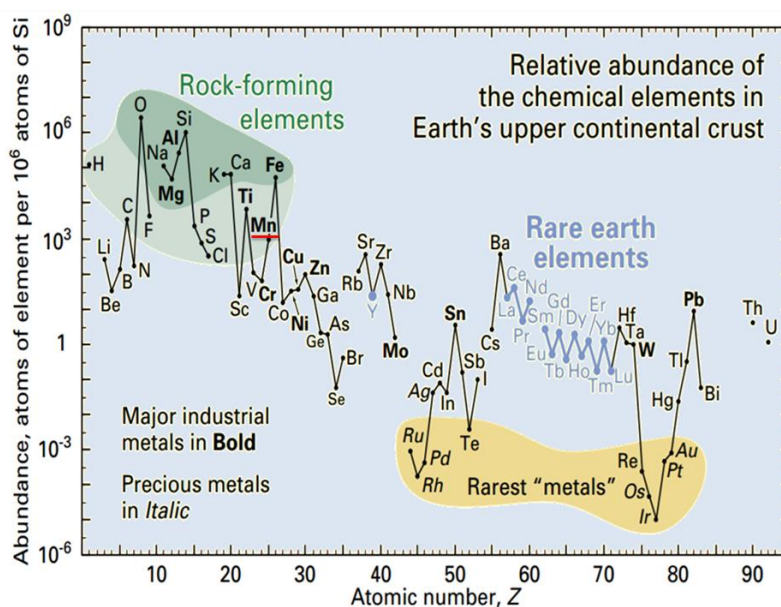
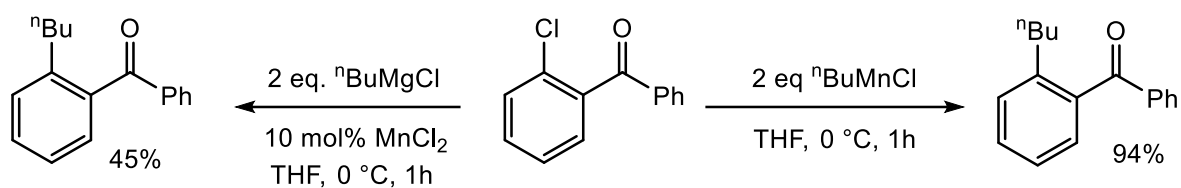


**Figure 1.9:** Relative abundance of the chemical elements in Earth's upper continental crust

In addition it is a biocompatible metal with a relatively low toxicity, which is particularly interesting for pharmaceutical applications.<sup>118</sup> Manganese most stable oxidation state is Mn(II), therefore the cation  $Mn^{2+}$  competes frequently with  $Mg^{2+}$  in biological systems.<sup>119</sup> The reactivity of organomanganese compounds can be compared to that of organomagnesium and organozinc compounds. This is due to the similarities between these compounds. Thus, the electronegativity of Mn has a value of 1.55 undimensional units, which is in between the electronegativity of Mg (1.31) and Zn (1.65) according to Pauling scale. In addition the ionic radius for  $Mg^{2+}$  and  $Mn^{2+}$  is very similar (0.8 Å and 0.83 Å respectively, in complexes where the metal has coordination number 6).<sup>119</sup> Differences include the available d-orbitals for manganese which indeed influence its reactivity. Although organomanganese species have been studied for more than half a century, recently there has been an increasing interest in the application of organomanganese complexes in synthesis. This increased attention is due to the

advantages they offer over conventional organolithiums, Grignards, organozincs and organocuprate compounds. Organomanganese can be classified in four types of compounds, organomanganese halides ( $\text{RMnX}$ ), diorganomanganese ( $\text{R}_2\text{Mn}$ ), triorganomanganates, ( $[\text{R}_3\text{Mn}]^-$ ), and tetraorganomanganates ( $[\text{R}_4\text{Mn}]^{2-}$ ).<sup>120</sup>

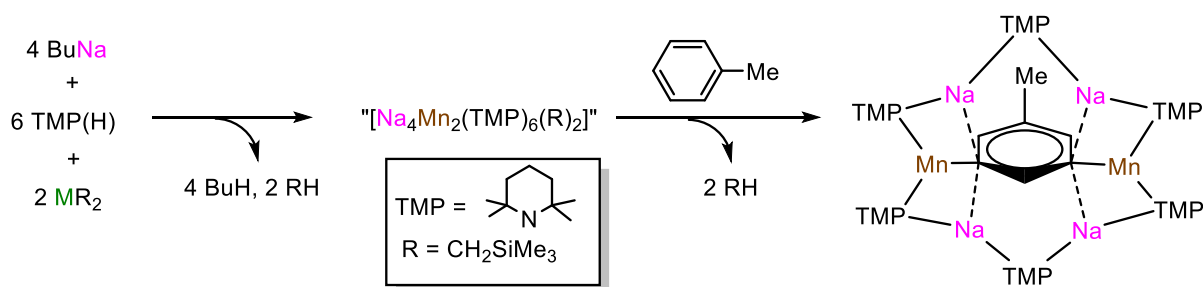
Organomanganese reagents can be quite often referred to as “soft” Grignard reagents. However, they can exhibit very different reactivity. In 2004 Cahiez developed the Mn/Cl exchange using *ortho*-chloroarylketones and the reaction can be performed even at low temperature (**Scheme 1.24**).<sup>121</sup>



**Scheme 1.24:** Cross coupling reaction between organomanganese reagents and *ortho*-chloroarylketones

When the reaction is carried out using two equivalents of  $^n\text{BuMgCl}$  and 10 mol% of  $\text{MnCl}_2$  in THF at  $0^\circ\text{C}$  the yield of coupling product is only 45% as the Grignard reagent mainly reacts with the ketone. When the reaction is carried out using two equivalents of  $^n\text{BuMnCl}$  under the same reaction conditions coupling product is obtained in an excellent 94% yield. To the best of my knowledge this was the first example of a direct coupling reaction between organomanganese reagents and aryl halides to be described. The reaction works even when the reactive *ortho*-chloroacetophenone is employed as a substrate with no evidence of addition products to the carbonyl group.

Similarly to what observed in diorganomagnesium compounds, diorganomanganese complexes on their own are generally too weakly basic to promote metal/hydrogen exchange reactions of arenes.<sup>120</sup> Activation of these compounds by combination with an alkali metal in heterobimetallic ate complexes increase their metallation power by several orders of magnitude. Thus similarly to what previously described for alkali metal magnesiates (See **Scheme 1.17** as an example), manganate complexes can also carry out alkali metal mediated manganation reactions ( $\text{AMMMn}$ ). Mixing  $\text{BuNa}$ ,  $\text{TMP(H)}$  and  $\text{Mn}(\text{CH}_2\text{SiMe}_3)_2$  in a 4:6:2 stoichiometry in hexane solution, and further reaction with one molar equivalent of toluene (**Scheme 1.25**), gives formation of product  $[(\text{TMP})_6\text{Na}_4(3,5\text{-Mn}_2\text{C}_6\text{H}_3\text{CH}_3)]$  where toluene has been dimanganated in the  $\text{C}_3$  and  $\text{C}_5$  position (**Scheme 1.25, Figure 1.10**).<sup>90</sup>



**Scheme 1.25:** dimetalation of toluene in position C<sub>3</sub> and C<sub>5</sub>, inverse-crown product [(TMP)<sub>6</sub>Na<sub>4</sub>(3,5-Mn<sub>2</sub>C<sub>6</sub>H<sub>3</sub>CH<sub>3</sub>)]

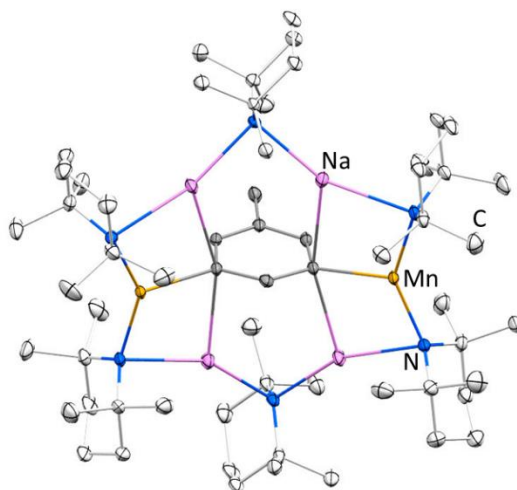
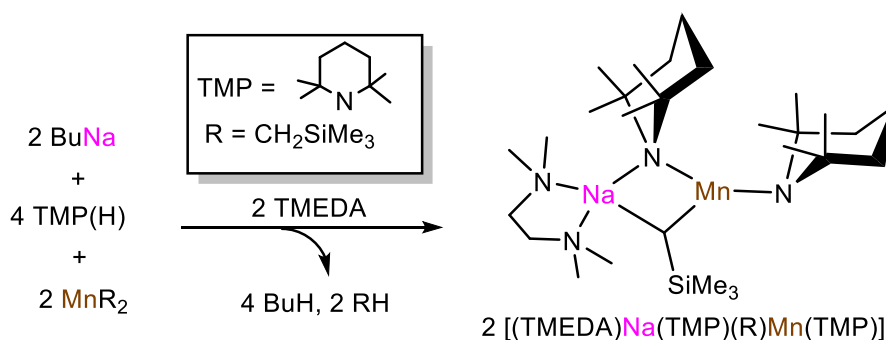


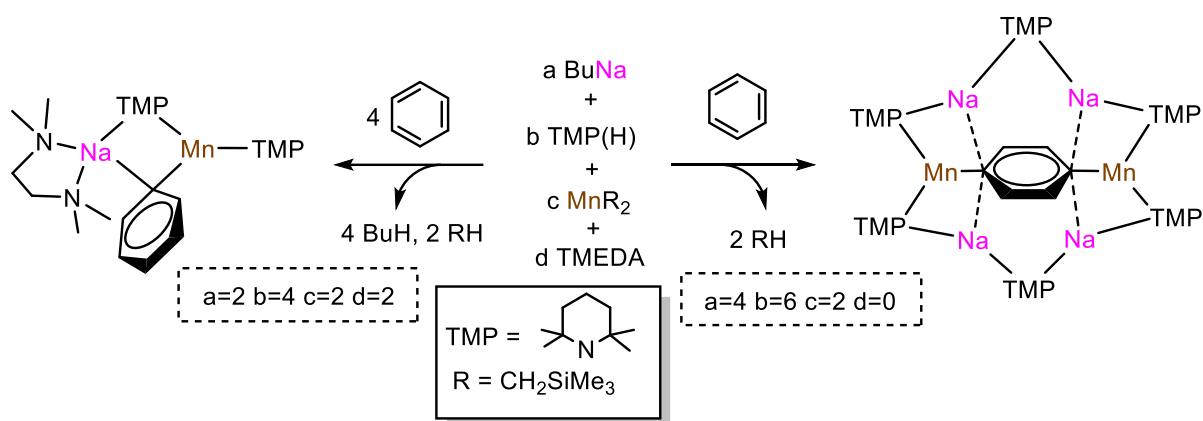
**Figure 1.10:** inverse-crown product [(TMP)<sub>6</sub>Na<sub>4</sub>(3,5-Mn<sub>2</sub>C<sub>6</sub>H<sub>3</sub>CH<sub>3</sub>)]

In 2007, Mulvey has shown that sodium manganese monoalkyl bisamido compound [(TMEDA)Na(TMP)(R)Mn(TMP)] can be prepared by direct co-complexation between 2 equivalents of BuNa, 4 equivalents of TMP(H), 2 equivalents of MnR<sub>2</sub> in the presence of 2 equivalents of TMEDA (**Scheme 1.26**).<sup>122</sup>



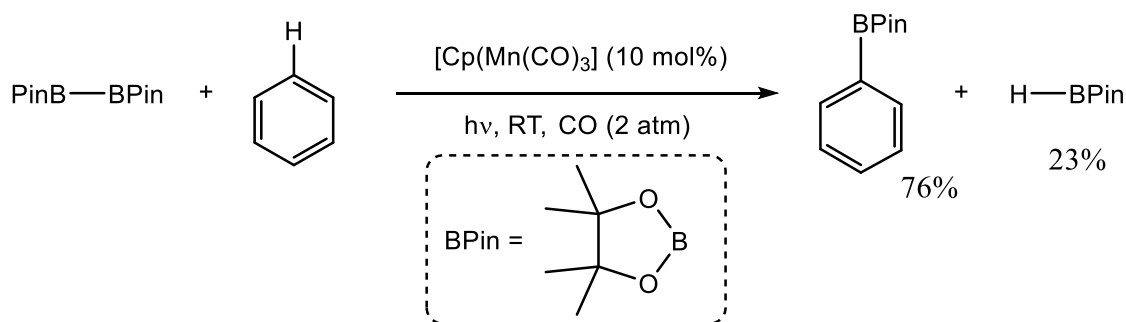
**Scheme 1.26:** direct synthesis of [(TMEDA)Na(TMP)(R)Mn(TMP)]

Further studies on the reactivity of related sodium manganese in direct metallation processes revealed these compounds can promote direct mono-metallation and di-metallation of benzene according to the stoichiometry employed (**Scheme 1.27**).<sup>122</sup>



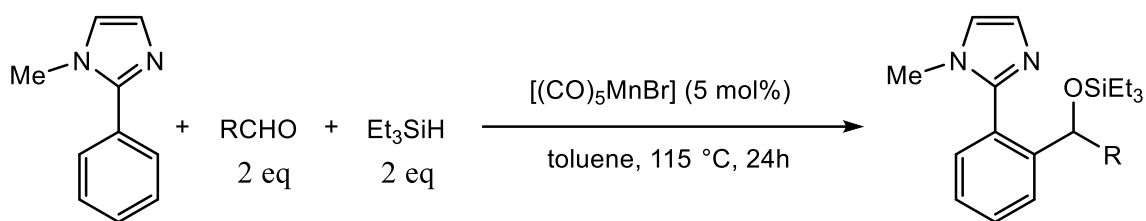
**Scheme 1.27:** Direct mono- and di-metallation of benzene using sodium manganates

Regarding the use of manganese in catalytic transformations a variety of Mn-catalysed methodologies can be found in the literature. Direct C–H bond activation and cross coupling reactions are amongst the most utilised processes for the generation of new C–C bonds. In 1999 Hartwig *et al* published the first catalytic C–H activation process based on an organometallic manganese complex. The reaction consists of a borylation of benzene with PinB–BPin using 10 mol% of Cp<sup>\*</sup>Mn(CO)<sub>3</sub> at RT in the presence of CO (2 atm) to give PhBPin and H-BPin in 76% and 23% yield respectively (**Scheme 1.28**).<sup>123</sup>



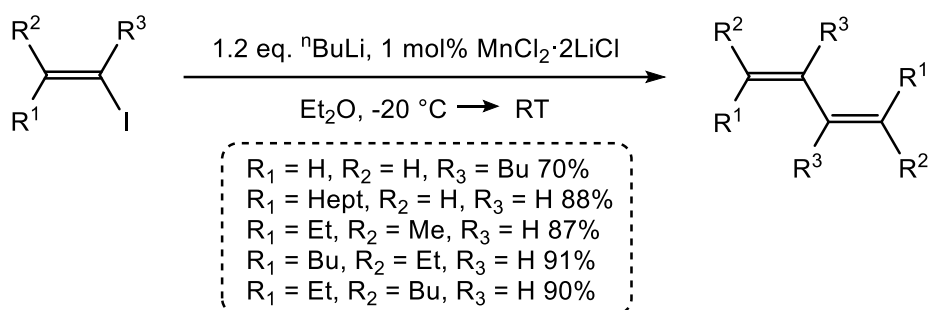
**Scheme 1.28:** Mn-catalysed borylation of benzene

In 2007 Kuninobu, Takai *et al* reported the Mn-catalysed C–H activation of C(sp<sup>2</sup>)-H bonds in substrates bearing a nitrogen donor directing group, in the presence of an aldehyde and a tertiary silane.<sup>124</sup> Good to excellent yields of silyl ethers were obtained using imidazole or imidazoline moiety as directing groups. Interestingly, whereas Mn<sub>2</sub>(CO)<sub>10</sub> and (CO)<sub>5</sub>MnMe exhibited the same efficiency as (CO)<sub>5</sub>MnBr, other pre-catalysts such as MnCl<sub>2</sub> or Mn(acac)<sub>3</sub>, remained totally inactive (**Scheme 1.29**).<sup>124</sup>



**Scheme 1.29:** Mn-catalysed C-H activation of benzene bearing an imidazole moiety as directing group

In 1976 Cahiez, Normant and collaborators developed the first efficient application of manganese catalysed cross-coupling reaction.<sup>125</sup> The authors reported the homo-coupling of alkenyl lithium reagents, to give the corresponding conjugated dienes in high yield and excellent *E*-selectivity (**Scheme 1.30**).



**Scheme 1.30:** Cahiez and Normant approach as the first Mn-catalysed cross-coupling reaction

## 1.5 Aims

The general aim of this PhD project is to assess the applications of some of the structurally defined mixed-metal reagents in organic synthesis and catalysis. Alkali metal magnesiates have been chosen for this study; their synergistic behavior together with the high availability and extremely low toxicity are key features for the application of these compounds in organic synthesis.

Aiming to expand the scope of direct Mg/H exchange reactions, Chapter 2 of this thesis presents a systematic study on the application of novel potassium magnesiates previously synthesised in our group for the deprotonation of challenging aromatic and heterocyclic substrates.

Expanding the synthetic potential of these cooperative bimetallics in catalysis, Chapter 3 presents our findings on sodium-magnesiate catalysed reaction formation of 1,5-disubstituted triazole molecules by cycloaddition reaction between alkynes and azides. These studies combine the synthesis and structural elucidation of the novel bimetallic catalysts with a comprehensive screening of the substrate scope of this method and insightful kinetic studies that shed some light in the intriguing mechanisms involved in these transformations.

Chapter 4 assesses the ability of sodium magnesiates to catalyse the guanilation of amines with carbodiimides. Studies on the possible mechanism of this ate-catalysed transformation involved the synthesis and characterization of sodium magnesium amido intermediates.

Finally, chapter 5 will focus on the application of lithium manganate complexes to promote C-I exchange and C-C bond forming processes.

## 1.6 References:

- (1) Weiss, E. *Angew. Chemie Int. Ed.* **1993**, 32 (11), 1501–1523.
- (2) Mulvey, R. E. *Organometallics* **2006**, 25, 1060–1075.
- (3) Mulvey, R. *Chem. Soc. Rev.* **1991**, 20, 167–209.
- (4) Mulvey, R. E. *Acc. Chem. Res.* **2009**, 42 (6), 743.
- (5) Wanklyn, J. A. *Ann. der Chemie und Pharm.* **1858**, 108 (1), 67–79.
- (6) Wittig, G.; Meyer, F. J.; Lange, G. *Justus Liebigs Ann. Chem.* **1951**, 571 (3), 167–201.
- (7) Wittig, G. *Angew. Chemie Int. Ed.* **1958**, 70, 65.
- (8) Seitz, L. M.; Brown, L. *J. Am. Chem. Soc.* **1966**, 88, 4140–4147.
- (9) Seitz, L. M.; Brown, L. *J. Am. Chem. Soc.* **1966**, 89, 1602–1607.
- (10) Weiss, E.; Thoennes, D. *Chem. Ber.* **1978**, 111, 3726.
- (11) Collum, B. *Acc. Chem. Res.* **1993**, 26 (5), 227–234.
- (12) *The chemistry of organolithium compounds*; Rappoport, Z., Marek, I., Eds.; Wiley: Chichester England, 2004.
- (13) Gilman, H.; Bebb, R. L. *J. Am. Chem. Soc.* **1939**, 61, 109.
- (14) Wittig, G.; Fuhrmann, G. *Berichte der Dtsch. Chem. Gesellschaft* **1940**, 73 (11), 1197–1218.
- (15) J. Clayden. *Organolithiums: Selectivity for synthesis*; Elsevier: Oxford, 2002.
- (16) Gilman, H.; Morton, J. W. *Org. React.* **1954**, 8, 258.
- (17) Rausch, M. D.; Ciappenelli, D. J. *J. Organomet. Chem.* **1967**, 10, 127.
- (18) Lewis, H. L.; Brown, T. L. *J. Am. Chem. Soc.* **1970**, 92, 4664–4670.
- (19) Snieckus, V. *Chem. Rev.* **1990**, 90 (6), 879–933.
- (20) Meyers, A. I.; Gant, T. G. *Tetrahedron* **1994**, 50, 2297.
- (21) Rodriguez, H. R.; Gschwend, H. W. *Org. React.* **1979**, 26, 1.
- (22) Snieckus, V.; Iwao, M.; Iihama, T.; Mahalanabis, K. K.; Perrier, H. *J. Org. Chem.* **1989**, 54, 24.
- (23) Clayden, J.; Cooney, J. J. A.; Julia, M. *J. Chem. Soc. Perkin Trans. 1* **1995**, 7.
- (24) Clayden, J.; Julia, M. *Chem. Commun.* **1993**, 1682.
- (25) Butenschon, H.; Winkler, M.; Vollhardt, K. P. *Chem. Commun.* **1986**, 388.
- (26) Hauser, C. R.; Ludt, R.; Griffiths, J.; McGrath, K. *J. Org. Chem.* **1973**, 38 (9), 1668–1674.
- (27) Hauser, C.; Puterbaugh, W. *J. Org. Chem.* **1964**, 29, 853.
- (28) Schlosser, M.; Moret, E. *Tetrahedron Lett.* **1984**, 25, 4491.
- (29) Zhang, P.; Gawley, R. E. *J. Org. Chem.* **1993**, 58, 3223–3224.
- (30) Lochmann, L. *Tetrahedron Lett.* **1966**, 257.
- (31) Schlosser, M. *J. Organomet. Chem.* **1967**, 8, 9.
- (32) Lubomir, L. *Eur. J. Inorg. Chem.* **2000**, 1115.

- (33) Kennedy, A. R.; Maclellan, J. G.; Mulvey, R. E. *Angew. Chemie Int. Ed.* **2001**, *40*, 3245–3247.
- (34) Masson, E.; Schlosser, M. *Org. Lett.* **2005**, *7* (10), 1923–1925.
- (35) Streitwieser, A.; Harder, S. *Angew. Chemie Int. Ed.* **1993**, *32* (7), 1066–1068.
- (36) Wei, X.; Dong, Q.; Tong, H.; Chao, J.; Liu, D.; Lappert, M. F. *Angew. Chemie Int. Ed.* **2008**, *47* (21), 3976–3978.
- (37) Unkelbach, C.; O’Shea, D. F.; Strohmman, C. *Angew. Chemie Int. Ed.* **2014**, *53* (2), 553–556.
- (38) Benrath, P.; Kaiser, M.; Limbach, T.; Mondeshki, M.; Klett, J. *Angew. Chemie Int. Ed.* **2016**, 10886–10889.
- (39) Morton, A. A.; Holden, M. E. *J. Am. Chem. Soc.* **1947**, *69*, 1675.
- (40) Morton, A. A. A.; Magat, E.; Letsinger, L. C. *J. Am. Chem. Soc.* **1947**, *69*, 950–961.
- (41) Morton, A.; Marsh, F. D.; Coombs, R. D.; Lyons, A. L.; Penner, S.; Ramsden, H.; Baker, V.; Little, E.; Letsinger, R. *J. Am. Chem. Soc.* **1950**, No. 72, 3785.
- (42) Schlosser, M. *Organometallics in synthesis*, 2nd ed.; J. Wiley and Sons: Chichester England, 2002.
- (43) Schlosser, M.; Zellner, A.; Leroux, F. *Synthesis (Stuttg.)* **2001**, 1830.
- (44) Schlosser, M. *Mod. Synth. Methods* **1992**, *6*, 27.
- (45) Schlosser, M.; Faigl, F. *Tetrahedron Lett.* **1991**, *32*, 3369.
- (46) Schlosser, M.; Choi, J. H.; Takagishi, S. *Tetrahedron* **1990**, *46* (16), 5633–5648.
- (47) Schlosser, M.; Marzi, E.; Spitaleri, A.; Mongin, F. *Eur. J. Org. Chem.* **2002**, No. 15, 2508.
- (48) Schlosser, M.; Katsoulos, G.; Sadahito, T. *Synlett* **1990**, 747.
- (49) Schlosser, M.; Mongin, F.; Porwisiak, J.; Dmowski, W.; Bükler, H. H.; Nibbering, N. *Chem. Eur. J.* **1998**, *4*, 1281–1286.
- (50) Schlosser, M.; Maccaroni, P.; Marzi, E. *Tetrahedron* **1998**, *54* (12), 2763–2770.
- (51) Hogan, A. L.; O’Shea, D. F. *Chem. Commun.* **2008**, 3839–3851.
- (52) Tricotet, T.; Fleming, P.; Cotter, J.; Hogan, A. L.; Strohmman, C.; Gessner, V. H.; O’Shea, D. F. *J. Am. Chem. Soc.* **2009**, *131*, 3142–3143.
- (53) Fleming, P.; O’Shea, D. F. *J. Am. Chem. Soc.* **2011**, *133* (6), 1698–1701.
- (54) Cotter, J.; Hogan, A. M. L.; O’Shea, D. F. *Org. Lett.* **2007**, *9* (8), 1493–1496.
- (55) Schlenk, W.; W. J., S. *Berichte der Dtsch. Chem. Gesellschaft* **1929**, 920–924.
- (56) Henderson, K. W.; Kerr, W. J. *Chem. Eur. J.* **2001**, *7*, 3430–3437.
- (57) Heathcock, C. H. In *Comprehensive Carbanion Chemistry Vol. B*; Buncl, E., Durst, T., Eds.; Elsevier: New York, 1980.
- (58) Wakefield, J. In *Comprehensive Organic Chemistry, Vol. 3*; Barton, D., Ollis, W., Eds.; Pergamon: Oxford, 1979; pp 943–967.
- (59) House, H.; Crumrine, D.; Teranishi, A.; Olmstead, H. *J. Am. Chem. Soc.* **1973**, *95*, 3310–3324.
- (60) Eaton, E. P.; Lee, C.-H.; Xiong, Y. *J. Am. Chem. Soc.* **1989**, *111*, 8016–8018.

- (61) Upton, C. J.; Beak, P. *J. Org. Chem.* **1975**, *40* (8), 1094–1098.
- (62) Kondo, Y.; Sakamoto, T.; Yoshida, A. *J. Chem. Soc. Perkin Trans. 1* **1996**, 2331–2332.
- (63) Knochel, P.; Krasovskiy, A. *Angew. Chemie Int. Ed.* **2004**, *43*, 3333–3336.
- (64) García-Alvarez, P.; Graham, D. V.; Hevia, E.; Kennedy, A. R.; Klett, J.; Mulvey, R. E.; O'Hara, C. T.; Weatherstone, S. *Angew. Chemie Int. Ed.* **2008**, *47* (42), 8079–8081.
- (65) Lin, W.; Baron, O.; Knochel, P. *Org. Lett.* **2006**, No. c.
- (66) Krasovskiy, A.; Krasovskaya, V.; Knochel, P. *Angew. Chemie Int. Ed.* **2006**, *45* (18), 2958–2961.
- (67) Rohbogner, C. J.; Clososki, G. C.; Knochel, P. *Angew. Chemie Int. Ed.* **2008**, *47* (8), 1503–1507.
- (68) Clososki, G. C.; Rohbogner, C. J.; Knochel, P. *Angew. Chemie Int. Ed.* **2007**, *46* (40), 7681–7684.
- (69) Knochel, P.; Rohbogner, C. J.; Wunderlich, S. H.; Clososki, G. C. *Eur. J. Org. Chem.* **2009**, No. 11, 1781–1795.
- (70) Greiser, T.; Kopf, J.; Thoennes, D. *Chem. Ber.* **1981**, *114*, 209–213.
- (71) Baillie, S. E.; Bluemke, T. D.; Clegg, W.; Kennedy, A. R.; Klett, J.; Russo, L.; De Tullio, M.; Hevia, E. *Chem. Commun.* **2014**, *50* (18), 12859–12862.
- (72) Hevia, E.; Kennedy, A. R.; Klett, J.; Baillie, S. E.; Clegg, W.; García-Álvarez, P.; Russo, L. *Organometallics* **2012**, *31*, 5131.
- (73) Baillie, S. E.; Clegg, W.; García-Álvarez, P.; Hevia, E.; Kennedy, A. R.; Klett, J.; Russo, L. *Chem. Commun.* **2011**, *47*, 388–390.
- (74) Forbes, G. C.; Kennedy, A. R.; Mulvey, R. E.; Rodger, P. J. a.; Rowlings, R. B. *Dalton Trans.* **2001**, No. 9, 1477–1484.
- (75) Hevia, E.; Gallagher, D. J.; Kennedy, A. R.; Mulvey, R. E.; O'Hara, C. T.; Talmard, C. *Chem. Commun.* **2004**, *791* (21), 2422–2423.
- (76) Barr, L.; Kennedy, A. R.; MacLellan, J. G.; Moir, J. H.; Mulvey, R. E.; Rodger, P. J. a. *Chem. Commun.* **2000**, *12* (18), 1757–1758.
- (77) Bonnet, V.; Mongin, F.; Trécourt, F.; Quéguiner, G. *J. Chem. Soc. Perkin Trans. 1* **2000**, No. 24, 4245–4249.
- (78) Awad, H.; Mongin, F.; Trécourt, F.; Quéguiner, G.; Marsais, F.; Blanco, F.; Abarca, B.; Ballesteros, R. *Tetrahedron Lett.* **2004**, *45* (36), 6697–6701.
- (79) Bayh, O.; Awad, H.; Mongin, F.; Hoarau, C.; Trécourt, F.; Quéguiner, G.; Marsais, F.; Blanco, F.; Abarca, B.; Ballesteros, R. *Tetrahedron* **2005**, *61* (20), 4779–4784.
- (80) Mongin, F.; Bucher, A.; Bazureau, J. P.; Bayh, O.; Awad, H.; Trécourt, F. *Tetrahedron Lett.* **2005**, *46* (46), 7989–7992.
- (81) Bayh, O.; Awad, H.; Mongin, F.; Hoarau, C.; Bischoff, L.; Trécourt, F.; Quéguiner, G.; Marsais, F.; Blanco, F.; Abarca, B.; Ballesteros, R. *J. Org. Chem.* **2005**, *70* (13), 5190–5196.
- (82) Bellamy, E.; Bayh, O.; Hoarau, C.; Trécourt, F.; Quéguiner, G.; Marsais, F. *Chem. Commun.* **2010**, *46*, 7043–7045.
- (83) Hawad, H.; Quéguiner, G.; Bayh, O.; Hoarau, C.; Trécourt, F.; Marsais, F.

- Tetrahedron* **2008**, *64* (14), 3236–3245.
- (84) Mulvey, R. E. *Chem. Commun.* **2001**, No. 12, 1049–1056.
- (85) Kennedy, A. R.; Klett, J.; Mulvey, R. E.; Newton, S.; Wright, D. S. *Chem. Commun.* **2008**, 308.
- (86) Kennedy, A. R.; Mulvey, R. E.; Rowlings, B. J. *Am. Chem. Soc.* **1998**, *120*, 7816–7824.
- (87) Kennedy, A. R.; Mulvey, R. E.; Raston, C. L.; Roberts, A.; Rowlings, R. B. *Chem. Commun.* **1999**, 353–354.
- (88) Andrews, P. C.; Kennedy, A. R.; Mulvey, R. E.; Raston, C. L.; Roberts, B. A.; Rowlings, R. B. *Angew. Chemie Int. Ed.* **2000**, *39* (11), 1960–1962.
- (89) Martínez-Martínez, A. J.; Armstrong, D. R.; Conway, B.; Fleming, B. J.; Klett, J.; Kennedy, A. R.; Mulvey, R. E.; Robertson, S. D.; O’Hara, C. T. *Chem. Sci.* **2014**, *5* (2), 771.
- (90) Blair, V. L.; Carrella, L. M.; Clegg, W.; Conway, B.; Harrington, R. W.; Hogg, L. M.; Klett, J.; Mulvey, R. E.; Rentschler, E.; Russo, L. *Angew. Chemie Int. Ed.* **2008**, *47* (33), 6208–6211.
- (91) Martínez-Martínez, A. J.; Kennedy, A. R.; Mulvey, R. E.; O’Hara, C. T. *Science* **2014**, *346* (6211), 834–837.
- (92) *United Nations Population Division and Human Mortality Database.*
- (93) *Catalysis in Perspective: Historic Review*; Van Santen, R., Ed.; Wiley, 2012.
- (94) Melen, R. L. *Chem. Soc. Rev.* **2016**, *45*, 775–788.
- (95) Hill, M. S.; Liptrot, D. J.; Weetman, C. *Chem. Soc. Rev.* **2016**, *45*, 972–988.
- (96) Crimmin, M. R.; Casely, I. J.; Hill, M. S. *J. Am. Chem. Soc.* **2005**, *127* (7), 2042–2043.
- (97) Spielmann, J.; Buch, F.; Harder, S. *Angew. Chemie Int. Ed.* **2008**, *47* (49), 9434–9438.
- (98) Cornils, B.; Herrmann, W. a. *Appl. Homog. Catal. with Organomet. Compd.* **2002**, 10–20.
- (99) Buchanan, W. D.; Allis, D. G.; Ruhlandt-Senge, K. *Chem. Commun.* **2010**, *46* (25), 4449–4465.
- (100) Corey, E. J.; Li, W.; Reichard, G. A. *J. Am. Chem. Soc.* **1998**, *120* (10), 2330–2336.
- (101) Kleine, V. J.; Kleine, H.-H. *Die Makromol. Chemie* **1959**, *30* (1), 23–38.
- (102) Arrowsmith, M.; Hill, M. S.; Hadlington, T.; Kociok-Köhn, G.; Weetman, C. *Organometallics* **2011**, *30* (21), 5556–5559.
- (103) Hill, M. S.; MacDougall, D. J.; Mahon, M. F. *Dalton Trans.* **2010**, *39* (46), 11129–11131.
- (104) Schwamm, R. J.; Day, B. M.; Mansfield, N. E.; Knowelden, W.; Hitchcock, P. B.; Coles, M. P. *Dalton Trans.* **2014**, *43* (38), 14302–14314.
- (105) Schwamm, R. J.; Coles, M. P. *Organometallics* **2013**, *32* (19), 5277–5280.
- (106) Barrett, A. G. M.; Crimmin, M. R.; Hill, M. S.; Hitchcock, P. B.; Procopiou, P. A. *Organometallics* **2007**, *26* (16), 4076–4079.
- (107) Sarish, S.; Nembenna, S.; Nagendran, S.; Roesky, H. W.; Pal, A.; Herbst-Irmer, R.; Ringe, A.; Magull, J. *Inorg. Chem.* **2008**, *47* (13), 5971–5977.

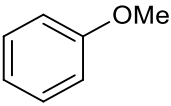
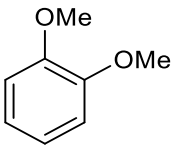
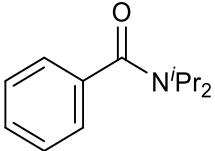
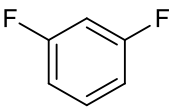
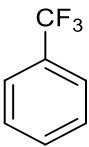
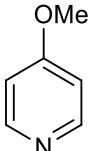
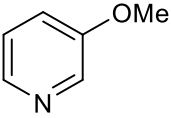
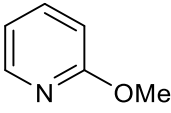
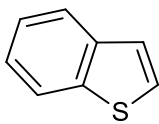
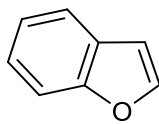
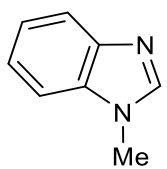
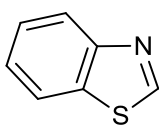
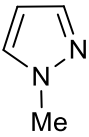
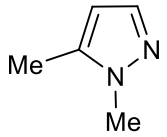
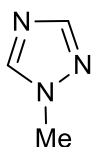
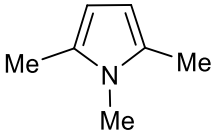
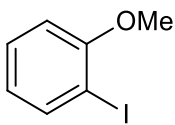
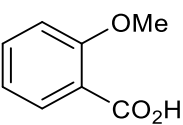
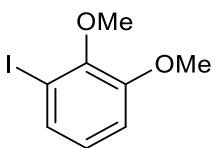
- (108) Crimmin, M. R.; Arrowsmith, M.; Barrett, A. G. M.; Casely, I. J.; Hill, M. S.; Procopiou, P. A. *J. Am. Chem. Soc.* **2009**, *131* (28), 9670–9685.
- (109) Barrett, A. G. M.; Brinkmann, C.; Crimmin, M. R.; Hill, M. S.; Hunt, P.; Procopiou, P. A. *J. Am. Chem. Soc.* **2009**, *131* (36), 12906–12907.
- (110) Brinkmann, C.; Barrett, A. G. M.; Hill, M. S.; Procopiou, P. A. *J. Am. Chem. Soc.* **2012**, *134* (4), 2193–2207.
- (111) Liu, B.; Roisnel, T.; Carpentier, J. F.; Sarazin, Y. *Angew. Chemie Int. Ed.* **2012**, *51* (20), 4943–4946.
- (112) Barrett, A. G. M.; Boorman, T. C.; Crimmin, M. R.; Hill, M. S.; Kociok-Köhn, G.; Procopiou, P. A. *Chem. Commun.* **2008**, 4356 (41), 5206–5208.
- (113) Arrowsmith, M.; Crimmin, M. R.; Hill, M. S.; Lomas, S. L.; Heng, M. S.; Hitchcock, P. B.; Kociok-Köhn, G.; Arrowsmith, M.; Hitchcock, P. B.; Crimmin, M. R.; Lomas, S. L.; Kociok-Köhn, G. *Dalton Trans.* **2014**, 43 (38), 14249–14256.
- (114) Hernán-Gómez, A.; Bradley, T. D.; Kennedy, A. R.; Livingstone, Z.; Robertson, S. D.; Hevia, E. *Chem. Commun.* **2013**, 49 (77), 8659–8661.
- (115) Cotton, F. A.; Wilkinson, G. *Advanced Inorganic Chemistry a Comprehensive Text*, John Wiley.; New York, 1980.
- (116) Christianson, D. W. *Prog. Biophys. Mol. Biol.* **1997**, *67*, 217–252.
- (117) Haxel, G. B.; Hedrick, J. B.; Orris, G. J. *United States Geological Survey (USGS) Fact Sheet: Rare Earth Elements — Critical Resources for High Technology*; 2002; Vol. 087–02.
- (118) Valyaev, D. A.; Lavigne, G.; Lugan, N. *Coord. Chem. Rev.* **2016**, *308*, 191–235.
- (119) Bock, C. W.; Katz, A. K.; Markham, G. D.; Glusker, J. P. *J. Am. Chem. Soc.* **1999**, *121* (32), 7360–7372.
- (120) Layfield, R. A. *Chem. Soc. Rev.* **2008**, *37* (6), 1098–1107.
- (121) Cahiez, G.; Luart, D.; Lecomte, F. *Org. Lett.* **2004**, *6* (24), 4395–4398.
- (122) Carrella, L. M.; Clegg, W.; Graham, D. V.; Hogg, L. M.; Kennedy, A. R.; Klett, J.; Mulvey, R. E.; Rentschler, E.; Russo, L. *Angew. Chemie Int. Ed.* **2007**, *46* (25), 4662–4666.
- (123) Chen, H.; Hartwig, J. F. *Angew. Chemie Int. Ed.* **1999**, *38* (22), 3391–3393.
- (124) Kuninobu, Y.; Nishina, Y.; Takeuchi, T.; Takai, K. *Angew. Chemie Int. Ed.* **2007**, *46* (34), 6518–6520.
- (125) Cahiez, G.; Bernard, D. *J. Organomet. Chem.* **1976**, *113* (2), 99–106.

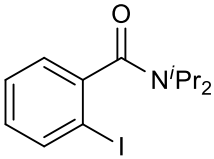
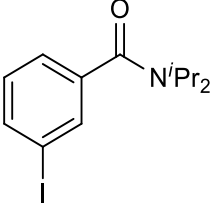
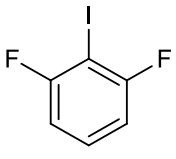
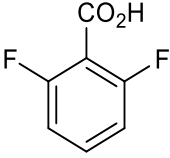
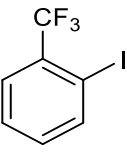
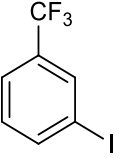
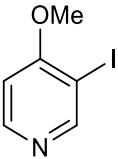
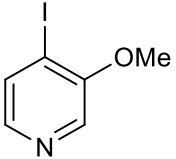
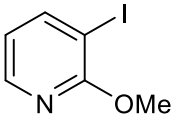
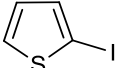
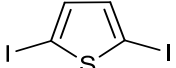
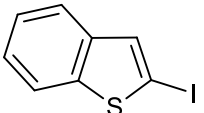
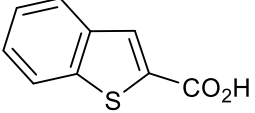
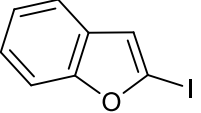
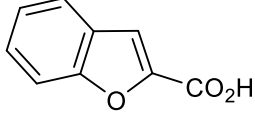
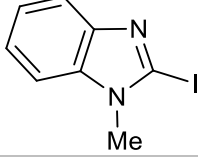
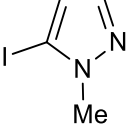
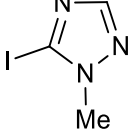
## **CHAPTER 2**

# **Alkali-Metal Mediated Magnesiations of Aromatic and N-heterocyclic Substrates Using Homoleptic Higher-Order Potassium Magnesiates.**

## II. Table of compounds

<b>1a</b>	$[\{(KMg(CH_2SiMe_3)_3)_3\}_\infty]$	<b>1b</b>	$[(PMDETA)_2K_2Mg(CH_2SiMe_3)_4]$
<b>1c</b>	$[(TMEDA)_2K_2Mg(CH_2SiMe_3)_4]$	<b>1d</b>	$[(TMEDA)_2Na_2Mg(CH_2SiMe_3)_4]$
<b>1e</b>	$[(TMEDA)_2Li_2Mg(CH_2SiMe_3)_4]$		

<b>2a</b>		<b>2b</b>		<b>2c</b>	
<b>2d</b>		<b>2e</b>		<b>2f</b>	
<b>2g</b>		<b>2h</b>		<b>2i</b>	
<b>2j</b>		<b>2k</b>		<b>2l</b>	
<b>2m</b>		<b>2n</b>		<b>2o</b>	
<b>2p</b>		<b>2q</b>			
<b>3a</b>		<b>3a'</b>		<b>3b</b>	

<b>3c</b>		<b>3c'</b>		<b>3d</b>	
<b>3d'</b>		<b>3e</b>		<b>3e'</b>	
<b>3f</b>		<b>3g</b>		<b>3h</b>	
<b>3i</b>		<b>3i'</b>		<b>3j</b>	
<b>3j'</b>		<b>3k</b>		<b>3k'</b>	
<b>3l</b>		<b>3n</b>		<b>3p</b>	

## 2.1 Summary

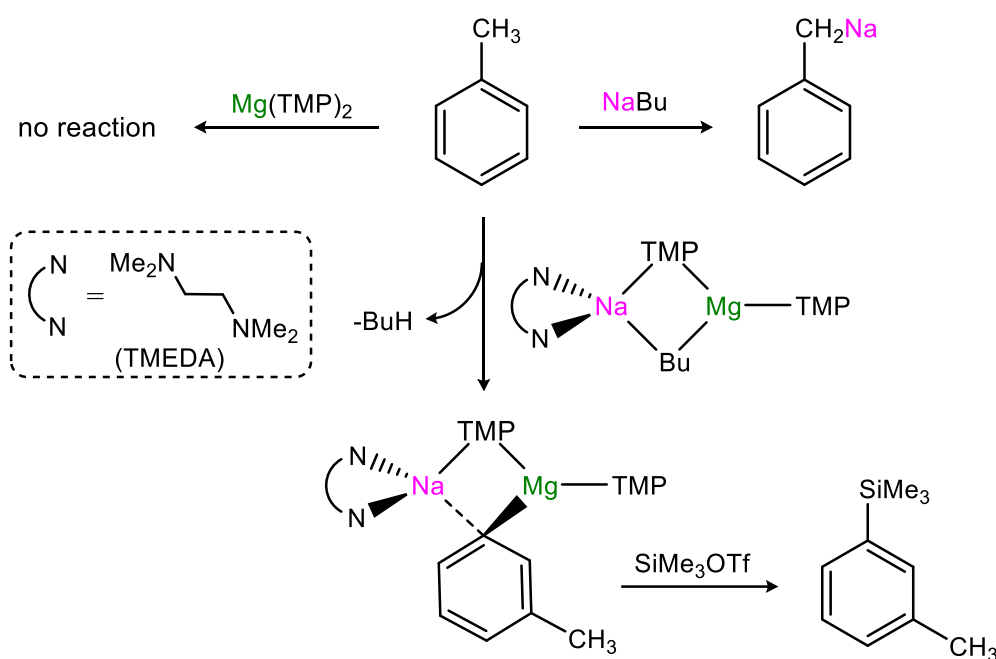
Looking to expand the scope and applications of potassium magnesiates in organic synthesis, this chapter of the PhD thesis presents a systematic study on the metallating ability of several homoleptic alkyl potassium magnesiates with a wide range of aromatic and N-heterocyclic substrates.

The bimetallic bases employed for this study are  $[\{(\text{KMg}(\text{CH}_2\text{SiMe}_3)_3)_\infty]$  (**1a**),  $[(\text{PMDETA})_2\text{K}_2\text{Mg}(\text{CH}_2\text{SiMe}_3)_4]$  (**1b**) and  $[(\text{TMEDA})_2\text{K}_2\text{Mg}(\text{CH}_2\text{SiMe}_3)_4]$  (**1c**), which can be easily prepared by co-complexation reactions of their homometallic components. Using aromatic ether anisole as a case study, show that while higher order magnesiates **1b** and **1c** can efficiently deprotonate this organic molecule at room temperature in hexane, giving 2-iodoanisole (**3a**) after iodine quenching whereas lower-order magnesiate **1a** is inert towards the metallation. The enhanced reactivity of **1b** and **1c** contrasts with the results obtained when the same substrate **2a** is confronted with  $\text{Mg}(\text{CH}_2\text{SiMe}_3)_2$  or  $\text{KCH}_2\text{SiMe}_3$ , which are sluggish to react, affording only traces of **3a**. A dramatic alkali-metal effect is observed, as closely related lithium magnesiates  $[(\text{TMEDA})_2\text{Li}_2\text{Mg}(\text{CH}_2\text{SiMe}_3)_4]$  **1d** fails to deprotonate anisole. Furthermore, reactivity studies using variable amounts of the substrate have revealed the ability of **1b** to metallate up to 3 molecules of **2a** disclosing its ability to exhibit polybasic behaviour. Thus, extending this method to other substrates **1b** can *ortho*-deprotonate 1,2-dimethoxybenzene (**2b**), *N,N*-diisopropylbenzamide (**2c**), 1,3-difluorobenzene (**2d**) and trifluorotoluene (**2e**) in yields ranging from 74% to 94%. When heterocyclic substrates were employed, selective deprotonations of methoxy substituted pyridines could be accomplished in good yields (58-75%).  $\alpha$ -Metallation of 5-membered unsaturated heterocycles such as thiophene (**2i**), benzothiophene (**2j**), benzofuran (**2k**), and methylbenzimidazole (**2l**) can also be accomplished in excellent yields (ranging from 81 to 92%) under very mild reaction conditions. In the case of 1-methyl-1H-pyrazole (**2n**) and 1-methyl-1H-1,2,4-triazole (**2p**), the deprotonation occurs exclusively at the C<sub>5</sub> position, affording 5-iodo-1-methyl-1H-pyrazole (**3n**) and 5-iodo-1-methyl-1H-1,2,4-triazole (**3p**) respectively in almost quantitative yields. Carboxylation reactions of selected substrates have also been studied, by treating the relevant aromatic molecule with 0.33 eq. of the potassium base **1b**, followed by exposure of the relevant aryl magnesiate intermediate to CO<sub>2</sub> gas and hydrolysis step, which led to the isolation of several carboxylic acids, in good yields (52-95%) at room temperature without the need of transition metal catalysts or long reaction times.

## 2.2 Introduction

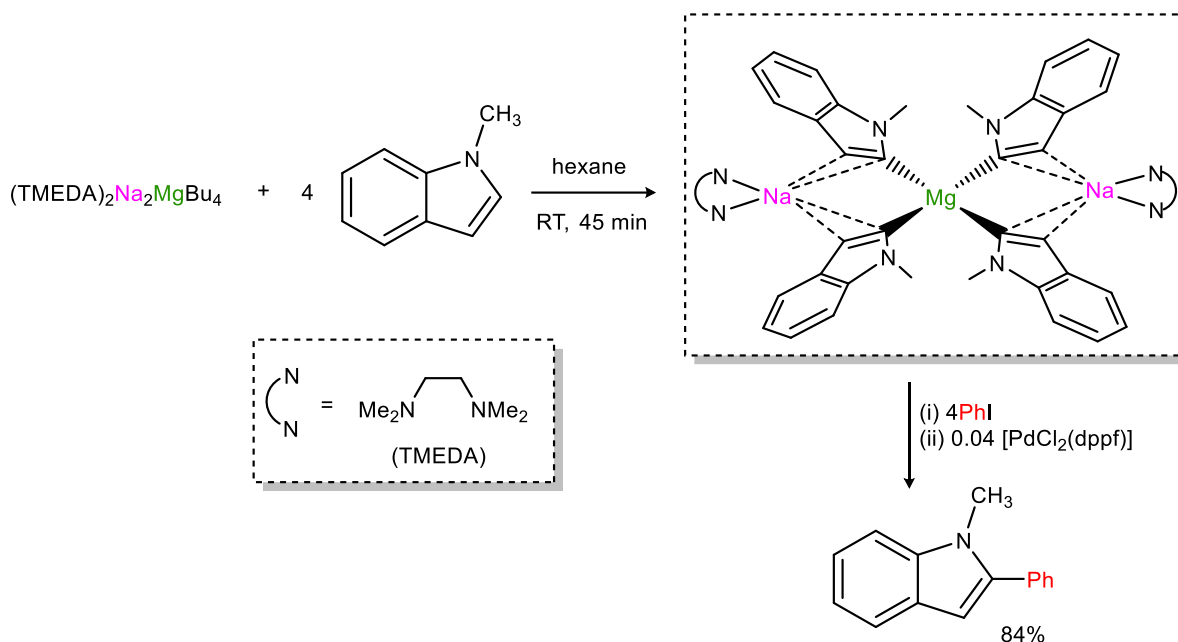
### 2.2.1 Alkali-Metal-Mediated-Magnesiations (AMMMg)

Studies by Mulvey *et al.* on the reactivity of alkali-metal magnesiates containing alkyl and amido ligands have established the concept of AMMg, where Magnesium-H exchange reactions are promoted by the synergistic effect of the two metals. For example using toluene as a substrate, when reacted with heteroleptic magnesiate [(TMEDA)Na(Bu)(TMP)Mg(TMP)] it is possible to promote the unprecedented *meta*-magnesylation of toluene (**Scheme 2.1**) affording [(TMEDA)Na(C<sub>6</sub>H<sub>4</sub>CH<sub>3</sub>)(TMP)Mg(TMP)] in almost quantitative yield, whose structure could be established by X-Ray crystallographic studies.<sup>1</sup> Interestingly although this reaction is formally a magnesylation, Mg(TMP)<sub>2</sub> fails to deprotonate toluene, whereas BuNa induces the formation of benzylna leaving the aromatic hydrogen atoms intact.



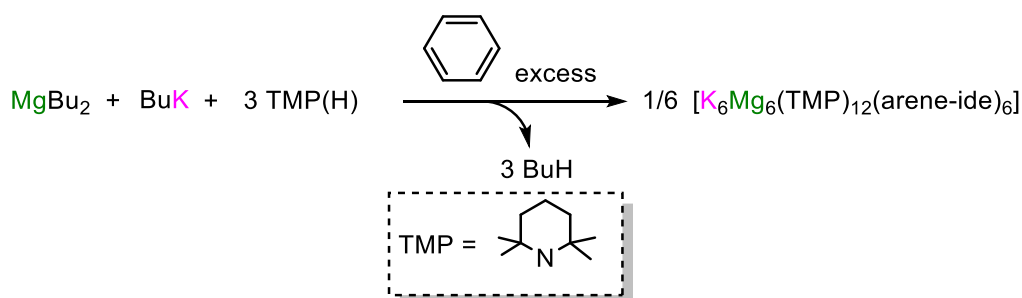
**Scheme 2.1:** *Meta*-metallation of toluene using the [(TMEDA)Na(Bu)(TMP)Mg(TMP)] base.

The intermediate was also quenched with SiMe<sub>3</sub>OTf (trimethylsilyl trifluoromethanesulfonate) in order to obtain the final trimethyl *meta*-tolylsilane in a quantitative yield. Interestingly this method can also be applied to N-heterocyclic molecules, such as indoles which are important building blocks in pharmaceutical synthesis.<sup>2,3</sup> Thus, the sodium-alkyl tetraorgano-magnesiate [(TMEDA)<sub>2</sub>Na<sub>2</sub>MgBu<sub>4</sub>] reacts with four equivalents of *N*-methyl-indole to afford [(TMEDA)<sub>2</sub>Na<sub>2</sub>Mg(C<sub>9</sub>H<sub>8</sub>N)<sub>4</sub>] (**Scheme 2.2**).<sup>4</sup>



**Scheme 2.2:** [(TMEDA)<sub>2</sub>Na<sub>2</sub>MgBu<sub>4</sub>] mediate magnesiation of N-methyl-indole.

This straightforward procedure contrasts with previous indirect approaches where lithiation of the heterocycle was carried out at subambient temperature to avoid side reactions (-78 °C), followed by metathesis with MgCl<sub>2</sub>.<sup>5</sup> Development of alkali metal magnesiations involve mainly the use of lithium and sodium analogues, potassium magnesiates have received considerably less attention. Mulvey's breakthrough in potassium mediated magnesiations of arenes with the corresponding monometallation of benzene or toluene using a 1:1:3 mixture of <sup>n</sup>BuK, Bu<sub>2</sub>Mg, and TMPH respectively to form a 24-atom polymetallic host ring [K<sub>6</sub>Mg<sub>6</sub>(TMP)<sub>12</sub>(arene-ide)<sub>6</sub>] (**Scheme 2.3, Figure 2.1**).<sup>6</sup>



**Scheme 2.3:** Reaction formation of potassium magnesiumate inverse crown [K<sub>6</sub>Mg<sub>6</sub>(TMP)<sub>12</sub>(arene-ide)<sub>6</sub>]<sup>6</sup>

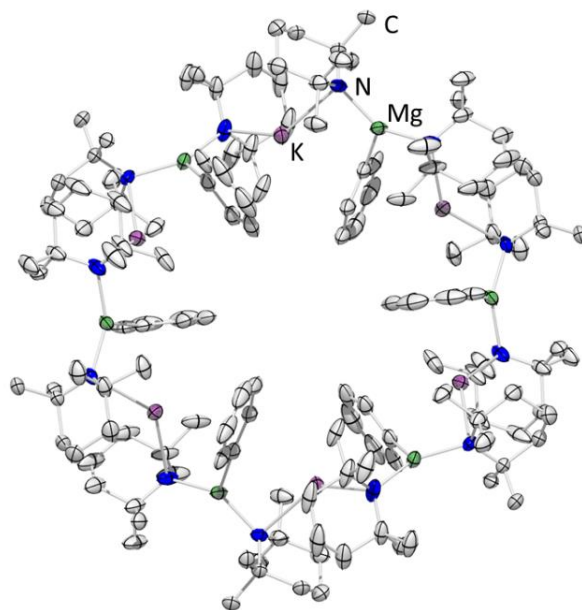
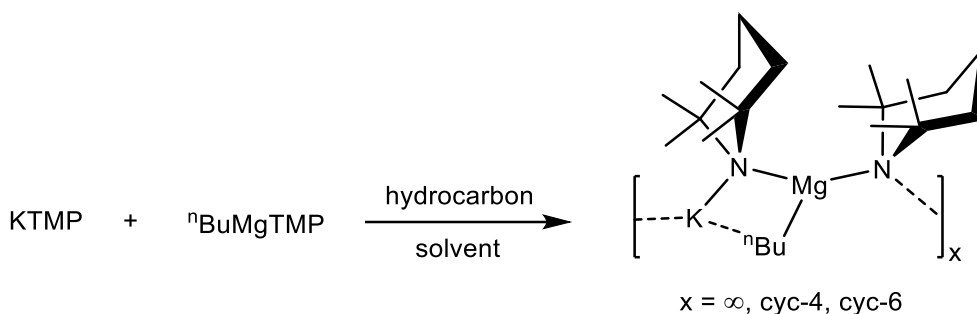


**Figure 2.1:** Inverse crown  $[K_6Mg_6(TMP)_{12}(C_6H_5)_6]$

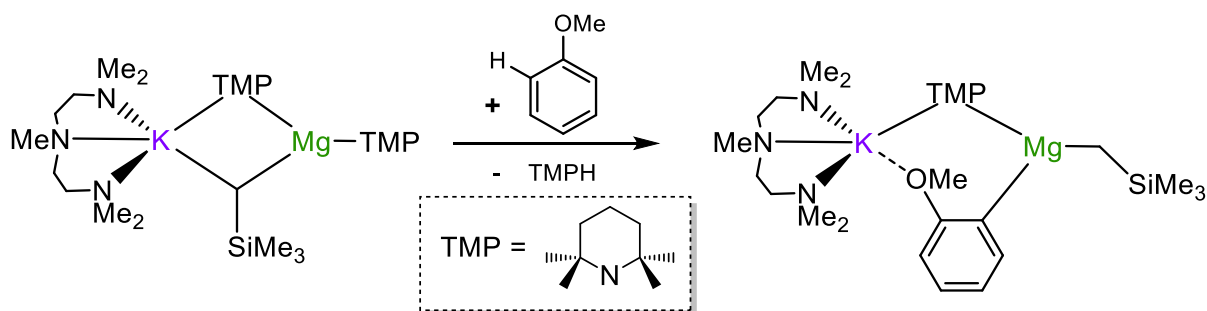
This 24-atom polymetallic compound is an example of potassium magnesiate inverse crown. Notwithstanding, these reactions suffer from drawbacks, for example, the arene has to be employed in high excess and generally moderate yields are obtained. Recently in order to overcome these limitations recent work carried out in our group has shown the possibility to synthesise potassium magnesiates *pre*-inverse-crowns, and further react these compounds with arenes such as benzene, toluene or naphthalene to promote Mg/H exchange reactions to form the already mentioned  $[K_6Mg_6(TMP)_{12}(\text{arene-ide})_6]$  *inverse crowns*.<sup>7</sup> Pre-inverse crowns are well defined unsolvated alkali metal magnesiates. O'Hara has studied the co-complexation reaction between KTMP and <sup>n</sup>BuMgTMP which leads to the formation of different oligomers depending on the solvent employed for the crystallisation.  $[KMg(TMP)_2{}^nBu]_{\infty}$ ,  $[KMg(TMP)_2{}^nBu]_4$  and  $[KMg(TMP)_2{}^nBu]_6$  can be obtained when the reaction between KTMP and <sup>n</sup>BuMgTMP is allowed to crystallise respectively from deuterated cyclohexane and methylcyclohexane at ambient temperature and cyclohexane at 8 °C (**Scheme 2.4**).<sup>7</sup>



**Scheme 2.4:** Synthesis of potassium magnesiate pre-inverse crowns  $[\text{KMg}(\text{TMP})_2^n\text{Bu}]_\infty$ ,  $[\text{KMg}(\text{TMP})_2^n\text{Bu}]_4$  and  $[\text{KMg}(\text{TMP})_2^n\text{Bu}]_6$

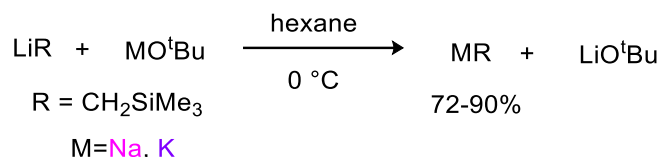
The reaction of the pre-inverse-crown  $[\text{KMg}(\text{TMP})_2^n\text{Bu}]_\infty$  with equimolar amounts of benzene and toluene at ambient temperature formed inverse crown  $[\text{K}_6\text{Mg}_6(\text{TMP})_{12}(\text{C}_6\text{H}_4(\text{R}))_6]$  ( $\text{R}=\text{H}$ ,  $\text{CH}_3$ ) respectively in a 44% and 93% yield.<sup>7</sup> These findings provided strong evidence for a base template approach mechanism in this transformations. This work has recently been extended by O'Hara, Mulvey *et al.* in the template base metalation approach using sodium magnesiate “[ $\text{Na}_4\text{Mg}_2(\text{TMP})_6(\text{nBu})_2$ ]” (See **Chapter 1.3.3** for further detail).<sup>8</sup>

Monomeric solvated potassium magnesiate compounds have also shown promise for Mg-H exchange reactions as Mulvey and co-workers demonstrated using PMDETA solvated potassium magnesiate  $[(\text{PMDETA})\text{K}(\text{TMP})_2\text{Mg}(\text{CH}_2\text{SiMe}_3)]$  for the *ortho*-magnesiation reaction of anisole (**Scheme 2.5, Figure 2.2**).



**Scheme 2.5:**  $[(\text{PMDETA})\text{K}(\text{TMP})_2\text{Mg}(\text{CH}_2\text{SiMe}_3)]$  *ortho*-magnesiation of anisole.





**Scheme 2.7:** Synthesis of  $\text{MCH}_2\text{SiMe}_3$

Both Mg and K analogues can be prepared with an array of alkyl substituents. Particularly interesting are the compounds containing silyl-substituted methyl groups, such as  $\text{CH}_2\text{SiMe}_3$ . Lacking hydrogens at the beta positions these alkyl groups, coupled with their bulkiness and electronic stabilisation,<sup>10,11</sup> have allowed the isolation and structural elucidation of several organopotassium species (**Figure 2.3**).<sup>12–19</sup>

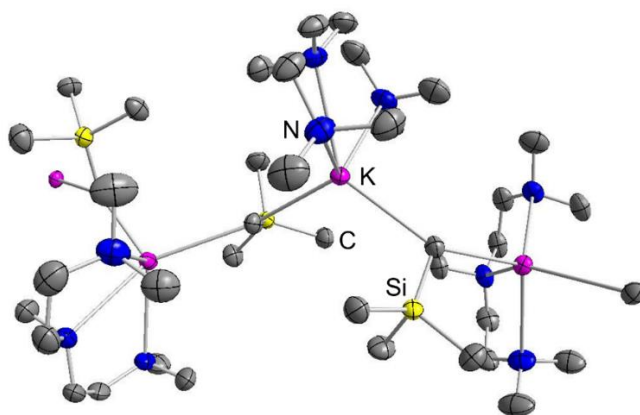
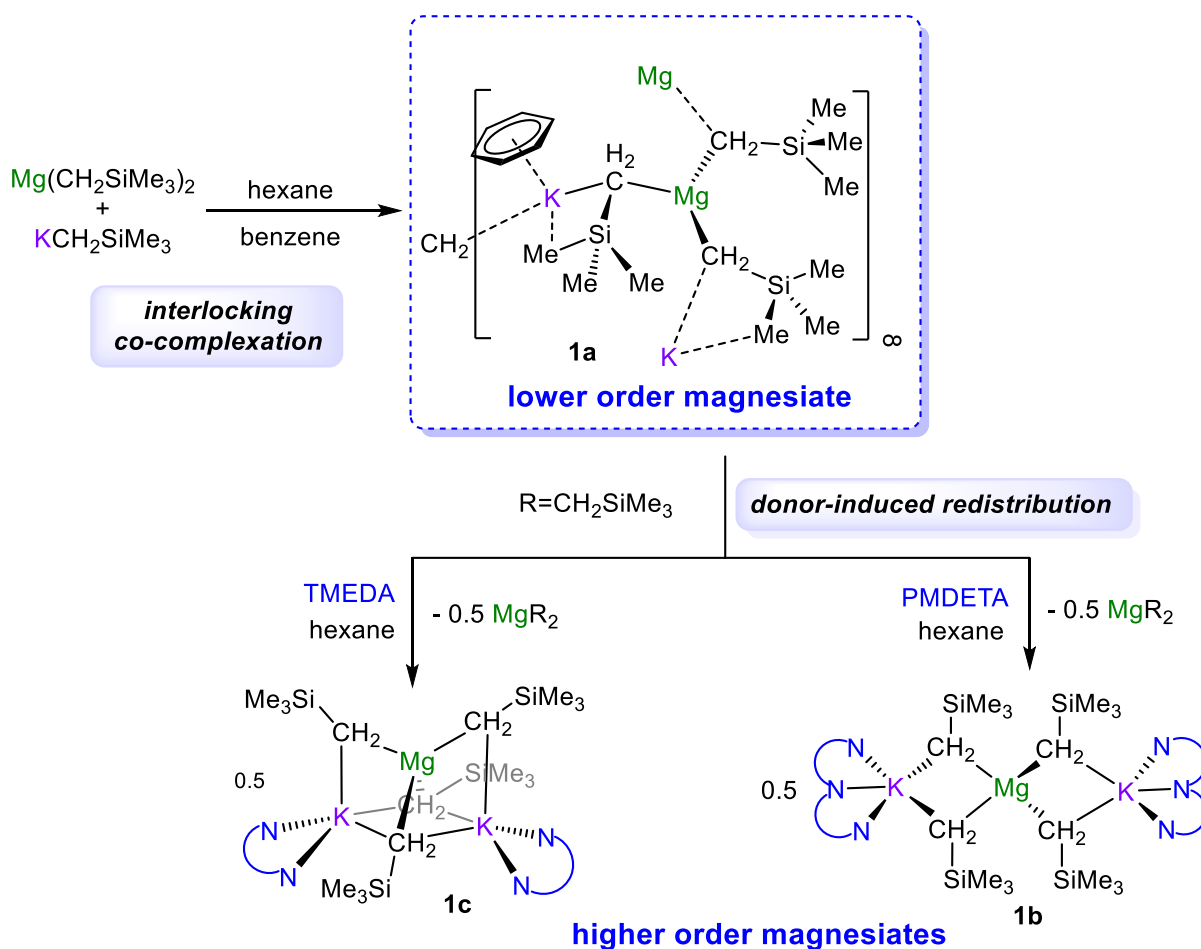


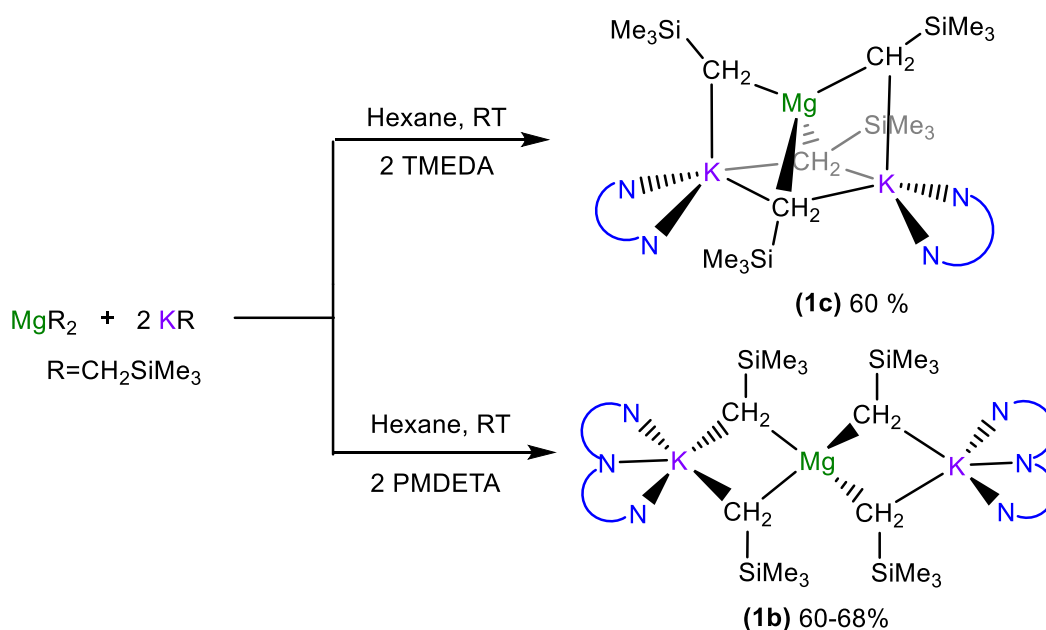
**Figure 2.3:** Monomeric unit of the polymeric structure of PMDETA solvated  $\text{KCH}_2\text{SiMe}_3$

Mixing together equimolar amounts of  $\text{Mg}(\text{CH}_2\text{SiMe}_3)_2$  and  $\text{KCH}_2\text{SiMe}_3$  results in a co-complexation reaction to form the lower order magnesiate  $[\{(\text{KMg}(\text{CH}_2\text{SiMe}_3)_3)_\infty]$  (**1a**) which in the solid state exhibits an intricate tridimensional network.<sup>20</sup>  $^1\text{H}$ -DOSY NMR studies have shown that this supramolecular structure is not retained in  $d_6$ -benzene solution, suggesting the presence of more simple monomeric units of  $[\text{KMg}(\text{CH}_2\text{SiMe}_3)_3(\text{benzene})_X]$  ( $X=1\text{-}2$ ) solvated by deuterated benzene.<sup>21</sup> The addition of nitrogen Lewis donors such as PMDETA or TMEDA favours a redistribution facilitating the formation of higher order tetraorganomagnesiates,  $[(\text{PMDETA})_2\text{K}_2\text{Mg}(\text{CH}_2\text{SiMe}_3)_4]$  (**1b**) and  $[(\text{TMEDA})_2\text{K}_2\text{Mg}(\text{CH}_2\text{SiMe}_3)_4]$  (**1c**) (**Scheme 2.8**).



**Scheme 2.8:** Chem draw representation of lower and higher order potassium magnesiates.

Considering the stoichiometries of **1b** and **1c** the maximum possible yield for these compounds following this methodology is 50%. However these bases can be isolated in much greater crystalline yields (typical yields 60-68%) when a more rational approach is employed by reacting two molar equivalents of  $\text{K}(\text{CH}_2\text{SiMe}_3)$  with  $\text{Mg}(\text{CH}_2\text{SiMe}_3)_2$  in the presence of two equivalents of Lewis donors (**Scheme 2.9, Figure 2.4**).



**Scheme 2.9:** Rational synthesis of potassium magnesiumate bases **1b** and **1c**.

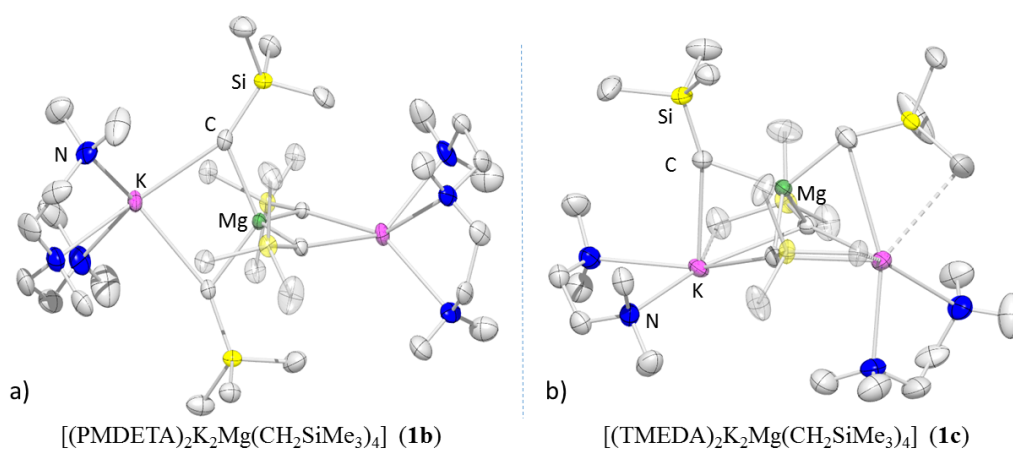


**Figure 2.4:** Monomeric units of a) **1b** and b) **1c**

Both compounds display a central C4-coordinated Mg atom flanked by two donor-solvated K cations. Interestingly, the different hapticities of the N-ligands impose remarkable differences in their structural motifs. Thus, PMDETA ligated **1b** displays a linear KMgK arrangement [174.18(3)°] with each R group bridging Mg with a K centre (**Figure 2.4 (a)**). Contrastingly, in TMEDA-solvate **1c**, in order to attain coordinative saturation, each K needs to bind to three monosilyl groups. Thus two of the four R groups in **1c** bridge between the three metals through their CH<sub>2</sub> heads, while the remaining ones connect Mg with only one K atom (**Figure 2.4 (b)**).

### 2.3.2 Assessing metallating ability of alkyl potassium magnesiate 1a, 1b and 1c.

Our initial studies to test the metallating ability of these novel potassium magnesium reagents focussed on the aromatic ether anisole (**2a**), a benchmark molecule in direct *ortho*-metallation reactions (see Introduction **chapter 1.2.2**).<sup>22</sup> There are a wide number of publications in the literature describing the metallation of anisole employing different metal agents. Early in the 1939 and 1940 the independent work of Gilman and Wittig on direct *ortho*-metallation of **2a** proved to be an efficient method for the selective functionalization of this aromatic ether. Wittig used PhLi as a metallating agent<sup>23,24</sup> whereas Gilman studied the reactions using *n*-BuLi, *n*-BuNa and PhNa.<sup>25</sup> The authors suggested that the regioselectivity of the reaction is due to the acidifying effect of the OMe on the *ortho*-hydrogens.<sup>26</sup> Further work carried out by Collum *et al* on *ortho*-lithiation of anisole using a 1:1 mixture of *n*-BuLi/TMEDA in toluene as a solvent at 0 °C gave quantitative yields of (2-methoxyphenyl)trimethylsilane after quenching with Me<sub>3</sub>SiCl. DFT calculations indicate that the reaction takes place via [(<sup>n</sup>BuLi)<sub>2</sub>(TMEDA)<sub>2</sub>(anisole)] intermediate.<sup>27-29</sup>

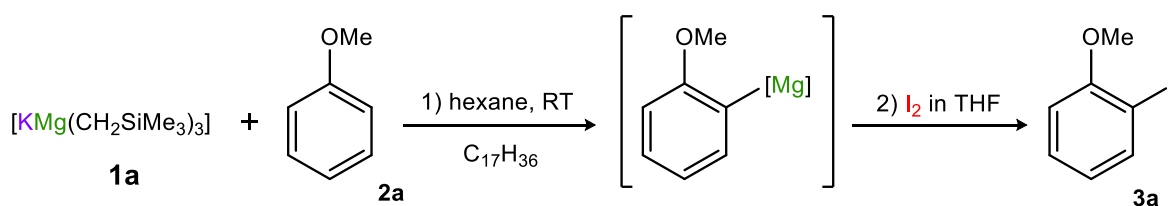
Knochel and co-workers have reported the use of (TMP)MgCl·LiCl for regioselective deprotonation of a wide variety of arenes and heteroarenes.<sup>30</sup> The reaction occurs at ambient temperature and the metallated intermediate can be intercepted with electrophiles giving the relevant *ortho*-substituted products in good yields (81-98%).

Closely related to our work, as mentioned above mixed alkyl amido potassium magnesiate [(PMDETA)KMg(CH<sub>2</sub>SiMe<sub>3</sub>)(TMP)<sub>2</sub>] reacts with **2a** to give [(PMDETA)K(C<sub>7</sub>H<sub>7</sub>O)Mg(CH<sub>2</sub>SiMe<sub>3</sub>)(TMP)] resulting from the *ortho*-magnesiation of anisole. This is unequivocally established by determining the structure of this intermediate by x-ray crystallography (See introduction of this chapter section 2.2.1, **Figure 2.2**). The metallating reagent acts as amido base with the concomitant elimination of TMP(H).

Building on this work we first decided to test the metallation ability of the tris(alkyl) magnesiate **1a** towards **2a** in a 1:1 stoichiometry. The reaction was carried out in hexane at ambient temperature. Aliquots of the reaction mixture were analysed at different periods of time by gas chromatography (GC) with the purpose to study the reaction over time. These experiments also allowed gathering very useful information with regards to the kinetics of the deprotonative metallation process. Mixed metal reagent **1a** was dissolved in hexane in an oven dried Schlenk (**S1**). Another Schlenk was filled with 1 equivalent of **2a** and 3 drops of

heptadecane (**S<sub>2</sub>**) which was used as an internal standard to estimate the final conversion of the reaction. Time zero ( $t_0$ ) was given by analysis of one aliquot of (**S<sub>2</sub>**) before the reaction started. Then (**S<sub>2</sub>**) was added dropwise to (**S<sub>1</sub>**) with a needle allowing the reaction to start. Aliquots were then quenched with iodine at different times and analysed by GC. The amount of **2a** (**I<sub>A</sub>**) and internal standard (**I<sub>S</sub>**) left would be obtained by integrations of the corresponding signals in the GC. Taking into account that internal standard did not react, conversions are obtained by comparison between the ratios  $I_A/I_S$  at a time  $t_n$  with the same ratio at the time over  $t_0$  (**Table 2.1**).

**Table 2.1:** Estimated reaction conversion percentages of the reaction between **1a** and **2a**.



time (min)	$I_A$	$I_S$	$I_A/I_S$	Conv. (%)
$t_0 = 0$	68.21	31.79	2.15	0
$t_1 = 15$	66.73	33.27	2.01	6.5
$t_2 = 30$	66.34	33.66	1.97	8.1
$t_3 = 60$	65.83	34.17	1.93	10.2
$t_4 = 120$	64.47	35.53	1.81	15.4

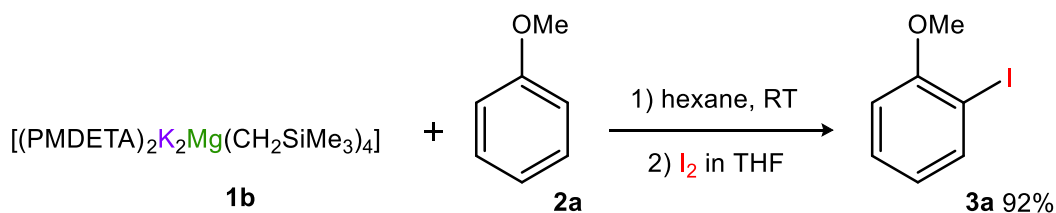
The conversions could then be estimated using mathematical equation 1:

$$\text{Conversion } (t_n) = \left[ 1 - \left( \frac{\left( \frac{I_A}{I_S} \right)_{t_n}}{\left( \frac{I_A}{I_S} \right)_{t_0}} \right) \right] 100$$

**Equation 2.1:** Formula employed to obtain the final conversions of the *ortho*-metallation reactions.

Mixing compound **1a** in hexane, resulted in a white suspension. After the addition of **2a** the suspension turned yellow. The suspensions stayed yellow even when allowing to stir over 20 hours (18% conversion after 20 hour reaction time). The method employed measured the conversion in terms of consumption of **2a**, the same result could be obtained when looking at the values of the signals for the formation of 2-iodoanisole (**3a**), as this was the only product formed in this reaction.

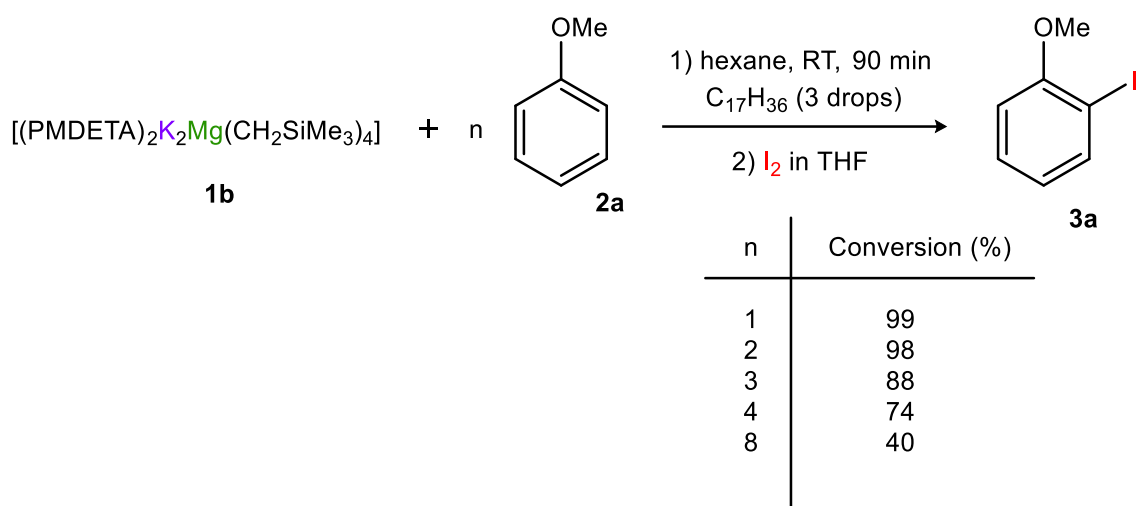
We then looked at the reactivity of higher-order magnesiate **1b**. Equimolar amounts of **2a** and *in situ* prepared compound **1b** in hexane were mixed, affording a clear solution which after 5 minutes deposited a colourless oil. The reaction was quenched after 90 minutes with excess of iodine. Product **3a** was obtained selectively in a quantitative 99% conversion by GC. The product was isolated as a colourless oil (isolated yield 92%) and characterised by <sup>1</sup>H and <sup>13</sup>C NMR and GC-MS and elemental analysis (Scheme 2.10).<sup>31</sup>



**Scheme 2.10:** *Ortho*-metallation of anisole using base **1b** under stoichiometric reaction conditions.

Considering the homoleptic alkyl constitution of **1b** we then decided to assess the potential of this bimetallic system to display polybasicity employing some of its remaining alkyl groups. It should be noted that although it is not common, polybasic behaviour has been previously noted in other bimetallic systems. Thus for example [Li<sub>2</sub>Mg(TMP)Bu<sub>3</sub>] can react with 3 equivalents of 1,3-difluorobenzene (**2d**), at -10 °C, for 2 hours followed by iodine quenching, allowing the relevant 1,3-difluoro-2-iodobenzene product (**3d**) in good yield (73%).<sup>32</sup>

Therefore, to explore this possibility, potassium magnesiate **1b** was reacted with variable amounts of **2a**. The same procedure as described for the studies of compound **1a** was employed to assess the conversion of **2a** to **3a** (Scheme 2.11).



**Scheme 2.11:** Reactivity study of potassium magnesiate **1b** towards variable amounts of **2a**.

As previously described when using equimolar amounts of **1b** and **2a**, full conversion is observed. Similarly employing two and three molar excess of the substrate, led to the formation of **3a** in excellent yields (98 and 88% respectively). Slightly lower conversions (74%) are obtained when using four equivalents of **2a**. These findings evidence the ability of **1b** to display polybasicity, using at least three of its four potential basic arms. Thus, the co-complexation of  $\text{Mg}(\text{CH}_2\text{SiMe}_3)_2$  with two equivalents of  $\text{K}(\text{CH}_2\text{SiMe}_3)$  in the presence of a Lewis donor leads to the formation of a new metallating reagent with three active basic sites, capable to effectively promote regioselective direct magnesiation of **2a** under mild reaction conditions. Since only 0.33 equivalents of **1b** are required to quantitatively *ortho*-metallate one equivalent of **2a**, this bimetallic approach can be described as atom-efficient.<sup>33</sup> The reaction of base **1b** with three equivalents of **2a** was also monitored by GC over different periods of time (**Figure 2.5**).

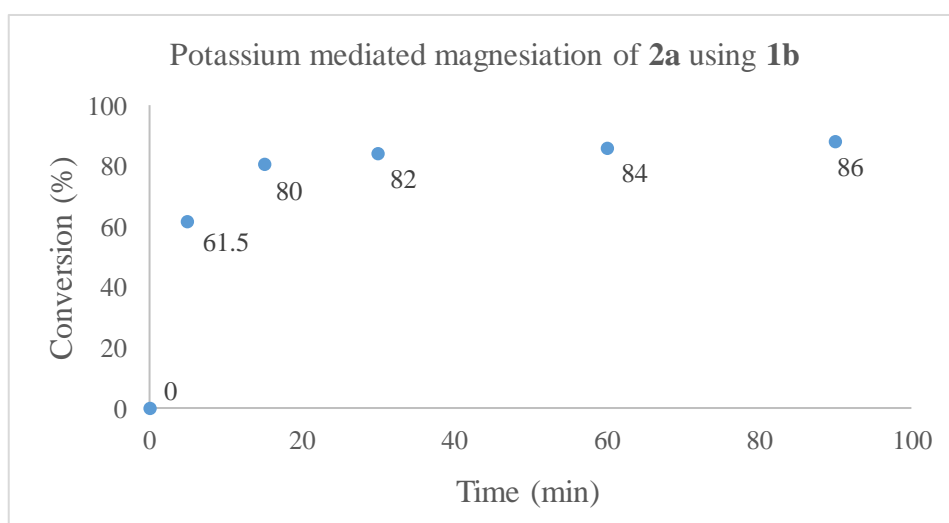
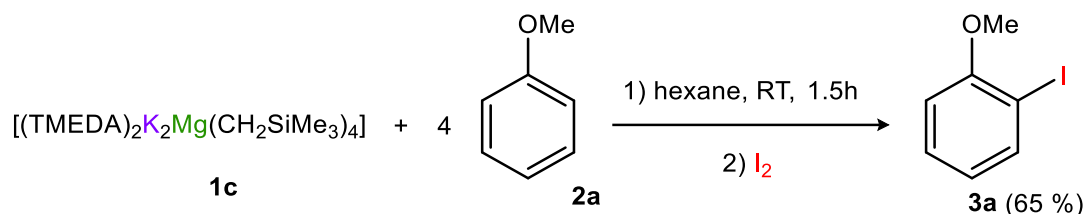


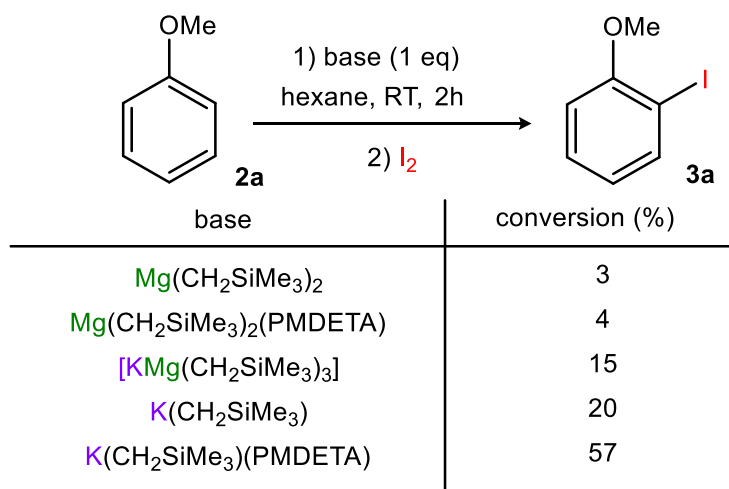
**Figure 2.5:** GC monitored reaction of **1b** with 3 equivalents of **2a**.

After only five minutes, 62% of **2a** was efficiently *ortho*-metallated (**Figure 2.5**). The rest of **2a** left in solution undergoes metallation more slowly to a maximum of 88% after 90 minutes. In order to assess the effect that Lewis base present in the tetraorganomagnesiates can have in its reactivity, we also carried out the reaction of 4 equivalents of **2a** with one equivalent of the TMEDA-solvate **1c** (**Scheme 2.12**).



**Scheme 2.12:** Reactivity of bimetallic compound **1c** towards anisole metallation

Compound **1c** successfully *ortho*-metallates **2a**, obtaining **3a** in good conversions (65% conversion obtained by GC using internal standard). A comparison of this conversion with that obtained using PMDETA-derivative **1b**, shows that under the same conditions **1b** is a slightly better base (74% conversion, **Scheme 2.11**). The reactivity of these bimetallic systems was compared to those exhibited by their homometallic counterparts  $\text{K}(\text{CH}_2\text{SiMe}_3)$  and  $\text{Mg}(\text{CH}_2\text{SiMe}_3)_2$ . Thus following the same approach **2a** was confronted with  $\text{Mg}(\text{CH}_2\text{SiMe}_3)_2$  in hexane, stir at ambient temperature for 2 hours followed by iodine quenching. An aliquot of the reaction mixture was then analysed by GC (**Scheme 2.13**).



**Scheme 2.13:** Reactivity of  $\text{Mg}(\text{CH}_2\text{SiMe}_3)_2$ ,  $\text{Mg}(\text{CH}_2\text{SiMe}_3)_2(\text{PMDETA})$ ,  $\text{K}(\text{CH}_2\text{SiMe}_3)$ ,  $\text{K}(\text{CH}_2\text{SiMe}_3)(\text{PMDETA})$  and **1a** towards **2a**.

Since the addition of a Lewis donors can greatly increase the reactivity of single-metal organometallic reagents<sup>34</sup> the reaction of equimolar amounts of  $\text{K}(\text{CH}_2\text{SiMe}_3)$  and PMDETA with anisole at ambient temperature was also investigated (**Figure 2.6**).

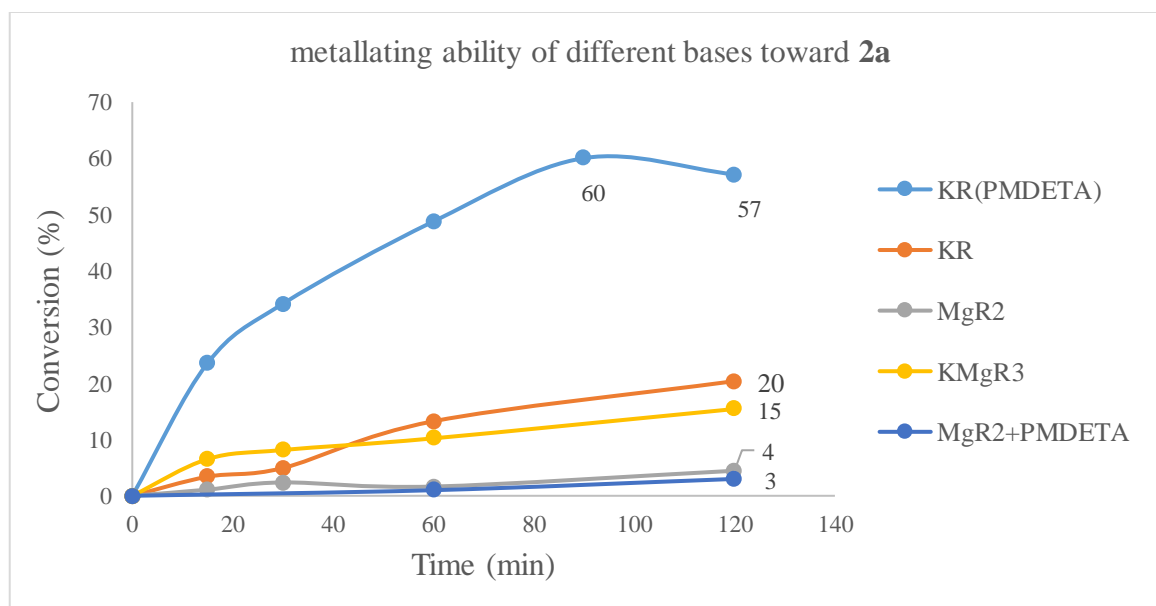


**Figure 2.6:** Comparison of reactivity between monometallic reagents  $\text{K}(\text{CH}_2\text{SiMe}_3)$ ,  $\text{Mg}(\text{CH}_2\text{SiMe}_3)_2$ ,  $(\text{PMDETA})\text{K}(\text{CH}_2\text{SiMe}_3)$  and the bimetallic base **1a** towards metallation of one equivalent of **2a**.

$\text{Mg}(\text{CH}_2\text{SiMe}_3)_2$  fails to deprotonate anisole under these reaction conditions (**Scheme 2.13**), the same happens with an equimolar mixture of  $\text{Mg}(\text{CH}_2\text{SiMe}_3)_2$  and PMDETA, which does not greatly enhance the reactivity of this compound. The mixed metal compound **1a** and  $\text{K}(\text{CH}_2\text{SiMe}_3)$  exhibit poor reactivity, whereas when a 1:1 mixture of  $\text{K}(\text{CH}_2\text{SiMe}_3)$  and

PMDETA is employed 57% conversions are observed after 2h (**Figure 2.6**), showing that the addition of PMDETA truly activates  $\text{K}(\text{CH}_2\text{SiMe}_3)$  towards deprotonation of anisole. This can be rationalised in terms of the Lewis-donor activation. This effect has been previously described for the metallation of anisole using BuLi. On the addition of TMEDA the reaction occurs quantitatively however in the absence of this Lewis base, BuLi forms a donor-complex with anisole, and no metallation takes place.<sup>27–29</sup> Although the structure of  $\text{K}(\text{CH}_2\text{SiMe}_3)$  is not known, it can be expected to be a high aggregate species (i.e.  $\text{Li}(\text{CH}_2\text{SiMe}_3)$  is a hexamer, whereas  $\text{Na}(\text{CH}_2\text{SiMe}_3)$  forms a polymeric chain made up of  $\{\text{Na}(\text{CH}_2\text{SiMe}_3)\}_4$  tetramers), as by the addition of PMDETA this supramolecular structure can be broken down to form a smaller polymeric aggregate that will be more reactive (**Figure 2.7**).

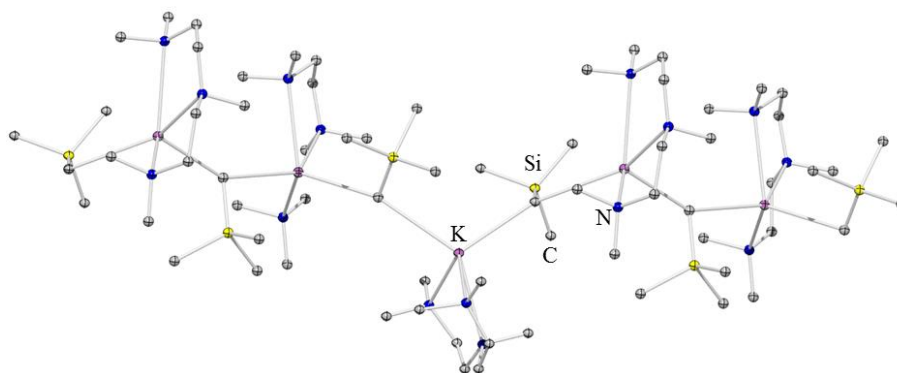


**Figure 2.7:** Portion of the polymeric structure of PMDETA solvated  $\text{KCH}_2\text{SiMe}_3$ .

It should be noted that although  $[(\text{PMDETA})\text{K}(\text{CH}_2\text{SiMe}_3)]$  can deprotonate **2a** at ambient temperature, the relevant potassium aryl organometallic intermediate appears to decompose in solution overtime. Thus, while GC analysis of the reaction crude showed a 60% conversion after 90 minutes of the addition time, when a new aliquot of the reaction mixture was analysed after 16h the conversion to **3a** decreased to 34%. This lack of stability contrasts with the results found using the bimetallic combination  $[(\text{PMDETA})_2\text{K}_2\text{Mg}(\text{CH}_2\text{SiMe}_3)_4]$  **1b** as a base where the relevant organometallic intermediate is stable in solution under argon atmosphere over significantly longer periods of time, without observing any substantial difference in the conversion rates between 3 hours and 72 hours, this can be rationalised by the formation of an aryl magnesium species rather than a potassium aryl intermediate, which would be expected to be more stable due to the more covalent (or less polar) character of the Mg-C bonds versus K-C bonds.

In order to study the alkali-metal effect in these bimetallic reagents, the reactivity of  $[(\text{TMEDA})_2\text{Na}_2\text{Mg}(\text{CH}_2\text{SiMe}_3)_4]$  (**1d**) and  $[(\text{TMEDA})_2\text{Li}_2\text{Mg}(\text{CH}_2\text{SiMe}_3)_4]$  (**1e**) was studied.

Compound **1e** has been previously prepared and structurally defined in our group<sup>35</sup> and exhibits the same linear motif AM...Mg...AM as that described for compound **1b** where magnesium is bonded to four alkyl groups (**Figure 2.8**).

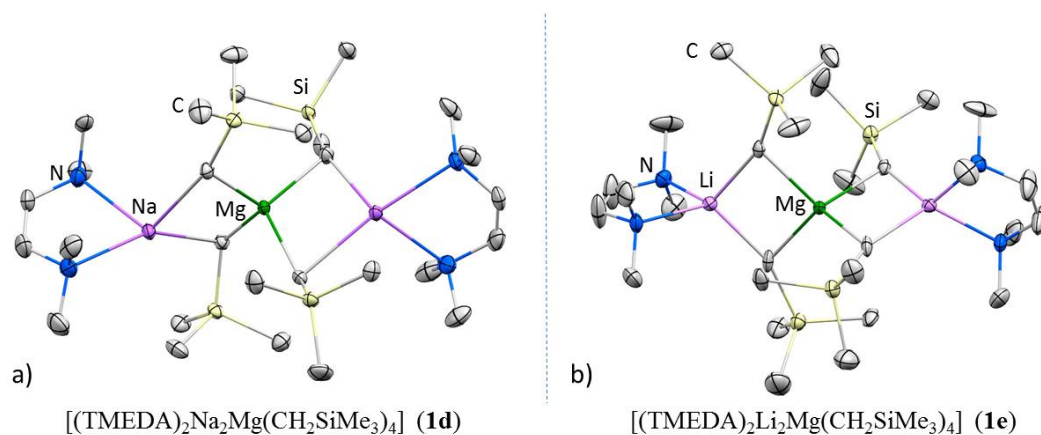
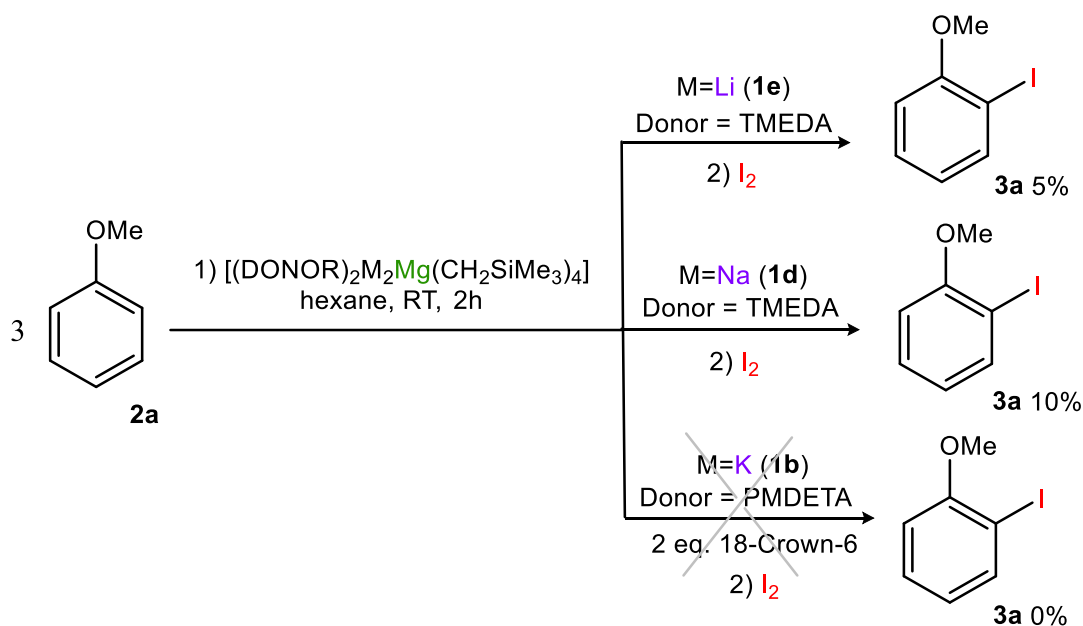


**Figure 2.8:** Monomeric units of a) **1d** and b) **1e**

Interestingly, using **1d** and **1e** under the same conditions previously described for the reactions of **1b** and **1c**, no substantial metallation of anisole was detected (**Scheme 2.14**).



**Scheme 2.14:** Reactivity of **1d** and **1e** towards metallation of **2a**.

This lack of reactivity illustrates the important role of the alkali metal counterpart in these magnesiate systems. Furthermore when the reaction of **1b** with anisole is carried out in the presence of two equivalents of 18-crown-6 which presumably captures the K cations, no iodoanisole is observed after quenching with iodine. These findings suggest that these reactions must operate via contacted-ion pair mixed-metal intermediates (CIP), being genuine examples

of potassium-mediated magnesiations. The enhanced reactivity of **1b** can be rationalised by the synergic partnership between the metals. By forming a higher-order magnesiate, the low kinetic basicity of the Mg–C bonds in MgR<sub>2</sub> can be overcome, but the K cations also play a major role in the process, coordinating to anisole, bringing its *ortho*-H in close proximity to the activated magnesiate anion.

### 2.3.3 Magnesiation of substituted aromatic substrates

The results and substrates screened in this section are summarised in **Table 2.2**:

**Table 2.2:** Reaction conditions and yields for the deprotonation reaction of different substituted aromatic substrates using **1b**.

Entry	substrate	Eq of <b>1b</b>	conditions	Product (Yield %) <sup>a</sup>
1	 <b>2a</b>	0.33	20 °C 1.5 h	 <b>3a</b> (78%) E = I <b>3a'</b> (84%) E = CO <sub>2</sub> H
2	 <b>2b</b>	0.33	20 °C 2 h	 <b>3b</b> (70%)
3	 <b>2c</b>	0.33	0 °C 1.5 h	 <b>3c</b> (52%) <b>3c'</b> (12%)
4	 <b>2c</b>	1	0 °C 1.5 h	 <b>3c</b> (94%)
5	 <b>2d</b>	0.33	0 °C 1.5 h	 <b>3d</b> (64%) <sup>b</sup> E = I <b>3d'</b> (52%) E = CO <sub>2</sub> H

6		0.33	0 °C 1.5 h	<b>3e</b> (43%) <sup>b</sup> <b>3e'</b> (4%) <sup>b</sup>
7		1	0 °C 1.5 h	<b>3e</b> (85%) <sup>b</sup> <b>3e'</b> (5%) <sup>b</sup>

<sup>a</sup>Yields refer to isolated yields of analytically pure products (>95% purity determined by NMR or GC-analysis) unless otherwise stated. <sup>b</sup>Yield was determined by <sup>1</sup>H-NMR analysis using ferrocene as internal standard.

As previously mentioned, metallation of relatively inert C-H bonds is one of the most useful synthetic methodologies. Benzene can be considered a challenging substrate towards metallation reaction, primarily due to the high  $pK_a$  value of its hydrogen atoms ( $pK_a = 44.7$ ) (**Figure 2.9**)<sup>36</sup> as well as the lack of activating directing groups. Previous work by Mulvey has shown that sodium magnesiate reagents can promote two-fold metallation of benzene at its sterically optimum positions 1 and 4.<sup>37,38</sup>

The presence of substituents in the aromatic molecule can affect dramatically the acidity of the aromatic protons of the ring due to electronic (resonance and inductive) effects. These substituents can greatly influence the regioselectivity of the metallation process (**Figure 2.9**).<sup>36</sup>

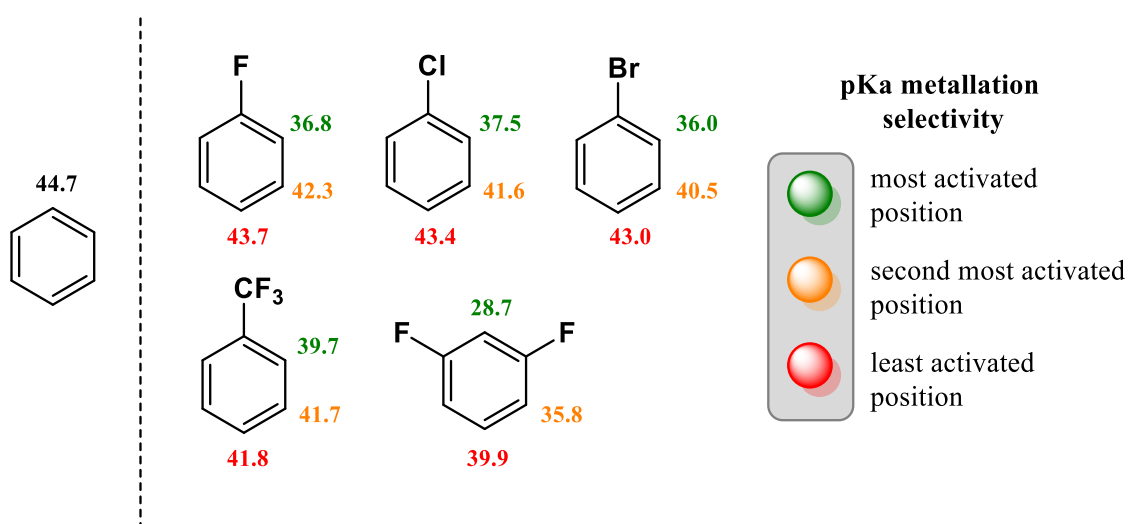
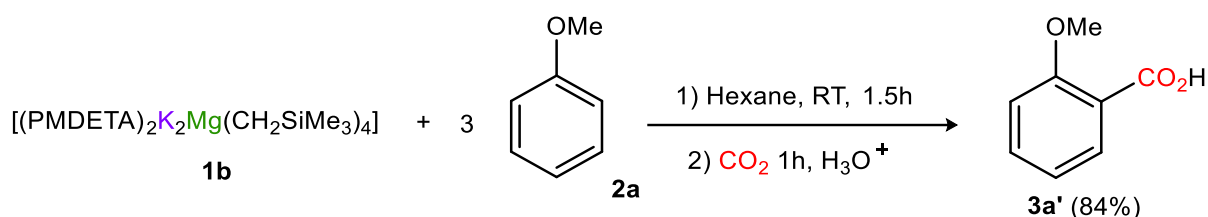


**Figure 2.9:** Theoretical predicted  $pK_a$  values of different substituted aromatic substrates.<sup>36</sup>

**Figure 2.9** depicts several aromatic molecules and the calculated  $pK_a$  values for their corresponding hydrogen atoms in DMSO solution. It is important to take into account that  $pK_a$

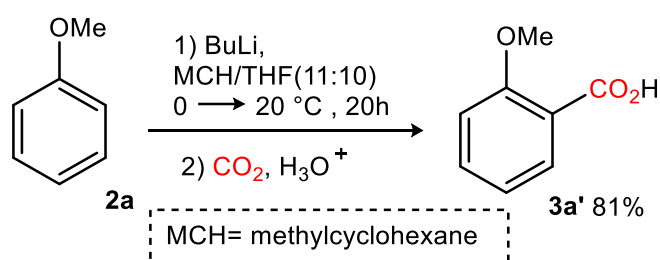
values vary according to the solvent used for the reaction, thus these values will be used principally for information purposes.

Based on the magnesiation efficiency of the bimetallic compound **1b** towards anisole we also decided to investigate the insertion reaction of CO<sub>2</sub> through different aryl and hetero-aryl magnesiate intermediates. The reaction of three equivalents of anisole with one equivalent of **1b** was quenched after 1.5 hours with an excess of CO<sub>2</sub> resulting from the evaporation of solid CO<sub>2</sub> (dry ice) which was bubbled through the reaction mixture via cannula. The reaction gave 2-methoxybenzoic acid (**3a'**) after acid/basic extraction selectively in a good 84% isolated yield (**Scheme 2.15**).<sup>39</sup>



**Scheme 2.15:** Magnesiation of **2a** using **1b** followed by insertion reaction of CO<sub>2</sub>.

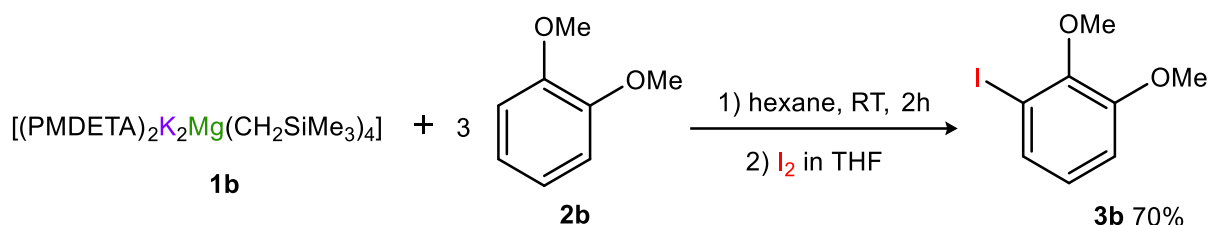
The yield of the isolated pure product is similar compared to the pure 2-iodoanisole (**3a**) obtained by iodination of the *ortho*-magnesiated intermediate under the same reaction conditions (78% yield obtained of **3a**). In the literature different ways have been described for the preparation of compound (**3a'**). A deprotonation approach has been described by Screttas regarding the use of organolithium reagents in methylcyclohexane/THF solutions at 0 °C for 20 hours (**scheme 2.16**).<sup>39</sup>



**Scheme 2.16:** Screttas *ortho*-lithiation approach of **2a** for the synthesis of **3a'**.

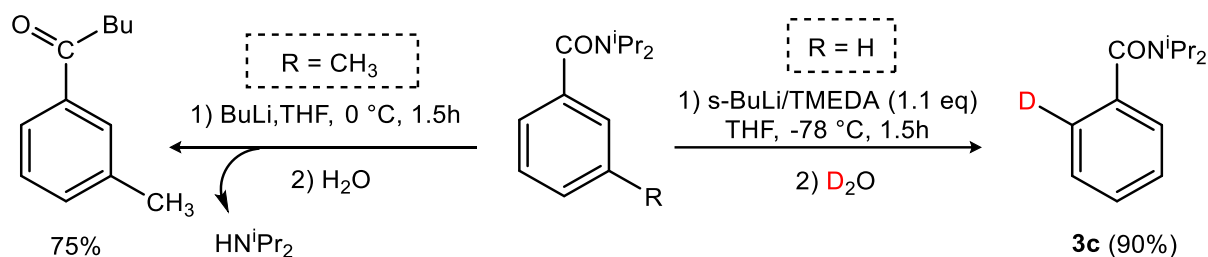
Thrilled by our initial results on the reactivity studies of **1b** with anisole (**2a**), we next explored the reactivity of **1b** towards metallation of 1,2-dimethoxybenzene (**2b**). This substrate has been previously studied in direct *ortho*-metalation chemistry. For example M. Uchiyama *et al* described the *ortho*-aluminum of **2b** at 0 °C for 4h using <sup>i</sup>Bu<sub>3</sub>Al(TMP)Li and after iodine quenching 1-iodo-2,3-dimethoxybenzene (**3b**) was isolated in good yields (74%).<sup>40</sup> Despite the

good outcome of this reaction procedure excess of the Li-aluminate complex (2.2 eq) is required for the reaction to take place. When we reacted **1b** with 3 equivalents of **2b** at ambient temperature for 2 h followed by iodine quenching, **3b** was isolated in a good yield (70%) (**Scheme 2.17**).



**Scheme 2.17:** Magnesiumation of **2b** using **1b**.

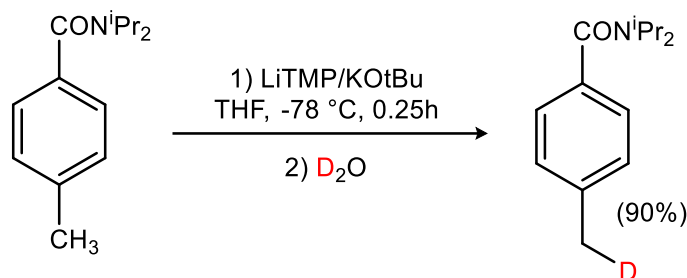
We then moved to an aromatic substrate containing an electron withdrawing group ( $\text{CON}^i\text{Pr}_2$ ) such as *N,N*-diisopropylbenzamide (**2c**). This aromatic substrate has been widely studied in metallation reactions due to the strong *ortho*-directing effect of the *N,N*-diisopropylbenzamide substituent.<sup>41</sup> For example, in the case of lithiations, tertiary amides stabilise the intermediate by interaction between the Lewis basic moiety (lone pair electrons of the nitrogen) with the Lewis acidic lithium cation, favouring the deprotonation in the vicinal *ortho*-position to the amide group. As a drawback these compounds suffer from addition to the amide, especially when organolithium reagents are employed. Sub-ambient temperatures ( $-78^\circ\text{C}$ ) are required along with the use of hindered substituents such as the  $\text{CON}^i\text{Pr}_2$  group to hinder the addition to the amide, thus favouring the *ortho*-metallation (**Scheme 2.18**).<sup>42–45</sup>



**Scheme 2.18:** Reactivity of different organolithium compounds with substrates containing the  $\text{CON}^i\text{Pr}_2$  group.

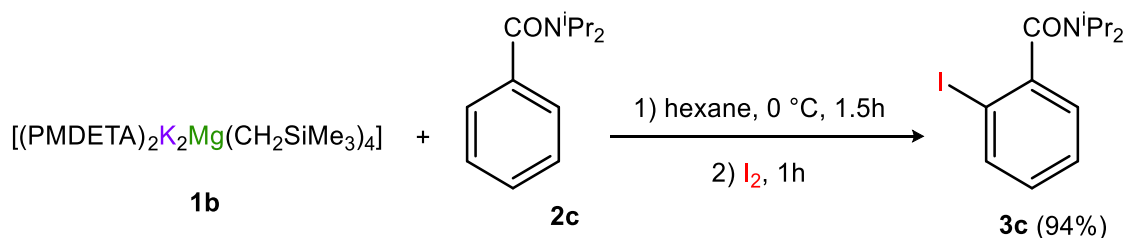
Work by Kondo, Uchiyama and Mulvey using mixed  $\text{Li/Al}$ ,<sup>31,40</sup>  $\text{Li/Zn}$ <sup>46</sup> and  $\text{Na/Zn}$ <sup>47,48</sup> reagents demonstrated that *ortho*-metallation of this sensitive substrate can be effectively carried out at room temperature, without observing side reactions at the  $\text{C=O}$  bond. Particularly interesting is to compare these results with the selective benzylic activation of *N,N*-diisopropyl-4-

methylbenzamide using LiTMP/KOtBu as described by O'Shea, where no *ortho*-metallation product was obtained (**Scheme 2.19**).<sup>49</sup>



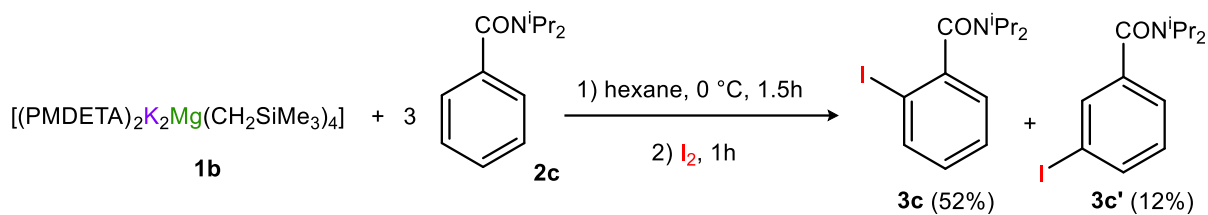
**Scheme 2.19:** O'Shea benzylic activation of *N,N*-diisopropyl-4-methylbenzamide using LiTMP/KOtBu

The reaction of **1b** with one equivalent of **2c** for 1.5 hours at ambient temperature followed by electrophilic quenching with iodine was also studied. Under these reaction conditions a mixture of 2-iodo-*N,N*-diisopropylbenzamide (**3c**) and other unknown by-products were formed. When the reaction was carried out at 0°C, followed by treatment with iodine, compound **3c** was obtained in excellent isolated yield (94%) (**Scheme 2.20**).



**Scheme 2.20:** Magnesiumation of **2c** using **1b**.

Interestingly when the reaction was carried out using 1 equivalent of base **1b** and 3 equivalents of diisopropylbenzamide for 1.5 hours at 0 °C followed by electrophilic quenching with iodine a mixture of two distinct products was formed which could be separated by column chromatography. <sup>1</sup>H and <sup>13</sup>C NMR analysis revealed the 3-iodo-*N,N*-diisopropylbenzamide (**3c'**) in 12% yield along with **3c** as the major product 52% yield (**Scheme 2.21**).

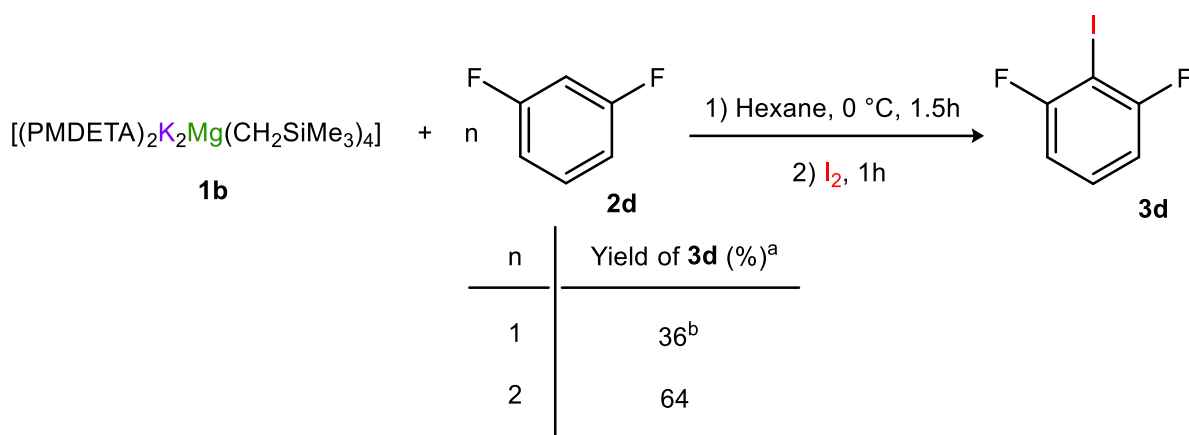


**Scheme 2.21:** Magnesiumation of **2c** using **1b** under sub-stoichiometric conditions.

This result is somehow surprising as the  $\text{CON}(\text{iPr})_2$  group in substrate **2c** is a very strong *ortho*-directing group, and as far as we are aware, there are no examples in the literature of *meta*-deprotonation of this substrate. Attempts to increase the yield of **3c'** by controlling the regioselectivity of the reaction were made by carrying out the reaction at lower temperatures and also by changing the reaction times, however in all cases **3c'** was observed as a minor product.

Another interesting aromatic substrate we looked at was 1,3-difluorobenzene (**2d**). Fluorine is the most electronegative of all the elements and it has one of the highest ionisation potentials, which means that a fluorine substituent has a strong electron-withdrawing effect on chemical bonds, making the C-F bond much more polar than the corresponding C-H bonds.<sup>50</sup> As a result, replacement of hydrogen with fluorine in C-H bonds of an organic molecule greatly polarises the bond with variation on the steric properties of the compound which can lead to significantly different physical properties and biological activity.<sup>51–54</sup>

Potassium magnesiate **1b** was employed for the metallation of **2d** at 0 °C for 1.5 hours. Iodine quench gave 1,3-difluoro-2-iodobenzene (**3d**) selectively in a 64% <sup>1</sup>H NMR yield. Attempts to isolate the product by column chromatography resulted in decomposition. The yield was therefore obtained by <sup>1</sup>H NMR analysis of the crude with addition of 10 mol% of ferrocene as internal standard after extraction of the final product (**Scheme 2.22, Figure 2.10**).



<sup>a</sup>Yield determined by integration of corresponding signals for the iodinated product in the <sup>1</sup>H NMR with the addition of 10 mol% of ferrocene as internal standard to the iodinated product. <sup>b</sup>decomposition of product observed

**Scheme 2.22:** Magnesium of 1,3-difluorobenzene using base **1b**.

The reaction was also carried out with 1 equivalent of base **1b** and 1 equivalent of **2d** at 0 °C, however after just 5 minutes of reaction a black precipitate was observed in solution. The iodine quenching after 1.5 hours yielded **3d** in a poor 36% yield (obtained by <sup>1</sup>H NMR) confirming the decomposition of the metallated intermediate **3d** under these reaction conditions.

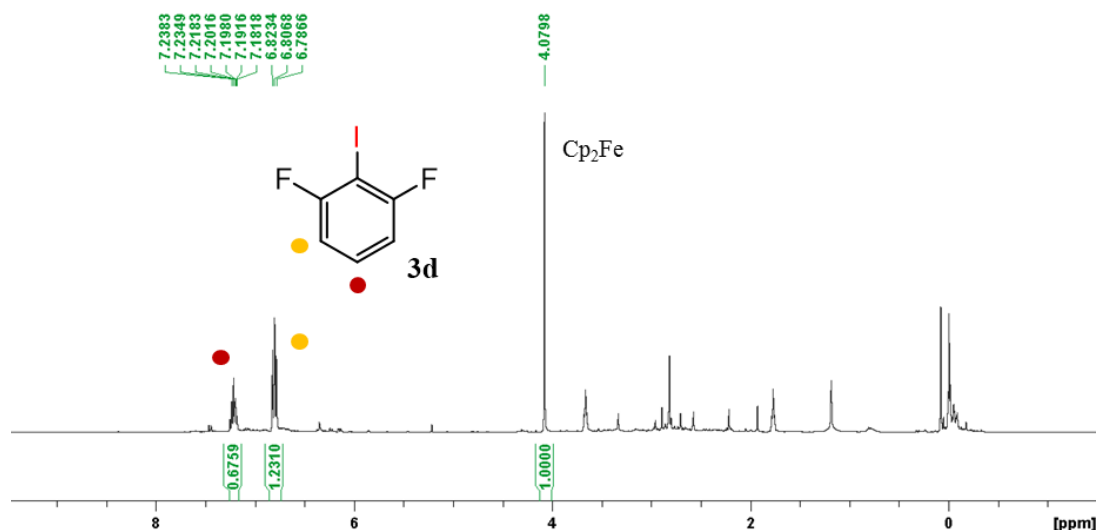
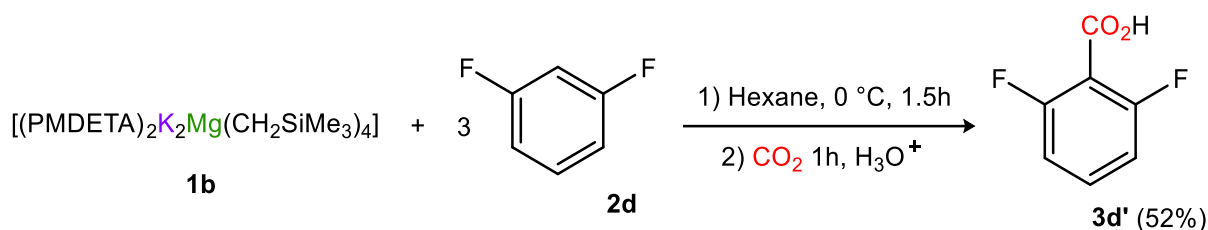


**Figure 2.10:** <sup>1</sup>H NMR yield for the magnesium of **2d** using **1b**.

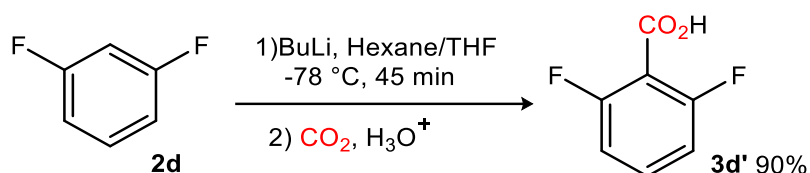
Despite the moderate yield obtained no other by-products or starting material were observed in the <sup>1</sup>H NMR spectrum. The fact that no starting material can be detected is due to the high volatility of **2d** (boiling point = 83.9 °C at atmospheric pressure) which can then be easily removed under vacuum while removing solvents after extraction in the Schlenk line. When the reaction was carried out between **1b** and 3 equivalents of **2d** at 0 °C followed by electrophilic

quenching with CO<sub>2</sub> (dry ice), which after acid/basic work up gave a moderate isolated 52% yield of 2,6-difluorobenzoic acid (**3d'**) (**Scheme 2.23**). This result is similar when compared to the yield obtained for the formation of 1,3-difluoro-2-iodobenzene (**3d**) (64% yield obtained by <sup>1</sup>H NMR) (**Scheme 2.23**).



**Scheme 2.23:** Magnesiumation of **2d** using **1b** for the synthesis of **3d'**

Carboxylic acid (**3d'**) has been previously synthesised using BuLi, in a 1:2.2 mixture of hexane and THF solution at -78 °C for 45 minutes (**Scheme 2.24**).<sup>55</sup>



**Scheme 2.24:** BuLi promoted deprotonation of 1,3-difluorobenzene

Despite the high yield of **3d'**, generally a more polar (and therefore nucleophilic) aryl lithium intermediate imposes the use of very low temperature (-78 °C). Potassium magnesiate **1b** was also employed for the metallation of trifluorotoluene (**2e**) at 0 °C. This substrate is frequently employed as a solvent in synthesis.<sup>56</sup> It is also a common fragment present in more complex molecules with relevance in the preparation of pharmaceuticals and agrochemicals.<sup>57</sup> Considering the strong electron withdrawing effect of the CF<sub>3</sub>, this group can be described as *ortho*-directing group, however due to its relative large size,<sup>58,59</sup> in some cases the deprotonation of **2e** can give mixtures of *ortho*, *meta* and *para*-substituted products.<sup>34</sup> Thus for example **2e** when treated with BuLi in ether at 35 °C followed by electrophilic quenching with CO<sub>2</sub> affords a mixture of *ortho*- and *meta*-carboxylic acids in a combined 48% yield and in a ratio of 5:1, respectively, along with trace amounts of the *para*-isomer.<sup>60</sup> In contrast, using the bimetallic “LIC-KOR” base BuLi·KO<sup>t</sup>Bu in THF solvent at -78°C,<sup>61-64</sup> Schlosser observed regioselective *ortho*-deprotonation.<sup>65</sup>

In our laboratory it has been recently shown that the direct zincation of **2e** at ambient temperature using the zincate [(TMEDA)NaZn(TMP)(<sup>t</sup>Bu)<sub>2</sub>] results in a mixture of *ortho*-,

*meta*-, and *para*-zincated ring products in a respective ratio of 20:11:1.<sup>66</sup> Also studies by Uchiyama of the alumination of **2e** through reaction with aluminate [LiAl(TMP)(*t*Bu)<sub>3</sub>] at 0 °C revealed the *meta*-product to be the predominant regioisomer (20% isolated yield), along with 10% *ortho*- and 10% *para*-metallation products.<sup>31</sup> Showing the importance that the donor solvent or Lewis bases added as additives play in the metallation of this substrate, recently a synthetic study carried out in our group for the deprotonation of **2e** by single-metal bases BuLi and BuNa revealed that the yield and regioselectivity of the metal-hydrogen exchange process can be controlled by the Lewis donors present in the reaction media (**Table 2.3**).<sup>34</sup>

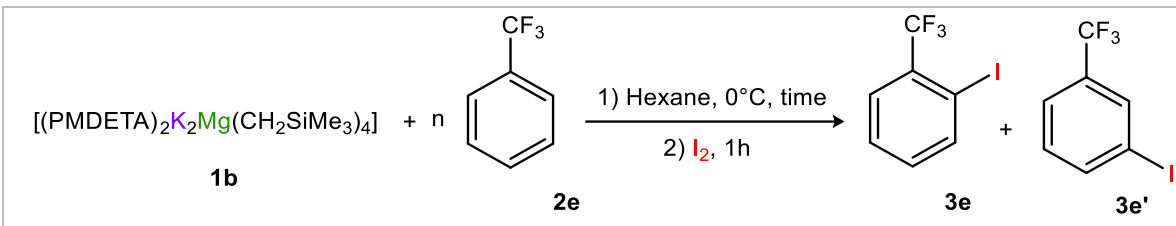
**Table 2.3:** Effect of varying the metal reagent and the donor solvent in the ratio of the Iodo-trifluorotoluene regioisomers.

Entry	metal alkyl	donor	Iodinated products Yield(%) <sup>a</sup>			
			ortho	meta	para	total
1	BuLi	none	0	0	0	0
2	BuLi	THF	30	26	13	69
3	BuLi	TMEDA	65	10	6	81
4	BuNa	none	8	0	0	8
5	BuNa	THF	43	0	0	43
6	BuNa	TMEDA	72	0	0	72
7	BuNa	PMDETA	80	1	1	82

<sup>a</sup>Yield determined by integration of corresponding signals for the iodinated product in the <sup>1</sup>H NMR with the addition of 10 mol% of ferrocene as internal standard to the iodinated product.

Building on these precedents we studied the magnesiation of **2e** using mixed potassium-magnesiate reagent **1b**. Using 3 equivalents of the organic substrate **2e** in hexane at 0 °C for 30 mins, followed by electrophilic quenching with iodine led to the formation of the *ortho* and *meta*-substituted products 1-iodo-2-(trifluoromethyl)benzene (**3e**) and 1-iodo-3-(trifluoromethyl)benzene (**3e'**) respectively in a 8:1 ratio with a combined yield of 43%. It should be noted that this yield was established by integration of the representative signals for each compound in the aromatic region using 10 mol% of ferrocene as an internal standard. The reaction was studied over different periods of time (**Table 2.4**).

**Table 2.4:** Magnesiumation of trifluorotoluene using base **1b**.

				
Entry	n	Time (h)	Ratio (3e:3e')	Yield (%) <sup>a</sup>
1	3	0.5	8:1	43
2	3	1.5	11:1	47
3	3	4	10:1	44
4	1	1.5	17:1	90

<sup>a</sup>Yield determined by integration of corresponding signals for the iodinated product in the <sup>1</sup>H NMR with the addition of 10 mol% of ferrocene as internal standard to the iodinated product.

Base **1b** was allowed to react with trifluorotoluene for 0.5 hours, 1.5 and 4 hours respectively before iodine was added to the reaction mixture. The reaction time does not affect the reactivity of **1b** towards deprotonation of **2e**, as the yields (43%, 47% and 44% entries 1,2 and 3 **Table 2.4**) are similar in all cases. In addition there is also no increase in formation of product **3e'** with respect to **3e**. Repeating this reaction using 1 equivalent of **2e** rather than 3 gave an improved yield of metallated product (90%) along with a greater control of the regioselectivity (17:1 of *ortho* and *meta*-products respectively) (**Figure 2.11**).

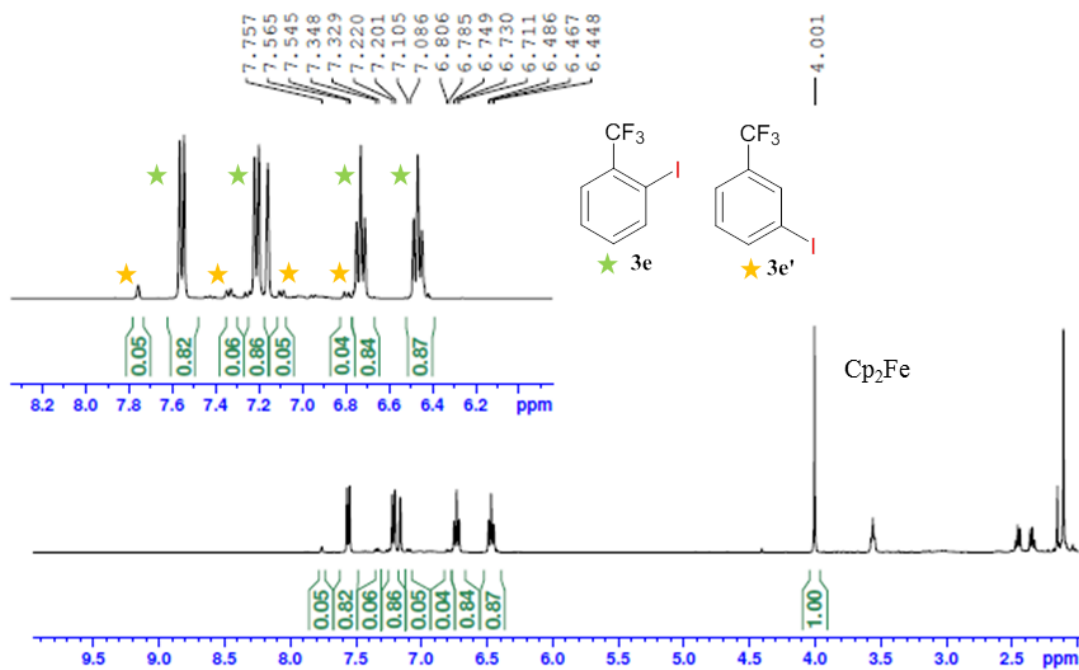


**Figure 2.11:**  $^1\text{H}$  NMR yield for the magnesianation of **2d** using **1b**.

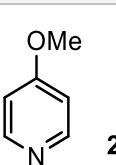
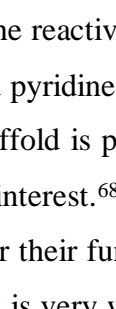
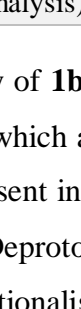
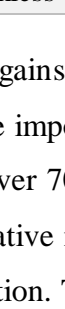
These results suggest that for this substrate **1b** may not be effectively acting as a polybasic reagent employing 3 of its 4 basic arms as we have previously seen for substrate **2a**.

## 2.4 Magnesium studies on N-heterocyclic substrates.

### 2.4.1 Studies using methoxy substituted pyridines.

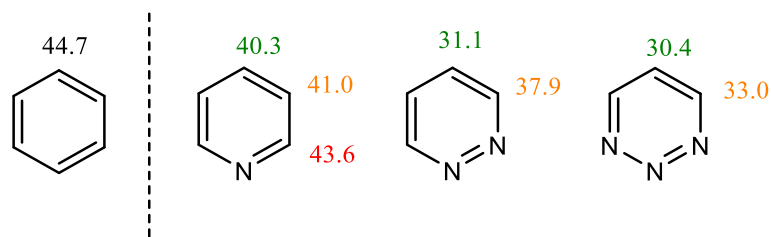
The results and substrates screened in this section are summarised in **Table 2.5**.

**Table 2.5:** Reaction conditions and yields for the deprotonation of different substituted pyridines using **1b**.

Entry	Substrate	Eq. of <b>1b</b>	Product (Yield %) <sup>a</sup>
1	 <b>2f</b>	0.33	 <b>3f</b> (70%)
2	 <b>2g</b>	0.33	 <b>3g</b> (75%)
3	 <b>2h</b>	0.33	 <b>3h</b> (58%)

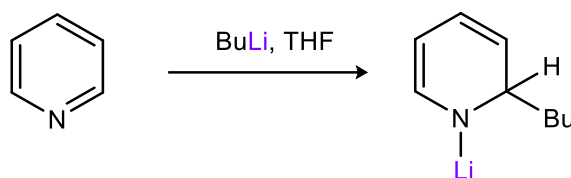
<sup>a</sup>Yields refer to isolated yields of analytically pure products (>95% purity determined by NMR or GC-analysis) unless otherwise stated.

We then decided to study the reactivity of **1b** against a series of heterocyclic molecules. We first focussed on substituted pyridines which are important building blocks in pharmaceutical industry.<sup>67</sup> The pyridine scaffold is present in over 7000 existing drugs, thus the methods for their synthesis are of great interest.<sup>68</sup> Deprotonative metallation is one of the most important methodologies employed for their functionalisation. The acidity of hydrogens in benzene and pyridine without substituent is very weak ( $pK_a > 40$ )<sup>36</sup> however the hydrogens in pyridine are more activated than in benzene (in terms of  $pK_a$ ), nevertheless their acidity is still weak. The high  $pK_a$  value is related to the highly-conjugated p-orbitals in the ring, therefore, if more nitrogen atoms are introduced into the ring, there is a decrease in aromaticity leading to more acidic protons (**Scheme 2.25**).



**Scheme 2.25:** Theoretical predicted acidities  $pK_a$  of 6-membered aromatic heterocycles.

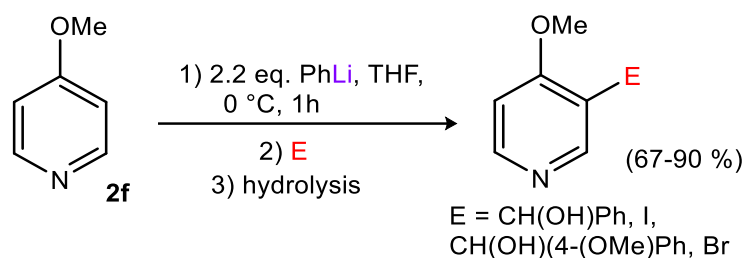
Hydrogens in C<sub>4</sub> position of a pyridine are 700 times more acidic than hydrogens in the C<sub>2</sub> position. Selective direct lithiation of electron deficient heteroaromatics such as pyridines can be difficult, as the competitive nucleophilic addition process to the C=N bond can take place rather than the metallation reaction (**Scheme 2.26**).<sup>69</sup>



**Scheme 2.26:** General reactivity observed in lithiation of pyridines.

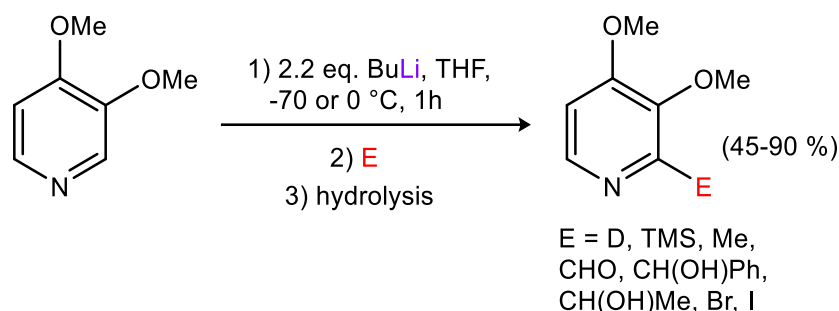
A solution to this problem can be the use of ligands with donor groups to enhance the basicity of the alkyllithium reagent. For example LiDMAE = Me<sub>2</sub>N(CH<sub>2</sub>)<sub>2</sub>OLi can be employed with two molar equivalents of *n*-butyllithium (at -78°C) in hexane solution to successfully lithiate pyridine in the 2-position, and further obtain the 2-substituted pyridines after electrophilic quenching in yields from 25-80%.<sup>70</sup> Sterically demanding lithium amides, such as LDA and LiTMP can also be used to deprotonate pyridines in good yields.<sup>71</sup>

In the early 90's different methods were reported for the deprotonation of methoxypyridines.<sup>71</sup> The lithiation of 4-methoxypyridine (**2f**) was optimised by Comins<sup>72</sup> and Quéguiner<sup>73</sup> using an excess of PhLi as a metallating reagent at 0°C, which has a lower nucleophilicity than BuLi but it is still basic enough to favour the deprotonation process (**Scheme 2.27**).



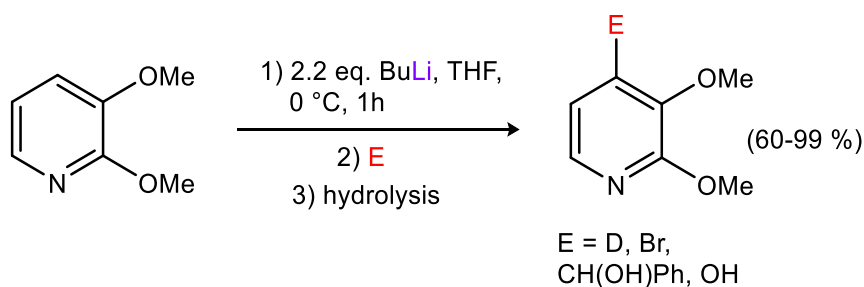
**Scheme 2.27:** Lithiation of **2f** in the C<sub>3</sub> position using PhLi.<sup>72,73</sup>

The same approach can be used for the lithiation of 3,4-dimethoxypyridine using <sup>n</sup>BuLi although in this case lower temperatures (-70°C) need to be employed (**Scheme 2.28**).<sup>73</sup>



**Scheme 2.28:** Lithiation of 3,4-dimethoxypyridine in the C<sub>2</sub> position using BuLi.<sup>73</sup>

Lithiation of the C<sub>4</sub> position was also achieved using the same conditions but having methoxy groups in the C<sub>2</sub> and C<sub>3</sub> positions (**Scheme 2.29**).<sup>74</sup>

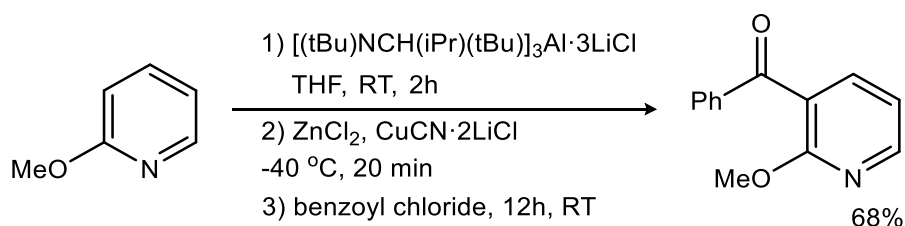


**Scheme 2.29:** Lithiation of 2,3-dimethoxypyridine in the C<sub>4</sub> position using BuLi.<sup>74</sup>

Remarkably when these reactions were carried out using 1.2 equivalents of BuLi low metallation yields were obtained (15%). The authors state that an excess of the organolithium reagent is required as the first equivalent coordinates to both methoxy substituent and nitrogen atom, whereas the second one carries out the Li-H exchange process. In order to expand the reactivity of base **1b** we decided to investigate its reactivity towards different methoxypyridines such as 4-methoxypyridine (**2f**), 3-methoxypyridine (**2g**) and 2-methoxypyridine (**2h**) (**Table 2.5**). In pyridine itself, the relative acidities around the ring are

700:72:1 (C<sub>4</sub>:C<sub>3</sub>:C<sub>2</sub> positions).<sup>75</sup> The metallation of 4-methoxypyridine (**2f**) at ambient temperature gave small quantities of unknown by-product, however when the reaction was carried out at 0 °C only *ortho*-metallation product was observed. This regioselectivity is directed by the acidity of the pyridine hydrogens as well as the *ortho*-directing effect of the OMe group. It should be noted that this regioselectivity has been previously described in the literature for the metallation of **2f** by mesityllithium at -23 °C followed by quenching with MeSSMe.<sup>76</sup>

In the case of 3-methoxypyridine (**2g**) the metallation occurs at the C<sub>4</sub> position which is the most acidic position, rather than C<sub>2</sub> position. The isolated yield obtained after separation by column chromatography was 75% which is slightly higher when compared to the isolated yields of 4-methoxypyridine (**2f**) (70%) and 2-methoxypyridine (**2h**) (58%). The methoxy group in the C<sub>3</sub> position favours the deprotonation in the C<sub>4</sub> position, not only because C<sub>4</sub> contains the most acidic proton of the pyridine, but also because the methoxy group increases its acidity with its *ortho*-directing effect. In the case of 4-methoxypyridine (**2f**) the most acidic proton of the pyridine is blocked, so the metallation takes place in the C<sub>3</sub> position. In the case of 2-methoxypyridine (**2h**) the regioselectivity of the reaction is particularly interesting as the metallation occurs exclusively in the C<sub>3</sub> position, suggesting that the regioselectivity is driven preferentially by the directing effect of the methoxy group. The metallation product **3h** in this case is obtained in a lower isolated yield (58%) compared to the other methoxypyridines studied. In a related reaction Knochel *et al* have reported the selective acylation of 2-methoxypyridine (25°C, 2h) at the C<sub>3</sub> position using the LiCl-complexed aluminate base [(<sup>t</sup>Bu)NCH(<sup>i</sup>Pr)(<sup>t</sup>Bu)]<sub>3</sub>Al·3LiCl in 68% yield (**Scheme 2.30**).<sup>77</sup>

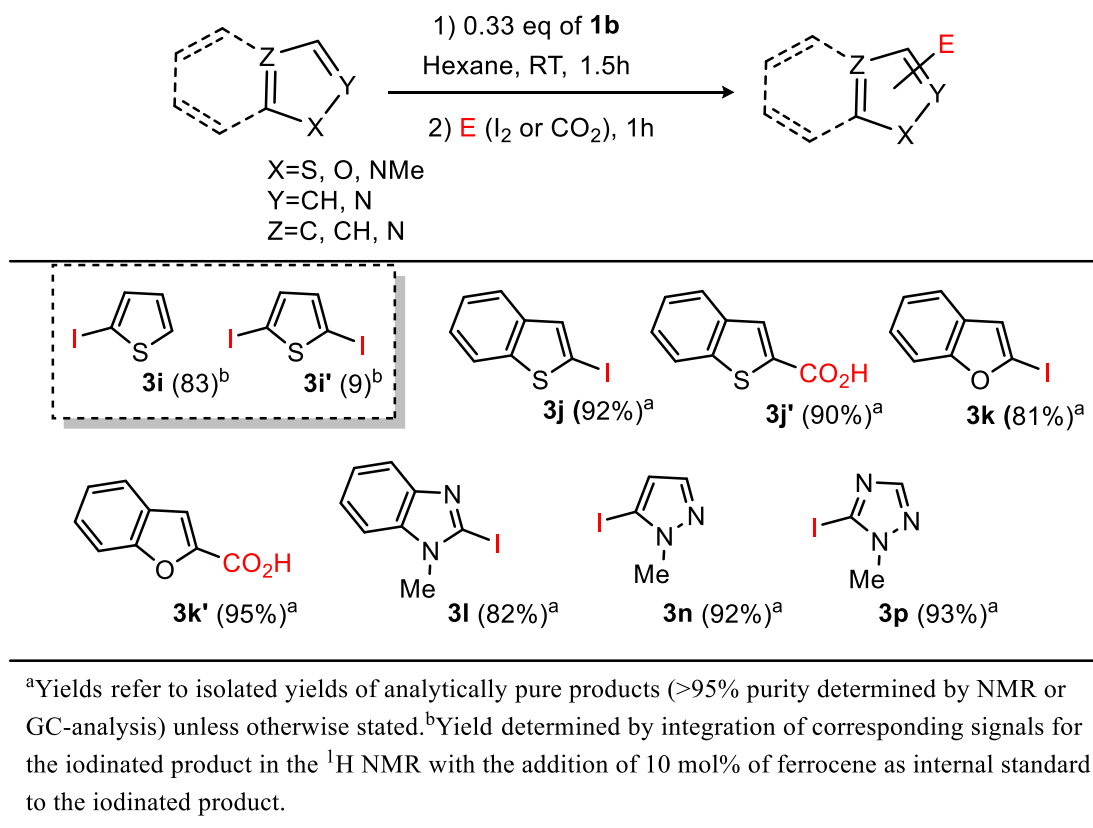


**Scheme 2.30:** Knochel's [(<sup>t</sup>Bu)NCH(<sup>i</sup>Pr)(<sup>t</sup>Bu)]<sub>3</sub>Al·3LiCl mediated deprotonation of **2g**.<sup>77</sup>

## 2.4.2 Magnesiumation of aromatic five-membered ring heterocycles.

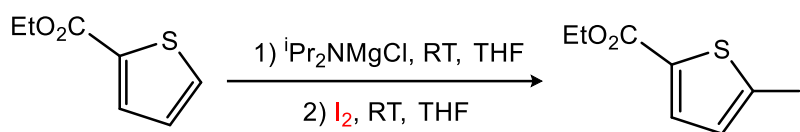
The results and substrates screened in this section are summarised in **Table 2.6**.

**Table 2.6:** Metallation of different 5-membered ring heterocycles using **1b**.



Substituted five-membered ring heterocycles such as thiophene (**2i**), benzothiophene (**2j**), benzofuran (**2k**), 1-methylbenzimidazole (**2l**), benzothiazole (**2m**), 1-methyl-1H-pyrazole (**2n**) and 1-methyl-1H-1,2,4-triazole (**2p**) are structural units present in many natural products and pharmaceutical synthetic intermediates.<sup>78,79</sup> Thus their functionalisation is particularly important. Kondo and Sakamoto described the magnesiumation of thiophenes and thiazoles using the amido base <sup>t</sup>Pr<sub>2</sub>NMgCl (**Table 2.7**).<sup>80</sup>

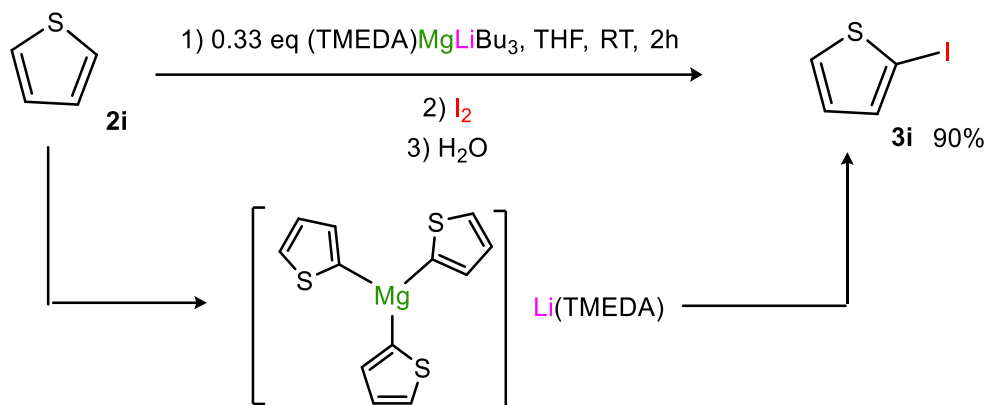
**Table 2.7:** Kondo's magnesiation of thiophene using  $i\text{Pr}_2\text{NMgCl}$  base.



$i\text{Pr}_2\text{NMgCl}$ (mol eq.)	time	Yield (%) <sup>a</sup>
1.0	1 h	21 (73)
1.0	24 h	0 (90)
2.0	10 min	77
2.0	30 min	60
2.0	1 h	52
2.0	24 h	0

<sup>a</sup>values in parentheses are recovery yields of starting material

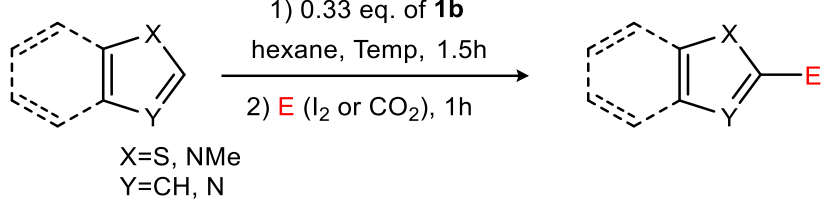
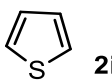
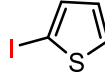
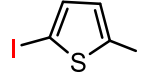
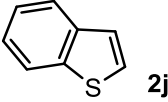
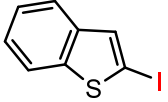
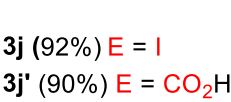
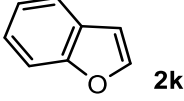
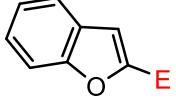
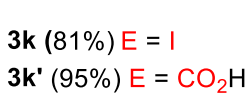
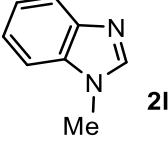
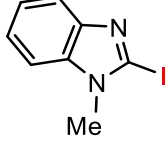
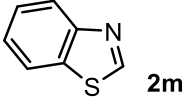
These studies showed that in order to get good conversions of thiophene (**2i**) into 2-iodothiophene (**3i**) an excess of the base reagent is required (2 equivalents). Furthermore the relevant metallated intermediate appeared to decompose over longer period of times since the yield of the reaction after 24 h is 0%. The monodeprotonation of **2i** at ambient temperatures can be also achieved selectively using  $(\text{TMP})\text{MgCl}\cdot\text{LiCl}$  as reported by Knochel and collaborators.<sup>30</sup> Furthermore when 1.1 equivalents of this base is employed  $\text{C}_2$  metallation of benzothiophene (**2j**) can be obtained at ambient temperatures for 24 hours.<sup>30</sup> Despite these efficient  $\text{C}_2$  magnesiations longer reaction times are required to quantitatively metallate **2i** and **2j** using this approach. Recently Mongin also reported selective metallation of **2i** using the lower order lithium magnesiate  $(\text{TMEDA})\text{LiMgBu}_3$ , obtaining 2-iodothiophene (**3i**) in a 90% yield. A proposed tris(thiophenyl) lithium magnesiate intermediate was proposed, although no experimental evidence was provided for its formation (**Scheme 2.31**).<sup>81</sup>



**Scheme 2.31:** Mongin's magnesiation of **2i** using (TMEDA)LiMgBu<sub>3</sub> base.

In this case LiMgBu<sub>3</sub> displays polybasic behaviour since almost quantitative yield of **3i** (90%) is observed when using 0.33 equivalents of the bimetallic reagent. The reaction of the higher order potassium magnesiate **1b** and thiophene ( $pK_a = 33.5$  see **Scheme 2.34**) at ambient temperatures followed by iodine quenching, it resulted in the formation of a mixture of two products. <sup>1</sup>H NMR analysis of the crude of the reaction mixture showed the formation of **3i** and 2,5-diiodothiophene (**3i'**) (**Table 2.8**).

**Table 2.8:** Thiophene magnesiation using **1b**.

 X=S, NMe Y=CH, N			
Entry	Substrate	Temp (°C)	Product (Yield %) <sup>a</sup>
1	 <b>2i</b>	20	 <b>3i</b> (83) <sup>b</sup>  <b>3i'</b> (9) <sup>b</sup>
2	 <b>2j</b>	20	 <b>3j</b> (92%) E = I  <b>3j'</b> (90%) E = CO <sub>2</sub> H
3	 <b>2k</b>	20	 <b>3k</b> (81%) E = I  <b>3k'</b> (95%) E = CO <sub>2</sub> H
4	 <b>2l</b>	20	 <b>3l</b> (82)
5	 <b>2m</b>	0	- <sup>c</sup>

<sup>a</sup>Yields refer to isolated yields of analytically pure products (>95% purity determined by NMR or GC-analysis) unless otherwise stated. <sup>b</sup>Yield determined by integration of corresponding signals for the iodinated product in the <sup>1</sup>H NMR with the addition of 10 mol% of ferrocene as internal standard to the iodinated product. <sup>c</sup>Unknown mixture of products observed

The reaction was repeated under the same reaction conditions in order to obtain the yield of the two products by <sup>1</sup>H NMR using ferrocene as an internal standard giving 83% and 9% yield of 2-iodothiophene (**3i**) and 2,5-diiodothiophene respectively (**3i'**) (**Figure 2.12**).

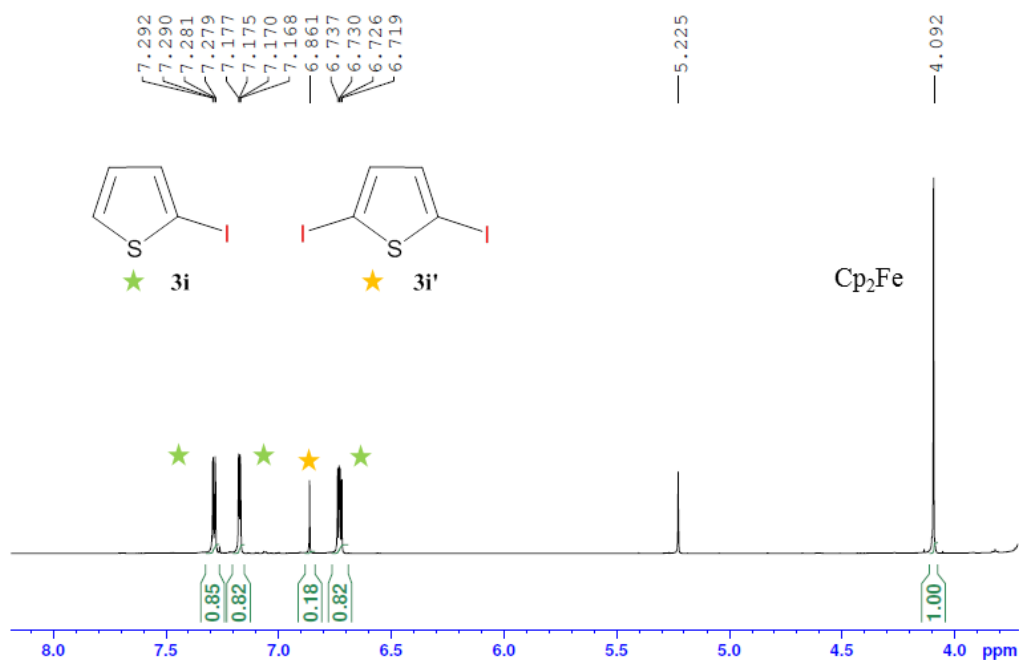


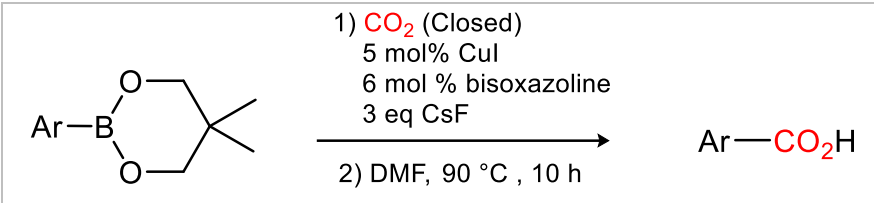
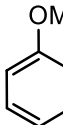
**Figure 2.12:** <sup>1</sup>H NMR yield for the magnesianation of **2i** using **1b**.

These results suggest that for this substrate all four alkyl groups on magnesium in **1b** may be active towards the deprotonation process. When the reaction of one equivalent of **1b** with 4 equivalents of **2i** followed by iodine quenching 73% yield of **3i** along with 4% yield of **3i'** were obtained by <sup>1</sup>H NMR. Interestingly when the C<sub>5</sub> position is blocked as in the case of benzothiophene (**2j**), **1b** selectively metallates this substrate in the C<sub>2</sub> position obtaining the iodinated product **3i** almost quantitatively (92% yield) after iodine quenching (entry 1, **Table 2.8**). Recent work published in our group has shown the ability to metallate thiophene using alkali metal ate complexes as deprotonative agents.<sup>82</sup> Regarding O-related analogues of this sulfur-containing heterocycle, it was reported that sodium magnesiate base [(TMEDA)Na(TMP)<sub>2</sub>Mg(CH<sub>2</sub>SiMe<sub>3</sub>)] undergoes a remarkable reaction with furan at room temperature to produce a spectacular octadecametallate complex [(TMEDA)<sub>6</sub>Na<sub>12</sub>Mg<sub>6</sub>(CH<sub>2</sub>SiMe<sub>3</sub>)<sub>2</sub>(C<sub>4</sub>H<sub>3</sub>O)<sup>-10</sup>(C<sub>4</sub>H<sub>3</sub>O)<sup>2-6</sup>], which contains ten α-monometallated and six α, α'-dideprotonated furan molecules.<sup>83</sup>

In order to expand the scope of the potassium mediated magnesianation reactions we investigated the reactivity of **1b** towards the metallation of different heteroaromatic compounds. Mongin demonstrated that benzofuran (**2k**) can be successfully metallated in the C<sub>2</sub> position using higher order lithium magnesiate compound Li<sub>2</sub>MgBu<sub>4</sub> (1/3 equivalents) at ambient temperature after electrophilic interception with I<sub>2</sub> or benzaldehyde, the relevant C<sub>2</sub> substituted benzofuran can be obtained in good yields (ranging from 85 to 89%).<sup>84</sup> The reaction of one equivalent of

**1b** with three equivalents of **2k** gave 2-iodobenzofuran (**3k**) as a unique product after iodolysis with a good 81% isolated yield (entry 3, **Table 2.8**). The reaction between **1b** and substrates **2k** and **2j** was carried out followed by the heterogeneous reaction of CO<sub>2</sub> which was bubbled through the reaction mixture. Different carboxylic acids were obtained selectively after acidic work up. The yields of the carboxylation reactions are similar to the yields obtained by iodine quenching (92% for **3j**, 90% for **3j'**, and 81% for **3k** and 95% for **3k'**, entry 2 and 3, **Table 2.8**). Compounds **3j'** and **3k'** have been previously prepared in a copper (I) catalysed reaction of aryl-boronic esters, in DMF solution, at 90 °C for 10 hours (**Table 2.9**).<sup>85</sup>

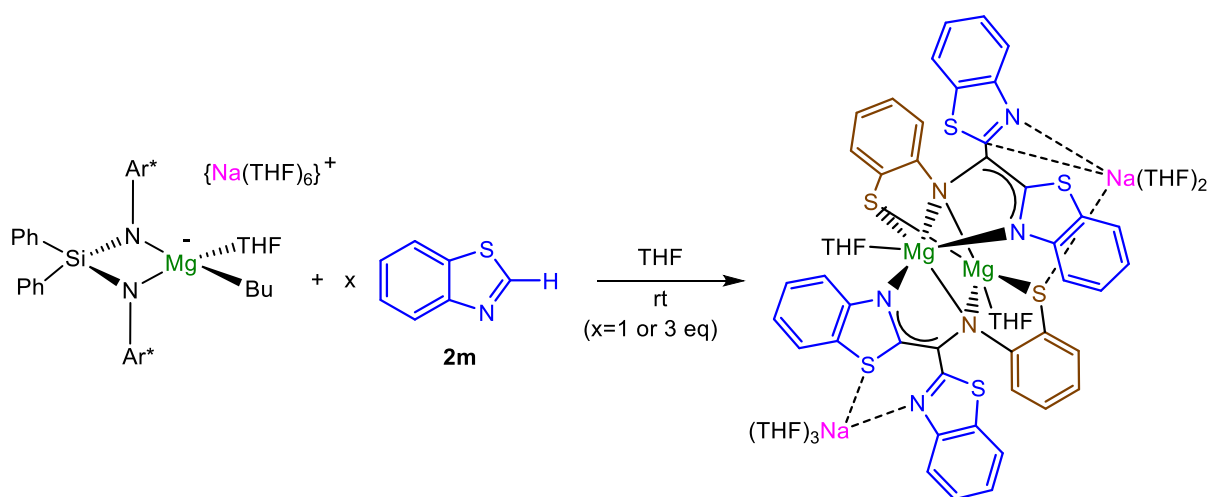
**Table 2.9:** Copper (I) catalysed carboxylation of aryl-boronic esters.

		
Entry	Aryl group	Yield (%)
1		72
2		82
3		78

Despite the high yields obtained, this procedure has some major drawbacks. On one hand, the high temperatures and the long reaction times employed (90 °C and 10 hours respectively), on the other hand, the preparation of the aryl-boronic esters in this methodology requires the use of BuLi at low temperature (-40 °C).

The reactions with other benzo-fused five membered-ring heterocycles such as 1-methyl-1H-benzimidazole (**2l**) and benzothiazole (**2m**) were also investigated. Surprisingly when one equivalent of **1b** reacts with three equivalents of **2m** at ambient temperature a dramatic colour change can be observed (from pale yellow to dark red) immediately after the reactions starts. Iodine quenching gave unknown mixture of products which were analysed by <sup>1</sup>H NMR spectroscopy (entry 5, **Table 2.8**). Related to this it has been previously reported in our group

that the use of solvent-separated sodium magnesiate compound  $[\{\text{Na}(\text{THF})_6\}^+\{\text{(Ph}_2\text{SiN}(\text{Ar}_2)\text{Mg}(\text{Bu})(\text{THF})\}^-]$  ( $\text{Ar} = 2,6\text{-}i\text{-Pr}_2\text{-C}_6\text{H}_3$ ) which contains highly bulky bis(amido) ligands, promotes activation of 3 equivalents of **2m** at ambient temperature, in a complicated cascade process which involves at least five distinct type of reactions such as  $\text{C}_2$  magnesiation, C-C coupling between two benzothiazoles, ring-opening, nucleophilic addition and intramolecular deprotonation (**Scheme 2.32**).<sup>86</sup>

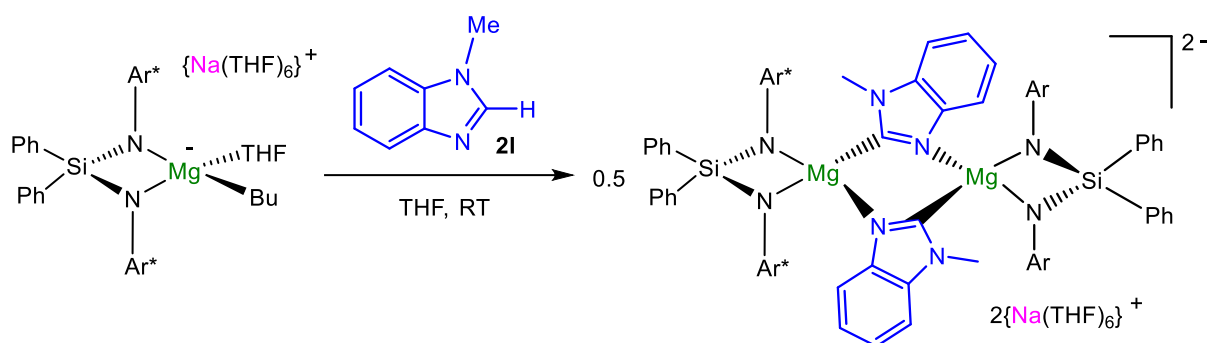


**Scheme 2.32:** Cascade process described for the activation of **2q**.<sup>86</sup>

This reaction takes place with a dramatic colour change, from light yellow to bright red. With this approach two of the benzothiazole molecules couple to each other whereas the third molecule suffers from  $\text{C}_2\text{-S}$  bond cleavage. Although no enough experimental evidence was gathered, a similar activation process could be taken in place here, which would explain the apparent complex mixture of products observed.

The magnesiation of **2l** was then investigated, which was successfully achieved in the  $\text{C}_2$  position using 0.33 equivalents of **1b**, at ambient temperature for 1.5 hours. Iodolysis of the magnesium intermediate resulted in 82% isolated yield of 2-iodo-1-methyl-1H-benzo[d]imidazole (**3l**) (entry 4, **Table 2.8**).

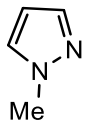
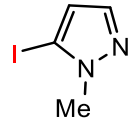
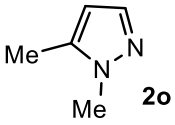
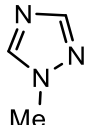
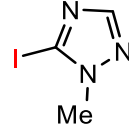
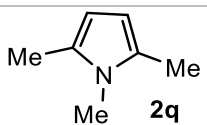
Closely related as recently shown in our group the use of solvent-separated sodium magnesiate compound  $[\{\text{Na}(\text{THF})_6\}^+\{\text{(Ph}_2\text{SiN}(\text{Ar}_2)\text{Mg}(\text{Bu})(\text{THF})\}^-]$  ( $\text{Ar} = 2,6\text{-}i\text{-Pr}_2\text{-C}_6\text{H}_3$ ) can promote quantitative magnesiation of **2l** as unequivocally established by X-ray characterisation of the relevant magnesium intermediate (**Scheme 2.33**).<sup>87</sup>



**Scheme 2.33:** Magnesiumation of **21** using a solvent separated sodium magnesiate.<sup>87</sup>

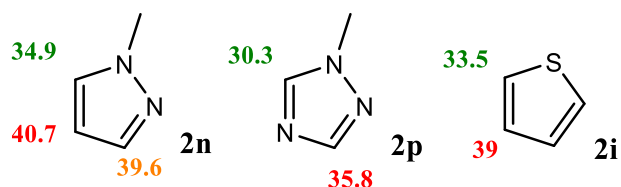
Building on these results, the reactivity of **1b** towards the metallation of different nitrogen-containing heteroaromatic 5-membered ring systems was next investigated. The reaction of one equivalent of **1b** with three equivalents of 1-methyl-1H-pyrazole (**2n**) at ambient temperature was quenched after 1.5 hours with iodine to afford 5-iodo-1-methyl-1H-pyrazole (**3n**) in almost quantitative isolated yield (92%) (Entry 1, **Table 2.10**). Similarly the reaction of one equivalent of **1b** and three equivalents of 1-methyl-1H-1,2,4-triazole (**2p**) under the same reaction conditions gave 5-iodo-1-methyl-1H-1,2,4-triazole (**3p**) in almost quantitative isolated yield (93%) (**Table 2.10**).

**Table 2.10:** Magnesiumation of **2n**, **2o**, **2p**, **2q** using **1b**.

Entry	Substrate	Product (Yield %) <sup>a</sup>
1	 <b>2n</b>	 <b>3n</b> (92)
2	 <b>2o</b>	No reaction <sup>b</sup>
3	 <b>2p</b>	 <b>3p</b> (93)
4	 <b>2q</b>	- <sup>c</sup>

<sup>a</sup>Yields refer to isolated yields of analytically pure products (>95% purity determined by NMR or GC-analysis) unless otherwise stated. <sup>b</sup>Full recovery of starting material. <sup>c</sup>Decomposition of product observed

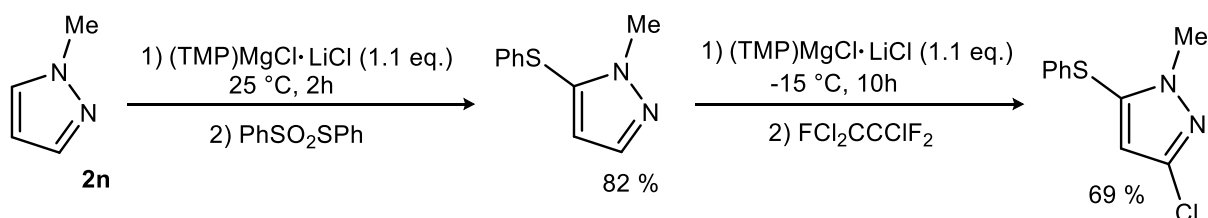
Interestingly the reaction of one equivalent of **1b** with 3 equivalents of **2q** at ambient temperature for 1.5 hours resulted in the formation of a black solid after quenching with iodine. <sup>1</sup>H NMR analysis of the crude suggested decomposition of the substrate due to the formation of multiple unknown signals with no evidence of metallation at all. In both substrates **2n** and **2p** the metallation took place in the  $\alpha$ -position (C<sub>5</sub> position) of the nitrogen atom bonded to a methyl group which can be considered “pyrrole” type, as its lone pair is involved in the  $\pi$ -system of the heterocycle whereas the remaining N atoms are like that present in pyridine, with their lone pair lying in the same plane as the aromatic ring and therefore been not involved in the electronic delocalization of the heterocyclic substrate. The regioselectivity observed for these reactions is consistent with the calculated  $pK_a$  values for these substrates in DMSO (Scheme 2.34).<sup>36</sup>



**Scheme 2.34:** Theoretical predicted  $pK_a$  of **2n**, **2p** and **2i**.

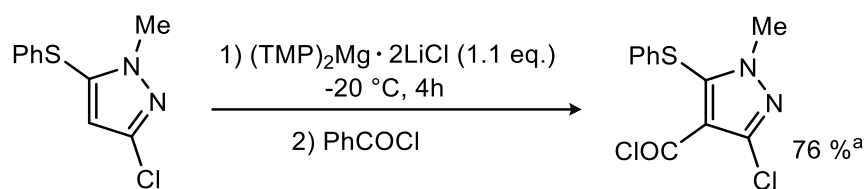
Interestingly for 1,5-dimethyl-1H-pyrazole **2o** where the C<sub>5</sub> position is blocked by a methyl group (entry 2, **Table 2.10**) no metallation is observed at all with full recovery of starting material, showing that under these mild reaction conditions, **1b** cannot remove the hydrogen bonded to C<sub>3</sub> which are significantly less activated in terms of  $pK_a$ . Closely related to these findings our group has recently reported the successful zincation of **2n** and **2p** and other N-heterocyclic substrates at ambient temperature using the lithium zincate complex (THF)Li(TMP)Zn(<sup>t</sup>Bu)<sub>2</sub> obtaining the iodinated products **3n** and **3p** after iodine quenching in 89% and 98% yields respectively.<sup>88</sup> However it should be noted that in these reactions excess of the amido/alkyl zincate (2 equivalents) were needed to quantitatively zincate **2n** and **3p**.

Within the context of magnesiation chemistry Knochel *et al* have reported the selective metallation of a range of *N*-methyl substituted pyrazoles at ambient temperature using (TMP)MgCl·LiCl and (TMP)<sub>2</sub>Mg·2LiCl (**Scheme 2.35**).<sup>89</sup>



**Scheme 2.35:** Knochel metallation of **2n** using (TMP)MgCl·LiCl.<sup>89</sup>

In this case, using a sequence of metallation/quenching steps the authors have managed to functionalise all three H-positions present in **2n**. This includes the hydrogen attached to C<sub>3</sub> which is the less activated in terms of  $pK_a$ , of this molecule, although in this case the reaction only works using the amido-rich base (TMP)<sub>2</sub>Mg·2LiCl (**Scheme 2.36**).<sup>89</sup>



<sup>a</sup> transmetallation with 1.1 eq of  $\text{CuCN} \cdot 2\text{LiCl}$

**Scheme 2.36:**  $(\text{TMP})\text{MgCl} \cdot \text{LiCl}$  and  $(\text{TMP})_2\text{Mg} \cdot 2\text{LiCl}$  mediated metallation of N-methyl substituted pyrazoles.<sup>89</sup>

It should be noted that in these substrates the presence of substituents at the  $\text{C}_4$  and  $\text{C}_2$  positions in the ring may greatly activate the  $\text{C}_4\text{-H}$ , in comparison to parent unsubstituted **2n**.

## 2.5 Conclusions

The following conclusions can be made resulting from the work presented in this chapter.

- 1) Using anisole as a case study, the synergic effect of potassium and magnesium in the higher order magnesiates **1b** and **1c** has been demonstrated. Thus, while both bimetallic species can promote the efficient *ortho*-deprotonation of this aromatic ether, their homometallic components  $\text{KCH}_2\text{SiMe}_3$  and  $\text{Mg}(\text{CH}_2\text{SiMe}_3)_2$  fail to do so, affording only negligible amounts of 2-iodoanisole (**3a**). Demonstrating their enhanced metallating power, the high reactivity of these compounds contrasts with the inertness of triorganomagnesiates  $[\{\text{KMg}(\text{CH}_2\text{SiMe}_3)_3\}_\infty]$  (**1a**) which fails to deprotonate this substrate.
- 2) Studies using variable amounts of anisole and mixed-metal base **1b** show the ability of the latter to exhibit polybasic behaviour employing three of its four potential basic arms. A moderate donor effect has also been observed as both mixed metal compounds  $[(\text{PMDETA})_2\text{K}_2\text{Mg}(\text{CH}_2\text{SiMe}_3)_4]$  (**1b**) and  $[(\text{TMEDA})_2\text{K}_2\text{Mg}(\text{CH}_2\text{SiMe}_3)_4]$  (**1c**) promote the *ortho*-metallation of anisole (**2a**) to form (**3a**) in similar yields.
- 3) A marked alkali-metal effect has been observed. Further studies for the reactivity of this novel mixed metal compounds towards the metallation of **2a** showed that when switching to the similar bimetallic compound  $[(\text{TMEDA})_2\text{Na}_2\text{Mg}(\text{CH}_2\text{SiMe}_3)_4]$  (**1d**) and  $[(\text{TMEDA})_2\text{Li}_2\text{Mg}(\text{CH}_2\text{SiMe}_3)_4]$  (**1e**) suppress the magnesiation process. Despite the close structural futures of **1b** and **1d**, replacing K for Li dramatically influences the reactivity of these mixed-metal compounds.
- 4) These compounds are able to promote the efficient and selective magnesiation of a wide range of aromatic and heteroaromatic substrates at room temperature under mild reaction conditions as pleasingly observed for the metallation of different compounds from **2a** to **2p**. Electrophilic interception of the metallated intermediates using  $\text{I}_2$ , allowed the isolation of **3a-3p** in good to excellent yields (ranging from 52-94%) These results show the potential application of **1b** in contrast with K-related compound LIC-KOR where cryogenic conditions must strictly be employed. Thereby different substrates have been metallated using **1b** and then reacted with  $\text{CO}_2$  to obtain different carboxylic acids. This resulted to be a straightforward method for the synthesis of different aryl substituted carboxylic acids with  $\text{CO}_2$  as an attractive environmentally friendly chemical feedstock.

## 2.6 Experimental section

**General Considerations.** All reactions were performed under a protective argon atmosphere using standard Schlenk techniques. Hexane, benzene and THF were dried by heating to reflux over sodium benzophenone ketyl and distilled under nitrogen or they were passed through a column of activated alumina (Innovative Tech.), degassed under nitrogen and stored over molecular sieves in the glove-box prior to use.  $\text{LiCH}_2\text{SiMe}_3$  and organic substrates were purchased from Sigma Aldrich chemicals and used as received. TMEDA and PMDETA were purchased from Sigma Aldrich chemicals, distilled over  $\text{CaH}_2$  and stored in a Schlenk with activated molecular sieves. NMR spectra were recorded on a Bruker DPX400 MHz spectrometer, operating at 400.13 MHz for  $^1\text{H}$ , 100.62 MHz for  $^{13}\text{C}$  or on a Varian FT-400 spectrometer using standard VARIAN-FT software. Elemental analyses were carried out using a Perkin Elmer 2400 elemental analyser.

### 2.6.1 Synthesis of inorganic compounds

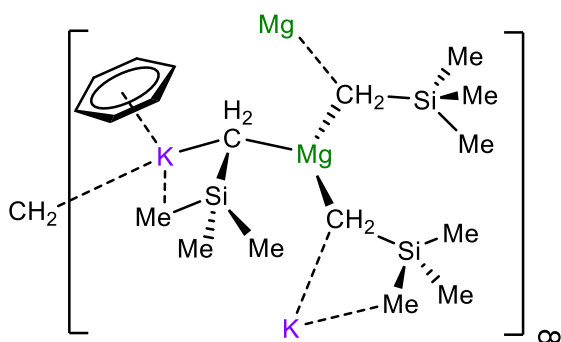
#### 2.6.1.1 Synthesis of $\text{KCH}_2\text{Si}(\text{CH}_3)_3$

To a suspension of  $\text{KO}^t\text{Bu}$  (2.75 g, 25 mmol) in hexane (50 mL) at 0 °C was added dropwise  $\text{LiCH}_2\text{SiMe}_3$  (26 mL of a 1M solution of  $\text{LiCH}_2\text{SiMe}_3$  in hexane). The reaction was left stirring overnight. The resultant off-white suspension was filtered, washed with hexane (3 x 20 mL) and dried under vacuum to afford a white solid (typical yield 2.4-2.55 g, 76-81%).  $^1\text{H NMR}$  (400 MHz,  $\text{CDCl}_3$ )  $\delta$  (ppm) = -2.21 (s, 2H,  $\text{CH}_2$ ), -0.15 (s, 9H,  $\text{CH}_3$ ).  $^{13}\text{C}\{^1\text{H}\}$  NMR (101 MHz,  $\text{CDCl}_3$ )  $\delta$  (ppm) = 0.9 ( $\text{CH}_2$ ), 7.2 ( $\text{CH}_3$ )

#### 2.6.1.2 Synthesis of $\text{Mg}(\text{CH}_2\text{SiMe}_3)_2$

To an oven-dried 500 mL round bottom flask were added Mg turnings (4.00 g, 136 mmol) and  $\text{Et}_2\text{O}$  (110 mL).  $\text{ClCH}_2\text{SiMe}_3$  (19 mL, 136 mmol) was suspended in  $\text{Et}_2\text{O}$  (60 mL) and added drop wise. The resulting grey solution was refluxed for 1h. To the cooled suspension was added 1,4-dioxane (9 mL, 106 mmol) and the pale grey mixture stirred for 16 hours. The suspension was then filtered through glass wool and washed with  $\text{Et}_2\text{O}$  (2 x 40 mL) giving a pale straw filtrate. Removal of the solvent *in vacuo* afforded a white solid which was purified by sublimation at 170 °C to obtain pure  $\text{Mg}(\text{CH}_2\text{SiMe}_3)_2$  as a white solid (typical yield 8 g, 58%).  $^1\text{H NMR}$  (400 MHz, THF)  $\delta$  (ppm) = -1.73 (s, 9H,  $\text{CH}_3$ ) -0.07 (s, 2H,  $\text{CH}_2$ )

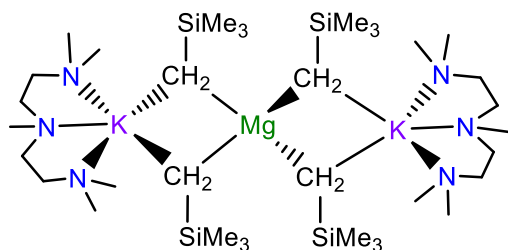
### 2.6.1.3 Synthesis of $[\{(KMg(CH_2SiMe_3)_3)\}_\infty]$ (1a)



To a suspension of  $KCH_2SiMe_3$  (0.12 g, 1 mmol) in hexane (5 mL)  $Mg(CH_2SiMe_3)_2$  (0.20 g, 1 mmol) was added and the resulting suspension stirred for 1 hour and benzene (4 mL) was added. Gentle heating resulted in a clear colourless solution. The Schlenk was left in the freezer at  $-30\text{ }^\circ\text{C}$  for 16h and a crop

of clear colourless crystals was isolated (0.18 g, 45%). mp:  $66\text{ }^\circ\text{C}$ .  $^1\text{H NMR}$  (400 MHz, 298 K,  $d_8$ -toluene)  $\delta$  -1.72 (6H, s,  $SiCH_2$ ), 0.28 (27H, s,  $Si(CH_3)_3$ ), 7.13 (2H, CH, benzene).  $^1\text{H NMR}$  (400 MHz, 298 K,  $C_6D_6$ )  $\delta$  (ppm) -1.75 (6H, s,  $SiCH_2$ ), 0.34 (27H, s,  $Si(CH_3)_3$ ).  $^{13}\text{C}\{^1\text{H}\}$  NMR (101 MHz, 298 K,  $C_6D_6$ )  $\delta$  (ppm) 5.66 ( $Si(CH_3)_3$ ), 0.97 ( $SiCH_2$ ).  $^{29}\text{Si}\{^1\text{H}\}$  NMR (79.475 MHz, 298K,  $C_6D_6$ )  $\delta$  -1.04 **Elemental analysis (CHN)**: Due to the extreme air-sensitivity of compound **1r** satisfactory analyses could not be obtained.

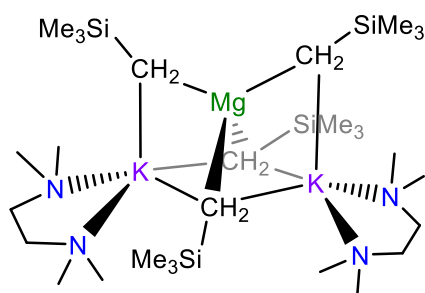
### 2.6.1.4 Synthesis of $[(PMDETA)_2K_2Mg(CH_2SiMe_3)_4]$ (1b)



To a suspension of  $KCH_2SiMe_3$  (0.12 g, 1 mmol) in hexane (15 mL)  $Mg(CH_2SiMe_3)_2$  (0.1 g, 0.5 mmol) was added and the suspension stirred for 1 hour. PMDETA (0.21mL, 1.0 mmol) was then added giving a clear solution with a yellow oil

deposited at the bottom of the Schlenk. The Schlenk was transferred to the freezer ( $-28\text{ }^\circ\text{C}$ ) overnight. A crop of clear, colourless crystals was isolated (0.31 g, 78%). mp:  $78\text{ }^\circ\text{C}$ .  $^1\text{H NMR}$  (400 MHz, 298 K,  $C_6D_6$ )  $\delta$  -1.70 (8H, s,  $SiCH_2$ ), 0.52 (36H, s,  $Si(CH_3)_3$ ), 1.80-1.87 (16H, m,  $NCH_2$ , PMDETA), 1.94 (6H, s,  $NCH_3$ , PMDETA), 2.01 (24H, s,  $N(CH_3)_2$ , PMDETA).  $^{13}\text{C}\{^1\text{H}\}$  NMR (101 MHz, 298 K,  $C_6D_6$ )  $\delta$  1.11 ( $SiCH_2$ ), 6.19 ( $Si(CH_3)_3$ ), 42.18 ( $CH_3$ , PMDETA), 45.47 ( $(CH_3)_2$ , PMDETA), 55.25 ( $CH_2$ , PMDETA), 57.09 ( $CH_2$ , PMDETA).  $^{29}\text{Si}\{^1\text{H}\}$  NMR (79.475 MHz, 298K,  $C_6D_6$ )  $\delta$  -0.99 **Elemental analysis (CHN)**: Due to the extreme air-sensitivity of compound **1r** satisfactory analyses could not be obtained.

### 2.6.1.5 Synthesis of [(TMEDA)<sub>2</sub>K<sub>2</sub>Mg(CH<sub>2</sub>SiMe<sub>3</sub>)<sub>4</sub>] (1c)

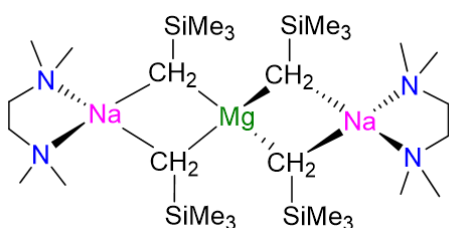


To a suspension of KCH<sub>2</sub>SiMe<sub>3</sub> (0.24 g, 2 mmol) in hexane (15 mL) Mg(CH<sub>2</sub>SiMe<sub>3</sub>)<sub>2</sub> (0.20 g, 1 mmol) was added and the suspension stirred for 1 hour. TMEDA (0.30 mL, 2 mmol) was then added and the almost clear solution transferred to the freezer (-28 °C). After 16 hours a crop of peach crystals was isolated (0.41 g,

60%). mp: 63°C (decomposition observed at 82°C). <sup>1</sup>H NMR (400 MHz, 298 K, C<sub>6</sub>D<sub>6</sub>)

<sup>a</sup> = -1.74 and -1.70 (2H, overlapping s, SiCH<sub>2</sub>), 0.40 and 0.41 (9H, overlapping s, Si(CH<sub>3</sub>)<sub>3</sub>), 1.93 and 1.94 (8H, overlapping s, TMEDA). <sup>13</sup>C{<sup>1</sup>H} NMR (101 MHz, 298 K, C<sub>6</sub>D<sub>6</sub>) -0.03 (SiCH<sub>2</sub>), 1.67 (SiCH<sub>2</sub>), 5.64 (Si(CH<sub>3</sub>)<sub>3</sub>), 45.53 (N(CH<sub>3</sub>)<sub>2</sub>, TMEDA), 57.31 (NCH<sub>2</sub>, TMEDA). <sup>29</sup>Si{<sup>1</sup>H} NMR (79.5 MHz, 298K, C<sub>6</sub>D<sub>6</sub>) δ -0.56 □ **Elemental analysis (CHN):** Due to the extreme air-sensitivity of compound **1r** satisfactory analyses could not be obtained.

### 2.6.1.6 Synthesis of [(TMEDA)<sub>2</sub>Na<sub>2</sub>Mg(CH<sub>2</sub>SiMe<sub>3</sub>)<sub>4</sub>] (1d).

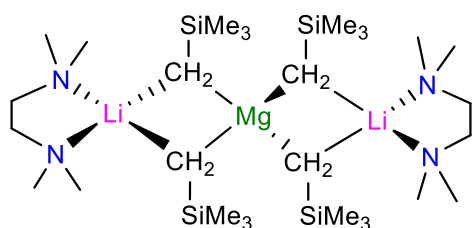


To a suspension of NaCH<sub>2</sub>SiMe<sub>3</sub> (0.22 g, 2 mmol) in hexane (15 mL) Mg(CH<sub>2</sub>SiMe<sub>3</sub>)<sub>2</sub> (0.20 g, 1 mmol) was added and the suspension stirred for 1 hour. TMEDA (0.30 mL, 2 mmol) was then added and gently heated to form a clear solution which was

transferred to the freezer (-28 °C). After 16 hours a crop of clear, colourless crystals was isolated (0.35 g, 54%). <sup>1</sup>H NMR (400 MHz, 298 K, C<sub>6</sub>D<sub>6</sub>) δ (ppm) = -1.78 (2H, s, SiCH<sub>2</sub>), 0.47 (9H, s, Si(CH<sub>3</sub>)<sub>3</sub>), 1.67 (2H, s, NCH<sub>2</sub>, TMEDA), 1.92 (6H, s, N(CH<sub>3</sub>)<sub>2</sub>, TMEDA). <sup>13</sup>C{<sup>1</sup>H} NMR (101 MHz, 298 K, C<sub>6</sub>D<sub>6</sub>) δ (ppm) = -3.14 (SiCH<sub>2</sub>), 5.63 (Si(CH<sub>3</sub>)<sub>3</sub>), 45.80 (N(CH<sub>3</sub>)<sub>2</sub>, TMEDA), 56.76 (NCH<sub>2</sub>, TMEDA). **Elemental analysis (CHN):** Expected value, C=51.62, H=11.76, N=8.60 found, C=51.12, H=11.54, N=8.93.

<sup>a</sup> For **1c** it is possible to distinguish between the two different types ( $\mu_2$  and  $\mu_3$ ) R ligands, as evidenced by the two distinct set of resonances observed for the monosilyl groups in its <sup>1</sup>H and <sup>13</sup>C NMR spectra.

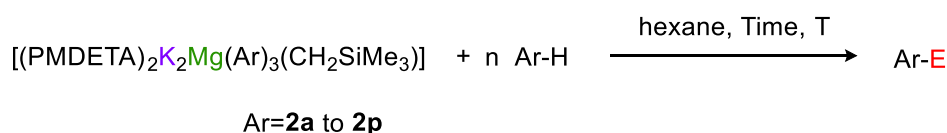
### 2.6.1.7 Synthesis of [(TMEDA)<sub>2</sub>Li<sub>2</sub>Mg(CH<sub>2</sub>SiMe<sub>3</sub>)<sub>4</sub>] (1e)



A solution of LiCH<sub>2</sub>SiMe<sub>3</sub> (1 mL of a 1 M solution in hexane, 1 mmol) was added to a suspension of Mg(CH<sub>2</sub>SiMe<sub>3</sub>)<sub>2</sub> (99mg, 0.5 mmol) in hexane (10 mL) to afford an almost clear solution which was left stirring for 30 minutes. TMEDA (116 mg, 1 mmol) was then added giving a white precipitate. The solution was transferred to the freezer and left at -30 °C for 16h to afford a higher amount of white precipitate, which was filtered and transferred to the glove box. (0.15g 48%). <sup>1</sup>H NMR (400 MHz, 298 K, C<sub>6</sub>D<sub>6</sub>) δ (ppm) = -1.98 (8H, s, SiCH<sub>2</sub>), 0.46 (36H, s, Si(CH<sub>3</sub>)<sub>3</sub>), 1.65 (8H, s, NCH<sub>2</sub>, TMEDA), 2.02 (24H, s, N(CH<sub>3</sub>)<sub>2</sub>, TMEDA). <sup>13</sup>C{<sup>1</sup>H} NMR (101 MHz, 298 K, C<sub>6</sub>D<sub>6</sub>) δ (ppm) = -3.1 (SiCH<sub>2</sub>), 5.7 (Si(CH<sub>3</sub>)<sub>3</sub>), 46.3 (N(CH<sub>3</sub>)<sub>2</sub>, TMEDA), 57.0 (NCH<sub>2</sub>, TMEDA). The values are consistent with previous data reported in the literature.<sup>35</sup>

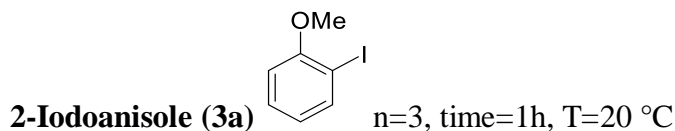
## 2.6.2 Synthesis of iodoaryl derivatives

### General synthesis for compounds 3a-3k

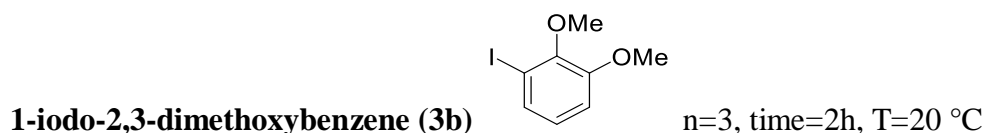


**Scheme 2.37:** General synthesis for compounds 3a-3k

A dry Schlenk flask was charged with KCH<sub>2</sub>SiMe<sub>3</sub> (126 mg, 1 mmol) and Mg(CH<sub>2</sub>SiMe<sub>3</sub>)<sub>2</sub> (99 mg, 0.5 mmol). The mixture was suspended in hexane (10 mL) and the suspension stirred for 1 h at 20 °C. PMDETA (173 mg, 1 mmol) was then added resulting in a clear solution with yellow oil deposited at the bottom of the flask. The organic substrate (n equivalents) was then introduced at temperature, T, and stirred for the given time (t) before I<sub>2</sub> (5 eq) was added. After stirring for 1 h the excess iodine was removed using sat. aqueous Na<sub>2</sub>S<sub>2</sub>O<sub>3</sub> solution. The phases were separated and the organic phase was extracted three times with DCM. The combined organic extracts were dried over MgSO<sub>4</sub> and the solvent removed under reduced pressure.



Manual column chromatographical purification (SiO<sub>2</sub>, hexane/EtOAc = 9:1) afforded 2-iodoanisole **3a** as a colorless oil (274 mg, 78% yield).<sup>b</sup> **<sup>1</sup>H NMR** (400 MHz, CDCl<sub>3</sub>) δ (ppm) = 3.88 (s, 3H), 6.70-6.74 (dt, *J* = 7.6 Hz, 1.2 Hz, 1H), 6.82-6.84 (dd, *J* = 8.0 Hz, 1.2 Hz, 1H), 7.29-7.33 (ddd, *J* = 8.8 Hz, 7.6 Hz, 1.6 Hz, 1H), 7.77-7.79 (dd, *J* = 8.0 Hz, 1.6 Hz, 1H); **<sup>13</sup>C{<sup>1</sup>H} NMR** (125 MHz, CDCl<sub>3</sub>) δ (ppm) = 56.5, 86.2, 111.2, 122.7, 129.7, 139.7, 158.2; **MS (EI, 70 eV)**: *m/z* (%) = 234 [M<sup>+</sup>] (100), 219 (22), 92 (43), 77 (31), 63 (31), 51 (23), 50 (20). The values are consistent with previous data reported in the literature.<sup>90</sup>



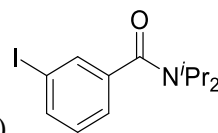
Column chromatographical purification using the combi flash (SiO<sub>2</sub>, hexane/EtOAc = 20:1) afforded 1-iodo-2,3-dimethoxybenzene **3b** as a pale yellow oil (278 mg, 70% yield). **<sup>1</sup>H NMR** (400 MHz, CDCl<sub>3</sub>) δ (ppm) = 3.86 (s, 3H), 3.87 (s, 3H), 6.81 (t, *J* = 8.1 Hz, 1H), 6.99 (dd, *J* = 8.1 Hz, 1.5 Hz, 1H), 7.36 (dd, *J* = 8.1 Hz, 1.5 Hz, 1H); **<sup>13</sup>C{<sup>1</sup>H} NMR** (100 MHz, CDCl<sub>3</sub>) δ (ppm) = 55.9, 60.3, 92.4, 112.7, 125.8, 130.4, 148.9, 152.8; **MS (EI, 70 eV)**: *m/z* (%) = 264 [MP + P] (100), 249 (32), 232 (2), 178 (16), 167 (5), 166 (26), 138 (69), 107 (5), 79 (2), 51 (1). (20). The values are consistent with previous data reported in the literature.<sup>40</sup>



Manual column chromatographical purification (SiO<sub>2</sub>, hexane/EtOAc = 8:1) afforded 2-iodo-N,N-diisopropylbenzamide (**3c**) as colourless crystals (156 mg, 94% Yield). **<sup>1</sup>H NMR** (500 MHz, CDCl<sub>3</sub>) δ (ppm) = 1.05 (d, 3H), 1.27 (d, 3H), 1.60 (m, 6H), 3.56 (m, 2H), 7.02 (dt, <sup>4</sup>*J*=1.6 Hz, <sup>3</sup>*J*=7.6 Hz 1H), 7.13 (dd, <sup>4</sup>*J*=1.6 Hz, <sup>3</sup>*J*=7.6 Hz, 1H), 7.34 (dt, <sup>4</sup>*J*=1.2 Hz, <sup>3</sup>*J*=7.2 Hz, 1H), 7.8 (dd, <sup>4</sup>*J*=1 Hz, <sup>3</sup>*J*=8 Hz, 1H); **<sup>13</sup>C{<sup>1</sup>H} NMR** (125 MHz, CDCl<sub>3</sub>) δ (ppm) = 21.0, 46.3, 51.5,

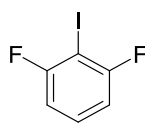
<sup>b</sup> No significant changes in the isolated yield of **3a** were observed when isolated crystals of the base **3** were employed.

92.61, 126.2, 128.5, 129.8, 139.7, 144.6, 170.1; **MS (EI, 70 eV)**: m/z (%) = 330 [M<sup>+</sup>] (27), 288 (18), 231 (100), 204 (45), 203 (11); **Elemental analysis (%)**: Calculated for C<sub>13</sub>H<sub>18</sub>INO: C, 47.14; H, 5.48; N, 4.23. Found: C, 47.16; H, 5.36; N, 4.34.



**Synthesis of 3-iodo-N,N-diisopropylbenzamide (3c')** n=3, time=1.5h, T=0 °C

Manual column chromatographical purification (SiO<sub>2</sub>, hexane/EtOAc = 8:1 to 4:1) afforded 3-iodo-N,N-diisopropylbenzamide (**3c'**) as a yellow solid (62 mg, 12% yield). **<sup>1</sup>H NMR** (500 MHz, CDCl<sub>3</sub>) δ (ppm) = 1.25-1.45 (broad peak, 12H), 3.56 (broad peak, 2H), 7.11 (t, *J*=8 Hz, 1H), 7.25 (dt, *J*=1.2, 7.6 Hz, 1H), 7.65 (t, *J*=1.6 Hz, 1H), 7.69 (dt, *J*=1.2, 8 Hz, 1H). **<sup>13</sup>C{<sup>1</sup>H} NMR** (125 MHz, CDCl<sub>3</sub>) δ (ppm) = 20.9, 31.2, 94.6, 124.9, 130.5, 134.8, 137.9, 141.1, 169.3; **MS (EI, "70 eV")**: m/z (%) = 331 [M<sup>+</sup>] (10), 330, (10), 288 (52), 231 (100), 203 (10), 76 (11); **Elemental analysis (%)**: Calculated for C<sub>13</sub>H<sub>18</sub>INO: C, 47.14; H, 5.48; N, 4.23. Found: C, 46.17; H, 5.45; N, 4.00.

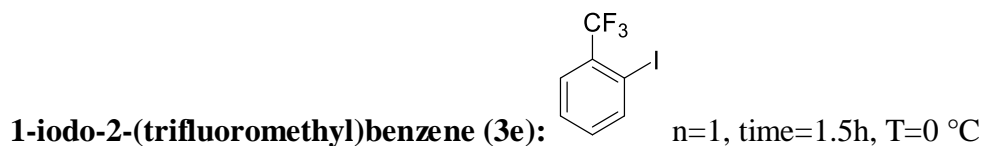


**Synthesis of 1,3-difluoro-2-iodobenzene (3d)** n=3, time=1.5h, T=0 °C

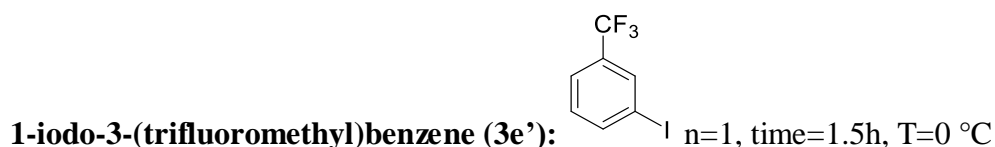
[(PMDETA)<sub>2</sub>K<sub>2</sub>MgR<sub>4</sub>] **1b** was prepared in situ as described for the synthesis **3a**. To a 0.5 mmols of **1b** was added 1,3-difluorobenzene (126 mg, 1.5 mmol) and the resultant yellowish solution allowed to stir at room temperature for 1.5 hours. The solution was then quenched with excess of I<sub>2</sub> (1,015 g, in 5 mL THF) and allowed to stir for 1 hour. Next a 10%-5% mixture solution of Na<sub>2</sub>S<sub>2</sub>O<sub>3</sub> and NH<sub>4</sub>Cl respectively was added until bleaching and the product extracted with DCM (3 x 1 mL). The combined organic extracts were dried over MgSO<sub>4</sub> and the solvent removed using the rotary evaporator to obtain a yellowish oil as a product. The product was then dissolved in CH<sub>2</sub>Cl<sub>2</sub> and ferrocene was added to the solution (29.7 mg, 10 mol%). The yield obtained by integration of the corresponding signals for **3d** by <sup>1</sup>H NMR was 64%. **<sup>1</sup>H NMR** (400 MHz, CDCl<sub>3</sub>) δ (ppm) = 6.88 (m, *J*= 6.4,2 Hz, 2H), 7.30 (m, *J*=6, 2 Hz, 1H). **<sup>13</sup>C{<sup>1</sup>H} NMR** (125 MHz, CDCl<sub>3</sub>) δ (ppm) = 71.4 (t, *J*=28.6), 111.5 (dd, *J*= 24.3, 3 Hz), 130.8 (t, *J*=9.3 Hz), 161.8-164.2 (dd, *J*=247, 5.3 Hz). **<sup>19</sup>F NMR** (376 MHz, CDCl<sub>3</sub>) δ (ppm) = -91.4

**Synthesis of 1-iodo-2-(trifluoromethyl)benzene (3e) and 1-iodo-3-(trifluoromethyl)benzene (3e').**

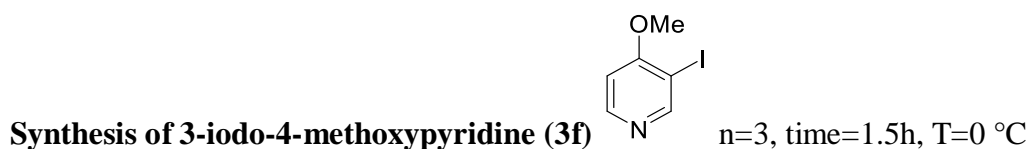
[(PMDETA)<sub>2</sub>K<sub>2</sub>MgR<sub>4</sub>] **1b** was prepared in situ as described for the synthesis **3a**. To 0.5 mmols of **1b** this solution was added (trifluoromethyl)benzene (73 mg, 0.5 mmol) leading to a formation of an oil after 5 minutes. The Schlenk was wrapped with kitchen foil to avoid light induced decomposition of the product. The resultant solution allowed to stir at 0 °C for 1.5 hours. The solution was then quenched with excess of I<sub>2</sub> (1,015 g, in 5 mL THF) and allowed to stir for 1 hour. Next a 10%-5% mixture solution of Na<sub>2</sub>S<sub>2</sub>O<sub>3</sub> and NH<sub>4</sub>Cl respectively was added until bleaching and the product extracted with DCM (3 x 1 mL). The combined organic extracts were dried over MgSO<sub>4</sub> and the solvent removed using the rotary evaporator to obtain a mixture of products as a yellowish oil. The products were then dissolved in CH<sub>2</sub>Cl<sub>2</sub> and ferrocene was added to the solution (29.7 mg, 10 mol%). The yield obtained by integration of the corresponding signals for **3e** and **3e'** <sup>1</sup>H NMR was 93% with 17:1 ratio of products **3e**\3e'.



<sup>1</sup>H NMR (400 MHz, CDCl<sub>3</sub>) δ (ppm) = 6.45 (t, *J*= 7 Hz, 1H), 6.71 (t, *J*=8 Hz, 1H), 7.20 (dd, *J*=8 Hz, *J*= 1.5 Hz, 1H), 7.54 (d, *J*= 8 Hz, 1H).



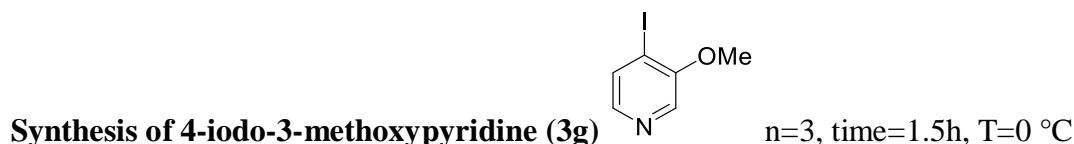
<sup>1</sup>H NMR (400 MHz, CDCl<sub>3</sub>) δ (ppm) = 6.78 (t, *J*= 8 Hz, 1H), 7.00 (t, *J*=8 Hz, 1H), 7.24 (dd, *J*=8 Hz, 1H), 7.76 (s, 1H).



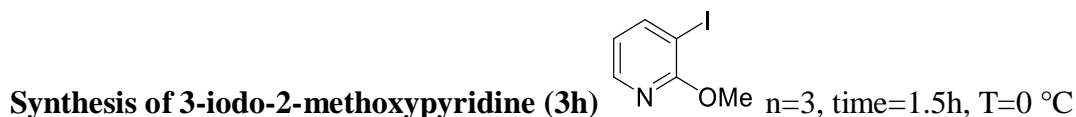
Column chromatographical purification by SiO<sub>2</sub> was carried out using the comby flash with Hexane:DCM as eluent (60:40) to give **3e** as a yellowish solid (247 mg, 70% yield).

<sup>1</sup>H NMR (400 MHz, CDCl<sub>3</sub>) δ (ppm) = 3.97 (s, 3H), 6.70 (d, *J*=5.6 Hz, 1H),

8.33 (d,  $J=5.6$  Hz, 1H), 8.70 (s, 1H).  $^{13}\text{C}\{^1\text{H}\}$  NMR (100 MHz,  $\text{C}_6\text{D}_6$ )  $\delta$  (ppm) = 56.4, 85.3, 107.3, 151.2, 158.1, 164.4. **MS (EI, “70 eV”):**  $m/z$  (%) = 235 [ $\text{M}^+$ ] (100), 93 (21), 78 (83), 51 (84), 50 (48). **Elemental analysis (%):** Calculated for  $\text{C}_6\text{H}_6\text{INO}$ : C, 30.66; H, 2.57; N, 5.96. Found: C, 30.39; H, 2.37; N, 6.40. Values consistent with previous data reported in the literature.<sup>40</sup>



Column chromatographical purification by  $\text{SiO}_2$  was carried out using the comby flash with Hexane:AcOEt as eluent (1:1) to give **3f** as a white solid (263 mg, 75% yield).  $^1\text{H}$  NMR (500 MHz,  $\text{CDCl}_3$ )  $\delta$  (ppm) = 3.96 (s, 3H), 7.70 (d,  $J=5$  Hz 1H), 7.86 (d,  $J=5$  Hz, 1H), 8.09 (s, 1H).  $^{13}\text{C}\{^1\text{H}\}$  NMR (125 MHz,  $\text{CDCl}_3$ )  $\delta$  (ppm) = 57.1, 97.3, 133.3, 134.5, 143.4, 155.4. **MS (EI, “70 eV”):**  $m/z$  (%) = 235 [ $\text{M}^+$ ] (100), 93 (27), 78 (13). **Elemental analysis (%):** Calculated for  $\text{C}_6\text{H}_6\text{INO}$ : C, 30.66; H, 2.57; N, 5.96. Found: C, 31.01; H, 2.43; N, 5.81. Values consistent with previous data reported in the literature.<sup>88</sup>

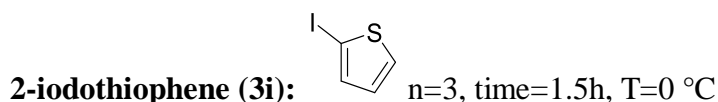


Column chromatographical purification by  $\text{SiO}_2$  was carried out using the comby flash with Hexane:DCM as eluent (20:80) to give **3g** as a colourless oil (204 mg, 58% yield).  $^1\text{H}$  NMR (500 MHz,  $\text{CDCl}_3$ )  $\delta$  (ppm) = 3.98 (s, 3 H), 6.62-6.65 (dd,  $J=7.5$  Hz,  $J=5$  Hz, 1 H), 8.01 (dd,  $J=7.5$ , 1.5 Hz, 1 H), 8.11 (dd,  $J=5$ , 1.5 Hz, 1 H).  $^{13}\text{C}\{^1\text{H}\}$  NMR (125 Mhz,  $\text{CDCl}_3$ )  $\delta$  (ppm) = 54.9, 80.1, 118.5, 146.8, 148.3, 162.2. **MS (EI, “70 eV”):**  $m/z$  (%) = 235 [ $\text{M}^+$ ] (23), 234 (72), 205 (32), 107 (18), 93 (31), 78 (42), 51 (26), 50 (48). Values consistent with previous data reported in the literature.<sup>88</sup>

### Synthesis of 2-iodothiophene (3i) and 2,5 diiodothiophene (3i’).

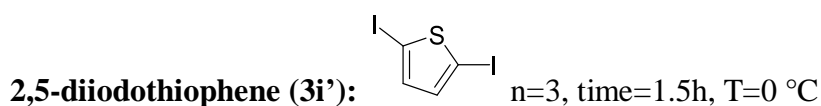
$[(\text{PMDETA})_2\text{K}_2\text{Mg}(\text{CH}_2\text{SiMe}_3)_4]$  **1b** was prepared in situ as described for the synthesis **3a**. To 0.5 mmols of **1b** was added thiophene (126 mg, 1.5 mmol) and the resultant yellowish solution allowed to stir at 0 °C for 1.5 hours. The solution was then quenched with excess of  $\text{I}_2$  (1,015 g, in 5 mL THF) and allowed to stir for 1 hour. Next a 10% -5% mixture solution of  $\text{Na}_2\text{S}_2\text{O}_3$

and NH<sub>4</sub>Cl respectively was added until bleaching and the product extracted with DCM (3 x 1 mL). The combined organic extracts were dried over MgSO<sub>4</sub> and the solvent removed using the rotary evaporator to obtain a mixture of both described products as a yellowish oil and yellowish crystals. The product was then dissolved in CH<sub>2</sub>Cl<sub>2</sub> and ferrocene was added to the solution (29.7 mg, 10 mol%). The yield obtained by integration of the corresponding signals for **3i** and **3i'** by <sup>1</sup>H NMR was 83% for **3i** and 9% for **3i'**.



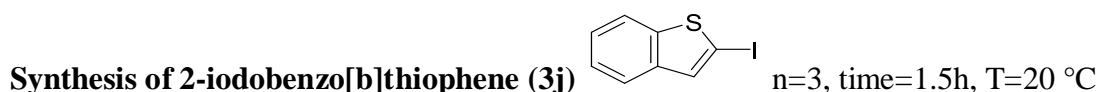
<sup>1</sup>H NMR (500 MHz, CDCl<sub>3</sub>) δ (ppm) = 6.73 (m, *J*=4 Hz, *J*=1.5 Hz, 1H), 7.17 (dd, *J*=3.5, 1 Hz, 1H), 7.28 (dd, *J*=5.5, 1 Hz, 1H).

<sup>13</sup>C{<sup>1</sup>H} NMR (125 MHz, CDCl<sub>3</sub>) δ (ppm) = 73.3, 129.0, 131.6, 137.0,

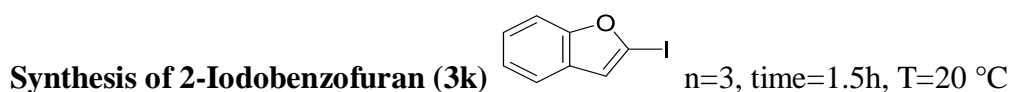


<sup>1</sup>H NMR (500 MHz, CDCl<sub>3</sub>) δ (ppm) = 6.86 (s, 2H)

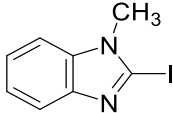
<sup>13</sup>C{<sup>1</sup>H} NMR (125 MHz, CDCl<sub>3</sub>) δ (ppm) = 76.5, 138.9.



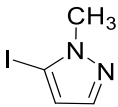
Column chromatographical purification using the combi flash (SiO<sub>2</sub>, hexane/EtOAc = 70:30) afforded **3j** as a pale yellow solid (359 mg, 92% Yield). <sup>1</sup>H NMR (500 MHz, CDCl<sub>3</sub>) δ (ppm) = 7.30-7.32(m, 2H), 7.54 (s, 1H), 7.71-7.73 (m, 1H), 7.76-7.78 (m, 1H). <sup>13</sup>C{<sup>1</sup>H} NMR (125 MHz, CDCl<sub>3</sub>) δ (ppm) = 78.7, 121.5, 122.5, 124.6, 124.7, 134.0, 141.0, 144.6 **MS (EI, “70 eV”):** m/z (%) = 260 [M<sup>+</sup>] (100), 133 (50), 89 (97), 63 (20). **Elemental analysis (%):** Calculated for C<sub>8</sub>H<sub>5</sub>IS: C, 36.94; H, 1.94. Found: C, 37.58; H, 1.91.



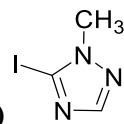
Column chromatographical purification using the combi flash (SiO<sub>2</sub>, hexane/EtOAc = 70:30) afforded **3k** as a pale yellow oil (296 mg, 81% Yield). <sup>1</sup>H NMR (400 MHz, CDCl<sub>3</sub>) δ (ppm) = 6.98 (s, 1H), 7.25-7.27 (m, 2H), 7.52-7.77 (m, 2H). <sup>13</sup>C{<sup>1</sup>H} NMR (101 MHz, CDCl<sub>3</sub>) δ (ppm) = 95.3, 110.0, 116.5, 118.9, 122.4, 123.5, 128.4, 132.5, 157.4. MS (EI, “70 eV”): m/z (%) = 244 [M<sup>+</sup>] (65), 89 (100), 63 (30), 62 (23).

**Synthesis of 2-iodo-1-methylbenzo[d]imidazole (3l)**  n=3, time=1.5h, T=20 °C

Column chromatographical purification using the combi flash (SiO<sub>2</sub>, hexane/EtOAc = 70:30) afforded **3l** as a colourless solid (318 mg, 82% Yield). <sup>1</sup>H NMR (500 MHz, CDCl<sub>3</sub>) δ (ppm) = 3.76 (s, 3H), 7.21-7.26 (m, 2H), 7.31-7.33 (d, <sup>3</sup>J=7.5 Hz 1H), 7.70-7.72 (d, <sup>3</sup>J=7.5 Hz, 1H). <sup>13</sup>C{<sup>1</sup>H} NMR (125 MHz, CDCl<sub>3</sub>) δ (ppm) = 34, 104.5, 109.7, 119.5, 122.5, 123.4, 136.6, 145.8. MS (EI, “70 eV”): m/z (%) = 260 [M<sup>+</sup>] (100), 133 (50), 89 (97), 63 (20). **Elemental analysis (%)**: Calculated for C<sub>8</sub>H<sub>7</sub>IN<sub>2</sub>: C, 37.23; H, 2.73; N, 10.86. Found: C, 36.91; H, 2.64; N, 10.81.

**Synthesis of 5-Iodo-1-methylpyrazole (3n)**  n=3, time=1.5h, T=20 °C

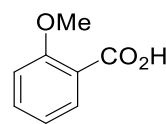
Column chromatographical purification using the combi flash (SiO<sub>2</sub>, hexane first, EtOAc after) afforded **3k** as pale yellow crystals (287 mg, 92% yield). <sup>1</sup>H NMR (500 MHz, C<sub>6</sub>D<sub>6</sub>) δ (ppm) = 3.34 (s, 3H), 6.16 (d, J=1.5 Hz, 1H), 7.34 (d, J=2 Hz, 1H). <sup>13</sup>C{<sup>1</sup>H} NMR (125 MHz, C<sub>6</sub>D<sub>6</sub>) δ (ppm) = 39.8, 81.2, 116.1, 141.8. MS (EI, “70 eV”): m/z (%) = 208 [M<sup>+</sup>] (100), 181 (65), 54 (16), 52 (16). **Elemental analysis (%)**: Calculated for C<sub>4</sub>H<sub>5</sub>IN<sub>2</sub>: C, 23.10; H, 2.42; N, 13.47. Found: C, 24.35; H, 2.65; N, 12.98.



**Synthesis of 5-Iodo-1-methyl-1,2,4-triazole (3p)**  $n=3$ , time=1.5h, T=20 °C

Column chromatographical purification using the combi flash (SiO<sub>2</sub>, hexane first, EtOAc after) afforded **3p** as yellowish crystals (290 mg, 93% yield). <sup>1</sup>H NMR (500 MHz, CDCl<sub>3</sub>) δ (ppm) = 3.86 (s, 3H), 7.83 (s, 1H). <sup>13</sup>C{<sup>1</sup>H} NMR (125 MHz, CDCl<sub>3</sub>) δ (ppm) = 38.1, 100.5, 154.3. **MS (EI, “70 eV”)**: m/z (%) = 209 [M<sup>+</sup>] (100), 182 (7), 56 (10). **Elemental analysis (%)**: Calculated for C<sub>3</sub>H<sub>4</sub>IN<sub>3</sub>: C, 17.24; H, 1.93; N, 20.11 Found: C, 18.23; H, 1.88; N, 20.20.

## 2.6.3 Synthesis of aromatic and heterocyclic substituted carboxylic acids



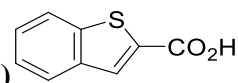
### 2.6.3.1 Synthesis of 2-methoxybenzoic acid (3a')

[(PMDETA)<sub>2</sub>K<sub>2</sub>Mg(CH<sub>2</sub>SiMe<sub>3</sub>)<sub>4</sub>] **1b** was prepared in situ by mixing together K(CH<sub>2</sub>SiMe<sub>3</sub>) (126 mg, 1 mmol) and Mg(CH<sub>2</sub>SiMe<sub>3</sub>)<sub>2</sub> (99mg, 0.5 mmol) in hexane solution and living stirring for 30 minutes. To the white suspension was added PMDETA (173 mg, 1 mmol) to afford a clear solution with an oil deposited at the bottom of the schlenk. Anisole (162 mg, 1.5 mmol) was then added to this solution and allowed to stir for 1.5 hours. Solid blocks of CO<sub>2</sub> were added to a second oven dried Schlenk (flushed with argon 3 times), and the CO<sub>2</sub> was bubbled through the first solution using a cannula for 1h. Instantly a white precipitate was observed. Next a basic saturated solution of Na<sub>2</sub>CO<sub>3</sub> in water was added (2 mL) and the product was dissolve in the water solution. The resultant water solution was washed with DCM (3 x 1 mL) and then acidified adding a 2M solution of HCl dropwise until pH = 2 (a white precipitate was observed). The final product was extracted from the water solution with diethyl ether (3 x 1 mL). The organic extract was dried over MgSO<sub>4</sub> and the solvent removed using the rotary evaporator to obtain **3a'** as a white solid (190 mg, 83% yield). <sup>1</sup>H NMR (400 MHz, DMSO) δ (ppm) = 3.80 (s, 3H), 6.97 (t, *J* = 7.5 Hz, 1H), 7.10 (d, *J* = 8 Hz, 1H), 7.49 (dt, *J* = 2 Hz, 7.5 Hz, 1H), 7.64 (dd, *J* = 1.5 Hz, 7.5 Hz, 1H), 12.61 (broad s, 1H). <sup>13</sup>C{<sup>1</sup>H} NMR (125 MHz, DMSO) δ (ppm) = 56.2, 112.9, 120.5, 121.8, 131.1, 133.5, 158.5, 167.8. **MS (EI, “70 eV”)**: m/z (%) = 151 [M<sup>+</sup>] (19), 135 (17), 123 (100), 105 (77), 79 (73), 77 (85), 63 (19). **Elemental analysis (%)**: Calculated for C<sub>8</sub>H<sub>8</sub>O<sub>3</sub>: C, 63.15; H, 5.30. Found: C, 62.84; H, 5.05.



### 2.6.3.2 Synthesis of 2,6-difluorobenzoic acid (3d)

[(PMDETA)<sub>2</sub>K<sub>2</sub>Mg(CH<sub>2</sub>SiMe<sub>3</sub>)<sub>4</sub>] **1b** was prepared in situ by mixing together K(CH<sub>2</sub>SiMe<sub>3</sub>) (126 mg, 1 mmol) and Mg(CH<sub>2</sub>SiMe<sub>3</sub>)<sub>2</sub> (99mg, 0.5 mmol) in hexane solution and living stirring for 30 minutes. To the white suspension was added PMDETA (173 mg, 1 mmol) to afford a clear solution with an oil deposited at the bottom of the schlenk. 1,3-Difluorobenzene (171 mg, 1.5 mmol) was then added to this solution and allowed to stir for 1.5 hours. Solid blocks of CO<sub>2</sub> were added to a second oven dried Schlenk (flushed with argon 3 times), and the CO<sub>2</sub> was bubbled through the first solution using a cannula for 1h. Instantly a white precipitate is observed. Next a basic saturated solution of Na<sub>2</sub>CO<sub>3</sub> in water is added (2 mL) and the allowing the product to dissolve in the water solution. The resultant water solution is washed with DCM (3 x 1 mL) and then acidified adding a 2M solution of HCl dropwise until pH = 2. The final product is extracted from the water solution with diethyl ether (3 x 1 mL). The organic extract was dried over MgSO<sub>4</sub> and the solvent removed using the rotary evaporator to obtain **3d'** as a white solid (123 mg, 52% yield). <sup>1</sup>H NMR (400 MHz, DMSO) δ (ppm) = 7.20 (t, *J*= 8 Hz, 2H), 7.58 (m, <sup>4</sup>*J*= 2 Hz, 1H), 13.94 (broad s, 1H). <sup>13</sup>C{<sup>1</sup>H} NMR (125 MHz, DMSO) δ (ppm) = 112.4 (dd, *J*= 5 Hz, 20 Hz), 133.0 (t, *J*= 10 Hz), 160.0 (dd, *J*=250, 7 Hz), 162.2. <sup>19</sup>F{<sup>1</sup>H} NMR (376 MHz, DMSO) δ (ppm) = -112.4. MS (EI, "70 eV"): *m/z* (%) = 158 [M<sup>+</sup>] (52), 141 (100), 113 (30), 63 (20). **Elemental analysis (%)**: Calculated for C<sub>7</sub>H<sub>4</sub>F<sub>2</sub>O<sub>2</sub>: C, 53.18; H, 2.55. Found: C, 54.60; H, 2.15.

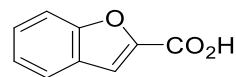


### 2.6.3.3 Synthesis of benzo[b]thiophene-2-carboxylic acid (3j')

[(PMDETA)<sub>2</sub>K<sub>2</sub>Mg(CH<sub>2</sub>SiMe<sub>3</sub>)<sub>4</sub>] **1b** was prepared in situ by mixing together K(CH<sub>2</sub>SiMe<sub>3</sub>) (126 mg, 1 mmol) and Mg(CH<sub>2</sub>SiMe<sub>3</sub>)<sub>2</sub> (99mg, 0.5 mmol) in hexane solution and living stirring for 30 minutes. To the white suspension was added PMDETA (173 mg, 1 mmol) to afford a clear solution with an oil deposited at the bottom of the schlenk. Benzothiophene (201 mg, 1.5 mmol) was then added to this solution and allowed to stir for 1.5 hours. Solid blocks of CO<sub>2</sub> were added to a second oven dried Schlenk (flushed with argon 3 times), and the CO<sub>2</sub> was bubbled through the first solution using a cannula for 1h. Instantly a yellowish precipitate is observed which is filtered with a Buchner funnel. The resultant filtrate was washed with DCM

(3 x 1 mL) and then acidified adding a 2M solution of HCl dropwise until pH = 2. The final product was extracted from the water solution with DCM (3 x 1 mL). The organic extract was dried over MgSO<sub>4</sub> and the solvent removed using the rotary evaporator to obtain **4o** acid as a yellowish solid (240 mg, 90% yield). <sup>1</sup>H NMR (400 MHz, DMSO) δ (ppm) = 7.48 (m, 2H), 8.00 (m, 2H), 8.10 (s, 1H). <sup>13</sup>C{<sup>1</sup>H} NMR (125 MHz, DMSO) δ (ppm) = 122.9, 125.0, 125.7, 126.9, 130.1, 134.9, 138.7, 141.3, 163.5. MS\* (EI, “70 eV”): m/z (%) = 192 [M<sup>+</sup>] (69), 161 (100), 133 (22), 89 (31).

\* The GC MS sample was made dissolving the product in methanol due to the low solubility of benzo[b]thiophene-2-carboxylic acid in chloroform. The mass obtained corresponds to methyl benzo[b]thiophene-2-carboxylate the ester derivative of the carboxylic acid previously formed.



#### 2.6.3.4 Synthesis of benzofuran-2-carboxylic acid (**3k'**)

[(PMDETA)<sub>2</sub>K<sub>2</sub>Mg(CH<sub>2</sub>SiMe<sub>3</sub>)<sub>4</sub>] **1b** was prepared in situ by mixing together K(CH<sub>2</sub>SiMe<sub>3</sub>) (126 mg, 1 mmol) and Mg(CH<sub>2</sub>SiMe<sub>3</sub>)<sub>2</sub> (99mg, 0.5 mmol) in hexane solution and living stirring for 30 minutes. To the white suspension was added PMDETA (173 mg, 1 mmol) to afford a clear solution with an oil deposited at the bottom of the schlenk. Benzofuran (177 mg, 1.5 mmol) was then added to this solution and allowed to stir for 1.5 hours. Solid blocks of CO<sub>2</sub> were added to a second oven dried Schlenk (flushed with argon 3 times), and the CO<sub>2</sub> was bubbled through the first solution using a cannula for 1h. Instantly a yellowish precipitate is observed. Next a basic saturated solution of Na<sub>2</sub>CO<sub>3</sub> in water is added (2 mL) and the allowing the product to dissolve in the water solution. The resultant water solution was washed with DCM (3 x 1 mL) and then acidified adding a 2M solution of HCl dropwise until pH = 2. The final product was extracted from the water solution with DCM (3 x 1 mL). The organic extract was dried over MgSO<sub>4</sub> and the solvent removed using the rotary evaporator to obtain **4n** as a white solid (231 mg, 95% yield). <sup>1</sup>H NMR (400 MHz, DMSO) δ (ppm) = 7.33 (t, 1H), 7.48 (t, 1H), 7.66 (s, 1H), 7.68 (d, 1H), 7.78 (d, 1H), 13.6 (broad s, 1H). <sup>13</sup>C{<sup>1</sup>H} NMR (125 MHz, DMSO) δ (ppm) = 112.0, 113.5, 123.1, 123.8, 126.9, 127.6, 146.2, 155.0, 160.1. MS (EI, “70 eV”): m/z (%) = 162 [M<sup>+</sup>] (100), 145 (43), 134 (27), 89 (39), 78 (19).

## 2.7 References:

- (1) Andrikopoulos, P. C.; Armstrong, D. R.; Graham, D. V.; Hevia, E.; Kennedy, A. R.; Mulvey, R. E.; O'Hara, C. T.; Talmard, C. *Angew. Chemie Int. Ed.* **2005**, *44* (22), 3459–3462.
- (2) Barden, T. C. *Top. Heterocycl. Chem.* **2011**, *26*, 31–46.
- (3) Kaushik, N. K.; Kaushik, N.; Attri, P.; Kumar, N.; Kim, C. H.; Verma, A. K.; Choi, E. H. *Molecules* **2013**, *18* (6), 6620–6662.
- (4) Conway, B.; Hevia, E.; Kennedy, A. R.; Mulvey, R. E. *Chem. Commun.* **2007**, No. 27, 2864–2866.
- (5) Frischmuth, A.; Fernández, M.; Barl, N. M.; Achrainger, F.; Zipse, H.; Berionni, G.; Mayr, H.; Karaghiosoff, K.; Knochel, P. *Angew. Chemie Int. Ed.* **2014**, *53* (30), 7928–7932.
- (6) Andrews, P. C.; Kennedy, A. R.; Mulvey, R. E.; Raston, C. L.; Roberts, B. A.; Rowlings, R. B. *Angew. Chemie Int. Ed.* **2000**, *39* (11), 1960–1962.
- (7) Martínez-Martínez, A. J.; Armstrong, D. R.; Conway, B.; Fleming, B. J.; Klett, J.; Kennedy, A. R.; Mulvey, R. E.; Robertson, S. D.; O'Hara, C. T. *Chem. Sci.* **2014**, *5* (2), 771.
- (8) Martínez-Martínez, A. J.; Kennedy, A. R.; Mulvey, R. E.; O'Hara, C. T. *Science* **2014**, *346* (6211), 834–837.
- (9) Schlenk, W.; W. J. S. *Berichte der Dtsch. Chem. Gesellschaft* **1929**, 920–924.
- (10) Klett, J.; Clegg, W.; Conway, B.; Kennedy, A. R.; Mulvey, R. E.; Russo, L. *Eur. J. Inorg. Chem.* **2011**, No. 5, 721–726.
- (11) Davidson, P. J.; Lappert, M. F.; Pearce, R. *Acc. Chem. Res.* **1974**, *7* (7), 209–217.
- (12) Corbelin, S.; Lorenzen, N. P.; Koph, J.; Weiss, E. *J. Organomet. Chem.* **1991**, *415*, 293.
- (13) Schumann, H.; Freckmann, D. M. M.; Dechert, S. *Organometallics* **2006**, *25*, 2696–2699.
- (14) Hitchcock, P.; Lappert, M. F.; Leung, W.; Diansheng, L.; Shun, T. *Chem. Commun.* **1993**, 1386–1387.
- (15) Boesveld, W. M.; Hitchcock, P. B.; Lappert, M. F.; Liu, D.-S.; Tian, S. *Organometallics* **2000**, *19*, 4030–4035.
- (16) Hitchcock, P. B.; Kh, A. V.; Lappert, M. F. *J. Organomet. Chem.* **2002**, *663*, 263–268.
- (17) Al-juaid, S. S.; Eaborn, C.; Hitchcock, P. B.; Izod, K.; Mallien, M.; Smith, J. D. *Angew. Chemie Int. Ed.* **1994**, *33*, 1268–1270.
- (18) Eaborn, C.; Hitchcock, P. B.; Izod, K.; Jaggar, A. J.; Smith, J. D. *Organometallics* **1994**, *13*, 753–754.
- (19) Eaborn, C.; Clegg, W.; Hitchcock, P. B.; Hopman, M.; Izod, K.; Shaughnessy, P. N. O.; Smith, J. D. *Organometallics* **1997**, *16*, 4728–4736.
- (20) Baillie, S. E.; Bluemke, T. D.; Clegg, W.; Kennedy, A. R.; Klett, J.; Russo, L.; De Tullio, M.; Hevia, E. *Chem. Commun.* **2014**, *50* (18), 12859–12862.

- (21) Sharon E. Baillie. PhD thesis: Novel synthetic and structural advances in magnesiate and zincate chemistry, University of Strathclyde, 2012.
- (22) Snieckus, V. *Chem. Rev.* **1990**, *90* (6), 879–933.
- (23) Wittig, G.; Pockels, U.; Drodge, H. *Berichte der Dtsch. Chem. Gesellschaft* **1938**, *71* (9), 1903.
- (24) Wittig, G.; Fuhrmann, G. *Berichte der Dtsch. Chem. Gesellschaft* **1940**, *73* (11), 1197–1218.
- (25) Gilman, H.; Bebb, R. L. *J. Am. Chem. Soc.* **1939**, *61*, 109.
- (26) Whisler, M. C.; MacNeil, S.; Snieckus, V.; Beak, P. *Angew. Chemie Int. Ed.* **2004**, *43* (17), 2206–2225.
- (27) Rennels, R. A.; Maliakal, A. J.; Collum, D. B. *J. Am. Chem. Soc.* **1998**, *120*, 421–422.
- (28) Chadwick, S. T.; Rennels, R. A.; Rutherford, J. L.; Collum, D. B. *J. Am. Chem. Soc.* **2000**, *122*, 8640–8647.
- (29) Collum, B. *Acc. Chem. Res.* **1993**, *26* (5), 227–234.
- (30) Krasovskiy, A.; Krasovskaya, V.; Knochel, P. *Angew. Chemie Int. Ed.* **2006**, *45* (18), 2958–2961.
- (31) Uchiyama, M.; Naka, H.; Matsumoto, Y.; Ohwada, T. *J. Am. Chem. Soc.* **2004**, *126* (34), 10526–10527.
- (32) Awad, H.; Mongin, F.; Trécourt, F.; Quéguiner, G.; Marsais, F.; Blanco, F.; Abarca, B.; Ballesteros, R. *Tetrahedron Lett.* **2004**, *45* (36), 6697–6701.
- (33) Trost, B. M. *Science* **1991**, *254*, 1471–1477.
- (34) Garden, J. A.; Armstrong, D. R.; Clegg, W.; Garcia-Alvarez, J.; Hevia, E.; Kennedy, A. R.; Mulvey, R. E.; Robertson, S. D.; Russo, L. *Organometallics* **2013**, *32*, 5481.
- (35) Hevia, E.; Kennedy, A. R.; Klett, J.; Baillie, S. E.; Clegg, W.; García-Álvarez, P.; Russo, L. *Organometallics* **2012**, *31*, 5131.
- (36) Shen, K.; Fu, Y.; Li, J.-N.; Liu, L.; Guo, Q.-X. *Tetrahedron* **2007**, *63* (7), 1568–1576.
- (37) Armstrong, D. R.; Kennedy, A. R.; Mulvey, R. E. *Angew. Chemie Int. Ed.* **1999**, *38*, 131.
- (38) Armstrong, D. R.; Clegg, W.; Dale, S. H.; Graham, D. V.; Hevia, E.; Hogg, L. M.; Honeyman, G. W.; Kennedy, A. R.; Mulvey, R. E. *Chem. Commun.* **2007**, No. 6, 598–600.
- (39) Screttas, C. G.; Steele, B. R. *J. Org. Chem.* **1989**, *54* (12), 1013–1017.
- (40) Uchiyama, M.; Naka, H.; Matsumoto, Y.; Wheatley, A. E. H.; McPartlin, M.; Morey, J. V.; Kondo, Y. *J. Am. Chem. Soc.* **2007**, *129* (7), 1921–1930.
- (41) Snieckus, V.; Beak, P. *Acc. Chem. Res.* **1982**, *15*, 306.
- (42) Beak, P.; Brubaker, G. R.; Farney, R. F. *J. Am. Chem. Soc.* **1976**, *98*, 3621.
- (43) Upton, C. J.; Beak, P. *J. Org. Chem.* **1975**, *40* (8), 1094–1098.
- (44) Beak, P.; Kerrick, S. T.; Gallagher, D. J. *J. Am. Chem. Soc.* **1993**, *115* (23), 10628–10636.
- (45) Hauser, C. R.; Ludt, R.; Griffiths, J.; McGrath, K. *J. Org. Chem.* **1973**, *38* (9), 1668–1674.

- (46) Kondo, Y.; Shilai, M.; Uchiyama, M.; Sakamoto, T. *J. Am. Chem. Soc.* **1999**, No. 8, 3539–3540.
- (47) Clegg, W.; Dale, S. H.; Hevia, E.; Honeyman, G. W.; Mulvey, R. E. *Angew. Chemie Int. Ed.* **2006**, 45 (15), 2370–2374.
- (48) Clegg, W.; Dale, S. H.; Hevia, E.; Honeyman, G. W.; Mulvey, R. E.; Harrington, R. W.; Hevia, E.; Honeyman, G. W.; Mulvey, R. E. *Angew. Chemie Int. Ed.* **2006**, 45 (15), 2374–2377.
- (49) Fleming, P.; O’Shea, D. F. *J. Am. Chem. Soc.* **2011**, 133 (6), 1698–1701.
- (50) Smart, B. E. *J. Fluor. Chem.* **2001**, 109 (1), 3–11.
- (51) Müller, K.; Faeh, C.; Diederich, F. *Science* **2007**, 317 (5846), 1881–1886.
- (52) Schlosser, M.; Michel, D. *Tetrahedron* **1996**, 52 (1), 99–108.
- (53) Gouverneur, V.; Purser, S.; Moore, P. R.; Swallow, S. *Chem. Soc. Rev.* **2008**, 37 (2), 237–432.
- (54) Ojima, I. *J. Org. Chem.* **2013**, 78 (13), 6358–6383.
- (55) Schlosser, M.; Heiss, C. *Eur. J. Org. Chem.* **2003**, No. 23, 4618–4624.
- (56) Ogawa, A.; Curran, D. P. *J. Org. Chem.* **1997**, 62 (3), 450–451.
- (57) Banks, R. E. *Organofluorine Chemicals and their Industrial Applications*; Ellis Horwood LTD: Chichester, 1979.
- (58) De Riggi, I.; Virgili, A.; De Moragas, M.; Jaime, C. *J. Org. Chem.* **1995**, 60, 27–31.
- (59) Charton, M. *J. Org. Chem.* **1976**, 41, 2217.
- (60) Roberts, J. D.; Curtin, D. Y. *J. Am. Chem. Soc.* **1946**, 68, 1658.
- (61) Morton, A.; Marsh, F. D.; Coombs, R. D.; Lyons, A. L.; Penner, S.; Ramsden, H.; Baker, V.; Little, E.; Letsinger, R. *J. Am. Chem. Soc.* **1950**, No. 72, 3785.
- (62) Morton, A. A.; Holden, M. E. *J. Am. Chem. Soc.* **1947**, 69, 1675.
- (63) Morton, A. A.; Patterson, H. G.; Donovan, J. J.; Ernest, L. L. *J. Am. Chem. Soc.* **1946**, 68, 93–96.
- (64) Schlosser, M.; Choi, J. H.; Takagishi, S. *Tetrahedron* **1990**, 46 (16), 5633–5648.
- (65) Schlosser, M.; Katsoulos, G.; Sadahito, T. *Synlett* **1990**, 747.
- (66) Hevia, E.; Armstrong, D. R.; Blair, V. L.; Clegg, W.; Dale, S. H.; Garcia-Alvarez, J.; Honeyman, G. W.; Mulvey, R. E.; Russo, L. *J. Am. Chem. Soc.* **2010**, 132 (27), 9480–9487.
- (67) Knochel, P.; Mongin, F.; Trécourt, F.; Bonnet, V.; Breton, G.; Marsais, F.; Quéguiner, G. *Synlett* **2002**, 6, 1008–1010.
- (68) Hermann, J. R.; Kleemann, A. *Pharmaceutical Chemistry, Vol 1: Drug synthesis*, Prentice H.; Europe, London, 1988.
- (69) Mongin, F.; Queguiner, G. *Tetrahedron* **2001**, 57 (564), 4059–4090.
- (70) Gros, P. C.; Fort, Y.; Caubère, P. *J. Chem. Soc.* **1997**, 3597.
- (71) Quéguiner, G.; Marsais, F.; Snieckus, V.; Epsztajn, J. *Adv. Heterocycl. Chem.* **1991**, 52, 187.
- (72) Comins, D. L.; Joseph, S. P.; Goehring, R. R. *J. Am. Chem. Soc.* **1994**, 116 (11), 4719–

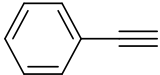
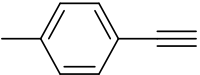
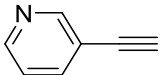
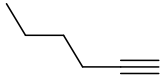
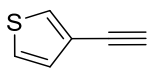
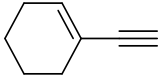
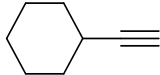
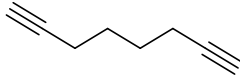
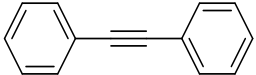
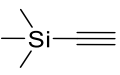
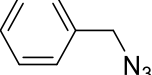
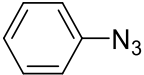
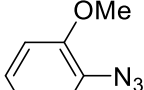
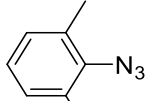
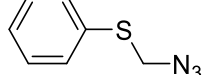
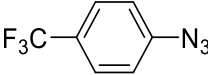
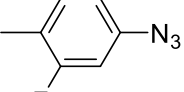
- 4728.
- (73) Trécourt, F.; Mallet, M.; Mongin, O.; Gervais, B.; Quéguiner, G. *Tetrahedron* **1993**, *49* (37), 8373–8380.
- (74) Trecourt, F.; Mallet, M.; Mongin, O.; Quéguiner, G. *J. Org. Chem.* **1994**, *59* (21), 6173–6178.
- (75) J. Clayden. *Organolithiums: Selectivity for synthesis*; Elsevier: Oxford, 2002.
- (76) Comins, D. L.; LaMunyon, D. H. *Tetrahedron Lett.* **1988**, *29*, 773.
- (77) Jaric, M.; Haag, B. a; Unsinn, A.; Karaghiosoff, K.; Knochel, P. *Angew. Chemie Int. Ed.* **2010**, *49* (32), 5451–5455.
- (78) Nicolaou, K. C.; Sorensen, E. J. *Classics in Total Synthesis*; Wiley-VCH: Weinheim, 1996.
- (79) Wipf, P.; Xu, W. *J. Org. Chem.* **1996**, *61*, 6556–6562.
- (80) Shilai, M.; Kondo, Y.; Sakamoto, T. *J. Chem. Soc. Perkin Trans. I* **2001**, No. 4, 442–444.
- (81) Bayh, O.; Awad, H.; Mongin, F.; Hoarau, C.; Trécourt, F.; Quéguiner, G.; Marsais, F.; Blanco, F.; Abarca, B.; Ballesteros, R. *Tetrahedron* **2005**, *61* (20), 4779–4784.
- (82) Mulvey, R. E.; Mongin, F.; Uchiyama, M.; Kondo, Y. *Angew. Chemie Int. Ed.* **2007**, *46* (21), 3802–3824.
- (83) Blair, V. L.; Kennedy, A. R.; Klett, J.; Mulvey, R. E. *Chem. Commun.* **2008**, 5426–5428.
- (84) Mongin, F.; Bucher, A.; Bazureau, J. P.; Bayh, O.; Awad, H.; Trécourt, F. *Tetrahedron Lett.* **2005**, *46* (46), 7989–7992.
- (85) Takaya, J.; Tadami, S.; Ukai, K.; Iwasawa, N. *Org. Lett.* **2008**, *10* (13), 2697–2700.
- (86) Blair, V. L.; Clegg, W.; Kennedy, A. R.; Livingstone, Z.; Russo, L.; Hevia, E. *Angew. Chemie Int. Ed.* **2011**, *50* (42), 9857–9860.
- (87) Armstrong, D. R.; Clegg, W.; Hernán-Gómez, A.; Kennedy, A. R.; Livingstone, Z.; Robertson, S. D.; Russo, L.; Hevia, E. *Dalton Trans.* **2014**, *43*, 4361.
- (88) Blair, V. L.; Blakemore, D. C.; Hay, D.; Hevia, E.; Pryde, D. C. *Tetrahedron Lett.* **2011**, *52* (36), 4590–4594.
- (89) Despotopoulou, C.; Klier, L.; Knochel, P. *Org. Lett.* **2009**, *11* (15), 3326–3329.
- (90) Tilly, D.; Snégaroff, K.; Dayaker, G.; Chevallier, F.; Gros, P. C.; Mongin, F. *Tetrahedron* **2012**, *68* (42), 8761–8766.

## **CHAPTER 3**

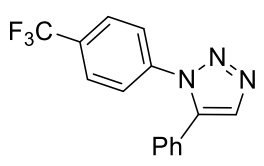
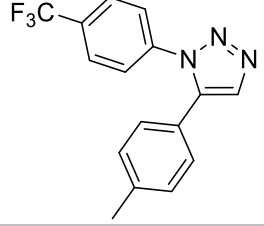
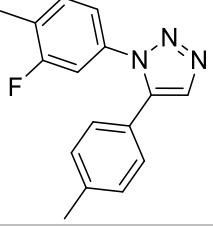
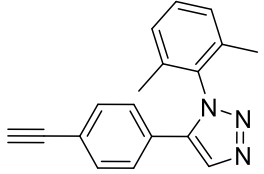
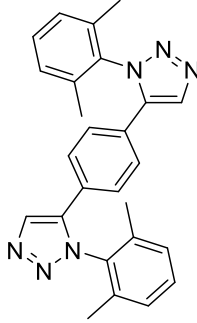
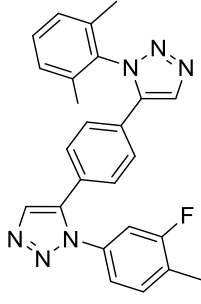
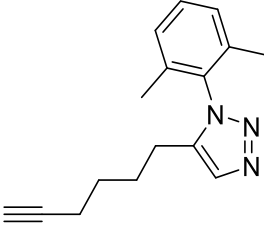
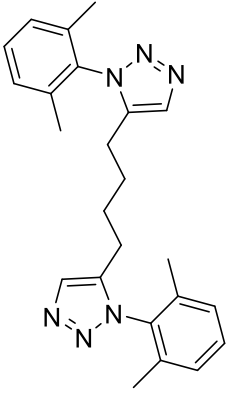
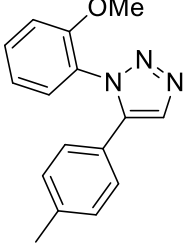
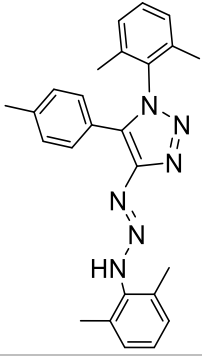
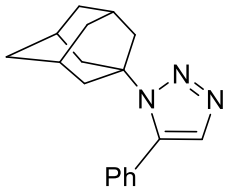
### **Sodium-magnesiate catalysed synthesis of 1,5-disubstituted-1,2,3-triazoles**

### III. Table of compounds

<b>1a</b>	$[\{(\text{KMg}(\text{CH}_2\text{SiMe}_3)_3)_\infty]$	<b>1b</b>	$[(\text{PMDETA})_2\text{K}_2\text{Mg}(\text{CH}_2\text{SiMe}_3)_4]$
<b>1d</b>	$[(\text{TMEDA})_2\text{Na}_2\text{Mg}(\text{CH}_2\text{SiMe}_3)_4]$	<b>1e</b>	$[(\text{TMEDA})_2\text{Li}_2\text{Mg}(\text{CH}_2\text{SiMe}_3)_4]$
<b>1f</b>	$[\text{NaMg}(\text{CH}_2\text{SiMe}_3)_3]$	<b>1g</b>	$[\text{LiMg}(\text{CH}_2\text{SiMe}_3)_3]$
<b>1h</b>	$[(\text{TMEDA})\text{NaMg}\{\text{C}\equiv\text{C}(p\text{-tolyl})\}_3]_2$	<b>1i</b>	$[(\text{TMEDA})\text{NaMg}\{\text{C}\equiv\text{C}(\text{SiMe}_3)\}_3]_2$
<b>1j</b>	$[(\text{THF})_4\text{Na}_2\text{Mg}\{\text{C}\equiv\text{C}(p\text{-tolyl})\}_4]$	<b>1k</b>	$[(\text{THF})\text{Na}(\text{C}_{25}\text{H}_{25}\text{N}_6)]$
<b>1l</b>	$[\{\text{C}\equiv\text{C}(p\text{-tolyl})\}_2\text{Mg}\{(\text{THF})\text{Na}(\text{C}_{23}\text{H}_{21}\text{N}_6\text{O}_2)\}_2]$		

<b>4a</b>		<b>4b</b>		<b>4c</b>	
<b>4d</b>		<b>4e</b>		<b>4f</b>	
<b>4g</b>		<b>4h</b>		<b>4i</b>	
<b>4j</b>		<b>4k</b>		<b>5a</b>	
<b>5b</b>		<b>5c</b>		<b>5d</b>	
<b>5e</b>		<b>5f</b>		<b>5g</b>	

<b>5h</b>		<b>5i</b>		<b>6a</b>	
<b>6b</b>		<b>6c</b>		<b>6d</b>	
<b>6e</b>		<b>6f</b>		<b>6g</b>	
<b>6h</b>		<b>6i</b>		<b>6j</b>	
<b>6k</b>		<b>6l</b>		<b>6m</b>	
<b>6n</b>		<b>6o</b>		<b>6p</b>	
<b>6q</b>		<b>6r</b>		<b>6s</b>	

<b>6t</b>		<b>6u</b>		<b>6v</b>	
<b>6w</b>		<b>6x</b>		<b>6y</b>	
<b>6z</b>		<b>6z'</b>		<b>6a</b>	
<b>6β</b>		<b>6ah</b>			

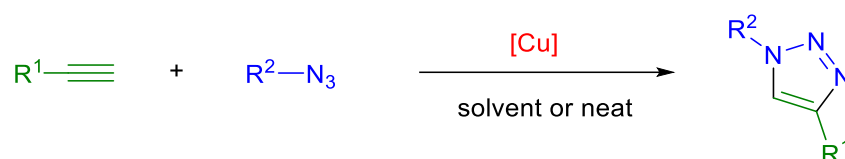
### 3.1 Summary

Unveiling new catalytic behaviour in cooperative bimetallic chemistry, this chapter reports the synthesis of 1,5-disubstituted-1,2,3-triazoles via ligation of terminal alkynes and organic azides using substoichiometric amounts (5-10 mol%) of the homoalkyl sodium magnesiates  $[\text{NaMg}(\text{CH}_2\text{SiMe}_3)_3]$  (**1f**) and  $[(\text{TMEDA})_2\text{Na}_2\text{Mg}(\text{CH}_2\text{SiMe}_3)_4]$  (**1d**). Combining reactivity, spectroscopic, structural and kinetic studies new light has been shed on the possible mechanism and constitution of the intermediates involved in these transformations. To access alkali-metal effects of lithium and potassium analogues of **1f** and **1d** was also assessed. The influence that donor solvents play in these transformations were also investigated. Studies show the importance of sodium in these transformations which acts in a synergistic manner with Mg to decrease the activation energy of these transformation.

Stoichiometric studies suggest sodium alkynyl magnesiates are intermediates in these catalyses. Reactivity and kinetic studies imply this novel reaction procedure occurs via (tris)- and (tetra)alkynyl intermediates that react with organic azides in insertion steps. The rate law for the reaction of 1-ethynylcyclohexene (**4g**) and 1-azido-2-methoxybenzene (**5c**) catalysed by **1d** is order 0 in [alkyne], order 1 in [azide] and [catalyst] which is consistent with the rate-determining azide insertion/intramolecular nucleophilic attack transition state. Being the first examples of an ate catalysed synthesis of 1,5-disubstituted-1,2,3-triazoles this procedure opens new ground on further applications in this area.

## 3.2 Introduction

*N*-Heterocyclic [1,2,3]-triazoles are molecules of great synthetic relevance due to their presence in many biologically active molecules,<sup>1-3</sup> materials<sup>4</sup> and natural products.<sup>5</sup> Amongst the different synthetic approaches to access [1,2,3]-triazoles Cu-catalysed alkyne azide cycloaddition reactions (CuAAC) constitute one of the most versatile and widely used methods, allowing the synthesis of a great variety of 1,4-disubstituted triazoles in excellent yields and substrate scope (**Scheme 3.1**).<sup>5,6</sup>



**Scheme 3.1:** General Cu-catalysed alkyne azide cycloaddition reaction with corresponding formation of 1,4-disubstituted triazoles

Since the discovery of this catalytic procedure, there has been an increasing interest in the synthesis of biological active triazoles which can be utilised as HIV inhibitors<sup>2,7</sup> as well as glycosidase inhibitors<sup>8</sup> which prevent the digestion of carbohydrates for type 2 diabetic patients and also as antifungal agents since they can mimic peptide bonds. For example when replacing the peptidic bond “CONH” of a known natural product with antifungal activity by a triazole moiety it leads to an increased antifungal activity of the novel cyclotetrapeptide triazole analogue (**Figure 3.1**).<sup>9</sup>

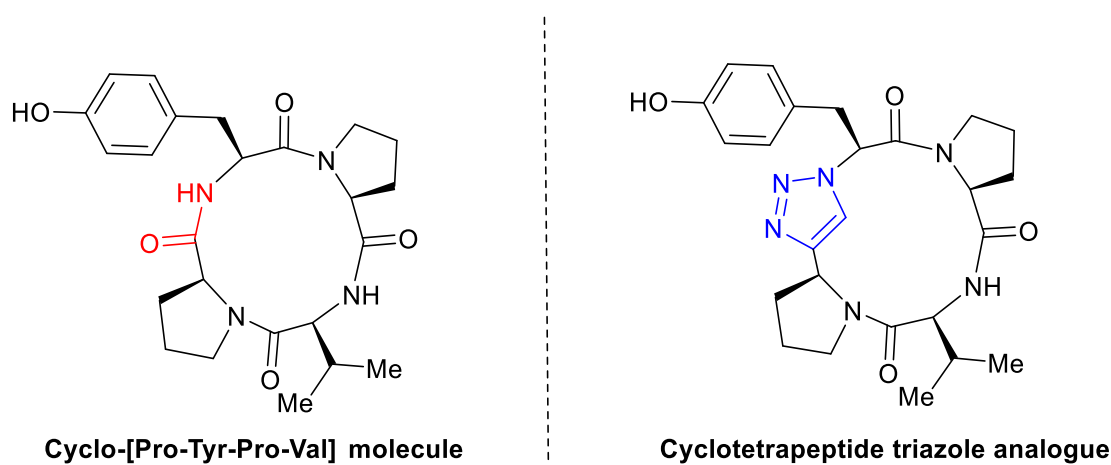


**Figure 3.1:** Example of 1,4-disubstituted triazole as an antifungal agent.

Contrasting with this well-developed methodology, the methods to give 1,5-substituted isomers have been significantly less well developed.<sup>10–12</sup> Therefore the applications of 1,5-disubstituted triazoles are significantly less well known when compared to 1,4-disubstituted triazoles. Finding new synthetic procedures to facilitate the formation of such important heterocycles will ultimately increase their applications in different areas. Other transition metals have succeeded in the formation of 1,5-disubstituted-1,2,3-triazoles with a wider reaction scope. In 2005 Fokin and collaborators developed a Ru-catalysed selective approach for the synthesis of both 1,5- and 1,4-regioisomers according to the ligands employed around the Ru center (**Table 3.1**).<sup>13</sup>

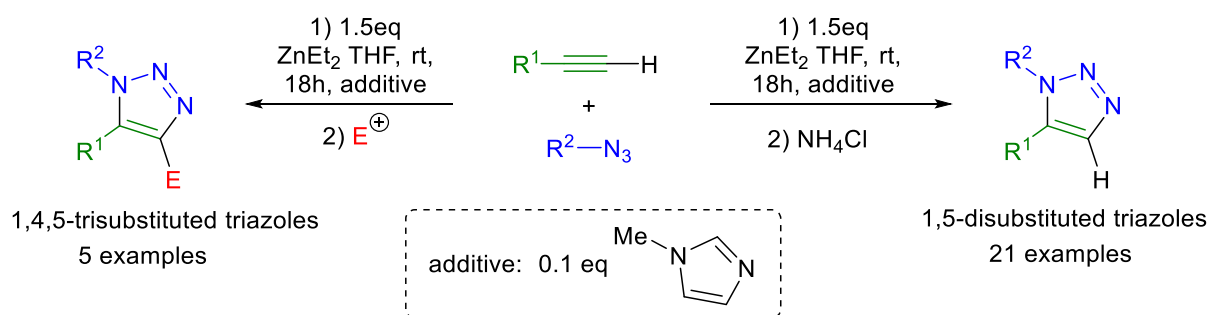
**Table 3.1:** Ru-catalysed 1,5- and 1,4-triazole regioisomers according to the ligands employed around the Ru center

Entry	[Ru]	Yield (%) <sup>a</sup> of 1,5-triazole	Yield (%) <sup>a</sup> of 1,4-triazole		
1	Ru(OAc) <sub>2</sub> (PPh <sub>3</sub> ) <sub>2</sub>	-	100		
2	RuCl <sub>2</sub> (PPh <sub>3</sub> ) <sub>3</sub>	-	20		
3	CpRuCl(PPh <sub>3</sub> ) <sub>2</sub>	85	15		
4	Cp <sup>*</sup> RuCl(PPh <sub>3</sub> ) <sub>2</sub>	100	-		
[a] Yields determined by <sup>1</sup> H NMR analysis					

In this procedure the regioselectivity of the reaction can be tuned depending on the electronic environment around the ruthenium center. In fact when a mixture of benzyl azide and phenylacetylene (1:1.5 equiv, respectively) react in benzene at 80 °C for 4 hours in the presence of 5 mol% of Ru(OAc)<sub>2</sub>(PPh<sub>3</sub>)<sub>2</sub>, 1,4-disubstituted triazole products can be obtained quantitatively (Entry 1, **Table 3.1**). Other complexes such as RuCl<sub>2</sub>(PPh<sub>3</sub>)<sub>3</sub> were found to be rather inactive, with only 20% yield for formation of 1,4-disubstituted-1,2,3-triazole (entry 2, **Table 3.1**). However when the reaction was carried out using a CpRuCl(PPh<sub>3</sub>)<sub>2</sub> ruthenium complex a mixture of 1,5 and 1,4 regioisomers were obtained (85% and 15% yields

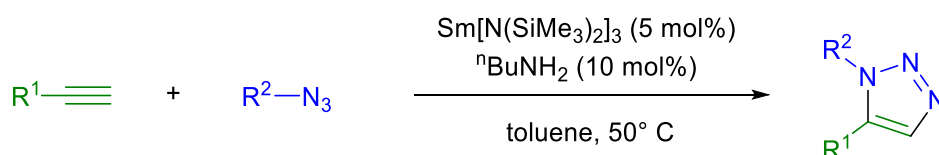
respectively, entry 3, **Table 3.1**). The regioselectivity of the reaction can be totally switched toward the formation of the 1,5-disubstituted-1,2,3-triazole when using  $\text{Cp}^*\text{RuCl}(\text{PPh}_3)_2$  as a catalyst. These results show that ruthenium complexes can effectively promote the synthesis of both 1,4 and 1,5-triazoles, however this approach requires of relatively long reaction times (2 to 12 hours) and high temperature (80 °C) for the reaction to get to completion. In addition ruthenium is a rare transition metal, thus there is a need for the preparation of 1,5-disubstituted-1,2,3-triazoles using cheap and abundant reagents.

Other known synthetic routes for their synthesis involve reactions of azides with polar organometallic reagents such as sodium, lithium or magnesium acetylides.<sup>14</sup> Recently, Greaney has shown that lower polarity organometallic reagents such as  $\text{ZnEt}_2$  can also promote the formation of a range of 1,5-disubstituted triazoles by in-situ formation of zinc acetylides which can undergo [3+2] cycloaddition reactions with organic azides (**Scheme 3.2**).<sup>15</sup>



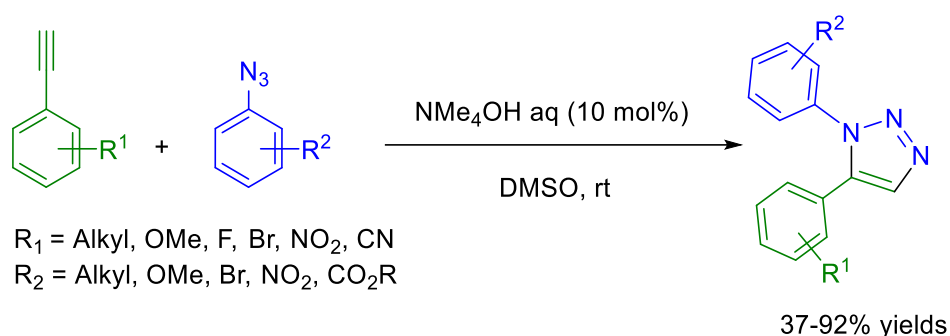
**Scheme 3.2:**  $\text{ZnEt}_2$  mediated azide-alkyne ligation to 1,5- and 1,4,5-substituted-1,2,3-triazoles

In many of these studies, the reactions require the use of stoichiometric amounts or an excess of the polar organometallic reagents which can be particularly problematic if for example the substrate contains other sensitive functional groups. Related to this work, in 2013 Zhou employed a new approach using rare earth metals such as Nd, Sm, Gd and Yb amides as catalysts in cycloaddition reactions of terminal alkyne to azides for the formation of 1,5-disubstituted triazoles (**Scheme 3.3**).



**Scheme 3.3:** Lanthanide catalysed cycloaddition reactions to form 1,5-disubstituted-1,2,3-triazoles

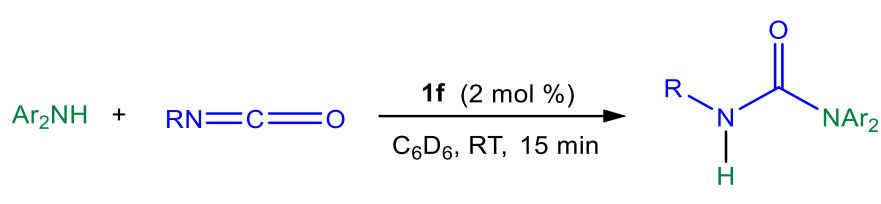
This approach shows a good substrate scope although long reaction times (up to 24 h at 50 °C) and careful control of the temperature are required, in order to avoid decomposition of the organometallic intermediates involved.<sup>12</sup> In addition, Fokin reported a metal-free base-catalysed approach, using a quaternary ammonium hydroxide (NMe<sub>4</sub>OH) where the use of a highly reactive polar organometallic reagent is not required. However this method is limited to aryl acetylenes and aryl azides (**Scheme 3.4**).<sup>10</sup>



**Scheme 3.4:** Fokin's metal-free base-catalysed approach for the synthesis of 1,5-triazoles

These methodologies demonstrate the ability of s-block organometallic reagents to promote the formation of 1,5-triazoles under stoichiometric conditions but so far there are no precedents in using these systems under catalytic regimes. **Chapter 2** of this PhD thesis has unveiled primarily the ability of alkali metal magnesiates to promote direct Mg-H exchange reactions of a wide range of substituted aromatic molecules with excellent levels of selectivity and a remarkable functional group tolerance.<sup>16</sup> Furthermore, preliminary studies have revealed the ability of NaMg(CH<sub>2</sub>SiMe)<sub>3</sub> (**1f**) to catalyse hydroamination/cyclotrimerisation processes of isocyanates, providing the first glimpses of the untapped potential of cooperative bimetallic reagents to effect catalytic transformations (**Table 3.2**).<sup>17</sup>

**Table 3.2:** NaMg(CH<sub>2</sub>SiMe)<sub>3</sub> (**1f**) catalysed hydroamination/cyclotrimerisation of isocyanates

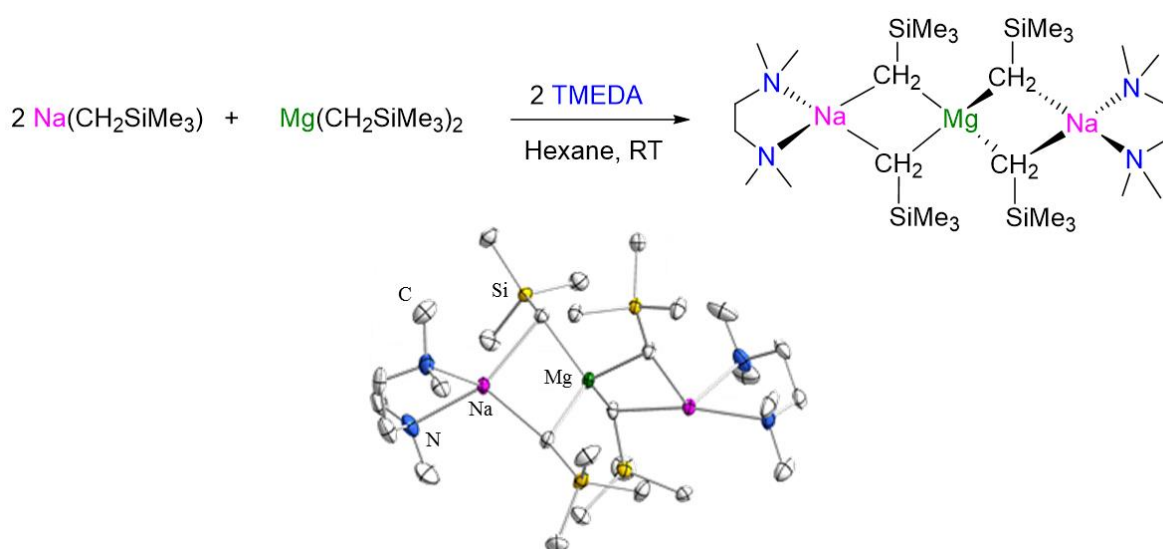
			
Entry	Ar <sub>2</sub> NH	R	Yield (%)
1	Ph <sub>2</sub> NH	<sup>t</sup> Bu	97
2	Ph <sub>2</sub> NH	Cy	98
3	Ph <sub>2</sub> NH	Ad	90
4	<i>p</i> -Tol <sub>2</sub> NH	<sup>t</sup> Bu	99
5	<i>p</i> -Tol <sub>2</sub> NH	Cy	98
6	<i>p</i> -Tol <sub>2</sub> NH	Ad	92
7	Ph(Me)NH	<sup>t</sup> Bu	99
8	Ph(Me)NH	Ad	99

Building on these initial studies, in this chapter we will discuss another catalytic application of these bimetallic systems assessing their ability to promote cycloaddition reactions of terminal alkynes to azide to yield 1,5-disubstituted 1,2,3-triazoles.

### 3.3 Results and discussion: Synthesis of starting materials

#### 3.3.1 Synthesis of bimetallic pre-catalysts

This chapter builds on previous synthetic and structural work carried out in our research group using homoleptic alkyl sodium magnesiate  $[\text{NaMg}(\text{CH}_2\text{SiMe}_3)_3]$  (**1f**), and  $[(\text{TMEDA})_2\text{Na}_2\text{Mg}(\text{CH}_2\text{SiMe}_3)_4]$  (**1d**)<sup>a</sup>. In addition to this, other bimetallic complexes such as  $[\text{KMg}(\text{CH}_2\text{SiMe}_3)_3]$  (**1a**),  $[\text{LiMg}(\text{CH}_2\text{SiMe}_3)_3]$  (**1g**),  $[(\text{TMEDA})_2\text{Li}_2\text{Mg}(\text{CH}_2\text{SiMe}_3)_4]$  (**1e**) and  $[(\text{PMDETA})_2\text{K}_2\text{Mg}(\text{CH}_2\text{SiMe}_3)_4]$  (**1b**) will be employed to assess the alkali metal effect of this catalytic transformation. For the synthesis of the homometallic components  $\text{MgR}_2$  and  $\text{MR}$  (M=alkali metal) see **Chapter 2.4** of this thesis. Homoleptic sodium magnesiate **1f** can be synthesised by simple co-complexation reaction between  $\text{NaCH}_2\text{SiMe}_3$  and  $\text{Mg}(\text{CH}_2\text{SiMe}_3)_2$  in a solvent mixture of hexane/toluene according to the literature procedure.<sup>18</sup> Similarly to the previously described synthesis of **1b**, sodium magnesiate  $[(\text{TMEDA})_2\text{Na}_2\text{Mg}(\text{CH}_2\text{SiMe}_3)_4]$  (**1d**) can be prepared in crystalline form by mixing  $\text{NaCH}_2\text{SiMe}_3$  and  $\text{Mg}(\text{CH}_2\text{SiMe}_3)_2$  in 2:1 ratio in the presence of the bidentate TMEDA Lewis base in hexane (typical yield 0.35 g, 54%) (**Scheme 3.5**).



**Scheme 3.5:** Synthesis and X-Ray structure of higher order sodium magnesiate **1d**.

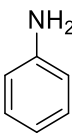
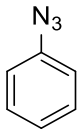
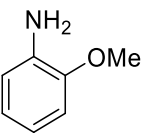
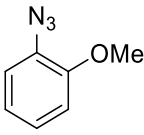
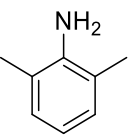
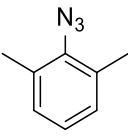
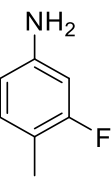
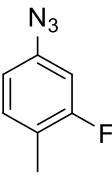
<sup>a</sup> Compound  $[(\text{TMEDA})_2\text{Na}_2\text{Mg}(\text{CH}_2\text{SiMe}_3)_4]$  (**1d**) was synthesised for the first time by Dr Sharon Baillie during the development of her PhD project

Compound (**1d**) exhibits a contacted ion pair structure with a central C<sub>4</sub>-coordinated Mg atom flanked by two TMEDA-solvated Na cations. This "Weiss" motif type of structure features four potentially active Mg-C sites to promote deprotonation of alkyne followed by addition to azide to form 1,2,3-triazoles.<sup>19</sup>

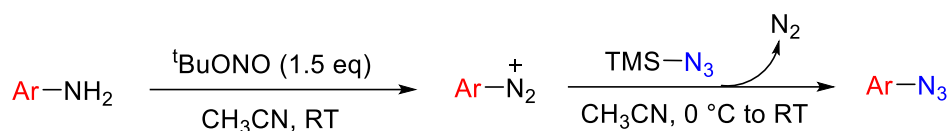
### 3.3.2 Synthesis of organic azides

A variety of substituted aryl amines can be transformed into aryl azides **5b-5e** by using *tert*-butyl nitrite (TBN) and azidotrimethylsilane (TMS-N<sub>3</sub>) under mild conditions according to the literature procedure described below (**Table 3.3**):<sup>20</sup>

**Table 3.3:** Synthesis of substituted aryl azides according to literature procedure

$\text{Ar-NH}_2 + \text{TMS-N}_3 \xrightarrow[\text{CH}_3\text{CN, 0 }^\circ\text{C to RT}]{\text{}^t\text{BuONO (1.5 eq)}} \text{Ar-N}_3$			
Entry	Ar-NH <sub>2</sub>	Ar-N <sub>3</sub>	Yield(%) <sup>a</sup>
1		 <b>5b</b>	74
2		 <b>5c</b>	90
3		 <b>5d</b>	87
4		 <b>5e</b>	90
[a] Yields refer to isolated yields of analytically pure products (>95% purity determined by NMR or GC-analysis)			

Following this methodology different azides were prepared in good to excellent yields such as azidobenzene (**5a**, 74% yield, entry 1, **Table 3.3**), 1-azido-2-methoxybenzene (**5c**, 90% yield, entry 2, **Table 3.3**), 2-azido-1,3-dimethylbenzene (**5d**, yield 87%, entry 3, **Table 3.3**) and 4-azido-2-fluoro-1-methylbenzene (**5e**, yield 90%, entry 4, **Table 3.3**). The mechanism of this reaction was not described by the corresponding authors, however it can be anticipated to be a diazotisation type mechanism (**Scheme 3.6**).



**Scheme 3.6:** Synthesis of organic azides from aryl amines.

In fact *tert*-butyl nitrite is an efficient NO source, which can react with the amine to generate a diazonium compound which then undergoes aromatic substitution type reaction with TMS-N<sub>3</sub> to generate the corresponding aryl azide.<sup>21</sup> This reaction is thermodynamically favoured as nitrogen gas is a produced (N<sub>2</sub> gas evolution can be observed after addition of TMS-N<sub>3</sub> in solution). An interesting feature of organic azides is that these compounds can react with both electrophiles and nucleophiles (**Figure 3.2**).<sup>22</sup>

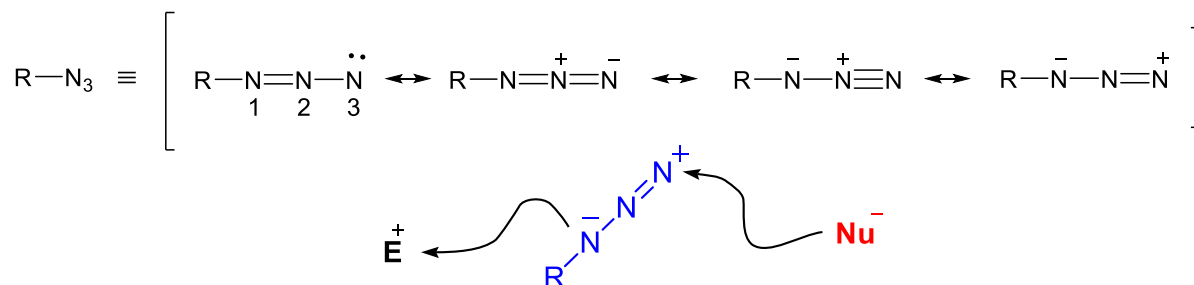


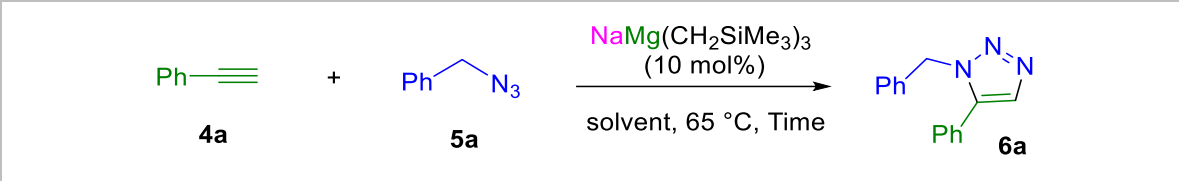
**Figure 3.2:** Different mesomeric structures for organic azides and their general reactivity with electrophiles (E<sup>+</sup>) and nucleophiles (Nu<sup>-</sup>).

The regioselectivity of their reactions with electrophiles and nucleophiles can be explained looking at the last mesomeric structure in **Figure 3.2** where N(1) is negatively charged and N(3) is positively charged. Thus, nucleophiles attack on N(3) whereas electrophiles are attacked by N(1).<sup>22</sup>

### 3.4 Assessing catalytic ability of homoleptic alkyl sodium magnesiumates **1f**, **1d**.

Studies begun on using sodium-magnesiates  $\text{NaMg}(\text{CH}_2\text{SiMe}_3)_3$  (**1f**) in a 10 mol% for the reaction of phenylacetylene (**4a**) and benzyl azide (**5a**) under different reaction conditions. Monitoring the reaction by  $^1\text{H}$  NMR spectroscopy showed that in  $\text{C}_6\text{D}_6$  at  $80^\circ\text{C}$ , full conversion to 1-benzyl-5-phenyl-1*H*-1,2,3-triazole (**6a**) was observed after 10 hours (entry 1, **Table 3.4**). Contrastingly disclosing a remarkable solvent effect using more polar and coordinating  $d_8$ -THF the quantitative formation of (**6a**) is observed after just 2h at  $65^\circ\text{C}$  (entry 2, **Table 3.4**).

**Table 3.4:** Solvent effect in the catalytic synthesis of (**6a**).

				
Entry	Solvent	Time (h)	Yield(%) <sup>a</sup>	
1	$\text{C}_6\text{D}_6$	10	99 <sup>b</sup>	
2	$d_8$ -THF	2	99	
[a] Yields obtained via spectroscopic $^1\text{H}$ NMR integration of signals for the triazole product <b>6a</b> with addition of ferrocene (10 mol %) as internal standard. Reaction carried out using 0.5 mL of solvent, 0.6 mmol of <b>4a</b> and 0.5 mmol of <b>5a</b> . [b] Reaction carried out at $80^\circ\text{C}$				

Studies in **chapter 2** have shown that higher order (or tetraorgano) magnesiumates  $\text{M}_2\text{MgR}_4$  (M=alkali metal, R=anionic group) can exhibit greatly enhanced performances in deprotonative metalation processes over their lower order (or tetraorgano) analogues  $\text{MMgR}_3$ .<sup>16,23,24</sup> To compare the catalytic ability of (**1f**) in the synthesis of (**6a**) with that of a higher order magnesiates we prepared  $[(\text{TMEDA})_2\text{Na}_2\text{Mg}(\text{CH}_2\text{SiMe}_3)_4]$  (**1d**) by co-complexation of a 2:1 mixture of the sodium and magnesium alkyls in the presence of two equivalents of the Lewis base TMEDA (TMEDA= *N,N,N',N'*-tetramethylethylenediamine) as described in **Scheme 3.5**. Compound (**1d**) was characterised by  $^1\text{H}$  and  $^{13}\text{C}$  NMR spectroscopy in  $\text{C}_6\text{D}_6$  solutions and its solid state structure was established by X-ray crystallographic studies (see experimental section for further details). Using the newly synthesised higher order

magnesiates (**1b**) in  $d_8$ -THF in a 10 mol% the formation of (**6a**) takes place in just 15 minutes (yield  $\geq 99\%$ , entry 5, **Table 3.5**).

**Table 3.5:** Comparison of the catalytic ability of different monometallic and bimetallic catalysts

Entry	Catalyst (mol%)	Time (h)	Yield of <b>6a</b> (%) <sup>a</sup>
1	-	48	traces <sup>b</sup>
2	[NaMg(CH <sub>2</sub> SiMe <sub>3</sub> ) <sub>3</sub> ] ( <b>1f</b> ) (10 mol%)	2	99
3	[NaCH <sub>2</sub> SiMe <sub>3</sub> ] (10 mol%)	24	traces
4	[Mg(CH <sub>2</sub> SiMe <sub>3</sub> ) <sub>2</sub> ] (10 mol%)	2	99
5	[(TMEDA) <sub>2</sub> Na <sub>2</sub> Mg(CH <sub>2</sub> SiMe <sub>3</sub> ) <sub>4</sub> ] ( <b>1d</b> ) (10 mol%)	0.25	99
6	[(TMEDA) <sub>2</sub> Na <sub>2</sub> Mg(CH <sub>2</sub> SiMe <sub>3</sub> ) <sub>4</sub> ] ( <b>1d</b> ) (5 mol%)	0.75	99
7	[(TMEDA) <sub>2</sub> Na <sub>2</sub> Mg(CH <sub>2</sub> SiMe <sub>3</sub> ) <sub>4</sub> ] ( <b>1d</b> ) (2 mol%)	2	48
8	[(TMEDA) <sub>2</sub> Li <sub>2</sub> Mg(CH <sub>2</sub> SiMe <sub>3</sub> ) <sub>4</sub> ] ( <b>1e</b> ) (5 mol%)	0.75	99
9	[(PMDETA) <sub>2</sub> K <sub>2</sub> Mg(CH <sub>2</sub> SiMe <sub>3</sub> ) <sub>4</sub> ] ( <b>1b</b> ) (5 mol%)	2-24 <sup>c</sup>	64

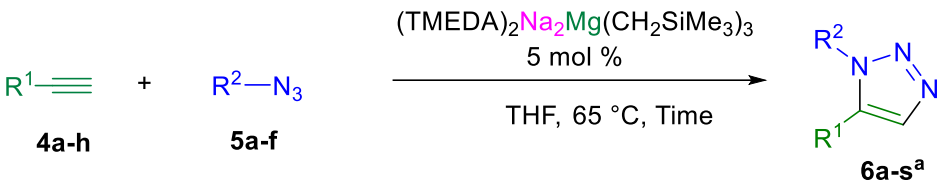
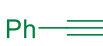
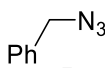
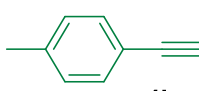
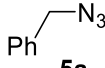
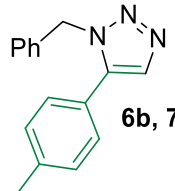
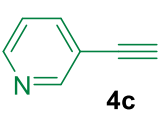
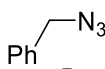
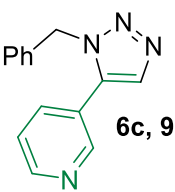
[a] Yields obtained via spectroscopic <sup>1</sup>H NMR integration of signals for the triazole product **6a** with addition of ferrocene (10 mol%) as internal standard. Reaction carried out using 0.5 mL of solvent, 0.6 mmol of **4a** (1.2M in THF) and 0.5 mmol of **5a** (1M in THF). [b] 1:1 formation of 1,5 and 1,4-disubstituted-1,2,3-triazole regioisomers could be observed by <sup>1</sup>H NMR spectroscopic analysis. [c] maximum yield of 64% observed after 2h, increasing reaction time to 24h does not improve the yield to any extent.

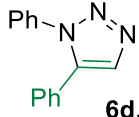
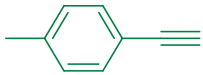
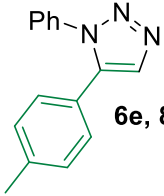
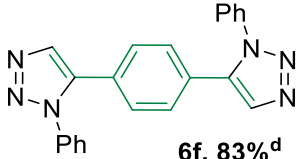
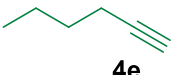
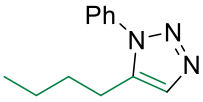
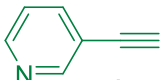
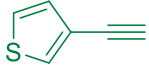
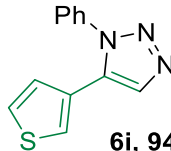
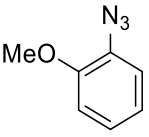
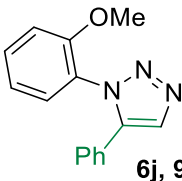
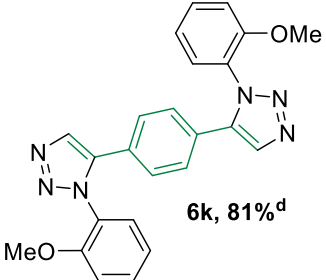
Furthermore the catalyst loading can be reduced to 5 mol% without affecting the conversion of the overall process although longer reaction times (45 min) are required to observe full conversion (entry 6, **Table 3.5**). Interestingly when the reaction of alkyne (**4a**) and azide (**5a**) was carried out in the absence of sodium magnesiates (**1f-1d**) after 48 h at 65 °C only traces of triazole **6a** could be detected (conversion  $\leq 6\%$  by <sup>1</sup>H NMR analysis) however with poor selectivity as 1:1 mixture of 1,4 and 1,5-regioisomers was obtained (Entry 1, **Table 3.5**). This result is consistent with the high kinetic barrier and lack of selectivity of the process in the absence of a catalyst.<sup>25</sup> To compare the catalytic activity of mixed-metal (**1f-1d**) with those of their homometallic components, the reaction of (**4a**) and (**5a**) was also repeated using 10 mol% of NaCH<sub>2</sub>SiMe<sub>3</sub> and Mg(CH<sub>2</sub>SiMe<sub>3</sub>)<sub>2</sub> as a pre-catalyst (entry 3-4, **Table 3.5**). While the alkali metal alkyl showed traces amount of triazole **6a** even when increasing the reaction time to 24

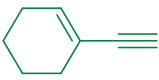
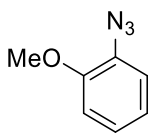
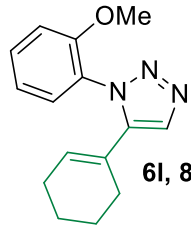
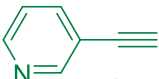
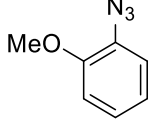
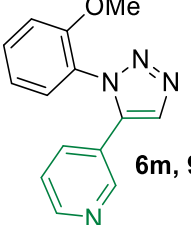
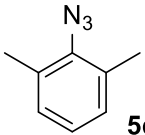
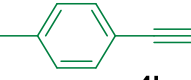
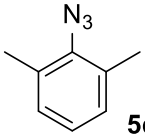
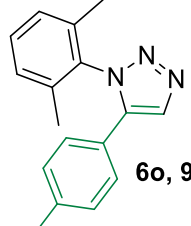
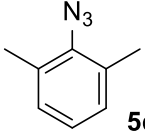
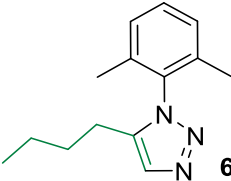
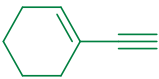
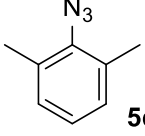
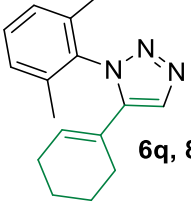
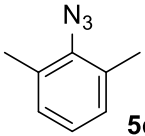
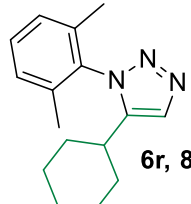
hours (conversion  $\leq$  8% of **6a** by  $^1\text{H}$  NMR) in the case of the Mg reagent compound (**6a**) can be obtained almost quantitatively although the reaction requires longer reaction times (2 h vs 15 min for **1d**). The effect of the alkali-metal in the higher order magnesiate was also assessed (entries 8 and 9, **Table 3.5**). Interestingly while Li derivative  $[(\text{TMEDA})_2\text{Li}_2\text{Mg}(\text{CH}_2\text{SiMe}_3)_4]$  (**1e**) shows similar behaviour to that described for **1d** the heavier alkali-metal  $[(\text{PMDETA})_2\text{K}_2\text{Mg}(\text{CH}_2\text{SiMe}_3)_4]$  (**1b**) appears to be less effective affording **6a** in a 64% yield after 2h at 65 °C and the yield did not improve after 24 h. In addition when the reaction is carried out using 5 mol% of **1d** and 10 mol% of 15-crown-5 which presumably captures the Na atoms the reaction is completely inhibited. This shows the crucial role that the alkali metal has in this methodology.

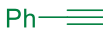
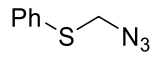
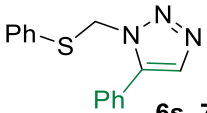
In order to study the substrate scope of this ate-mediated catalytic process, different 1,5-disubstituted-1,2,3-triazoles (**6a-s**) were synthesised from reactions of aromatic and aliphatic alkynes (**4a-h**) with different aromatic and aliphatic substituted azides (**5a-d**) (**Table 3.6**).

**Table 3.6:** Substrate scope when the reaction was carried out at 65 °C using pre-catalyst **1d**

$\text{R}^1\text{—C}\equiv\text{C} + \text{R}^2\text{—N}_3 \xrightarrow[\text{THF, 65 }^\circ\text{C, Time}]{(\text{TMEDA})_2\text{Na}_2\text{Mg}(\text{CH}_2\text{SiMe}_3)_3, 5 \text{ mol } \%}$ 				
Entry	Alkyne	Azide	Time <sup>a</sup>	Product, Yield (%) <sup>b</sup>
1	 <b>4a</b>	 <b>5a</b>	2 h	 <b>6a, 79%</b>
2	 <b>4b</b>	 <b>5a</b>	2 h	 <b>6b, 71%</b>
3	 <b>4c</b>	 <b>5a</b>	1 h	 <b>6c, 93%<sup>c</sup></b>

4	 4a	Ph-N <sub>3</sub> 5b	0.5 h	 6d, 96%
5	 4b	Ph-N <sub>3</sub> 5b	0.5 h	 6e, 86%
6	 4d	Ph-N <sub>3</sub> 5b	1 h	 6f, 83% <sup>d</sup>
7	 4e	Ph-N <sub>3</sub> 5b	1 h	 6g, 71%
8	 4c	Ph-N <sub>3</sub> 5b	0.5 h	 6h, 92%
9	 4f	Ph-N <sub>3</sub> 5b	0.5 h	 6i, 94%
10	 4a	 5c	0.5 h	 6j, 99%
11	 4d	 5c	1 h	 6k, 81% <sup>d</sup>

12	 4g	 5c	0.5 h	 6l, 89%
13	 4c	 5c	0.5 h	 6m, 99%
14	 4a	 5d	0.5 h	 6n, 92%
15	 4b	 5d	0.5 h	 6o, 93%
16	 4e	 5d	0.5 h	 6p, 76%
17	 4g	 5d	0.5 h	 6q, 87%
18	 4h	 5d	0.5 h	 6r, 89%

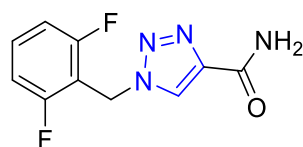
<b>19</b>	 <b>4a</b>	 <b>5e</b>	3 h	 <b>6s, 73%</b>
<p>[a] Reaction carried out using 1.2 mmol of corresponding alkyne and 1 mmol of corresponding azide [b] Yields refer to isolated yields of analytically pure products (&gt;95% purity determined by NMR or GC-analysis) [c] Reaction was carried out using 0.6 mmols of 4c and 0.5 mmols of 5c [d] Reaction carried out using 1.2 mmols of alkyne <b>4d</b> and 2 mmols of corresponding azide (5b or 5c)</p>				

This methodology allowed the formation of 1,5-disubstituted-1,2,3-triazoles (**6a-s**, **Table 3.6**) in good to excellent yields (ranging from 71-99%) at 65 °C for short reaction times (0.5 to 3 h) which contrasts with other related methods, such as those using rare-earth metal catalysis which require harsher reaction conditions (24 h at 50 °C).<sup>12</sup> Good yields were obtained when using benzyl azide (**5a**) which furnished triazoles **6a**, **6b** and **6c** in good to excellent yields (79%, 71% and 93% yield respectively) upon reaction with corresponding alkynes (entries 1, 2 and 3, **Table 3.6**). Shorter reaction times were observed for aromatic azides which efficiently react with both aromatic and aliphatic alkynes (entry 4-9, **Table 3.6**). For example when using phenyl azide (**5b**) with ethynylbenzene (**4a**), 1-ethynyl-4-methylbenzene (**4b**) and 1,4-diethynylbenzene (**4c**) good to excellent yields of triazoles **6d** (96% yield), **6e** (86% yield) and **6f** (83% yield) were obtained in only 30 minutes (entries 4,5 and 6, **Table 3.6**). We were pleased to find that azide **5b** and aliphatic alkyne 1-hexyne (**4e**) gave triazole (**6g**) in 71% yield (entry 7, **Table 3.6**) in 30 minutes. Heteroaromatic alkynes such as 3-ethynylpyridine (**4d**), 3-ethynylthiophene (**4f**) worked very well and triazoles (**6h**) and (**6i**) were both obtained in 92% and 94% yields respectively (entries 8 and 9, **Table 3.6**).

The same methodology was repeated using aromatic substituted azides bearing electron donating groups. For example when 1-azido-2-methoxybenzene (**5c**) was used with alkynes (**4a**, **4d**, 1-ethynylcyclohexene (**4g**) and **4c**) yielding triazoles (**6j**, **6k**, **6l**, **6m**) in 99%, 81%, 89% and 99% yields respectively (entries 10, 11, 12 and 13, **Table 3.6**) in short periods of time (0.5 to 1h). Other electron-rich and sterically more demanding aromatic substituted azides were tested such as 2-azido-1,3-dimethylbenzene (**5d**), with both aromatic and aliphatic alkynes (**4a**, **4b**, **4e**, **4g**) and ethynylcyclohexane (**4h**) to form triazoles (**6n**, **6o**, **6p**, **6q**, **6r**) in 92%, 93%, 76%, 87% and 89% yields respectively (entries 14, 15, 16, 17 and 18, **Table 3.6**). Particularly interesting was the use of (azidomethyl)(phenyl)sulfane (**5e**) as a substrate which upon reaction with alkyne (**4a**) formed the final corresponding triazole (**6s**) in good yield (73% yield, entry

19, **Table 3.6**) and 3 hours reaction time. This contrasts with most of the Cu-catalysed methodologies in which molecules containing free donor atoms (such as the thioether group) are known to deactivate the active Cu-catalyst, although few exceptions to this problems have recently been developed.<sup>26,27</sup>

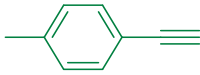
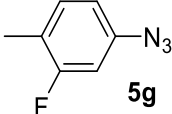
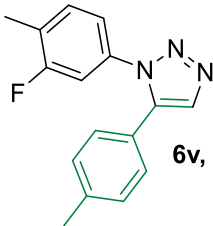
To further investigate the substrate scope of this approach we next looked at aromatic substituted azides containing electron withdrawing groups in particular azides containing fluorine groups (**Table 3.7**). As previously mentioned in **Chapter 2**, replacement of hydrogen with fluorine in C-H bonds of an organic molecule can lead to significantly different physical properties and biological activity.<sup>28-31</sup> Triazole molecules containing fluorine atoms have also emerged as new protagonists in biological chemistry. For example Rufinamide is used as antiepileptic drugs which contains two fluorine atoms on a 1,4-disubstituted triazole molecule (**Figure 3.3**).



**Figure 3.3:** 1-(2,6-difluorobenzyl)-1H-1,2,3-triazole-4-carboxamide, also known as Rufinamide.

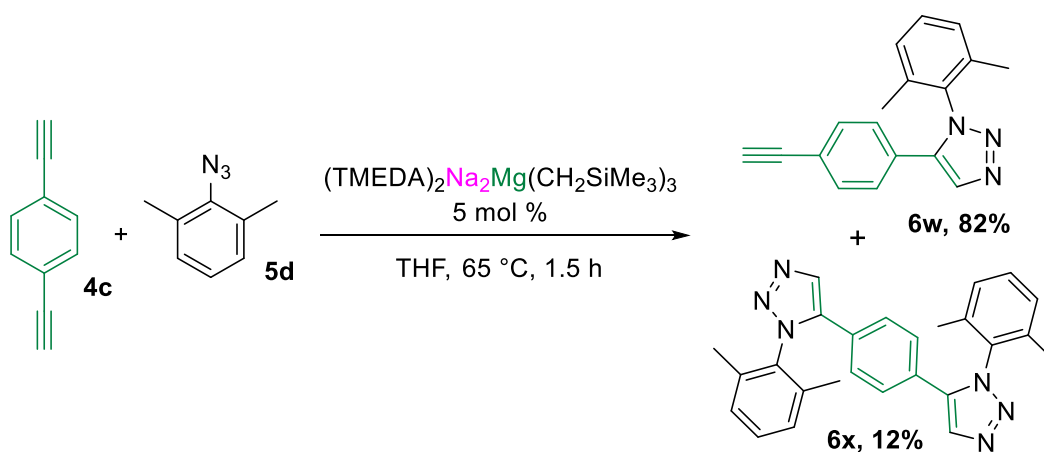
**Table 3.7:** Substrate scope using **1d** with fluoro substituted aromatic substrates

$\text{R}^1\text{-}\equiv\text{C-C}\equiv\text{C} + \text{R}^2\text{-N}_3 \xrightarrow[\text{THF, 65 }^\circ\text{C, Time}]{(\text{TMEDA})_2\text{Na}_2\text{Mg}(\text{CH}_2\text{SiMe}_3)_3, 5 \text{ mol } \%}$				
Entry	Alkyne	Azide	Time <sup>a</sup>	Product (Yield %) <sup>b</sup>
1	 4a	 5f	1 h	 6t, 98%
2	 4b	 5f	1 h	 6u, 97%

<b>3</b>	 <b>4b</b>	 <b>5g</b>	1 h	 <b>6v, 83%</b>
<p>[a] Reaction carried out using 1.2 mmol of corresponding alkyne and 1 mmol of corresponding azide [b] Yields refer to isolated yields of analytically pure products (&gt;95% purity determined by NMR or GC-analysis)</p>				

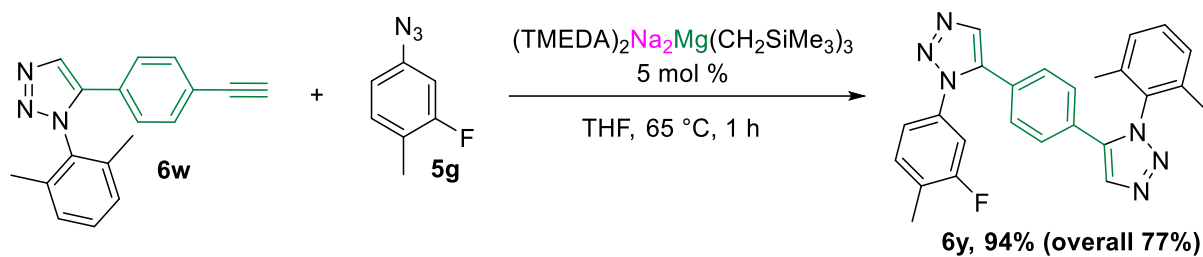
Reactions of alkynes **4a** and **4b** with 1-azido-4-(trifluoromethyl)benzene (**5f**) for 1 hour at 65 °C gave formation of triazoles **6t** and **6u** in excellent yields (98% and 97% respectively, entries 1 and 2, **Table 3.7**). In addition to this, the reaction of 4-azido-2-fluoro-1-methylbenzene (**5g**) with alkyne **4b** was also carried out under the same reaction conditions and triazole **6v** was obtained in good yield (83%, entry 3, **Table 3.7**).

Furthermore the synthesis of di-triazole molecules containing two different disubstituted triazole derivatives was also studied. Thus, the reaction of 1,4-diethynylbenzene (**4c**) with one equivalent of azide **5d** allowed formation of triazole **6w** in 82% yield along with 12% yield of ditriazole **6x** (**Scheme 3.7**).



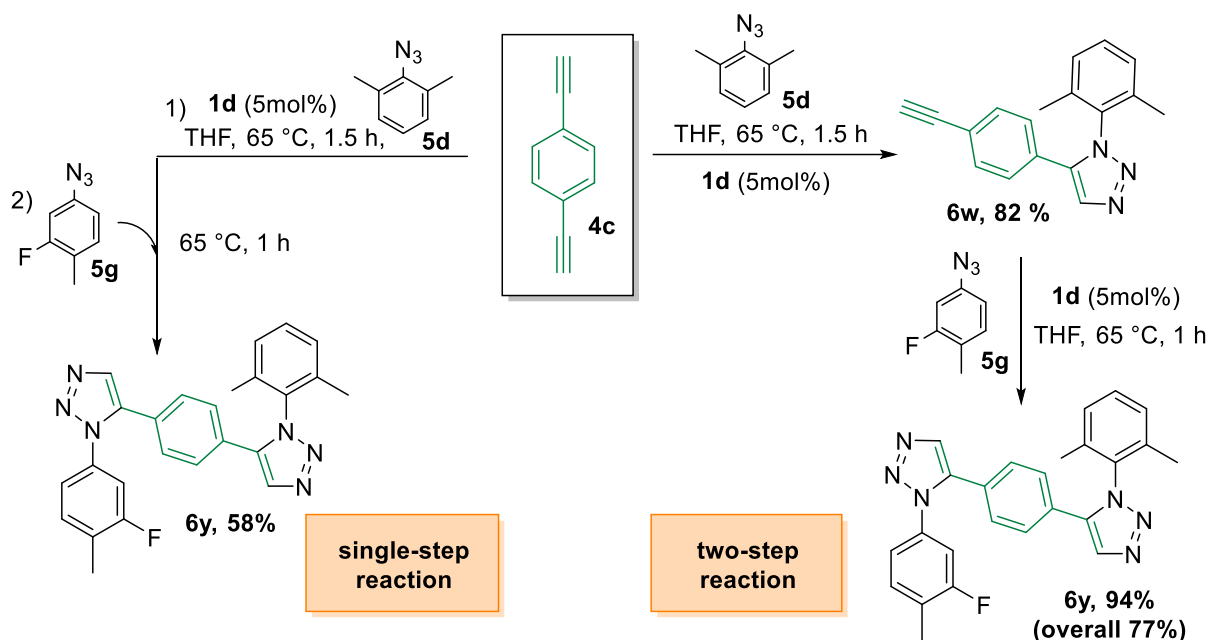
**Scheme 3.7:** **1d** catalysed reaction formation of **6w** and **6x**

Further reaction of triazole alkynyl substrate **6w** with azide **5g** in 1 hour at 65 °C afforded asymmetric ditriazole **6y** in 94% yield (considering the two reactions the overall yield for the synthesis of **6y** was 77%) (**Scheme 3.8**).



**Scheme 3.8:** **1d** catalysed reaction formation of asymmetric ditriazole **6y**

The reaction was then repeated in a single-step procedure, using one equivalent of 1,4-diethynylbenzene (**4c**) with one equivalent of azide **5d** at 65 °C for 1.5 hours followed by insertion of one equivalent of azide **5g** for 1 hour at 65 °C to obtain ditriazole **6y** in 58% yield (**Scheme 3.9**).



**Scheme 3.9:** Single and two step reaction procedures for the synthesis of unsymmetrical di-triazole **6y**

This approach allows the synthesis of di-triazole molecules and it enables the formation of unsymmetrical triazoles. This can be particularly interesting for the synthesis of biologically active triazole molecules. Thus generation of two different triazoles on the same molecule can lead to a combination of properties from each of the triazoles molecules. In all cases the reaction was regioselective towards the 1,5-disubstituted regioisomer, no formation of 1,4-triazole regioisomer was observed. The 1,5 selectivity for the formation of the triazoles was confirmed by X-ray diffraction studies of triazoles (**Figure 3.4**).

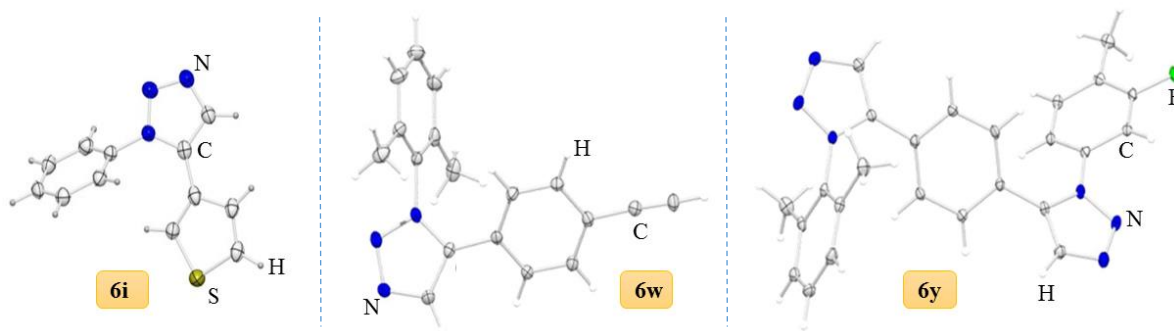
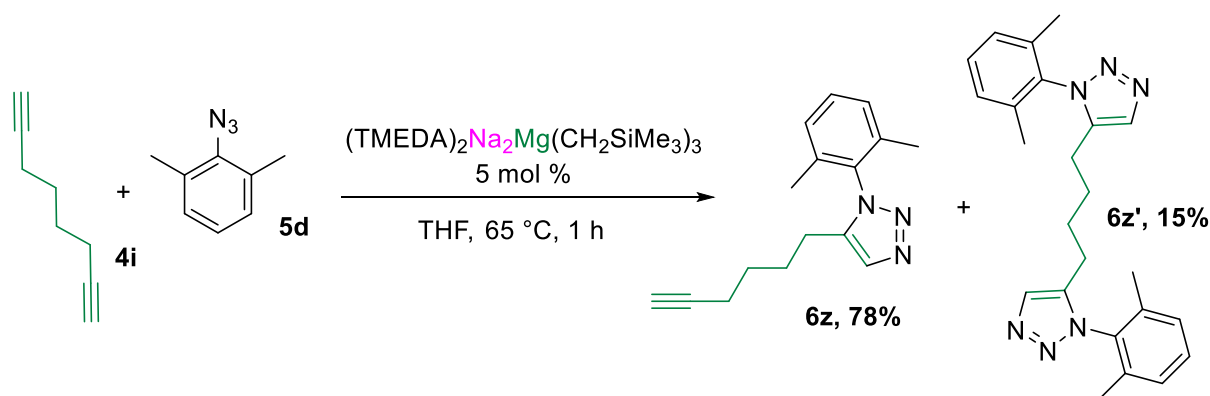


**Figure 3.4:** Molecular structures of organic triazoles **6i**, **6w** and unsymmetrical di-triazole **6y** with displacement ellipsoids at the 50% of probability.

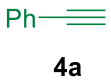
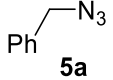
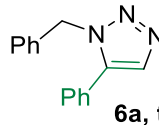
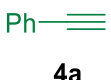
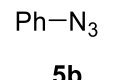
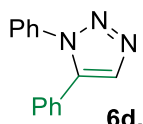
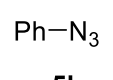
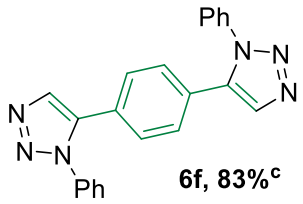
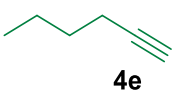
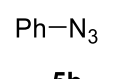
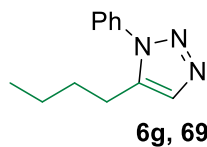
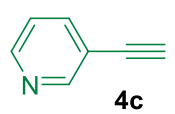
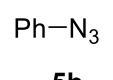
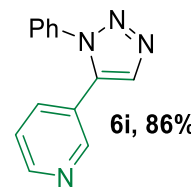
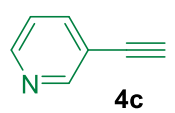
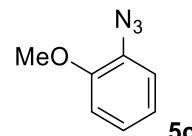
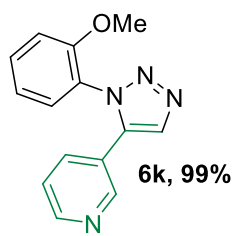
These reactions were also expanded to aliphatic dialkynes such as octa-1,7-diyne (**4i**), thus reaction of **1d** with **4i** and 2-azido-1,3-dimethylbenzene (**5d**) in THF at 65°C gave formation of triazole 1-(2,6-dimethylphenyl)-5-(hex-5-yn-1-yl)-1H-1,2,3-triazole (**6z**) in good yield (78%) along with formation of ditriazole **6z'** (Scheme 3.10).

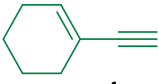
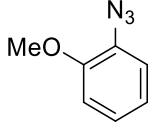
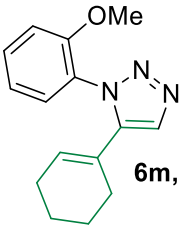
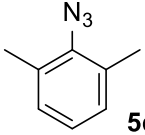
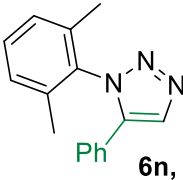
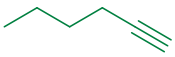
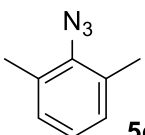
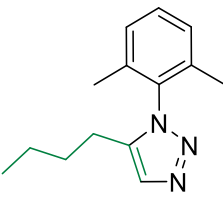


**Scheme 3.10:** **1d** catalysed reaction formation of **6z** and **6z'**

Furthermore we were pleased to find that some combinations of substrates were found to react at room temperature depending on the nature of the alkyne and azide employed (Table 3.8):

**Table 3.8:** Substrate scope using **1d** at ambient temperature.

Entry	Alkyne	Azide	Time <sup>a</sup>	Product (Yield %) <sup>b</sup>
$  \begin{array}{c}  \text{R}^1\text{—}\equiv\equiv\equiv + \text{R}^2\text{—N}_3 \\  \text{4a, 4c-e, 4g} \quad \quad \quad \text{5a-d} \\  \xrightarrow[\text{THF, 20 }^\circ\text{C, Time}]{(\text{TMEDA})_2\text{Na}_2\text{Mg}(\text{CH}_2\text{SiMe}_3)_3, 5 \text{ mol } \%} \\  \begin{array}{c}  \text{R}^2 \\    \\  \text{N} \\  / \quad \backslash \\  \text{N} \quad \text{N} \\    \\  \text{R}^1  \end{array} \\  \text{6a, 6d, 6f-g, 6i, 6k, 6m-n, 6p}  \end{array}  $				
1	 4a	 5a	24 h	 6a, traces
2	 4a	 5b	5 h	 6d, 90%
3	 4d	 5b	8 h	 6f, 83% <sup>c</sup>
4	 4e	 5b	3 h	 6g, 69%
5	 4c	 5b	4 h	 6i, 86%
6	 4c	 5c	5 h	 6k, 99%

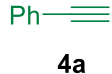
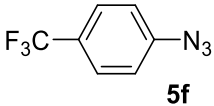
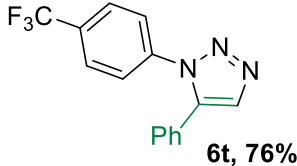
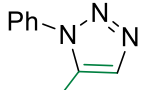
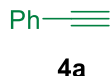
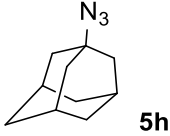
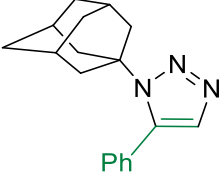
7	 4g	 5c	5 h	 6m, 87%
8	 4a	 5d	4 h	 6n, 95%
9	 4e	 5d	4 h	 6p, 77%
[a] Reaction carried out using 1.2 mmol of corresponding alkyne and 1 mmol of corresponding azide [b] Yields refer to isolated yields of analytically pure products (>95% purity determined by NMR or GC-analysis) [c] Reaction carried out using 1.2 mmols of alkyne <b>4d</b> and 2 mmols of azide <b>5b</b>				

The reactions of alkyne **4a** and azide **5a** were carried out at room temperature but only traces of triazole **6a** were detected even after long periods of times (conversion  $\leq 8\%$  by  $^1\text{H}$  NMR analysis, entry 1, **Table 3.8**). The reaction of different aromatic azides with both aromatic and aliphatic alkynes was then studied. For example the reaction of azide **5b** with alkynes **4a**, **4c**, **4d** and **4e** gave formation of final corresponding triazoles **6d** (90%), **6f** (83%), **6g** (69%), **6i** (86%) in good to excellent yields at ambient temperature and periods of time ranging from 4-8 hours (entries 2, 3, 4 and 5, **Table 3.8**). In addition to this we carried out the reaction between azide **5c** with alkynes **4c** and **4g** to generate triazoles **6k** and **6m** in excellent yields (99% and 87% yields respectively, entries 6 and 7, **Table 3.8**). Furthermore when **1d** was confronted with azide **5d** and alkynes **4a** and **4e** at room temperature triazoles **6n** and **6p** were obtain in good to excellent yields (95% and 77% yields respectively, entries 8 and 9, **Table 3.8**).

It should be noted this magnesiate catalysed approach works well with aliphatic alkynes such as (**4e**) and (**4h**) even when the reaction is carried out at room temperature, which is in sharp contrast with Fokin's work using ( $\text{NMe}_4\text{OH}$ ) as a catalyst (vide supra) which is limited to aromatic alkynes.<sup>10</sup>





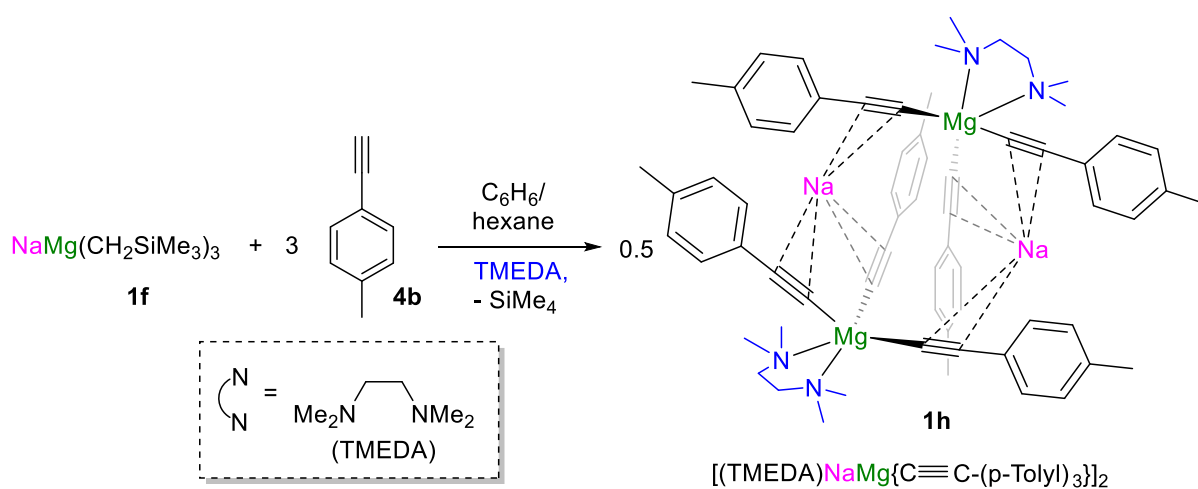
7	 4a	 5f	65 °C, 3 h	 6t, 76%
8	 4k	 5b	65 °C, 12 h	 TMS not observed
9	 4a	 5h	65 °C, 12 h	 Ph not observed
[a] Reaction carried out using 1.2 mmol of corresponding alkyne and 1 mmol of corresponding azide [b] Yields refer to isolated yields of analytically pure products (>95% purity determined by NMR or GC-analysis) [c] Reaction carried out using 1.2 mmols of alkyne <b>4d</b> and 2 mmols of corresponding azide <b>5b</b>				

Thus, using 10 mol% of **1f** to catalyse the reaction between alkyne **4a** with azide **5a** at 65 °C in 2 hours allowed the formation of triazole **6a** in 77% yield (entry 1, **Table 3.10**). This result is very similar to the one obtained using higher order magnesiate **1d** (79% yield of **6a** obtained using **1d** under the same reaction conditions, see **Table 3.6** for comparison). However in the case of lower order **1f** higher amounts of catalyst loading had to be employed (10 mol% of **1f** compared to 5 mol% with **1d**). Reaction between alkyne **4b** and azide **5a** led to formation of triazole **6b** in 68% yield after 3 hours reaction time at 65 °C (entry 2, **Table 3.10**). A similar yield was obtained using **1d** as a pre-catalyst (71% yield of **6b**, see **Table 3.6** for comparison) although the reaction was carried out using lower catalyst loading (5 mol% of **1d**) and 2 hour reaction time. Catalytic activity of **1f** was then tested using the more reactive azide **5b** upon reaction with alkynes **4a**, **4b** and **4d** which afforded triazoles **6d** (in 1h), **6e** (3h), and **6f** (6h) in 95% 84% and 72% yield respectively (entry 3,5 and 6 respectively, **Table 3.10**). For comparison (details in **Table 3.6**), pre-catalyst **1d** gave formation of triazoles **6d** (96% yield in 0.5h), **6e** (85% yield in 0.5h), and **6f** (83% in 1h). In addition to that, reaction of alkyne **4a** and azide **5b** could also be carried out at room temperature to yield triazole **6d** in 82% yield although longer reaction time was required (12 hours) (entry 4, **Table 3.10**) when compared to

the result obtained using **1d** (90% yield of **6d** after 5h at RT, see entry 2, **Table 3.8** for further details). Furthermore reaction of alkyne **4a** with azide **5f** allowed formation of triazole **6t** in 76% yield after 3 hours (entry 7, **Table 3.10**). For comparison when using 5 mol% of **1d** the same reaction afforded triazoles **6t** in higher yield (98% yield after 1 hour, see entry 1, **Table 3.7** for further details). No triazole formation was observed from the reactions between alkyne **4k** and azide **5b** (entry 9, **Table 3.10**) as well as using 1-azidoadamantane (**5i**) with alkyne **4a** (entry 10, **Table 3.10**). Both reactions resulted in full recovery of starting materials after 12 h reaction at 65 °C. In summary these results clearly show the higher activity of higher order sodium magnesiate **1d** to carry out the aforementioned cyclisation reaction between alkynes and azides to form 1,5-disubstituted triazoles. Despite lower order sodium magnesiate **1f** efficiently catalysing these procedure it requires longer periods of time for the reaction to get to completion and higher amounts of pre-catalyst (5 mol% of **1d** compared to 10 mol% of **1f**). Furthermore, yields of the corresponding final triazoles are generally lower in most cases.

### 3.5 Stoichiometric studies

To gain some insights into the possible constitution of the bimetallic species involved in these transformations the stoichiometric reaction of sodium magnesiate (**1f**) with *p*-tolylacetylene (**4b**) was also investigated. Thus, reaction of one molar equivalent of **1f** with 3 equivalents of **4b** in hexane at ambient temperature, followed by addition of TMEDA, led to crystallisation of sodium magnesiate  $[(\text{TMEDA})\text{NaMg}\{\text{C}\equiv\text{C}(p\text{-tolyl})\}_3]_2$  (**1h**) (38% crystalline yield, 78% as a white solid) (**Scheme 3.11**).



**Scheme 3.11:** **1f** mediated metalation of alkyne **4b**.

X-ray crystallographic studies of **1h** confirmed the protonolysis of the 3 alkyl groups of alkyne **4b** forming a contacted ion-pair bimetallic species (**Figure 3.5**).

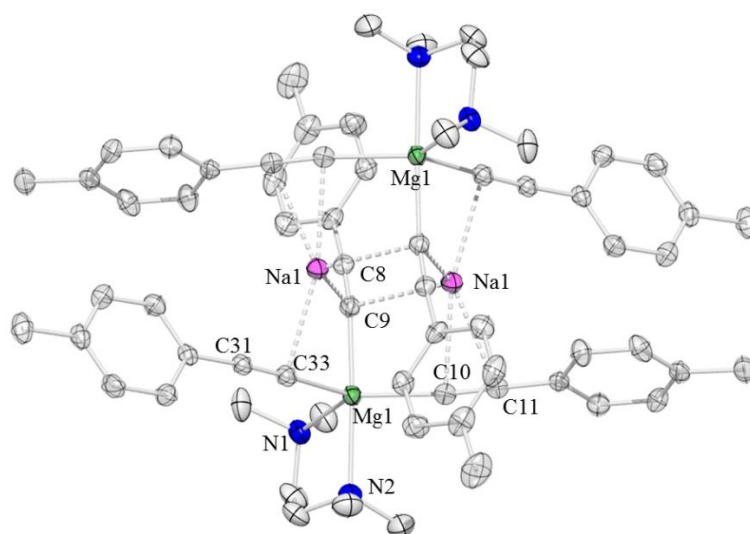


**Figure 3.5:** Dimeric unit for  $[(\text{TMEDA})\text{NaMg}\{\text{C}\equiv\text{C}(p\text{-tolyl})\}_3]_2$  (**1h**), **Selected bond distances** (Å), Mg(1)-N(1) 2.264(2); Mg(1)-N(2) 2.334(2); Mg(1)-C(33) 2.162(2); Mg(1)-C(10) 2.196(2); Mg(1)-C(9) 2.257(2); Na(1)-C(9) 2.584(2); Na(1)-C(8) 3.108 (2); Na(1)-C(33) 2.586(2); Na(1)-C(31) 2.679 (2);

Na(1)-C(10) 2.570(2); Na(1) C(11) 2.909(2); C(8)-C(9) 1.221(2); C(10)-C(11) 1.217(2); C(31)-C(33) 1.212(2). **Selected angles** ( $^{\circ}$ ), C(33)-Mg(1)-C(10) 126.42(7); C(33)-Mg(1)-C(9) 93.72(6); C(10) Mg(1) C(9) 95.35(6); C(33)-Mg(1)-N(1) 129.13(7); C(10)-Mg(1)-N(1) 103.57(6); C(9)-Mg(1)-N(1) 90.01(6); C(33)-Mg(1)-N(2) 90.12(6); C(10)-Mg(1)-N(2) 92.27(6); C(9)-Mg(1)-N(2) 167.07(7); N(1)-Mg(1)-N(2) 78.03(6); C(11)-C(10)-Mg(1), 166.30 (15); C(31)-C(33)-Mg(1) 174.31(14); C(8)-C(9)-Mg(1), 166.76(15); C(11)-C(10)-Na(1) 93.41(12); C(31)-C(33)-Na(1) 81.05(11); C(8)-C(9)-Na(1) 103.71(13)

The new lower order sodium trisalkynyl magnesiate exhibits a dimeric arrangement through  $\pi$ -Na-C interactions. Interestingly, the Mg atoms occupy a slightly distorted trigonal bipyramidal environment (coordination number 5), solvated by one molecule of TMEDA and bonded to the three tolyl-alkynyl groups [C(33)-Mg(1)-C(10) 126.42(7); C(33)-Mg(1)-C(9) 93.72(6); C(10) Mg(1) C(9) 95.35(6); C(33)-Mg(1)-N(1) 129.13(7); C(10)-Mg(1)-N(1) 103.57(6); C(9)-Mg(1)-N(1) 90.01(6); C(33)-Mg(1)-N(2) 90.12(6); C(10)-Mg(1)-N(2) 92.27(6); C(9)-Mg(1)-N(2) 167.07(7); N(1)-Mg(1)-N(2) 78.03(6)], Na forms a series of  $\pi$ -Na-C interactions ( $\eta^2$  fashion) with two of the alkynes, while the third alkyne interacts with another sodium atom to form a dimer. Further detail can be given looking at the inorganic core of the structure (**Figure 3.6**).

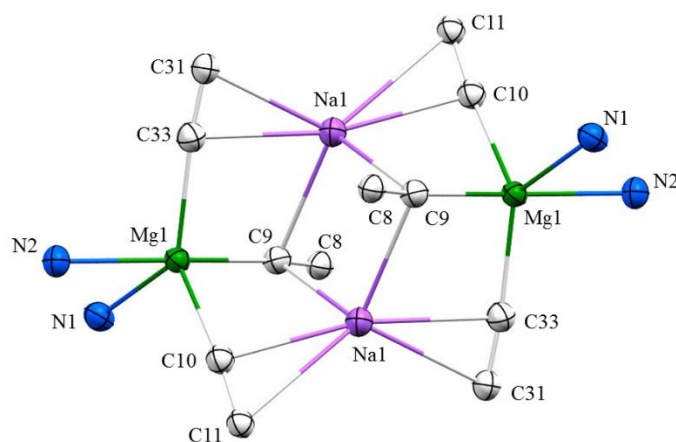


**Figure 3.6:** Inorganic core of **1h** including alkynyl groups

Compound **1h** exhibits different Mg-N bond distances, in fact the Mg-N bond in the axial position is larger than the Mg-N bond in the equatorial position [Mg(1)-N(2) 2.334(2) larger than Mg(1)-N(1) 2.264(2)] as expected. Interestingly looking at the asymmetric unit of **1h** the three Mg-C bonds with acetylide ligands exhibit bond angles which deviate slightly from the desired linear geometry to Mg [C(11)-C(10)-Mg(1), 166.30 (15); C(31)-C(33)-Mg(1) 174.31(14); C(8)-C(9)-Mg(1), 166.76(15);], and the perpendicular geometries to Na [C(11)-C(10)-Na(1) 93.41(12); C(31)-C(33)-Na(1) 81.05(11); C(8)-C(9)-Na(1) 103.71(13)], furthermore the Mg-C distance to the axial tolyl-C $\equiv$ C ligand is considerably longer than the

two Mg-C distances to the alkynyl ligands in the equatorial position [Mg(1)-C(9) 2.257(2) longer than Mg(1)-C(10) 2.196(2) and Mg(1)-C(33) 2.162(2)]. This is due to the extra stabilisation of the terminal anionic C(9) of the the axial tolyl-C≡C ligand from two Na cations [Na(1)-C(9) 2.584(2); Na(1)-C(8) 3.108 (2); Na(1)-C(33) 2.586(2); Na(1)-C(31) 2.679 (2); Na(1)-C(10) 2.570(2); Na(1) C(11) 2.909(2)], this weakens the corresponding Mg-C bond, whereas in the two equatorial tolyl-C≡C ligands C(33) and C(10) there is only interaction with one Na cation (**Figure 3.6**).

The same reaction was carried out using trimethylsililacetylene (**4k**) at ambient temperature in hexane for 1 hour. Addition of benzene allowed the crystallisation of sodium magnesiate [(TMEDA)NaMg{C≡C(SiMe<sub>3</sub>)<sub>3</sub>]<sub>2</sub> (**1i**) in moderate yield (42% crystalline yield, **Figure 3.7**)

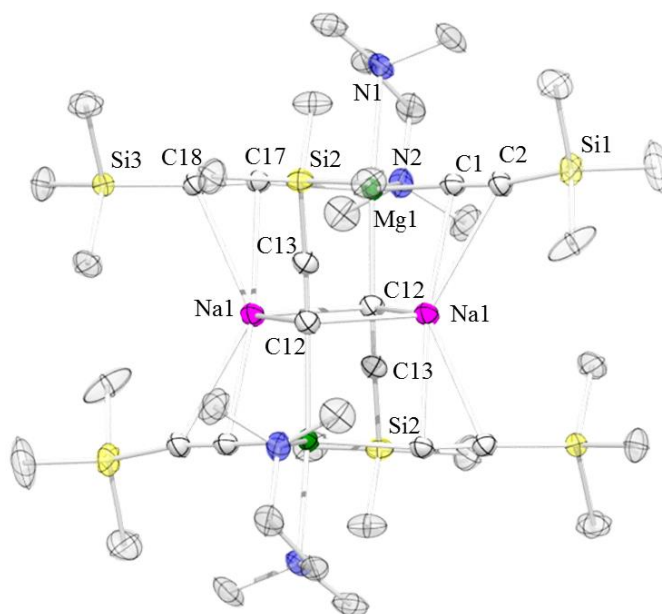


**Figure 3.7:** Dimeric unit for [(TMEDA)NaMg{C≡C(SiMe<sub>3</sub>)<sub>3</sub>]<sub>2</sub> (**1i**) **Selected bond distances** (Å), N(1)-Mg(1) 2.369(1), N(2)-Mg(1) 2.260(2), Mg(1)-C(1) 2.189(2), Mg(1)-C(12) 2.254(2), Mg(1)-C(17) 2.167(2), Na(1)-C(1) 2.673(1), Na(1)-C(2) 2.792(2), Na(1)-C(12) 2.592(2), Na(1)-C(13) 3.016(2), Na(1)-C(17) 2.608(2), Na(1)-C(18) 2.857(2), C(1)-C(2) 1.216(2), C(12)-C(13) 1.218(2), C(17)-C(18) 1.215(2). **Selected angles** (°), N(2)-Mg(1)-N(1) 78.30(5), N(1)-Mg(1)-C(1) 91.42(5), N(1)-Mg(1)-C(12) 166.69(6), N(1)-Mg(1)-C(17) 90.43(5), N(2)-Mg(1)-C(1) 109.47(5), N(2)-Mg(1)-C(12) 88.45(5), N(2)-Mg(1)-C(17) 119.59(6), C(1)-Mg(1)-C(12) 94.27(5), C(17)-Mg(1)-C(1) 130.18(6); C(17)-Mg(1)-C(12) 95.04(6); C(18)-C(17)-Mg(1) 177.3(1); Mg(1)-C(12)-C(13) 163.2(1); Mg(1)-C(1)-C(2) 172.4(1); Na(1)-C(1)-C(2) 82.6(1); Na(1)-C(12)-C(13) 98.2(1); Na(1)-C(17)-C(18) 88.9(1)

Sodium magnesiate **1i** exhibits an almost identical structural motif to that of **1h**. Once again the Mg atoms occupy a distorted trigonal bipyramidal environment (coordination number 5), solvated by one molecule of TMEDA and bonded to the three TMS-alkynyl groups, the Na

atom joins two asymmetric units by a series of  $\pi$ -Na-C interactions with two of the alkynes and the third alkyne interacts with another sodium atom to form a dimer (**Figure 3.8**)

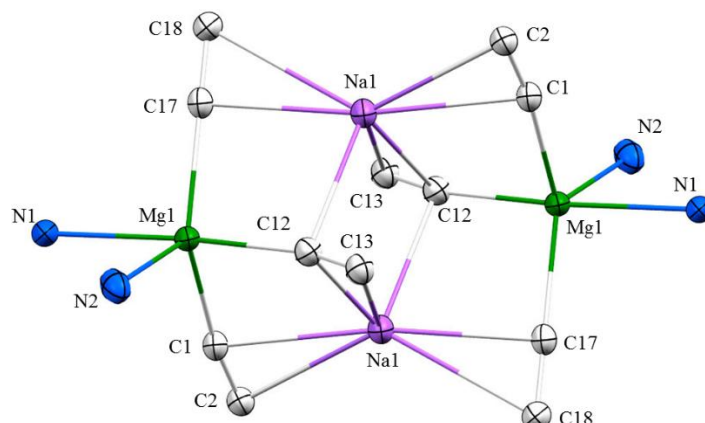


**Figure 3.8:** Inorganic core of **1i** including alkynyl groups

The structures of (**1h**, **1i**) have a strong resemblance to that described by Weiss for [(TMEDA)LiMg{C≡C(Ph)}<sub>3</sub>]<sub>2</sub> (**Figure 3.9**).

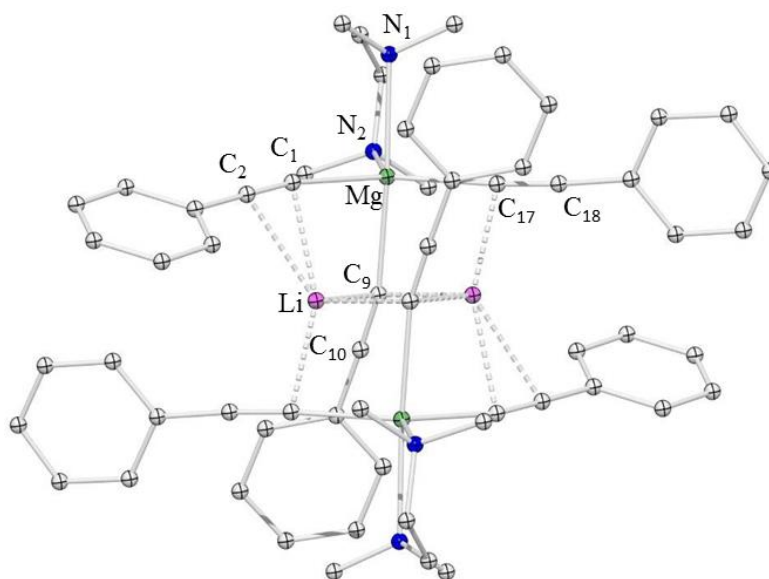


**Figure 3.9:** Weiss's lower order alkynyl lithium magnesiate [(TMEDA)LiMg{C≡C(Ph)}<sub>3</sub>]<sub>2</sub>

Li atoms in Weiss's structure also form electrostatic interactions with the alkyne anions.<sup>32</sup> Weiss described his alkynyl lithium magnesiate structure as a "bipyramidal trigonal magnesium atom coordinated by three acetylide ligands and one chelating TMEDA which dimerises through alkali-C interactions." These structures are almost identical to the ones of **1h** and **1i**. A comparison between bond distances and angles of compound **1h** and **1i** and Weiss's lithium magnesiate (**Li-Weiss**) is given in **Table 3.11**:

**Table 3.11:** Comparison of key bond lengths (Å) and bond angles (°) in crystal structures of **1h** and **1i** and Weiss's alkynyl lithium magnesiate;

<b>bond</b>	<b>1h</b>	<b>1i</b>	<b>Li-Weiss</b>
<b>-C≡C- (Å)</b>	C(8)-C(9) 1.221(2) C(10)-C(11) 1.217(2) C(31)-C(33) 1.212(2)	C(12)-C(13) 1.218(2) C(1)-C(2) 1.216(2) C(17)-C(18) 1.215(2)	C(1)-C(2) 1.220(7) C(17)-C(18) 1.219(6) C(9)-C(10) 1.198(6)
<b>-C≡C-A<sub>m</sub> (Å)</b>	Na(1)-C(33) 2.586(2) Na(1)-C(31) 2.679 (2) Na(1)-C(10) 2.570(2) Na(1) C(11) 2.909(2) Na(1)-C(9) 2.584(2) Na(1)-C(8) 3.108 (2)	Na(1)-C(1) 2.673(1) Na(1)-C(2) 2.792(2) Na(1)-C(17) 2.608(2) Na(1)-C(18) 2.857(2) Na(1)-C(12) 2.592(2) Na(1)-C(13) 3.016(2)	Li(1)-(C1) 2.342(8) Li(1)-C(9) 2.301(10) Li(1)-C(9)' 2.315 Li(1)-C(17)' 2.257
<b>-C≡C-Mg (Å)</b>	Mg(1)-C(33) 2.162(2) Mg(1)-C(10) 2.196(2) Mg(1)-C(9) 2.257(2)	Mg(1)-C(17) 2.167(2) Mg(1)-C(1) 2.189(2) Mg(1)-C(12) 2.254(2)	Mg-C(17) 2.183(5) Mg-C(1) 2.188(5) Mg-C(9) 2.307(4)
<b>C-Mg-N (°)</b>	C(33)-Mg(1)-C(10) 126.42(7)	C(17)-Mg(1)-C(1) 130.18(6)	C(1)-Mg-C(17) 132.8(2)
<b>C-Mg-C (°)</b>	C(33)-Mg(1)-C(9) 93.72(6)	C(1)-Mg(1)-C(12) 94.27(5)	C(1)-Mg-C(9) 89.3(2)
	C(10) Mg(1) C(9) 95.35(6)	C(17)-Mg(1)-C(12) 95.04(6)	C(1)-Mg-N(1) 92.2(2)
	C(33)-Mg(1)-N(1) 129.13(7)	N(2)-Mg(1)-C-(17) 119.59(6)	C(1)-Mg-N(2) 116.8(2)
	C(9)-Mg(1)-N(2) 167.07(7)	N(1)-Mg(1)-C(12) 166.69(6)	C(9)-Mg-N(1) 172.1(2)
	C(10)-Mg(1)-N(1) 103.57(6)	N(2)-Mg(1)-C(1) 109.47(5)	C(17)-Mg-N(2) 110.3(2)
	C(9)-Mg(1)-N(1) 90.01(6)	N(2)-Mg(1)-C(12) 88.45(5)	C(9)-Mg-N(2) 92.0(2)
	C(33)-Mg(1)-N(2) 90.12(6)	N(1)-Mg-(1)-C(17) 90.43(5)	C(17)-Mg-C(9) 92.6(2)
	C(10)-Mg(1)-N(2) 92.27(6)	N(1)-Mg(1)-C(1) 91.42(5)	C(17)-Mg-N(1) 92.0(2)

	N(1)-Mg(1)-N(2) 78.03(6)	N(2)-Mg(1)-N(1) 78.30(5)	N(1)-Mg-N(2) 80.2(2)
C≡C-Mg (°)	Mg(1)-C(10)-C(11) 166.30 (15)	Mg(1)-C(17)-C(18) 177.3(1)	Mg-C(17)-C(18) 176.1(3)
	Mg(1)-C(33)-C(31) 174.31(14)	Mg(1)-C(1)-C(2) 172.4(1)	Mg-C(1)-C(2) 167.8(4)
	Mg(1)-C(9)-C(8) 166.76(15)	Mg(1)-C(12)-C(13) 163.2(1)	Mg-C(9)-C(10) 162.0(4)
C≡C-A <sub>m</sub> (°)	C(11)-C(10)-Na(1) 93.41(12)	Na(1)-C(1)-C(2) 82.6(1)	Li-C(17)-C(18) 98.4
	C(31)-C(33)-Na(1) 81.05(11)	Na(1)-C(12)-C(13) 98.2(1)	Li-C(1)-C(2) 81.9
	C(8)-C(9)-Na(1) 103.71(13)	Na(1)-C(17)-C(18) 88.9(1)	Li-C(9)-C(10) 117.1

Previous work by Wright and co-workers has established the possibility of accessing alkali-metal zincates containing acetylide groups. The structure  $[(\text{TMEDA})_2\text{Li}_2\text{Mg}\{\text{C}\equiv\text{C}(\text{Ph})\}_4]$  presented in their work feature the low polarity Zn forming  $\sigma$ -bonds with the  $\alpha$ -C whereas the alkali-metals  $\pi$ -interact with both acetylenic C atoms (**Figure 3.10**).<sup>33</sup>

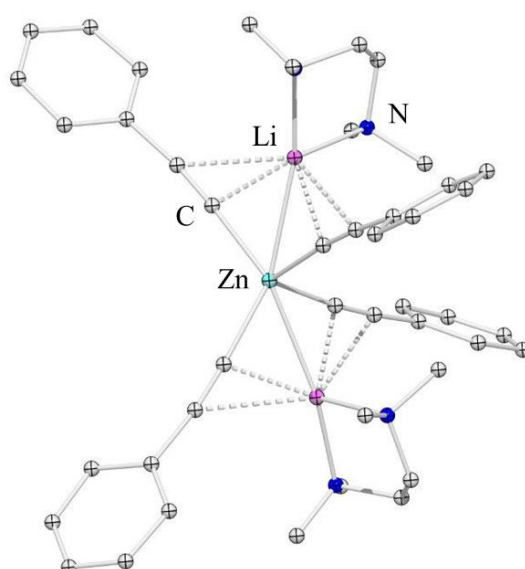
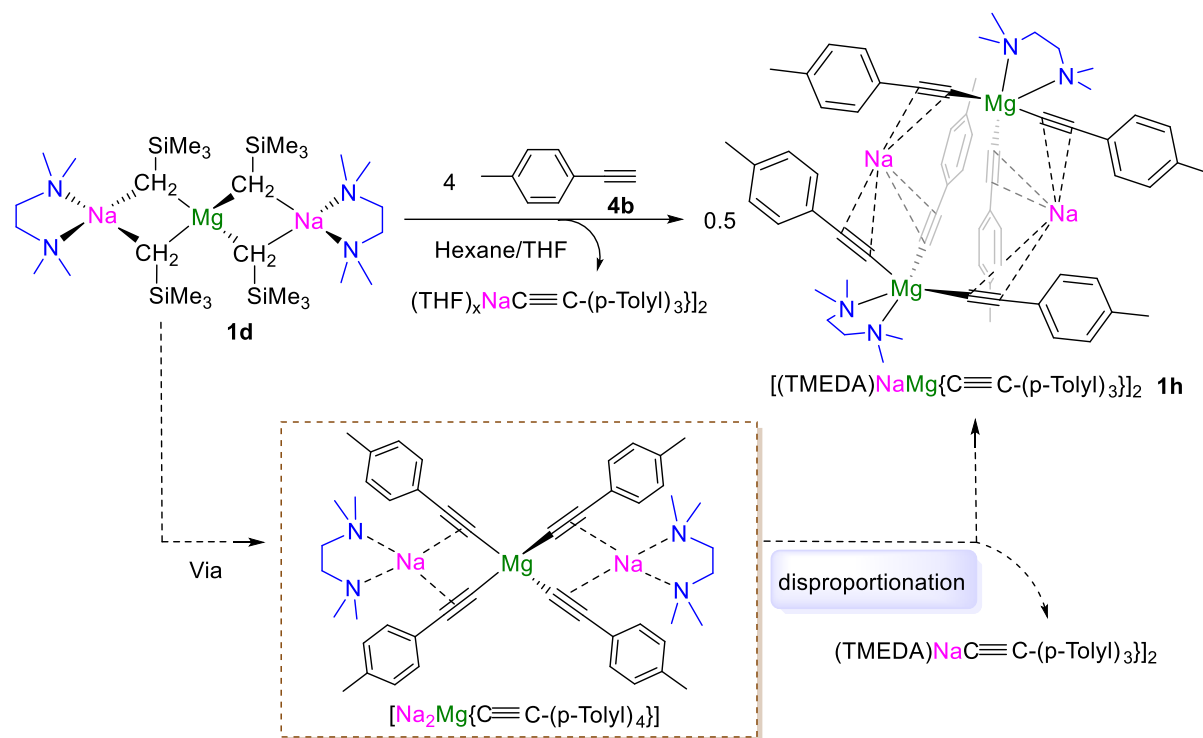


**Figure 3.10:** Higher order alkynyl lithium zincate  $[(\text{TMEDA})_2\text{Li}_2\text{Mg}\{\text{C}\equiv\text{C}(\text{Ph})\}_4]$

In addition to this, similar type of dual  $\sigma$ -bonds  $\pi$ -bonded to the acetylide involving two Cu centers has recently been proposed by Fokin, as the catalytically active complex in CuAAC.<sup>34</sup>

The stoichiometric reaction of **1d** with 4 equivalents of *p*-tolylacetylene (**4b**) was also carried out at ambient temperature in hexane. After 30 minutes addition of toluene allowed the crystallisation of the final product, [(TMEDA)NaMg{C≡C(*p*-tolyl)}<sub>3</sub>]<sub>2</sub> (**1h**) (**Scheme 3.12**).



**Scheme 3.12:** **1d** stoichiometric reaction with alkyne **4b**.

A possible explanation for the isolation of **1h** could be the disproportionation reaction of a putative higher order alkynyl magnesiate intermediate  $[\text{Na}_2\text{Mg}\{\text{C}\equiv\text{C}(\textit{p}\text{-tolyl})_4\}]$  to generate **1h** and sodium *p*-tolylacetylene (**Scheme 3.12**). As previously discussed in **chapter 3.4** the catalytic ability of sodium magnesiates **1f** and **1d** to form 1,5-triazoles is different, in particular **1f** shows lower activity in the formation of a variety of 1,5-disubstituted triazoles (See **Table 3.6**, **Table 3.7**, and **Table 3.10** for comparison). However, stoichiometric reactions between **1f** or **1d** and *p*-tolylacetylene led to the crystallisation of lower order alkynyl sodium magnesiate **1h** in both cases. In the subsequent NMR spectroscopic analysis for compound **1h** and **1j** a downfield shift of the acetylenic <sup>13</sup>C-signals was observed. Acetylenic <sup>13</sup>C-signals were originally situated at 77.8: 84.1 ppm (for *p*-tolylacetylene in d<sub>8</sub>-THF) and shifted to 108.6: 128.8 ppm for (**1h** in d<sub>8</sub>-THF), 109.0: 130.7 ppm for (**1j** in d<sub>8</sub>-THF) (**Table 3.12**):

**Table 3.12:**  $^1\text{H}$  and  $^{13}\text{C}$  NMR chemical shifts for acetylenic and methyl carbon atoms in compounds **1h**, **1j** and free *p*-tolylacetylene (**4b**).

Compound	$\delta^{1\text{H}}$ Me ( <i>p</i> -tol) (ppm)	$\delta^{13\text{C}}$ Mg-C $\equiv$ C (ppm)	$\delta^{13\text{C}}$ Mg-C $\equiv$ C (ppm)
H-C $\equiv$ C( <i>p</i> -tolyl)	2.31	77.8	84.2
1h	2.23	108.6	128.8
1j	2.23	109	130.7

[a]  $^1\text{H}$  and  $^{13}\text{C}$  NMR studies were carried out dissolving 30 mg of product in  $d_8$ -THF.

Bearing in mind the dramatic effect that the donor ability of the solvent has in these transformations,  $^1\text{H}$  DOSY NMR studies were carried out to get further information about the possible active species of the catalytic cycle.  $^1\text{H}$  DOSY NMR is a well-known technique used to predict the constitution of species in solution according to their diffusion coefficient and molecular weights.<sup>35,36</sup> The Stokes-Einstein equation can be used to estimate molecular size of large molecules<sup>b</sup>:

$$D = \frac{kT}{6\pi\eta R_h}$$

However one of the most powerful classes of relations which correlate the molecular weight (Mw) and the diffusion coefficient (D) is an empirically derived power law of the Stokes-Einstein equation:

$$D = KM_w^\alpha$$

This power law is restricted to a specific class of compounds (oligosaccharides, denaturated peptides or polyethylene oxides) and in some cases it can be used for small molecules however high errors are associated with the prediction of their molecular weights. Li, Williard *et al* have developed an analogous approach of the power law and with the introduction of at least three internal references to one NMR sample a calibration curve can be obtained which allows the prediction of the size of small molecules with a lower associated error.<sup>36</sup> Although this method has been vastly employed,<sup>37-40</sup> it contains different experimental difficulties. To name few, the

<sup>b</sup>  $D = (kT)/(6\pi\eta R_h)$ , where D is the diffusion coefficient, k is the Boltzman constant, T is the temperature,  $\eta$  is the viscosity, and  $R_h$  is the hydrodynamic radius.

internal references have to be inert to analyte, the resonances in the  $^1\text{H}$  NMR spectrum of the analyte should not overlap with those from the internal reference. Furthermore, the calibration curve is only useful for one NMR sample. Recently Stalke *et al* have made a further development in the field showing that  $^1\text{H}$  DOSY NMR studies can be carried out using external calibration curves (ECC).<sup>41</sup> This method requires only TMS as internal standard reducing most of the complications previously mentioned.

Using Stalke's ECC novel method,  $^1\text{H}$  DOSY NMR analysis of **1h** (35 mM) was performed in  $d_8$ -THF solution. These studies suggested that its dimeric solid state structure is not retained in  $d_8$ -THF solution, favouring instead monomeric  $[(\text{THF})_2\text{NaMg}(\text{THF})_2\{\text{C}\equiv\text{C}(p\text{-tolyl})\}_3]$  ( $M_w=681.19\text{ g mol}^{-1}$ ) which affords an excellent correlation with the calculated molecular weight ( $M_w=673\text{ g mol}^{-1}$ , 1% error, **Figure 3.11**)

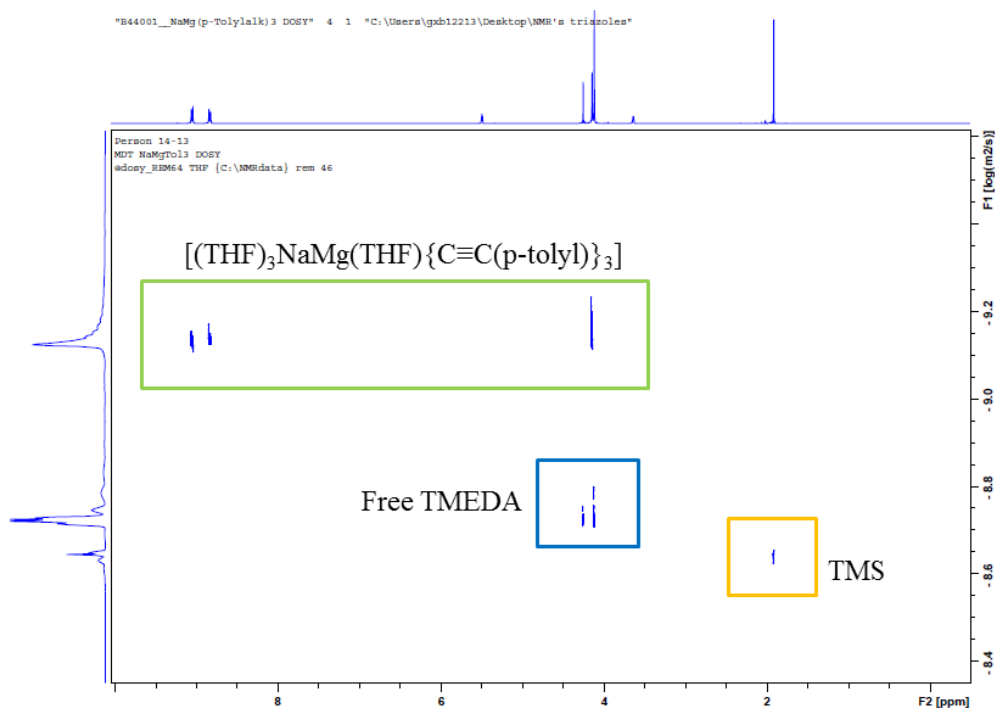


**Figure 3.11:**  $^1\text{H}$  DOSY NMR of lower order sodium magnesiate **1h** in  $d_8$ -THF solution

These results suggest that THF has higher affinity towards solvation of Na atoms in **1h** as free TMEDA is observed in  $d_8$ -THF solution. Excess of THF (used as a solvent) favors displacement of TMEDA which was present in solid state structure of **1h** (**Figure 3.12**).

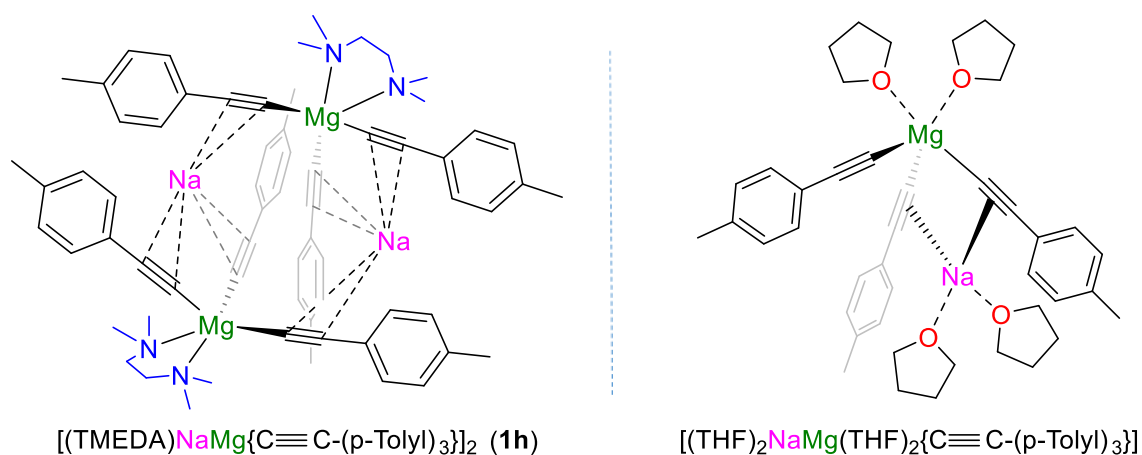
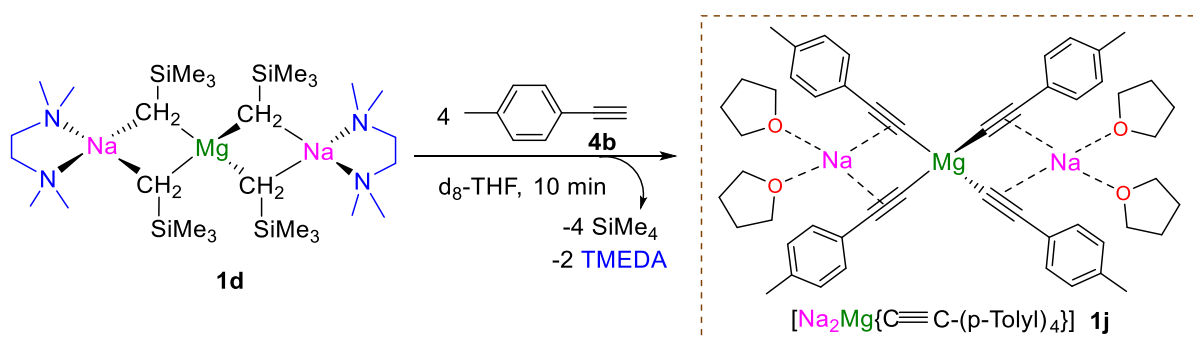


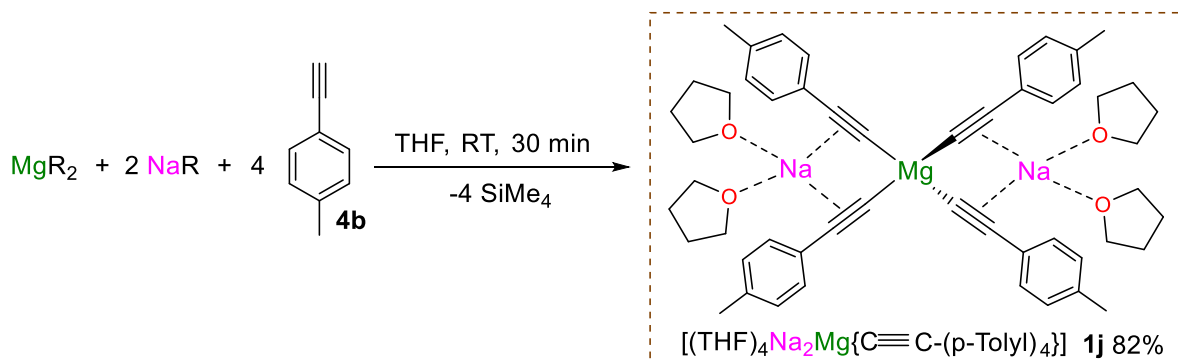
**Figure 3.12:** Chem Draw comparison between the solid state dimeric structure of **1h** and the proposed composition of **1h** in  $d_8$ -THF solution

The reaction of **1d** with 4 equivalents of *p*-tolylacetylene in  $d_8$ -THF was also studied.  $^1\text{H}$ ,  $^{13}\text{C}$  NMR studies suggested formation of one product only and no disproportionation to **1h** was observed (**Scheme 3.13**).



**Scheme 3.13:** Stoichiometric reaction of **1d** with 4 equivalents of *p*-tolylacetylene (**4b**) in  $d_8$ -THF

Furthermore, in situ mixture of NaR,  $\text{MgR}_2$  and 4 equivalents of *p*-tolylacetylene in THF at room temperature for 30 minutes afforded [(THF)<sub>4</sub>Na<sub>2</sub>Mg{C≡C(*p*-tolyl)}<sub>4</sub>] (**1j**) in excellent yield (82%) which could be stored in the glovebox as a yellow solid after removing solvent under vacuum (**Scheme 3.14**)



**Scheme 3.14:** Synthesis and isolation of **1j** as white solid

Contrasting with solid state studies,  $^1\text{H}$  DOSY NMR spectroscopic investigations revealed the retention of the higher order configuration of **1j**. Thus, compound  $[(\text{THF})_4\text{Na}_2\text{Mg}\{\text{C}\equiv\text{C}(p\text{-tolyl})\}_4]$  ( $M_w=819.33 \text{ g mol}^{-1}$ ) affords an excellent correlation with the calculated molecular weight ( $M_w=792 \text{ g mol}^{-1}$ , error 3%, **Figure 3.13**).

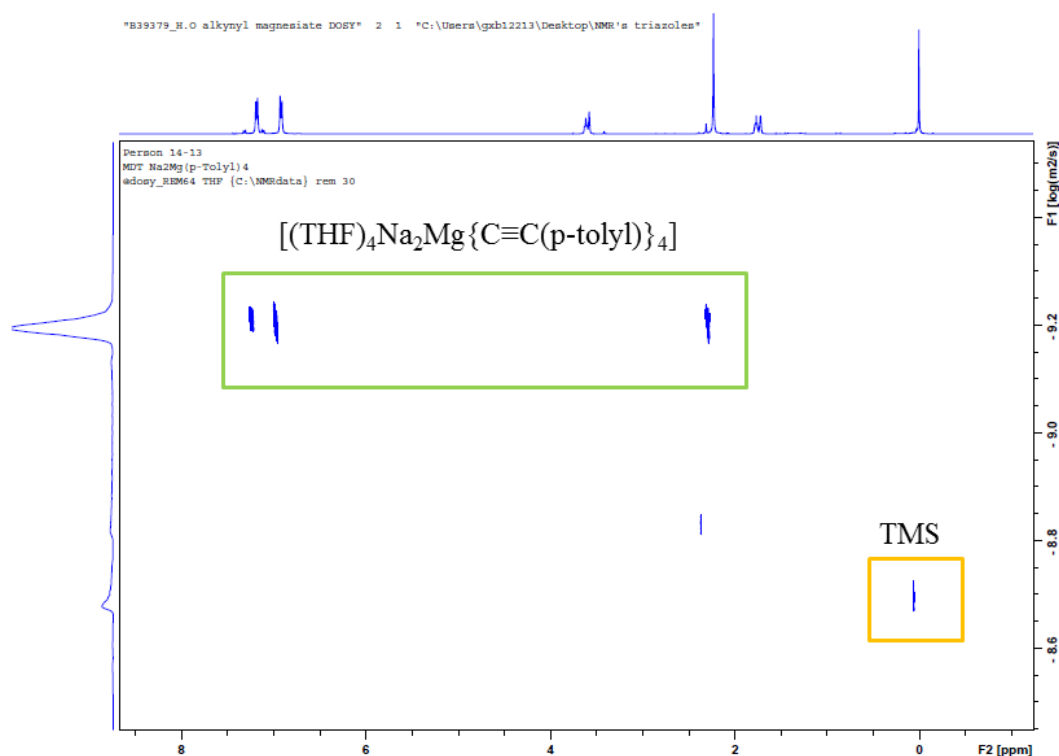
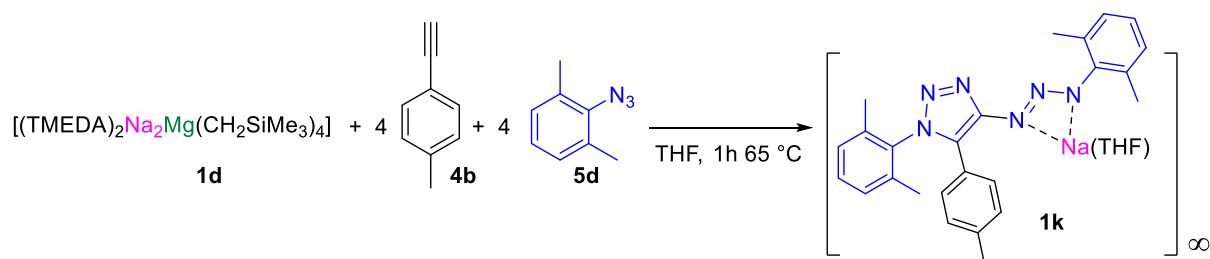


**Figure 3.13:**  $^1\text{H}$  DOSY NMR of higher order sodium magnesiate **1j** in  $d_8$ -THF solution

No evidence of disproportionation to **1h** and sodium *p*-tolylacetylene were observed in THF solution. This is particularly interesting as THF is the solvent used for catalytic studies.

The stoichiometric reaction between alkyne **4b** and azide **5d** was then studied. One equivalent of higher order sodium magnesiate **1d** reacted with four equivalents of alkyne **4b** and four equivalents of azide **5d** in THF at 65 °C for 1 hour which allowed the formation of polymeric product  $[(\text{THF})\text{Na}(\text{C}_{25}\text{H}_{25}\text{N}_6)]$  (**1k**) with the absence of a  $\text{C}^4\text{-H}$   $^1\text{H}$  NMR signal (**Scheme 3.15**).



**Scheme 3.15:** Reaction formation of product **1k**.

Compound **1k** was crystallised by dissolving it in refluxing THF and leaving the solution cooling down slowly in a warm water bath (28% yield, **Figure 3.14**).

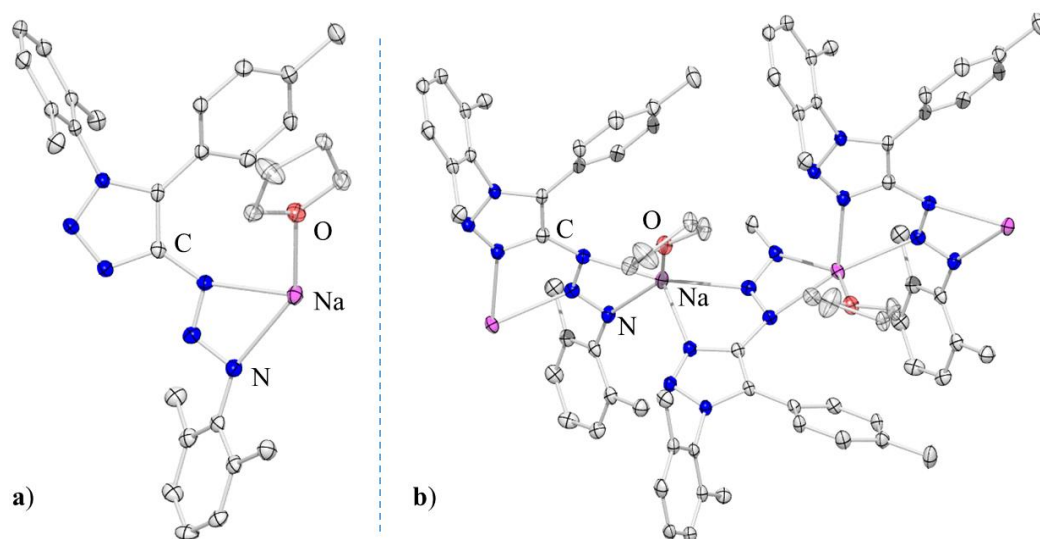
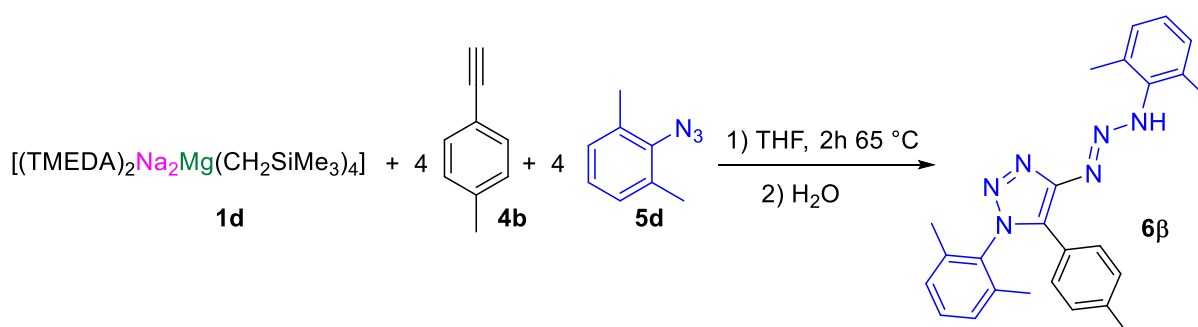


**Figure 3.14:** a) Asymmetric unit of **1k** b) Section (3 asymmetric units) of the polymeric chain structure for **1k**, in both cases the H atoms and the THF minor disorder component have been omitted for clarity. The chain runs along the *c* axis.

Compound **1k** exhibits a series of N-Na-N interactions to form a polymeric chain (along the *c* axis). In addition the sodium atom exhibits a trigonal bipyramidal arrangement with four Na-N interactions and one O-Na interaction. Product **1k** could also be synthesised in higher yield by reacting equimolar amounts of  $\text{NaCH}_2\text{SiMe}_3$  with one equivalent of alkyne **4b** and two equivalents of azide **5d** (65% Yield). A possible explanation for the isolation of **1k** relies on the dual behavior of organic azides as electrophiles and nucleophiles (See section 3.3.2, **Figure 3.2**). A proposed mechanism for the formation of **1k** will be discussed in section 3.6.4, **Scheme**

**3.20.** The stoichiometric reaction between **1d**, alkyne **4b** and azide **5d** was repeated under the same reaction conditions and it was quenched with H<sub>2</sub>O after 2 hours (**Scheme 3.16**).

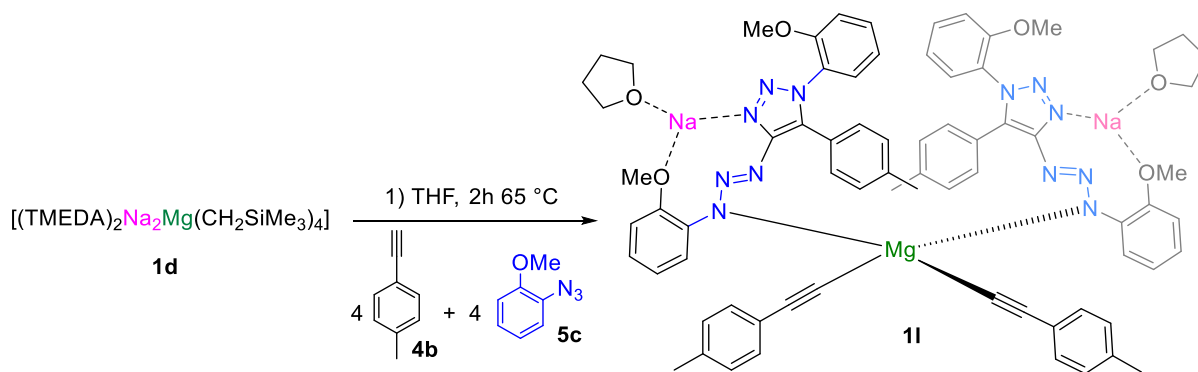


**Scheme 3.16:** Reaction formation of **6β** by quenching product **1k**

GC analysis of the reaction mixture revealed no formation of triazoles **6o**, instead only free alkyne **4b** was recovered along with formation of product (E)-1-(2,6-dimethylphenyl)-4-(3-(2,6-dimethylphenyl)triaz-1-en-1-yl)-5-(*p*-tolyl)-1H-1,2,3-triazole (**6β**)<sup>c</sup>. In contrast to this when the reaction was carried out under catalytic conditions (5 mol% of **1d**), with one equivalent of alkyne **4b** and one equivalent of azide **5d** full conversion of triazole **6o** was obtained (93% isolated yield, entry 15, **Table 3.6**) while no by-product **6β** was observed at all. <sup>1</sup>H and <sup>13</sup>C NMR analysis of the same reaction carried out in d<sub>8</sub>-THF gave a complex NMR spectrum and products could not be identified.

The reaction was repeated changing the azide. Thus **1j** and 4 equivalents of azide **5c** were mixed in d<sub>8</sub>-THF and allowed to react for 1h at 65 °C. <sup>1</sup>H, <sup>13</sup>C NMR analysis revealed formation of one product only [ $\{C\equiv C(p\text{-tolyl})\}_2Mg\{(THF)Na(C_{23}H_{21}N_6O_2)\}_2$ ] (**1l**) (**Scheme 3.17**)

<sup>c</sup> The E configuration of **6β** is assumed considering the retention of the configuration from product **1k** after quenching with H<sub>2</sub>O.



**Scheme 3.17:** Reaction formation of product **11**

$^1\text{H}$  DOSY NMR spectroscopic investigations are in agreement with proposed formation of **11** ( $M_w=1271.73 \text{ g mol}^{-1}$ ) which affords an excellent correlation with the calculated molecular weight ( $M_w=1376 \text{ g mol}^{-1}$ , error 8%, **Figure 3.15**).

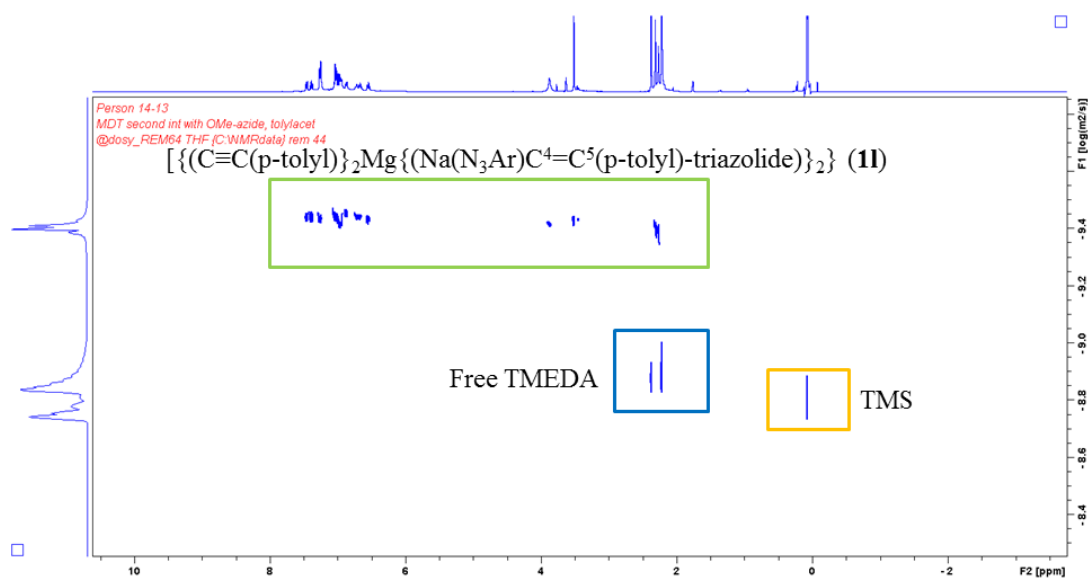
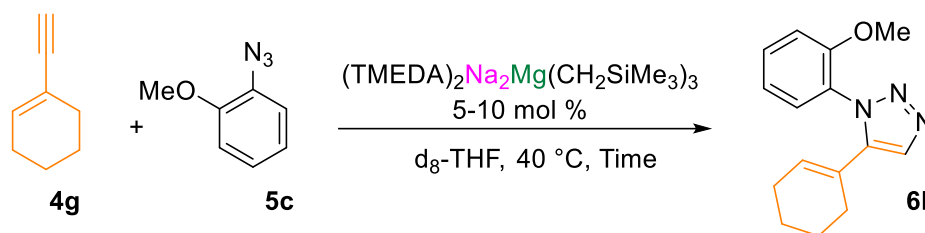


**Figure 3.15:**  $^1\text{H}$  DOSY NMR of product **11** in  $d_8$ -THF solution

### 3.6 Kinetic Analysis

In order to get a better insight into the mechanisms of these reaction, kinetic studies were carried out utilising  $^1\text{H}$  NMR spectroscopy. The reaction between 1-ethynylcyclohexene (**4g**) and 1-azido-2-methoxybenzene (**5c**) was chosen as a model reaction for the kinetic studies (Scheme 3.18).



**Scheme 3.18:** Reaction between 1-ethynylcyclohexene (**4g**) and 1-azido-2-methoxybenzene (**5c**) for kinetic studies

The reaction mixture was heated to 40 °C and periodically monitored by  $^1\text{H}$  NMR spectroscopy (one  $^1\text{H}$  NMR was collected every 30 seconds). This led to reaction completion in timeframes ranging from 10 to 40 minutes (depending on the loading of catalyst employed). Absolute concentrations of alkyne and azide were determined using FeCp<sub>2</sub> (10 mol%) as an internal standard. The reaction kinetics were usually monitored from the intensity changes in the azide resonance -OMe (3.82 ppm) over three or more half-lives on the basis of azide consumption. All data collected could be fit by natural logarithm to the following equation:

$$\ln([Azide] - [Azide]_0) = mt$$

where  $[Azide]_0$  is the initial substrate concentration and  $[Azide]$  the substrate concentration at the specific reaction time,  $t$  is the time and  $m$  the slope of the graph. The effect of  $[azide]$  on the reaction rate was investigated by monitoring the reaction between alkyne **4g** (4.14 M) and azide **5c** (0.36 M) catalysed by **1d** (7.5 mol%), therefore the molar ratio of alkyne to azide was 11:1 maintaining approximately zero-order conditions. The rate of the reaction follows a linear dependence of  $[azide]$  on reaction time till 86% conversion of triazole **6l**, at conversions >86% the reaction rate speeds up remarkably (Figure 3.16).

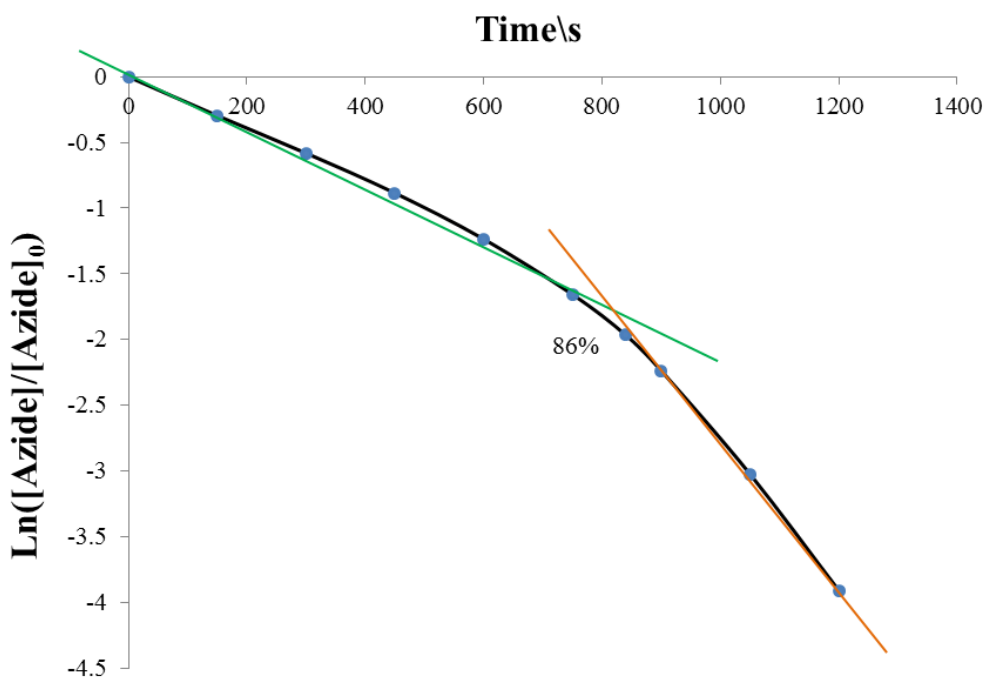


**Figure 3.16:** Plot of  $\text{Ln}([\text{Azide}]/[\text{Azide}]_0)$  vs reaction time for the cycloaddition of alkyne (4.14 M) to azide (0.36 M) catalysed by **1d** at 0.02628 M. Rate of reaction increases after yield of **6I** >86%

Further kinetic studies were carried out on the same reaction with data collection over three half lives (<86% conversion of triazole **6I**). Data collection was excluded for the conversions >86% as the rate changes.

### 3.6.1 Azide order

To analyse the order of the azide a reaction with a molar ratio 11:1 of alkyne and azide was carried out at 40 °C using **1d** (7.5 mol%). **Figure 3.17** reveal a linear dependence of [azide] on reaction time, which agrees with an essentially order one dependence of the catalytic rate on azide concentration.

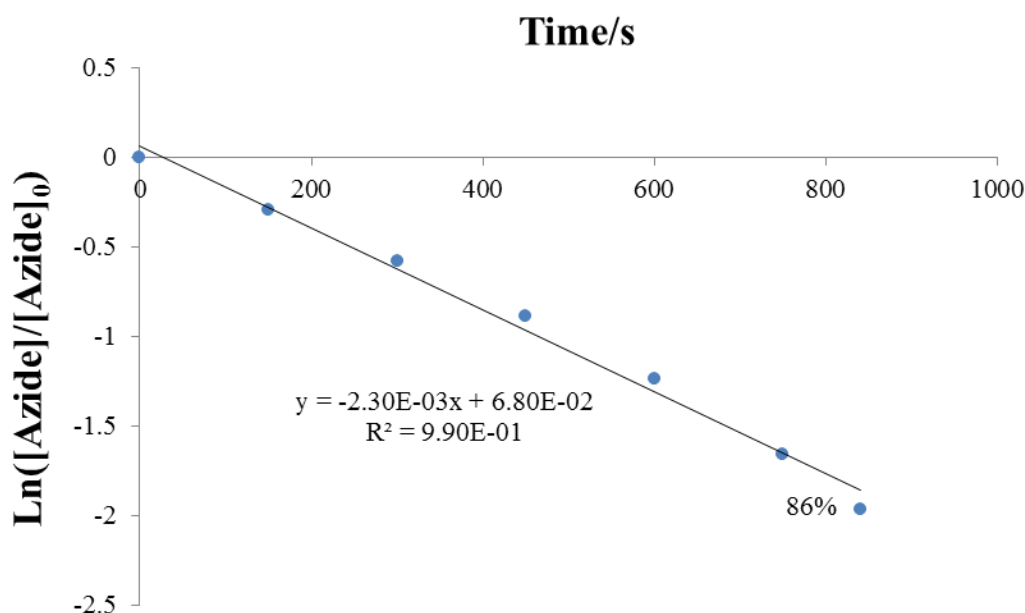


**Figure 3.17:** Plot of  $\text{Ln}([\text{Azide}]/[\text{Azide}]_0)$  vs reaction time for the cycloaddition of alkyne (4.14 M) to azide (0.36 M) catalysed by **1d** at 0.02628 M

Initial attempts to study the order of alkyne failed. Using the same approach we carried out a reaction with a molar ratio alkyne to azide 1:11 maintaining approximately zero-order conditions reaction in azide. However no reaction conversion was observed as the reaction is inhibited by high concentrations of azide. Similarly to what is observed when the reaction is carried out using 15-crown-5 where the reaction was completely inhibited, a similar outcome of the reaction is observed under high concentrations of azide. The synergistic effect of the Mg and Na atoms within the same molecule can be broken as the azide can act as Lewis base capturing the Na atoms (similarly to what happens with 15-crown-5). Once more this shows the crucial role of the alkali metal in this transformation.

### 3.6.2 Alkyne order

The effect of alkyne **4g** was studied through four experiment sets varying the concentration of only alkyne while keeping constant the concentration of the other two components of the mixture, and always at an alkyne to azide molar ratio greater than 11:1. Kinetic plots for the catalytic reaction rate as a function of [alkyne] (concentration range [alkyne] = 3.80 – 5.60 M; [alkyne]:[azide] > 11:1, [azide]:[1d] > 10:1, **Figure 3.18 and Figure 3.19**) indicate that the reaction rate is zero-order in alkyne.

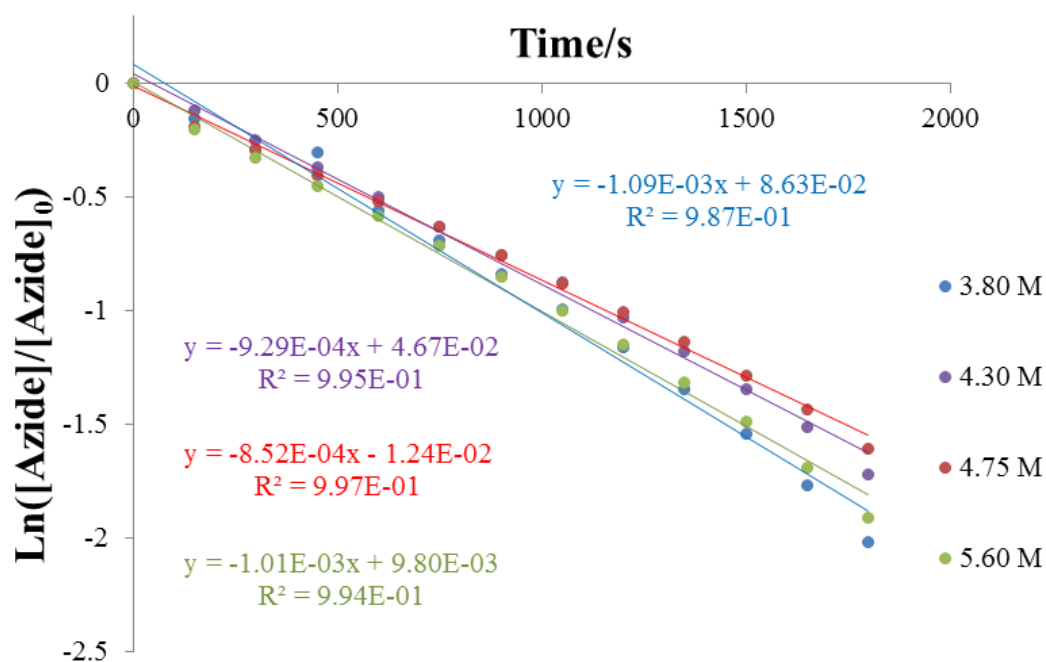


**Figure 3.18:** Plot of  $\ln([Azide]/[Azide]_0)$  vs reaction time for the cycloaddition of four different concentrations of alkyne (3.80, 4.30, 4.75 and 5.60 M) to azide (0.36 M) catalysed by **1d** (0.01803 M).

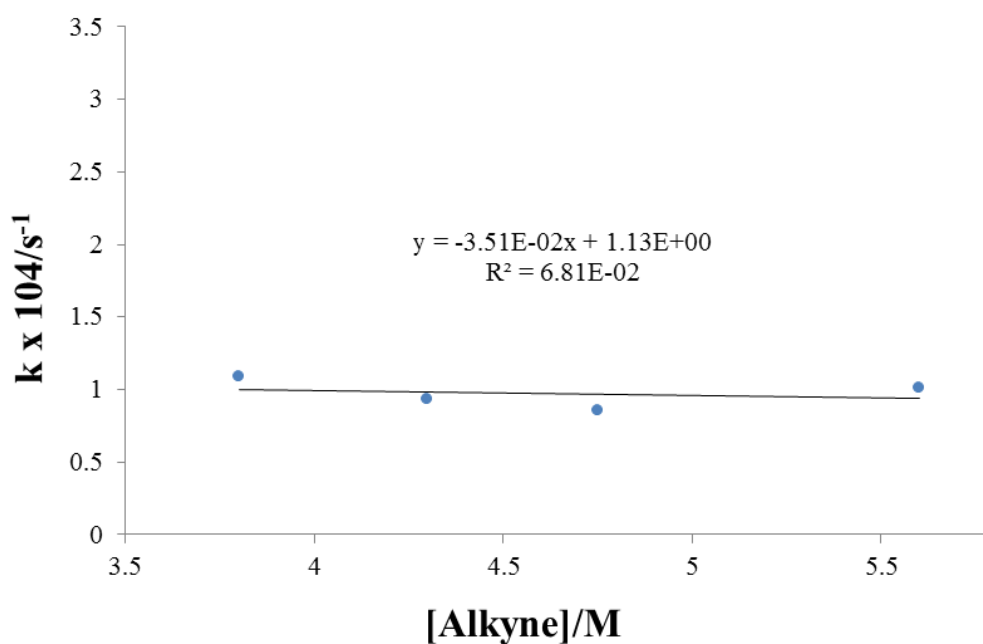


**Figure 3.19:** Plot of  $k$  values obtained for the cycloaddition of four different concentrations of alkyne (3.80, 4.30, 4.75 and 5.60 M) to azide (0.36 M) catalysed by **1d** (0.01803 M).

This result indicates that formation of alkynyl sodium magnesiate from the reaction between **1d** and alkyne is not the rate determining step of the triazole reaction formation.

### 3.6.3 Catalyst order

Similarly to what is discussed in **chapter 3.6.2**, the effect of catalyst **1d** was studied through four experiment sets varying the concentration of only catalyst **1d** while keeping constant the concentration of the alkyne **4g** and azide **5d** in the mixture, and always with a ratio alkyne to azide greater than 11:1. Kinetic plots for the catalytic reaction rate as a function of the concentration of catalyst precursor **1d** varied from 0.0234 M to 0.0322 M (**Figure 3.20** and **Figure 3.21**) indicate that the reaction rate is first order in catalyst.

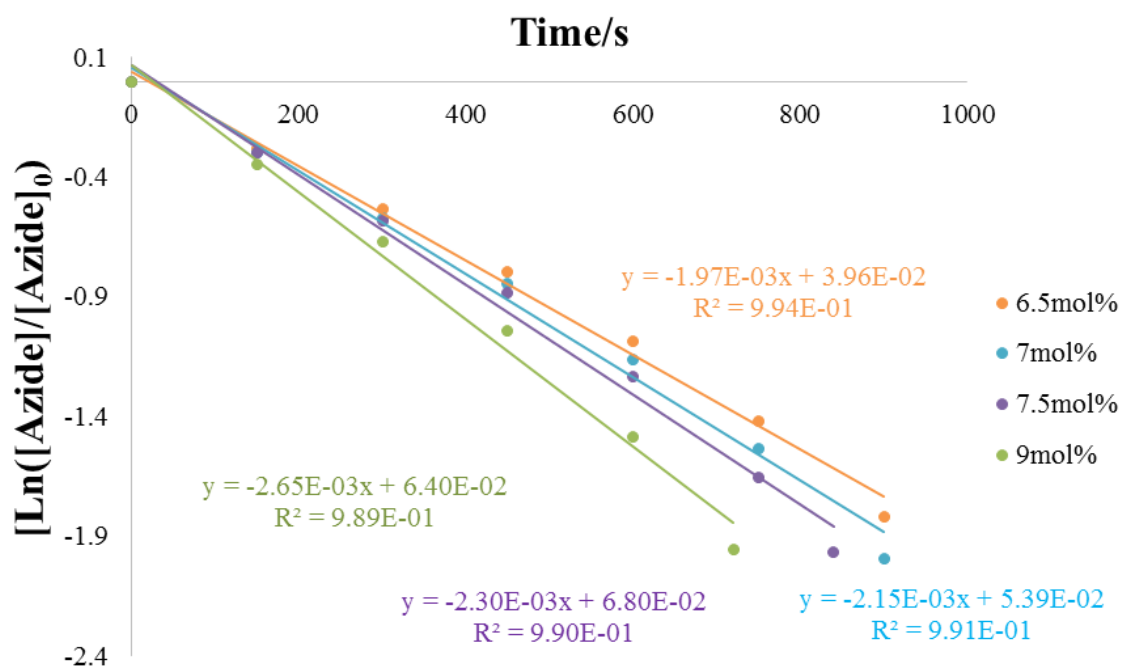


**Figure 3.20:** Plot of  $\ln([Azide]/[Azide]_0)$  vs reaction time for the cycloaddition of four different concentrations of catalyst [0.0234 M (6.5 mol%), 0.0251 M (7 mol%), 0.0278 M (7.5 mol%), 0.0322 M (9 mol%)] with a constant [alkyne]:[azide]=11:1, [azide]=0.36 M

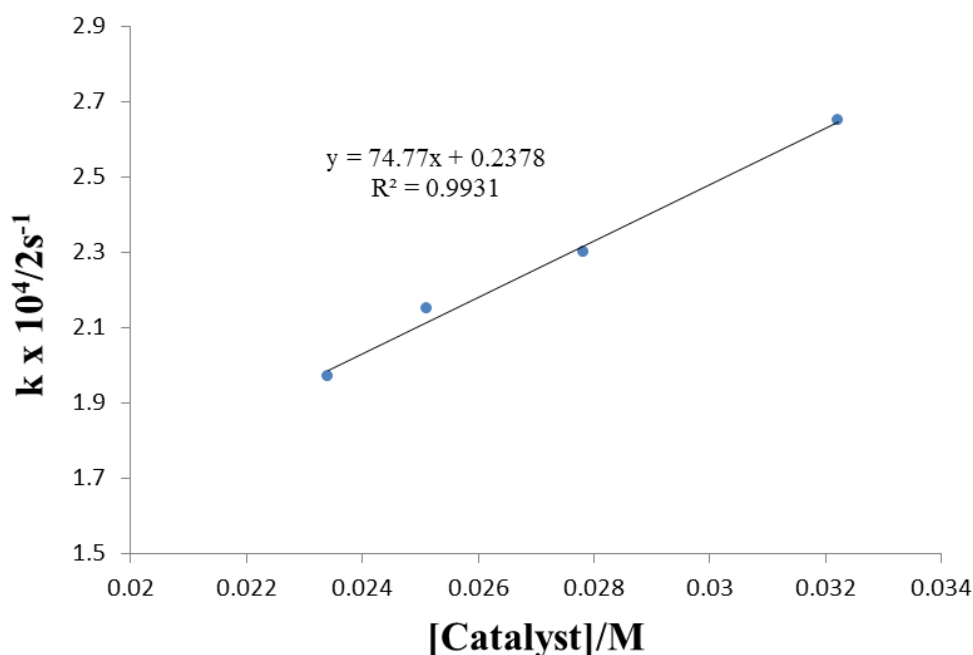


**Figure 3.21:** Plot of  $k$  vs [catalyst] for the cycloaddition reaction of alkyne (4.14 M) to azide (0.36 M) catalysed by **1d** at four different concentrations [0.0234 M (6.5 mol%), 0.0251 M (7 mol%), 0.0278 M (7.5 mol%), 0.0322 M (9 mol%)] with a constant [alkyne]:[azide]=11:1, [azide]=0.36 M

Taken all the kinetic information together, the empirical rate law is given in the following equation.

$$v = k[\text{Alkyne}]^0[\text{Azide}]^1[\text{Cat}]^1$$

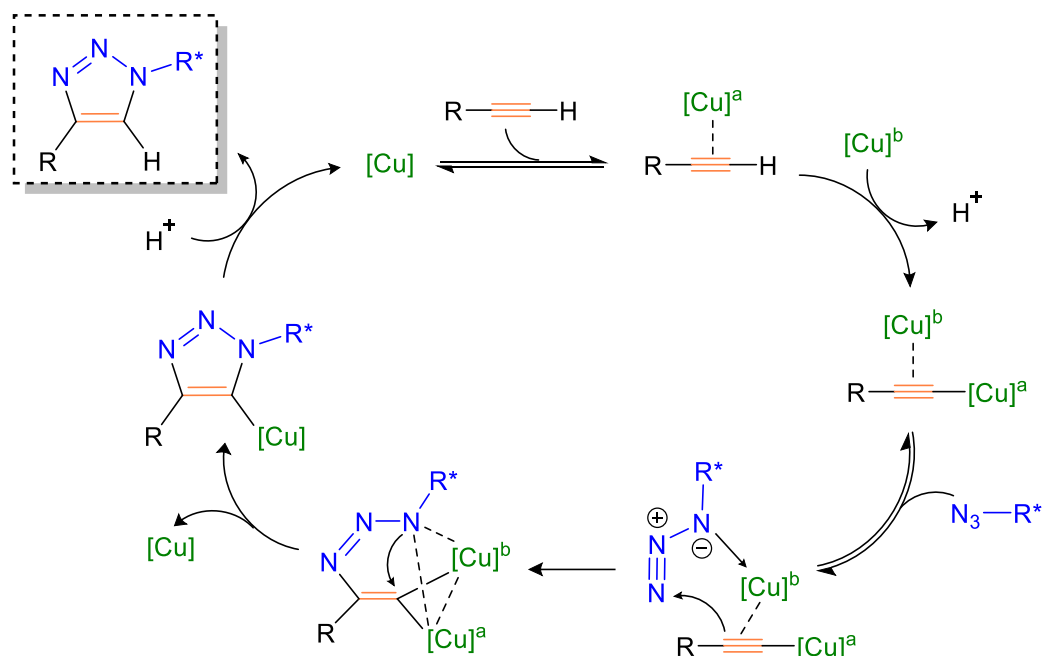
The key points evidenced by kinetic studies can be summarised as follows:

1. Metallation of alkyne is not the rate determining step of the reaction
2. Insertion/intramolecular nucleophilic attack is the rate determining step
3. Only one substituent of the higher order magnesiate **1** is active in the catalytic process

### 3.6.4 Proposed mechanism:

Regarding the synthesis of 1,4-triazoles in CuAAC, previous theoretical studies suggested possible involvement of more than one Cu center in the mechanism of this type of transformations.<sup>42,43</sup> Prior to Fokin and collaborators discovery no evidence of experimental

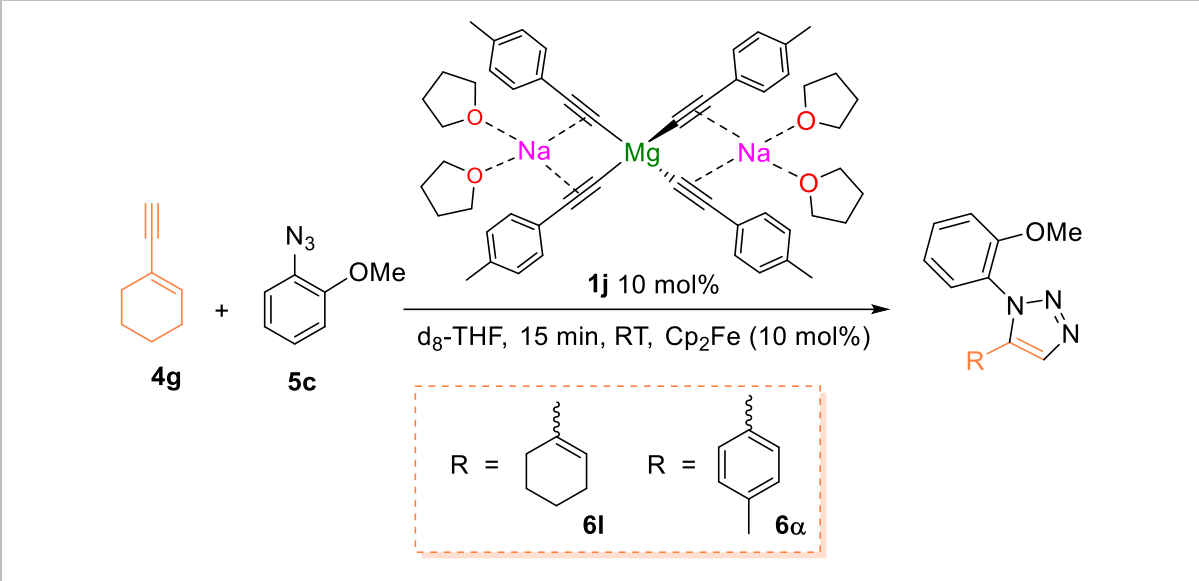
data backed up these theoretical studies. Using enriched  $^{63}\text{Cu}$  catalysts Fokin and collaborators designed a reaction procedure which allowed them to assign the cycloaddition step as the part of the reaction where two copper centers act simultaneously to yield 1,4-triazoles (**Scheme 3.19**).<sup>34</sup>



**Scheme 3.19:** Fokin *et al* proposed mechanism with the presence of two Cu centers for CuAAC.

The authors propose a mechanism in which the first step is the formation of a dual  $\sigma$ -bonded copper acetylide intermediate, it follows the insertion of azide and nucleophilic attack to form a triazolyl copper intermediate. Furthermore the protonolysis of the triazolyl copper intermediate generates the final 1,4-triazole moiety and it regenerates the Cu catalyst which can start a new cycle.

These results raised new questions on the possible mechanism of the **1d** catalysed 1,5-triazole procedure, which could potentially proceed via  $\pi$ -interactions between Mg or Na with both acetylenic C atoms rather than the intuitive  $\sigma$ -bond activation. To exclude this possibility a cross over type reaction was carried out (**Table 3.13**).

**Table 3.13:** **1j** catalysed cross over reaction between alkynes **4g** and azide **5c**

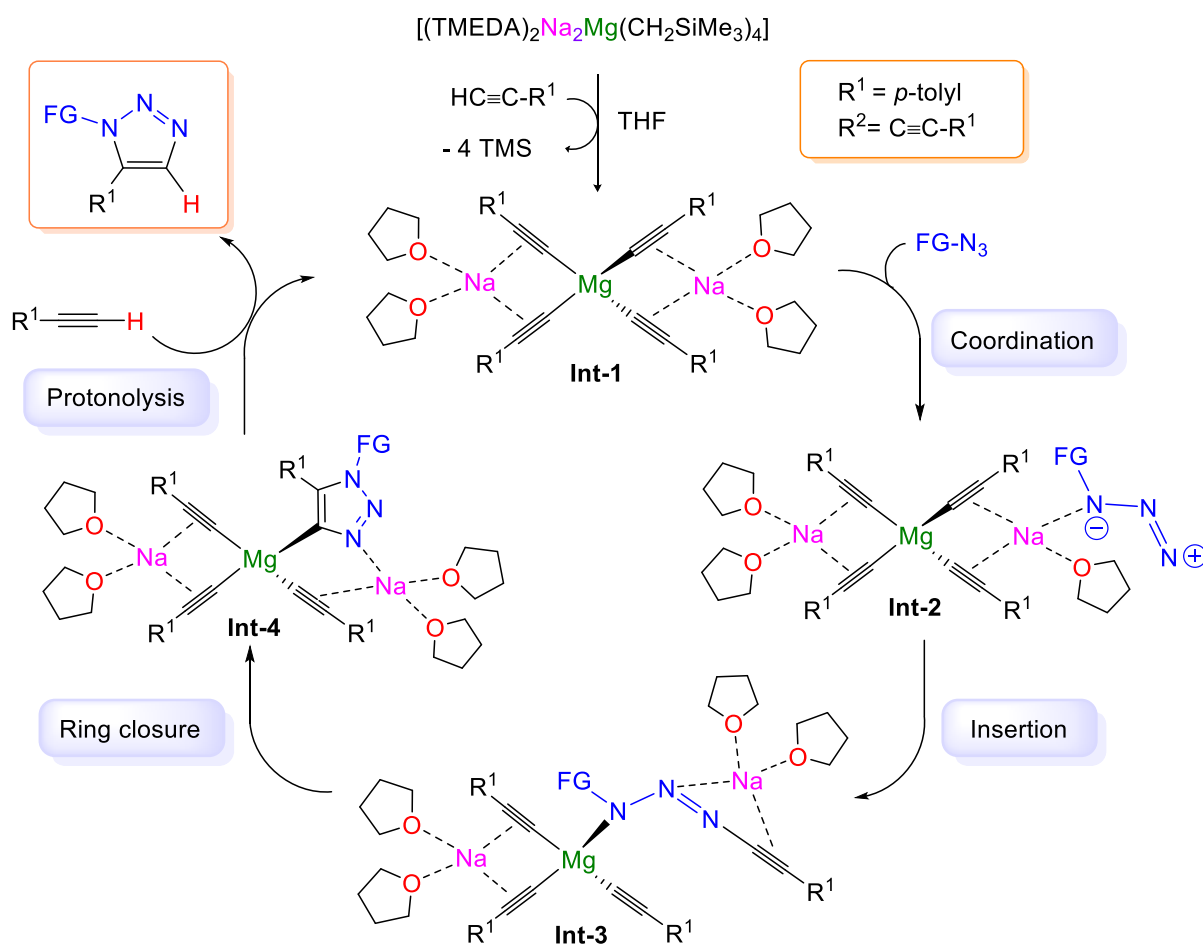
Entry	alkyne <b>4g</b> (mmol)	azide <b>5c</b> (mmol)	<b>6l</b> (mmol)	<b>6a</b> (mmol)
<b>1</b> ( <b>t0</b> )	0.35	0.42	0	0
<b>2</b> ( <b>t1</b> )	traces	0	0.30	0.12

[a] <sup>1</sup>H and <sup>13</sup>C NMR studies were carried out using 10 mol% of catalyst **1t** which is equivalent to (0.14 mmols of *p*-tolylacetylene) in d<sub>8</sub>-THF.

Confronting alkyne **4g** (0.37 mmols) and azide **5c** (0.42 mmols) with 10 mol% of alkynyl sodium magnesiate **1j** resulted in formation of triazole **6a** in 0.12 mmols and triazole **6l** in 0.30 mmols. This result demonstrates that the efficiency of **1j** to promote the catalytic formation of 1,5 triazoles and the reaction proceeds through magnesiate  $\sigma$ -bond activation of the terminal acetylenic C atom. With the course of the reaction as soon as *p*-tolyl alkynyl moiety has been transformed into triazoles **6a** by insertion reaction with azide **5c**, a different alkyne such as **4g** can be activated and further insertion with azide **5c** gives formation of a different triazole **6a**. Supporting this proposal, internal alkynes such as diphenylacetylene (**4j**) fail to react with azides under the conditions studied. In the case of a promoted  $\pi$ -activation as the only force of the reaction procedure the only product expected would be triazole **6l**.

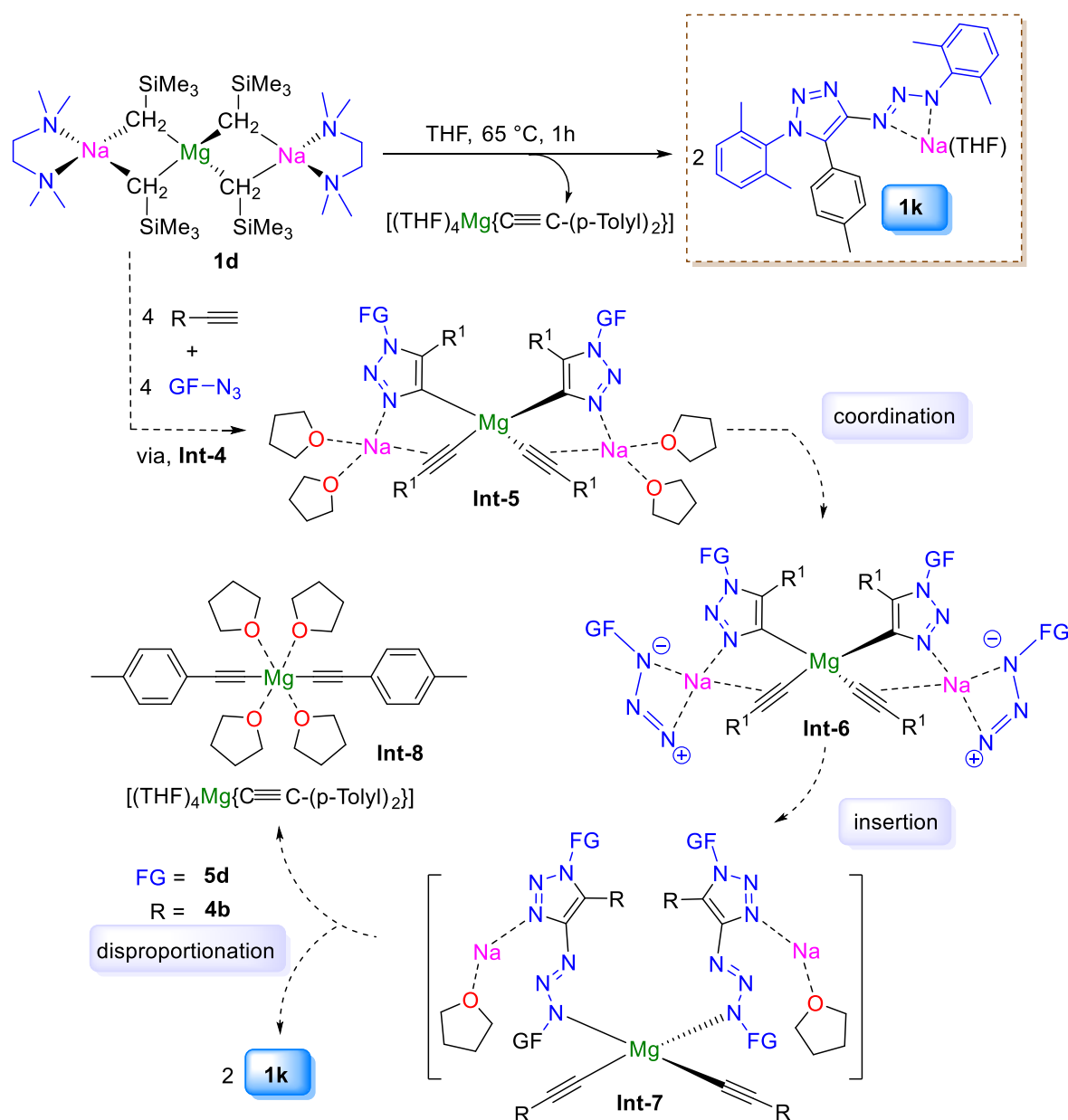
Based on all the compiled results, a plausible mechanism for the cycloaddition of terminal alkynes to azides mediated by the higher order sodium magnesiate **1d** is shown in **Scheme 3.20**. In a first step terminal alkyne is metallated by **1d** giving rise to a magnesiate acetylide (**Int-1**, **Scheme 3.20**). <sup>1</sup>H DOSY NMR studies on the stoichiometric reaction between **1d** and

**4b** confirmed the formation of intermediate **1j**. Coordination of azide acting as a Lewis base with the Na cation forms magnesiate **Int-2** (**Scheme 3.20**). Thus, one of the activated alkynyl species ( $\text{Mg-C}\equiv\text{C-R}$ ) can act as a nucleophile, and by attacking the terminal nitrogen atom in organic azide, intermediate **3** is formed (**Int-3**, **Scheme 3.20**). Furthermore, **INT-3** undergoes an intramolecular nucleophilic attack of the far nucleophilic nitrogen atom to the  $\pi$ -coordinated alkyne moiety leading to the formation of triazolite intermediate **4** (**Int-4**, **Scheme 3.20**). Although intermediates **2**, **3** and **4** could not be detected the empirical rate law obtained with the kinetic studies suggests that only one triazolite intermediate is formed at a time on each catalytic cycle. Protonation by the excess of alkyne releases the organic product and recycles the active catalyst (**Int-1**, **Scheme 3.20**).



**Scheme 3.20:** Proposed mechanism for the **1d** catalyzed 1,5-disubstituted-1,2,3-triazole formation reaction.

As previously discussed, the stoichiometric reaction between **1d** and alkyne **4b** and azide **5d** gave formation of product **1k**. A plausible formation of **1k** is proposed in **Scheme 3.21**.



**Scheme 3.21:** Plausible mechanism for the formation of **1k** under stoichiometric conditions

Following the same mechanism as in **Scheme 3.20**, intermediate 4 can be formed (**Int-4**, **Scheme 3.20**). The absence of free alkyne due to stoichiometric conditions and the presence of free organic azide in solution allows formation of di-triazolate intermediate (**Int-5**, **Scheme 3.21**). Furthermore free organic azide in solution can coordinate to the Na center to form intermediate 6 (**Int-6**, **Scheme 3.21**). Furthermore, nucleophilic attack of Mg-C bond from the triazolate intermediate to the electrophilic terminal N atom of the organic azide allows formation of intermediate 7 (**Int-7**, **Scheme 3.21**).  $^1\text{H}$  DOSY NMR studies on the

stoichiometric reaction between **1d** alkyne **4d** and azide **5c** confirmed the formation of intermediate **1l** (**Int-7**) in  $d_8$ -THF solution. This does not happen under catalytic conditions as the triazolate intermediate (**Int-4**, **Scheme 3.21**) quickly reacts with free alkyne in solution to form the final triazoles and to regenerate intermediate **1**. Furthermore, disproportionation reaction forms product **1k** and Mg alkynyl intermediate **8** (**Int-8**, **Scheme 3.21**).

### 3.7 Conclusions

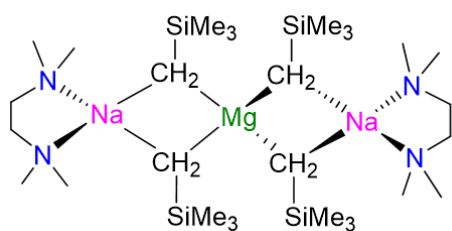
In conclusion a versatile new ate-mediated catalytic method for the cycloaddition reactions of alkynes to azides to form 1,5-disubstituted-1,2,3-triazoles has been developed. This first catalytic method using s-block metal pairs, works in a concerted synergistic manner as a more sustainable method to the already known transition metal catalysts. Despite the high kinetic barrier of this type of transformation, the process exhibits broad substrate scope and mild reaction conditions when compared to other methods. Both kinetic and stoichiometric studies helped to elucidate the mechanism of the catalytic transformation.

### 3.8 Experimental section

**General Considerations.** All reactions were performed under a protective argon atmosphere using standard Schlenk techniques. Hexane and THF were dried by heating to reflux over sodium benzophenone ketyl and distilled under nitrogen prior to use. The synthesis of  $[\{(\text{KMg}(\text{CH}_2\text{SiMe}_3)_3)_\infty\}]$  (**1a**),  $[(\text{PMDETA})_2\text{K}_2\text{Mg}(\text{CH}_2\text{SiMe}_3)_4]$  (**1b**), was carried out according to the literature procedure<sup>16</sup> (see experimental section of **Chapter 2** Section 2.7.1.3 for **1a** and section 2.7.1.4 for **1b**). The synthesis of  $[(\text{TMEDA})_2\text{Li}_2\text{Mg}(\text{CH}_2\text{SiMe}_3)_4]$  (**1e**) and  $[\text{LiMg}(\text{CH}_2\text{SiMe}_3)_3]$  (**1g**) was carried out according to the literature procedure<sup>18</sup> (see experimental section of **Chapter 2** section 2.7.1.7 for **1e**). The synthesis of  $[\text{NaMg}(\text{CH}_2\text{SiMe}_3)_3]$  (**1f**) was carried out according to the literature procedure.<sup>17</sup> TMEDA and PMDETA were distilled over  $\text{CaH}_2$  and stored in a Schlenk with activated molecular sieves prior to use. NMR spectra were recorded on a Bruker DPX 400 MHz spectrometer operating at 400.13 MHz for  $^1\text{H}$  and 100.62 MHz for  $^{13}\text{C}$ . Elemental analyses were obtained using a Perkin Elmer 2400 elemental analyser. High resolution mass spectra for products (**6a-6z**, **6a** and **6b**) were recorded on a thermo scientific LTQ ORBITRAP XL spectrometer (HRMS ESI, nanoelectrospray) coupled to an Advion TriVersa NanoMate 3 in positive or negative ionization mode (samples were diffused in a stream of MeOH:  $\text{NH}_4\text{OAc}$  9:1).

### 3.8.1 Synthesis of inorganic compounds

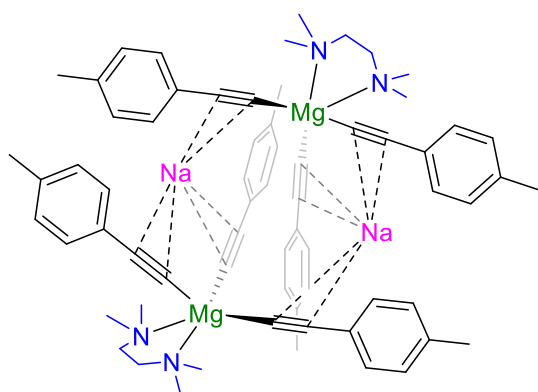
#### 3.8.1.1 Synthesis of [(TMEDA)<sub>2</sub>Na<sub>2</sub>Mg(CH<sub>2</sub>SiMe<sub>3</sub>)<sub>4</sub>] (1d).



To a suspension of NaCH<sub>2</sub>SiMe<sub>3</sub> (0.22 g, 2 mmol) in hexane (15 mL) Mg(CH<sub>2</sub>SiMe<sub>3</sub>)<sub>2</sub> (0.20 g, 1 mmol) was added and the suspension stirred for 1 hour. TMEDA (0.30 mL, 2 mmol) was then added and the solution was gently heated to form a clear solution

which was transferred to the freezer (-28 °C). After 16 hours a crop of clear, colourless crystals was isolated (0.35 g, 54%). <sup>1</sup>H NMR (400 MHz, 298 K, C<sub>6</sub>D<sub>6</sub>) δ (ppm) = -1.78 (2H, s, SiCH<sub>2</sub>), 0.47 (9H, s, Si(CH<sub>3</sub>)<sub>3</sub>), 1.67 (2H, s, NCH<sub>2</sub>, TMEDA), 1.92 (6H, s, N(CH<sub>3</sub>)<sub>2</sub>, TMEDA). <sup>13</sup>C{<sup>1</sup>H} NMR (101 MHz, 298 K, C<sub>6</sub>D<sub>6</sub>) δ (ppm) = -3.14 (SiCH<sub>2</sub>), 5.63 (Si(CH<sub>3</sub>)<sub>3</sub>), 45.80 (N(CH<sub>3</sub>)<sub>2</sub>, TMEDA), 56.76 (NCH<sub>2</sub>, TMEDA). **Elemental analysis (CHN):** Expected value, C=51.62, H=11.76, N=8.60 found, C=51.12, H=11.54, N=8.93.

#### 3.8.1.2 Synthesis of [(TMEDA)NaMg{C≡C(*p*-tolyl)}<sub>3</sub>]<sub>2</sub> (1h).

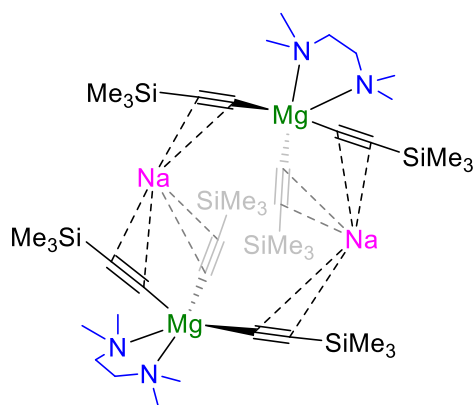


To a suspension of **1f** (309 mg, 1 mmol) in hexane (10 mL), 4-ethynyltoluene (348 mg, 3 mmol) was added and the white suspension was stirred for 1h. TMEDA (0.15 mL, 1 mmol) was then added, giving a clear solution for few seconds which rapidly precipitates. A white precipitate was isolated (396 mg, 78% yield) and characterised by <sup>1</sup>H and <sup>13</sup>C NMR

as **1h**. Crystalline **1h** can be prepared following a similar procedure. To a suspension of **1f** (309 mg, 1 mmol) in hexane (10 mL) 4-Ethynyltoluene (348 mg, 3 mmol) was added and the white suspension was stirred for 1h. After addition of TMEDA (0.15 mL, 1 mmol), C<sub>6</sub>H<sub>6</sub> (6 mL) were added, the solution was gently heated to form a clear solution which was kept in a warm water bath. After 16 hours a crop of clear, colourless crystalline needles were isolated (193 mg, 38% yield). No substantial difference in the <sup>1</sup>H and <sup>13</sup>C NMR of the product was observed from the two preparation methods employed for the synthesis of **1h**. <sup>1</sup>H NMR (400 MHz, 298 K, C<sub>6</sub>D<sub>6</sub>) δ (ppm) = 1.96 (broad s, 4H, NCH<sub>2</sub>, TMEDA), 2.07 (s, 9H), 2.39 (broad

s, 12H, N(CH<sub>3</sub>)<sub>2</sub>, TMEDA), 6.89 (d, *J*=8 Hz, 6H), 7.60 (d, *J*=8 Hz, 6H). <sup>13</sup>C{<sup>1</sup>H} NMR (101 MHz, 298 K, C<sub>6</sub>D<sub>6</sub>) δ (ppm) = 14.9, 21.9, 47.5, 56.8, 112.4, 125.6, 129.5, 129.6, 132.8, 135.8.

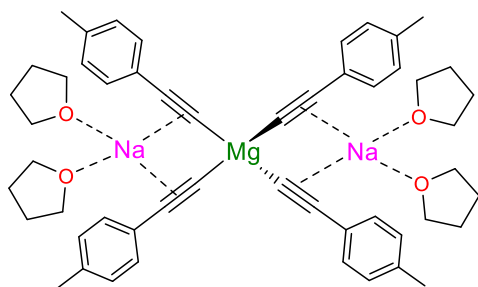
### 3.8.1.3 Synthesis of [(TMEDA)NaMg{C≡C(SiMe<sub>3</sub>)<sub>3</sub>}<sub>2</sub>] (1i)



To a suspension of **1f** (309 mg, 1 mmol) in hexane (10 mL) ethynyltrimethylsilane (295 mg, 3 mmol) was added and the white suspension was stirred for 1h. TMEDA (0.15 mL, 1 mmol) was then added and the solvent was removed under vacuum. Toluene (3 mL) was then added to give a clear solution which was transferred to the freezer (-28 °C). After 16h a crop of colourless crystals were isolated (147 mg, 32% yield)

and characterised by <sup>1</sup>H and <sup>13</sup>C NMR as **1i**. <sup>1</sup>H NMR (400 MHz, 298 K, d<sub>8</sub>-THF) δ (ppm) = 0.46 (s, 27H, Si(CH<sub>3</sub>)<sub>3</sub>), 1.92 (s, 4H, NCH<sub>2</sub>, TMEDA), 2.41 (s, 12H, N(CH<sub>3</sub>)<sub>2</sub>, TMEDA). <sup>13</sup>C{<sup>1</sup>H} NMR (101 MHz, 298 K, C<sub>6</sub>D<sub>6</sub>) δ (ppm) = 2.0, 46.9, 56.3, 116.9, 160.5.

### 3.8.1.4 Synthesis of [(THF)<sub>4</sub>Na<sub>2</sub>Mg{C≡C(*p*-tolyl)}<sub>4</sub>] (1j)

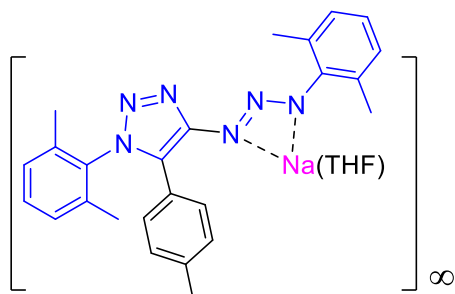


To a suspension of NaCH<sub>2</sub>SiMe<sub>3</sub> (220 mg, 2 mmol) and Mg(CH<sub>2</sub>SiMe<sub>3</sub>)<sub>2</sub> (198 mg, 1 mmol) in hexane (10 mL) 4-Ethynyltoluene (464 mg, 4 mmol) was added and the white suspension was stirred for 1h. THF was then added to afford a colourless solution. Solvent was then removed and a white precipitate was

isolated (493 mg, 82% Yield) and characterised by <sup>1</sup>H, <sup>13</sup>C and <sup>1</sup>H DOSY NMR as [(THF)NaMg(C≡C-*p*-tolyl)<sub>4</sub>] (**1j**) in d<sub>8</sub>-THF (see <sup>1</sup>H DOSY NMR experiments for further detail). <sup>1</sup>H NMR (400 MHz, 298 K, d<sub>8</sub>-THF) δ (ppm) = 1.77 (m, 4H, THF), 2.23 (s, 12H, CH<sub>3</sub>), 3.62 (m, 4H, THF), 6.92 (d, *J*=7.8 Hz, 8H, CH), 7.19 (d, *J*=7.8 Hz, 8H). <sup>13</sup>C{<sup>1</sup>H} NMR (101 MHz, 298 K, C<sub>6</sub>D<sub>6</sub>) δ (ppm) = 21.0, 26.1 (THF), 68.0 (THF), 109.0, 126.6, 128.8, 130.7,

131.6, 134.5. **Elemental analysis (CHN)**<sup>d</sup>: Expected value, C=79.67, H=6.02 found, C=78.77, H=5.87

### 3.8.1.5 Synthesis of [(THF)Na(C<sub>25</sub>H<sub>25</sub>N<sub>6</sub>)] (1k)



To a suspension of NaCH<sub>2</sub>SiMe<sub>3</sub> (110 mg, 1 mmol) in hexane (5 mL) 4-Ethynyltoluene (116 mg, 1 mmol) was added and the white suspension was stirred for 30 min. 2-azido-1,3-dimethylbenzene **4d** (294 mg, 2 mmol) was added and the temperature was increased until reflux (68 °C) for 1 hour. The solvent was then

removed to afford a yellowish precipitate which was redissolved in THF (5 mL) to afford a yellowish solution which was left cooling down in a warm water bath to allow the formation of small pale yellow crystals (373 mg obtained, 65% yield). <sup>1</sup>H NMR (400 MHz, 298 K, d<sub>8</sub>-THF) δ (ppm) = 1.72 (m, 4H, THF), 1.77-2.14 (overlapping s, 15H, CH<sub>3</sub>), 3.62 (m, 4H, THF), 6.57-6.90 (three overlapping sets of multiplets, 5H, aromatic CH), 7.06-7.31 (three overlapping sets of multiplets, 5H, aromatic CH). <sup>13</sup>C{<sup>1</sup>H} NMR (101 MHz, 298 K, C<sub>6</sub>D<sub>6</sub>) δ (ppm) = 17.9, 20.2, 21.1, 26.4 (THF), 68.2 (THF), 121.9, 122.6, 123.7, 127.0, 127.3, 127.7, 128.6, 128.9, 128.9, 129.4, 130.1, 136.9, 137.2, 152.2. **Elemental analysis (CHN)**: Expected value, C=69.43, H=5.83, N=19.43 found, C=68.48, H=5.99, N=18.74.

---

<sup>d</sup> It corresponds to the elemental analysis for the same compound with only one THF molecule, as by <sup>1</sup>H NMR it can be observed that only one molecule of THF is present. THF can be removed under high vacuum.

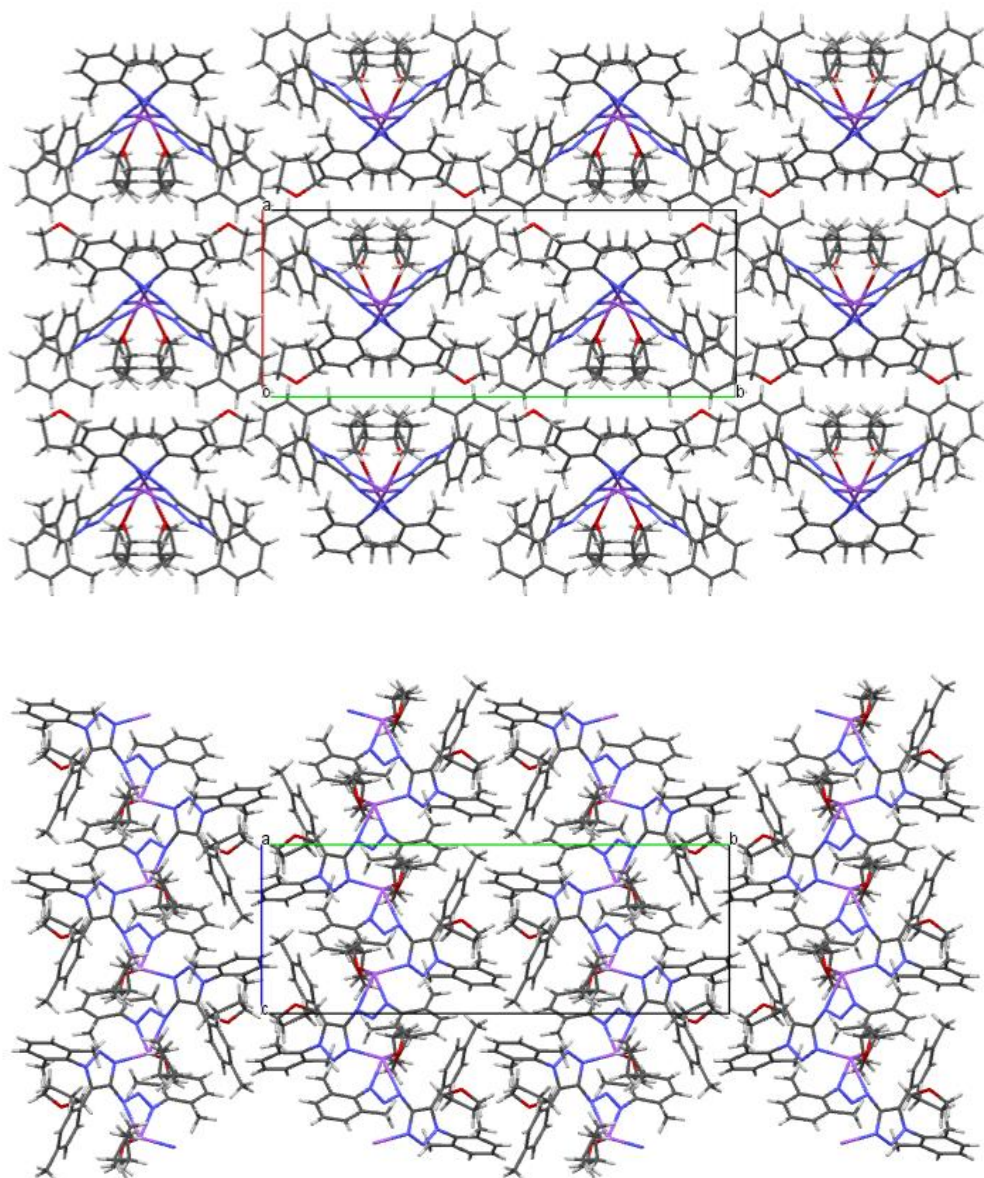
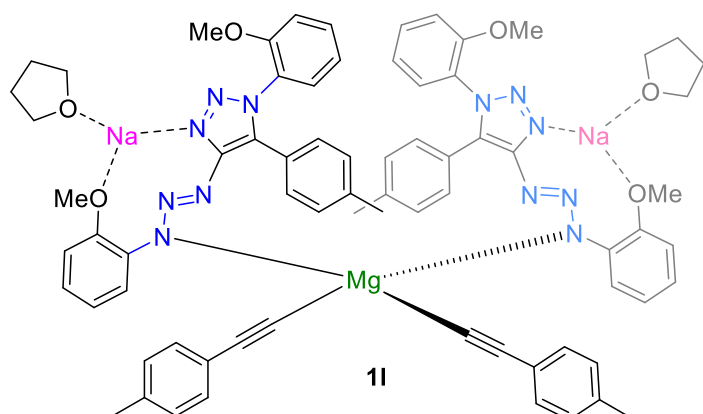


**Figure 3.22:** Packing diagrams (including H atoms and disorder), viewed along the *a* (top) and *c* (bottom) axes for polymeric structure of **1k**

### 3.8.1.6 Synthesis of $[\{(C\equiv C(p\text{-tolyl})\}_2Mg\{(THF)Na(C_{23}H_{21}N_6O_2)\}_2)]$ (**11**)



One equivalent of (16 mg, 0.019 mmols, **1j**) was charged in a Young NMR tube and dissolved in  $d_8$ -THF (0.5 mL). 4 equivalents of 1-azido-2-methoxybenzene (**5c**) were added (11 mg, 0.076 mmol) and the mixture was allowed to react at 65 °C for 1 hour.  $^1H$ ,  $^{13}C$  NMR and  $^1H$

DOSY NMR analysis revealed formation of one product only  $[\{(C\equiv C(p\text{-tolyl})\}_2Mg\{(THF)Na(C_{23}H_{21}N_6O_2)\}_2)]$  (**11**).  $^1H$  NMR (400 MHz, 298 K,  $d_8$ -THF)  $\delta$  (ppm) = 2.22 (s, 6H,  $CH_3$ ), 2.26 (s, 6H,  $CH_3$ ), 3.46 (s, 6H,  $OCH_3$ ), 3.82 (broad s, 6H,  $OCH_3$ ), 6.47-6.51 (m, 2H, aromatic  $CH$ ), 6.60-6.63 (m, 2H, aromatic  $CH$ ), 6.66(m, 2H, aromatic  $CH$ ), 6.82 (d, 2H,  $J=7.8$  Hz, aromatic  $CH$ ), 6.89-6.99 (m, overlapping signals, 14H, aromatic  $CH$ ), 7.21 (d, 6H,  $J=7.9$  Hz, aromatic  $CH$ ), 7.31-7.36 (m, 2H, aromatic  $CH$ ), 7.40 (d, 2H,  $J=7.9$  Hz, aromatic  $CH$ ).  $^{13}C\{^1H\}$  NMR (101 MHz, 298 K,  $C_6D_6$ )  $\delta$  (ppm) = 110.6, 112.9, 116.4, 120.6, 120.9, 121.2, 124.6, 127.9, 128.4, 128.7, 128.8, 129.4, 130.3, 131.8, 134.7, 137.0, 144.3, 151.2, 155.1

#### Synthesis of 1-phenyl-5-(thiophen-3-yl)-1H-1,2,3-triazole (**6i**).

An oven dried Schlenk tube was charged with sodium magnesiate (**1b**) (33 mg, 0.05 mmol, 5 mol %) and THF (2 mL). 1-ethynyl-4-methylbenzene (139 mg, 1.2 mmol) was then added and the mixture was stirred for 30 minutes. 2-azido-1,3-dimethylbenzene (147 mg, 1 mmol) was added and the reaction mixture was heated in an oil bath until reflux (66 °C) for 30 minutes. The reaction mixture was then quenched with brine 2 mL. The crude was extracted using ethyl acetate and brine (3 x 5 mL), the organic solution was dried over magnesium sulphate and the product was purified by flash column chromatography using hexane/EtOAc 8:2 to obtain product (**5o**), which was isolated as a pale yellow solid (245 mg, 93% yield). Crystalline (**5h**) can be obtained by dissolving the product in ether and slow evaporation of the solvent to afford colourless crystals.

**Selected crystal parameters and refinement data:**

	<b>1h</b>	<b>1i</b>	<b>1k</b>	<b>6i</b>
Empirical formula	C <sub>66</sub> H <sub>74</sub> Mg <sub>2</sub> N <sub>4</sub> Na <sub>2</sub>	C <sub>42</sub> H <sub>86</sub> Mg <sub>2</sub> N <sub>4</sub> Na <sub>2</sub> Si <sub>6</sub>	C <sub>33</sub> H <sub>41</sub> N <sub>6</sub> NaO <sub>2</sub>	C <sub>13</sub> H <sub>9</sub> N <sub>3</sub> S
Molecular Weight	1017.89	910.28	576.71	239.29
Temperature (K)	123(2)	123(2)	100(2)	123(2)
Wavelength (Å)	0.71073	0.71073	0.6889	1.5418
Crystal system	triclinic	monoclinic	monoclinic	orthorhombic
Space group	P-1	C 2/c	P2 <sub>1</sub> /c	P2 <sub>1</sub> 2 <sub>1</sub> 2 <sub>1</sub>
<i>a</i> (Å)	8.9002(7)	22.3697(9)	11.217(4)	6.1315(5)
<i>b</i> (Å)	13.1281(11)	13.0744(6)	27.774(10)	8.9338(7)
<i>c</i> (Å)	13.9110(12)	20.9706(14)	10.323(4)	19.3334(12)
$\alpha$ (°)	71.457(8)	90	90	90
$\beta$ (°)	79.030(7)	99.930(4)	102.739(4) <sup>o</sup>	90
$\gamma$ (°)	88.345(7)	90	90	90
Cell volume (Å <sup>3</sup> )	1512.0(2)	6041.4(6)	3137(2)	1059.04(14)
Z	1	4	4	4
$\rho_{calc}$ (g.cm <sup>-3</sup> )	1.118	1.001	1.221	1.501
$\mu$ (mm <sup>-1</sup> )	0.096	0.201	0.084	2.517
2 $\theta$ max(°)	60.36	60.52	49.60	145.92
Index ranges	-12 ≤ <i>h</i> ≤ 12 -18 ≤ <i>k</i> ≤ 17 -19 ≤ <i>l</i> ≤ 14	-30 ≤ <i>h</i> ≤ 31-- 17 ≤ <i>k</i> ≤ 18 -27 ≤ <i>l</i> ≤ 27	-13 ≤ <i>h</i> ≤ 13 -33 ≤ <i>k</i> ≤ 31 -12 ≤ <i>l</i> ≤ 11	-7 ≤ <i>h</i> ≤ 5 -10 ≤ <i>k</i> ≤ 107 -23 ≤ <i>l</i> ≤ 20
Reflections collected	15524	19711	22798	4269
Reflections unique	7912	8095	3834	1902
Reflections obs.	5546	6074	5814	1671

$R_{\text{int}}$	0.0365	0.0418	0.0932	0.0371
No. Parameters	341	282	395	145
Goodness-of-fit-on $F^2$ (GOF)	1.041	1.023	1.035	1.055
Final $R$ indices [ $I > 2\sigma(I)$ ]	0.0526	0.0932	0.0723	0.0458
$R$ indices (all data)	0.1431	0.0644	0.1826	0.1206
Largest diff. peak and hole ( $e \text{ \AA}^{-3}$ )	0.335 and -0.318	0.378 and -0.189	0.91 and -0.39	0.320 and -0.226

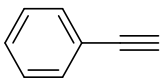
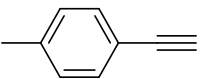
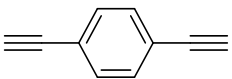
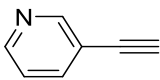
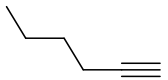
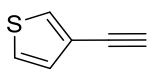
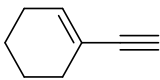
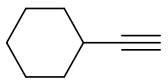
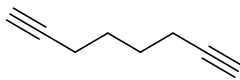
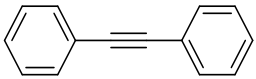
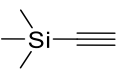
	<b>6w</b>	<b>6y</b>
Empirical formula	$\text{C}_{18}\text{H}_{30}\text{Cl}_2\text{N}_3$	$\text{C}_{25}\text{H}_{21}\text{FN}_6$
Molecular Weight	359.35	424.48
Temperature (K)	123(2)	123(2)
Wavelength ( $\text{\AA}$ )	1.54184	0.71073
Crystal system	monoclinic	monoclinic
Space group	C 2/c	P 21
$a$ ( $\text{\AA}$ )	23.1431(6)	6.9755(4)
$b$ ( $\text{\AA}$ )	8.1966(2)	6.4828(4)
$c$ ( $\text{\AA}$ )	17.7543(4)	23.2389(14)
$\alpha$ ( $^\circ$ )	90	90
$\beta$ ( $^\circ$ )	90.017(2)	94.781(6)
$\gamma$ ( $^\circ$ )	90	90
Cell volume ( $\text{\AA}^3$ )	3367.90(14)	1047.22(11)
$Z$	8	2
$\rho_{\text{calc}}$ ( $\text{g.cm}^{-3}$ )	1.240	1.346
$\mu$ ( $\text{mm}^{-1}$ )	3.042	0.090
$2\theta$ max( $^\circ$ )	146.14	60.34
Index ranges	$-28 \leq h \leq 28$	$-9 \leq h \leq 9$

	-9≤k≤7 -21≤l≤22	-8≤k≤9 -26≤l≤32
Reflections collected	11066	5922
Reflections unique	3296	4721
Reflections obs.	2700	3992
$R_{\text{int}}$	0.0954	0.0468
No. Parameters	197	292
Goodnes-of-fit-on $F^2$ (GOF)	1.197	1.027
Final $R$ indices [ $I > 2\sigma(I)$ ]	0.2065	0.0951
$R$ indices (all data)	0.2103	0.1022
Largest diff. peak and hole ( $\text{e \AA}^{-3}$ )	0.754 and -0.312	0.245 and -0.220

### 3.8.2 Synthesis of organic compounds

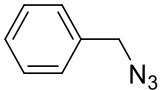
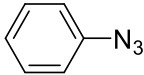
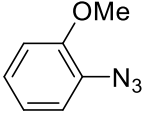
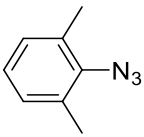
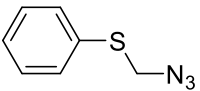
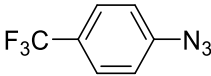
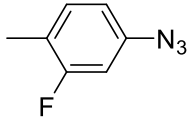
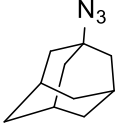
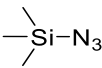
#### General considerations for the use of Alkynes 4a-k:

**Alkynes 4a-k:** Alkynes 3a-k were purchased from Alfa Aesar or Sigma Aldrich chemicals. Alkynes **4a, b, e, f, h** were distilled under inert argon atmosphere and stored over molecular sieves prior to use. Alkynes **4c, d, g, h, i, j** were degassed and stored over molecular sieves prior to use.

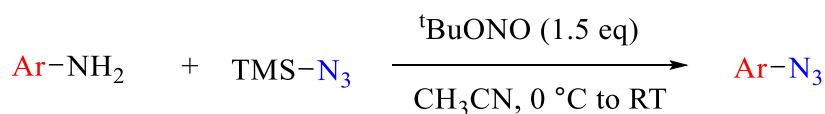
<b>4a</b>		<b>4b</b>		<b>4c</b>	
<b>4d</b>		<b>4e</b>		<b>4f</b>	
<b>4g</b>		<b>4h</b>		<b>4i</b>	
<b>4j</b>		<b>4k</b>			

### 3.8.3 Synthesis of azides:

Although no accidents were reported while using azides throughout the development of this project, it should be noted that azides must be handled carefully as they are potentially explosive compounds. The list of azides used in this chapter are the following:

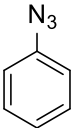
<b>5a</b>		<b>5b</b>		<b>5c</b>	
<b>5d</b>		<b>5e</b>		<b>5f</b>	
<b>5g</b>		<b>5h</b>		<b>5i</b>	

Benzyl azide (**5a**), 1-azido-4-(trifluoromethyl)benzene (**5f**), (azidomethyl)(phenyl)sulfane (**5e**), 1-azidoadamantane (**5h**) and azidotrimethylsilane (**5i**) were purchased from Alfa Aesar, degassed over 2Å molecular sieves and stored under inert argon atmosphere prior to use. Azides **5b,c,d,g** were synthesised according to reaction procedure described below, degassed under inert argon atmosphere and stored over 2Å molecular sieves prior to use.<sup>20</sup>



Scheme 3.22: Synthesis of azides according to literature procedure.<sup>20</sup>

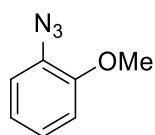
#### 3.8.3.1 Phenyl azide (**5b**):

 Aniline (2 g, 21.5 mmol) was dissolved in CH<sub>3</sub>CN (40 mL) in a 100 ml round-bottomed flask and cooled to 0 °C. To this mixture was added <sup>t</sup>BuONO (3.31 g, 3.8 mL, 32.1 mmol) followed by TMSN<sub>3</sub> (3 g, 3.4 mL, 25.6 mmol) dropwise. The resulting solution was stirred for 1 h at room temperature. The solvent was then removed under vacuum and the crude product was purified by silica-gel chromatography (hexane as

eluent) to give product **5b** as a pale yellow oil (1.9 g 74% Yield).  $^1\text{H NMR}$  (400MHz, 298 K,  $\text{CDCl}_3$ )  $\delta$  (ppm) = 7.06 (m,  $J$  = 8 and 1 Hz, 2H), 7.17 (td,  $J$  = 8 and 1 Hz, 1H), 7.37(t,  $J$  = 8 Hz, 2H).  $^{13}\text{C}\{\text{H}\}$  NMR (101 MHz, 298 K,  $\text{CDCl}_3$ )  $\delta$  (ppm) = 120.1, 126.0, 130.8, 141.1.

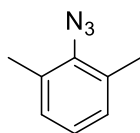
The values are consistent with previously reported data in the literature.<sup>20</sup>

### 3.8.3.2 1-azido-2-methoxybenzene (**5c**):



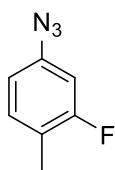
*O*-anisidine (2g, 16.2 mmol) was dissolved in  $\text{CH}_3\text{CN}$  (30 mL) in a 100 mL round-bottomed flask and cooled to 0 °C. To this mixture was added  $^t\text{BuONO}$  (2.5g, 24.4 mmol), followed by  $\text{TMSN}_3$  (1.9g, 2.18 mL, 19.4 mmol) dropwise. The resulting solution was stirred for 1h at room temperature. The solvent was then removed under vacuum and the crude product was purified by silica-gel chromatography (hexane as eluent) to give product **5c** as a yellow oil (2.1g, 87% Yield).  $^1\text{H NMR}$  (400 MHz,  $\text{CDCl}_3$ )  $\delta$  (ppm) = 3.87 (s, 3H), 6.91 (m, 2H), 7.00 (dd,  $J$  = 8 and 1 Hz, 1H), 7.09 (t,  $J$  = 8 Hz, 1H).  $^{13}\text{C}\{\text{H}\}$  NMR (101 MHz,  $\text{CDCl}_3$ )  $\delta$  (ppm) = 60.0, 112.2, 120.4, 121.4, 125.7, 128.4, 152.0

### 3.8.3.3 2-azido-1,3-dimethylbenzene (**5d**):



2,6-dimethylaniline (2g, 16.5 mmol) was dissolved in  $\text{CH}_3\text{CN}$  (30 mL) in a 100 mL round-bottomed flask and cooled to 0 °C. To this mixture was added  $^t\text{BuONO}$  (2.58 g, 2.98 mL, 25 mmol) followed by  $\text{TMSN}_3$  (1.95g, 2.2 mL, 19.8 mmol) dropwise. The resulting solution was stirred for 1h at room temperature. The solvent was then removed under vacuum and the crude product was purified by silica-gel chromatography (hexane as eluent) to give product **5d** as a pale yellow oil (2.2g, 90% Yield).  $^1\text{H NMR}$  (400 MHz, 298 K,  $\text{CDCl}_3$ )  $\delta$  (ppm) = 2.45 (s, 6H), 7.08 (m, 3H).  $^{13}\text{C}\{\text{H}\}$  NMR (101 MHz, 298 K,  $\text{CDCl}_3$ )  $\delta$  (ppm) = 18.1, 125.8, 128.9, 132.2, 137.1.

### 3.8.3.4 4-azido-2-fluoro-1-methylbenzene (**5g**):



3-fluoro-4-methylaniline (1g, 8 mmol) was dissolved in  $\text{CH}_3\text{CN}$  (15 mL) in a 50 mL round-bottomed flask and cooled to 0 °C. To this mixture was added  $^t\text{BuONO}$  (1.25g, 12.2 mmol), followed by  $\text{TMSN}_3$  (0.95g, 1.09 mL, 9.7 mmol) dropwise. The resulting solution was stirred for 1h at room temperature. The solvent was then removed under vacuum and the crude product was purified by silica-gel chromatography (hexane as eluent) to give product **5g** as a yellow oil (1.09g, 90% Yield).  $^1\text{H NMR}$  (400 MHz,

$\text{CDCl}_3$ )  $\delta$  (ppm) = 2.25 (s, 3H), 6.71(m, 2H), 7.15 (t,  $J=8$  Hz, 1H).  $^{13}\text{C}\{\text{H}\}$  NMR (101 MHz,  $\text{CDCl}_3$ )  $\delta$  (ppm) = 161.8 (d,  $J_{\text{CF}}=245$  Hz), 139.2 (d,  $J_{\text{CF}}=10$  Hz), 132.3 (d,  $J_{\text{CF}}=6$  Hz), 121.6 (d,  $J_{\text{CF}}=18$  Hz), 114.5 (d,  $J_{\text{CF}}=3$  Hz), 106.4 (d,  $J_{\text{CF}}=25$  Hz), 14.1 (d,  $J_{\text{CF}}=4$ Hz).  $^{19}\text{F}$  NMR (376.5 MHz,  $\text{CDCl}_3$ )  $\delta$  (ppm) = -114.6

### 3.8.4 Synthesis of 1,5-disubstituted-1,2,3-triazoles:

#### General procedure for reactions at NMR tube scale.

- **Using 1f as a catalyst:**

Catalytic reactions were performed in an NMR scale using the following standard procedure. A Young NMR tube was charged in the glove box with 0.65 mmol of acetylene (1.3 eq) a 10 mol% of ferrocene (9 mg, 0.05 mmol), which was employed as an internal standard one equivalent of corresponding azide and 0.5 mL of  $d_8$ -THF. The initial ratio of starting materials was determined by integration of their resonances in the  $^1\text{H}$  NMR spectrum. 10 mol% of precatalyst **1d** (15 mg, 0.05 mmol) or 10 mol% of precatalyst **1f** (15 mg, 0.05 mmol) was introduced and reactions times were measured from this point. Yields were determined by integration of the products resonances relative to the resonance of the internal standard in the  $^1\text{H}$  NMR spectrum.

- **Using 1d as a catalyst:**

Catalytic reactions were performed in an NMR scale using the following standard procedure. A Young NMR tube was charged in the glove box with 0.60 mmol of acetylene (1.2 eq) a 10 mol% of ferrocene (9 mg, 0.05 mmol), which was employed as an internal standard one equivalent of corresponding azide and 0.5 mL of  $d_8$ -THF. The initial ratio of starting materials was determined by integration of their resonances in the  $^1\text{H}$  NMR spectrum. 10 mol% of precatalyst **1d** (15 mg, 0.05 mmol) or 5 mol% of precatalyst **1d** (16 mg, 0.025 mmol) was introduced and reactions times were measured from this point. Yields were determined by integration of the products resonances relative to the resonance of the internal standard in the  $^1\text{H}$  NMR spectrum.

### General procedure for reactions at Schlenk tube scale.

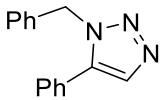
- **Using 1f as a catalyst:**

An oven dried Schlenk tube was charged with sodium magnesiate **1f** (30 mg, 0.1 mmol, 10 mol %) and THF (2 mL). Alkyne (1.3 mmol) was added and the mixture was stirred for 30 mins. Azide (1 mmol) was added and the reaction mixture was heated in an oil bath until reflux (66 °C) for the needed period of time. The reaction mixture was then quenched with brine 2 mL and each triazoles was extracted as described in the following section.

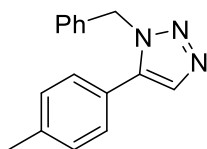
- **Using 1d as a catalyst:**

An oven dried Schlenk tube was charged with sodium magnesiate **1d** (32 mg, 0.05 mmol, 5 mol %) and THF (2 mL). Alkyne (1.2 mmol) was added and the mixture was stirred for 15 min. Azide (1 mmol) was added and the reaction mixture was left reacting at room temperature or heated in an oil bath until reflux (66 °C) for the needed period of time. The reaction mixture was then quenched with brine 2 mL and each triazoles was extracted as described in the following section.

#### 3.8.4.1 Synthesis of 1-benzyl-5-phenyl-1H-1,2,3-triazole (**6a**).

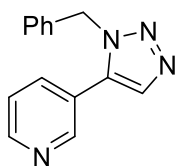
 An oven dried Schlenk tube was charged with sodium magnesiate **1d** (33 mg, 0.05 mmol, 5 mol %) and THF (2 mL). Phenylacetylene (123 mg, 1.2 mmol) was added and the mixture was stirred for 30 mins. Benzylazide (133 mg, 1 mmol) was added and the reaction mixture was heated in an oil bath until reflux (66 °C) for 2 hours. The reaction mixture was then quenched with brine 2 mL. The crude was extracted using diethyl ether and brine (3 x 5 mL), the organic solution was dried over magnesium sulphate and the product was purified by flash column chromatography using hexane/EtOAc 1:1 as eluente. **6a** was isolated as a yellowish solid (185 mg, 79% yield). **<sup>1</sup>H NMR** (400 MHz, CDCl<sub>3</sub>) δ (ppm) = 5.54 (s, 2H), 7.04-7.08 (m, 2H), 7.24 (m, 5H), 7.42 (m, 3H), 7.73 (s, 1H). **<sup>13</sup>C{<sup>1</sup>H} NMR** (101 MHz, CDCl<sub>3</sub>) δ (ppm) = 52.0, 127.2, 127.4, 128.4, 129.0, 129.1, 129.2, 129.8, 133.5, 135.8, 138.4. **HRMS (ESI):** *m/z* calcd. for [M+H]<sup>+</sup>: C<sub>15</sub>H<sub>14</sub>N<sub>3</sub> = 236.1182, found 236.1182 error (-0.1 ppm).

### 3.8.4.2 1-benzyl-5-(*p*-tolyl)-1H-1,2,3-triazole (6b)



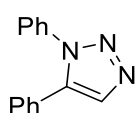
An oven dried Schlenk tube was charged with sodium magnesiate **1d** (33 mg, 0.05 mmol, 5 mol %) and THF (2 mL). *p*-Tolylacetylene (139 mg, 1.2 mmol) was then added and the mixture was stirred for 30 minutes. Benzylazide (133 mg, 1 mmol) was added and the reaction mixture was heated in an oil bath until reflux (66 °C) for 2 hours. The reaction mixture was then quenched with brine 2 mL. The crude was extracted using diethyl ether and brine (3 x 5 mL), the organic solution was dried over magnesium sulphate and the product was purified by flash column chromatography using hexane/EtOAc 8:2 to obtain product **6b**, which was isolated as a pale yellow oil (177 mg, 71% yield). <sup>1</sup>H NMR (400 MHz, CDCl<sub>3</sub>) δ (ppm) = 5.54 (s, 2H), 7.04-7.08 (m, 2H), 7.24 (m, 5H), 7.42 (m, 3H), 7.73 (s, 1H). <sup>13</sup>C{<sup>1</sup>H} NMR (101 MHz, CDCl<sub>3</sub>) δ (ppm) = 52.0, 127.2, 127.4, 128.4, 129.0, 129.1, 129.2, 129.8, 133.5, 135.8, 138.4. HRMS (ESI): *m/z* calcd. for [M+H]<sup>+</sup>: C<sub>15</sub>H<sub>14</sub>N<sub>3</sub> = 250.1339, found 250.1340 error (0.5 ppm).

### 3.8.4.3 3-(1-benzyl-1H-1,2,3-triazol-5-yl)pyridine (6c)



An oven dried Schlenk tube was charged with sodium magnesiate **1d** (33 mg, 0.05 mmol, 5 mol %) and THF (2 mL). 3-ethynylpyridine (62 mg, 0.6 mmol) was then added and the mixture was stirred for 30 minutes. Benzylazide (67 mg, 1 mmol) was added and the reaction mixture was heated in an oil bath until reflux (66 °C) for 1 hour. The reaction mixture was then quenched with brine 2 mL. The crude was extracted using diethyl ether and brine (3 x 5 mL), the organic solution was dried over magnesium sulphate and the product was purified by flash column chromatography using hexane/EtOAc 8:2 to obtain product **6c**, which was isolated as a yellow oil (110 mg, 93% yield). <sup>1</sup>H NMR (400 MHz, CDCl<sub>3</sub>) δ (ppm) = 5.56 (s, 2H), 7.03 (d, *J*=7.3 Hz, 2H), 7.27 (s, 3H), 7.33 (d, *J*=7.9 Hz, 1H), 7.44 (d, *J*=7.9 Hz, 1H), 7.79 (s, 1H), 8.52 (s, 1H), 8.65 (m, 1H). <sup>13</sup>C{<sup>1</sup>H} NMR (101 MHz, CDCl<sub>3</sub>) δ (ppm) = 51.4, 122.6, 122.8, 126.3, 133.2, 134.1, 135.5, 148.6, 149.9. HRMS (ESI): *m/z* calcd. for [M+H]<sup>+</sup>: C<sub>14</sub>H<sub>13</sub>N<sub>4</sub> = 237.1135, found 237.1135 error (0.1 ppm).

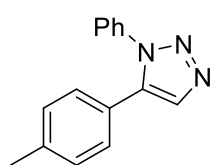
### 3.8.4.4 Synthesis of 1,5-diphenyl-1H-1,2,3-triazole (6d).



An oven dried Schlenk tube was charged with sodium magnesiate **1d** (33 mg, 0.05 mmol, 5 mol %) and THF (2 mL). Phenylacetylene (123 mg, 1.2 mmol) was added

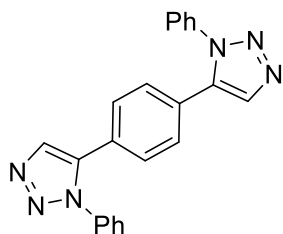
and the mixture was stirred for 30 minutes. Phenylazide (119 mg, 1 mmol) was added and the reaction mixture was heated in an oil bath until reflux (66 °C) for 30 mins. The reaction mixture was then quenched with brine 2 mL. The crude was extracted using diethyl ether and brine (3 x 5 mL), the organic solution was dried over magnesium sulphate and the product was purified by flash column chromatography using hexane/EtOAc 1:1 as eluente. **6d** was isolated as a yellowish solid (212 mg, 96% yield). <sup>1</sup>H NMR (400 MHz, CDCl<sub>3</sub>) δ (ppm) = 7.22 (m, 2H), 7.33 (m, 5H), 7.37 (m, 3H), 7.86 (s, 1H). <sup>13</sup>C{<sup>1</sup>H} NMR (101 MHz, CDCl<sub>3</sub>) δ (ppm) = 125.5, 127.1, 128.9, 129.2, 129.5, 129.7, 133.7, 136.9, 138.0. HRMS (ESI): *m/z* calcd. for [M+H]<sup>+</sup>: C<sub>14</sub>H<sub>12</sub>N<sub>3</sub> = 222.1026, found 222.1026 error (0.1 ppm).

### 3.8.4.5 1-phenyl-5-(*p*-tolyl)-1H-1,2,3-triazole (**6e**)



An oven dried Schlenk tube was charged with sodium magnesiate **1d** (33 mg, 0.05 mmol, 5 mol %) and THF (2 mL). *p*-Tolylacetylene (139 mg, 1.2 mmol) was added and the mixture was stirred for 30 minutes. Phenylazide (119 mg, 1 mmol) was added and the reaction mixture was heated in an oil bath until reflux (66 °C) for 30 mins. The reaction mixture was then quenched with brine 2 mL. The crude was extracted using diethyl ether and brine (3 x 5 mL), the organic solution was dried over magnesium sulphate and the product was purified by flash column chromatography using hexane/EtOAc 3:1 as eluente. **6e** was isolated as a yellowish solid (202 mg, 86% yield). <sup>1</sup>H NMR (400 MHz, CDCl<sub>3</sub>) δ (ppm) = 2.35 (s, 3H), 7.12 (m, 4H), 7.37 (m, 2H), 7.43 (m, 3H), 7.83 (s, 1H). <sup>13</sup>C{<sup>1</sup>H} NMR (101 MHz, CDCl<sub>3</sub>) δ (ppm) = 21.6, 124.2, 125.6, 128.8, 129.5, 129.7, 129.9, 133.6, 137.1, 138.1, 139.7. HRMS (ESI): *m/z* calcd. for [M+H]<sup>+</sup>: C<sub>15</sub>H<sub>14</sub>N<sub>3</sub> = 236.1182, found 236.1182 error (-0.1 ppm).

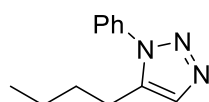
### 3.8.4.6 1,4-bis(1-phenyl-1H-1,2,3-triazol-5-yl)benzene (**6f**)



An oven dried Schlenk tube was charged with sodium magnesiate **1d** (33 mg, 0.05 mmol, 5 mol %) and THF (2 mL). 1,4-diethynylbenzene (151 mg, 1.2 mmol) was added and the mixture was stirred for 30 minutes. Phenylazide (238 mg, 2 mmol) was added and the reaction mixture was heated in an oil bath until reflux (66 °C) for 1 hour. The reaction mixture was then quenched with brine 2 mL. The crude was extracted using ethyl acetate and brine (3 x 5 mL), the organic solution was dried over magnesium sulphate and the product was purified by flash column chromatography using EtOAc to obtain **6f**, which was

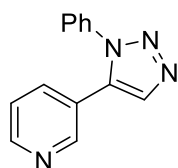
isolated as a brown solid (302 mg, 83% yield).  $^1\text{H NMR}$  (400 MHz,  $\text{CDCl}_3$ )  $\delta$  (ppm) = 7.2 (s, 4H), 7.33 (m, 4H), 7.44 (m, 6H), 7.89 (s, 2H).  $^{13}\text{C}\{\text{H}\}$  NMR (101 MHz,  $\text{CDCl}_3$ )  $\delta$  (ppm) = 125.6, 127.9, 129.2, 129.8, 129.9, 133.9, 136.7, 137.0. **HRMS (ESI):**  $m/z$  calcd. for  $[\text{M}+\text{H}]^+$ :  $\text{C}_{22}\text{H}_{17}\text{N}_6 = 365.1509$ , found 365.1509 error (-0.1 ppm).

#### 3.8.4.7 5-butyl-1-phenyl-1H-1,2,3-triazole (6g)



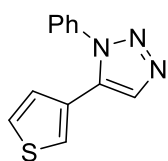
An oven dried Schlenk tube was charged with sodium magnesiate **1d** (33 mg, 0.05 mmol, 5 mol %) and THF (2 mL). hex-1-yne (99 mg, 1.2 mmol) was then added and the mixture was stirred for 15 minutes. Phenylazide (133 mg, 1 mmol) was added and the reaction mixture was heated in an oil bath until reflux (66 °C) for 1 hours. The reaction mixture was then quenched with brine 2 mL. The crude was extracted using diethyl ether and brine (3 x 5 mL), the organic solution was dried over magnesium sulphate and the product was purified by flash column chromatography using hexane/EtOAc 8:2 to obtain product **6g**, which was isolated as a yellow oil (143 mg, 71% yield).  $^1\text{H NMR}$  (400 MHz,  $\text{CDCl}_3$ )  $\delta$  (ppm) = 0.84 (t,  $J=7.4$  Hz, 3H), 1.29 (m, 2H), 1.55 (m, 2H), 2.63 (t,  $J=7.6$  Hz, 2H), 7.41 (m, 2H), 7.49 (m, 3H), 7.56 (s, 1H).  $^{13}\text{C}\{\text{H}\}$  NMR (101 MHz,  $\text{CDCl}_3$ )  $\delta$  (ppm) = 12.8, 21.4, 22.6, 29.6, 124.5, 128.7, 135.8, 137.5. **HRMS (ESI):**  $m/z$  calcd. for  $[\text{M}+\text{H}]^+$ :  $\text{C}_{12}\text{H}_{16}\text{N}_3 = 202.1339$ , found 202.1342 error (1.6 ppm).

#### 3.8.4.8 3-(1-phenyl-1H-1,2,3-triazol-5-yl)pyridine (6h)



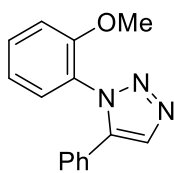
An oven dried Schlenk tube was charged with sodium magnesiate **1d** (33 mg, 0.05 mmol, 5 mol %) and THF (2 mL). 3-ethynylpyridine (124 mg, 1.2 mmol) was then added and the mixture was stirred for 30 minutes. Phenylazide (133 mg, 1 mmol) was added and the reaction mixture was heated in an oil bath until reflux (66 °C) for 30 minutes. The reaction mixture was then quenched with brine 2 mL. The crude was extracted using diethyl ether and brine (3 x 5 mL), the organic solution was dried over magnesium sulphate and the product was purified by flash column chromatography using hexane/EtOAc 8:2 to obtain product **6h**, which was isolated as a yellow solid (204 mg, 92% yield).  $^1\text{H NMR}$  (400 MHz,  $\text{CDCl}_3$ )  $\delta$  (ppm) = 7.28 (m, 1H), 7.36 (m, 2H), 7.48 (m, 4H), 7.95 (s, 1H), 8.56 (m, 1H), 8.61 (m, 1H).  $^{13}\text{C}\{\text{H}\}$  NMR (101 MHz,  $\text{CDCl}_3$ )  $\delta$  (ppm) = 122.5, 122.8, 124.6, 129.0, 133.0, 134.0, 135.0, 135.2, 148.4, 149.6. **HRMS (ESI):**  $m/z$  calcd. for  $[\text{M}+\text{H}]^+$ :  $\text{C}_{13}\text{H}_{11}\text{N}_4 = 223.0978$ , found 223.0979 error (0.3 ppm).

### 3.8.4.9 1-phenyl-5-(thiophen-3-yl)-1H-1,2,3-triazole (6i)



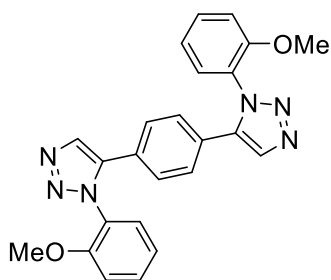
An oven dried Schlenk tube was charged with sodium magnesiate **1d** (33 mg, 0.05 mmol, 5 mol %) and THF (2 mL). 3-ethynylthiophene (130 mg, 1.2 mmol) was then added and the mixture was stirred for 15 minutes. Phenylazide (133 mg, 1 mmol) was added and the reaction mixture was heated in an oil bath until reflux (66 °C) for 30 minutes. The reaction mixture was then quenched with brine 2 mL. The crude was extracted using diethyl ether and brine (3 x 5 mL), the organic solution was dried over magnesium sulphate and the product was purified by flash column chromatography using hexane/EtOAc 8:2 to obtain product **6i**, which was isolated as a yellow solid (209 mg, 94% yield). **<sup>1</sup>H NMR** (400 MHz, CDCl<sub>3</sub>) δ (ppm) = 6.92 (d, *J*=5 Hz, 1H), 7.14 (d, *J*=2.4 Hz, 1H), 7.32 (m, 1H), 7.41 (m, 2H), 7.50 (m, 3H), 7.87 (s, 1H). **<sup>13</sup>C{<sup>1</sup>H} NMR** (101 MHz, CDCl<sub>3</sub>) δ (ppm) = 125.0, 125.9, 127.1, 127.3, 129.8, 130.0, 133.1, 133.9, 137.0 **HRMS (ESI):** *m/z* calcd. for [M+H]<sup>+</sup>: C<sub>12</sub>H<sub>10</sub>N<sub>3</sub>S = 228.0590, found 228.0590 error (0.0 ppm).

### 3.8.4.10 1-(2-methoxyphenyl)-5-phenyl-1H-1,2,3-triazole (6j)



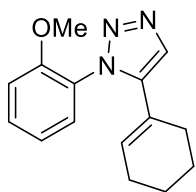
An oven dried Schlenk tube was charged with sodium magnesiate **1d** (33 mg, 0.05 mmol, 5 mol %) and THF (2 mL). Phenylacetylene (123 mg, 1.2 mmol) was then added and the mixture was stirred for 30 minutes. 1-azido-2-methoxybenzene (149 mg, 1 mmol) was added and the reaction mixture was heated in an oil bath until reflux (66 °C) for 30 minutes. The reaction mixture was then quenched with brine 2 mL. The crude was extracted using ethyl acetate and brine (3 x 5 mL), the organic solution was dried over magnesium sulphate and the product was purified by flash column chromatography using EtOAc to obtain product **6j**, which was isolated as a brown oil (248 mg, 99% yield). **<sup>1</sup>H NMR** (400 MHz, CDCl<sub>3</sub>) δ (ppm) = 3.42 (s, 3H), 6.90 (m, 1H), 7.05 (m, 1H), 7.23 (m, 5H), 7.41 (m, 2H), 7.85 (s, 1H). **<sup>13</sup>C{<sup>1</sup>H} NMR** (101 MHz, CDCl<sub>3</sub>) δ (ppm) = 55.6, 112.6, 121.1, 125.9, 128.7, 128.8, 128.9, 130.0, 131.9, 132.0, 139.5, 153.9. **HRMS (ESI):** *m/z* calcd. for [M+H]<sup>+</sup>: C<sub>15</sub>H<sub>14</sub>N<sub>3</sub>O = 252.1131, found 252.1126 error (-2.1 ppm).

### 3.8.4.11 1,4-bis(1-(2-methoxyphenyl)-1H-1,2,3-triazol-5-yl)benzene (6k)



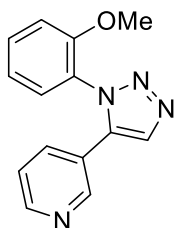
An oven dried Schlenk tube was charged sodium magnesiate **1d** (33 mg, 0.05 mmol, 5 mol %) and THF (2 mL). 1,4-diethynylbenzene (151 mg, 1.2 mmol) was added and the mixture was stirred for 30 minutes. 1-azido-2-methoxybenzene (298 mg, 2 mmol) was added and the reaction mixture was heated in an oil bath until reflux (66 °C) for 1 hour. The reaction mixture was then quenched with brine 2 mL. The insoluble product in THF was washed with diethyl ether (3x5mL) to obtain **6k** as a brown solid (344 mg, 81% yield). **<sup>1</sup>H NMR** (400 MHz, CDCl<sub>3</sub>) δ (ppm) = 3.45 (s, 6H), 6.92 (d, *J*=8.3Hz, 2H), 7.07 (t, *J*=7.6 Hz, 1H), 7.15 (s, 4H), 7.41 (m, 4H), 7.86 (s, 2H). **<sup>13</sup>C{<sup>1</sup>H} NMR** (101 MHz, CDCl<sub>3</sub>) δ (ppm) = 55.8, 112.7, 121.4, 126.0, 127.0, 127.2, 128.3, 131.9, 138.7, 154.0. **HRMS (ESI):** *m/z* calcd. for [M+H]<sup>+</sup>: C<sub>24</sub>H<sub>21</sub>N<sub>6</sub>O<sub>2</sub> = 425.1721, found 425.1708 error (-2.9 ppm).

### 3.8.4.12 5-(cyclohex-1-en-1-yl)-1-(2-methoxyphenyl)-1H-1,2,3-triazole (6l)



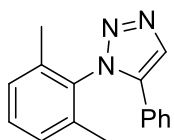
An oven dried Schlenk tube was charged with sodium magnesiate **1d** (33 mg, 0.05 mmol, 5 mol %) and THF (2 mL). 1-ethynylcyclohexene (127 mg, 1.2 mmol) (127 mg, 1.2 mmol) was then added and the mixture was stirred for 30 minutes. 1-azido-2-methoxybenzene (149 mg, 1 mmol) was added and the reaction mixture was heated in an oil bath until reflux (66 °C) for 30 minutes. The reaction mixture was then quenched with brine 2 mL. The crude was extracted using diethyl ether and brine (3 x 5 mL), the organic solution was dried over magnesium sulphate and the product was purified by flash column chromatography using hexane/EtOAc 1:2 to obtain product **6l**, which was isolated as a yellow solid (227mg, 89% yield). **<sup>1</sup>H NMR** (400 MHz, CDCl<sub>3</sub>) δ (ppm) = 1.47 (m, 2H), 1.57 (m, 2H), 1.92 (m, 2H), 2.05 (m, 2H), 3.67 (s, 3H), 5.61 (broad s, 1H), 6.97 (m, 2H), 7.27 (m, 1H), 7.4 (m, 1H), 7.55 (s, 1H). **<sup>13</sup>C{<sup>1</sup>H} NMR** (101 MHz, CDCl<sub>3</sub>) δ (ppm) = 21.4, 22.2, 25.3, 27.3, 55.6, 112.0, 120.7, 124.5, 126.3, 128.1, 128.9, 131.0, 131.3, 140.5, 153.9. **HRMS (ESI):** *m/z* calcd. for [M+H]<sup>+</sup>: C<sub>15</sub>H<sub>17</sub>N<sub>3</sub>O = 256.1444, found 256.1443 error (-0.5 ppm).

### 3.8.4.13 3-(1-(2-methoxyphenyl)-1H-1,2,3-triazol-5-yl)pyridine (6m)



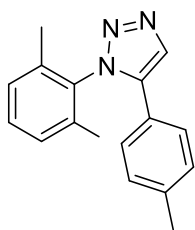
An oven dried Schlenk tube was charged with sodium magnesiate **1d** (33 mg, 0.05 mmol, 5 mol %) and THF (2 mL). 3-ethynylpyridine (124 mg, 1.2 mmol) was then added and the mixture was stirred for 30 minutes. 1-azido-2-methoxybenzene (149 mg, 1 mmol) was added and the reaction mixture was heated in an oil bath until reflux (66 °C) for 30 minutes. The reaction mixture was then quenched with brine 2 mL. The crude was extracted using diethyl ether and brine (3 x 5 mL), the organic solution was dried over magnesium sulphate and the product was purified by flash column chromatography using hexane/EtOAc 6:4 to obtain product **6m**, which was isolated as a yellow solid (250mg, 99% yield). <sup>1</sup>H NMR (400 MHz, CDCl<sub>3</sub>) δ (ppm) = 3.47 (s, 3H), 6.91 (d, *J*=8.7 Hz, 1H), 7.07 (t, *J*=7.6 Hz, 1H), 7.21 (m, 1H), 7.46 (m, 3H), 7.92 (s, 1H), 8.5 (m, 2H). <sup>13</sup>C{H} NMR (101 MHz, CDCl<sub>3</sub>) δ (ppm) = 55.7, 112.6, 121.4, 123.5, 124.2, 124.8, 132.1, 132.7, 134.7, 135.6, 148.5, 150.2, 153.6. HRMS (ESI): *m/z* calcd. for [M+H]<sup>+</sup>: C<sub>13</sub>H<sub>11</sub>N<sub>4</sub> = 253.1084, found 253.1084 error (0.0 ppm).

### 3.8.4.14 1-(2,6-dimethylphenyl)-5-phenyl-1H-1,2,3-triazole (6n)



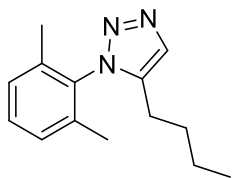
An oven dried Schlenk tube was charged with sodium magnesiate **1d** (33 mg, 0.05 mmol, 5 mol %) and THF (2 mL). Phenylacetylene (123 mg, 1.2 mmol) was then added and the mixture was stirred for 30 minutes. 2-azido-1,3-dimethylbenzene (147 mg, 1 mmol) was added and the reaction mixture was heated in an oil bath until reflux (66 °C) for 30 minutes, and then quenched with brine 2 mL. The crude was extracted using ethyl acetate and brine (3 x 5 mL), the organic solution was dried over magnesium sulphate and the product was purified by flash column chromatography using hexane/EtOAc 8:2 to obtain product **6n**, which was isolated as a pale yellow solid (229 mg, 92% yield). <sup>1</sup>H NMR (400 MHz, CDCl<sub>3</sub>) δ (ppm) = 1.94 (s, 6H), 7.18 (m, 4H), 7.31 (m, 4H), 8.02 (s, 1H). <sup>13</sup>C{H} NMR (101 MHz, CDCl<sub>3</sub>) δ (ppm) = 17.9, 126.8, 127.2, 128.9, 129.3, 129.5, 130.4, 132.5, 135.6, 136.2, 138.5. HRMS (ESI): *m/z* calcd. for [M+H]<sup>+</sup>: C<sub>16</sub>H<sub>15</sub>N<sub>3</sub> = 250.1339, found 250.1337 error (-0.7 ppm).

### 3.8.4.15 1-(2,6-dimethylphenyl)-5-(*p*-tolyl)-1H-1,2,3-triazole (6o)



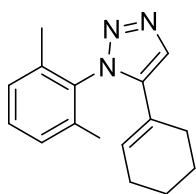
An oven dried Schlenk tube was charged with sodium magnesiate **1d** (33 mg, 0.05 mmol, 5 mol %) and THF (2 mL). 1-ethynyl-4-methylbenzene (139 mg, 1.2 mmol) was then added and the mixture was stirred for 30 minutes. 2-azido-1,3-dimethylbenzene (147 mg, 1 mmol) was added and the reaction mixture was heated in an oil bath until reflux (66 °C) for 30 minutes. The reaction mixture was then quenched with brine 2 mL. The crude was extracted using ethyl acetate and brine (3 x 5 mL), the organic solution was dried over magnesium sulphate and the product was purified by flash column chromatography using hexane/EtOAc 8:2 to obtain product **6o**, which was isolated as a pale yellow solid (245 mg, 93% yield). <sup>1</sup>H NMR (400 MHz, CDCl<sub>3</sub>) δ (ppm) = 1.93 (s, 6H), 2.31 (s, 3H), 7.07 (m, 4H), 7.16 (d, *J*=7.6 Hz, 2H), 7.31 (m, 1H), 7.98 (s, 1H). <sup>13</sup>C{<sup>1</sup>H} NMR (101 MHz, CDCl<sub>3</sub>) δ (ppm) = 17.9, 21.6, 124.0, 127.1, 128.9, 130.0, 130.4, 132.3, 135.8, 136.3, 138.6, 139.6. HRMS (ESI): *m/z* calcd. for [M+H]<sup>+</sup>: C<sub>17</sub>H<sub>18</sub>N<sub>3</sub> = 264.1495, found 264.1491 error (-1.6 ppm).

### 3.8.4.16 5-butyl-1-(2,6-dimethylphenyl)-1H-1,2,3-triazole (6p)



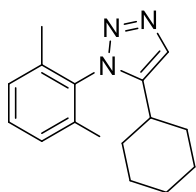
An oven dried Schlenk tube was charged with sodium magnesiate **1d** (33 mg, 0.05 mmol, 5 mol %) and THF (2 mL). hex-1-yne (99 mg, 1.2 mmol) was then added and the mixture was stirred for 15 minutes. 2-azido-1,3-dimethylbenzene (147 mg, 1 mmol) was added and the reaction mixture was heated in an oil bath until reflux (66 °C) for 30 minutes. The reaction mixture was then quenched with brine 2 mL. The crude was extracted using diethyl ether and brine (3 x 5 mL), the organic solution was dried over magnesium sulphate and the product was purified by flash column chromatography using hexane/EtOAc 8:2 to obtain product **6p**, which was isolated as a colourless oil (174 mg, 76% yield). <sup>1</sup>H NMR (400 MHz, CDCl<sub>3</sub>) δ (ppm) = 0.78 (t, *J*=7.2 Hz, 3H), 1.25 (m, 2H), 1.49 (m, 2H), 1.84 (s, 6H), 2.28 (t, *J*=8 Hz, 2H), 7.11 (d, *J*=7.6 Hz, 2H), 7.23 (t, *J*=7.6 Hz, 1H), 7.56 (s, 1H). <sup>13</sup>C{<sup>1</sup>H} NMR (101 MHz, CDCl<sub>3</sub>) δ (ppm) = 13.7, 17.3, 22.2, 22.8, 30.0, 128.6, 130.1, 131.7, 134.6, 136.0, 138.7. HRMS (ESI): *m/z* calcd. for [M+H]<sup>+</sup>: C<sub>14</sub>H<sub>20</sub>N<sub>3</sub> = 230.1652, found 230.1650 error (-0.8 ppm).

### 3.8.4.17 5-(cyclohex-1-en-1-yl)-1-(2,6-dimethylphenyl)-1H-1,2,3-triazole (6q)



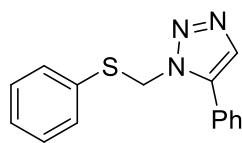
An oven dried Schlenk tube was charged with sodium magnesiate **1d** (33 mg, 0.05 mmol, 5 mol %) and THF (2 mL). 1-ethynylcyclohex-1-ene (127 mg, 1.2 mmol) was then added and the mixture was stirred for 30 minutes. 2-azido-1,3-dimethylbenzene (147 mg, 1 mmol) was added and the reaction mixture was heated in an oil bath until reflux (66 °C) for 30 minutes. The reaction mixture was then quenched with brine 2 mL. The crude was extracted using ethyl acetate and brine (3 x 5 mL), the organic solution was dried over magnesium sulphate and the product was purified by flash column chromatography using hexane/EtOAc 8:2 to obtain product **6q**, which was isolated as a pale yellow solid (220 mg, 87% yield). <sup>1</sup>H NMR (400 MHz, CDCl<sub>3</sub>) δ (ppm) = 1.51 (m, 2H), 1.61 (m, 2H), 1.92 (s, 6H), 1.94 (m, 2H), 2.10 (m, 2H), 5.59 (m, 1H), 7.12 (d, J=7.6 Hz, 2H), 7.27 (t, J=7.6 Hz, 1H), 7.68 (s, 1H). <sup>13</sup>C{<sup>1</sup>H} NMR (101 MHz, CDCl<sub>3</sub>) δ (ppm) = 17.7, 21.6, 2.4, 25.8, 27.2, 124.4, 128.7, 129.2, 129.6, 131.8, 135.9, 136.4, 139.5. HRMS (ESI): *m/z* calcd. for [M+H]<sup>+</sup>: C<sub>16</sub>H<sub>19</sub>N<sub>3</sub> = 254.1651, found 254.1652 error (-0.3 ppm).

### 3.8.4.18 5-cyclohexyl-1-(2,6-dimethylphenyl)-1H-1,2,3-triazole (6r)



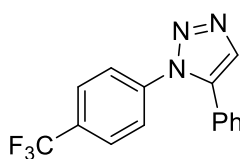
An oven dried Schlenk tube was charged with sodium magnesiate **1d** (33 mg, 0.05 mmol, 5 mol %) and THF (2 mL). Ethynylcyclohexane (130 mg, 1.2 mmol) was then added and the mixture was stirred for 30 minutes. 2-azido-1,3-dimethylbenzene (147 mg, 1 mmol) was added and the reaction mixture was heated in an oil bath until reflux (66 °C) for 30 minutes. The reaction mixture was then quenched with brine 2 mL. The crude was extracted using ethyl acetate and brine (3 x 5 mL), the organic solution was dried over magnesium sulphate and the product was purified by flash column chromatography using hexane/EtOAc 8:2 to obtain product **6r**, which was isolated as a pale yellow solid (230 mg, 90% yield). <sup>1</sup>H NMR (400 MHz, CDCl<sub>3</sub>) δ (ppm) = 1.12 (m, 3H), 1.29 (m, 2H), 1.60 (m, 5H), 1.86 (s, 6H), 2.17 (m, 1H), 7.12 (d, J=7.6 Hz, 2H), 7.24 (t, J=7.6 Hz, 1H), 7.56 (s, 1H). <sup>13</sup>C{<sup>1</sup>H} NMR (101 MHz, CDCl<sub>3</sub>) δ (ppm) = 17.5, 25.6, 26.0, 32.8, 33.5, 128.7, 130.0, 130.5, 134.8, 136.0, 143.9. HRMS (ESI): *m/z* calcd. for [M+H]<sup>+</sup>: C<sub>16</sub>H<sub>19</sub>N<sub>3</sub> = 256.1808, found 256.1807 error (-0.5 ppm).

### 3.8.4.19 5-phenyl-1-((phenylthio)methyl)-1H-1,2,3-triazole (6s)



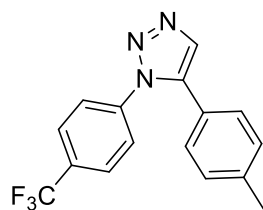
An oven dried Schlenk tube was charged with sodium magnesiate **1d** (33 mg, 0.05 mmol, 5 mol %) and THF (2 mL). Phenylacetylene (123 mg, 1.2 mmol) was then added and the mixture was stirred for 15 minutes. Azidomethyl phenyl sulfide (165 mg, 1 mmol) was added and the reaction mixture was heated in an oil bath until reflux (66 °C) for 3 hours. The reaction mixture was then quenched with brine 2 mL. The crude was extracted using diethyl ether and brine (3 x 5 mL), the organic solution was dried over magnesium sulphate and the product was purified by flash column chromatography using hexane/EtOAc 7:3 as eluent to give triazole **6s** as a brown oil (195 mg, 73% yield). <sup>1</sup>H NMR (400 MHz, CDCl<sub>3</sub>) δ (ppm) = 5.62 (s, 2H, CH<sub>2</sub>) 7.23-7.35 (m, overlapping signals, 7H, aromatic CH), 7.43-7.45 (m, 3H, aromatic CH) 7.67(s, 1H, CH triazole). <sup>13</sup>C{H} NMR (101 MHz, CDCl<sub>3</sub>) δ (ppm) = 52.4, 126.6, 128.7, 129.0, 129.1, 129.3, 129.6, 131.9, 133.2, 133.3, 138.1. HRMS (ESI): *m/z* calcd. for [M+H]<sup>+</sup>: C<sub>15</sub>H<sub>14</sub>N<sub>3</sub>S = 268.0903, found 268.0903 error (0 ppm).

### 3.8.4.20 5-phenyl-1-(4-(trifluoromethyl)phenyl)-1H-1,2,3-triazole (6t)



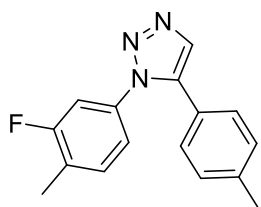
An oven dried Schlenk tube was charged with sodium magnesiate **1d** (33 mg, 0.05 mmol, 5 mol %). Phenylacetylene (123 mg, 1.2 mmol) was then added neat and the mixture was stirred for 15 minutes. 1-azido-4-(trifluoromethyl)benzene (2 mL of 0.5 M solution in *tert*-butyl methyl ether, 1 mmol) was added and the reaction mixture was heated in an oil bath until reflux (66 °C) for 1 hour. The reaction mixture was then quenched with brine 2 mL. The crude was extracted using diethyl ether and brine (3 x 5 mL), the organic solution was dried over magnesium sulphate and the product was purified by flash column chromatography using hexane/EtOAc 8:2 as eluent, **6t** was isolated as a yellowish oil (284 mg, 98% yield). <sup>1</sup>H NMR (400 MHz, CDCl<sub>3</sub>) δ (ppm) = 7.21-7.23 (m, 2H), 7.38-7.40 (m, 3H), 7.49-7.51 (m, 2H), 7.67-7.69 (m, 2H), 7.85 (s, 1H). <sup>13</sup>C{H} NMR (101 MHz, CDCl<sub>3</sub>) δ (ppm) = 123.6 (q, J=271 Hz), 125.3, 126.7 (m), 128.8, 129.2, 129.8, 131.2 (q, J=33 Hz), 134.0, 138.0, 139.4. HRMS (ESI): *m/z* calcd. for [M+H]<sup>+</sup>: C<sub>15</sub>H<sub>11</sub>F<sub>3</sub>N<sub>3</sub> = 290.0900, found 290.0899 error (-0.2 ppm).

### 3.8.4.21 5-(*p*-tolyl)-1-(4-(trifluoromethyl)phenyl)-1H-1,2,3-triazole (**6u**)



An oven dried Schlenk tube was charged with sodium magnesiate **1d** (33 mg, 0.05 mmol, 5 mol %). *p*-Tolylacetylene (139 mg, 1.2 mmol) was then added neat and the mixture was stirred for 15 minutes. 1-azido-4-(trifluoromethyl)benzene (2 mL of 0.5 M solution in *tert*-butyl methyl ether, 1 mmol) was added and the reaction mixture was heated in an oil bath until reflux (66 °C) for 1 hour. The reaction mixture was then quenched with brine 2 mL. The crude was extracted using diethyl ether and brine (3 x 5 mL), the organic solution was dried over magnesium sulphate and the product was purified by flash column chromatography using hexane/EtOAc 8:2 as eluent, **6u** was isolated as a pale yellow solid (295 mg, 97% yield). <sup>1</sup>H NMR (400 MHz, CDCl<sub>3</sub>) δ (ppm) = 2.38 (s, 3H), 7.11 (d, J=8 Hz, 2H), 7.19 (d, J=8 Hz, 2H), 7.51 (d, J=8.3 Hz, 2H), 7.71 (d, J=8.4 Hz, 2H), 7.83 (s, 1H). <sup>13</sup>C{<sup>1</sup>H} NMR (101 MHz, CDCl<sub>3</sub>)<sup>e</sup> δ (ppm) = 123.5, 125.3, 126.7 (m), 128.7, 130.0, 131.2 (q, J=33 Hz), 133.8, 138.1, 139.6, 140.0. HRMS (ESI): *m/z* calcd. for [M+H]<sup>+</sup>: C<sub>16</sub>H<sub>13</sub>F<sub>3</sub>N<sub>3</sub> = 304.1056, found 304.1055 error (-0.4 ppm).

### 3.8.4.22 1-(3-fluoro-4-methylphenyl)-5-(*p*-tolyl)-1H-1,2,3-triazole (**6v**)

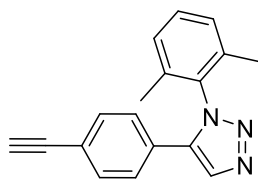


An oven dried Schlenk tube was charged with sodium magnesiate **1d** (33 mg, 0.05 mmol, 5 mol %) and THF (2 mL). *p*-Tolylacetylene (139 mg, 1.2 mmol) was then added neat and the mixture was stirred for 15 minutes. 4-azido-2-fluoro-1-methylbenzene (151 mg, 1 mmol) was added and the reaction mixture was heated in an oil bath until reflux (66 °C) for 1 hour. The reaction mixture was then quenched with brine 2 mL. The crude was extracted using diethyl ether and brine (3 x 5 mL), the organic solution was dried over magnesium sulphate and the product was purified by flash column chromatography using hexane/EtOAc 8:2 as eluent to give triazole **6v** as a pale yellow solid (222 mg, 83% yield). <sup>1</sup>H NMR (400 MHz, CDCl<sub>3</sub>) δ (ppm) = 2.30 (s, 3H), 2.35 (s, 3H), 7.02 (m, 1H), 7.04 (m, 1H), 7.07 (m, 2H), 7.11 (m, 2H), 7.16 (m, 1H), 7.79 (s, 1H). <sup>13</sup>C{<sup>1</sup>H} NMR (101 MHz, CDCl<sub>3</sub>) δ (ppm) = 14.7, 21.6, 112.6 (d, J=26 Hz), 120.8, 123.8, 126.4 (d, J=20 Hz), 128.7, 129.9, 132.1, 132.2, 133.5, 139.8, 161.1 (d,

<sup>e</sup> Quaternary carbons (CF<sub>3</sub>, and C<sub>5</sub>) could not be detected

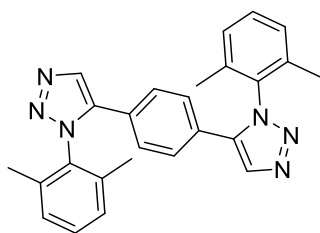
$J=246$ ).  $^{19}\text{F}\{\text{H}\}$  NMR (376.5 MHz,  $\text{CDCl}_3$ )  $\delta$  (ppm) = -114.10. HRMS (ESI):  $m/z$  calcd. for  $[\text{M}+\text{H}]^+$ :  $\text{C}_{16}\text{H}_{15}\text{FN}_3$  = 268.1245, found 268.1243 error (-0.6 ppm).

### 3.8.4.23 1-(2,6-dimethylphenyl)-5-(4-ethynylphenyl)-1H-1,2,3-triazole (6w)



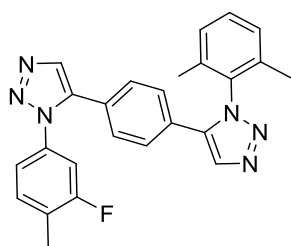
An oven dried Schlenk tube was charged sodium magnesiate **1d** (33 mg, 0.05 mmol, 5 mol %) and THF (2 mL). 1,4-diethynylbenzene (151 mg, 1.2 mmol) was added and the mixture was stirred for 30 minutes. 2-azido-1,3-dimethylbenzene (147 mg, 1 mmol) was added and the reaction mixture was heated in an oil bath until reflux (66 °C) for 30 minutes.. The reaction mixture was then quenched with brine 2 mL. The product was extracted with diethyl ether and brine (3x5mL), the organic solution was dried over magnesium sulphate and the product was purified by flash column chromatography using hexane/ $\text{Et}_2\text{O}$  2:1 as eluent to give colourless needles (224 mg, 82% yield) along with 12% yield of **6x** which will be described as follows.  $^1\text{H}$  NMR (400 MHz,  $\text{CDCl}_3$ )  $\delta$  (ppm) = 1.91 (s, 6H), 3.12 (s, 1H), 7.10 (d,  $J=8.5$  Hz, 2H), 7.15-7.17 (m, 2H), 7.32 (t,  $J=7.6$  Hz, 1H), 7.38 (d,  $J=8.5$  Hz, 2H), 8.02 (s, 1H).  $^{13}\text{C}\{\text{H}\}$  NMR (101 MHz,  $\text{CDCl}_3$ )  $\delta$  (ppm) = 17.7, 79.2, 82.7, 123.1, 126.8, 126.9, 128.9, 130.4, 132.5, 132.8, 135.2, 135.9, 137.6.

### 3.8.4.24 1,4-bis(1-(2,6-dimethylphenyl)-1H-1,2,3-triazol-5-yl)benzene (6x)



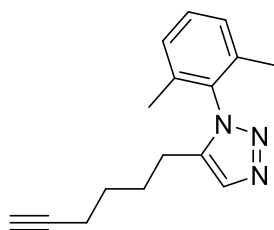
An oven dried Schlenk tube was charged sodium magnesiate **1d** (33 mg, 0.05 mmol, 5 mol %) and THF (2 mL). 1,4-diethynylbenzene (151 mg, 1.2 mmol) was added and the mixture was stirred for 30 minutes. 2-azido-1,3-dimethylbenzene (294 mg, 2 mmol) was added and the reaction mixture was heated in an oil bath until reflux (66 °C) for 1 hour. The reaction mixture was then quenched with brine 2 mL. The product was extracted with diethyl ether (3x5mL), the organic solution was dried over magnesium sulphate and the product was purified by flash column chromatography using  $\text{EtOAc}$  to give **6x** as a brown solid (328 mg, 78% yield).  $^1\text{H}$  NMR (400 MHz,  $\text{CDCl}_3$ )  $\delta$  (ppm) = 1.89 (s, 12H), 7.01 (s, 4H), 7.16-7.18 (m, 4H), 7.31-7.35 (m, 2H), 7.99 (s, 2H).  $^{13}\text{C}\{\text{H}\}$  NMR (101 MHz,  $\text{CDCl}_3$ )  $\delta$  (ppm) = 17.7, 127.4, 128.9, 130.4, 132.5, 135.2, 135.8, 137.2. HRMS (ESI):  $m/z$  calcd. for  $[\text{M}+\text{H}]^+$ :  $\text{C}_{26}\text{H}_{25}\text{N}_6$  = 421.2135, found 421.2133 error (-0.5 ppm).

### 3.8.4.25 1-(2,6-dimethylphenyl)-5-(4-(1-(3-fluoro-4-methylphenyl)-1H-1,2,3-triazol-5-yl)phenyl)-1H-1,2,3-triazole (6y)

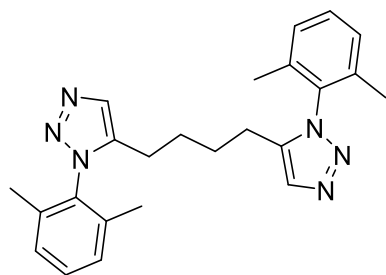


An oven dried Schlenk tube was charged sodium magnesiate **1d** (33 mg, 0.05 mmol, 5 mol %) and THF (2 mL). **6w** (328 mg, 1.2 mmol) was added and the mixture was stirred for 15 minutes. 4-azido-2-fluoro-1-methylbenzene (151 mg, 1 mmol) was added and the reaction mixture was heated in an oil bath until reflux (66 °C) 1 hour. The reaction mixture was then quenched with brine 2 mL. The product was extracted with diethyl ether and brine (3x5mL), the organic solution was dried over magnesium sulphate and the product was purified by flash column chromatography using hexane/Et<sub>2</sub>O 2:1 as eluent to give colourless needles (399 mg, 94% yield). <sup>1</sup>H NMR (400 MHz, CDCl<sub>3</sub>) δ (ppm) = 1.91 (s, 6H), 2.32 (s, 3H), 6.97-7.01 (m, 2H), 7.16-7.18 (s, overlapping signals, 6H), 7.21-7.25 (m, 1H), 7.31-7.34 (m, 1H), 7.82 (s, 1H), 8.04 (s, 1H). <sup>13</sup>C{<sup>1</sup>H} NMR (101 MHz, CDCl<sub>3</sub>) δ (ppm) = 14.5, 17.7, 112.3, 112.5, 120.6, 127.3, 127.4, 127.6, 128.9, 129.2, 130.4, 132.2 (d, J=6 Hz), 132.6, 133.7, 135.0, 135.1, 135.8, 136.7, 137.2, 160.9 (d, J=246 Hz). <sup>19</sup>F{<sup>1</sup>H} NMR (376.5 MHz, CDCl<sub>3</sub>) δ (ppm) = -113.6. HRMS (ESI): *m/z* calcd. for [M+H]<sup>+</sup>: C<sub>25</sub>H<sub>22</sub>FN<sub>6</sub> = 425.1884, found 425.1879 error (-1.3 ppm).

### 3.8.4.26 1-(2,6-dimethylphenyl)-5-(hex-5-yn-1-yl)-1H-1,2,3-triazole (6z)

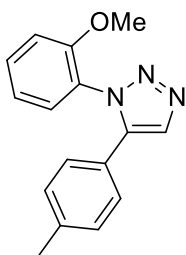


An oven dried Schlenk tube was charged sodium magnesiate **1d** (33 mg, 0.05 mmol, 5 mol %) and THF (2 mL). Octa-1,7-diyne (127.4 mg, 1.2 mmol) was added and the mixture was stirred for 15 minutes. 2-azido-1,3-dimethylbenzene (147 mg, 1 mmol) was added and the reaction mixture was heated in an oil bath until reflux (66 °C) 1 hour. The reaction mixture was then quenched with brine 2 mL. The product was extracted with diethyl ether and brine (3x5mL), the organic solution was dried over magnesium sulphate and the product was purified by flash column chromatography using hexane/Et<sub>2</sub>O 2:1 as eluent to give **6z** as a colourless oil (198 mg, 78% yield) as well as **6z'** as a pale yellow solid (60 mg, 15% Yield). <sup>1</sup>H NMR (400 MHz, CDCl<sub>3</sub>) δ (ppm) = 1.48-1.55 (m, 2H), 1.66-1.72 (m, 2H), 1.92 (s, two overlapping signals, 7H), 2.14-2.18 (m, 2H), 2.36-2.40 (m, 2H), 7.17-7.19 (m, 2H), 7.29-7.33 (m, 1H), 7.66 (s, 1H). <sup>13</sup>C{<sup>1</sup>H} NMR (101 MHz, CDCl<sub>3</sub>) δ (ppm) = 17.3, 18.0, 22.7, 26.8, 27.7, 68.9, 83.5, 128.6, 130.1, 131.8, 134.4, 136.0, 138.1.



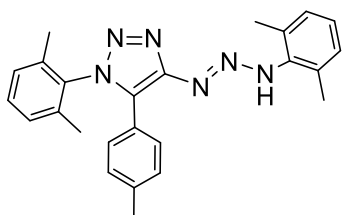
**6z'**:  $^1\text{H NMR}$  (400 MHz,  $\text{CDCl}_3$ )  $\delta$  (ppm) = 1.51-1.55 (m, 4H), 1.84 (s, 12H), 2.29-2.33 (m, 4H), 7.14-7.16 (m, 4H), 7.28-7.32 (m, 2H) 7.53 (s, 2H).  $^{13}\text{C}\{\text{H}\}$  NMR (101 MHz,  $\text{CDCl}_3$ )  $\delta$  (ppm) = 17.3, 22.8, 27.4, 128.6, 130.2, 131.7, 134.3, 135.9, 137.7.

### 3.8.4.27 1-(2-methoxyphenyl)-5-(*p*-tolyl)-1H-1,2,3-triazole (**6 $\alpha$** )



This compound was characterised only by  $^1\text{H NMR}$  as it was obtained from a cross over reaction discussed in **Table 3.13**. The cross over reaction was carried out as follows. An oven dried Young NMR tube was charged sodium magnesiate **1j** (29 mg, 0.035 mmol, 10 mol %) and THF (2 mL). 1-ethynylcyclohex-1-ene (37 mg, 0.35 mmol) was added and the mixture was stirred for 15 minutes. 1-azido-2-methoxybenzene (62 mg, 1 mmol) was added and the reaction mixture was heated in an oil bath until reflux (66 °C) 1 hour. NMR analysis of the reaction mixture allowed to obtained yields for the two products formed in this reaction, namely **6l** and **6 $\alpha$**  (detailed discussion and yields obtained can be found in **Table 3.13**). Yields of the two products formed were determined using ferrocene as internal standard.

### 3.8.4.28 (E)-1-(2,6-dimethylphenyl)-4-(3-(2,6-dimethylphenyl)triaz-1-en-1-yl)-5-(*p*-tolyl)-1H-1,2,3-triazole (**6 $\beta$** )



An oven dried Schlenk tube was charged  $\text{NaCH}_2\text{SiMe}_3$  (110 mg, 1 mmol) and THF (2 mL). *p*-Tolylacetylene (116 mg, 1 mmol) was added and the mixture was stirred for 15 minutes. 2-azido-1,3-dimethylbenzene (294 mg, 2 mmol) was added and the reaction mixture was heated in an oil bath until reflux (66 °C) 1 hour. The reaction mixture was then quenched with brine 2 mL. The product was extracted with diethyl ether and brine (3x5mL), the organic solution was dried over magnesium sulphate and the product was purified by flash column chromatography using hexane/ $\text{Et}_2\text{O}$  2:1 as eluent to give **6 $\beta$**  as a white solid (324 mg, 79% yield).  $^1\text{H NMR}$  (400 MHz,  $\text{CDCl}_3$ )  $\delta$  (ppm) = 1.98 (s, 6H), 2.30 (s, 3H), 2.33 (s, 6H), 7.08-7.30 (m, overlapping signals, 10H), 9.47 (broad s, 1H, NH).  $^{13}\text{C}\{\text{H}\}$  NMR (101 MHz,  $\text{CDCl}_3$ )  $\delta$  (ppm) = 17.9, 19.1, 21.4, 123.4, 128.5 (overlapping signals), 128.7, 129.3, 130.2, 135.6, 136.1, 139.1. **HRMS (ESI):**  $m/z$  calcd. for  $[\text{M}+\text{H}]^+$ :  $\text{C}_{25}\text{H}_{27}\text{N}_6 = 411.2292$ , found 411.2294 error (0.6 ppm).

### 3.9 References:

- (1) Alvarez, R.; Velázquez, S.; San-felix, A.; Aquaro, S.; De Clercq, E.; Perno, C.; Karlsson, A.; Balzarini, J.; Camarasa, M. J. *J. Med. Chem.* **1994**, *37*, 4185–4194.
- (2) Velázquez, S.; Alvarez, R.; Pérez, C.; Gago, F.; De Clercq, E.; Balzarini, J.; Camarasa, M. *Antivir. Chem. Chemother.* **1997**, *9*, 481–489.
- (3) Duan, Y.-C.; Ma, Y.-C.; Zhang, E.; Shi, X.-J.; Wang, M.-M.; Ye, X.-W.; Liu, H.-M. *Eur. J. Med. Chem.* **2013**, *62*, 11–19.
- (4) Golasa L, P.; Matyjaszewski, K. *soci* **2010**, No. 39, 1338.
- (5) Tornøe, C. W.; Christensen, C.; Meldal, M. *J. Org. Chem.* **2002**, *67* (9), 3057–3064.
- (6) Rostovtsev, V. V.; Green, L. G.; Fokin, V. V.; Sharpless, K. B. *Angew. Chemie Int. Ed.* **2002**, *41* (14), 2596–2599.
- (7) da Silva, F. de C.; de Souza, M. C. B. V; Frugulhetti, I. I. P.; Castro, H. C.; Souza, S. L. de O.; de Souza, T. M. L.; Rodrigues, D. Q.; Souza, A. M. T.; Abreu, P. A.; Passamani, F.; Rodrigues, C. R.; Ferreira, V. F. *Eur. J. Med. Chem.* **2009**, *44* (1), 373–383.
- (8) Périon, R.; Ferrières, V.; García-Moreno, M. I.; Mellet, C. O.; Duval, R.; García Fernández, J. M.; Plusquellec, D. *Tetrahedron* **2005**, *61* (38), 9118–9128.
- (9) Bock, V. D.; Speijer, D.; Hiemstra, H.; van Maarseveen, J. H. *Org. Biomol. Chem.* **2007**, *5* (6), 971–975.
- (10) Kwok, S. W.; Fotsing, J. R.; Fraser, R. J.; Rodionov, V. O.; Fokin, V. V. *Org. Lett.* **2010**, *12*, 4217–4219.
- (11) Krasinski, A.; Fokin, V. V.; Sharpless, K. B. *Org. Lett.* **2004**, *6* (8), 1237–1240.
- (12) Hong, L.; Lin, W.; Zhang, F.; Liu, R.; Zhou, X. *Chem. Commun.* **2013**, *49*, 5589–5591.
- (13) Zhang, L.; Chen, X.; Xue, P.; Sun, H. H. Y.; Williams, I. D.; Sharpless, K. B.; Fokin, V. V.; Jia, G. *J. Am. Chem. Soc.* **2005**, *127* (46), 15998–15999.
- (14) Casarrubios, L.; de la Torre, M. C.; Sierra, M. *Chem. Eur. J.* **2013**, *19* (11), 3534–3541.
- (15) Smith, C. D.; Greaney, M. F. *Org. Lett.* **2013**, *15* (c), 3–6.
- (16) Baillie, S. E.; Bluemke, T. D.; Clegg, W.; Kennedy, A. R.; Klett, J.; Russo, L.; De Tullio, M.; Hevia, E. *Chem. Commun.* **2014**, *50* (18), 12859–12862.
- (17) Hernán-Gómez, A.; Bradley, T. D.; Kennedy, A. R.; Livingstone, Z.; Robertson, S. D.; Hevia, E. *Chem. Commun.* **2013**, *49* (77), 8659–8661.
- (18) Baillie, S. E.; Clegg, W.; García-Álvarez, P.; Hevia, E.; Kennedy, A. R.; Klett, J.; Russo, L. *Chem. Commun.* **2011**, *47*, 388–390.
- (19) Weiss, E. *Angew. Chemie Int. Ed.* **1993**, *32* (11), 1501–1523.
- (20) Barral, K.; Moorhouse, A. D.; Moses, J. E. *Org. Lett.* **2007**, *9* (9), 1809.
- (21) Liu, Y. *Synlett* **2011**, No. 8, 1184–1185.
- (22) Brase, S.; Gil, C.; Knepper, K.; Zimmermann, V. *Angew. Chemie Int. Ed.* **2005**, *44* (33), 5188–5240.

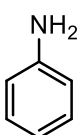
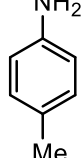
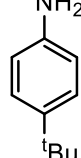
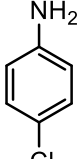
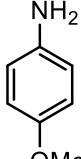
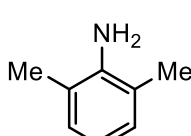
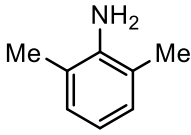
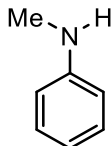
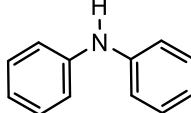
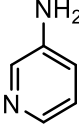
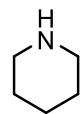
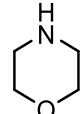
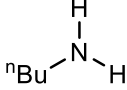
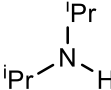
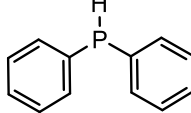
- (23) Martínez-Martínez, A. J.; Kennedy, A. R.; Mulvey, R. E.; O'Hara, C. *Science* **2014**, *346*, 834.
- (24) Martínez-Martínez, A. J.; Armstrong, D. R.; Conway, B.; Fleming, B. J.; Klett, J.; Kennedy, a. R.; Mulvey, R. E.; Robertson, S. D.; O'Hara, C. T. *Chem. Sci.* **2014**, *5* (2), 771.
- (25) Hein, J. E.; Fokin, V. V. *Chem Soc Rev* **2010**, *39* (4), 1302–1315.
- (26) Vidal, C.; Garcia-Alvarez, J. *Green Chem.* **2014**, *16*, 3515–3521.
- (27) García-Álvarez, J.; Díez, J.; Gimeno, J. *Green Chem.* **2010**, *12* (12), 2127.
- (28) Müller, K.; Faeh, C.; Diederich, F. *Science* **2007**, *317* (5846), 1881–1886.
- (29) Schlosser, M.; Michel, D. *Tetrahedron* **1996**, *52* (1), 99–108.
- (30) Gouverneur, V.; Purser, S.; Moore, P. R.; Swallow, S. *soci* **2008**, *37* (2), 237–432.
- (31) Ojima, I. *J. Org. Chem.* **2013**, *78* (13), 6358–6383.
- (32) Weiss, E.; Schubert, B. *Chem. Ber.* **1984**, *117*, 366–375.
- (33) Edwards, A. J.; Fallaize, A.; Raithby, P. R.; Rennie, M.; Steiner, A.; Verhorevoort, K. L.; Wright, D. S. *Dalton Trans.* **1996**, 133–137.
- (34) Fokin, V. V.; Malik, J. A.; Worrell, B. T. *Science* **2013**, *340*, 457.
- (35) Macchioni, A.; Ciancaleoni, G.; Zuccaccia, C.; Zuccaccia, D. *Chem. Soc. Rev.* **2008**, No. 37, 479–489.
- (36) Li, D.; Keresztes, I.; Hopson, R.; Williard, P. G. *Acc. Chem. Res.* **2009**, *42* (2), 270–280.
- (37) Rutherford, J. L.; Collum, D. B. *J. Am. Chem. Soc.* **1999**, *121* (43), 10198–10202.
- (38) Durand, E.; Clemancey, M.; Quoineaud, A.; Verstraete, J.; Espinat, D.; Lancelin, J.-M. *Energy & Fuels* **2008**, *22* (4), 2604–2610.
- (39) Li, W.; Chung, H.; Daeffler, C.; Johnson, J. A.; Grubbs, R. H. *Macromolecules* **2012**, *45* (24), 9595–9603.
- (40) Jin, K. J.; Collum, D. B. *J. Am. Chem. Soc.* **2015**, *137* (45), 14446–14455.
- (41) Neufeld, R.; Stalke, D. *Chem. Sci.* **2015**, *6*, 3354–3364.
- (42) Straub, B. F. *Chem. Commun.* **2007**, 3868–3870.
- (43) Ahlquist, M.; Fokin, V. V. *Organometallics* **2007**, *26* (18), 4389–4391.

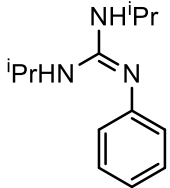
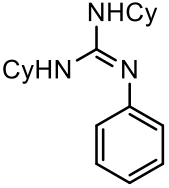
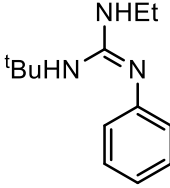
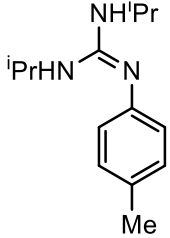
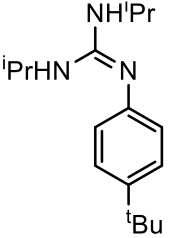
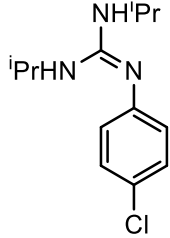
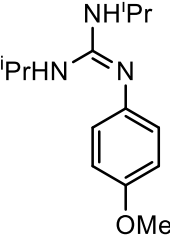
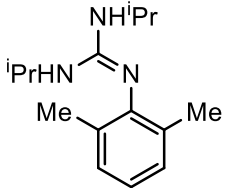
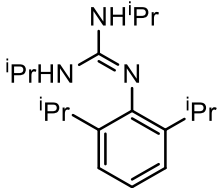
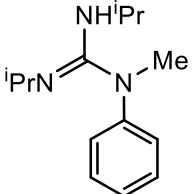
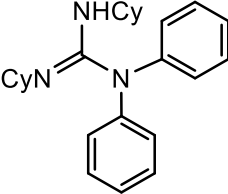
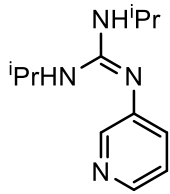
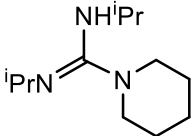
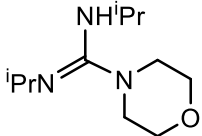
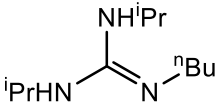
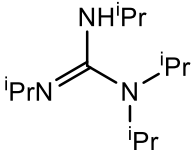
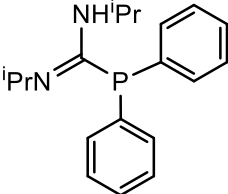
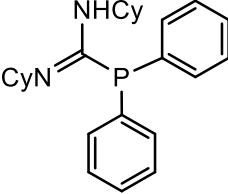
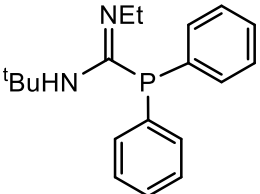
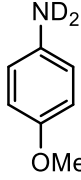
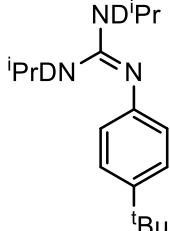
## **CHAPTER 4**

### **Structural and mechanistic insights into s-block bimetallic catalysis: sodium magnesiate catalysed guanylation of amines**

#### IV. Table of compounds

<b>1f</b>	[NaMg(CH <sub>2</sub> SiMe <sub>3</sub> ) <sub>3</sub> ]	<b>1m</b>	[{(THF) <sub>3</sub> NaMg(NHAr <sub>3</sub> )} <sub>2</sub> ] (Ar = 2,6-Me <sub>2</sub> C <sub>6</sub> H <sub>3</sub> )
<b>1n</b>	[(THF) <sub>2</sub> NaMg(NPh <sub>2</sub> ) <sub>3</sub> ]	<b>1o</b>	[Na(THF) <sub>6</sub> ] <sup>+</sup> [Mg{(CyN) <sub>2</sub> C(NPh <sub>2</sub> )} <sub>2</sub> (NPh <sub>2</sub> )] <sup>-</sup>
<b>1p</b>	[Mg{( <sup>i</sup> PrN)C(NAr)(HN <sup>i</sup> Pr)} <sub>2</sub> (THF)]	<b>1q</b>	[Na{( <sup>i</sup> PrNC(HN <sup>i</sup> Pr)N(2,6-Me <sub>2</sub> C <sub>6</sub> H <sub>3</sub> ))}(THF) <sub>2</sub> ]
<b>1r</b>	[{(THF) <sub>2</sub> Na(NHAr)} <sub>2</sub> ]		

<b>7a</b>		<b>7b</b>		<b>7c</b>	
<b>7d</b>		<b>7e</b>		<b>7f</b>	
<b>7g</b>		<b>7h</b>		<b>7i</b>	
<b>7j</b>		<b>7k</b>		<b>7l</b>	
<b>7m</b>		<b>7n</b>		<b>7o</b>	
<b>8a</b>	<sup>i</sup> PrN=C=N <sup>i</sup> Pr	<b>8b</b>	CyN=C=NCy	<b>8c</b>	EtN=C=N <sup>i</sup> Bu

<b>9a</b>		<b>9b</b>		<b>9c</b>	
<b>9d</b>		<b>9e</b>		<b>9f</b>	
<b>9g</b>		<b>9h</b>		<b>9i</b>	
<b>9j</b>		<b>9k</b>		<b>9l</b>	
<b>9m</b>		<b>9n</b>		<b>9o</b>	
<b>9p</b>		<b>9q</b>		<b>9r</b>	
<b>9s</b>		<b>d2-7e</b>		<b>d2-9e</b>	

## 4.1 Summary

Advancing catalytic applications of s-block mixed-metal complexes, sodium magnesiate  $[\text{NaMg}(\text{CH}_2\text{SiMe}_3)_3]$  (**1f**) is reported as an efficient precatalyst for guanylation of a variety of anilines and secondary amines with carbodiimides. The first examples of hydrophosphination of carbodiimides using a Mg catalyst are also described in this chapter. The mixed-metal systems catalytic ability is much greater than those of its homometallic components  $[\text{NaCH}_2\text{SiMe}_3]$  and  $[\text{Mg}(\text{CH}_2\text{SiMe}_3)_2]$ . Stoichiometric studies suggest magnesiate amido and guanidinate complexes are intermediates in these catalyses. Reactivity and kinetic studies imply these guanylation reactions occur via (tris)amide intermediates that react with carbodiimides in insertion steps. The rate law for the guanylation of *N,N'*-diisopropylcarbodiimide with 4-*tert*-butylaniline catalysed by **1f** is order 1 in [amine], [carbodiimide] and [catalyst], showing a large kinetic isotopic effect, consistent with an amine-assisted rate-determining carbodiimide insertion transition state. Studies assessing the effect of sodium in these transformations denote a secondary role with little involvement in the catalytic cycle (**Figure 4.1**).

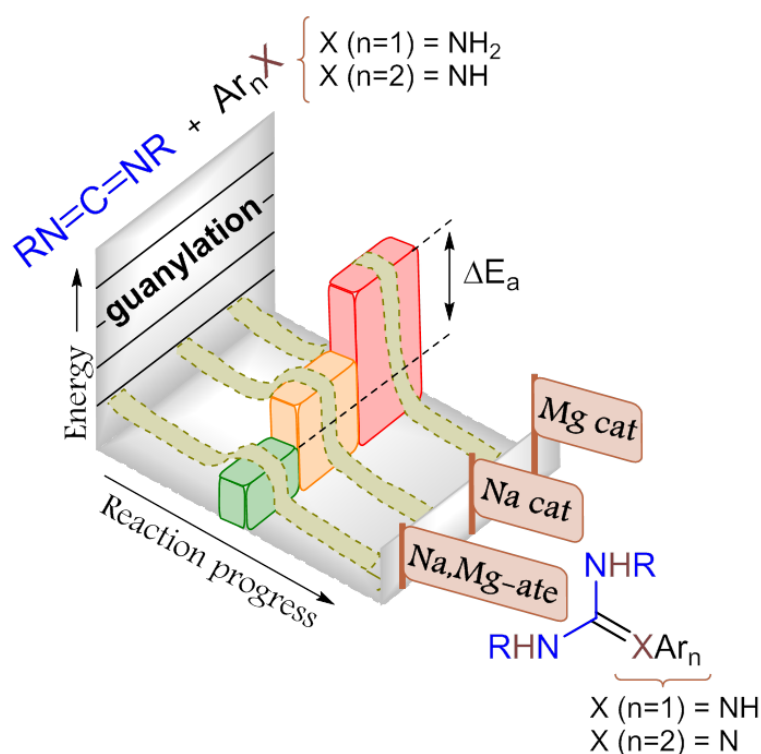


**Figure 4.1:** General overview for chapter 4

## 4.2 Introduction

The synthesis of guanidines has received considerable attention,<sup>1</sup> as these simple nitrogen-containing molecules are valuable building blocks present in numerous natural products and pharmaceuticals.<sup>2</sup> Furthermore, they also find extensive applications as precursors of ancillary ligands for numerous transition, lanthanoid, and main group metal complexes<sup>3</sup> and they can also be employed as organocatalysts (**Figure 4.2**).<sup>4</sup>

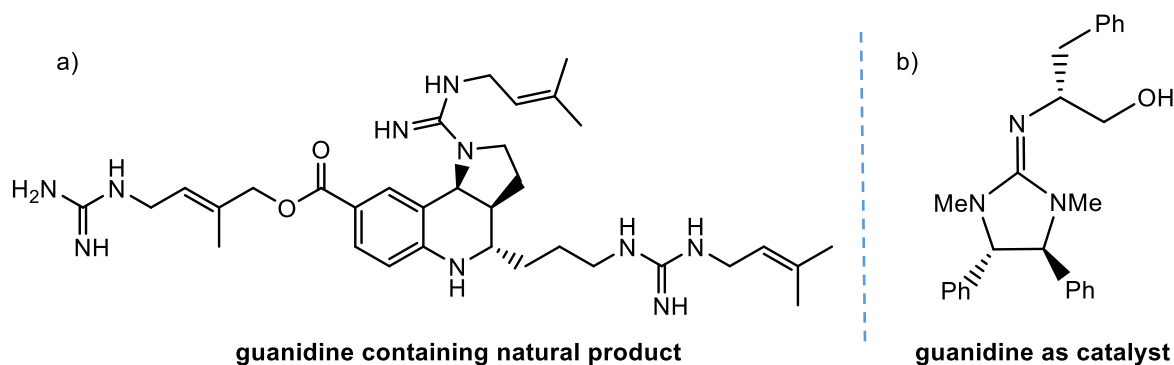
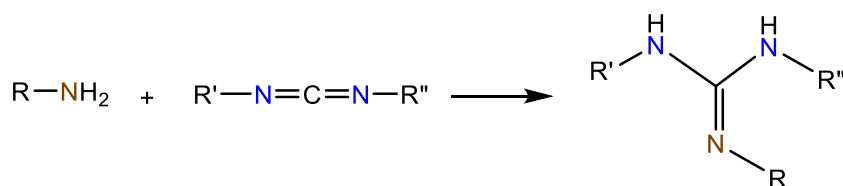


**Figure 4.2:** a) ChemDraw representation of Martinelline, a guanidine containing natural product which has been identified as the first naturally occurring nonpeptidic bradykinin B2 receptor antagonist b) ChemDraw representation of guanidine containing compound (4*S*,5*S*)-1,3-dimethyl-4,5-diphenyl-2-[(*R*)-1-hydroxyethyl-2-phenylethylimino]imidazolidine which is an effective catalyst in Michael type reactions.

Atom-economical catalytic addition of amines to carbodiimides, guanylation reaction (**Scheme 4.1**) constitutes one of the most straightforward routes to access *N*-substituted guanidines.<sup>1</sup>



**Scheme 4.1:** Guanylation of primary amines with carbodiimides.

Although certain guanylations can be accomplished catalyst-free, these processes have high kinetic barriers requiring the use of harsh reaction conditions as well as restricting their applications to activated primary aliphatic amines.<sup>5</sup> Thus, metal-catalysis is required when using anilines or secondary amines, and even so, high temperatures are needed, with only a select few catalytic systems facilitating these processes at room temperature.<sup>1</sup> The vast majority of these studies have focussed on transition-metal and rare-earth metal catalysis.<sup>6</sup> Richeson and collaborators developed the Ti-mediated guanylation of amines and transamination of

guanidines using the imido titanium complex  $[(\text{Me}_2\text{N})\text{C}(\text{N}^i\text{Pr})_2]_2\text{Ti}=\text{N}(2,6\text{-Me}_2\text{C}_6\text{H}_3)$  which had previously been reported by the same authors (**Table 4.1**).<sup>14a</sup>

**Table 4.1:** Ti-Mediated guanylation of amines and transamination of guanidines.

Entry	ArNH <sub>2</sub>	R	Yield (%) <sup>a</sup>
1	2,6-Me <sub>2</sub> C <sub>6</sub> H <sub>3</sub>	<i>i</i> Pr	81.5 <sup>c</sup>
2	C <sub>6</sub> F <sub>5</sub>	<i>i</i> Pr	92.3 <sup>c</sup>
3	<i>para</i> -MeOC <sub>6</sub> H <sub>4</sub>	<i>i</i> Pr	82.8 <sup>c</sup>
4	<i>ortho</i> -MeOC <sub>6</sub> H <sub>4</sub>	<i>i</i> Pr	87.2 <sup>b</sup>
5	<i>para</i> -ClC <sub>6</sub> H <sub>4</sub>	<i>i</i> Pr	96.6 <sup>b</sup>
6	<i>para</i> -NCCH <sub>2</sub> C <sub>6</sub> H <sub>4</sub>	<i>i</i> Pr	47.6 <sup>b</sup>
7	<i>para</i> -C <sub>6</sub> H <sub>4</sub> NH <sub>2</sub>	<i>i</i> Pr	97.2 <sup>b</sup>
8	2,6-Me <sub>2</sub> C <sub>6</sub> H <sub>3</sub> NH <sub>2</sub>	Cy	92

[a] All reactions were carried to 100% conversion. [b] Yields determined by integration of <sup>1</sup>H NMR relative to internal standard of either 1,3-(MeO)<sub>2</sub>C<sub>6</sub>H<sub>4</sub> or O(SiMe<sub>3</sub>)<sub>2</sub>. [c] Isolated yields.

Some recent studies using lithium,<sup>7</sup> or magnesium (and heavier group 2 elements)<sup>8</sup> have already demonstrated the potential of s-block metal complexes to catalyse these reactions.<sup>a</sup> MgBu<sub>2</sub> can be used as a catalyst for these reactions (**Table 4.2**).<sup>8a</sup>

(a) To best of my knowledge, only three examples of magnesium complexes have been described so far in the literature as catalysts for guanylation reactions: Mg(*n*Bu)<sub>2</sub>, [MgBz<sub>2</sub>(THF)<sub>2</sub>], and an *N*-heterocyclic carbene (NHC) supported magnesium amide, see references **8a,8b** and **8c** respectively.

**Table 4.2:** Optimisation of the reaction conditions

$\text{Ar}-\text{NH}_2 + \text{iPrN}=\text{C}=\text{N}^{\text{iPr}} \xrightarrow[\text{Toluene, 50 }^\circ\text{C, 0.5h}]{\text{MgBu}_2 (1.5 \text{ mol}\%)} \text{iPrHN}-\text{C}(\text{NAr})-\text{NH}^{\text{iPr}}$		
Entry	Ar	Yield (%) <sup>a</sup>
1	Ph	99
2	2,4,5-trimethylbenzene	99
3	4-tert-butylbenzene	99
4	4-bromobenzene	99
5	3-pyridine	62
6	3,5-dimethyl-2-pyridine	traces

Although this reaction requires the use of high temperatures (50 °C), in addition when the reaction is carried out using different substituted pyridines low yields or no reaction is obtained (Entries 5 and 6, **Table 4.2**).

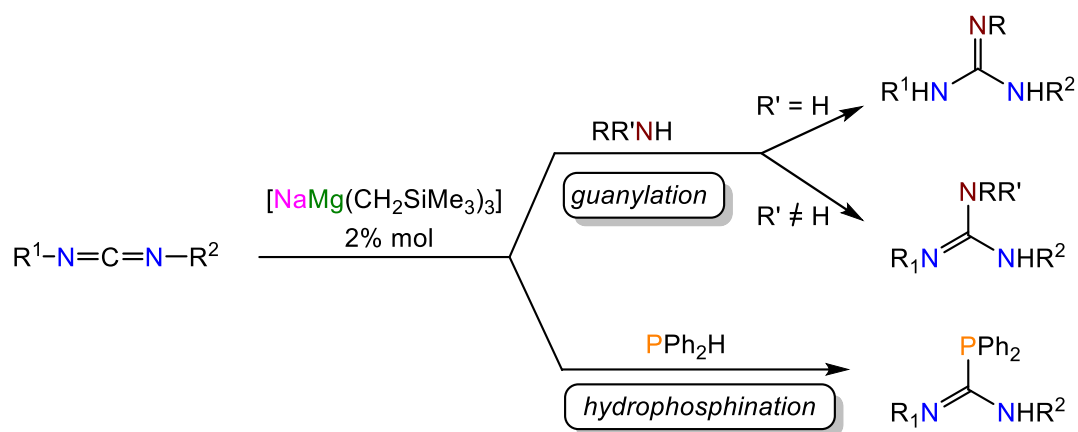
Related studies investigating the synthesis of phosphaguanidines have revealed the ability of heavier alkaline-earth metal amides to catalyse the direct addition of secondary phosphines to carbodiimides.<sup>9</sup>

Aiming to expand the scope of s-block cooperative catalysis, the first catalytic applications of alkali-metal magnesiates for the synthesis of guanidines will be reported in this chapter. Combining kinetic experiments with stoichiometric reactivity studies, informative mechanistic insights into these new ate-catalysed transformations will be assessed.

## 4.3 Results and discussion

### 4.3.1 Catalytic synthesis of guanidines and phosphaguanidines

Studies began by testing the efficacy of homoleptic sodium magnesiate  $[\text{NaMg}(\text{CH}_2\text{SiMe}_3)_3]$  (**1f**)<sup>10</sup> in the intermolecular hydroamination reaction of different carbodiimides with a variety of aromatic, aliphatic and secondary cyclic amines (guanylation process). In addition, compound **1f** was tested in the hydrophosphination reaction of the same carbodiimide substrates with the secondary phosphine  $\text{PPh}_2\text{H}$  (**Scheme 4.2**).



**Scheme 4.2:** Catalytic guanylation and hydrophosphination reactions.

Firstly, as a model reaction, the guanylation of 2,6-dimethylaniline **7f** with  $N,N'$ -diisopropylcarbodiimide (DIC) **8a** was investigated (**Table 4.2**), in  $\text{C}_6\text{D}_6$ , using 2 mol% of **1f**. At room temperature, the reaction yielded 90% of the corresponding guanidine **9h** in 3 hours. An important solvent effect was noted and when the more polar ethereal solvent  $d_8$ -THF, with its greater coordination ability, was employed, guanidine **9h** was obtained in a 99% yield after just 15 minutes. Contrastingly, illustrating the synergic reactivity of **1f**, when its single-metal components were tested as catalysts under the same reaction conditions lower conversions for guanidine **9h** were observed after 15 minutes, with  $\text{Mg}(\text{CH}_2\text{SiMe}_3)_2$  being significantly less efficient (44% conversion) than the more polar, more reactive  $\text{NaCH}_2\text{SiMe}_3$  (72% conversion) (**Table 4.3**).

**Table 4.3:** Optimisation of the reaction conditions

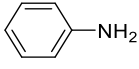
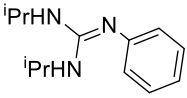
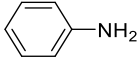
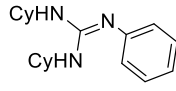
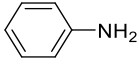
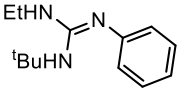
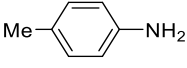
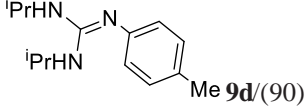
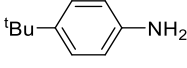
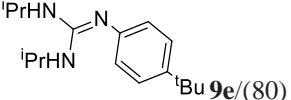
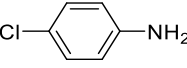
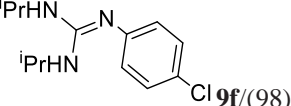
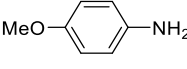
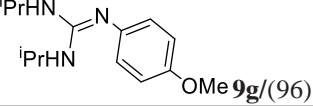
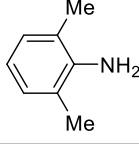
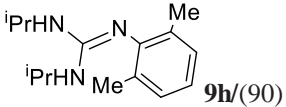
Entry	Catalyst (2 mol%)	Solvent	Time (h)	Yield (%) <sup>a</sup>
1	[NaCH <sub>2</sub> SiMe <sub>3</sub> ]	d <sub>8</sub> -THF	0.25	72
2	[NaCH <sub>2</sub> SiMe <sub>3</sub> ]	d <sub>8</sub> -THF	1	84
3	[Mg(CH <sub>2</sub> SiMe <sub>3</sub> ) <sub>2</sub> ]	d <sub>8</sub> -THF	0.25	44
4	[Mg(CH <sub>2</sub> SiMe <sub>3</sub> ) <sub>2</sub> ]	d <sub>8</sub> -THF	16	99
5	[NaMg(CH <sub>2</sub> SiMe <sub>3</sub> ) <sub>3</sub> ] ( <b>1f</b> )	d <sub>8</sub> -THF	0.25	99
6	[NaMg(CH <sub>2</sub> SiMe <sub>3</sub> ) <sub>3</sub> ] ( <b>1f</b> )	C <sub>6</sub> D <sub>6</sub>	3	90

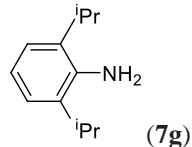
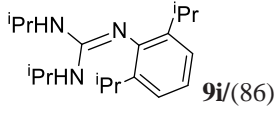
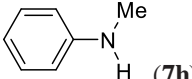
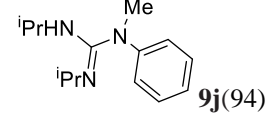
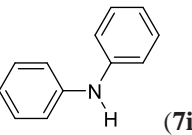
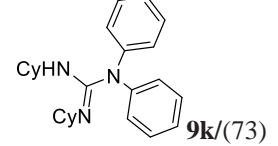
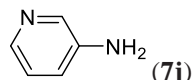
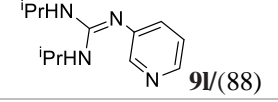
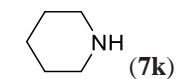
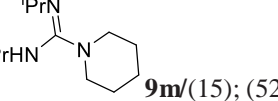
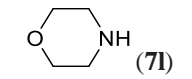
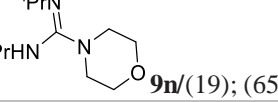
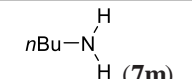
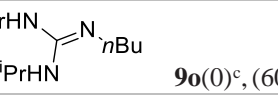
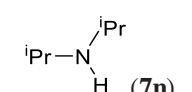
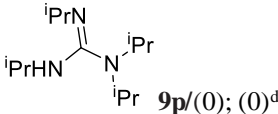
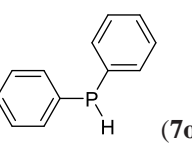
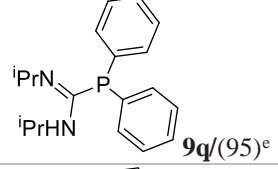
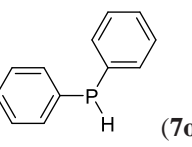
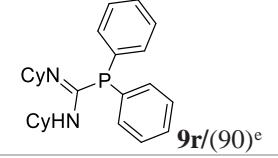
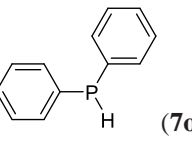
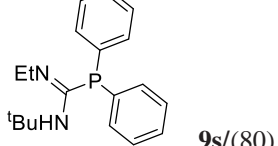
[a] Yields obtained via spectroscopic <sup>1</sup>H NMR integration of signals for the guanidine product 4h with addition of ferrocene (10 mol %) as internal standard. Reactions carried out using 0.5 mL of solvent, 0.55 mmol of 2,6-dimethylaniline, 0.5 mmol of DIC, and 0.01 mmol of catalyst.

Subsequently, the catalytic activity of **1f** was investigated for a range of amines and carbodiimides (Table 4.4, see also Experimental Section). Aniline (**7a**) reacts with *N,N'*-diisopropylcarbodiimide DIC (**8a**), *N,N'*-dicyclohexylcarbodiimide (DCC) (**8b**), and EtNCNEt (**8c**), affording guanidines **9a-c** in high yields (80% to 96%, Table 4.4, entries 1-3). It is noteworthy that precatalyst **1f** was compatible with both electron-donating and electron-withdrawing substituents on the phenyl ring of the amine such as Me-, *t*-butyl-, MeO-, or Cl- (Table 4.4, entries 4-7) affording the corresponding substituted guanidines **9d-9g** in excellent yields (80-98%). Furthermore, **1f** also effectively facilitated the room temperature addition of hindered anilines with substituents at their *ortho*-positions (**7f-7g**) or even of the secondary aniline *N*-methylaniline (**7h**) (86-94% yield, Table 4.4, entries 8, 9, and 10) and low activated diphenylamine (**7i**) (73% yield, Table 4.4, entry 11). Interestingly, and despite the presence of a pyridyl substituent, which could potentially coordinate to the bimetallic intermediates involved in this process, inhibiting their catalytic activity, the reaction of 3-aminopyridine (**7j**) with DIC afforded guanidine **9l** in an 88% yield (Table 4.4, entry 12). This versatility and functional group tolerance are remarkable when compared with other s-block catalytic systems where anilines with large substituents or coordinating groups give lower yields than when employing non-substituted substrates.<sup>1c, 7</sup> Using cyclic amines, morpholine and piperidine, and *n*-butylamine required the used of forcing reaction conditions, higher temperatures (70 °C), or a longer reaction time (24 h), to furnish the relevant guanidines **9m-9o** in moderate yields (52-

65%, **Table 4.4**, entries 13-15). Contrastingly no reaction is observed when diisopropylamine (**7n**) is employed which can be rationalised in terms of the significant increase steric bulk in this amine when compared with the rest of the substrates studied (**Table 4.4**, entry 16). Although previous studies have shown the feasibility of homometallic magnesium complexes to catalyse guanylation processes employing, unhindered amines,<sup>[8a,8b]</sup> **1f** offers a significant improvement for secondary amines and substituted anilines,<sup>[8a,8c]</sup> enabling these processes to take place at room temperature in short periods of time. Interestingly, hydrophosphination of carbodiimides **8a-c** with diphenylphosphine (**7o**) could also be achieved at room temperature using catalyst loadings as low as 2 mol%, affording the relevant phosphoguanidines **9q-9s** in high yields (80-95%, **Table 4.4**, entries 17-19). To the best of my knowledge, this represents the first example of a magnesium complex catalysing this process, showing an activity comparable to those reported by Hill using heavier alkaline earth metal amides, where efficiency of the catalyst correlates directly with the increase in size of the metal cation.<sup>9</sup>

**Table 4.4:** Guanylation and hydrophosphination of carbodiimides.<sup>[a]</sup>

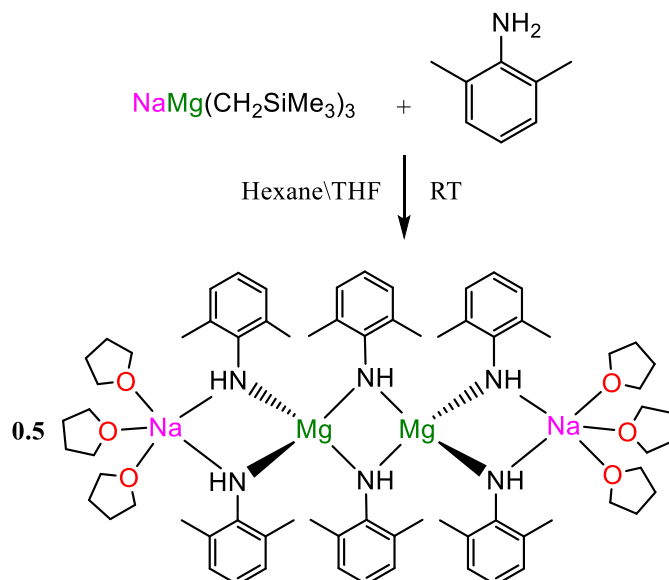
Entry	Amine/Phosphine	Carbodiimide	Compound/Yield (%) <sup>b</sup>
1	 <b>(7a)</b>	$i\text{PrN}=\text{C}=\text{N}i\text{Pr}$ ( <b>8a</b> )	 <b>9a</b> /(96)
2	 <b>(7a)</b>	$\text{CyN}=\text{C}=\text{NCy}$ ( <b>8b</b> )	 <b>9b</b> /(90)
3	 <b>(7a)</b>	$\text{EtN}=\text{C}=\text{N}^t\text{Bu}$ ( <b>8c</b> )	 <b>9c</b> /(80)
4	 <b>(7b)</b>	$i\text{PrN}=\text{C}=\text{N}i\text{Pr}$ ( <b>8a</b> )	 <b>9d</b> /(90)
5	 <b>(7c)</b>	$i\text{PrN}=\text{C}=\text{N}i\text{Pr}$ ( <b>8a</b> )	 <b>9e</b> /(80)
6	 <b>(7d)</b>	$i\text{PrN}=\text{C}=\text{N}i\text{Pr}$ ( <b>8a</b> )	 <b>9f</b> /(98)
7	 <b>(7e)</b>	$i\text{PrN}=\text{C}=\text{N}i\text{Pr}$ ( <b>8a</b> )	 <b>9g</b> /(96)
8	 <b>(7f)</b>	$i\text{PrN}=\text{C}=\text{N}i\text{Pr}$ ( <b>8a</b> )	 <b>9h</b> /(90)

Entry	Amine/Phosphine	Carbodiimide	Compound/Yield (%) <sup>b</sup>
9	 (7g)	$iPrN=C=NiPr$ (8a)	 <b>9i</b> /(86)
10	 (7h)	$iPrN=C=NiPr$ (8a)	 <b>9j</b> /(94)
11	 (7i)	$CyN=C=NCy$ (8b)	 <b>9k</b> /(73)
12	 (7j)	$iPrN=C=NiPr$ (8a)	 <b>9l</b> /(88)
13	 (7k)	$iPrN=C=NiPr$ (8a)	 <b>9m</b> /(15); (52) <sup>c</sup>
14	 (7l)	$iPrN=C=NiPr$ (8a)	 <b>9n</b> /(19); (65) <sup>c</sup>
15	 (7m)	$iPrN=C=NiPr$ (8a)	 <b>9o</b> (0) <sup>c</sup> , (60) <sup>d</sup>
16	 (7n)	$iPrN=C=NiPr$ (8a)	 <b>9p</b> /(0); (0) <sup>d</sup>
17	 (7o)	$iPrN=C=NiPr$ (8a)	 <b>9q</b> /(95) <sup>e</sup>
18	 (7o)	$CyN=C=NCy$ (8b)	 <b>9r</b> /(90) <sup>e</sup>
19	 (7o)	$EtN=C=N^tBu$ (8c)	 <b>9s</b> /(80)

[a] Conditions: amine/phosphine (1.00 mmol), carbodiimide (1.00 mmol), catalyst **1f** (2% mol), THF (3 mL), 1h, 25°C. [b] Isolated yields. [c] 1h, 70°C. [d] 24 h, 70°C. [e] 30 min, 25°C.

### 4.3.2 Stoichiometric investigations

To gain mechanistic insights into these promising catalytic processes a series of stoichiometric reactions were carried out. Addition of three molar equivalents of  $\text{NH}_2\text{Ar}$  ( $\text{Ar} = 2,6\text{-Me}_2\text{C}_6\text{H}_3$ ) (**7f**) to tris(alkyl)magnesiates **1f** afforded colourless crystals of tris(amido)magnesiates  $[\{(\text{THF})_3\text{NaMg}(\text{NHAr}_3)\}_2]$  (**1m**) in a 58% yield (**Scheme 4.3**).



**Scheme 4.3:** Synthesis of sodium magnesiates  $[\{(\text{THF})_3\text{NaMg}(\text{NHAr}_3)\}_2]$  (**1m**).

Determined by X-ray crystallography, the molecular structure of **1m** is dimeric, comprising a tetranuclear  $\text{Na}\dots\text{Mg}\dots\text{Mg}\dots\text{Na}$  chain arrangement connected by six anilide bridges (**Figure 4.3**).<sup>11</sup> This gives rise to three planar four-membered rings made up of two outer  $\{\text{NaN}_2\text{Mg}\}$  heterometallic rings, which are linked through a central  $\{\text{Mg}_2\text{N}_2\}$  homometallic ring, that is orthogonal to the outer rings. Each Mg atom in **1m** is bonded to four amido groups with Mg-N distances similar [mean value, 2.08(5) Å] to those found in other reported tris(amido) alkali-metal magnesiates.<sup>11</sup> Three molecules of THF complete the coordination sphere of each sodium atom which is also coordinated by two amido groups, exhibiting Na-N distances [mean value, 2.54(4) Å] which are significantly elongated compared to that reported for the homometallic sodium anilide  $[\{(\text{PMDETA})\text{NaNHPh}\}_2]$  [mean value, 2.42(3) Å].<sup>12</sup> The structure of **1m** contrasts to that previously reported in our group for  $[(\text{THF})_2\text{NaMg}(\text{NPh}_2)_3]$  (**1n**). Resulting from a similar reaction of **1f** with three equivalents of diphenylamine, **1n** displays a monomeric arrangement with the amido groups coordinating terminally to Mg via their N atoms; whereas the Na center  $\pi$ -engages with two phenyl groups in addition to binding to two THF ligands.<sup>6</sup>

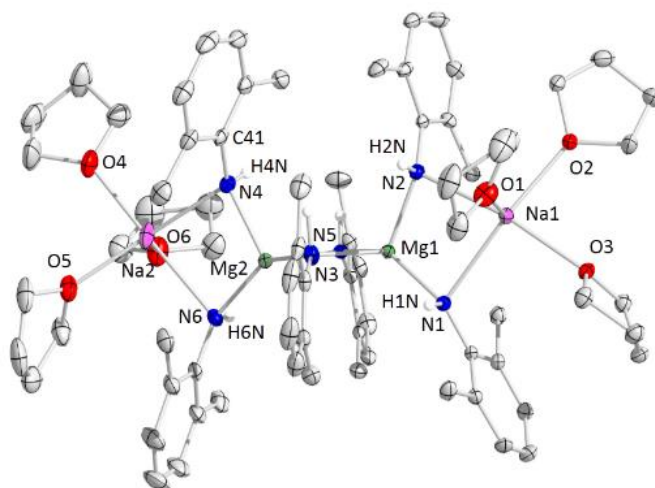


**Figure 4.3:** Molecular structure of  $[\{(THF)_3NaMg(NAr_3)\}_2]$  (**1m**) with displacement ellipsoids at the 30% probability level. Disorder and hydrogen atoms except those attached to nitrogen atoms are omitted for clarity. Selected bond distances (Å) and angles ( $^\circ$ ), Mg(1)-N(1) 2.032(2), Mg(1)-N(2) 2.051(2), Mg(1)-N(3) 2.159(2), Mg(1)-N(5) 2.111(2), Mg(2)-N(3) 2.078(2), Mg(2)-N(4) 2.057(2), Mg(2)-N(5) 2.160(2), Mg(2)-N(6) 2.028(2), Na(1)-N(1) 2.590(2), Na(1)-N(2) 2.539(2), Na(1)-O(1) 2.40(2), Na(1)-O(2) 2.362(2), Na(1)-O(3) 2.356(2), Na(2)-N(4) 2.488(2), Na(2)-N(6) 2.562(2); N(1)-Mg(1)-N(2) 105.38(9), N(1)-Mg(1)-N(3) 106.75(9), N(1)-Mg(1)-N(5) 136.73(9), N(2)-Mg(1)-N(3) 102.89(8), N(2)-Mg(1)-N(5) 109.60(8), N(3)-Mg(1)-N(5) 89.58(7), N(3)-Mg(2)-N(4) 107.65(9), N(3)-Mg(2)-N(5) 90.45(8), N(3)-Mg(2)-N(6) 137.49(9), N(4)-Mg(2)-N(5) 101.10(9), N(4)-Mg(2)-N(6) 105.43(9), N(5)-Mg(2)-N(6) 108.59(8).

Multinuclear NMR spectroscopy characterisation of compound **1m** was performed in  $C_6D_6$  solution.  $^1H$  NMR analysis revealed a complex spectrum with multiple signals in the aromatic, aliphatic and NH regions. More informatively, the  $^{13}C$  NMR spectrum showed six different signals (ranging from 157.0 to 152.7 ppm) which can be assigned to the *ipso*-C atoms of the 2,6-Me<sub>2</sub>-C<sub>6</sub>H<sub>4</sub> groups, suggesting the lack of equivalence between the anilide groups present in **1m**. This is consistent with retention in  $C_6D_6$  solution of the dimeric structure of **1m** in the solid state, with six non-equivalent anilide fragments, derived from four chiral nitrogen atoms and two pro-chiral nitrogen atoms.<sup>b</sup> Further confirmation of the retention of the dimeric arrangement of **1m** in  $C_6D_6$  solution was gained by  $^1H$  DOSY NMR studies. Thus, investigation of a deuterated toluene solution of **1m** (40 mM), using tetramethylsilane (TMS) as an internal

(b) X-ray analysis shows only three non-equivalent anilide fragments with R, S, R, S configuration for N4, N6, N2 and N1. However, during the identification of the hydrogen atoms on the Fourier map possible disorder was noticed, precluding an accurate establishment of the real configuration. Thus, two different possibilities can be found, a diastereomer with a configuration of the type R, R, R, S which would show six inequivalent anilide fragments or a mixture of diastereomers such as R, S, R, S and R, R, S, S which similarly would display a total of six signals for the anilide fragments.

reference, revealed D (diffusion coefficient) values of  $5.076 \times 10^{-10} \text{ m}^2/\text{s}$  and  $2.262 \times 10^{-9} \text{ m}^2/\text{s}$  respectively (**Figure 4.4**).

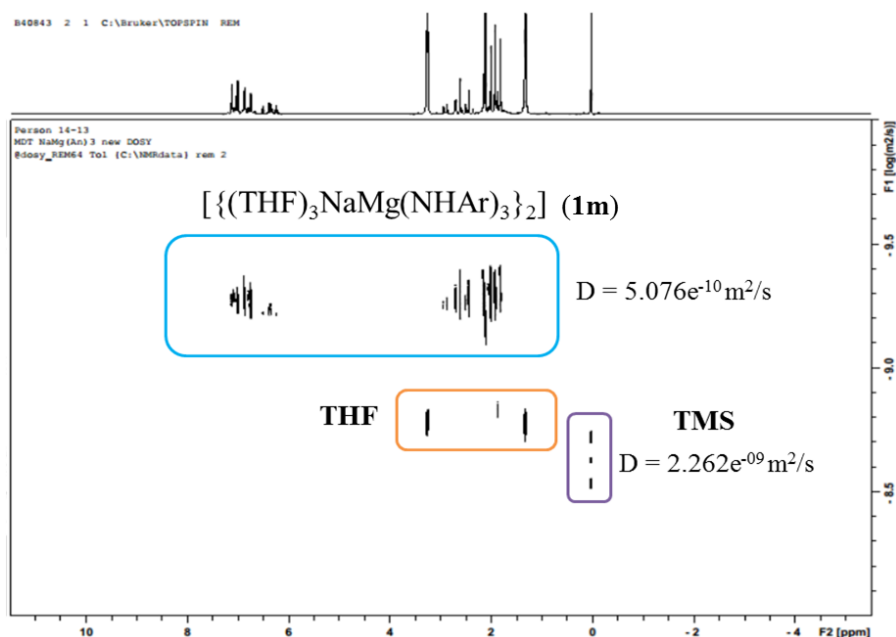


**Figure 4.4:**  $^1\text{H}$  DOSY NMR spectrum of  $[(\text{THF})_3\text{NaMg}(\text{NHAr})_3]_2$  (**1m**) and TMS in  $\text{C}_7\text{D}_8$  at 298K.

Using the external calibration curve (ECC) for dissipated spheres and ellipsoids elaborated by Stalke<sup>13</sup> the molecular weight of compound **1m** in solution was estimated to be  $1183 \text{ g mol}^{-1}$ . This result deviates only 5% when compared to the dimeric structure observed for **1m** in the solid state. Interestingly, using donor  $\text{d}_8$ -THF as solvent, DOSY experiments indicate the formation of solvent-separated ion pair species (**Figure 4.5**).

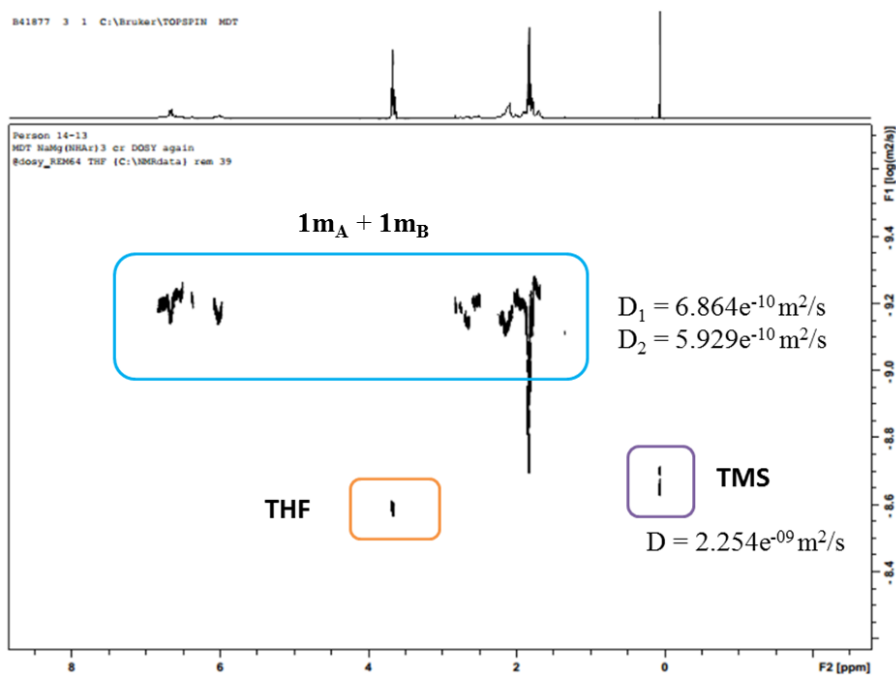


**Figure 4.5:**  $^1\text{H}$  DOSY NMR spectrum of  $[\{(\text{THF})_3\text{NaMg}(\text{NHAr}_3)_2\}]$  (**1m**) and TMS in  $d_8$ -THF at 298K.

In this case two different diffusion coefficients were observed for **1m** ( $D_1 = 6.864 \times 10^{-10} \text{ m}^2/\text{s}$  and  $D_2 = 5.929 \times 10^{-10} \text{ m}^2/\text{s}$ ). From these values two molecular weights were calculated ( $Mw_1 = 773 \text{ g mol}^{-1}$  and  $Mw_2 = 994 \text{ g mol}^{-1}$ ) which are consistent with the presence in solution of monoanionic  $[(\text{THF})_3\text{NaMg}_2(\text{NHAr})_6]^-$  (**1mA**) ( $Mw = 1008.97 \text{ g/mol}$ ) and dianionic  $[\text{Mg}_2(\text{NHAr})_6]^{2-}$  (**1mB**) ( $Mw = 769.66 \text{ g/mol}$ ) species (1% error for both species) (**Figure 4.6**).<sup>14</sup>

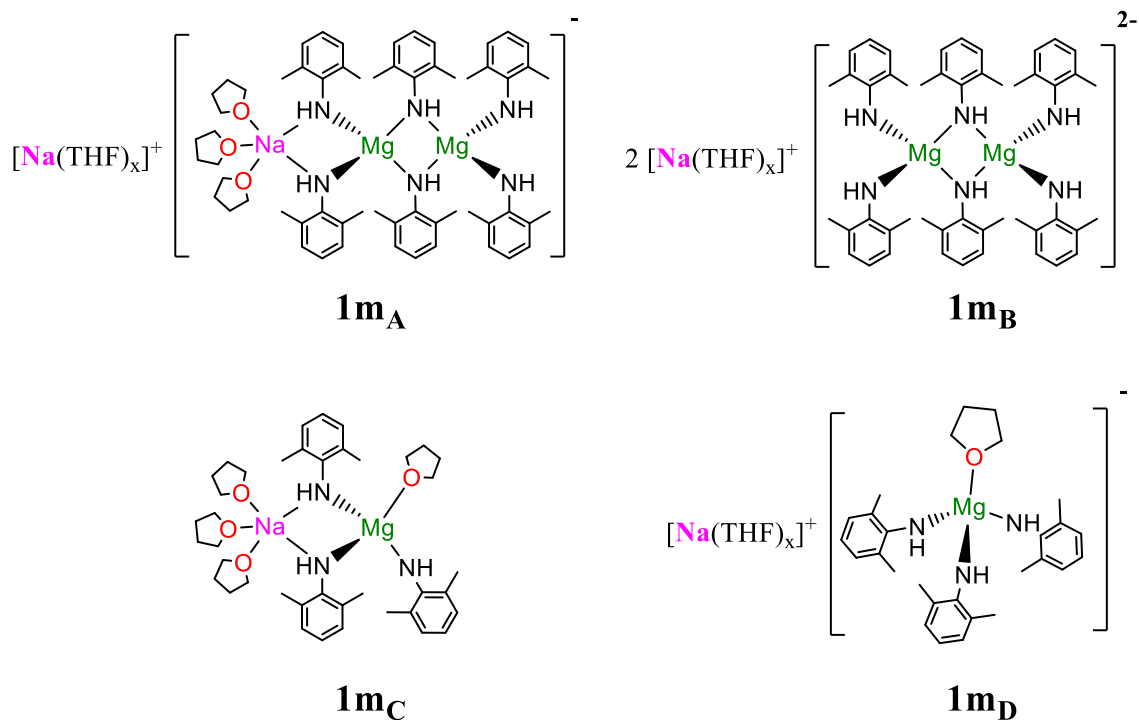


**Figure 4.6:** Chem Draw representation of possible species for  $[(\text{THF})_3\text{NaMg}(\text{NHAr}_3)]_2$  (**1m**) in  $\text{C}_7\text{D}_8$  and  $d_8$ -THF solution.

Furthermore 2D  $[\text{}^1\text{H}-\text{}^1\text{H}]$  EXSY NMR data (**Figures 4.7** and **4.8** and **Scheme 4.4**) established that slow exchange takes place between **1m<sub>A</sub>** and **1m<sub>B</sub>** in  $d_8$ -THF solution.

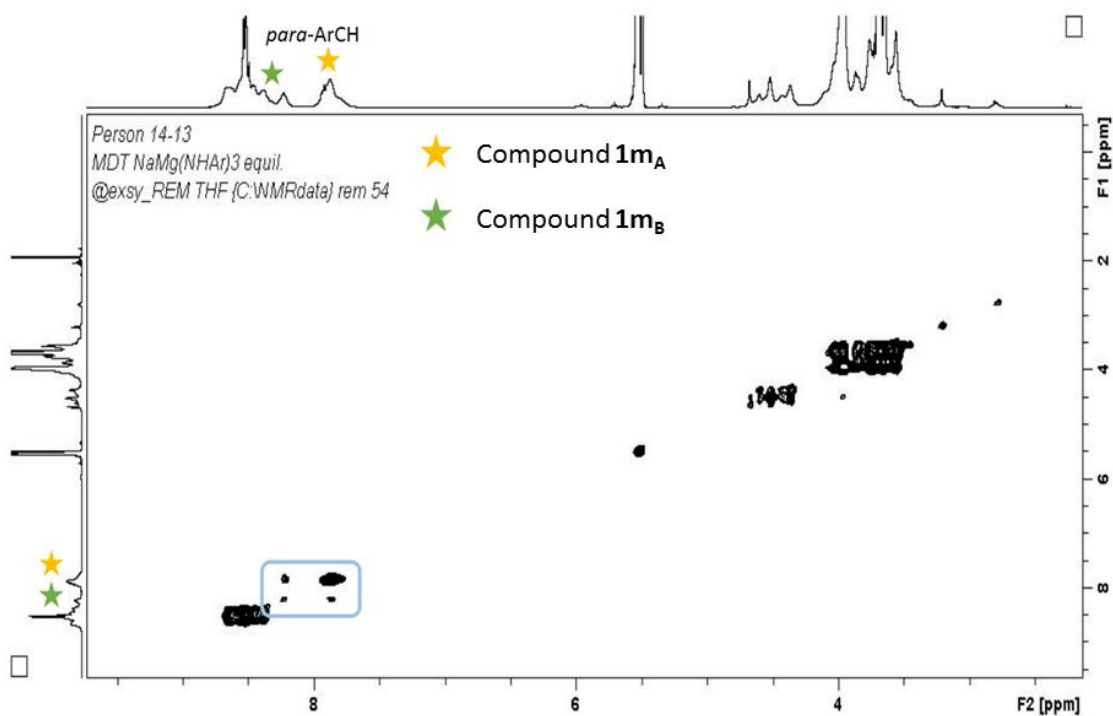


**Figure 4.7:** EXSY NMR spectrum of  $[(\text{THF})_3\text{NaMg}(\text{NHAr}_3)]_2$  (**1m**) in  $d_8$ -THF at 298K.

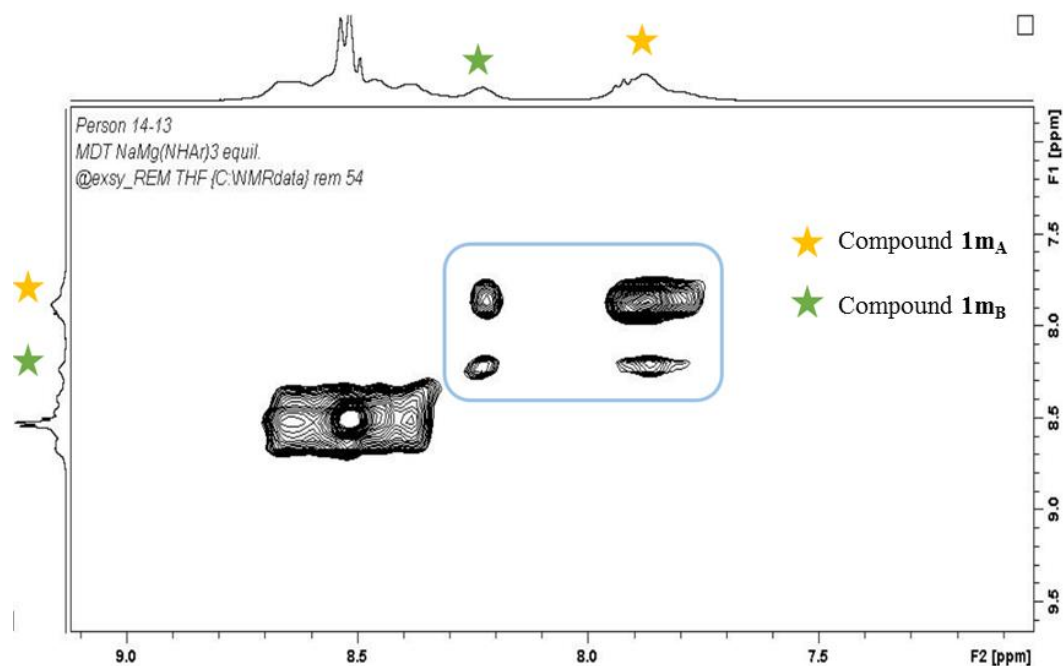
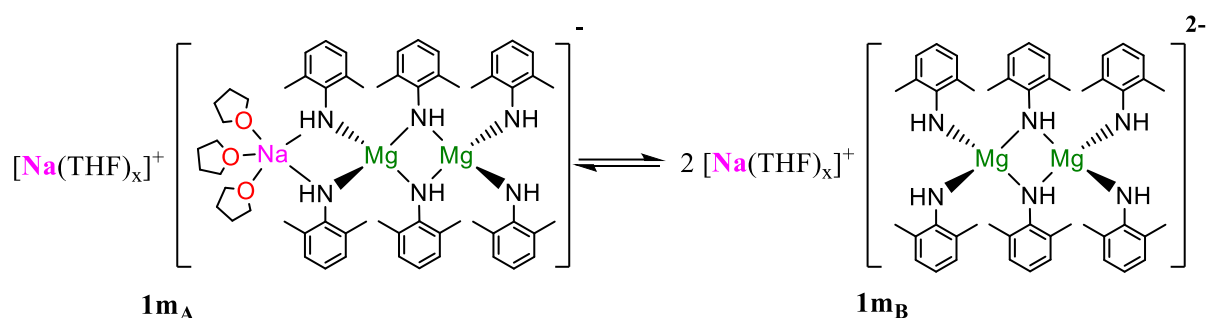


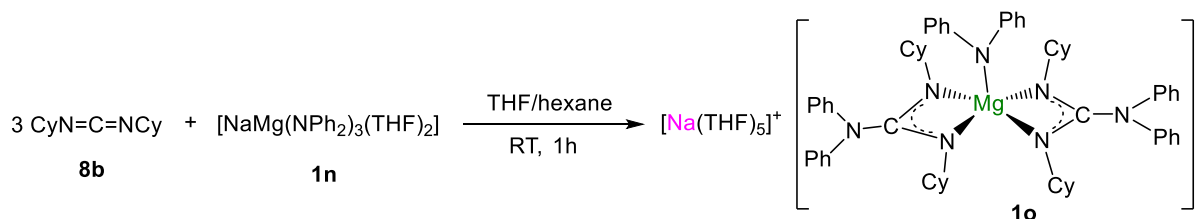
**Figure 4.8:** Aromatic region for EXSY NMR spectrum of  $[(\text{THF})_3\text{NaMg}(\text{NHAr}_3)]_2$  (**1m**) in  $d_8$ -THF at 298K.



**Scheme 4.4:** Equilibrium between species **1m<sub>A</sub>** and **1m<sub>B</sub>** observed in  $d_8$ -THF solution.

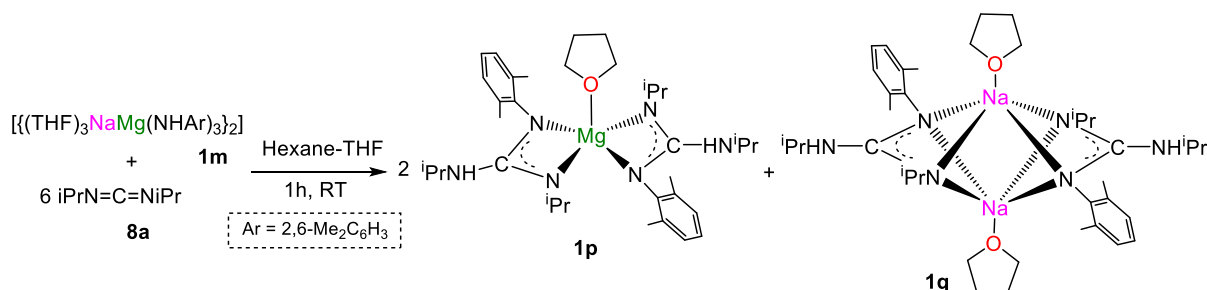
$^1\text{H}$  NMR monitoring of the reaction of an equimolar mixture of carbodiimide **8a** and aniline **7f** in the presence of 2 mol% of tris(amido) magnesiate **1m** indicated the formation of guanidine **9h** in a 99% yield after 15 minutes at room temperature, showing an identical efficiency to that found for tris(alkyl)magnesiate **1f** (99%, **Table 1**, entry 3). This hints at a possible involvement of (amido)magnesiate **1m** as an intermediate in the catalytic cycle (vide supra). If this is the case, the higher catalytic activity of **1f** in donor solvent THF when compared with benzene (**Table 4.2**) can be rationalised in terms of the different constitution of the relevant tris(amido) ate species in these solvents, with THF favouring the formation of solvent-separated- ion pair (SSIP) species which can be anticipated to be more powerful nucleophiles (containing terminal Mg-N bonds) than the analogous contacted-ion pair (CIP) ates where all the ligands are bridging between two metals.

The insertion reactions of tris(amido) magnesiate  $[\text{NaMg}(\text{NPh}_2)_3(\text{THF})_2]$  (**1n**) and **1m** with three molar equivalents of carbodiimide **8b** and **8a** respectively (Schemes 4.5 and 4.6 respectively) was next investigated. Interestingly, completely different outcomes were observed depending on the amido group present on the magnesiate. Thus (**1n**), previously prepared in our group by reaction of **1f** with 3 equivalents of **7i**, which contains diphenylamido groups, can insert only two molecules of carbodiimide **8b**, affording heteroleptic mixed amido/guanidinate sodium magnesiate **1o** in a 78% yield (Scheme 4.5).



**Scheme 4.5:** Insertion reaction of **8b** with tris(amido) magnesiate **1n**.

Contrastingly, **1m** can react effectively with three equivalents of **8a** furnishing a 1:1 mixture of the homometallic magnesium and sodium guanidinate **1p** and **1q**, which contain the unsymmetrical guanidinate ligand  $[\text{iPrNC}(\text{NH}^{\text{iPr}})\text{NAr}]$ , resulting from the formal insertion of the carbodiimide into the N-H bonds of the anilide groups present in **1m** (Scheme 4.6).



**Scheme 4.6:** Insertion reaction of **8a** with tris(amido) magnesiate **1m**

The formation of  $[\text{iPrNC}(\text{NH}^{\text{iPr}})\text{NAr}]$  can be rationalised as a result of a proton transfer from the arylamino nitrogen atom to an isopropylamido nitrogen, followed by the dissociation of the resultant  $\text{NH}^{\text{iPr}}$  group and formation of a new  $\text{M-NAr}$  bond (where  $\text{M} = \text{Mg}$  or  $\text{Na}$ ). This isomerisation not only allows a better stabilisation of the negative charge of the ligand (due to the conjugation effect between the aromatic ring and the  $\text{C}=\text{N}$  bond), but also a relief on the steric hindrance around the metal, by replacing one bulky  $\text{N}^{\text{iPr}}$  arm of the guanidinate ligand by a  $\text{NAr}$  substituent.<sup>15</sup> Conversion of **1m** into a 1:1 mixture of **1p** and **1q** occurs quantitatively, as indicated by  $^1\text{H}$  NMR monitoring of the reaction (Figure 4.9).

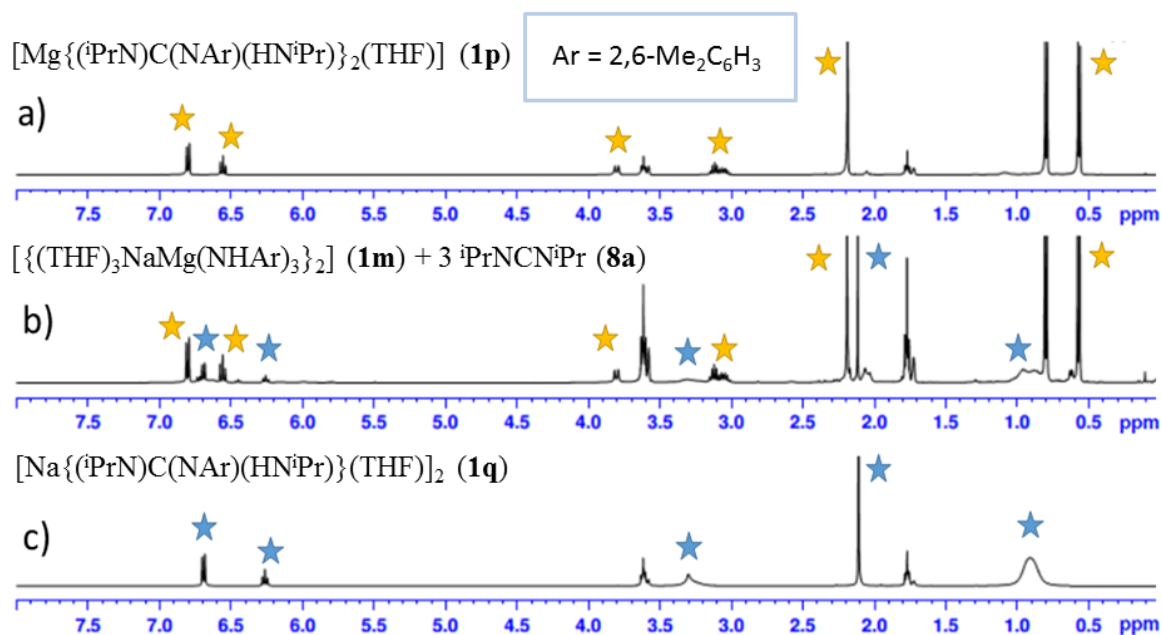


**Figure 4.9:** Comparison of  $^1\text{H}$  NMR spectra of a)  $[\text{Mg}\{(\text{iPrN})\text{C}(\text{NAr})(\text{HN}^i\text{Pr})\}_2(\text{THF})]$  (**1p**), b) reaction mixture of  $[\{(\text{THF})_3\text{NaMg}(\text{NHAr})_3\}_2]$  (**1m**) and **8a** and c)  $[\text{Na}\{(\text{iPrN})\text{C}(\text{NAr})(\text{HN}^i\text{Pr})\}(\text{THF})]_2$  (**1q**).

Compound **1p** could be crystallised from the reaction mixture in a 38% yield. Compound **1q** could alternatively be prepared by insertion of **8a** in sodium amide  $[\{(\text{THF})_2\text{Na}(\text{NHAr})\}_2]$  (**1r**) which was prepared by reacting  $\text{NaCH}_2\text{SiMe}_3$  with equimolar amounts of the amine **7f**. These results suggest that under stoichiometric conditions, in the case of **1m**, the insertion of a third equivalent carbodiimide into the remaining anilide group induces the disproportionation of putative magnesiate  $[\{\text{Na}(\text{THF})_x\}[\text{Mg}\{(\text{iPrN})\text{C}(\text{NH}^i\text{Pr})\text{NAr}\}_3]]$  into its monometallic guanidinate components **1p** and **1q**. This process is probably driven by the large steric congestion around Mg when coordinated by three guanidinate ligands. Attempts to prepare the relevant products of insertion resulting from the reactions of one and two equivalents of DIC with **1m** furnished, in all cases, variable amounts of **1p** and **1q** (in a 1:1 ratio) along with the recovery of unreacted **1m**. Thus under the conditions of this study, it appears that the three-fold activation of the Mg-NHAr bonds of **1m** is significantly favoured over a possible sequential reactivity. Contrastingly, sodium magnesiate **1o** does not react with a further equivalent of carbodiimide even under forcing reaction conditions (12h,  $60^\circ\text{C}$ ). This lack of reactivity can be attributed to the steric congestion around Mg in **1o**, which should compromise not only the approach of the heterocumulene to the magnesiate anion but also the availability of the remaining  $\text{NPh}_2$  amido group to act as a nucleophile, with its N atom sheltered by the cyclohexyl scaffolding of the guanidinate ligands (see **Figure 4.12b** for a space filling model)

which is also further stabilised by delocalisation of its lone pair across its two Ph substituents (sum of the angles around N7, 359.9°, see **Figure 4.12a**).

X-ray crystallographic studies established the molecular structures of **1o**, **1p**, **1q** (**Figures 4.12**, **4.11**, and **4.13** respectively) and **1r** (**Figure 4.10**). Sodium anilide **1r** is a dimeric species derived from the deprotonation of 2,6-dimethylaniline, forming a (NaN)<sub>2</sub> ring where each Na atom is coordinated by two anilide fragments and two molecules of THF (**Figure 4.10**).

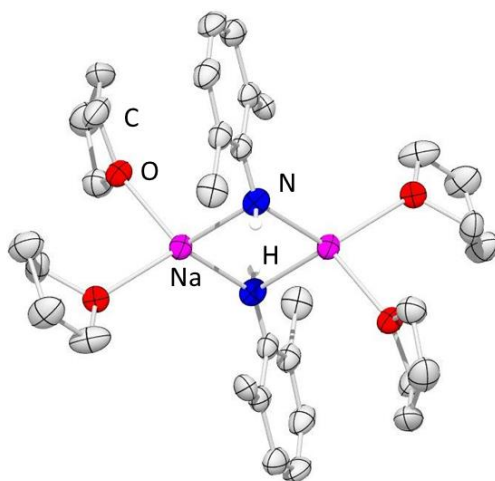


**Figure 4.10:** Solid state structure of  $[(\text{THF})_2\text{Na}(\text{NHAr})]_2$  (**1r**) with thermal ellipsoids at 30% of probability. Hydrogens atoms except those attached to nitrogen atoms and disorder are omitted for clarity.

Similarly to other alkali-metal anilide species reported in the literature such as  $[(\text{THF})_2\text{Li}(\text{NHPh})]_2$ <sup>16</sup> and  $[(\text{PMDETA})\text{Na}(\text{NHPh})]_2$ <sup>12</sup> the (NaN)<sub>2</sub> ring is planar ( $\Sigma$  angles = 360°), however the disordered nature of the substituents around sodium precludes further discussion of the angle and bond distances.

Compound **1p** exhibits a contacted ion pair structure with the Mg center in a distorted square pyramidal geometry, formed by four nitrogen atoms of two chelate guanidinate ligands in the equatorial position ( $\Sigma$  angles around Mg in equatorial plane = 345°), whereas the apical position is occupied by one molecule of THF. It should be noted that the guanidinate ligands present in **1p** are unsymmetrical, with one of the chelating N' atoms attached to <sup>i</sup>Pr (N2), whereas the remaining N (N1) binds to 2,6-dimethylphenyl (Ar). This lack of symmetry, translates in the formation of noticeably shorter Mg-NR bonds when R = <sup>i</sup>Pr [2.066(2) Å] than for the aromatic substituent [2.158(2) Å].

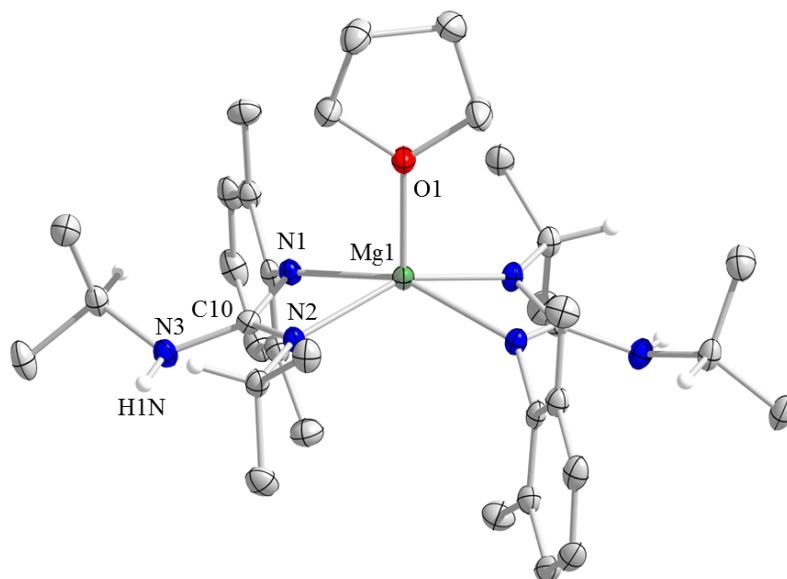


**Figure 4.11:** Molecular structure of  $[\text{Mg}\{(\text{iPrNC}(\text{NAr}))\}(\text{HN}^{\text{iPr}})]_2(\text{THF})$  (**1p**) ( $\text{Ar} = 2,6\text{-Me}_2\text{C}_6\text{H}_3$ ) with displacement ellipsoids at the 30% of probability. Hydrogen atoms, except those attached to nitrogens and those from the CH groups of the isopropyl substituents, are omitted for clarity. Selected bond distances ( $\text{\AA}$ ) and angles ( $^\circ$ )  $\text{Mg}(1)\text{-O}(1)$  2.039(2),  $\text{Mg}(1)\text{-N}(1)$  2.158(2),  $\text{Mg}(1)\text{-N}(2)$  2.066(2),  $\text{N}(1)\text{-C}(10)$  1.344(3),  $\text{N}(2)\text{-C}(10)$  1.326(3),  $\text{N}(3)\text{-C}(10)$  1.385(3),  $\text{N}(3)\text{-H}(1\text{N})$  0.84(4);  $\text{O}(1)\text{-Mg}(1)\text{-N}(1)$  163.65(6),  $\text{O}(1)\text{-Mg}(1)\text{-N}(2)$  104.94(7),  $\text{N}(1)\text{-Mg}(1)\text{-N}(2)$  64.01(8),  $\text{N}(2)\text{-Mg}(1)\text{-N}(1')$  108.45(8).

In addition, bond distances  $\text{N}(1)\text{-C}(10)$  [1.344(3)  $\text{\AA}$ ] and  $\text{N}(2)\text{-C}(10)$  (1.326(3)  $\text{\AA}$ ] are shorter than that one displayed by  $\text{N}(3)\text{-C}(10)$  1.385(3) in agreement with the delocalisation of the negative charge of the ligand across the bond system  $\text{N}(1)\text{-C}(10)\text{-N}(2)$ . In this context, the  $\text{sp}^2$  hybridisation of  $\text{C}(10)$  is confirmed by the sum of angles with a value of  $360^\circ$ . Related structures to that of **1p** have recently being reported by Kays for magnesium guanidates obtained using an alternative synthetic approach, by  $\text{MgnBu}_2$  deprotonation of guanidines containing highly sterically demanding groups.<sup>[16,17]</sup>

Sodium magnesiate **1o** constitutes, as far as I am aware, the first example of an alkali-metal magnesiate containing guanidinate ligands to be structurally defined. This compound was previously described in our group by Dr Zoe Livingston as part of her PhD project and it will only be mentioned in this section for discussion purposes. Compound **1o** exhibits a SSIP structure, comprising a sodium cation solvated by THF molecules balanced by a magnesiate anion where the magnesium center is bound by two chelating guanidinate ligands and a terminal  $\text{NPh}_2$  group (**Figure 4.12**).

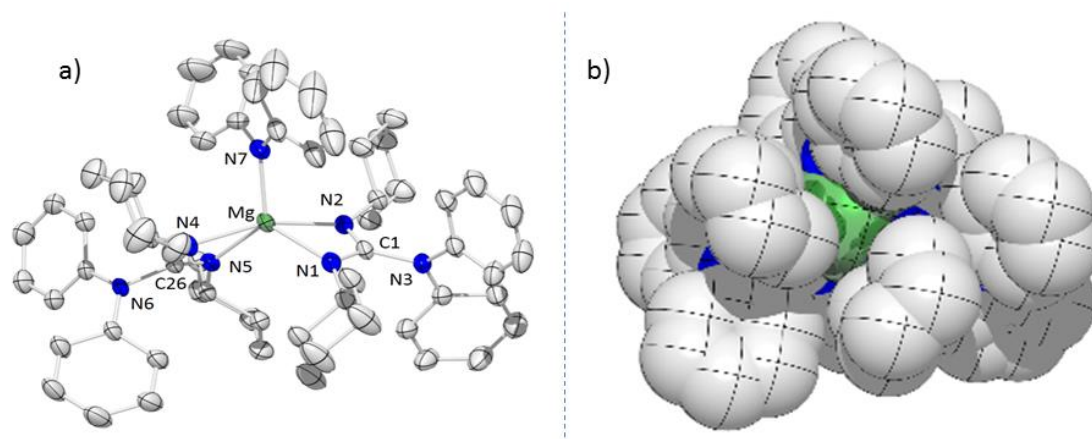


**Figure 4.12:** (a) Molecular structure of the anion  $[\text{Mg}\{(\text{CyN})_2\text{C}(\text{NPh}_2)\}_2(\text{NPh}_2)]^-$  present in **1o** with displacement ellipsoids at the 30% probability level. Hydrogen atoms are omitted for clarity.

The magnesiate anion in **1o** bears a strong resemblance to that found for homometallic magnesium complex **1p**, though in the latter the apical position is filled by a molecule of the neutral donor THF. Sodium guanidinate **1q** shows a dimeric arrangement, with the two guanidinate ligands being parallel to each other (**Figure 4.13**)

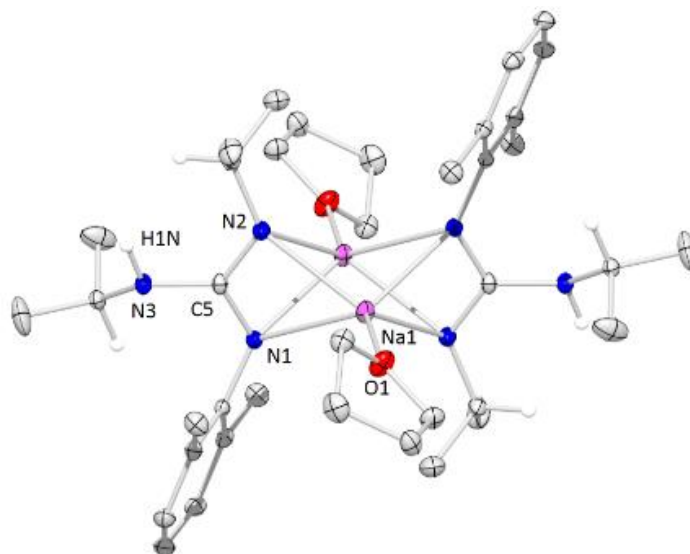
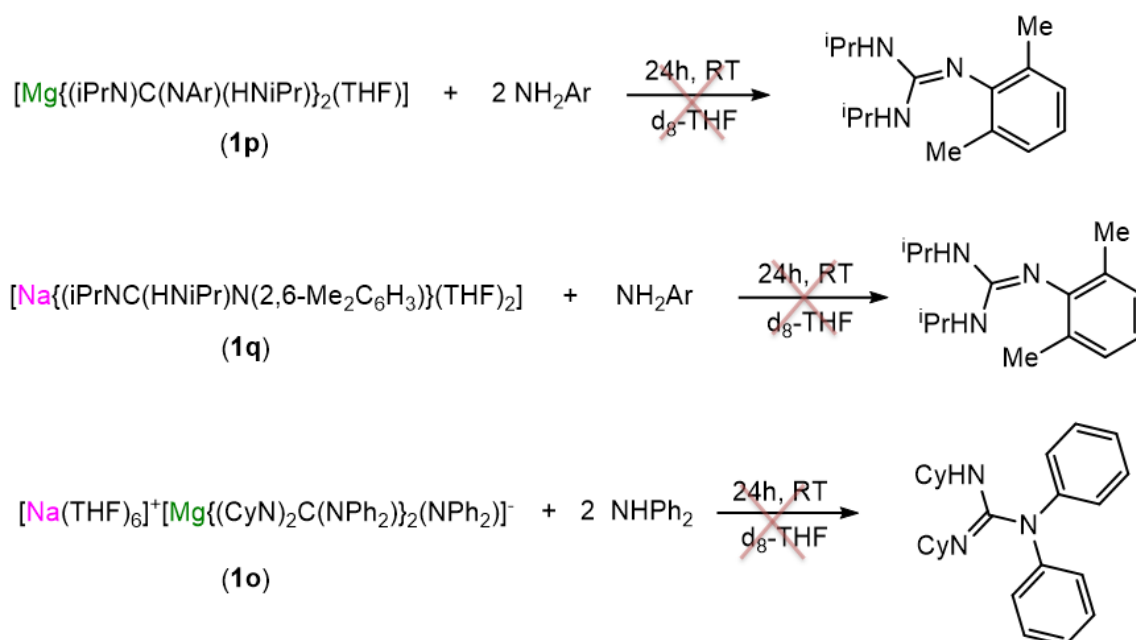


**Figure 4.13:** Molecular structure of  $[\text{Na}\{(\text{iPr})\text{NC}(\text{NAr})(\text{HNiPr})\}(\text{THF})]_2$  (**1q**) with displacement ellipsoids at the 30% of probability. Hydrogens atoms except those attached to nitrogens and those from the CH groups of the isopropyl substituents, are omitted for clarity. Selected bond distances (Å) and angles (°) Na(1)-O(1) 2.277(1), Na(1)-N(1) 2.453(1), Na(1)-N(2) 2.558(2), N(1)-C(5) 1.341(2), N(2)-C(5) 1.323(2), N(3)-C(5) 1.404(2), N(3)-H(1N) 0.9(2); O(1)-Na(1)-N(1) 122.19(4), O(1)-Na(1)-N(2) 123.79(4), O(1)-Na(1)-N(1') 122.27(5), O(1)-Na(1)-N(2') 120.48(4), N(1)-Na(1)-N(2) 53.57(4), N(2)-Na(1)-N(1') 89.20(5), N(2')-Na(1)-N(1) 93.88(5), N(1)-C(5)-N(2) 116.0(1), N(1)-C(5)-N(3) 120.4(1), N(2)-C(5)-N(3) 123.5(1).

Each sodium is coordinated by four N atoms of the Na<sub>2</sub>N<sub>4</sub> core [distances ranging from 2.453(1) to 2.558(2) Å] as well as a molecule of THF, with a Na...Na1 vector of length 2.671(2) Å, which lies perpendicular to the two guanidinate NCN planes. Containing the same unsymmetrical guanidinate ligand described above for **1p**, an opposite trend is observed for the length of its Na-N bonds [Na-N1, 2.453(1) Å vs Na-N2, 2.558(2) Å]. The structure of **1q** contrasts with that reported for trimeric guanidinate complex {Na[CyNC(N(SiMe<sub>3</sub>)<sub>2</sub>)NCy]}<sub>3</sub>, resulting from the reaction of DCC with NaN(SiMe<sub>3</sub>)<sub>2</sub>.<sup>18</sup>

Protonolysis of guanidinate complexes **1o**, **1p** and **1q** was attempted by treating them with variable amounts of the relevant amine (two equivalents of NHPH<sub>2</sub> for **1o**, and two and one equivalents of NH<sub>2</sub>Ar for **1p** and **1q** respectively) (**Scheme 4.7**).



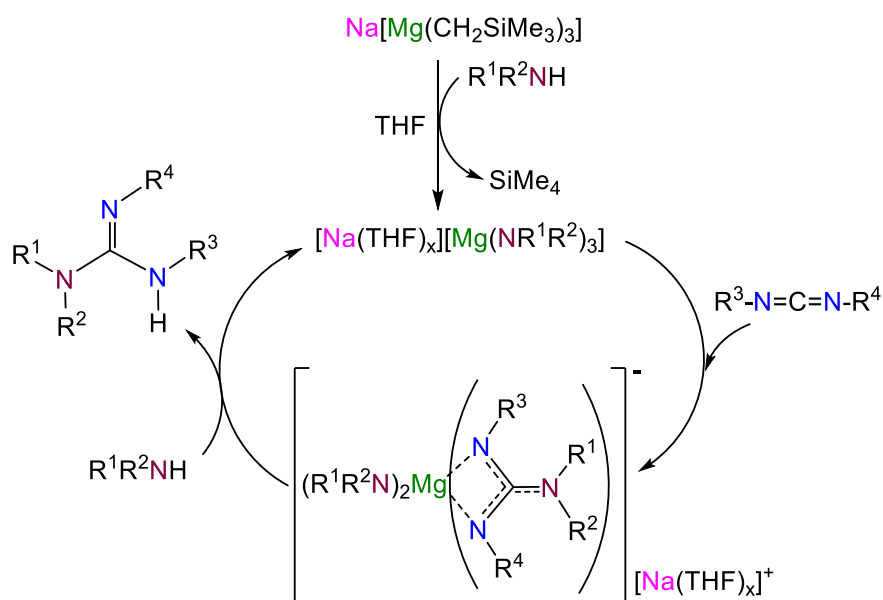
**Scheme 4.7:** Chem Draw representation of protonolysis reactions carried out on guanidinate complexes **1o**, **1p** and **1q**.

In all cases, no reaction was apparent after 24 hours at room temperature. The catalytic ability of these guanidinate complexes was also investigated. Interestingly, mixed-metal guanidinate **1o** was able to catalyse the guanylation of DCC with NHPH<sub>2</sub> affording guanidine in almost identical yields to those found when using sodium magnesiate **1f** (73% vs 75% using in both cases 2 mol% catalyst loading, RT, 1h). However, illustrating the synergistic capabilities in sodium magnesiate systems, single-metal guanidinates **1p** and **1q** displayed significant lower efficiencies for the reaction of DIC and NH<sub>2</sub>Ar than **1f**. Thus Mg complex **1p** afforded guanidine product in a modest 30% after 15 minutes, whereas the Na complex **1q** gave a 72% conversion under the same conditions. Even when an equimolar mixture of **1p** and **1q** was

employed as a catalyst for this reaction (using a 2 mol% loading, room temperature, 15 minutes), the conversions observed were still lower (76%) than when using preformed bimetallic precatalyst **1f** (99%). Collectively these results, and despite the isolation of single metal complexes in some of the stoichiometric studies, support the view that these guanylation reactions are indeed ate-catalysed transformations and highlight the limitations of comparing the results of stoichiometric reactions with the complex equilibria present during the catalytic process where variable excesses of reagents are present.

### 4.3.3 Mechanistic Studies

The observations from our stoichiometric studies, together with knowledge obtained from previous reports using s-block single-metal catalysts,<sup>1</sup> suggest that these ate-catalysed guanylation reactions of amines may take place via the mechanism presented in **Scheme 4.8**. Initially fast protonation of sodium tris(alkyl) magnesiate **1f** takes place to form a nucleophilic sodium tris(amido) magnesiate (as those seen for **1m** and **1n**), that in turn can undergo carbodiimide insertion affording a sodium magnesiate guanidinate complex. Protonolysis of this latter species with one equivalent of amine liberates the guanidine product and regenerates the active sodium tris(amido) magnesiate (**Scheme 4.8**).



**Scheme 4.8:** Proposed mechanism for the guanylation of amines with **1f**.

Previous insightful mechanistic studies by Richeson using LiHMDS as a catalyst have shown that the insertion step in these processes is initiated by coordination of the carbodiimide to the

Lewis acidic Li center.<sup>19</sup> Using bimetallic **1f** as a precatalyst, two potential sites are available for coordination, involving either the Na or Mg centers. Repeating the guanylation of DIC (**8a**) by 2,6-dimethylaniline (**7f**) using as a catalyst a 1:1 mixture of sodium magnesiate **1f** and the crown ether 15-crown-5 (which can block Na coordination sites) showed only a slight decrease in the yield obtained for guanidine **9h** (from 99% to 83%), which, coupled with the DOSY studies that show preference of these bimetallic compounds to exist as SSIP structures in THF solutions, suggest only a secondary role for sodium in this process, with the pre-coordination of the carbodiimide to Mg. Consistent with this interpretation of a minor involvement of the alkali-metal, rather than stabilising the magnesiate anion, using the lithium derivative  $[\text{LiMg}(\text{CH}_2\text{SiMe}_3)_3]^{20}$  as a precatalyst led to almost identical conversions (97%) to those observed using sodium-containing **1f**. Thus, the enhanced catalytic activity of these bimetallic systems seems to be a case of anionic activation,<sup>21</sup> where the formation of magnesiate anions, generates more powerful nucleophilic intermediates than when using charge-neutral organomagnesium precursors.<sup>8</sup>

Kinetic data was developed in collaboration with Dr Fernando Carrillo and co-workers from the University of Ciudad Real in Spain; the data obtained by our collaborators is used in this chapter for discussion purposes only. In order to obtain quantitative kinetic data, reactions of *N,N'*-diisopropylcarbodiimide with 4-*tert*-butylaniline in the presence of **1f** as catalyst were carried out, using *d*<sub>8</sub>-THF as solvent. Reaction rates of the guanylation were monitored over time by <sup>1</sup>H NMR spectroscopy using the integration changes in the substrate resonances over more than three half-lives. The order of the reaction was first determined with respect to amine concentration by keeping the concentration of other components virtually unaltered. Initially, the study started by using 2 mol% of catalyst **1f**, and the carbodiimide to amine molar ratio was maintained at 10:1 to maintain approximately zero-order conditions for carbodiimide. The plot of  $\ln([A]_0/[A]_t)$  versus reaction time is shown in **Figure 4.14**, where  $[A]_0$  is the initial amine concentration and  $[A]_t$  is the amine concentration after a given reaction time. An induction period was not observed, indicating that the catalyst was reactive from the beginning of the process. The data confirm a fit consistent with first-order kinetic behaviour with respect to amine concentration.

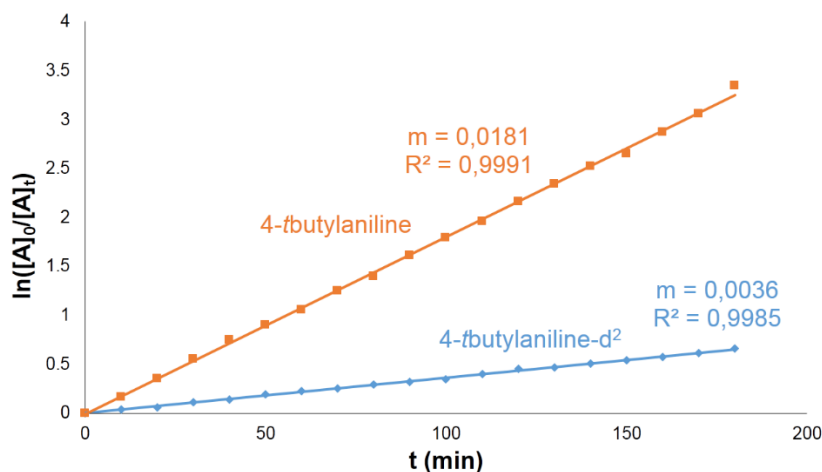


**Figure 4.14:** First-order kinetic analysis of the NMR-tube scale reaction of 4-*tert*-butylaniline (■) or 4-*tert*-butylaniline- $d^2$  (observed KIE=5) (◆) and di-isopropylcarbodiimide in  $d_8$ -THF with 2 mol% of **1** at room temperature.

Next, the order of the reaction with respect to the concentration of carbodiimide was determined. During this study a relative carbodiimide to amine ratio of 1:10 was maintained, and the linearity of the plot of  $\ln([C]_0/[C]_t)$ , where  $[C]$  is the carbodiimide concentration, versus the reaction time shows that the reaction was also first-order with respect to this reagent (**Figure 4.15**).

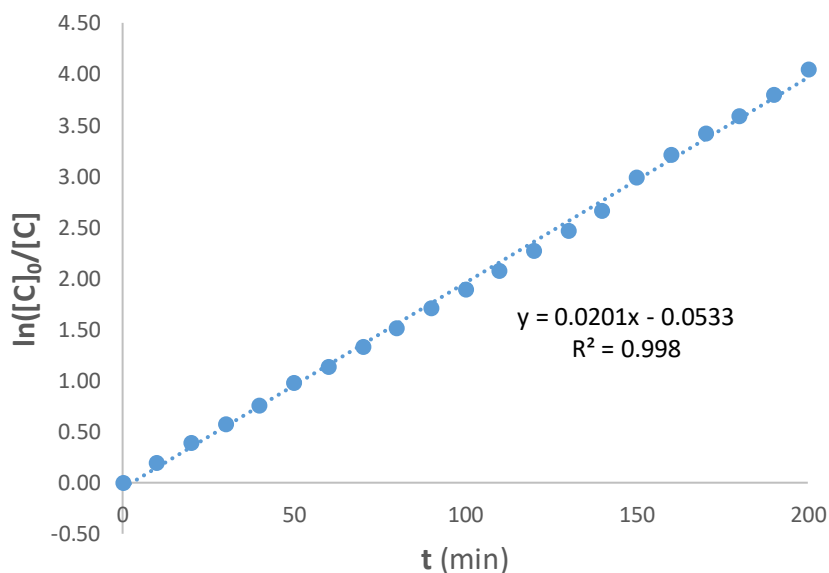
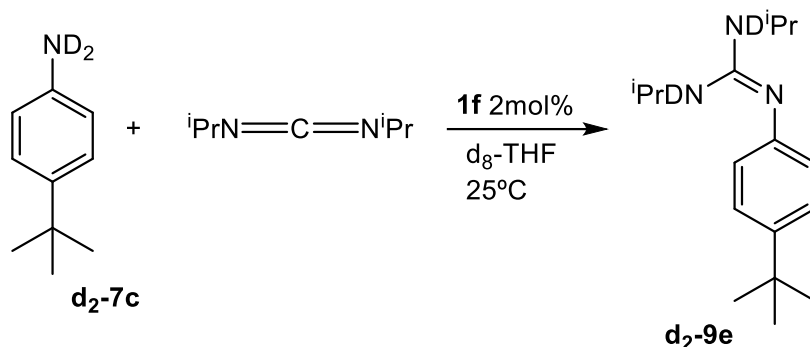


**Figure 4.15:** Pseudo-first order kinetic dependence for **8a**;  $k_{\text{obs}} = 0.0201 \text{ s}^{-1}$  error = 0.0002  
 $R^2 = 0.998$ .

Additionally, a H/D kinetic isotope effect (KIE) experiment using  $N,N'$ -diisopropylcarbodiimide and 4-*tert*-butylaniline- $d_2$  with catalyst **1f** was carried out. (KIE) was

studied monitoring by  $^1\text{H}$  NMR spectroscopy, at the described intervals, the disappearance of the deuterated amine **d2-7c** and formation of guanidine **d2-9e** over more than three half-lives (**Scheme 4.9**). The plot of  $\ln([\text{d}_2\text{-7c}]_0/[\text{d}_2\text{-7c}]_t)$  versus reaction time is shown in **Figure 4.16**, where  $[\text{d}_2\text{-7c}]_0$  is the initial deuterated amine concentration and  $[\text{d}_2\text{-7c}]_t$  is the deuterated amine concentration after a given reaction time. This study gave a KIE ( $k_H/k_D$ ) value of 5 (**Figure 4.16**).



**Scheme 4.9:** Reaction between deuterated amine **d2-7c** with formation of guanidine **d2-9e** for (KIE) studies.

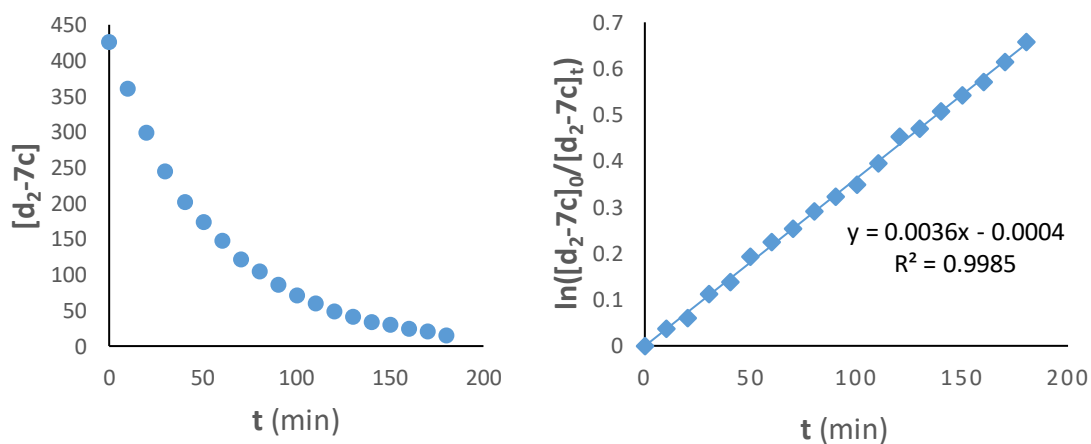


**Figure 4.16:**  $[\text{d}_2\text{-7c}]$  vs time and pseudo-first order kinetic;  $k_{\text{obs}} = 0.0036 \text{ s}^{-1}$  error = 0.00004  $R^2 = 0.998$

The maximum calculated kinetic isotope effect (KIE) at 25 °C for a reaction involving a N–H bond should be approximately 8.5. In our case of the guanylation reaction of *tert*-butylaniline, the magnitude of the measured value was clearly indicative of a primary KIE,<sup>22</sup> and indicates that a N–H bond is broken during the turnover-limiting step. While this observation would indicate that protonolysis by the amine of the starting alkyl compound could be the rate-determining step, it seems unlikely as stoichiometric reactions demonstrate that these protolytic

reactions occur instantaneously at room temperature. Thus, the more limiting protonolysis of chelate guanidinate intermediates could be responsible for this high KIE.

The dependence of the rate of reaction with respect to catalyst concentration was studied with different catalyst precursor concentrations, [1f] = 1 – 5 mol%, and fixing the carbodiimide to amine molar ratio at 10:1. A plot of reaction rate versus catalyst concentration reveals a linear increase of the reaction rate with catalyst concentration (**Figure 4.17** left).

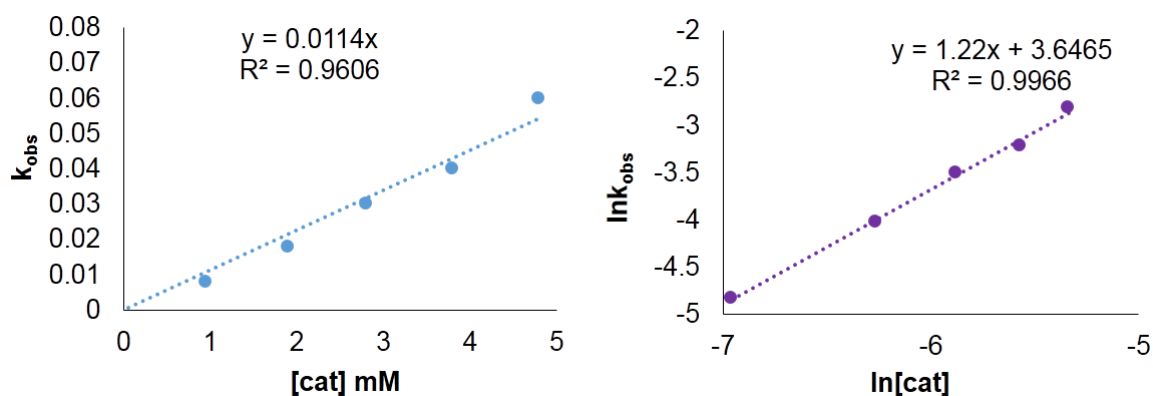


**Figure 4.17:** Plot of reaction rate versus concentration of the catalyst (left) and van't Hoff plot (right).

The first order rate of the reaction with respect to the catalyst concentration was further confirmed from the van't Hoff plot for the three first concentrations (**Figure 4.17** right). The value of the slope was determined to be close to 1. Thus, from the present study, the overall rate law for the guanylation of 4-*tert*-butylaniline with *N,N'*-diisopropylcarbodiimide catalysed by **1f** at low concentrations could be summarised as shown in **eqn (1)**. A similar rate law has been obtained for trinuclear zirconium alkyl diamido complexes.<sup>22</sup>



Values of  $k_{obs}$  at four different temperatures were measured. These  $k_{obs}$  values satisfactorily fit the Arrhenius plot (**Figure 4.18, left**), with a value of  $E_a = 20.7 \text{ kJ}\cdot\text{mol}^{-1}$ . The activation parameters were quantified by a plot of  $\ln(k_{obs}/T)$  versus  $1/T$ , which results in  $\Delta H^\ddagger = 18.1 \text{ kJ}\cdot\text{mol}^{-1}$  and  $\Delta S^\ddagger = -25.8 \text{ J}\cdot\text{mol}^{-1}\cdot\text{K}^{-1}$  (**Figure 4.18, right**).<sup>23</sup>

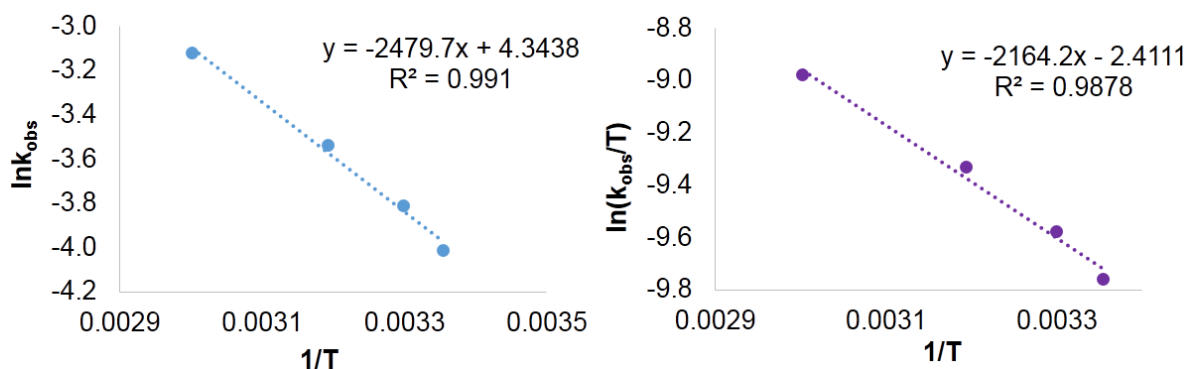


**Figure 4.18:** Arrhenius (left) and Eyring plots (right) for the guanylation reaction catalysed by **1f**

This last value could support the existence of a concerted transition state. Although the kinetic studies of guanylation process are scarce,<sup>16a,23</sup> several authors propose an amine-assisted concerted transition state in comparatively analogous alkene hydroamination processes with group 2 metal complexes, involving, as in this case, a large isotopic effect.<sup>24</sup> This amine-assisted state could also explain the first order observed in amine (and carbodiimide), in such a way that, under catalytic conditions, where an excess of amine is present through the main part of the process, it can be proposed that the magnesium amido complex formed in the first step could coordinate an amine molecule, where the negatively charged nitrogen atom of the incoming carbodiimide was stabilised favouring the attack of an amido ligand on the electrophilic carbon atom (**Figure 4.19**).

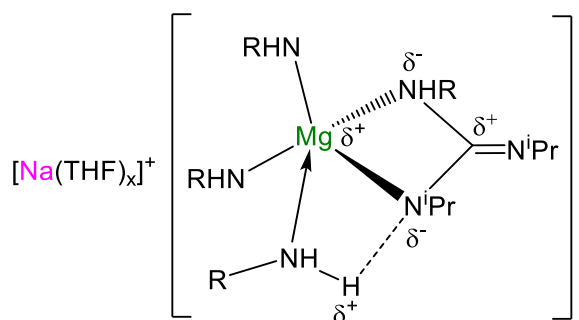


**Figure 4.19:** Proposed carbodiimide insertion transition state.

## 4.4 Conclusions

Here the first catalytic applications of alkali-metal magnesiate for guanylation and hydrophosphination reactions was reported. Homoleptic mixed Na/Mg complex  $[\text{NaMg}(\text{CH}_2\text{SiMe}_3)_3]$  (**1f**) has been found to offer significantly greater catalytic ability than those of its homometallic components  $[\text{NaCH}_2\text{SiMe}_3]$  and  $[\text{Mg}(\text{CH}_2\text{SiMe}_3)_2]$ , allowing guanylation of a range of substituted anilines and secondary amines under very mild reaction conditions (most cases at room temperature). Furthermore, by installing Mg within this sodium magnesiate platform, it is possible to activate it towards catalysing the hydrophosphination of carbodiimides at room temperature.

Stoichiometric investigations have allowed the isolation and structural elucidation of tris(amido) sodium magnesiate  $[\{(\text{THF})_3\text{NaMg}(\text{NHA}r_3)\}_2]$  (**1m**) and mixed amido/guanidinate sodium magnesiate  $[\text{Na}(\text{THF})_5]^+[\text{Mg}\{(\text{CyN})_2\text{C}(\text{NPh}_2)\}_2(\text{NPh}_2)]^-$  (**1o**). These appear to be intermediates in these catalytic transformations. Reactivity studies in these complexes, coupled with kinetic investigations, suggest these guanylation reactions occur by forming highly nucleophilic (tris)amide intermediates that can subsequently react with the carbodiimide in an insertion step, followed by amine protonolysis of the resultant guanidinate species. Interestingly, all these processes appear to take place in the coordination sphere of Mg, with Na taking a backseat in the catalytic cycle, stabilising the magnesiate anion intermediates, hinting that the enhanced catalytic activity of these systems is due to anionic activation.

The rate law for the guanylation of *N,N'*-diisopropylcarbodiimide with 4-*tert*-butylaniline catalysed by **1f** was deduced to be order 1 in [amine], [carbodiimide] and [catalyst], showing a large kinetic isotopic effect, which is consistent with the formation of an amine-assisted rate-determining carbodiimide insertion transition state.

## 4.5 Experimental Section

**General Considerations.** All reactions were performed under a protective argon atmosphere using standard Schlenk techniques. Hexane, benzene and THF were dried by heating to reflux over sodium benzophenone ketyl and distilled under nitrogen or they were passed through a column of activated alumina (Innovative Tech.), degassed under nitrogen and stored over molecular sieves in the glove-box prior to use.  $\text{Mg}(\text{CH}_2\text{SiMe}_3)_2$ ,  $\text{NaCH}_2\text{SiMe}_3$ ,  $[\text{NaMg}(\text{CH}_2\text{SiMe}_3)_3]$  and  $[(\text{THF})_2\text{NaMg}(\text{NPh}_2)_3]$  were prepared according to the literature.<sup>[6, 19, 25]</sup>  $\text{LiCH}_2\text{SiMe}_3$ , amines, phosphines and carbodiimides were purchased from Sigma Aldrich chemicals and used as received. NMR spectra were recorded on a Bruker DPX400 MHz spectrometer, operating at 400.13 MHz for  $^1\text{H}$ , 100.62 MHz for  $^{13}\text{C}$  or on a Varian FT-400 spectrometer using standard VARIAN-FT software. Elemental analyses were carried out using a Perkin Elmer 2400 elemental analyser.

**Preparative Scale Reaction of the guanidines and phosphaguanidines.** In the glovebox, a solution of compound **1f** (2% mol) in THF (3 mL) was added in a Schlenk tube. Amine (or phosphane) (1.00 mmol) and carbodiimide (1.00 mmol) were then added to the above reaction mixture. The Schlenk tube was taken outside the glovebox, and the reaction was stirred at the desired temperature. After carrying out the reaction for the desired time, the solution was concentrated under reduced pressure, and hexane was added and placed in a refrigerator at  $-30\text{ }^\circ\text{C}$  for 16 h. After filtration the products were obtained as white microcrystalline solids, characterised by comparing their NMR spectra with the literature data.<sup>[6e, 8a, 15, 25]</sup>

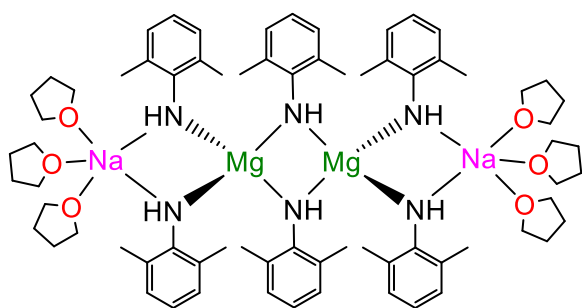
**X-ray crystallography.** Data for samples **1m**, **1p** and **1q** were measured on Oxford Diffraction diffractometers<sup>26</sup> with Mo  $\text{K}\alpha$  ( $\lambda = 0.71073\text{ \AA}$ ) or Cu  $\text{K}\alpha$  ( $\lambda = 1.5418\text{ \AA}$ ). Data for sample **1o** were measured at Beamline I19 of the Diamond Light Source using  $0.6889\text{ \AA}$  radiation and a Crystal Logics diffractometers with Rigaku Saturn 724+ CCD detector; data collection and processing used Rigaku and Bruker software. All structures were refined to convergence on  $F^2$  of all independent reflections by the full-matrix least-squares method using the SHELXL program.<sup>27</sup> Selected crystallographic and refinement details are given in **Table 4.5**:

**Table 4.5:** Selected crystallographic and refinement parameters.

	<b>1m</b>	<b>1o</b>	<b>1p</b>	<b>1q</b>
Empirical formula	$C_{72}H_{108}Mg_2N_6NaO_6$	$C_{86}H_{122}MgN_7NaO_6$	$C_{34}H_{56}MgN_6O$	$C_{38}H_{64}N_6Na_2O_2$
Molecular Weight	1248.24	1397.20	589.15	682.93
Temperature (K)	123(2)	150(2)	123(2)	123(2)
Wavelength (Å)	0.71073	0.6889	1.5418	0.71073
Crystal system,	Monoclinic	triclinic	Tetragonal	Monoclinic
Space group	P 21/c	P-1	I 41cd	C 2/c
<i>a</i> (Å)	24.4968(6)	13.921(5)	16.9555(2)	28.150(7)
<i>b</i> (Å)	12.0255(3)	14.508(4)	16.9555(2)	9.3222(9)
<i>c</i> (Å)	24.1965(6)	20.265(5)	24.5229(4)	20.248(5)
$\alpha$ (°)	90	84.113(3)	90	90
$\beta$ (°)	93.907(2)	81.093(3)	90	130.55(4)
$\gamma$ (°)	9	79.501(3)	90	90
Cell volume (Å <sup>3</sup> )	7111.4(3)	3964.0(19)	7050.1(2)	4037(2)
Z	4	2	8	4
$\rho_{calc}$ (g.cm <sup>-3</sup> )	1.166	1.171	1.11	1.124
$\mu$ (mm <sup>-1</sup> )	0.1	0.053	0.686	0.088
2 $\theta$ max(°)	54	42.5	146.6	60
Index ranges	-30 ≤ <i>h</i> ≤ 31 -15 ≤ <i>k</i> ≤ 15 -30 ≤ <i>l</i> ≤ 30	-14 ≤ <i>h</i> ≤ 11 -15 ≤ <i>k</i> ≤ 15 -21 ≤ <i>l</i> ≤ 21	-19 ≤ <i>h</i> ≤ 19 -20 ≤ <i>k</i> ≤ 21 -30 ≤ <i>l</i> ≤ 30	-39 ≤ <i>h</i> ≤ 37 -12 ≤ <i>k</i> ≤ 11 -26 ≤ <i>l</i> ≤ 27
Reflections collected	38901	18305	16891	15891
Reflections unique	15355	8870	3501	5494
Reflections obs.	10062	6093	3280	4235
<i>R</i> <sub>int</sub>	0.0359	0.0633	0.0319	0.0343
No. Parameters	904	1151	202	240

Goodnes-of-fit-on $F^2$ ( $GOF$ )	1.027	1.092	1.037	1.038
Final $R$ indices [ $I > 2\sigma(I)$ ]	0.061	0.1092	0.0353	0.044
$R$ indices (all data)	0.1509	0.2827	0.0936	0.1198
Largest diff. peak and hole ( $e \text{ \AA}^{-3}$ )	0.515 and -0.349	0.518 and -0.392	0.248 and -0.177	0.269 and -0.225

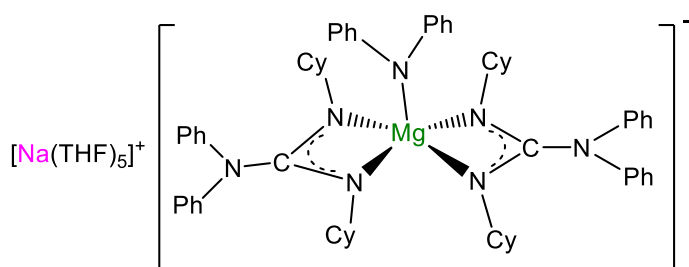
#### 4.5.1 Synthesis of $[\{(\text{THF})_3\text{NaMg}(\text{NHAr})_3\}_2]$ (**1m**) ( $\text{Ar} = 2,6\text{-Me}_2\text{C}_6\text{H}_3$ ).



To a  $\text{NaMg}(\text{CH}_2\text{SiMe}_3)_3$  (1 mmol, 0.309 g) suspension in hexane (10 mL) 2,6-dimethylaniline (3 mmol, 0.37 mL) was added. After 1h stirring at room temperature THF (2 mL) was introduced, affording a light brown solution. The solution was stored at -

20 °C overnight affording colorless crystals of sodium magnesiate **1m** (0.362 g, 58%).  $^1\text{H NMR}$  (400 MHz, 298 K,  $\text{C}_6\text{D}_6$ )  $\delta$  (ppm) = 1.24 (m, 24H, THF), 1.87, 1.98, 2.07, 2.18, 2.19, 2.22 (36H,  $\text{CH}_3$ ,  $\text{NHAr}$ ), 2.52, 2.57, 2.68, 2.76, 2.79, 2.81 (6H,  $\text{NHAr}$ ), 3.19 (m, 24H, THF), 6.3-7.1 (18H,  $\text{CH}$ ,  $\text{NHAr}$ ).  $^{13}\text{C}\{^1\text{H}\}$  NMR (101 MHz, 298 K,  $\text{C}_6\text{D}_6$ )  $\delta$  (ppm) = 18.8, 19.5, 19.7, 20.0, 20.9, 21.6 ( $\text{CH}_3$ ,  $\text{NHAr}$ ), 25.5 (THF), 67.8 (THF), 111.7, 111.8, 112.3, 112.6, 116.6, 121.4, 121.7, 122.0, 124.7, 125.3, 125.9, 128.6, 128.9, 129.0, 129.1, 129.3, 129.5, 129.8 ( $\text{CH}$ ,  $\text{NHAr}$ ), 152.7, 152.8, 156.1, 156.2, 156.6, 157 (*ipso-C*,  $\text{NHAr}$ ). **Anal Calcd for**  $\text{C}_{72}\text{H}_{108}\text{Mg}_2\text{N}_6\text{Na}_2\text{O}_6$ : C, 69.28; H, 8.72; N, 6.73. Found, C, 69.25; H, 8.85; N, 7.12.

#### 4.5.2 Synthesis of $[\text{Na}(\text{THF})_5]^+[\text{Mg}\{(\text{CyN})_2\text{C}(\text{NPh}_2)\}_2(\text{NPh}_2)]^-$ (**1o**)<sup>c</sup>

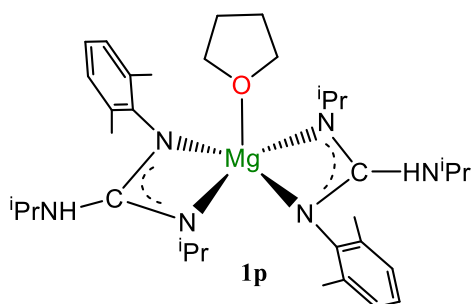


To a THF solution (4 mL) of sodium magnesiate  $[(\text{THF})_2\text{NaMg}(\text{NPh}_2)_3]$  (**1n**) (0.7 g, 1 mmol) *N,N'*-dicyclohexylcarbodiimide (**8b**)

(c) The synthesis of **1o** was carried out by Dr. Zoe Livingstone during her PhD studies within the Hevia group.

(0.62 g, 3 mmol) was added. After 1h stirring, hexane (4mL) was introduced, and the Schlenk was stored in the freezer (-30 °C) overnight to allow the formation of colorless crystals of  $[\text{Na}(\text{THF})_5]^+[\text{Mg}\{(\text{CyN})_2\text{C}(\text{NPh}_2)\}_2(\text{NPh}_2)]^-$  (**1o**) (1.03 g, 78%).  **$^1\text{H}$  NMR** (400 MHz, 298 K,  $\text{C}_6\text{D}_6$ )  $\delta$  (ppm) = 1.04-1.27, 1.47-1.73 (m, 40H,  $\text{CH}_2$ , CyN), 1.43 (m, 20H, THF), -3.40-4.48 (m, 4H, CH, CyN), 3.57 (m, 20H, THF), 6.71 (t,  $J=7.1\text{Hz}$ , 1H,  $\text{NPh}_2$ ), 6.79 (t,  $J=7.1\text{Hz}$ , 1H,  $\text{NPh}_2$ ), 6.85-6.90 (m, 4H, CH,  $\text{NPh}_2$ , guanidinate), 7.16-7.23, (m, 8H, CH,  $\text{NPh}_2$ , guanidinate), 7.28-7.38 (m, 4H, CH,  $\text{NPh}_2$ ), 7.44 (d,  $J=7.6\text{Hz}$ , 8H,  $\text{NPh}_2$ , guanidinate), 7.50 (d,  $J=7.6\text{ Hz}$ , 2H,  $\text{NPh}_2$ ), 7.67 (d,  $J=7.6\text{ Hz}$ , 2H,  $\text{NPh}_2$ ).  **$^{13}\text{C}\{\text{H}\}$  NMR** (101 MHz, 298 K,  $\text{C}_6\text{D}_6$ )  $\delta$  (ppm) = 25.7 (THF), 26.2, 26.5, 26.6, 26.8, 37.3, 37.4, ( $\text{CH}_2$ , CyN) 55, 56.1(CH, CyN), 67.9 (THF), 121.1, 129.3, 130.2 (CH,  $\text{NPh}_2$ , guanidinate), 145.8 (*ipso*-C,  $\text{NPh}_2$ , guanidinate), 122, 129.5, 130.3 (CH,  $\text{NPh}_2$ ), 146.3 (*ipso*-C,  $\text{NPh}_2$ ), 163.5 ( $\text{CN}_3$ ). **Anal Calcd** for  $\text{C}_{82}\text{H}_{114}\text{MgN}_7\text{NaO}_5$ : C, 74.32; H, 8.67; N, 7.40. Found, C, 74.48; H, 8.41; N, 8.37.

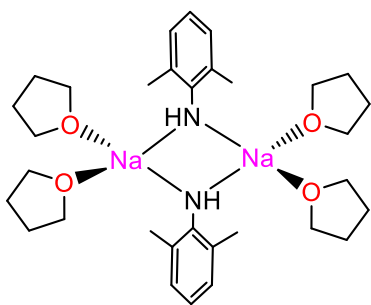
#### 4.5.3 Stoichiometric studies: reaction between $[\{(\text{THF})_3\text{NaMg}(\text{NHA}r_3)\}_2]$ (**1m**) ( $\text{Ar} = 2,6\text{-Me}_2\text{C}_6\text{H}_3$ ) and 3 equivalents of diisopropylcarbodiimide (**8a**).



Sodium magnesiate  $[\{(\text{THF})_3\text{NaMg}(\text{NHA}r_3)\}_2]$  (**1m**) (0.312g, 0.25 mmol) was reacted with N,N-diisopropylcarbodiimide (1.5 mmol, 0.23 mL) in THF (2 mL). The reaction mixture was stirred for 1 hour, then hexane (4 mL) was added (if a precipitate forms, it can be redissolved by gentle heating). The solution was

stored at -15 °C overnight to allow the formation of colorless crystals of compound  $[\text{Mg}\{(\text{iPrN})\text{C}(\text{NA}r)(\text{HNiPr})\}_2(\text{THF})]$  (**1p**) (112 mg, 38%).  **$^1\text{H}$  NMR** (400 MHz, 298 K,  $\text{d}_8\text{-THF}$ )  $\delta$  (ppm) = 0.56 (d,  $J=6.2\text{ Hz}$ , 12H,  $\text{CH}_3$ ,  $\text{iPr}$ ), 0.79 (d,  $J=6.4\text{ Hz}$ , 12H,  $\text{CH}_3$ ,  $\text{iPr}$ ), 1.77 (m, 4H, THF), 2.19 (s, 12H,  $\text{CH}_3$ ,  $\text{NA}r$ ), 3.02-3.15 (m, 4H, CH,  $\text{iPr}$ ), 3.61 (m, 4H, THF) 3.80 (br d, 2H,  $\text{NH}^{\text{iPr}}$ ), 6.56 (t,  $J=7.6\text{ Hz}$ , 2H, *para*-CH,  $\text{NA}r$ ), 6.80 (d,  $J=7.6\text{ Hz}$ , 4H, *meta*-CH,  $\text{NA}r$ ).  **$^{13}\text{C}\{\text{H}\}$  NMR** (101 MHz, 298 K,  $\text{d}_8\text{-THF}$ )  $\delta$  (ppm) = 19.7 ( $\text{CH}_3$ ,  $\text{NA}r$ ), 24.2 ( $\text{CH}_3$ ,  $\text{iPr}$ ), 25 ( $\text{CH}_3$ ,  $\text{iPr}$ ), 26.2 (THF), 44.7 (CH,  $\text{iPr}$ ), 45.0 (CH,  $\text{iPr}$ ), 68.0 (THF), 120.1 (*para*-CH,  $\text{NA}r$ ), 128.1 (*meta*-CH,  $\text{NA}r$ ), 132.6 (*ortho*-C,  $\text{NA}r$ ), 150.3 (*ipso*-C,  $\text{NA}r$ ), 163.5 ( $\text{CN}_3$ ). **Anal Calcd** for  $\text{C}_{34}\text{H}_{56}\text{MgN}_6\text{O}$ : C, 69.31; H, 9.58; N, 14.26. Found, C, 68.73; H, 9.26; N, 13.97.

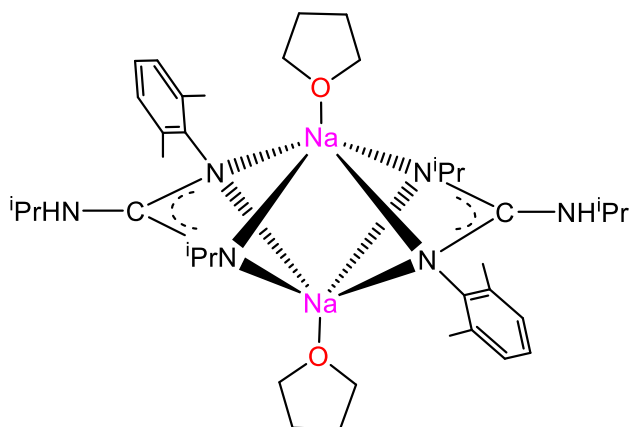
#### 4.5.4 Synthesis of dimer $[\{\text{Na}(\text{NHAr})\}_2]$ (**1r**) (Ar = 2,6-Me<sub>2</sub>C<sub>6</sub>H<sub>3</sub>)



$\text{Na}(\text{CH}_2\text{SiMe}_3)$  (0.11 g, 1 mmol) was charged in an oven dried Schlenk and suspended in hexane (4 mL). 2,6-dimethylaniline (0.12 mL, 1 mmol) was then added and the mixture was left stirring for 1h. After addition of THF (1 mL), the resulting solution was cooled down to  $-30\text{ }^\circ\text{C}$  affording sodium amide  $[\{\text{Na}(\text{NHAr})\}_2]$  (**1r**) (114 mg, 80% Yield) as a

white solid.  $^1\text{H NMR}$  (400 MHz, 298 K,  $\text{d}_8\text{-THF}$ )  $\delta$  (ppm) = 2.07 (s, 6H,  $\text{CH}_3$ ,  $\text{NHAr}$ ), 2.80 (s, 1H,  $\text{NHAr}$ ), 5.75 (t,  $J=7.2$  Hz, 1H, *para-CH*,  $\text{NHAr}$ ) 6.58 (d,  $J=7.2$  Hz, 2H, *meta-CH*,  $\text{NHAr}$ ).  $^{13}\text{C}\{\text{H}\}$  NMR (101 MHz, 298 K,  $\text{d}_8\text{-THF}$ )  $\delta$  (ppm) = 19.9 ( $\text{CH}_3$ ,  $\text{NHAr}$ ), 106.6 (*ortho-C*,  $\text{NHAr}$ ), 119.2 (*para-CH*,  $\text{NHAr}$ ), 128.1 (*meta-CH*,  $\text{NHAr}$ ), 161.4 (*ipso-C*,  $\text{NHAr}$ ). Due to the extreme air-sensitivity of compound **1r** satisfactory analyses could not be obtained.

#### 4.5.5 Synthesis of $[\text{Na}\{(\text{iPrN})\text{C}(\text{NAr})(\text{HNiPr})\}(\text{THF})_2]$ (**1q**) (Ar = 2,6-Me<sub>2</sub>C<sub>6</sub>H<sub>3</sub>).



To a solution of sodium (2,6-dimethylphenyl)amide  $[\{\text{Na}(\text{NHAr})\}_2]$  (**1r**) (0.143 g, 0.5 mmol) in hexane/THF (4 mL/1 mL) diisopropylcarbodiimide (0.08 mL, 0.5 mmol) was added. The resulting pale yellow solution was stored in the freezer ( $-30\text{ }^\circ\text{C}$ ) overnight to allow the formation of colorless crystals of

$[\text{Na}\{(\text{iPrN})\text{C}(\text{NAr})(\text{HNiPr})\}(\text{THF})_2]$  (**1q**) (0.108 g, 63%).  $^1\text{H NMR}$  (400 MHz, 298 K,  $\text{d}_8\text{-THF}$ )  $\delta$  (ppm) = 0.91 (s, 24H,  $\text{CH}_3$ ,  $\text{iPr}$ ), 1.78 (m, 4H, THF), 2.11 (s, 6H,  $\text{CH}_3$ ,  $\text{NAr}$ ), 3.30 (broad s, 4H + 2H,  $\text{CH}$ ,  $\text{iPr}$  +  $\text{NH}^{\text{iPr}}$ ), 3.61 (m, 4H, THF), 6.26 (t,  $J=7.2$  Hz, 2H, *para-CH*,  $\text{NAr}$ ), 6.69 (d,  $J=7.2$  Hz, 4H, *meta-CH*,  $\text{NAr}$ ).  $^{13}\text{C}\{\text{H}\}$  NMR (100 MHz, 298 K,  $\text{d}_8\text{-THF}$ )  $\delta$  (ppm) = 19.8 ( $\text{CH}_3$ ,  $\text{NAr}$ ), 24.4 ( $\text{CH}_3$ ,  $\text{iPr}$ ), 26.2 (THF), 27.0 ( $\text{CH}_3$ ,  $\text{iPr}$ ), 44.6 ( $\text{CH}$ ,  $\text{iPr}$ ), 46.7 ( $\text{CH}$ ,  $\text{iPr}$ ), 115.3 (*ortho-C*,  $\text{NAr}$ ), 127.7 (*meta-CH*,  $\text{NAr}$ ), 129.7 (*para-CH*,  $\text{NAr}$ ), 155.3 (*ipso-C*,  $\text{NAr}$ ), 160.2 ( $\text{CN}_3$ ). **Anal Calcd** for  $\text{C}_{34}\text{H}_{56}\text{N}_6\text{Na}_2\text{O}$  (one molecule of THF per dimer was considered, according to the NMR data): C, 66.85; H, 9.24; N, 13.76. Found, C, 67.14; H, 9.22; N, 14.51.

**General procedure for kinetic experiments.** Kinetic experiments were performed using a Varian FT-400 MHz spectrometer. A standard solution of catalyst **1f** in deuterated THF was made. The described kinetic experiments were carried out on the *N,N'*-disopropylcarbodiimide **8a** and 4-*t*-butylaniline **7c** to form the corresponding guanidine. Reactions were carried out in J-Young NMR tubes and the reaction rates were measured by monitoring the disappearance of amine (or carbodiimide) and formation of guanidine by <sup>1</sup>H NMR spectroscopy at the described intervals over more than three half-lives. All data were processed using Varian integral analysis software. Reaction rates were derived from the plot of Ln[substrate]<sub>0</sub>/[substrate] vs time (by fitting data to the eq. Ln[substrate]<sub>0</sub>/[substrate] = k<sub>obs</sub>.t) by using linear trend lines generated by Microsoft Excel software. To obtain Arrhenius and Eyring plots, kinetic analyses were conducted at four different temperatures, each separated by approximately 5-10 K.

**Determination of reaction order with respect aniline 7c and carbodiimide 8a.** The order of the reaction with respect to amine concentration was determined holding the concentration of the other components virtually unaltered, using 1.9 mM concentration solution of catalyst **1f**, and using a carbodiimide to amine molar ratio greater than 10:1. The excess of carbodiimide concentration maintains approximately zero-order conditions. The order of the reaction with respect to the concentration of carbodiimide was studied holding an amine to carbodiimide molar ratio greater than 10:1.

## 4.6 References:

- (1) For reviews in the area see: (a) C. Alonso–Moreno, A. Antiñolo, F. Carrillo–Hermosilla, A. Otero, *Chem. Soc. Rev.* **2014**, *43*, 3406. (b) W.–X. Zhang, L. Xu, Z. Xi, *Chem. Commun.* **2015**, *51*, 254. (c) L. Xu, W.–X. Zhang, F. Xi, *Organometallics* **2015**, *34*, 1787.
- (2) See, for example: (a) R. G. S. Berlinck, A. E. Trindade–Silva, M. F. C. Santos, *Nat. Prod. Rep.* **2012**, *29*, 1382. (b) D. Castagnolo, S. Schenone, M. Botta, *Chem. Rev.* **2011**, *111*, 5247. (c) S. Ekelund, P. Nygren, R. Larsson, *Biochem. Pharmacol.* **2001**, *61*, 1183. (d) P. P. Toth, *Postgrad Med.* **2014**, *126*, 7. (e) D. T. Nash, *J. Clin. Pharmacol.* **1973**, *13*, 416. (f) N. Scheinfeld, *Dermatol. Online J.* **2003**, *9*, 4. (g) M. von Itzstein, *Nat. Rev. Drug. Discov.* **2007**, *12*, 967. (h) Y. Hirata, I. Yanagisawa, Y. Ishii, S. Tsukamoto, N. Ito, Y. Isomura, M. Takeda, U.S. Patent **1981**, 4.283.408. (i) E. Buchdunger, J. Zimmermann, H. Mett, T. Meyer, M. Mueller, B. J. Druker, N. B. Lydon, *Cancer Res.* **1996**, *56*, 100. (j) L. Troncone, V. Rufini, *Anticancer Res.* **1997**, *17*, 1823. (k) C. Loesberg, H. Van Rooij, J. C. Romijm, L. A. Smets, *Biochem. Pharmacol.* **1991**, *42*, 793.
- (3) See, for example: (a) P. J. Bailey, S. Pace, *Coord. Chem. Rev.* **2001**, *214*, 91. (b) W. E. Piers, D.J.H. Emslie, *Coord. Chem. Rev.* **2002**, *233*, 131. (c) M. P. Coles, *Dalton Trans.* **2006**, 985. (d) P. C. Junk, M. L. Cole, *Chem. Commun.* **2007**, 1579. (e) F. T. Edelmann, *Adv. Organomet. Chem.* **2008**, *57*, 183. (f) F.T. Edelmann, *Adv. Organomet. Chem.* **2013**, *61*, 55. (g) J. Barker, M. Kilner, *Coord. Chem. Rev.* **1994**, *133*, 219. (h) F. T. Edelmann, *Coord. Chem. Rev.* **1994**, *137*, 403. (i) F. T. Edelmann, *Chem. Soc. Rev.* **2009**, *38*, 2253. (j) F.T. Edelmann, *Chem. Soc. Rev.* **2012**, *41*, 7657. (k) C. Jones, *Coord. Chem. Rev.* **2010**, *254*, 1273. (l) A. A. Trifonov, *Coord. Chem. Rev.* **2010**, *254*, 1327.
- (4) See, for example: (a) T. Ishikawa, T. Isobe, *Chem.–Eur. J.* **2002**, *8*, 553. (b) T. Ishikawa, T. Kumamoto, *Synthesis* **2006**, 737. (c) T. Ishikawa, *Superbases for Organic Synthesis: Guanidines, Amidines, Phosphazenes and Organocatalysts*, John Wiley & Sons, **2009**. (d) J. E. Taylor, S. D. Bull, J. M. J. Williams, *Chem. Soc. Rev.* **2012**, *41*, 2109. (e) D. Leow, C.–H. Tan, *Chem.–Asian J.* **2009**, *4*, 488. (f) P. Selig, *Synthesis* **2013**, 703. (g) M. P. Coles, *Chem. Commun.* **2009**, 3659. (h) X. Fu, C.–H. Tan, *Chem. Commun.* **2011**, *47*, 8210. (i) A. Avila, R. Chinchilla, E. Gómez–Bengoia, C. Nájera, *Eur. J. Org. Chem.* **2013**, 5085. (j) C. Thomasa, B. Bibal, *Green Chem.* **2014**, *16*, 1687.
- (5) (a) M. K. T. Tin, N. Thirupathi, G. P. A. Yap, D. S. Richeson, *J. Chem. Soc., Dalton Trans.* **1999**, 2947. (b) M. K. T. Tin, G. P. A. Yap, D. S. Richeson, *Inorg. Chem.* **1998**, *37*, 6728. (c) E. W. Thomas, E. E. Nishizawa, D. C. Zimmermann, D. J. Williams, *J. Med. Chem.* **1989**, *32*, 228.
- (6) (a) X. Zhang, C. Wang, C. Qian, F. Han, F. Xu, Q. Shen, *Tetrahedron*, **2011**, *67*, 8790. (b) X. Zhu, Z. Du, F. Xu, Q. Shen, *J. Org. Chem.*, **2009**, *74*, 6347. (c) T.–G. Ong, G. P. A. Yap, D. S. Richeson, *J. Am. Chem. Soc.*, **2003**, *125*, 8100.
- (7) T.–G. Ong, J. S. O’Brien, I. Korobkov, D. S. Richeson, *Organometallics*, **2006**, *25*, 4728.

- (8) (a) C. Alonso–Moreno, F. Carrillo–Hermosilla, A. Garcés, A. Otero, I. López–Solera, A. M. Rodríguez, A. Antiñolo, *Organometallics* **2010**, *29*, 2789. (b) D. Elorriaga, F. Carrillo–Hermosilla, A. Antiñolo, I. López–Solera, R. Fernández–Galán, A. Serrano, E. Villaseñor, *Eur. J. Inorg. Chem.* **2013**, 2940. (c) A. Baishya, M. Kr. Barman, T. Peddarao, S. Nembenna, *J. Organomet. Chem.* **2014**, 769, 112. (d) J. R. Lachs, A. G. M. Barrett, M. R. Crimmin, G. Kociok–Köhn, M. S. Hill, M. F. Mahon, P. A. Procopiou, *Eur. J. Inorg. Chem.* **2008**, 4173.
- (9) M. R. Crimmin, A. G.M. Barrett, M. S. Hill, P. B. Hitchcock, P. A. Procopiou, *Organometallics* **2008**, *27*, 497.
- (10) S. E. Baillie, W. Clegg, P. Garcia-Alvarez, E. Hevia, A. R. Kennedy, J. Klett, L. Russo, *Chem. Commun.* **2011**, *47*, 388.
- (11) For other examples of structurally defined tris(amido)magnesiates see: (a) E. Hevia, F. R. Kenley, A. R. Kennedy, R. E. Mulvey, R. B. Rowlings, *Eur. J. Inorg. Chem.* **2003**, 3347. (b) G C. Forbes, A. R. Kennedy, R. E. Mulvey, P. J. A. Rodger, R. B. Rowlings, *J. Chem. Soc., Dalton Trans.*, **2001**, 1477. (c) W. Clegg, K. W. Henderson, R. E. Mulvey, P. A. O’Neil, *J. Chem. Soc., Dalton Trans.*, **1994**, 769. (d) B. J. Fleming, P. García–Álvarez, E. Keating, A. R. Kennedy, C. T. O’Hara, *Inorg. Chim. Acta*, **2012**, *384*, 154. (e) J. Francos, B. J. Fleming, P. García–Álvarez, A. R. Kennedy, K. Reilly, G. M. Robertson, S. D. Robertson, C. T. O’Hara, *Dalton Trans.*, **2014**, *43*, 14424.
- (12) D. Barr, W. Clegg, L. Cowton, L. Horsburgh, F. M. Mackenzie, R. E. Mulvey, *J. Chem. Soc., Chem. Comm.*, **1995**, 891.
- (13) R. Neufeld, D. Stalke, *Chem. Sci.*, **2015**, *6*, 3354.
- (14) For examples of sodium magnesiates displaying a SSIP structure in which sodium is solvated by THF molecules see: (a) D. R. Armstrong, W. Clegg, A. Hernan-Gomez, A. R. Kennedy, Z. Livingstone, S. D. Robertson, L. Russo, E. Hevia, *Dalton Trans.*, **2014**, *43*, 4361. (b) V. L. Blair, W. Clegg, A. R. Kennedy, Z. Livingstone, L. Russo, E. Hevia, *Angew. Chem., Int. Ed.*, **2011**, *50*, 9857.
- (15) For other examples of structurally defined guanidates where a similar rearrangement has taken place see references 6g, 8a, 8d, and W. X. Zhang, M. Nishiura, Z. Hou, *Chem. Eur. J.* **2007**, *13*, 4037.
- (16) G. J. Moxey, A. J. Blake, W. Lewis, D. L. Kays, *Eur. J. Inorg. Chem.*, **2015**, 5892.
- (17) A similar motif has been also reported by Chang for the reaction of Mg[N(*i*Pr)<sub>2</sub>]<sub>2</sub> with 2 eq DIC, see: B. Srinivas, C.-C. Chang, C.-H. Chen, M. Y. Chiang, I.-T. Chen, Y. Wang, G.-H. Lee, *J. Chem. Soc., Dalton Trans.*, **1997**, 957.
- (18) G. R. Giesbrecht, A. Shafir, J. Arnold, *J. Chem. Soc., Dalton Trans.*, **1999**, 3601.
- (19) C. N. Rowley, T.-G. Ong, J. Priem, T. K. Woo, D. S. Richeson, *Inorg. Chem.*, **2008**, *47*, 9660.

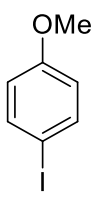
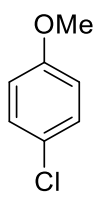
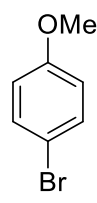
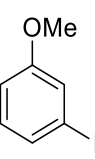
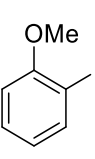
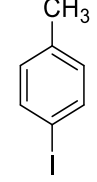
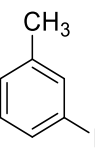
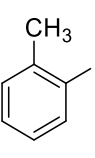
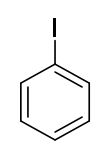
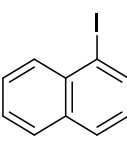
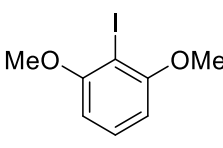
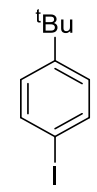
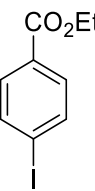
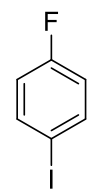
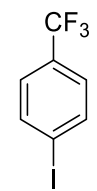
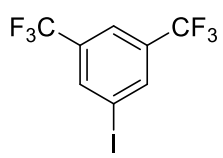
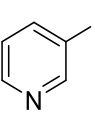
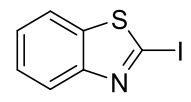
- (20) S. E. Baillie, W. Clegg, P. Garcia-Álvarez, E. Hevia, A. R. Kennedy, J. Klett, L. Russo, *Organometallics*, **2012**, 31, 5131.
- (21) For an example of anionic activation of magnesium reagents by forming mixed ammonium-magnesiates see: C. Vidal, J. Garcia-Alvarez, A. Hernan-Gomez, A. R. Kennedy, E. Hevia, *Angew. Chem. Int. Ed.* **2014**, 53, 5969.
- (22) A. Mukherjee, T. K. Sen, S. K. Mandal, B. Maity, D. Koley, *RSC Adv.* **2013**, 3, 125
- (23) J. H. Espenson, *Chemical kinetics and reaction mechanisms*, 2<sup>nd</sup> ed.; McGraw-Hill: New York, **1995**.
- (24) (a) J. F. Dunne, D. B. Fulton, A. Ellern, A. D. Sadow, *J. Am. Chem. Soc.* **2010**, 132, 17680; (b) C. Brinkmann, A. G. M. Barrett, M. S. Hill, P. A. Procopiu, *J. Am. Chem. Soc.* **2012**, 134, 2193.
- (25) (a) T. G. Ong, G. P. A. Yap, D. S. Richeson, *J. Am. Chem. Soc.* **2003**, 125, 8100; (b) Q. Li, S. Wang, S. Zhou, G. Yang, X. Zhu, Y. Liu, *J. Org. Chem.* **2007**, 72, 6763; (c) S4. Z. Du, W. Li, X. Zhu, F. Xu, Q. Shen, *J. Org. Chem.* **2008**, 73, 8966; (d) M. P. Coles, P. B. Hitchcock, *Chem. Commun.* **2002**, 2794.
- (26) *CrysAlisPro*; Oxford Diffraction: Oxford, UK **2008**.
- (27) G. Sheldrick, *Acta Cryst.* **2015**, C71, 3-8.

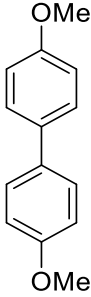
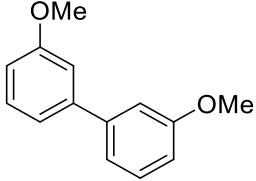
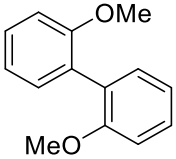
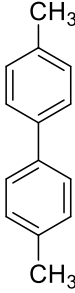
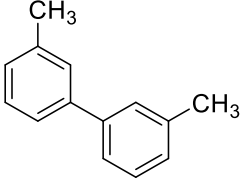
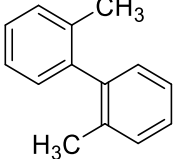
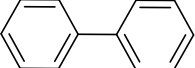
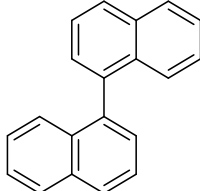
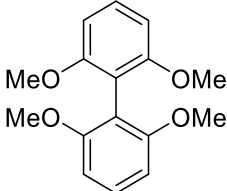
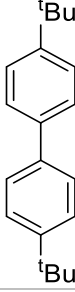
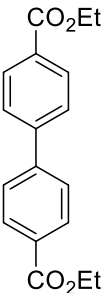
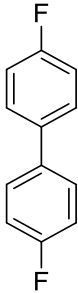
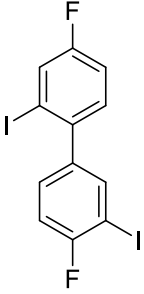
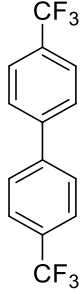
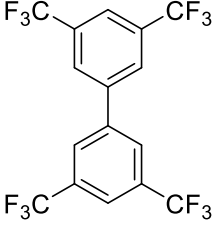
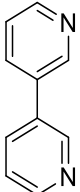
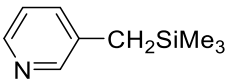
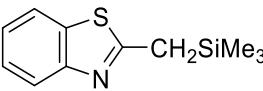
## **CHAPTER 5**

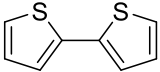
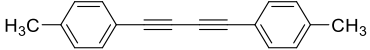
**Using Lithium Manganates to access symmetric biaryl  
compounds: Tandem Mn-I exchange, C-C homocoupling  
processes**

## V. Table of compounds

<b>1s</b>	[LiMn(CH <sub>2</sub> SiMe <sub>3</sub> ) <sub>3</sub> ]	<b>1t</b>	[(TMEDA) <sub>2</sub> Li <sub>2</sub> Mn(CH <sub>2</sub> SiMe <sub>3</sub> ) <sub>4</sub> ]
<b>1u</b>	[(THF) <sub>x</sub> Li <sub>2</sub> Mn(CH <sub>2</sub> SiMe <sub>3</sub> ) <sub>4</sub> ]		

<b>10a</b>		<b>10b</b>		<b>10c</b>	
<b>10d</b>		<b>10e</b>		<b>10f</b>	
<b>10g</b>		<b>10h</b>		<b>10i</b>	
<b>10j</b>		<b>10k</b>		<b>10l</b>	
<b>10m</b>		<b>10n</b>		<b>10o</b>	
<b>10p</b>		<b>10q</b>		<b>10r</b>	

<b>11a</b>		<b>11b</b>		<b>11c</b>	
<b>11d</b>		<b>11e</b>		<b>11f</b>	
<b>11g</b>		<b>11h</b>		<b>11i</b>	
<b>11j</b>		<b>11k</b>		<b>11l</b>	
<b>11l'</b>		<b>11m</b>		<b>11n</b>	
<b>11o</b>		<b>11o'</b>		<b>11p</b>	

<b>11q</b>	 <chem>C1=CC=C(S1)-C2=CC=C(S2)</chem>	<b>11r</b>	 <chem>Cc1ccc(cc1)C#CC#Cc2ccc(C)cc2</chem>	
------------	---	------------	---	--

## 5.1 Summary

Unveiling a new application of cooperative alkali metal manganates, this chapter describes the synthesis of symmetric biaryl compounds from a temperature controlled procedure which includes a direct Mn/I exchange reaction at sub-ambient temperature (-78 °C) followed by homocoupling reaction. The bimetallic reagents employed in this study are [(THF)<sub>x</sub>LiMn(CH<sub>2</sub>SiMe<sub>3</sub>)<sub>3</sub>] (**1s**) and [(TMEDA)<sub>2</sub>Li<sub>2</sub>Mn(CH<sub>2</sub>SiMe<sub>3</sub>)<sub>4</sub>] **1t** however in the vast majority of the reactions an in situ version of bimetallic complex **1t** will be employed, namely [(THF)<sub>x</sub>Li<sub>2</sub>Mn(CH<sub>2</sub>SiMe<sub>3</sub>)<sub>4</sub>] **1u** resulting from the reaction of an excess of LiCH<sub>2</sub>SiMe<sub>3</sub> with MnCl<sub>2</sub> in THF.

Using 4-iodoanisole (**10a**) as a case study, showed that while higher order lithium manganate **1t** and **1u** can efficiently promote Mn/I exchange at -78°C and homocoupling at ambient temperature to form 4,4'-dimethoxy-1,1'-biphenyl (**11a**) lower-order manganate **1s** displayed sluggish reactivity towards **10a** as only 22% formation of **11a** could be observed. The enhanced reactivity of **1t** and **1u** contrasts with the results obtained when the same substrate **10a** is confronted with Mn(CH<sub>2</sub>SiMe<sub>3</sub>)<sub>2</sub> which is completely inert towards Mn/I exchange or LiCH<sub>2</sub>SiMe<sub>3</sub>, which is able to promote Li/I exchange but it does not give any formation of homocoupled product **11a**. A dramatic lithium effect is observed, as when the reaction is carried out using 12-crown-4, which captures the Li atoms, **1u** fails to promote the Mn/I exchange and no product is observed at all. The methodology was extended to other substrates, thus reaction of **1u** with 3-iodoanisole (**10d**), 2-iodoanisole (**10e**), 4-iodotoluene (**10f**), 3-iodotoluene (**10g**) and 2-iodotoluene (**10h**) allowed formation of symmetric biaryl compounds **11a-11f** in yields ranging from 60% to 80%. Substitution effect showed *ortho*-substituted iodoaryl substrates to be the most reactive reagents. Both substrates containing electron donating groups such as 1-(*tert*-butyl)-4-iodobenzene (**10l**) and electron withdrawing groups such as 1-fluoro-4-iodobenzene (**10n**) worked well (84% and 69% yield respectively). Fluorinated substrates such as 1-fluoro-4-iodobenzene (**10n**), 1-iodo-4-(trifluoromethyl)benzene (**10o**) and 1-iodo-3,5-bis(trifluoromethyl)benzene (**10p**) worked well with yields of homocoupling products ranging from 68% to 73% yield. Particularly interesting is the reactivity of 3-iodopyridine (**10q**) which gave a mixture of homocoupled product **11o** and cross coupled product **11o'** with the CH<sub>2</sub>SiMe<sub>3</sub> group and 2-iodobenzothiazole (**10r**) were the cross coupled product **11p** was the major product of the reaction. Thus, **1u** was found to be a versatile reagent for the synthesis of a variety of symmetric biaryl compounds.

## 5.2 Introduction

Symmetric biaryl compounds are important building blocks in nature.<sup>1</sup> They are commonly present in many chiral biologically active natural products such as (+) Podototarín with antibacterial activity against gram-positive bacteria,<sup>2</sup> or atropisomers such as Michellamine B, a strong anti-HIV viral replication inhibitor<sup>3</sup> and Mastigophorene A which stimulates nerve growth<sup>4-6</sup> to name a few (**Figure 5.1**).

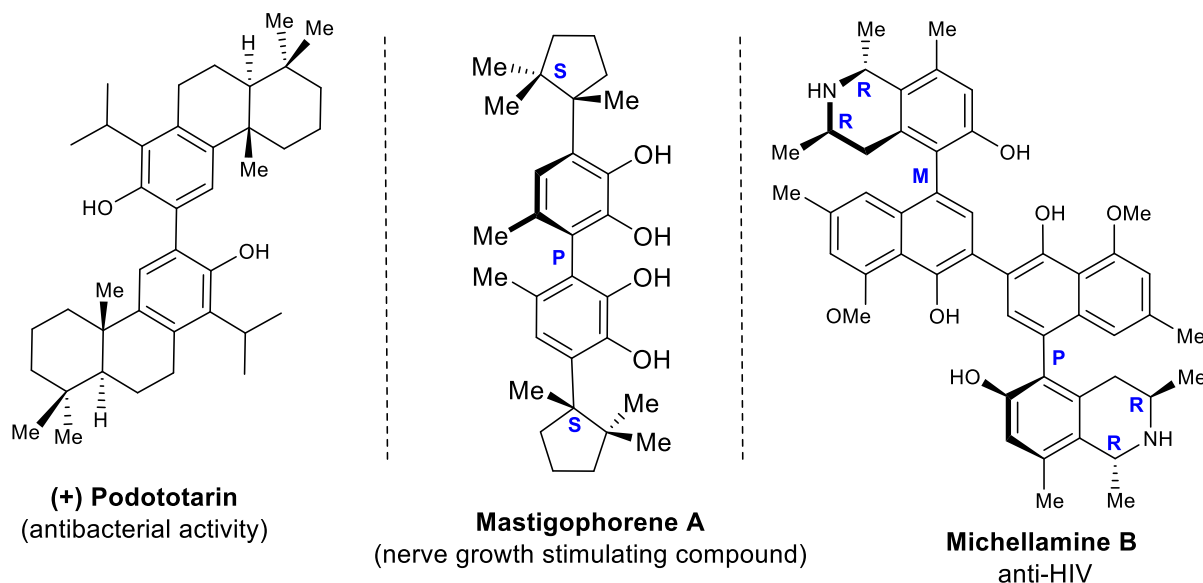
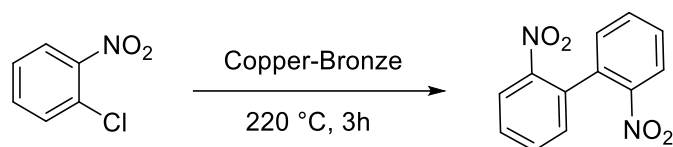


**Figure 5.1:** biologically active symmetric biaryl natural products

In addition biaryl substrates are present in ligands such as (R)-P-PHOS and R-BINAP which play a major role in catalysis.<sup>6,7</sup> Symmetric biaryl compounds can be prepared in different ways. Homocoupling reactions are amongst the most utilised methods for the generation of new C-C bonds in synthesis. This methodology represents one of the most useful methods for the synthesis of biaryl compounds. For more than 50 years along the 20<sup>th</sup> century copper was almost the only protagonist in the generation of aryl-aryl bonds. Initial research in this area involved the use of copper and copper-bronze alloy under stoichiometric conditions to carry out the reductive symmetrical coupling of aryl halides (Ullmann reaction, **Scheme 5.1**).<sup>8</sup>



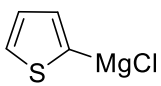
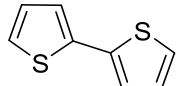
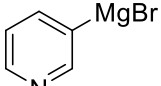
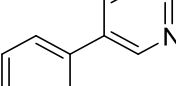
**Scheme 5.1:** example of Ullmann coupling type reaction

This methodology requires harsh reaction conditions therefore other methods have been discovered ever since.<sup>9</sup> Different versions of palladium-catalysed homocoupling reactions of aryl halides have been developed. Examples include the palladium-catalysed coupling reactions of chloroaryls in water,<sup>10</sup> the coupling of iodoaryls in supercritical carbon dioxide or under solvent free conditions<sup>11</sup> and Feringa's recent development in palladium-catalysed, *tert*-butyllithium-mediated dimerisation of of aryl halides.<sup>6</sup> This methodology allows to carry out the reaction at ambient temperatures and it enables the synthesis of a variety of symmetric biaryl compounds in high yields. In addition the authors carried out the atroposelective total synthesis of mastigophorene A in only eight reaction steps, a major improvement considering that the previous shorter methodology required more than 20 steps.

Manganese is a good alternative to generate C-C bonds in cross coupling reactions. Cahiez and Normant development of Mn-catalysed homocoupling reactions in 1976 was the first Mn-catalysed application in this field (see **chapter 1.4.3**) which was further developed in the following decades. Proof of concepts has been established by Cahiez who has reported the manganese-catalysed homocoupling of Grignard reagents.<sup>12,13</sup>

**Table 5.1:** Cahiez manganese-catalysed homocoupling of Grignard reagents

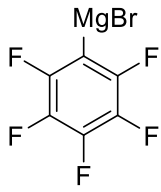
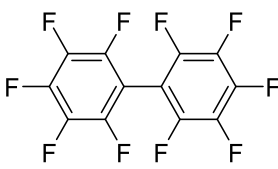
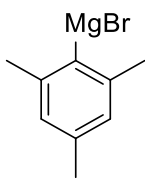
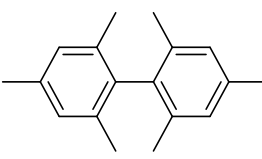
$\text{RMgX} \xrightarrow[\text{THF, RT, 45 min}]{\text{Dry air, 5 mol\% MnCl}_2 \cdot \text{LiCl}} \text{R-R}$			
Entry	RMgX	Product	Yield (%) <sup>a</sup>
1			95
2			76
3			80 <sup>b</sup>

Entry	RMgX	Product	Yield (%) <sup>a</sup>
4			91
5			80
6	Ph—C≡C—MgCl	Ph—C≡C—C≡C—Ph	89

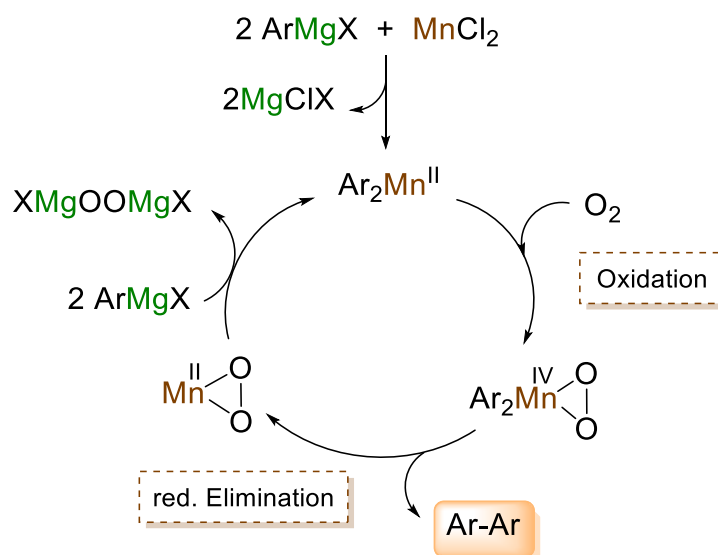
[a] Isolated yield. [b] The reaction was performed at -20 °C.

The reaction of an aryl Grignard reagent with air in the presence of manganese chloride readily forms a biaryl. In addition substrate scope can be expanded to alkynyl Grignard reagents with the corresponding formation of the 1,3-diyne species (**Table 5.1**). These procedure is highly dependent on both steric and electronic factors. The use of *ortho*-substituted aryl groups as substrates with high steric hindrance lead to lower yields in the formation of biaryls by homocoupling reaction. This detrimental effect is well established.<sup>9,14</sup> Thus, electron-poor pentafluorophenylmagnesium chloride does not give the expected homocoupling product, while hindered mesitylmagnesium bromide gives only traces of the coupled product (**Table 5.2**).

**Table 5.2:** Limitations of Cahiez Mn-catalysed homocoupling reaction

$\text{RMgX} \xrightarrow[\text{O}_2, \text{THF}, 0^\circ\text{C}, 1 \text{ hour}]{20 \text{ mol\% MnCl}_2 \cdot \text{LiCl}} \text{R-R}$			
Entry	RMgX	Product	Yield (%)
1			0
2			traces

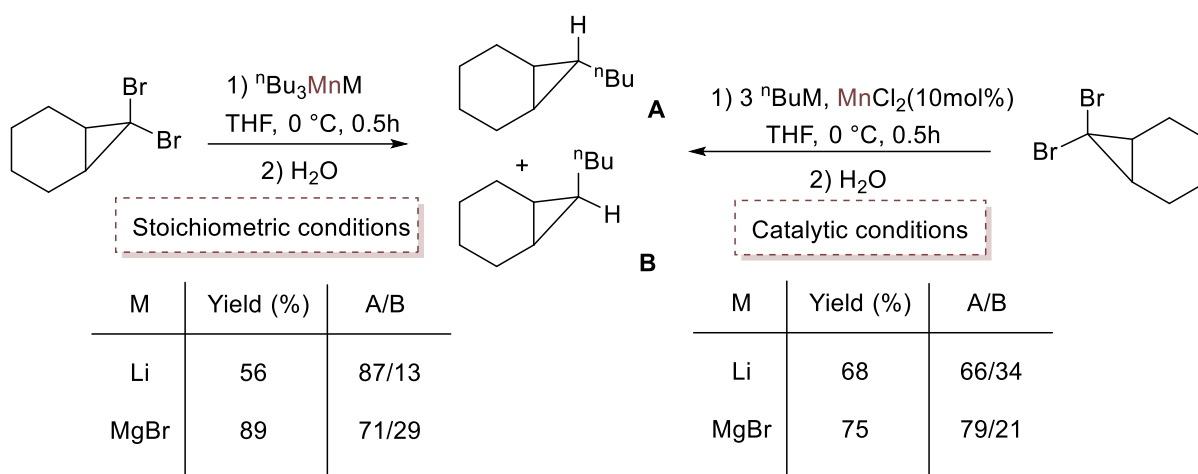
In 2009 Cahiez and collaborators carried out the manganese-catalysed oxidative cross-coupling of Grignard reagents.<sup>15</sup> In all cases oxygen was required as an oxidant for the reaction to take place. The proposed mechanism for this transformation involves the formation of Mn(II)-Mn(IV) intermediates (**Scheme 5.2**).

**Scheme 5.2:** Cahiez proposed mechanism for Mn-catalysed homocoupling of Grignard reagents.

The first step involves a transmetalation reaction between the aryl Grignard reagent  $\text{ArMgX}$  and  $\text{MnCl}_2$  to form  $\text{R}_2\text{Mn}^{\text{II}}$ . Then oxidation of  $\text{Ar}_2\text{Mn}^{\text{II}}$  species by molecular oxygen to form

the reactive and unstable  $\text{Ar}_2\text{Mn}^{\text{IV}}(\text{O}_2)$  species. Therefore reductive elimination of  $\text{Ar}_2\text{Mn}^{\text{IV}}(\text{O}_2)$  species quickly give rise to the formation of Ar-Ar coupling product and  $\text{Mn}^{\text{II}}(\text{O}_2)$ . The aryl Grignard reagent regenerates the active  $\text{Ar}_2\text{Mn}^{\text{II}}$  species which can further proceed with another reaction cycle. Despite of the presence of LiCl in the manganese reagent employed in this transformation, namely  $\text{MnCl}_2\cdot\text{LiCl}$ , authors do not include LiCl in the catalytic cycle, its presence was attributed merely to solubility reasons and was never included in proposed intermediates. Also it should be noted that the formation of mixed-metal ate intermediates is not proposed.

Furthermore, Oshima *et al* have reported the dialkylation of gem-dibromocyclopropanes using trialkylmanganates such as  $\text{MMnR}_3$  ( $\text{M} = \text{Li}, \text{MgX}$ ). In this case the reaction can be carried out both under stoichiometric and catalytic regimes (**Scheme 5.3**).<sup>16</sup>



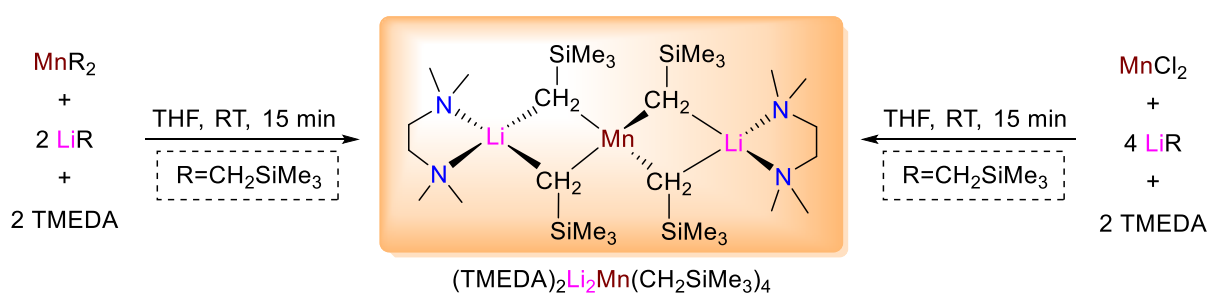
**Scheme 5.3:** Dialkylation of gem-dibromocyclopropanes using  $\text{MMnR}_3$  ( $\text{M} = \text{Li}, \text{MgX}$ )

Interestingly the same reaction was previously described by Corey *et al* using dibutylcuprate,<sup>17</sup> however the reaction required to be carried out a lower temperatures ( $-15\text{ }^\circ\text{C}$ ) and lower yields were obtained. Furthermore tributylzincate<sup>18</sup> was also described to promote the same reaction at  $-85\text{ }^\circ\text{C}$  to prevent decomposition. Although this is a very useful method for the synthesis of C-C bonds authors fail to propose a mechanism for this transformation. Furthermore, regarding the use of manganates, Corey described the synthesis of C-C bonds by methylation reaction of iodo-derivatives using  $\text{LiMnMe}_3$ .<sup>19</sup>

## 5.3 Results and discussion

### 5.3.1 Synthesis of starting material

This chapter builds on synthetic and structural work carried out by another member of the Hevia group who has studied the synthesis and structures of homoleptic alkyl alkali-metal manganates such as  $[\text{LiMn}(\text{CH}_2\text{SiMe}_3)_3]$  (**1s**),  $[(\text{TMEDA})_2\text{Li}_2\text{Mn}(\text{CH}_2\text{SiMe}_3)_4]$  (**1t**) as well as developed the in situ preparation of  $(\text{THF})_x\text{Li}_2\text{Mn}(\text{CH}_2\text{SiMe}_3)_4$  (**1u**).  $\text{Mn}(\text{CH}_2\text{SiMe}_3)_2$  was prepared according to the literature procedure.<sup>20,21</sup> Homoleptic lithium manganates  $[(\text{TMEDA})_2\text{Li}_2\text{Mn}(\text{CH}_2\text{SiMe}_3)_4]$  (**1t**) can be synthesised by co-complexation reaction between  $\text{LiCH}_2\text{SiMe}_3$  and  $\text{Mn}(\text{CH}_2\text{SiMe}_3)_2$  in hexane at room temperature using a 2:1 stoichiometric ratio, followed by the addition of 2 molar equivalents of Lewis donor TMEDA, this afforded an orange suspension. Gentle heating led to an orange solution which upon slow cooling yielded crystals of  $[(\text{TMEDA})_2\text{Li}_2\text{Mn}(\text{CH}_2\text{SiMe}_3)_4]$  (**1t**). In addition a salt metathesis approach can be employed for the synthesis of the same compound. Mixing  $\text{MnCl}_2$  and four equivalents of  $\text{LiCH}_2\text{SiMe}_3$  in THF at room temperature formed an orange solution after 15 minutes which suggests the formation of **1t**. The solvent was then removed under vacuum and hexane was added to precipitate the presumably formed  $\text{LiCl}$ ; the solution was then filtered and two equivalents of TMEDA were added. The product was solubilised with toluene and crystallised at  $-33\text{ }^\circ\text{C}$  to yield **1t** in 38% yield. Although the isolated crystalline yield for **1t** was lower (38%), these results confirmed that this mixed lithium manganese complex can be easily prepared in situ using two commercially available reagents (**Scheme 5.4**).



**Scheme 5.4:** Different approaches for the synthesis of  $[(\text{TMEDA})_2\text{Li}_2\text{Mn}(\text{CH}_2\text{SiMe}_3)_4]$  (**1t**)

Structural and synthetic studies carried out by Dr. M. Uzelac within our group have established the molecular structure of  $[(\text{TMEDA})_2\text{Li}_2\text{Mn}(\text{CH}_2\text{SiMe}_3)_4]$  **1t**, which displays a classical “Weiss motif”<sup>22,23</sup> contacted ion-pair structure where the four alkyl groups form bridges between the central Mn atom and the N-donor solvated alkali-metal (**Figure 5.2**).

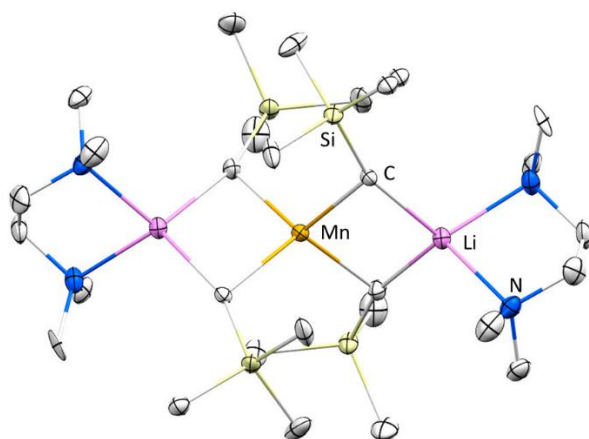
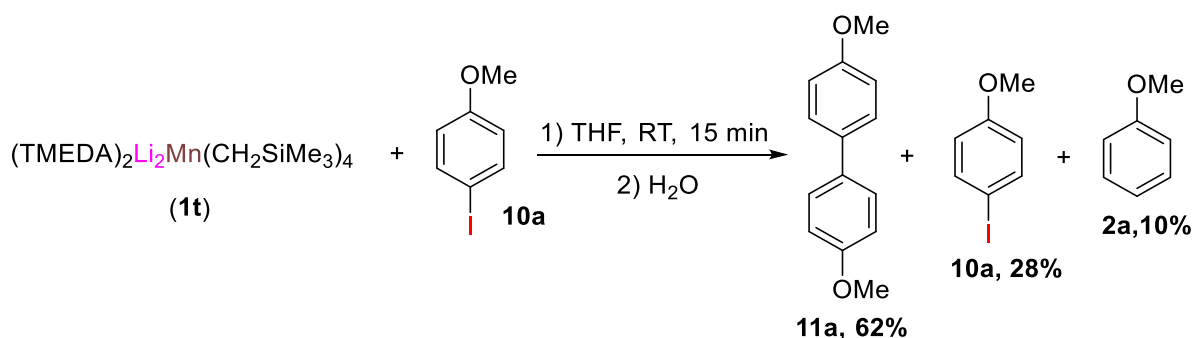


**Figure 5.2:** Monomeric structure of [(TMEDA)<sub>2</sub>Li<sub>2</sub>Mn(CH<sub>2</sub>SiMe<sub>3</sub>)<sub>4</sub>] (**1t**)

**1t** is isostructural with the structures [(TMEDA)<sub>2</sub>Li<sub>2</sub>Mn(R)<sub>4</sub>] (R=Me, Et, CH<sub>2</sub>CH<sub>2</sub>CMe<sub>3</sub>) reported by Girolami.<sup>24,25</sup> Similarly **1f** is isostructural with previously used and described alkali metal magnesiates [(TMEDA)<sub>2</sub>Am<sub>2</sub>Mg(CH<sub>2</sub>SiMe<sub>3</sub>)<sub>4</sub>] (Am = Na, Li for structures **1d** and **1e** respectively).<sup>26</sup>

### 5.3.2 Assessing the ability of lithium manganates to promote Mn/halogen exchange reactions followed by homocoupling.

Preliminary studies carried out in our group using [(TMEDA)<sub>2</sub>Li<sub>2</sub>Mn(CH<sub>2</sub>SiMe<sub>3</sub>)<sub>4</sub>] (**1t**) for the reaction of 4-iodoanisole (**10a**) revealed that Mn/I exchange and homocoupling quickly takes place; in fact GC-analyses of hydrolysed reaction aliquots carried out after 15 minutes reaction revealed 62% consumption of starting material and formation of two different products (**Scheme 5.5**).



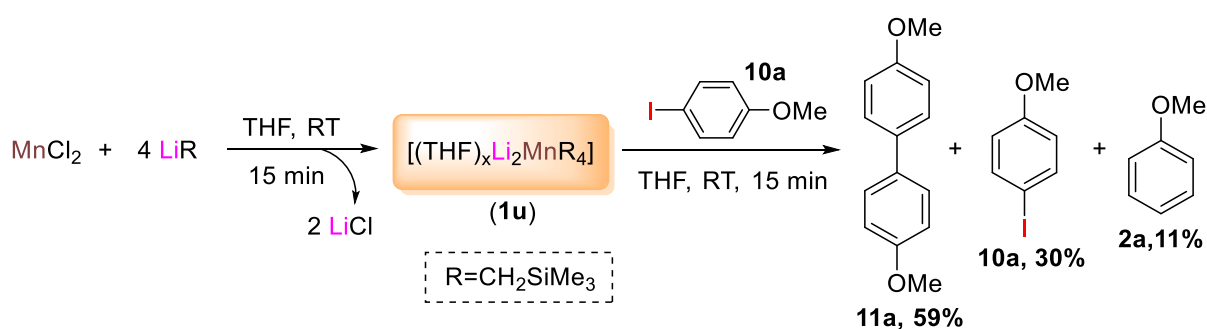
**Scheme 5.5:** Unoptimised Mn/I exchange and homocoupling reaction between **1t** with four equivalents of 4-iodoanisole followed by aqueous work-up.

Subsequent <sup>1</sup>H and <sup>13</sup>C NMR spectroscopic analysis of hydrolysed reaction mixture confirmed the identities of products and integration against hexamethylbenzene revealed 4,4'-dimethoxy-1,1'-biphenyl (**11a**) to be the main product (62%). Starting material 4-iodoanisole and anisole

as by product were recovered in 28% yield and 10% yield respectively. The presence of anisole has been confirmed in the  $^1\text{H}$  NMR spectra, but due to its volatility, the yield given is actually calculated as a difference up to 100%. This protocol shows good synthetic potential for the synthesis of symmetric biaryl compounds, under relatively mild reaction conditions, short reaction times and substoichiometric amount of lithium manganese **1t**. Therefore optimisation of reaction conditions and expansion of the substrate scope was then developed.

### 5.3.3 Optimisation of reaction conditions

First step in the optimisation of the reaction conditions was to compare the activity of isolated crystals of  $[(\text{TMEDA})_2\text{Li}_2\text{Mn}(\text{CH}_2\text{SiMe}_3)_4]$  (**1t**) with an in situ mixture of the base in THF. Reaction of  $\text{LiCH}_2\text{SiMe}_3$  and  $\text{MnCl}_2$  in a 4:1 ratio in THF at RT for 15 minutes allowed the formation of an orange solution, which is a sign of co-complexation to form the presumed  $[(\text{THF})_x\text{Li}_2\text{Mn}(\text{CH}_2\text{SiMe}_3)_4]$  (**1u**) as  $\text{MnCl}_2$  is not soluble in THF. The reaction in **Scheme 5.5** was repeated under the same reaction conditions using the in situ prepared  $[(\text{THF})_x\text{Li}_2\text{Mn}(\text{CH}_2\text{SiMe}_3)_4]$  complex (**1u**), therefore 1 equivalent of **1u** reacted with 4 equivalents of 4-iodoanisole at room temperature for 15 minutes.  $^1\text{H}$  NMR analysis after quenching with  $\text{H}_2\text{O}$  revealed formation of 59% yield of coupled product **11a** and 30% yield of starting material recovered along with 11% presumed formation of anisole as a by-product (**Scheme 5.6**).



**Scheme 5.6:** Reactivity of an in situ prepared  $(\text{THF})_x\text{Li}_2\text{MnR}_4$  with 4-Iodoanisole.

This result is similar when compared to the one obtained when using crystalline (**1t**) (62% yield obtained of **11a** **Scheme 5.5**). This allows to use commercially available reagents without observing any substantial decrease in yield of homocoupled product **11a**. Different reaction conditions for the Mn/I exchange step of these methodology were then studied initially the studies focused on the effect of the temperature and reaction time for the Mn/I exchange reaction, which is the first step of the reaction procedure (**Table 5.3**).

**Table 5.3:** Optimisation of the reaction conditions for the Mn/I exchange reaction step of the reaction procedure

	Entry	Ratio 1u: 10a	T (°C)	Time (min)	Yield (%) <sup>a</sup>			
					11a	10a	2a <sup>b</sup>	
	1	1:4	RT	15	59	30	11	
	2	1:4	0	15	64	26	10	
	3	1:4	-78	15	75	19	6	
	4	1:4	-78	60	76	19	5	
	5	1:3	-78	15	80	10	10	
	6	1:1	-78	15	90	0	10	

[a] Yields obtained via spectroscopic <sup>1</sup>H NMR integration of signals for product **11a**, starting material **10a** and by-product **2a** with addition of hexamethylbenzene (10 mol %) as internal standard. [b] The presence of **2a** has been confirmed in the <sup>1</sup>H NMR analysis, but due to its volatility, the amount in the table is calculated as a difference up to 100 %.

Therefore the reaction of [(THF)<sub>x</sub>Li<sub>2</sub>Mn(CH<sub>2</sub>SiMe<sub>3</sub>)<sub>4</sub>] (**1u**) with 4 equivalents of **10a** was carried out at low temperature (0 °C) for 15 minutes. Thereafter the temperature was raised to ambient temperature and the reaction mixture was left stirring for 15 minutes. <sup>1</sup>H NMR analysis after quenching with H<sub>2</sub>O revealed the formation of **11a** in moderate yield (64%) along with 26% yield of **10a** recovered and 10% yield of **2a** (Entry 2, **Table 5.3**). The reaction was then repeated at -78 °C following the exact same procedure as the reaction described above. Therefore the homocoupled product **11a** was obtained in 75% yield under these reaction conditions (Entry 3, **Table 5.3**). No substantial increase in the reaction yield was detected by increasing the reaction time, in fact when the reaction is carried out under the same reaction

conditions but leaving stirring at  $-78\text{ }^{\circ}\text{C}$  for 1 hour **11a** was obtained in 76% yield along with 19% yield of recovered starting material (Entry 4 **Table 5.3**). This result is very similar to the one obtained in entry 3 **Table 5.3** where the yield of **11a** was 75% in 15 minutes reaction time. Finally in order to further increase the yield of **11a** the reaction was carried out using a 1:3 ratio of **1u**:**10a** at  $-78\text{ }^{\circ}\text{C}$  for 15 minutes. This implies a slight excess (1.3 equivalents) of R groups with respect to the substrate **10a**. The temperature was then raised to ambient temperature and the reaction mixture was stirred for 15 minutes.  $^1\text{H}$  NMR analysis after quenching with  $\text{H}_2\text{O}$  revealed the formation of **11a** in 80% yield along with 10% yield of starting material recovered and 10% formation of **2a** (Entry 5, **Table 5.3**). Reaction of **1u** with **10a** using excess of the ate (1:1 ratio) gave formation of homocoupled product **11a** in 90% yield, however no starting material was observed in this case (Entry 6, **Table 5.3**).

Furthermore the effect of the temperature and reaction time on the second step of the reaction was studied, which refers to the C-C bond forming part of the reaction procedure through homocoupling (**Table 5.4**).

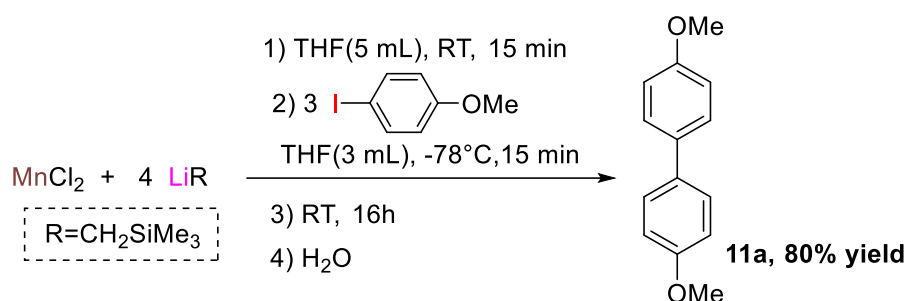
**Table 5.4:** Optimisation of the reaction conditions for the homocoupling step of the reaction procedure.

	Entry	T ( $^{\circ}\text{C}$ )	Time (h)	Yield (%) <sup>a</sup>			
				11a	10a	2a <sup>b</sup>	
	1	RT	0.25	80	10	10	
	2	RT	16	84	8	8	
	3	65	1	72	14	14	

[a] Yields obtained via spectroscopic  $^1\text{H}$  NMR integration of signals for product **11a**, starting material **10a** and by-product **2a** with addition of hexamethylbenzene (10 mol %) as internal standard. [b] The presence of **2a** has been confirmed in the  $^1\text{H}$  NMR analysis, but due to its volatility, the amount in the table is calculated as a difference up to 100 %.

Therefore the reaction of **1u** with 3 equivalents of **10a** was carried out at -78 °C for 15 minutes, after that the temperature was raised to ambient temperature and the reaction mixture was left stirring for 16 hours. <sup>1</sup>H NMR analysis after quenching with H<sub>2</sub>O revealed the formation of **11a** in excellent yield (84%) along with 8% yield of **10a** recovered and 8% yield of **2a** (Entry 2, **Table 5.4**). Repeating the reaction under the same conditions but increasing the temperature from -78 °C to 65 °C after Mn/I exchange took place, gave formation of coupled product **11a** in a lower yield (72%, entry 2, **Table 5.4**).

The reaction was repeated using optimised reaction conditions and compound **11a** was isolated in 80% yield by column chromatography (**Scheme 5.7**) and characterised by <sup>1</sup>H and <sup>13</sup>C NMR (See experimental section for further details).



**Scheme 5.7:** Optimised conditions for the reaction between  $(\text{THF})_x\text{Li}_2\text{MnR}_4$  with three equivalents of 4-iodoanisole.

The reactivity of  $[(\text{THF})_x\text{Li}_2\text{Mn}(\text{CH}_2\text{SiMe}_3)_4]$  **1u** was compared to those exhibited by their homometallic counterparts  $\text{Li}(\text{CH}_2\text{SiMe}_3)$  and  $\text{Mn}(\text{CH}_2\text{SiMe}_3)_2$  and other Mn-ate species. Thus following the same approach **10a** was confronted with  $\text{Li}(\text{CH}_2\text{SiMe}_3)$  in THF, stirred at -78 °C for 15 minutes. The temperature was then raised to ambient temperature and the solution was left stirring for 16 hours. An aliquot of the reaction mixture was then quenched with H<sub>2</sub>O and analysed by <sup>1</sup>H NMR analysis to give **2a** in 75% yield and 25% of starting material recovered. LiR promotes the expected Li/I exchange reaction however no homocoupling product **11a** was observed (Entry 1, **Table 5.5**). The ability of lithium reagents to promote Li/halogen exchange reactions was discovered in 1938 by Wittig and Gilman simultaneously and it has been one of the most powerful methods to functionalise aromatic halides in synthesis.<sup>27-29</sup>

**Table 5.5:** Comparison of the activity of  $(\text{THF})_x\text{Li}_2\text{MnR}_4$  and other species such as  $\text{Li}(\text{CH}_2\text{SiMe}_3)_2$ ,  $\text{Mn}(\text{CH}_2\text{SiMe}_3)_2$  towards Mn/I exchange reaction followed by homocoupling.

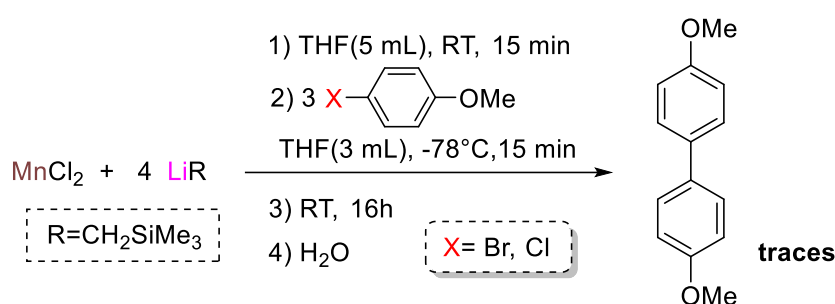
Entry	MxR (R=CH <sub>2</sub> SiMe <sub>3</sub> )	Yield (%) <sup>a</sup>		
		11a	10a	2a <sup>b</sup>
1	LiR <sup>c</sup>	0	25	75
2	MnR <sub>2</sub> <sup>c</sup>	0	92	8
3	[LiMnR <sub>3</sub> ] <sup>d</sup>	22	60	18
4	[(THF) <sub>x</sub> Li <sub>2</sub> MnR <sub>4</sub> ] <sup>e</sup>	84	8	8

[a] Yields obtained via spectroscopic <sup>1</sup>H NMR integration of signals for product **11a**, starting material **10a** and by-product **2a** with addition of hexamethylbenzene (10 mol %) as internal standard. [b] The presence of **2a** has been confirmed in the <sup>1</sup>H NMR analysis, but due to its volatility, the amount in the table is calculated as a difference up to 100 %. [c] Reaction carried out using a 1:1 stoichiometry between MxR:**10a**. [d] Reaction carried out using a 1:3 stoichiometry between LiMnR<sub>3</sub>:**10a** [e] Reaction carried out using optimised reaction conditions from **Scheme 5.5**.

When the reaction was carried out with  $\text{Mn}(\text{CH}_2\text{SiMe}_3)_2$  under the same reaction conditions almost full recovery of starting material was obtained (92% of **10a**) along with small quantity of **2a** formed (Entry 2, **Table 5.5**). Monometallic  $\text{Mn}(\text{CH}_2\text{SiMe}_3)_2$  fails to promote Mn/I exchange reaction therefore no homocoupling product is obtained. The activity of lower order lithium manganate  $\text{LiMn}(\text{CH}_2\text{SiMe}_3)_3$  (**1s**) was also studied. Reaction of **1s** with three equivalents of **10a** afforded 22% yield of homocoupled product along with 60% of starting material recovered and 18% presumed formation of **2a** (Entry 3, **Table 5.5**). This result shows a remarkably lower activity of  $\text{LiMn}(\text{CH}_2\text{SiMe}_3)_3$  compared to higher order lithium manganate **1u** (Entry 4, **Table 5.5**). The recovery of starting material in 60% yield indicates once more the difficulty of  $\text{LiMn}(\text{CH}_2\text{SiMe}_3)_3$  to promote Mn/I exchange reaction under the reaction conditions taken into account, therefore only a low amount of homocoupling product **11a** could

be observed (22%). These results highlight the higher activity of manganate species compared to the monometallic complexes.

The effect of the halogen atom was also investigated. Thus the activity of the lithium manganate towards Mn/X exchange was studied from the reaction between  $[(\text{THF})_x\text{Li}_2\text{Mn}(\text{CH}_2\text{SiMe}_3)_4]$  and 4-chloroanisole (**10b**), 4-bromoanisole (**10c**) and comparing these results with the one obtained for the reaction between **1u** and **10a**. It is worth mentioning that when 1 equivalent of **1u** reacts with 3 equivalents of **10b** following the optimised reaction conditions (see **Scheme 5.7** for details) no homocoupled product is obtained. Similarly when using **10c** only traces of homocoupled product were obtained under these reaction conditions (**Scheme 5.8**).



**Scheme 5.8:** Halogen effect on the reaction procedure.

These results are somehow expected especially taking into account the bond dissociation energy for the different Aryl-X bonds (**Table 5.6**).<sup>30</sup>

**Table 5.6:** Bond dissociation energies of aryl halides

Bond	Dissociation energy (KJ mol <sup>-1</sup> )
Ph-F	533
Ph-Cl	407
Ph-Br	346
Ph-I	280

$\text{C}_{\text{sp}2}$ -halogen bond dissociation energy decreases from top to bottom in group 17 of the periodic table, making very difficult the dissociation between  $\text{C}_{\text{sp}2}\text{-F}$  bond (533 KJ·mol<sup>-1</sup>) and more feasible the  $\text{C}_{\text{sp}2}\text{-I}$  rupture (280 KJ·mol<sup>-1</sup>). The stoichiometry of the reaction played an important role in this case, in fact when the reaction is carried out using a 1:1 ratio between **1u**

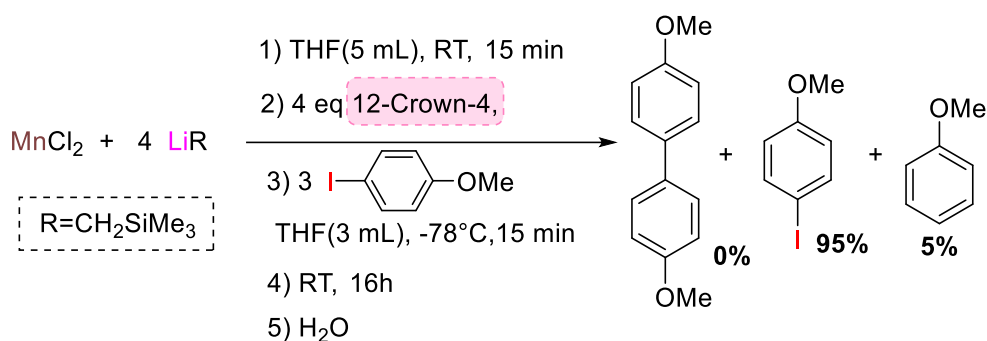
and **10c**, homocoupled product was obtained in low 30% yield along with 41% yield recovery of starting material (Entry 2, **Table 5.7**). However lithium manganate **1u** is unable to promote a noticeable Mn/Cl exchange upon reaction with **10b** even when using excess of the ate (1:1 ratio) as in this case only traces of homocoupled product are obtained (Entry 2, **Table 5.7**).

**Table 5.7:** Reactivity of  $(\text{THF})_x\text{Li}_2\text{MnR}_4$  in Mn/halogen exchange with different halogen atoms.

Entry	X	Yield (%) <sup>a</sup>		
		11a	10x	2a <sup>b</sup>
1	Cl	traces	78	18
2	Br	30	41	8
3	I	90	0	8

[a] Yields obtained via spectroscopic <sup>1</sup>H NMR integration of signals for product **11a**, starting material **10a** and by-product **2a** with addition of hexamethylbenzene (10 mol %) as internal standard. [b] The presence of **2a** has been confirmed in the <sup>1</sup>H NMR analysis, but due to its volatility, the amount in the table is calculated as a difference up to 100 %.

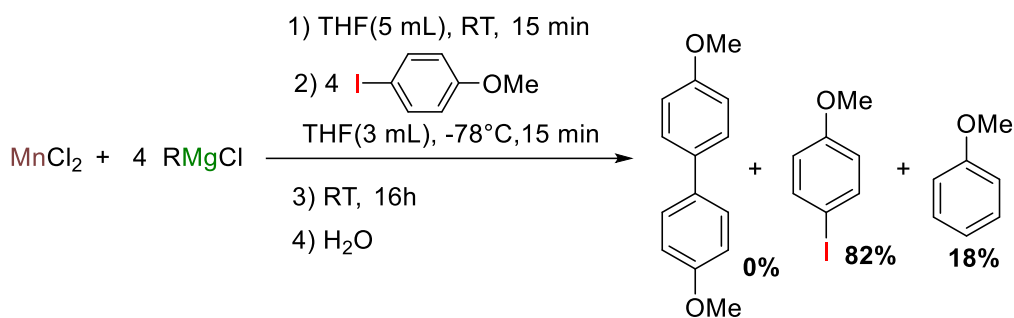
To assess the possible role of lithium in this process, lithium manganate **1u** was prepared in situ in THF solvent, four equivalents of 12-crown-4 were added to the reaction mixture and the solution was left stirring for 15 minutes at ambient temperature. The solution was then cooled to -78 °C and a solution of substrate **10a** in 3mL of THF were added at -78 °C. The mixture was left stirring at -78 C for 15 minutes, the temperature was then raised to ambient temperature and the mixture was left stirring for 16 hours (**Scheme 5.9**)



**Scheme 5.9:** LiCl effect on the fate of the reaction.

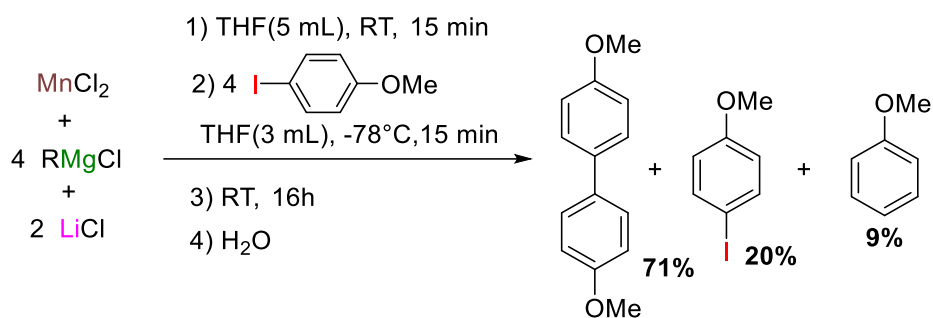
Surprisingly, using these reaction conditions 95% of starting material **10a** was recovered and no formation of **11a** could be observed. This result highlights the crucial effect of the alkali metal in these transformations and it suggests the reaction takes place via contacted ion pair intermediates. These findings raise an important question regarding the possible mechanism of these transformations. Going back to Cahiez MnCl<sub>2</sub>-LiCl catalysed homocoupling of aryl Grignard reagents, these transformations involve the formation of Mn(IV) intermediates as previously discussed (See **Scheme 5.2**). Results in **Scheme 5.7** contrast with Cahiez proposed mechanism and suggest that LiCl presence is crucial to facilitate the Mn/X exchange and the subsequent homocoupling process. Furthermore, all reactions using lithium manganate [(THF)<sub>x</sub>Li<sub>2</sub>Mn(CH<sub>2</sub>SiMe<sub>3</sub>)<sub>4</sub>] (**1u**) were carried out with no exposure to O<sub>2</sub>. This may suggest a reductive cross-coupling type mechanism.

In order to gain a better understanding on the effect of LiCl, the reaction was repeated under the same conditions using a Grignard reagent (CH<sub>2</sub>SiMe<sub>3</sub>)MgCl instead of Li(CH<sub>2</sub>SiMe<sub>3</sub>). Thus RMgCl and MnCl<sub>2</sub> were mixed in THF solvent and the reaction mixture was left stirring for 15 minutes at ambient temperature. The solution was then cooled to -78 °C and a solution of substrate **10a** in 3mL of THF was added at -78 °C. The mixture was left stirring at -78 °C for 15 minutes, the temperature was then raised to ambient temperature and the mixture was left stirring for 16 hours. Surprisingly, using this reaction conditions 82% of starting material **10a** was recovered and no formation of **11a** could be observed (**Scheme 5.10**).



**Scheme 5.10:** Reaction using RMgCl instead of LiR.

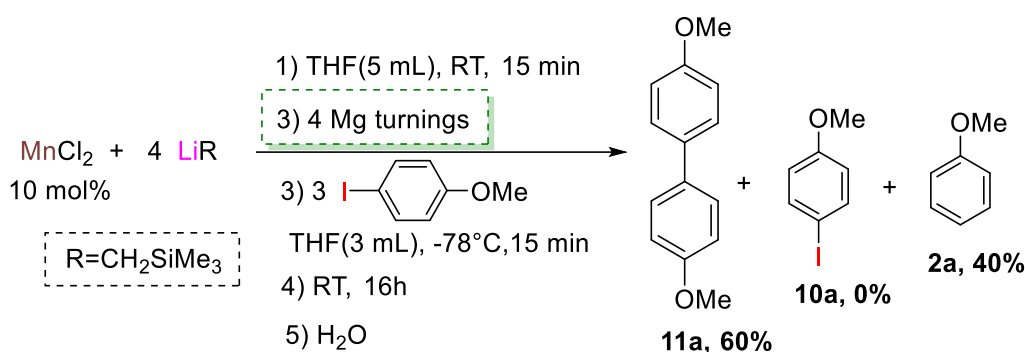
Furthermore, the same reaction was repeated with addition of LiCl. Thus, four equivalents of RMgCl were mixed with one equivalent of MnCl<sub>2</sub> in THF and two equivalents of LiCl were added, followed by the addition of three equivalents of 4-iodoanisole at -78 °C and organic work-up, allowed to obtain 71% yield of **11a** along with 20% of **10a** (**Scheme 5.11**).



**Scheme 5.11:** Reaction using RMgCl·LiCl to assess the effect of lithium.

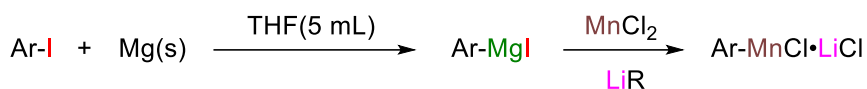
Results summarised in **Schemes 5.9, 5.10** and **5.11** suggest a crucial activating effect of LiCl to promote Mn-I exchange and the subsequent homocoupling reaction. Based on all these studies, it can be deduced that the mechanism of the Mn/I and C-C bond formation procedure here developed involves the formation of alkali metal manganate intermediates. Although a radical mechanism cannot be ruled out, results suggest the reaction proceeds via contacted ion pair intermediates where Li plays an important role.

The reaction was then carried out using catalytic amounts of MnCl<sub>2</sub>. Thus, four equivalents of LiR were mixed with 10 mol% of MnCl<sub>2</sub> in THF, and the solution was left stirring for 15 minutes at ambient temperature. Mg metal was then added to the reaction mixture, then the solution was cooled to -78 °C and 3 equivalents of substrate **10a** in 3mL of THF were added at -78 °C. The mixture was left stirring at -78 C for 15 minutes, the temperature was then raised to ambient temperature and the mixture was left stirring for 16 hours. Organic work-up, allowed to obtain 60% yield of **11a** however no starting material was left in the reaction mixture (**Scheme 5.12**).



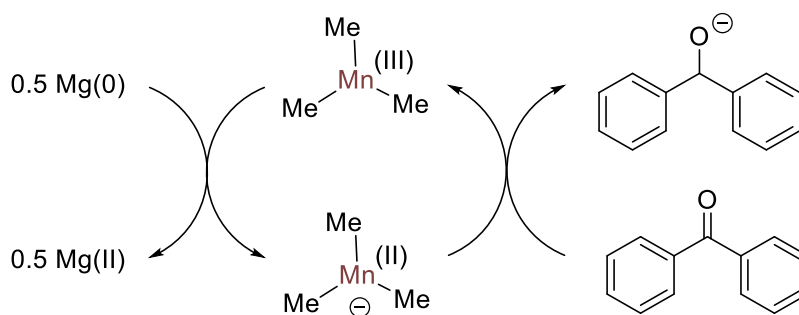
**Scheme 5.12:** Reaction carried out under catalytic conditions ( $\text{MnCl}_2$  10 mol%)

Two different roles can be assigned to magnesium: 1) the presence of magnesium can lead to formation of a Grignard reagent by reaction with the iodoaryl substrate. Thus, subsequent Mn transmetalation in the presence of LiR would form an aryl manganate  $\text{ArMnCl}\cdot\text{LiCl}$ . This methodology has been used in synthesis by Knochel and co-workers (**Scheme 5.13**).<sup>31,32</sup>



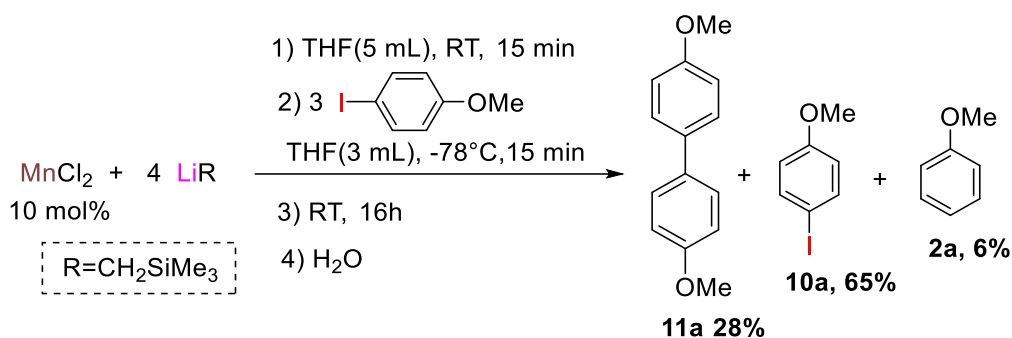
**Scheme 5.13:** Preparation of Aryl lithium manganates via transmetalation with Mg.

2) Magnesium turnings can also act as reducing agents. They have been previously employed as reducing agent in ate chemistry, thus Uchiyama *et al* developed a catalytic electron transfer system mediated by transition metal ate complexes for the reduction of ketones (**Scheme 5.14**).<sup>33</sup>



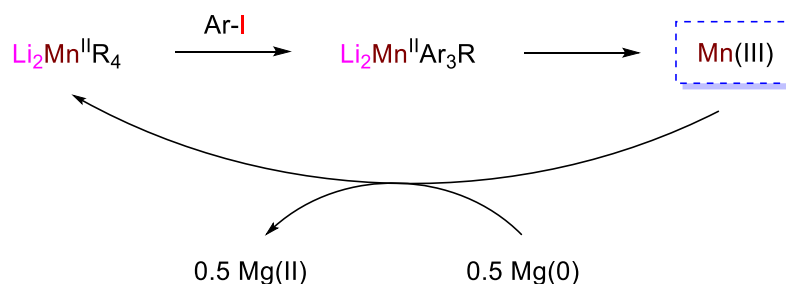
**Scheme 5.14:** Transition metal ate mediated reduction of ketones

When the same reaction is carried out in the absence of Mg turnings, under the same reaction conditions, **11a** was obtained in a lower 28% yield (**Scheme 5.15**).



**Scheme 5.15:** Reaction carried out under catalytic conditions (MnCl<sub>2</sub> 10 mol%) with no Mg turnings.

The presence of Mg(s) is key using catalytic amounts of MnCl<sub>2</sub> (10 mol%). These results show that the reaction can be carried out both under catalytic and stoichiometric conditions. Preliminary EPR spectroscopic studies<sup>a</sup> have shown that in the reaction Mn(II) oxidises to Mn(III), thus the effect of magnesium is to reduce it back to Mn(II) to restart the cycle. This allows to propose a simplistic view of a reductive cross coupling type mechanism for the **1u** mediated Mn/I exchange followed by homocoupling as follows (**Scheme 5.16**)



**Scheme 5.16:** Simplistic view of the proposed reductive cross coupling mechanism

Further studies to determine the mechanism of this reaction procedure are currently underway. Although other examples of C-C bond coupling processes using manganates were previously reported, the exact mechanism of these transformations is extremely complex.<sup>34</sup>

### 5.3.4 Substrate scope

In order to expand the scope of the lithium manganate mediated Mn/I exchange reactions followed by C-C bond formation by homocoupling, the reactivity of **1u** with different aromatic and heteroaromatic halogenated substrates was studied. Stoichiometric conditions were used in all cases as higher yields were obtained of the corresponding biaryl products

<sup>a</sup> EPR studies were carried out by Marina Uzelac a former member of Hevia's group in collaboration with the group of Prof Aromí at the Universitat de Barcelona.

compared to the catalytic conditions. The presence of a functional group in the aromatic molecule can drastically alter the final outcome of the reaction due to steric and electronic factors. Optimisation of the reaction was carried out using the same substrate (4-iodoanisole **10a**) therefore substitution effect was studied using 3-iodoanisole (**10d**) and 2-iodoanisole (**10e**) (Table 5.8).

**Table 5.8:** Effect of the substitution in the **1u** mediated Mn/I exchange and C-C coupling.

$\text{MnCl}_2 + 4 \text{LiR} \xrightarrow[\text{THF (3 mL), -78}^\circ\text{C, 15 min}]{\text{1) THF (5mL), -78}^\circ\text{C, 0.25 h}}$ $\text{Ar-Ar} \xrightarrow[\text{4) H}_2\text{O}]{\text{2) 3 Ar-I, 3) RT, 16 h}}$ <div style="border: 1px dashed black; padding: 2px; display: inline-block; margin: 5px;">R=CH<sub>2</sub>SiMe<sub>3</sub></div>				
Entry	Ar-I	Ar-Ar	Yield(%) <sup>a</sup>	
1	<b>10a</b>	<b>11a</b>	80	
2	<b>10d</b>	<b>11b</b>	68	
3	<b>10e</b>	<b>11c</b>	60	
4	<b>10f</b>	<b>11d</b>	74	
5	<b>10g</b>	<b>11e</b>	55	
6	<b>10h</b>	<b>11f</b>	33	

[a] Yields refer to isolated yields of analytically pure products (>95% purity determined by NMR or GC-analysis) unless otherwise stated.

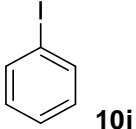
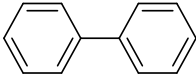
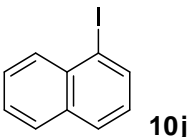
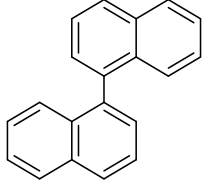
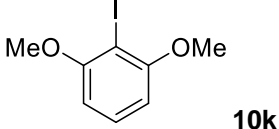
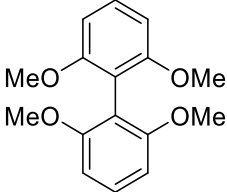
Reaction of **1u** with **10d** using optimised reaction conditions in **scheme 5.5** gave formation of homocoupled product 3,3'-dimethoxy-1,1'-biphenyl (**11b**) in 68% yield (Entry 2, **Table 5.8**). Reaction of **1u** with **10e** under the same reaction conditions gave formation of homocoupled product 2,2'-dimethoxy-1,1'-biphenyl (**11c**) in a lower 60% yield (Entry 3, **Table 5.8**). The position of the electro donating group such as the methoxy group has a modest effect on the reaction yield, the best result is obtained when the methoxy group is in the *para* position with respect to the iodine atom (80% yield of **11a**) whereas the worst result is obtained when the methoxy group is in *ortho* position with respect to the iodine atom (60% yield of **11c**). A similar study was carried out changing the substrate. A methyl group was employed this time as an electron donating substituent instead of methoxy. Thus when **1u** reacts with 4-iodotoluene (**10f**) under the same reaction conditions, homocoupled product 4,4'-dimethyl-1,1'-biphenyl (**11d**) was obtained in 74% yield. When the methyl group was in the *meta* position with respect to iodine, thus using 3-iodotoluene (**10g**), homocoupled product 3,3'-dimethyl-1,1'-biphenyl (**11e**) was obtained in a lower 55% yield. Furthermore when **1u** was confronted with 2-iodotoluene (**10h**) homocoupled product (**11f**) was obtained in a small 33% yield, with recovery of starting material as a major product. These results show that the position of the substituents in the aromatic ring have a major effect on the reaction outcome, electron donating substituents such as a methyl group in *para* position do not alter the reaction yield (74% yield of **11d**), however electron donating groups in *meta* and *para* have a clear detrimental effect on the reaction yield (55% and 35% yields for **11e** and **11f** respectively).

Comparing this results with Cahiez's manganese-catalysed homocoupling of Grignard reagents previously described in **Chapter 5.2 (Table 5.1)**, slightly better yields are obtain when using 4-(methoxyphenyl)magnesium bromide as substrate (95% yield obtained Entry 1, **Table 5.1**, compared to 80% yield obtained using **1u**, Entry 1, **Table 5.8**). Cahiez protocol also seemed to be affected by the substitution effect, thus when the reaction is carried out using more sterically hindered 2-(methoxyphenyl)magnesium bromide the biaryl product is obtained in a lower 76% yield (Entry 2, **Table 5.1**, compared to 60% yield obtained using **1u**, Entry 1, **Table 5.8**).

In order to study steric effects on the fate of the reaction, **1u** was confronted with both substrates containing sterically accessible iodine atoms and substrates containing sterically hindered iodine atoms (**Table 5.9**). For example the reaction between **1u** and iodobenzene (**10i**) under optimised reaction conditions gave formation of homocoupled product 1,1'-biphenyl (**11g**) in 85% yield (Entry 1, **Table 5.9**). When **1u** was confronted with 1-iodonaphthalene (**10j**) the homocoupled product 1,1'-binaphthalene (**11h**) was obtained in a good 70% yield (Entry 2,

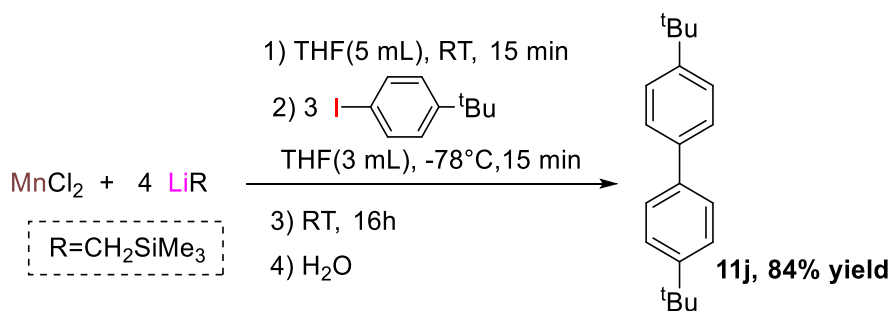
**Table 5.9).** Furthermore when **1u** reacts with the sterically hindered iodine atom present in 2-iodo-1,3-dimethoxybenzene (**10k**), the homocoupled product 2,2',6,6'-tetramethoxy-1,1'-biphenyl (**11i**) is obtained in a lower 67% yield (Entry 3, **Table 5.9**).

**Table 5.9:** Reactivity of  $(\text{THF})_x\text{Li}_2\text{MnR}_4$  with different substrates according to steric effects.

$\text{MnCl}_2 + 4 \text{LiR} \xrightarrow[\text{THF (3 mL), -78}^\circ\text{C, 15 min}]{\text{1) THF (5mL), -78}^\circ\text{C, 0.25 h}}$ $\text{Ar-Ar}$ <div style="border: 1px dashed black; padding: 2px; display: inline-block; margin: 5px;"> <math>\text{R}=\text{CH}_2\text{SiMe}_3</math> </div> $\text{2) 3 Ar-I}$ $\text{3) RT, 16 h}$ $\text{4) H}_2\text{O}$				
Entry	Ar-I	Ar-Ar	Yield(%) <sup>a</sup>	
1	 <b>10i</b>	 <b>11g</b>	85	
2	 <b>10j</b>	 <b>11h</b>	70	
3	 <b>10k</b>	 <b>11i</b>	67	

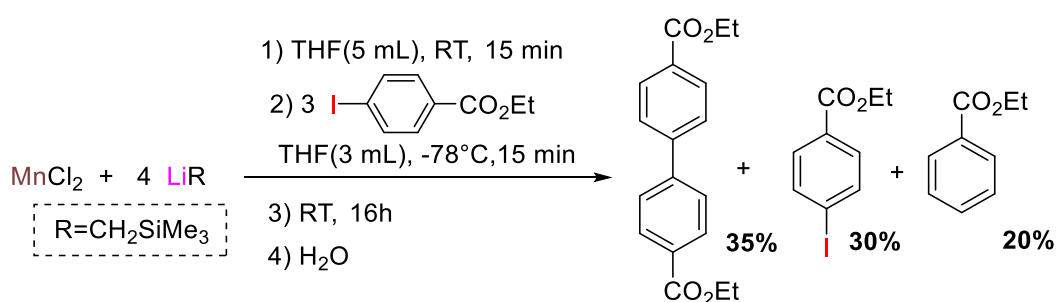
[a] Yields refer to isolated yields of analytically pure products (>95% purity determined by NMR or GC-analysis) unless otherwise stated.

These results show that lithium manganese  $[(\text{THF})_x\text{Li}_2\text{Mn}(\text{CH}_2\text{SiMe}_3)_4]$  is capable of promoting the homocoupling reaction in good yields both in sterically hindered and sterically accessible iodine atoms. This is in contrast with Cahiez's Mn-catalysed homocoupling of Grignard reagents in which homocoupling product was not observed using substrates containing sterically hindered iodine atoms (see **Table 5.2** for further details). Then a different electron donating substituent was tested. Thus reaction of **1u** with substrate 1-(*tert*-butyl)-4-iodobenzene (**10l**) under the optimised reaction conditions 4,4'-di-*tert*-butyl-1,1'-biphenyl (**11j**) was obtained in 84% yield after separation by column chromatography (**Scheme 5.17**).



**Scheme 5.17:** Reaction of **1u** with 1-(*tert*-butyl)-4-iodobenzene (**10l**)

A different outcome was obtained when using a strong electron withdrawing substituent in the *ortho* position. In fact reaction of **1u** with ethyl 4-iodobenzoate (**10m**) gave formation of homocoupled product diethyl [1,1'-biphenyl]-4,4'-dicarboxylate (**11k**) in a low 35% yield. Starting material **10m** and ethyl benzoate were obtained in 30% and 20% yield respectively (**Scheme 5.18**).



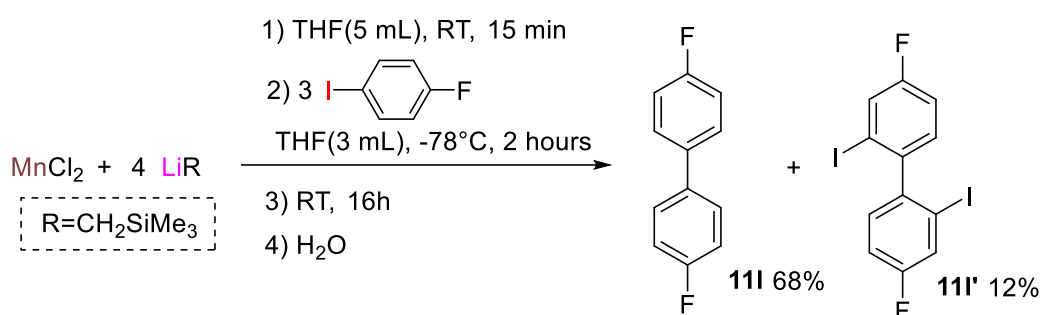
**Scheme 5.18:** Reaction of **1u** with 4-iodobenzoate (**10m**)

These results clearly show a drastically lowered yield when using substrates containing strong electron withdrawing groups such as esters. This result contrasts with what reported by Cahiez *et al* as when using (4-(ethoxycarbonyl)phenyl)magnesium bromide) the biaryl product is obtained in high 80% yield (Entry 4, **Table 5.1**).

Fluorine containing substrates were also studied. As previously mentioned in **chapter 2** of this thesis, replacement of hydrogen with fluorine in C-H bonds of an organic molecule can lead to significantly different physical properties and biological activity.<sup>35–38</sup> Surprisingly only few naturally occurring organic compounds that contain fluorine exist and only few examples of these natural products have been reported.<sup>39</sup> Contrastingly, substrates containing chlorine, bromine and even iodine, figure prominently in many natural products (more than 3000 have been reported to date).<sup>40</sup> The chemical properties of fluorine containing compounds make this molecules particularly interesting in pharmaceutical industry. The high electronegativity of fluorine atom has a large electronic effect at neighbouring carbon centres, as well as having a

substantial effect on the molecule's dipole moment and it can alter the acidity or basicity of other groups nearby. In addition insertion of fluorine atoms in a substrate can change the overall reactivity and stability of a molecule. Furthermore, fluorine centre can act as a hydrogen bond acceptors, and the presence of three lone pair electrons can enable it to act as a ligand for alkali metals.<sup>37</sup>

Thus reaction of **1u** with 3 equivalents of 1-fluoro-4-iodobenzene (**10n**) under the optimised reaction conditions afforded homocoupled product 4,4'-difluoro-1,1'-biphenyl (**11l**) in 68% yield along with formation of by-product 4,4'-difluoro-2,2'-diiodo-1,1'-biphenyl in 12% yield (**11l'**) (**Scheme 5.19**).

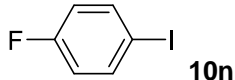
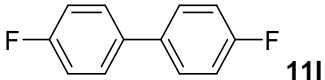
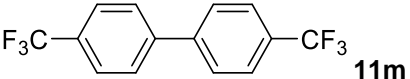
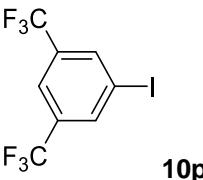
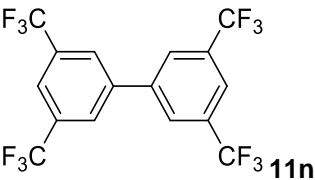


**Scheme 5.19:** Reaction of **1u** with 1-fluoro-4-iodobenzene (**10n**)

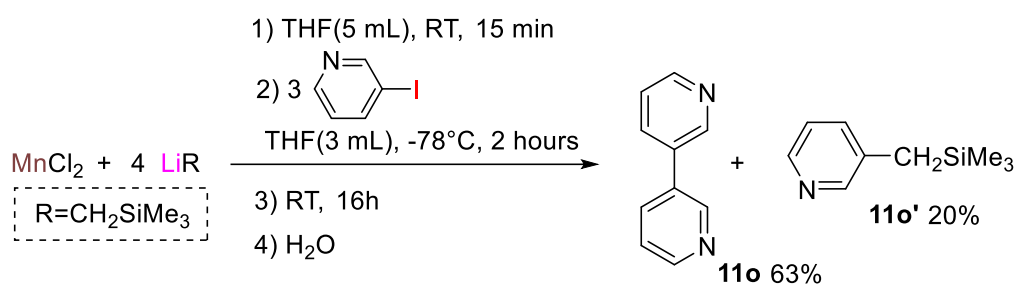
Further research is ongoing to give a plausible explanation for the formation of by-product **11l'**, although the mechanism is unknown to date, it can be anticipated to be an extremely complex processes where aryne formation might be involved,<sup>41</sup> in agreement with it is the fact that 1-fluoro-4-iodobenzene **10n** is a compound known as a precursor to arynes.<sup>42</sup>

Furthermore the same reaction using 1-iodo-4-(trifluoromethyl)benzene (**10o**) afforded homocoupled product 4,4'-bis(trifluoromethyl)-1,1'-biphenyl (**11m**) in 73% yield (Entry 2, **Table 5.10**). Similarly when the reaction is carried out using 1-iodo-3,5-bis(trifluoromethyl)benzene (**10p**) as a substrate formation of 3,3',5,5'-tetrakis(trifluoromethyl)-1,1'-biphenyl (**11n**) was obtained in 69% yield (Entry, **Table 5.10**).

**Table 5.10:** Substrate scope using fluorine containing substrates.

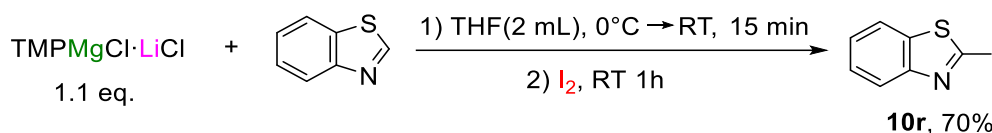
$\text{MnCl}_2 + 4 \text{LiR} \xrightarrow[\text{THF (3 mL), -78}^\circ\text{C, 15 min}]{\text{1) THF (5mL), -78}^\circ\text{C, 0.25 h}}$ 2) <b>3</b> Ar-I 3) RT, 16 h 4) H <sub>2</sub> O Ar-Ar			
$\text{R}=\text{CH}_2\text{SiMe}_3$			
Entry	Ar-I	Ar-Ar	Yield(%) <sup>a</sup>
1	 <b>10n</b>	 <b>11l</b>	68
2	 <b>10o</b>	 <b>11m</b>	73
3	 <b>10p</b>	 <b>11n</b>	69
[a] Yields refer to isolated yields of analytically pure products (>95% purity determined by NMR or GC-analysis) unless otherwise stated.			

The reaction was also expanded to aromatic heterocyclic molecules. Thus 3-iodopyridine (**10q**) was confronted to lithium manganate **1u**, the reaction was left stirring for 2 hours at -78 °C as no evidence of homocoupling was observed using optimised reaction conditions (15 min at -78 °C). After quenching with H<sub>2</sub>O two products were observed by GC-analysis. Separation by column chromatography gave 3,3'-bipyridine (**11o**) in 63% yield along with 20% formation of by-product 3-((trimethylsilyl)methyl)pyridine (**11o'**) (**Scheme 5.20**). Both products were characterised by <sup>1</sup>H and <sup>13</sup>C NMR spectroscopy.



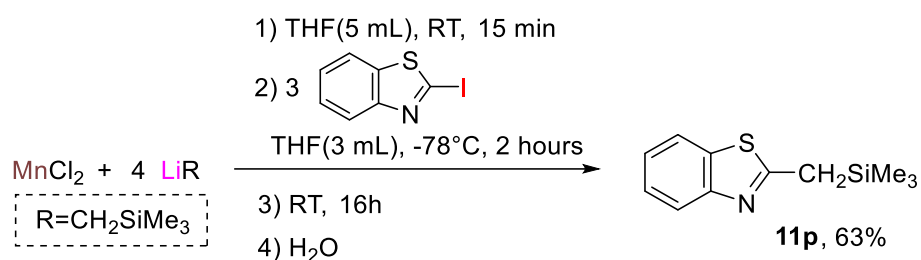
**Scheme 5.20:** Reaction of **1u** with 3,3'-bipyridine (**10q**)

A plausible explanation for the formation of **11o'** is given by a kinetically favoured cross coupling reaction between the  $\text{CH}_2\text{SiMe}_3$  group present in  $[(\text{THF})_x\text{Li}_2\text{Mn}(\text{CH}_2\text{SiMe}_3)_4]$  (**1u**) with a pyridyl group. The reaction between **1u** with 3-iodopyridine was repeated several times changing the reaction conditions. Longer reaction times (6 hours) and higher temperatures (25 °C) did not alter the ratio for the formation of products **11o** and **11o'**. Further research is needed to fulfil the information missing regards the mechanism of by product formation. Another heterocyclic substrate was then tested. Substrate 2-iodobenzothiazole (**10r**) was prepared by direct metalation reaction of benzothiazole **2m** using 1.5 equivalents of turbo Grignard base  $\text{iPrMgCl}\cdot\text{LiCl}$  followed by iodine quenching according to the literature procedure (**Scheme 5.21**).<sup>43</sup>



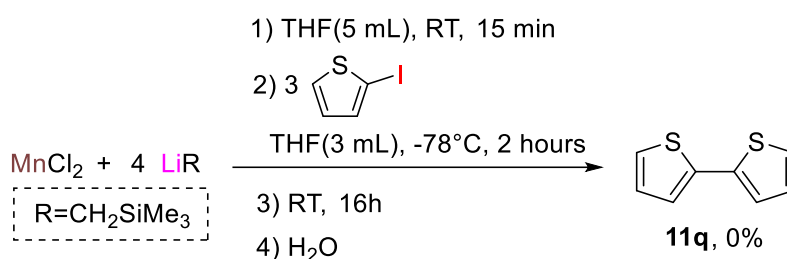
**Scheme 5.21:** Synthesis of **10r** using Knochell's Turbo Grignard  $\text{TMPMgCl}\cdot\text{LiCl}$

Reaction of **1u** with **10r** using reaction conditions in **Scheme 5.11**, gave formation of 2-((trimethylsilyl)methyl)benzothiazole (**11p**) in 63% yield. Product **11p** was isolated as the only product of the reaction along with recovery of starting material. No homocoupling product was observed in this case and the major product of the reaction is the cross coupling product between the  $\text{CH}_2\text{SiMe}_3$  group and the benzothiazolyl group (**Scheme 5.21**).



**Scheme 5.22:** Cross coupling reaction formation of **11p** between benzothiazolyl group and CH<sub>2</sub>SiMe<sub>3</sub>

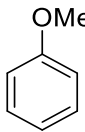
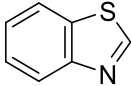
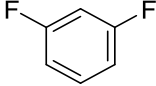
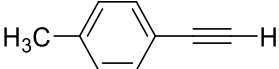
Furthermore reaction of **1u** with 2-iodothiophene (**10s**) was studied. However under these reaction conditions **1u** failed to promote the formation of homocoupling product 2,2'-bithiophene (**11q**) (**Scheme 5.22**).



**Scheme 5.23:** Reactivity of **1u** with 2-iodothiophene (**10s**)

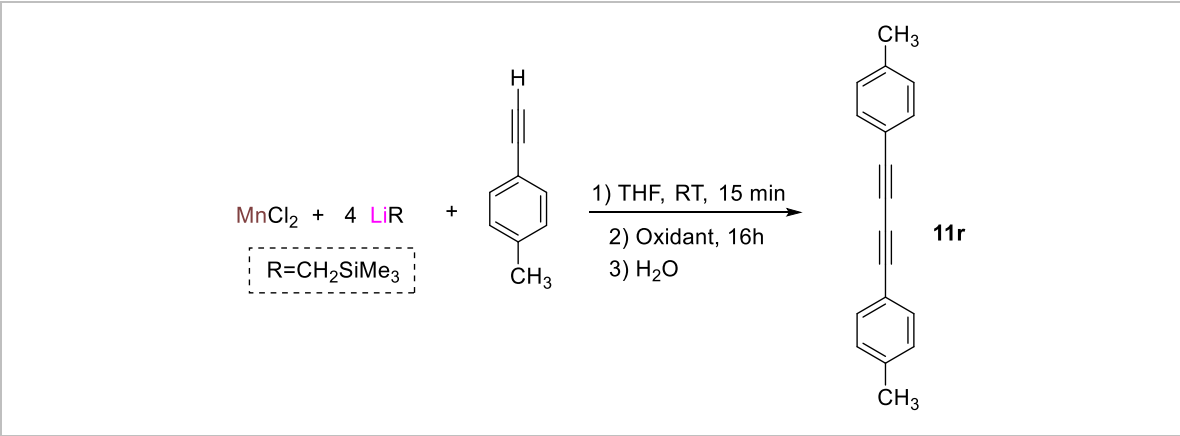
In order to test the reactivity of **1u** towards metal/hydrogen exchange reactions, and to find out if the homocoupling processes could be obtained with the absence of the Mn/I exchange reaction different aromatic substrates were tested. Thus **1u** was confronted with anisole (**2a**), benzothiazole (**2m**) and 1,3-difluorobenzene (**2d**) using the optimised reaction conditions. GC analysis of an aliquot from the reaction mixture gave a mixture of unknown products along with starting material recovered (Entry 1 and 2, **Table 5.11**). No homocoupled product was obtained in all cases.

**Table 5.11:** Reactivity of **1u** towards metal/hydrogen exchange reactions

		1) THF (5mL), -78°C, 0.25 h 2) <b>3</b> Ar-H THF (3 mL), -78°C, 15 min 3) RT, 16 h 4) H <sub>2</sub> O			
		MnCl <sub>2</sub> + 4 LiR	→	Ar-Ar	
		R=CH <sub>2</sub> SiMe <sub>3</sub>			
Entry	Ar-I		Ar-Ar		
1			-		
2			-		
3			-		
4			-		

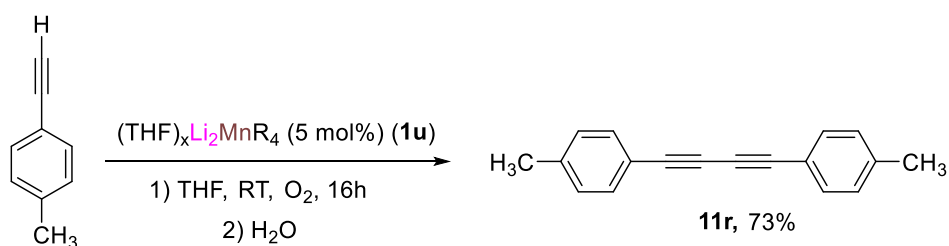
The reactions were repeated, exposing the reaction mixture to O<sub>2</sub> however no conversion to biaryl was observed in any case. Perhaps under these reaction conditions Mn/H exchange reaction does not take place. The reaction was repeated using *p*-tolylacetylene (**4b**) and full recovery of starting material was obtained following the exact same reaction in the absence of O<sub>2</sub>. A different outcome was obtained from the Mn/I exchange reaction between **1u** with *p*-tolylacetylene (**4b**) in the presence of O<sub>2</sub>. An aliquot from the reaction mixture was analysed by GC after hydrolysis revealing formation of 1,4-di-*p*-tolylbuta-1,3-diyne (**11r**) in good 82% yield (**Table 5.12**).

**Table 5.12:** Reaction of **1u** with *p*-tolylacetylene (**4b**) to form 1,4-di-*p*-tolylbuta-1,3-diyne (**11r**)

				
Entry	Oxidant	Yield (%) <sup>a</sup>		
1	O <sub>2</sub> (excess)	82		
2	-	0		

[a] Yields obtained via spectroscopic <sup>1</sup>H NMR integration of signals for product **11r** with addition of hexamethylbenzene (10 mol %) as internal standard.

In addition to this, **1u** was found to be active in catalytic amounts with the homocoupling reaction of alkynes, thus reaction of 5 mol% of **1u** with **4b** in the presence of O<sub>2</sub> in THF, at ambient temperature for 16 hours gave formation of 1,4-di-*p*-tolylbuta-1,3-diyne (**11r**) in 73% yield (**Scheme 5.23**).



**Scheme 5.24:** Reaction formation of 1,4-di-*p*-tolylbuta-1,3-diyne (**11r**) using catalytic amounts of **1u**

This reaction procedure contrasts with what described for the homocoupling of iodoaryl compounds where oxygen was not required. Thus this can be considered an oxidative coupling type of mechanism, where with no oxidant (O<sub>2</sub>) the reaction does not take place. Examples of oxidative coupling type reactions with alkynes have been reported previously using Cu<sup>44</sup> and Au<sup>45</sup> catalysts. In addition Cahiez's methodology also allowed formation of diynes.<sup>13</sup>

## 5.4 Conclusions

The last chapter of this PhD thesis reports the synthesis of symmetric biaryl compounds from a temperature controlled procedure which includes a Mn/I exchange reaction at sub-ambient temperature (-78 °C) followed by C-C bond formation by homocoupling reaction. Using iodoanisole as a case study, the synergic effect of lithium and manganese in higher order manganate **1t** and **1u** has been demonstrated. Thus, while both bimetallic species can promote the Mn/I exchange of this aromatic ether, their homometallic components exhibit different reactivity.  $\text{LiCH}_2\text{SiMe}_3$  promotes the Li/I exchange reaction however it is unable to form the give the biaryl product.  $\text{Mn}(\text{CH}_2\text{SiMe}_3)_2$  fail to give a substantial amount of Mn/I exchange reaction thus no biaryl product is observed under the same reaction conditions employed when using **1u**. Demonstrating their enhanced reactivity, the high reactivity of these compounds contrasts with the inertness of triorganomanganates [ $\{(\text{LiMn}(\text{CH}_2\text{SiMe}_3)_3)_\infty\}$ ] (**1s**) which gives homocoupled product in a lower 22% yield.

Li seems to play an important role in this methodology as further studies for the reactivity of this novel mixed metal compounds towards Mn/I exchange followed by C-C bond formation of **10a** showed that when the reaction is carried out using 12-crown-4 which captures the Li atoms the reaction is totally inhibited. These results suggest that the mechanism of the Mn/I and C-C bond formation procedure here developed involves the formation of alkali metal manganate intermediates. This methodology could also be upgraded to catalytic regimes, although Mg(s) as reducing agent was required. These findings along with preliminary magnetic studies which show Mn to go from Mn(II) to Mn(III) suggest the reaction might proceed via reductive coupling type mechanism. This is in contrast with Cahiez's methodology which proceeds through oxidative coupling type mechanism as it requires an oxidizing agent such as  $\text{O}_2$  to take place.

These compounds are able to promote the efficient Mn/I exchange of a wide range of aromatic and heteroaromatic substrates, including substrates containing electron donating and electron withdrawing groups. This methodology could be carried out using substrates containing sterically hindered I atoms such as **10k** (ranging from 52-94%), where the formation of the corresponding biaryl product **11i** was obtained in good yield (67% yield). Careful selection of substrates allowed to upgrade from homocoupling to cross-coupling the reaction procedure as when using 3-iodopyridine (**10q**) a mixture of homocoupled and cross-coupled products were

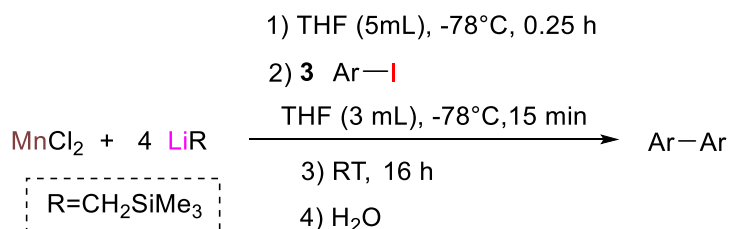
obtained (**11o** and **11o'** respectively) with the  $\text{CH}_2\text{SiMe}_3$  present in **1u**. In addition using 2-iodobenzothiazole (**10r**) resulted in the selective formation of cross-coupled product (**11p**) whereas homocoupled product was not observed. Furthermore the coupling of *p*-tolylacetylene was also carried out using catalytic amounts of Mn. In this case a totally different scenario is proposed as the reaction does only take place in the presence of an oxidizing agent such as  $\text{O}_2$ , thus the reaction might proceed via oxidative coupling type mechanism.

## 5.5 Experimental Section

**General Considerations.** All reactions were performed under a protective argon atmosphere using standard Schlenk techniques. Hexane and THF were dried by heating to reflux over sodium benzophenone ketyl and distilled under nitrogen or they were passed through a column of activated alumina (Innovative Tech.), degassed under nitrogen and stored over molecular sieves in the glove-box prior to use.  $\text{Mn}(\text{CH}_2\text{SiMe}_3)_2$  was prepared according to previously reported procedure.<sup>21</sup>  $\text{LiCH}_2\text{SiMe}_3$  was purchased from Sigma Aldrich chemicals as a 1M solution in hexane.  $\text{LiCH}_2\text{SiMe}_3$  was stored in the glove box as a white solid after solvent was removed under vacuum. Iodoaryls, alkynes and other organic substrates were purchased from Sigma Aldrich chemicals and used as received. NMR spectra were recorded on a Bruker DPX400 MHz spectrometer, operating at 400.13 MHz for  $^1\text{H}$ , 100.62 MHz for  $^{13}\text{C}$  or on a Varian FT-400 spectrometer using standard VARIAN-FT software.

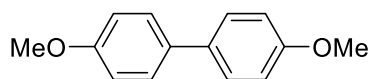
### 5.5.1 Synthesis of biaryl compounds.

Unless otherwise stated the synthesis of biaryl compounds **11a-11q** was carried out according to the following reaction procedure (**Scheme 5.25**):



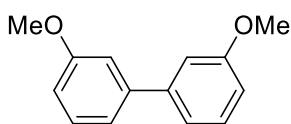
**Scheme 5.25:** General reaction procedure for the synthesis of biaryls using manganates

### 5.5.1.1 4,4'-dimethoxy-1,1'-biphenyl (11a)



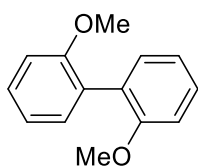
An oven dried Schlenk tube was charged with  $\text{LiCH}_2\text{SiMe}_3$  (188 mg, 2 mmol) and  $\text{MnCl}_2$  (63 mg, 0.5 mmol), THF (5 mL) was added and the reaction was left stirring at ambient temperature (20 °C) for 15 minutes, the temperature was then cooled down (-78 °C). A different oven dried Schlenk tube was charged with 4-iodoanisole (351 mg, 1.5 mmol), THF (3 mL) was added and the temperature was cooled to (-78 °C). The two solutions were mixed via cannula and the mixture was stirred for 15 minutes. The mixture was then allowed to stir at ambient temperature (20 °C) for 16 hours. The reaction mixture was then quenched with brine 2 mL. The crude was extracted using diethyl ether and brine (3 x 5 mL), the organic solution was dried over magnesium sulphate and the product was purified by flash column chromatography using hexane/DCM 3:1 as eluent to give **11a** as a pale yellow solid (128 mg, 80% yield).  $^1\text{H NMR}$  (600 MHz,  $\text{CDCl}_3$ )  $\delta$  (ppm) = 3.85 (s, 6H), 6.97 (d,  $J=8.6$  Hz, 4H), 7.48 (d,  $J=8.6$  Hz, 4H),  $^{13}\text{C}\{\text{H}\}$  NMR (101 MHz,  $\text{CDCl}_3$ )  $\delta$  (ppm) = 55.5, 114.2, 127.8, 133.6, 158.8. The values are consistent with previous data reported in the literature.<sup>12</sup>

### 5.5.1.2 3,3'-dimethoxy-1,1'-biphenyl (11b)



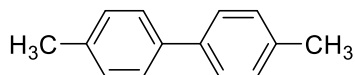
An oven dried Schlenk tube was charged with  $\text{LiCH}_2\text{SiMe}_3$  (188 mg, 2 mmol) and  $\text{MnCl}_2$  (63 mg, 0.5 mmol), THF (5 mL) was added and the reaction was left stirring at ambient temperature (20 °C) for 15 minutes, the temperature was then cooled down (-78 °C). A different oven dried Schlenk tube was charged with 3-iodoanisole (351 mg, 1.5 mmol), THF (3 mL) was added and the temperature was cooled to (-78 °C). The two solutions were mixed via cannula and the mixture was stirred for 15 minutes. The mixture was then allowed to stir at ambient temperature (20 °C) for 16 hours. The reaction mixture was then quenched with brine 2 mL. The crude was extracted using diethyl ether and brine (3 x 5 mL), the organic solution was dried over magnesium sulphate and the product was purified by flash column chromatography using hexane/ $\text{Et}_2\text{O}$  95:5 as eluent to give **11b** as a colourless oil (109 mg, 68% yield).  $^1\text{H NMR}$  (400 MHz,  $\text{CDCl}_3$ )  $\delta$  (ppm) = 3.87 (s, 6H), 6.90-6.93 (m, 2H), 7.14 (m, 2H), 7.18-7.21 (m, 2H), 7.63 (t,  $J=8$  Hz, 2H).  $^{13}\text{C}\{\text{H}\}$  NMR (101 MHz,  $\text{CDCl}_3$ )  $\delta$  (ppm) = 55.4, 112.9, 113.1, 119.8, 129.8, 142.8, 160.0.

### 5.5.1.3 2,2'-dimethoxy-1,1'-biphenyl (11c)



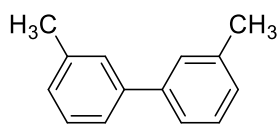
An oven dried Schlenk tube was charged with  $\text{LiCH}_2\text{SiMe}_3$  (188 mg, 2 mmol) and  $\text{MnCl}_2$  (63 mg, 0.5 mmol), THF (5 mL) was added and the reaction was left stirring at ambient temperature (20 °C) for 15 minutes, the temperature was then cooled down (-78 °C). A different oven dried Schlenk tube was charged with 2-iodoanisole (351 mg, 1.5 mmol), THF (3 mL) was added and the temperature was cooled to (-78 °C). The two solutions were mixed via cannula and the mixture was stirred for 15 minutes. The mixture was then allowed to stir at ambient temperature (20 °C) for 16 hours. The reaction mixture was then quenched with brine 2 mL. The crude was extracted using diethyl ether and brine (3 x 5 mL), the organic solution was dried over magnesium sulphate and the product was purified by flash column chromatography using hexane/ $\text{Et}_2\text{O}$  95:5 as eluent to give **11c** as a white solid (96 mg, 60% yield).  $^1\text{H NMR}$  (400 MHz,  $\text{CDCl}_3$ )  $\delta$  (ppm) = 3.79 (s, 6H), 6.99-7.04 (m, 4H), 7.26-7.28 (m, 2H), 7.32-7.38 (m, 2H).  $^{13}\text{C}\{\text{H}\}$  NMR (101 MHz,  $\text{CDCl}_3$ )  $\delta$  (ppm) = 55.8, 111.2, 120.5, 128.0, 128.7, 131.6, 157.2. The values are consistent with previous data reported in the literature.<sup>12</sup>

### 5.5.1.4 4,4'-dimethyl-1,1'-biphenyl (11d)



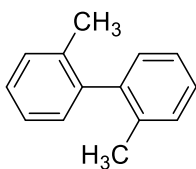
An oven dried Schlenk tube was charged with  $\text{LiCH}_2\text{SiMe}_3$  (188 mg, 2 mmol) and  $\text{MnCl}_2$  (63 mg, 0.5 mmol), THF (5 mL) was added and the reaction was left stirring at ambient temperature (20 °C) for 15 minutes, the temperature was then cooled down (-78 °C). A different oven dried Schlenk tube was charged with 4-iodotoluene (327 mg, 1.5 mmol), THF (3 mL) was added and the temperature was cooled to (-78 °C). The two solutions were mixed via cannula and the mixture was stirred for 15 minutes. The mixture was then allowed to stir at ambient temperature (20 °C) for 16 hours. The reaction mixture was then quenched with brine 2 mL. The crude was extracted using diethyl ether and brine (3 x 5 mL), the organic solution was dried over magnesium sulphate and the product was purified by flash column chromatography using hexane as eluent to give **11d** as a white solid (101 mg, 74% yield).  $^1\text{H NMR}$  (400 MHz,  $\text{CDCl}_3$ )  $\delta$  (ppm) = 2.66 (s, 6H), 7.51 (d,  $J=8.0$  Hz, 4H), 7.75 (d,  $J=8.6$  Hz, 4H).  $^{13}\text{C}\{\text{H}\}$  NMR (101 MHz,  $\text{CDCl}_3$ )  $\delta$  (ppm) = 21.2, 126.9, 129.6, 136.8, 138.4.

### 5.5.1.5 3,3'-dimethyl-1,1'-biphenyl (11e)



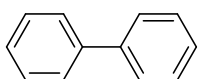
An oven dried Schlenk tube was charged with  $\text{LiCH}_2\text{SiMe}_3$  (188 mg, 2 mmol) and  $\text{MnCl}_2$  (63 mg, 0.5 mmol), THF (5 mL) was added and the reaction was left stirring at ambient temperature (20 °C) for 15 minutes, the temperature was then cooled down (-78 °C). A different oven dried Schlenk tube was charged with 3-iodotoluene (327 mg, 1.5 mmol), THF (3 mL) was added and the temperature was cooled to (-78 °C). The two solutions were mixed via cannula and the mixture was stirred for 15 minutes. The mixture was then allowed to stir at ambient temperature (20 °C) for 16 hours. The reaction mixture was then quenched with brine 2 mL. The crude was extracted using diethyl ether and brine (3 x 5 mL), the organic solution was dried over magnesium sulphate and the product was purified by flash column chromatography using hexane as eluent to give **11e** as a colourless liquid (75 mg, 55% yield).  $^1\text{H NMR}$  (400 MHz,  $\text{CDCl}_3$ )  $\delta$  (ppm) = 2.46 (s, 6H), 7.19-7.21 (m, 2H), 7.36 (t,  $J=7.5$  Hz, 2H), 7.42-7.45 (m, 4H).  $^{13}\text{C}\{\text{H}\}$  NMR (101 MHz,  $\text{CDCl}_3$ )  $\delta$  (ppm) = 21.7, 124.4, 128.0, 128.1, 128.7, 138.4, 141.5.

### 5.5.1.6 2,2'-dimethyl-1,1'-biphenyl (11f)



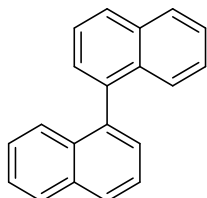
An oven dried Schlenk tube was charged with  $\text{LiCH}_2\text{SiMe}_3$  (188 mg, 2 mmol) and  $\text{MnCl}_2$  (63 mg, 0.5 mmol), THF (5 mL) was added and the reaction was left stirring at ambient temperature (20 °C) for 15 minutes, the temperature was then cooled down (-78 °C). A different oven dried Schlenk tube was charged with 3-iodotoluene (327 mg, 1.5 mmol), THF (3 mL) was added and the temperature was cooled to (-78 °C). The two solutions were mixed via cannula and the mixture was stirred for 15 minutes. The mixture was then allowed to stir at ambient temperature (20 °C) for 16 hours. The reaction mixture was then quenched with brine 2 mL. The crude was extracted using diethyl ether and brine (3 x 5 mL), the organic solution was dried over magnesium sulphate and the product was purified by flash column chromatography using hexane as eluent to give **11f** as a colourless liquid (45 mg, 33% yield).  $^1\text{H NMR}$  (400 MHz,  $\text{CDCl}_3$ )  $\delta$  (ppm) = 2.09 (s, 6H), 7.13-7.15 (m, 2H), 7.23-7.27 (m, 2H), 7.29-7.30 (m, 4H).  $^{13}\text{C}\{\text{H}\}$  NMR (101 MHz,  $\text{CDCl}_3$ )  $\delta$  (ppm) = 19.9, 125.7, 127.3, 129.4, 129.9, 135.9, 141.7.

### 5.5.1.7 1,1'-biphenyl (11g)



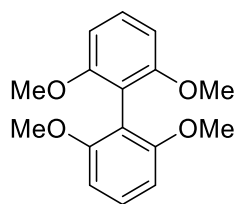
An oven dried Schlenk tube was charged with  $\text{LiCH}_2\text{SiMe}_3$  (188 mg, 2 mmol) and  $\text{MnCl}_2$  (63 mg, 0.5 mmol), THF (5 mL) was added and the reaction was left stirring at ambient temperature (20 °C) for 15 minutes, the temperature was then cooled down (-78 °C). A different oven dried Schlenk tube was charged with iodobenzene (306 mg, 1.5 mmol), THF (3 mL) was added and the temperature was cooled to (-78 °C). The two solutions were mixed via cannula and the mixture was stirred for 15 minutes. The mixture was then allowed to stir at ambient temperature (20 °C) for 16 hours. The reaction mixture was then quenched with brine 2 mL. The crude was extracted using diethyl ether and brine (3 x 5 mL), the organic solution was dried over magnesium sulphate and the product was purified by flash column chromatography using hexane as eluent to give **11g** as a pale yellow solid (98 mg, 85% yield).  $^1\text{H NMR}$  (400 MHz,  $\text{CDCl}_3$ )  $\delta$  (ppm) = 7.34-7.38 (m, 2H), 7.24 (m, 5H), 7.44-7.47 (m, 4H), 7.60-7.62 (m, 4H).  $^{13}\text{C}\{\text{H}\}$  NMR (101 MHz,  $\text{CDCl}_3$ )  $\delta$  (ppm) = 127.3, 127.4, 128.9, 141.4. The values are consistent with previous data reported in the literature.<sup>12</sup>

### 5.5.1.8 1,1'-binaphthalene (11h)



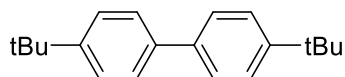
An oven dried Schlenk tube was charged with  $\text{LiCH}_2\text{SiMe}_3$  (188 mg, 2 mmol) and  $\text{MnCl}_2$  (63 mg, 0.5 mmol), THF (5 mL) was added and the reaction was left stirring at ambient temperature (20 °C) for 15 minutes, the temperature was then cooled down (-78 °C). A different oven dried Schlenk tube was charged with 1-iodonaphthalene (381 mg, 1.5 mmol), THF (3 mL) was added and the temperature was cooled to (-78 °C). The two solutions were mixed via cannula and the mixture was stirred for 15 minutes. The mixture was then allowed to stir at ambient temperature (20 °C) for 16 hours. The reaction mixture was then quenched with brine 2 mL. The crude was extracted using diethyl ether and brine (3 x 5 mL), the organic solution was dried over magnesium sulphate and the product was purified by flash column chromatography using pentane as eluent to give **11h** as a white solid (133 mg, 70% yield).  $^1\text{H NMR}$  (400 MHz,  $\text{CDCl}_3$ )  $\delta$  (ppm) = 7.29-7.33 (m, 2H), 7.42-7.44 (m, 2H), 7.48-7.53 (m, 4H), 7.60-7.64 (m, 4H), 7.96-7.99 (m, 2H).  $^{13}\text{C}\{\text{H}\}$  NMR (101 MHz,  $\text{CDCl}_3$ )  $\delta$  (ppm) = 125.5, 125.9, 126.1, 126.7, 128.0, 128.0, 128.3, 133.0, 133.7, 138.6.

### 5.5.1.9 2,2',6,6'-tetramethoxy-1,1'-biphenyl (11i)



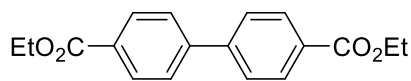
An oven dried Schlenk tube was charged with  $\text{LiCH}_2\text{SiMe}_3$  (188 mg, 2 mmol) and  $\text{MnCl}_2$  (63 mg, 0.5 mmol), THF (5 mL) was added and the reaction was left stirring at ambient temperature (20 °C) for 15 minutes, the temperature was then cooled down (-78 °C). A different oven dried Schlenk tube was charged with 2-iodo-1,3-dimethoxybenzene (396 mg, 1.5 mmol), THF (3 mL) was added and the temperature was cooled to (-78 °C). The two solutions were mixed via cannula and the mixture was stirred for 15 minutes. The mixture was then allowed to stir at ambient temperature (20 °C) for 16 hours. The reaction mixture was then quenched with brine 2 mL. The crude was extracted using diethyl ether and brine (3 x 5 mL), the organic solution was dried over magnesium sulphate and the product was purified by flash column chromatography using hexane/Et<sub>2</sub>O 9:1 as eluent to give **11i** as a colourless oil (138 mg, 68% yield). <sup>1</sup>H NMR (400 MHz, CDCl<sub>3</sub>) δ (ppm) = 3.81 (s, 6H), 6.53-6.56 (dd, *J*'=8.1 Hz, *J*<sup>2</sup>=2.4 Hz, 4H), 7.22 (t, *J*=8.1 Hz 2H), <sup>13</sup>C{<sup>1</sup>H} NMR (101 MHz, CDCl<sub>3</sub>) δ (ppm) = 55.3, 100.5, 106.2, 129.9, 161.0,

### 5.5.1.10 4,4'-di-*tert*-butyl-1,1'-biphenyl (11j)



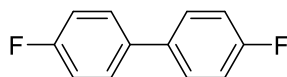
An oven dried Schlenk tube was charged with  $\text{LiCH}_2\text{SiMe}_3$  (188 mg, 2 mmol) and  $\text{MnCl}_2$  (63 mg, 0.5 mmol), THF (5 mL) was added and the reaction was left stirring at ambient temperature (20 °C) for 15 minutes, the temperature was then cooled down (-78 °C). A different oven dried Schlenk tube was charged with 1-(*tert*-butyl)-4-iodobenzene (390 mg, 1.5 mmol), THF (3 mL) was added and the temperature was cooled to (-78 °C). The two solutions were mixed via cannula and the mixture was stirred for 15 minutes. The mixture was then allowed to stir at ambient temperature (20 °C) for 16 hours. The reaction mixture was then quenched with brine 2 mL. The crude was extracted using diethyl ether and brine (3 x 5 mL), the organic solution was dried over magnesium sulphate and the product was purified by flash column chromatography using hexane as eluent to give **11j** as a white solid (168 mg, 84% yield). <sup>1</sup>H NMR (400 MHz, CDCl<sub>3</sub>) δ (ppm) = 1.41 (s, 18H), 7.50 (d, *J*=8.5 Hz 4H), 7.57 (d, *J*=8.5 Hz 4H). <sup>13</sup>C{<sup>1</sup>H} NMR (101 MHz, CDCl<sub>3</sub>) δ (ppm) = 31.5, 34.6, 125.8, 126.8, 138.3, 150.0

#### 5.5.1.11 diethyl [1,1'-biphenyl]-4,4'-dicarboxylate (**11k**)



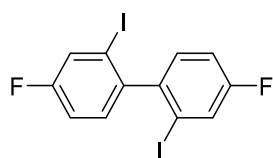
An oven dried Schlenk tube was charged with  $\text{LiCH}_2\text{SiMe}_3$  (188 mg, 2 mmol) and  $\text{MnCl}_2$  (63 mg, 0.5 mmol), THF (5 mL) was added and the reaction was left stirring at ambient temperature (20 °C) for 15 minutes, the temperature was then cooled down (-78 °C). A different oven dried Schlenk tube was charged with 4-iodobenzoate (414 mg, 1.5 mmol), THF (3 mL) was added and the temperature was cooled to (-78 °C). The two solutions were mixed via cannula and the mixture was stirred for 15 minutes. The mixture was then allowed to stir at ambient temperature (20 °C) for 16 hours. The reaction mixture was then quenched with brine 2 mL. The crude was extracted using diethyl ether and brine (3 x 5 mL), the organic solution was dried over magnesium sulphate and the product was purified by flash column chromatography using hexane/ $\text{Et}_2\text{O}$  8:2 as eluent to give **11k** as a white crystalline solid (78 mg, 35% yield).  $^1\text{H NMR}$  (400 MHz,  $\text{CDCl}_3$ )  $\delta$  (ppm) = 1.41 (t,  $J=7.1$  Hz, 6H), 4.40 (q,  $J=7.1$  Hz, 4H), 7.67 (d,  $J=8.5$  Hz, 4H), 8.12 (d,  $J=8.5$  Hz, 4H).  $^{13}\text{C}\{\text{H}\}$  NMR (101 MHz,  $\text{CDCl}_3$ )  $\delta$  (ppm) = 14.4, 61.2, 127.3, 130.1, 130.2, 144.4, 166.4. The values are consistent with previous data reported in the literature.<sup>12</sup>

#### 5.5.1.12 4,4'-difluoro-1,1'-biphenyl (**11l**)



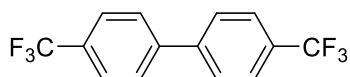
An oven dried Schlenk tube was charged with  $\text{LiCH}_2\text{SiMe}_3$  (188 mg, 2 mmol) and  $\text{MnCl}_2$  (63 mg, 0.5 mmol), THF (5 mL) was added and the reaction was left stirring at ambient temperature (20 °C) for 15 minutes, the temperature was then cooled down (-78 °C). A different oven dried Schlenk tube was charged with 1-fluoro-4-iodobenzene (333 mg, 1.5 mmol), THF (3 mL) was added and the temperature was cooled to (-78 °C). The two solutions were mixed via cannula and the mixture was stirred for 15 minutes. The mixture was then allowed to stir at ambient temperature (20 °C) for 16 hours. The reaction mixture was then quenched with brine 2 mL. The crude was extracted using diethyl ether and brine (3 x 5 mL), the organic solution was dried over magnesium sulphate and the product was purified by flash column chromatography using hexane as eluent to give **11l** as a white solid (97 mg, 68% yield) as well as **11l'** (39 mg, 12% yield).  $^1\text{H NMR}$  (400 MHz,  $\text{CDCl}_3$ )  $\delta$  (ppm) = 7.10-7.14 (m, 4H), 7.47-7.51 (m, 4H).  $^{13}\text{C NMR}$  (101 MHz,  $\text{CDCl}_3$ )  $\delta$  (ppm) = 115.7 (d,  $J=21$  Hz), 128.8, 136.5 (d,  $J=3$  Hz), 162.6 (d,  $J=245$  Hz).  $^{19}\text{F}\{\text{H}\}$  NMR (376 MHz,  $\text{CDCl}_3$ )  $\delta$  (ppm) = -115.8.

### 5.5.1.13 4,4'-difluoro-2,2'-diiodo-1,1'-biphenyl (11l')



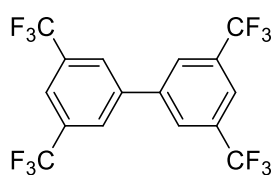
$^1\text{H NMR}$  (400 MHz,  $\text{CDCl}_3$ )  $\delta$  (ppm) = 7.14 (t,  $J=8.6$  Hz, 2H), 7.57-7.59 (m, 2H), 7.61 (s, 2H).  $^{13}\text{C}\{\text{H}\}$  NMR (101 MHz,  $\text{CDCl}_3$ )  $\delta$  (ppm) = 115.9 (d,  $J=21.5$  Hz), 127.6, 128.7 (d,  $J=8$  Hz), 136.9 (d,  $J=4$  Hz), 139.4, 162.7 (d,  $J=245$  Hz).  $^{19}\text{F}\{\text{H}\}$  NMR (376 MHz,  $\text{CDCl}_3$ )  $\delta$  (ppm) = -115.5.

### 5.5.1.14 4,4'-bis(trifluoromethyl)-1,1'-biphenyl (11m)



An oven dried Schlenk tube was charged with  $\text{LiCH}_2\text{SiMe}_3$  (188 mg, 2 mmol) and  $\text{MnCl}_2$  (63 mg, 0.5 mmol), THF (5 mL) was added and the reaction was left stirring at ambient temperature (20 °C) for 15 minutes, the temperature was then cooled down (-78 °C). A different oven dried Schlenk tube was charged with 1-iodo-4-(trifluoromethyl)benzene (408 mg, 1.5 mmol), THF (3 mL) was added and the temperature was cooled to (-78 °C). The two solutions were mixed via cannula and the mixture was stirred for 15 minutes. The mixture was then allowed to stir at ambient temperature (20 °C) for 16 hours. The reaction mixture was then quenched with brine 2 mL. The crude was extracted using diethyl ether and brine (3 x 5 mL), the organic solution was dried over magnesium sulphate and the product was purified by flash column chromatography using hexane as eluent to give **11m** as a white solid (159 mg, 73% yield).  $^1\text{H NMR}$  (400 MHz,  $\text{CDCl}_3$ )  $\delta$  (ppm) = 7.73 (m, 8H).  $^{13}\text{C}\{\text{H}\}$  NMR (101 MHz,  $\text{CDCl}_3$ )  $\delta$  (ppm) = 124.3 (q,  $J=271$  Hz), 126.1 (q,  $J=3$  Hz), 127.8, 130.5 (q,  $J=33$  Hz), 143.4.  $^{19}\text{F}\{\text{H}\}$  NMR (376 MHz,  $\text{CDCl}_3$ )  $\delta$  (ppm) = -62.6.

### 5.5.1.15 3,3',5,5'-tetrakis(trifluoromethyl)-1,1'-biphenyl (11n)

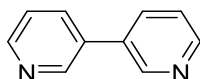


An oven dried Schlenk tube was charged with  $\text{LiCH}_2\text{SiMe}_3$  (188 mg, 2 mmol) and  $\text{MnCl}_2$  (63 mg, 0.5 mmol), THF (5 mL) was added and the reaction was left stirring at ambient temperature (20 °C) for 15 minutes, the temperature was then cooled down (-78 °C). A different oven dried Schlenk tube was charged with 1-iodo-3,5-bis(trifluoromethyl)benzene (510 mg, 1.5 mmol), THF (3 mL) was added and the temperature was cooled to (-78 °C). The two solutions were mixed via cannula and the mixture was stirred for 15 minutes. The mixture was then allowed to stir at ambient temperature (20 °C) for 16 hours. The reaction mixture was then quenched with brine 2 mL. The crude was extracted using diethyl ether and brine (3 x 5 mL),

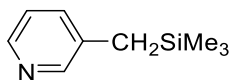
the organic solution was dried over magnesium sulphate and the product was purified by flash column chromatography using hexane as eluent to give **11n** as a white solid (220 mg, 69% yield).  $^1\text{H NMR}$  (400 MHz,  $\text{CDCl}_3$ )  $\delta$  (ppm) = 7.99 (broad s, 2H), 8.03 (broad s, 4H).  $^{13}\text{C}\{\text{H}\}$  NMR (101 MHz,  $\text{CDCl}_3$ )  $\delta$  (ppm) = 122.8 (m), 123.2 (q,  $J=271$  Hz), 127.7 (d,  $J=3$  Hz), 133.1 (q,  $J=34$  Hz), 140.6.

#### 5.5.1.16 3,3'-bipyridine (**11o**) and 3-((trimethylsilyl)methyl)pyridine (**11o'**)

An oven dried Schlenk tube was charged with  $\text{LiCH}_2\text{SiMe}_3$  (188 mg, 2 mmol) and  $\text{MnCl}_2$  (63 mg, 0.5 mmol), THF (5 mL) was added and the reaction was left stirring at ambient temperature (20 °C) for 15 minutes, the temperature was then cooled down (-78 °C). A different oven dried Schlenk tube was charged with 3-iodopyridine (308 mg, 1.5 mmol), THF (3 mL) was added and the temperature was cooled to (-78 °C). The two solutions were mixed via cannula and the mixture was stirred for 15 minutes. The mixture was then allowed to stir at ambient temperature (20 °C) for 16 hours. The reaction mixture was then quenched with brine 2 mL. The crude was extracted using diethyl ether and brine (3 x 5 mL), the organic solution was dried over magnesium sulphate and the product was purified by flash column chromatography using hexane/ $\text{Et}_2\text{O}$  6:4 as eluent to give **11o** as a pale yellow solid (74 mg, 63% yield) and **11o'** as a colourless oil (25 mg, 20% yield).

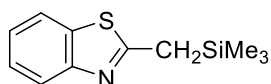


$^1\text{H NMR}$  (400 MHz,  $\text{CDCl}_3$ )  $\delta$  (ppm) = 7.38-7.42 (m, 2H), 7.86-7.89 (m, 2H), 8.64-8.65 (m, 2H), 8.83 (d,  $J=1.9$  Hz, 2H).  $^{13}\text{C}\{\text{H}\}$  NMR (101 MHz,  $\text{CDCl}_3$ )  $\delta$  (ppm) = 123.9, 133.6, 134.5, 148.3, 149.4.



$^1\text{H NMR}$  (400 MHz,  $\text{CDCl}_3$ )  $\delta$  (ppm) = 0.02 (s, 9H), 2.02 (s, 2H), 7.08-7.11 (m, 1H), 7.26-7.28 (m, 1H), 8.26-8.30 (m, 2H).  $^{13}\text{C}\{\text{H}\}$  NMR (101 MHz,  $\text{CDCl}_3$ )  $\delta$  (ppm) = -2.0, 24.0, 123.1, 135.2, 136.2, 145.5, 149.2.

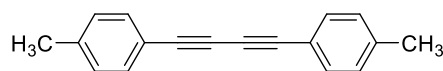
#### 5.5.1.17 2-((trimethylsilyl)methyl)benzothiazole (**11p**)



An oven dried Schlenk tube was charged with  $\text{LiCH}_2\text{SiMe}_3$  (188 mg, 2 mmol) and  $\text{MnCl}_2$  (63 mg, 0.5 mmol), THF (5 mL) was added and the reaction was left stirring at ambient temperature (20 °C) for 15 minutes, the temperature was

then cooled down (-78 °C). A different oven dried Schlenk tube was charged with 2-iodobenzothiazole (392 mg, 1.5 mmol), THF (3 mL) was added and the temperature was cooled to (-78 °C). The two solutions were mixed via cannula and the mixture was stirred for 15 minutes. The mixture was then allowed to stir at ambient temperature (20 °C) for 16 hours. The reaction mixture was then quenched with brine 2 mL. The crude was extracted using diethyl ether and brine (3 x 5 mL), the organic solution was dried over magnesium sulphate and the product was purified by flash column chromatography using hexane/EtOAc 9:1 as eluent to give **11p** as a white solid (209 mg, 63% yield). <sup>1</sup>H NMR (400 MHz, CDCl<sub>3</sub>) δ (ppm) = 0.14 (s, 9H), 2.68 (s, 2H), 7.26-7.30 (m, 1H), 7.38-7.42 (m, 1H), 7.76-7.78 (m, 1H), 7.88-7.90 (m, 1H). <sup>13</sup>C{<sup>1</sup>H} NMR (101 MHz, CDCl<sub>3</sub>) δ (ppm) = -1.5, 26.7, 121.2, 121.9, 124.1, 125.8, 135.3, 153.9, 170.2.

#### 5.5.1.18 1,4-di-*p*-tolylbuta-1,3-diyne (**11r**)



An oven dried Schlenk tube was charged with LiCH<sub>2</sub>SiMe<sub>3</sub> (188 mg, 2 mmol) and MnCl<sub>2</sub> (9 mg, 0.075 mmol), THF (5 mL) was added and the reaction was left stirring at ambient temperature (20 °C) for 15 minutes. *p*-tolylacetylene (174 mg, 1.5 mmol) was then added and the mixture was stirred for 15 minutes. The reaction mixture was exposed to dry O<sub>2</sub> for 16 hours using tube charged calcium hydride as a drying agent. The reaction mixture was then quenched with brine 2 mL. The crude was extracted using diethyl ether and brine (3 x 5 mL), the organic solution was dried over magnesium sulphate and the product was purified by flash column chromatography using hexane as eluent to give **11r** as a white solid (220 mg, 69% yield). <sup>1</sup>H NMR (400 MHz, CDCl<sub>3</sub>) δ (ppm) = 2.37 (s, 6H), 7.14 (d, *J*=7.9 Hz, 4H), 7.42 (d, *J*=1.9 Hz, 4H). <sup>13</sup>C{<sup>1</sup>H} NMR (101 MHz, CDCl<sub>3</sub>) δ (ppm) = 21.8, 73.6, 81.7, 118.9, 129.3, 132.5, 139.6.

## 5.6 References:

- (1) Bringman, G.; Günther, C.; Othse, M.; Schupp, O.; Tasler, S. *Progress in the chemistry of organic natural products*, Springer.; Hertz, W., Falk, H., Kirby, G. W., Moore, R. B., Eds.; 2001.
- (2) Miyake, T.; Kigoshi, H.; Akita, H. *Tetrahedron Asymm.* **2007**, *18* (24), 2915–2922.
- (3) Hobbs, P. D.; Upender, V.; Liu, J.; Pollart, D. J.; Thomas, D. W.; Dawson, M. I. *Chem. Commun.* **1996**, No. 8, 923–924.
- (4) Fukuyama, Y.; Asakawa, Y. *J. Chem. Soc. Perkin Trans. 1* **1991**, 2737–2741.
- (5) Degnan, A. P.; Meyers, A. I. *J. Am. Chem. Soc.* **1999**, *121* (12), 2762–2769.
- (6) Buter, J.; Heijnen, D.; Vila, C.; Hornillos, V.; Otten, E.; Giannerini, M.; Minnaard, A. J.; Feringa, B. L. *Angew. Chemie Int. Ed.* **2016**, *55* (11), 3620–3624.
- (7) Wu, J.; Chan, A. S. C. *Acc. Chem. Res.* **2006**, *39* (10), 711–720.
- (8) Ullmann, F.; Bielecki, J. *Chem. Ber.* **1901**, *31* (2), 1697–1698.
- (9) Hassan, J.; Se, M.; Gozzi, C.; Schulz, E.; Lemaire, M. *Chem. Rev.* **2002**, *102*, 1359–1469.
- (10) Mukhopadhyay, S.; Rothenberg, G.; Gitis, D.; Wiener, H.; Sasson, Y. *J. Chem. Soc. Perkin Trans. 2* **1999**, No. 11, 2481–2484.
- (11) Shezad, N.; Clifford, A. A.; Rayner, C. M. *Green Chem.* **2002**, *4* (1), 64–67.
- (12) Cahiez, G.; Moyeux, A.; Buendia, J.; Duplais, C. *J. Am. Chem. Soc.* **2007**, *129* (45), 13788–13789.
- (13) Bottoni, A.; Cahiez, G.; Calvaresi, M.; Moyeux, A.; Giacinto, P.; Miscione, G. Pietro. *J. Organomet. Chem.* **2016**, *814*, 25–34.
- (14) Littke, A. F.; Fu, G. C. *Angew. Chemie Int. Ed.* **2002**, *41*, 4176–4211.
- (15) Cahiez, G.; Duplais, C.; Buendia, J. *Angew. Chemie Int. Ed.* **2009**, *48* (36), 6731–6734.
- (16) Oshima, K.; Yorimitsu, H. In *The Chemistry of Organomagnesium Compounds*; Rapport, Z., Marek, I., Eds.; John Wiley & Sons, 2008; pp 681–715.
- (17) Huang, P. C. *J. Am. Chem. Soc.* **1967**, *89* (15), 3911.
- (18) Harada, T.; Katsuhira, T.; Hattori, K.; Oku, A. *J. Org. Chem.* **1993**, *58* (11), 2958–2965.
- (19) Corey, E. J.; Posner, G. H. *Tetrahedron Lett.* **1970**, 315–318.
- (20) Dalton, J. C. S.; Dialkyls, M.; Dialkyl, M.; Adducts, A.; Andersen, B. R. A.; Carmona-guzman, E.; Gibson, J. F.; Wilkinson, G. *Dalton Trans.* **1976**, 2204.
- (21) Alberola, A.; Blair, V. L.; Carrella, L. M.; Clegg, W.; Kennedy, A. R.; Klett, J.; Mulvey, R. E.; Newton, S.; Rentschler, E.; Russo, L. *Organometallics* **2009**, *28*, 2112–2118.
- (22) Weiss, E. *Angew. Chemie Int. Ed.* **1993**, *32* (11), 1501–1523.
- (23) Schubert, B.; Weiss, U. B. E.; Schubert, B.; Behrens, U. *Chem. Ber.* **1981**, *114*, 2640–2643.

- (24) Morris, R. J.; Girolami, G. S. *Organometallics* **1989**, 8 (20), 1478–1485.
- (25) Morris, R. J.; Girolami, G. S. *J. Am. Chem. Soc.* **1988**, 110 (9), 6245–6246.
- (26) Hevia, E.; Kennedy, A. R.; Klett, J.; Baillie, S. E.; Clegg, W.; García-Álvarez, P.; Russo, L. *Organometallics* **2012**, 31, 5131.
- (27) Wittig, G.; Fuhrmann, G. *Berichte der Dtsch. Chem. Gesellschaft* **1940**, 73 (11), 1197–1218.
- (28) Gilman, H.; Langham, W.; Jacoby, A. L. *J. Am. Chem. Soc.* **1939**, 61 (1), 106–109.
- (29) J. Clayden. *Organolithiums: Selectivity for synthesis*; Elsevier: Oxford, 2002.
- (30) Sheppard, T. D. *Org. Biomol. Chem.* **2009**, 7 (6), 1043.
- (31) Wunderlich, S. H.; Kienle, M.; Knochel, P. *Angew. Chemie Int. Ed.* **2009**, 48 (39), 7256–7260.
- (32) Peng, Z.; Knochel, P. *Org. Lett.* **2011**, 13 (12), 3198–3201.
- (33) Transformations, O. *J. Am. Chem. Soc.* **2004**, 126, 8755.
- (34) Valyaev, D. A.; Lavigne, G.; Lugan, N. *Coord. Chem. Rev.* **2016**, 308, 191–235.
- (35) Müller, K.; Faeh, C.; Diederich, F. *Science* **2007**, 317 (5846), 1881–1886.
- (36) Schlosser, M.; Michel, D. *Tetrahedron* **1996**, 52 (1), 99–108.
- (37) Gouverneur, V.; Purser, S.; Moore, P. R.; Swallow, S. *Chem. Soc. Rev.* **2008**, 37 (2), 237–432.
- (38) Ojima, I. *J. Org. Chem.* **2013**, 78 (13), 6358–6383.
- (39) O’Hagan, D.; B. Harper, D. *J. Fluor. Chem.* **1999**, 100 (1–2), 127–133.
- (40) Gribble, G. W. *J. Nat. Prod.* **1992**, 55 (10), 1353–1395.
- (41) *The chemistry of organolithium compounds*; Rappoport, Z., Marek, I., Eds.; Wiley: Chichester England, 2004.
- (42) Bunnett, J. F. *J. Chem. Educ.* **1961**, 38 (6), 278.
- (43) Krasovskiy, A.; Krasovskaya, V.; Knochel, P. *Angew. Chemie Int. Ed.* **2006**, 45 (18), 2958–2961.
- (44) Jia, X.; Yin, K.; Li, C.; Li, J.; Bian, H. *Green Chem.* **2011**, 13 (8), 2175.
- (45) Leyva-Pérez, A.; Doménech-Carbó, A.; Corma, A. *Nat. Commun.* **2015**, 6 (May 2014), 6703.

## Chapter 6

### Conclusions and Further Work

#### 6.1 Conclusions

The ultimate milestone for synthetic chemistry nowadays is the development of both new and existing routes using non-toxic and abundant elements. Although the use of single metal reagents has prevailed for many years, advances understanding synergistic effects in mixed-metal ates has propelled their applications in cornerstone organic transformations. Contrastingly their applications in catalytic transformations has hardly been explored. This thesis opens new ground in mixed-metal chemistry by pioneering the use of mixed-alkali metal magnesium reagents in catalytic transformations. Furthermore, it also provides new synthetic insights on exploring cooperative effects to promote direct regioselective Mg-H exchange reactions as well as homocoupling processes of aryl halides mediated by novel lithium manganate reagents.

Initial studies were based on the development of deprotonative metallation chemistry via potassium mediated magnesiation reactions, formally Mg/H exchange processes. Interestingly a variety of aromatic and heterocyclic substrates have been deprotonated at room temperature and under mild reaction conditions. Detailed GC and spectroscopic studies showed that substoichiometric amounts of the K-Magnesiates can perform direct *ortho*-metallations of aromatic and heterocyclic substrates at room temperature in hydrocarbon solvents. Since only 0.33 equivalents of  $(\text{PMDETA})_2\text{K}_2\text{Mg}(\text{CH}_2\text{SiMe}_3)_4$  (**1b**) are required to quantitatively *ortho*-metallate one equivalent of anisole (**2a**), this bimetallic approach is atom-efficient. Studies have suggested the involvement of CIP intermediates, with the presence of K being the key to facilitate these novel magnesiation reactions as when K is replaced by Li or Na atoms the magnesiation process is suppressed.

Upgrading from stoichiometric to catalytic applications has been accomplished using alkali metal magnesiates only once previously. Thus, it was very exciting to develop novel applications of alkali metal magnesiates as catalysts.  $(\text{TMEDA})_2\text{Na}_2\text{Mg}(\text{CH}_2\text{SiMe}_3)_4$  (**1d**) was employed to develop the first ever ate-catalysed cycloaddition reaction of alkynes to azides to form 1,5-disubstituted triazoles molecules. Structural, spectroscopic and new kinetic studies in this field revealed that this methodology works in a concerted synergistic manner as a more sustainable method to the already known transition metal catalysts. Thus, the use of catalysts

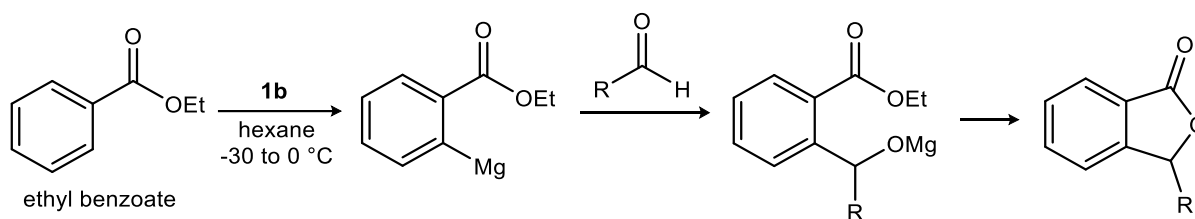
such as **1d** and  $\text{NaMg}(\text{CH}_2\text{SiMe}_3)_3$  (**1f**) containing both a Lewis acid (Na) which can anchor the azide and a Lewis base ( $\text{Mg}-\text{C}\equiv\text{C}-\text{R}$ ) with enhanced nucleophilicity both within the same molecule, dramatically reduces the activation energy for the reaction to take place. This is in agreement with the low reaction times and mild reaction conditions needed in this methodology compared to other method. Furthermore when the synergy between the two metals is broken using crown ethers which sequestered the Na atom the reaction does not occur. Kinetic studies have shown the reaction rate is independent from alkyne concentration, alkyne order is zero, thus the deprotonation of alkyne is not involved in the rate determining step of the reaction. Furthermore, the reaction is order one in azide and order one in catalyst. These result suggest that the rate determining step of the reaction is the Insertion/intramolecular nucleophilic attack. Furthermore only one arm of the potentially four within sodium magnesiate **1d** is active at a time in each catalytic cycle.

In addition, the first catalytic applications of alkali-metal magnesiates in guanylation and hydrophosphination reactions was developed using lower order sodium magnesiate  $\text{NaMg}(\text{CH}_2\text{SiMe}_3)_3$  (**1f**). Studies suggest that the enhanced catalytic activity of these systems is due to anionic activation.

Similarities between Mn and Mg atoms have allowed the structural elucidation of a variety of novel alkali metal manganates, formally Mn(II) compounds, which are isostructural to alkali metal magnesiates. Finally, the use of this compounds was studied in detail for the Mn/I exchange reaction followed by C-C bond formation to generate biaryl compounds. The reaction of substoichiometric amounts of  $[(\text{THF})_x\text{Li}_2\text{Mn}(\text{CH}_2\text{SiMe}_3)_4]$  (**1u**) with 3 equivalents of aryl halides allowed to obtain a variety of biaryl reagents in good yields. This reactivity could not be replicated by  $\text{Mn}(\text{CH}_2\text{SiMe}_3)_2$  which did not react with 4-iodoanisole, and  $\text{LiCH}_2\text{SiMe}_3$  which was able to promote the Li/I exchange reaction but was unable to furnish any substantial formation of homocoupled product. Although the mechanism involved in these type of transformation is still under debate, it is safe to say that these transformation proceeds through reductive coupling type mechanism. This has been confirmed by the need of a reducing agent such as Mg(s) when the reaction is carried out using catalytic amounts of Mn. This is in contrast with Cahiez's  $\text{MnCl}_2\cdot\text{LiCl}$  methodology which requires of an oxidizing agent such as  $\text{O}_2$  to take place.

## 6.2 Further work

The initial findings included in this report (**Chapter 2**) open new ground towards developing new synthetic applications of potassium magnesiate reagents. Further work in the area will include expanding the substrate scope of this approach. For example aromatic esters as ethyl benzoate will be studied. These substrates are particularly appealing as ortho-metallated species can lead to intramolecular cascade process in the presence of aldehydes to form lactones as final products (**Scheme 6.1**).



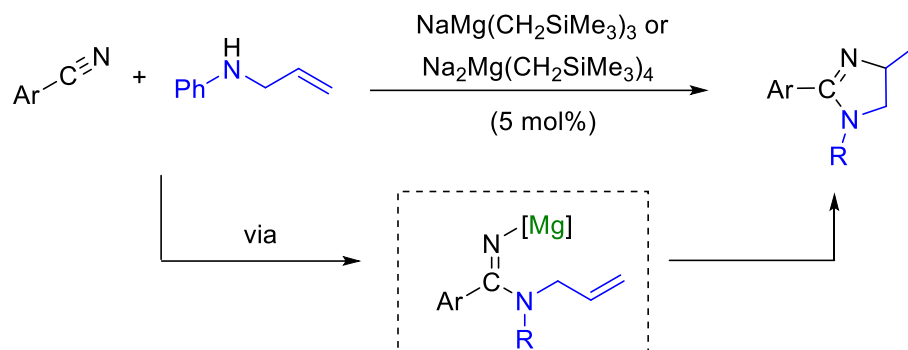
**Scheme 6.1:** Deprotonation reaction of aromatic ester

Furthermore, this approach could also be tested for the metallation of other challenging organic molecules such as non-aromatic and olefinic substrates whose deprotonation has proved significantly more challenging using single-metal bases. In addition, it will also be interesting to extend our electrophilic quenching studies to transition metal catalyzed C-C bond formation process. In this regard it is well-known that aryl magnesium reagents can undergo cross-coupling reaction with organic electrophiles RX in the presence of a Pd or Ni catalyst (Kumada coupling). However the use of arylmagnesiates species has hardly been explored. This leads to further applications. For example the functionalization of heterocyclic halides such as pyridines.

In addition, as reported in the literature, aryl magnesium reagents can react with alkyl halides under Fe(III) salt catalysis conditions to yield the relevant aryl-alkyl coupling product, investigations could be carried out to assess the effect of this chemistry with relation to potassium magnesiates and the potential transmetallation power of the magnesiate with the iron catalyst. This will be particularly attractive area to pursue, as iron-catalysis is regarded as a more sustainable alternative to other methods using Ni and Pd catalysts, which are significantly more expensive and also toxic.

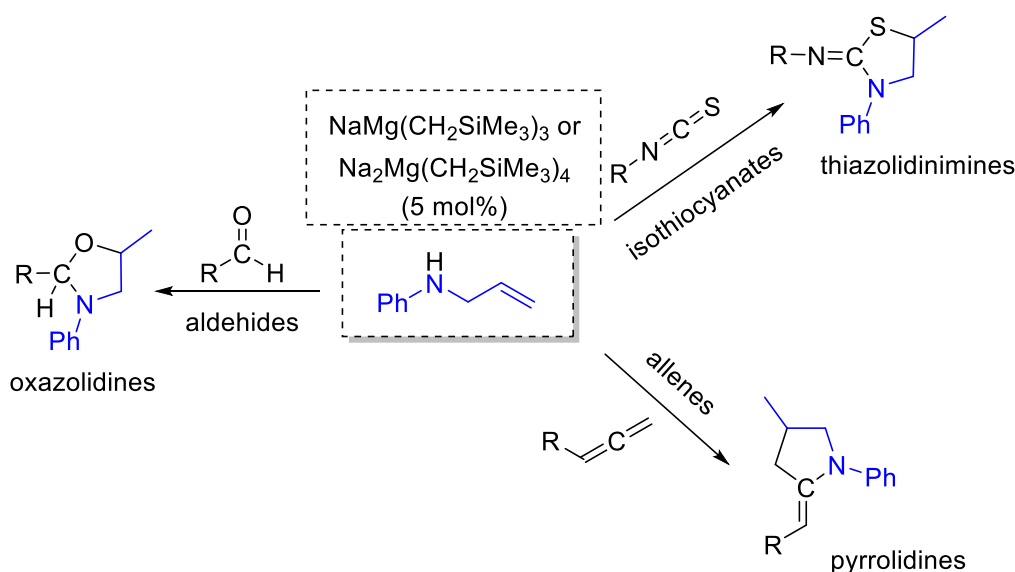
Reflecting on the activity of alkali metal magnesiates in catalytic applications (**Chapter 3** and **4**) a novel and wide open area of chemistry involving the use of both  $M^I\text{Mg}(\text{CH}_2\text{SiMe}_3)_3$  and

$M^I_2Mg(CH_2SiMe_3)_4$  ( $M^I = Li, Na, K$ ) will be studied. For example, the cycloamidation reaction between aminoalkenes and nitriles for the synthesis of substituted 2-imidazolines can be carried out using  $Ln[N(SiMe_3)_2]_3$  catalysts (**Scheme 6.2**).



**Scheme 6.2:** The cycloamidation reaction between aminoalkenes and nitriles

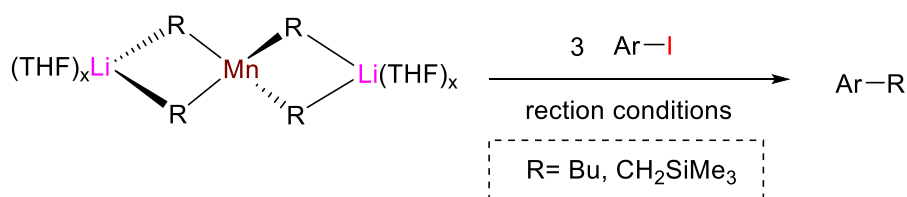
The reaction is sought to proceed via simple deprotonation of the aminoalkene derivative, thus forming a more nucleophilic Mg-N bond, further insertion of the nucleophilic N atom to the electrophilic C of the nitrile and attack to the alkene would generate the corresponding 2-imidazoline product. This is only a single example of the potential application of alkali metal ates in catalysis, although their use can be upgraded to a variety of transformations. By simply selecting different electrophiles a wide range of chemical transformations can be designed. Thus, reaction of N-allylaniline with isothiocyanates would give rise to cyclic thiazolidinimines, furthermore the use of aldehydes as electrophiles would generate oxazolidines. In addition using allenes would form benzylic substituted pyrrolidines (**Scheme 6.3**). In all cases the selection of a different electrophile would potentially allow to develop new elegant reaction procedures using alkali metal ates as catalysts.



**Scheme 6.3:** Potential uses of alkali metal magnesiates in catalytic applications

Similarly, other transformations can be developed by changing the nucleophilic substrate, a good example is the catalytic hydroacetylation of carbodiimides to form different substituted amidines, which has previously been studied by M. Hill using homoleptic alkaline earth hexamethyldisilazides.

In addition, the effect of the alkali metal in the Mn/I exchange methodology will be assessed by replacing the Li atom by Na and K and testing their efficiency in the generation of biaryl compounds. Further studies using alkali metal/main-group ate complexes for the development of novel cross coupling reactions will be studied. Carefull selection of substrates and reaction conditions will be studied to access new C-C bond formation reactions (**Scheme 6.4**):



**Scheme 6.4:** Development of new type of alkali metal manganates catalysed cross coupling reactions

In addition potassium manganates will be tested in ortho metallation reactions, similarly to what described in **Chapter 2** they will be also studied in the Mn/H exchange processes with potential noble TM free C-C bond forming reactions.

## Chapter 7

### General experimental techniques and procedures

#### 7.1 Schlenk line techniques

The organometallic reagents employed in this project are extremely air and moisture sensitive. For this reason an argon atmosphere was used for all organometallic reactions carried out in this project. Standard Schlenk techniques, involving the repeated use of high-vacuum Schlenk line (**figure 7.1**) were employed as a matter of routine.

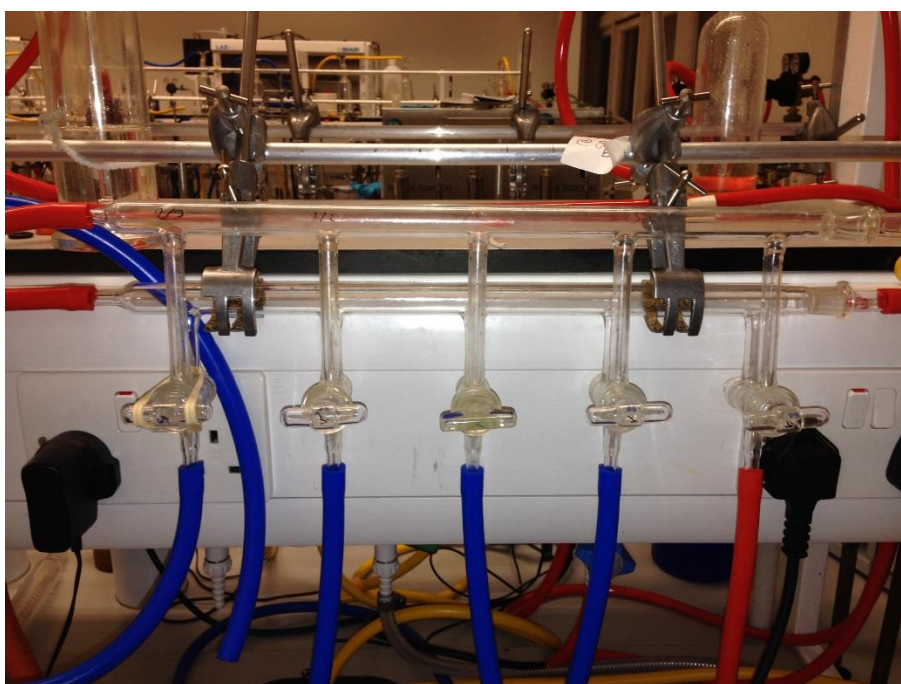


**Figure 7.1:** Standard Schlenk line

A typical Schlenk line consists of two independent paths: one of which is connected to a vacuum pump; and another which supplies dry and oxygen-free argon gas, with two oil bubblers en route to avoid a build-up of gas pressure. This also prevents air entering the system and contaminating the argon source. The one photographed in **Figure 7.1** contains five connections to Schlenk apparatus, primarily Schlenk tubes. Each connections has a two-way tap which can be adjusted so that the apparatus can be subjected to a vacuum or to an argon source. Air can be removed from the Schlenk tubes by evacuating them, and then subsequently refilling with argon gas, and this process is repeated three times as standard practice. A trap, which is placed in a liquid nitrogen-filled Dewar flask, is included to condense any volatile substances just before reaching, and will prevent the vacuum pump to get damaged.

## 7.2 Glove Box Techniques

The manipulation of all solid reactants and products, for example, for the determinations of weights of reactant solids and product yields, and also for NMR spectroscopic preparations, had to be carried out in an inert atmosphere, to prevent decontamination or decomposition. Hence, an argon-filled glove box was the best apparatus at hand to achieve this manipulations safely. A typical glove box is shown in (Figure 7.2)



**Figure 7.2:** Standard Glove box

The small port on the right-hand side of the box allows the transfer of chemicals and small pieces of apparatus in and out of the glove box. Once the item(s) of interest are placed in the port, the outer port door is closed and, as for the Schlenk line, a pattern of evacuating the port and then refilling with argon is followed twice. The inner port door can then be opened in the knowledge that no, or negligible quantities, of  $\text{H}_2\text{O}$  or  $\text{O}_2$  has entered the main body of the glove box.

